UNIVERSITEIT VAN PRETORIA
UNIVERSITY OF PRETORIA
YUNIBESITHI YA PRETORIA

Multimetal complexes of Fischer carbenes

by

Daniela Ina Bezuidenhout

Submitted in partial fulfilment of the requirements of the degree

Philosophiae Doctor

In the Faculty of Natural and Agricultural Sciences

University of Pretoria
Pretoria

Supervisors:	Professor Simon Lotz Doctor Marilé Landman

March 2010

Declaration

I declare that the thesis, which I hereby submit for the degree Philosophiae Doctor at the University of Pretoria, is my own work and has not previously been submitted by me for a degree at this or any other tertiary institution.

The X-ray structure determinations reported in this thesis were performed by Mr DC Liles at the University of Pretoria.

Results obtained from this study have also been published in:
D.I. Bezuidenhout, E. van der Watt, D.C. Liles, M. Landman, S. Lotz,
Organometallics **2008,** *27*, 2447-2456.

Signature:

Date:

Acknowledgements

I would like to thank the following people for their contributions towards this thesis:

My supervisors, Prof. Simon Lotz and Dr. Marilé Landman, for their guidance, support and friendship. Thank you also for your enthusiasm towards research, and the freedom you have allowed me in this project.

Prof. Dwight A. Sweigart, for the opportunity to work in his laboratories at Brown University, USA, and his guidance in my electrochemical studies.

Mr Dave Liles, who performed the data collections and structure determinations of my single crystal X-ray diffraction results. Your inputs were very valuable, and are much appreciated.

Mr Eric Palmer, who kindly assisted with the recording of the NMR data far beyond the call of duty.

Werner Barnard, for his assistance not only with the measurement and interpretation of the Raman spectra, but for his generous sharing of scientific knowledge in general. Thank you for your unfailing friendship, enthusiasm and endless supply of entertainment throughout all the years! I cannot imagine a more loyal friend and dedicated scientist.

My fellow lab workers: Andrew Olivier, Elisia Swart, Jacorien Coetzee, Belinda van der Westhuizen and Nina van Jaarsveld. At different times in my career, you have suffered, laughed, and have faced many fiery situations together with me. Thank you for all your different contributions.

My parents, Danie and Ina Bezuidenhout, and sister Annalie, who have always believed in me, and provided all the inspiration needed to complete this degree.

Sean, for your love, support and encouragement. I could not have done it without you.

Daniela

Table of Contents

Chapter 1 Introduction

Chapter 2 Group VI Transition Metal Carbene Cluster Complexes

Chapter 3 Group VII Transition Metal Carbene Cluster Complexes

Chapter 4 Investigation of substituent effect on carbene ligands

Chapter 5 Experimental

Appendices

Attached compact disk

Summary

Multimetal complexes of Fischer carbenes

by

Daniela Ina Bezuidenhout

Supervisor: Prof S Lotz
Co-supervisor: Dr M Landman
Submitted in partial fulfilment of the requirements for the degree Philosophiae Doctor, Department of Chemistry, University of Pretoria

Fischer carbene complexes of the Group VI transition metals (Cr, Mo and W) containing at least two or three different transition metal substituents, all in electronic contact with the carbene carbon atom, were synthesized and studied both in solution and in the solid state. For the complexes of the type $[M(CO)_5\{C(OR)R'\}]$, the substituents chosen included (hetero)aromatic (benzene or thiophene) rings π-bonded to a chromium tricarbonyl fragment or ferrocene as the R'-substituent, while the OR-substituent was systematically varied between an ethoxy or a titanoxy group, to yield the complexes **1** (M = Cr, R = Et, R' = Fc), **2** (M = W, R = Et, R' = Fc), **5** (M = Cr, R = $TiCp_2Cl$, R' = Fc), **6** (M = W, R = $TiCp_2Cl$, R' = Fc), **7** (M = Mo, R = $TiCp_2Cl$, R' = Fc), **12** (M = Cr, R = $TiCp_2Cl$, R' = 2-thienyl) and **13** (M = Cr, R = $TiCp_2Cl$, R' = $[Cr(CO)_3(\eta^6\text{-phenyl})]$).

Direct lithiation of the ferrocene with *n*-BuLi/TMEDA at elevated temperatures, followed by the Fischer method of carbene preparation, also resulted, in most cases, in the formation of the novel biscarbene complexes with bridging ferrocen-1,1'-diyl carbene ligands $[\mu\text{-Fe}\{C_5H_4C(OEt)M(CO)_5\}_2]$ (**3**: M = Cr, **4**: M = W) or the unusual bimetallacyclic bridged biscarbene complexes $[\{\mu\text{-TiCp}_2O_2\text{-O,O'}\}\{\mu\text{-Fe}(C_5H_4)_2\text{-C,C'}\}\{CM(CO)_5\}_2]$ (**8**: M = Cr, **9**: M = W, **10**: M = Mo). It was attempted to prepare the mixed heteronuclear biscarbene complex **11** $[W(CO)_5C\{\mu\text{-TiCp}_2O_2\text{-O,O'}\}\{\mu\text{-Fe}(C_5H_4)_2\text{-C,C'}\}CCr(CO)_5]$, however the complex could not be fully characterized.

The investigation was expanded to include Group VII transition metals Mn and Re, and using the same methodology, the manganese complexes isolated included [MnCp(CO)$_2${C(OR)Fc}] (**22**: R = Et, **24**: R = TiCp$_2$Cl), **23** [μ-Fe{C$_5$H$_4$C(OEt)MnCp(CO)$_2$}$_2$] and **25** [{μ-TiCp$_2$O$_2$-O,O'}{μ-Fe(C$_5$H$_4$)$_2$-C,C'}[CMnCp(CO)$_2$}$_2$]. The different reactivity of the binary dirhenium decacarbonyl precursor complex, compared to that of the Group VI complexes, resulted in the formation of a range of complexes. The target compounds [Re$_2$(CO)$_9${C(OR)Fc}] (**26**: R = Et, **31**: R = TiCp$_2$Cl), **27** [μ-Fe{C$_5$H$_4$C(OEt)Re$_2$(CO)$_9$}$_2$] and **33** [{μ-TiCp$_2$O$_2$-O,O'}{μ-Fe(C$_5$H$_4$)$_2$-C,C'}[CRe$_2$(CO)$_9$}$_2$] were isolated displaying a variety of different geometric isomers. In addition, acyl (**30**) and aldehyde (**32**) decomposition products, as well as hydrido (**29**), and hydrido acyl hydroxycarbene (**34**) complexes and the unique dichloro-bridged biscarbene complex (**28**) were also characterized. Most of these complexes displayed Re-Re bond breaking, and two probable mechanisms, either radical or ionic, were proposed involving either hydrogen transfer or protonation followed by hydrolysis.

Finally, the structural features and their relevance to bonding in the carbene cluster compounds of the Group VI transition metals were investigated as they represent indicators of possible reactivity sites in multimetal carbene assemblies. The possibility of using DFT calculations to quantify the effect of metal-containing substituents on the carbene ligands was tested and correlated with experimental parameters by employing methods such as vibrational spectroscopy, molecular orbital analysis, and cyclic voltammetry. The best results were obtained from the cyclic voltammetric studies, where the localized metal centre's oxidation potential correlated to both the calculated HOMO energy, and the effect of both the heteroatom substituent and the (hetero)arene substituent, as well as different combinations of the above.

List of Compounds

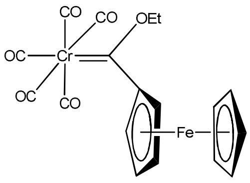

1 $[Cr(CO)_5\{C(OEt)Fc\}]$

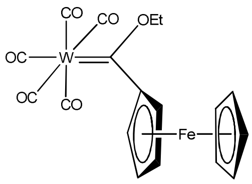

2 $[W(CO)_5\{C(OEt)Fc\}]$

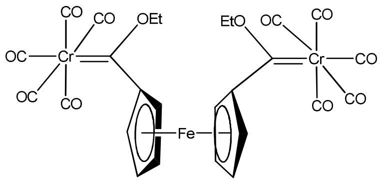

3 $[\mu\text{-}Fe\{C_5H_4C(OEt)Cr(CO)_5\}_2]$

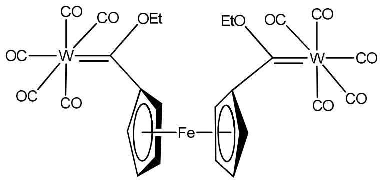

4 $[\mu\text{-}Fe\{C_5H_4C(OEt)W(CO)_5\}_2]$

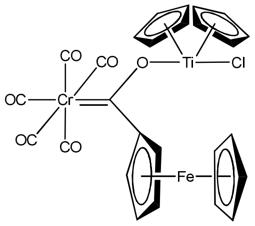

5 $[Cr(CO)_5\{C(OTiCp_2Cl)Fc\}]$

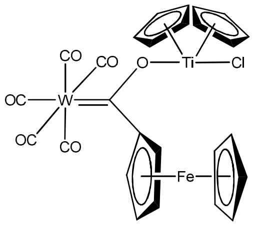

6 $[W(CO)_5\{C(OTiCp_2Cl)Fc\}]$

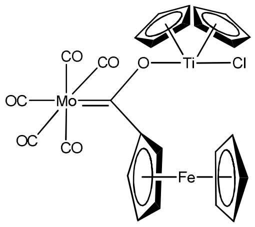

7 $[Mo(CO)_5\{C(OTiCp_2Cl)Fc\}]$

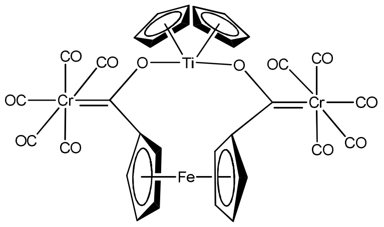

8 $[\{\mu\text{-}TiCp_2O_2\text{-}O,O'\}\{\mu\text{-}Fe(C_5H_4)_2\text{-}C,C'\}\{CCr(CO)_5\}_2]$

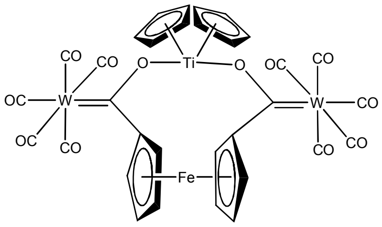

9 $[\{\mu\text{-TiCp}_2\text{O}_2\text{-O,O'}\}\{\mu\text{-Fe(C}_5\text{H}_4)_2\text{-C,C'}\}\{\text{CW(CO)}_5\}_2]$

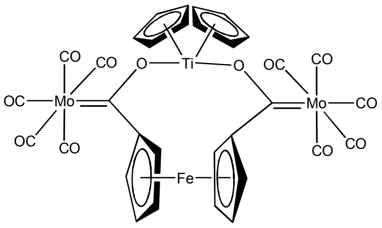

10 $[\{\mu\text{-TiCp}_2\text{O}_2\text{-O,O'}\}\{\mu\text{-Fe(C}_5\text{H}_4)_2\text{-C,C'}\}\{\text{CMo(CO)}_5\}_2]$

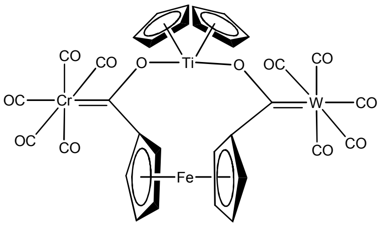

11 $[\text{W(CO)}_5\text{C}\{\mu\text{-TiCp}_2\text{O}_2\text{-O,O'}\}\{\mu\text{-Fe(C}_5\text{H}_4)_2\text{-C,C'}\}\text{CCr(CO)}_5]$

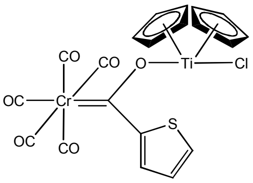

12 $[\text{Cr(CO)}_5\{\text{C(OTiCp}_2\text{Cl)(C}_4\text{H}_3\text{S)}\}]$

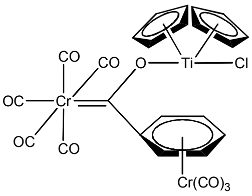

13 $[\text{Cr(CO)}_5\{\text{C(OTiCp}_2\text{Cl)}(\eta^1\text{:}\eta^6\text{-C}_6\text{H}_5)\text{Cr(CO)}_3]$

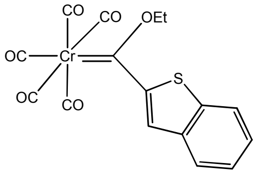

14 $[\mathrm{Cr(CO)_5\{C(OEt)(C_8H_5S)}]$

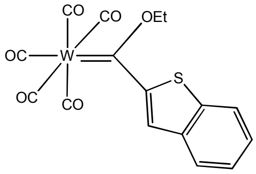

15 $[\mathrm{W(CO)_5\{C(OEt)(C_8H_5S)}]$

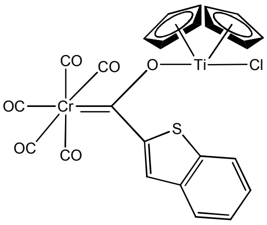

16 $[\mathrm{Cr(CO)_5\{C(OTiCp_2Cl)(C_8H_5S)}]$

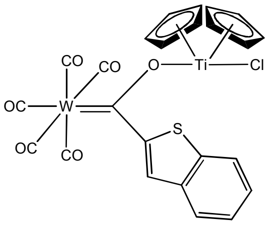

17 $[\mathrm{W(CO)_5\{C(OTiCp_2Cl)(C_8H_5S)}]$

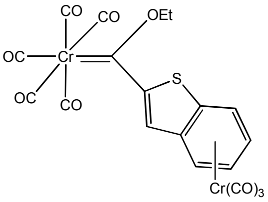

18 $[\mathrm{Cr(CO)_5\{C(OEt)(\eta^1{:}\eta^6\text{-}C_8H_5S)Cr(CO)_3}]$

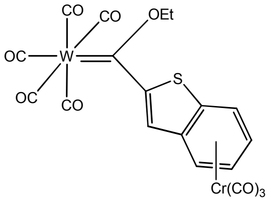

19 $[\mathrm{W(CO)_5\{C(OEt)(\eta^1{:}\eta^6\text{-}C_8H_5S)Cr(CO)_3}]$

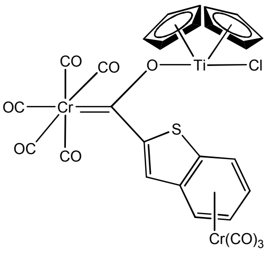

20 $[\mathrm{Cr(CO)_5\{C(OTiCp_2Cl)(\eta^1{:}\eta^6\text{-}C_8H_5S)Cr(CO)_3}]$

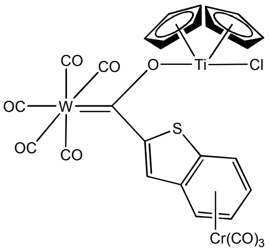

21 $[\mathrm{W(CO)_5\{C(OTiCp_2Cl)(\eta^1{:}\eta^6\text{-}C_8H_5S)Cr(CO)_3}]$

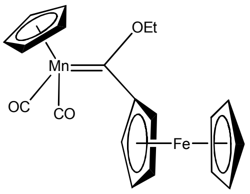

22 $[MnCp(CO)_2\{C(OEt)Fc\}]$

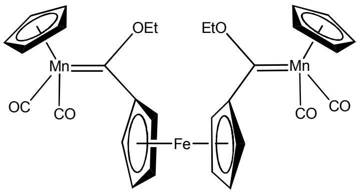

23 $[\mu\text{-}Fe\{C_5H_4C(OEt)MnCp(CO)_2\}_2]$

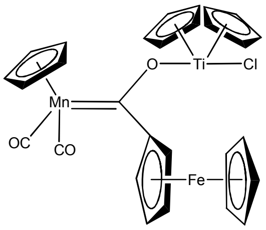

24 $[MnCp(CO)_2\{C(OTiCp_2Cl)Fc\}]$

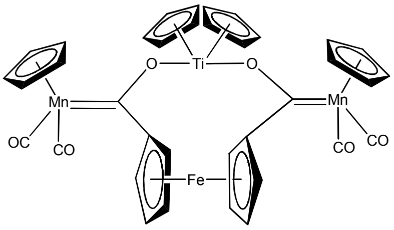

25 $[\{\mu\text{-}TiCp_2O_2\text{-}O,O'\}\{\mu\text{-}Fe(C_5H_4)_2\text{-}C,C'\}[CMnCp(CO)_2\}_2]$

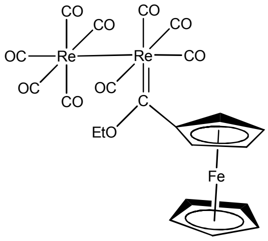

26 $[Re_2(CO)_9\{C(OEt)Fc\}]$

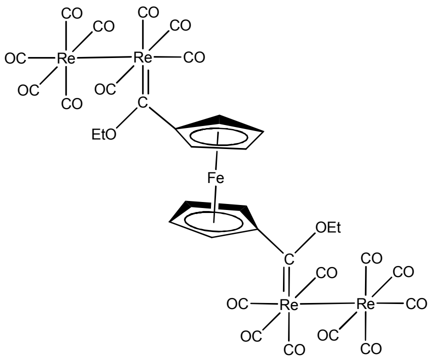

27 *eq,eq*-$[\mu\text{-}Fe\{C_5H_4C(OEt)Re_2(CO)_9\}_2]$

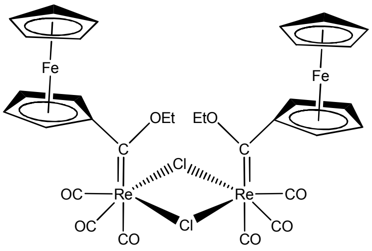

28 *fac*-$[(\mu\text{-}Cl)_2\text{-}(Re(CO)_3\{C(OEt)Fc\})_2]$

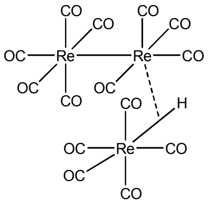

29 $[Re_3(CO)_{14}H]$

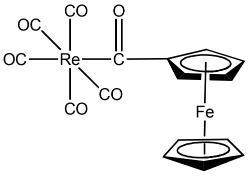

30 $[Re(CO)_5\{C(O)Fc\}]$

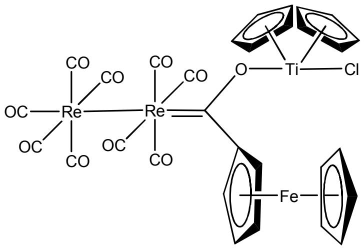

31 *ax*-$[Re_2(CO)_9\{C(OTiCp_2Cl)Fc\}]$

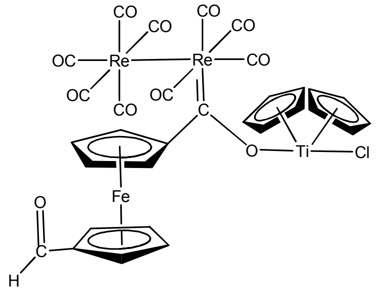

32 *eq*-$[Re_2(CO)_9\{C(OTiCp_2Cl)(Fc'CHO)\}]$

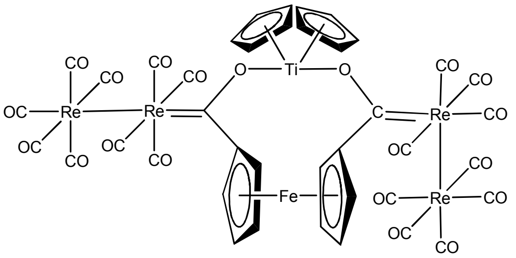

33 *ax, eq*-$[\{\mu\text{-}TiCp_2O_2\text{-}O,O'\}\{\mu\text{-}Fe(C_5H_4)_2\text{-}C,C'\}\{CRe_2(CO)_9\}_2]$

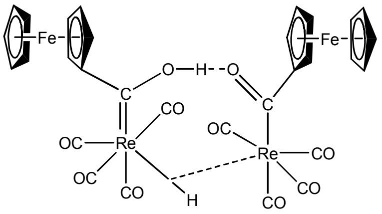

34 $[(\mu\text{-}H)_2\text{-}(Re(CO)_4\{C(O)Fc\})_2]$

List of Abbreviations

ax	:	axial
Bu	:	butyl
br	:	broad (IR, NMR)
BT	:	benzothienyl
Cp	:	η^5-C_5H_5
d	:	doublet
DCM	:	dichloromethane
DEE	:	diethyl ether
dd	:	doublet of doublets
ddd	:	doublet of doublets of doublets
DFT	:	density functional theory
Et	:	ethyl
eq	:	equatorial
eq	:	equivalent
Fc	:	ferrocenyl
Fc’	:	ferrocen-1,1’-diyl
η^n	:	hapticity of C_nH_n
HOMO	:	highest occupied molecular orbital
IR	:	infrared spectroscopy
J	:	coupling constant
LUMO	:	lowest unoccupied molecular orbital
m	:	medium (IR)
Me	:	methyl
MLCT	:	metal-to-ligand charge transfer
MO	:	molecular orbital
MS	:	mass spectrometry
NBO	:	natural bond orbital
NMR	:	nuclear magnetic resonance spectroscopy

n.o. : not observed
Ph : phenyl
R : alkyl group
RT : room temperature
s : singlet (NMR)
s : strong (IR)
T : thienyl
THF : tetrahydrofuran
TMEDA : *N, N, N’. N’*-tetramethylethylenediamine
UV : ultraviolet
Vis : visible
vs : very strong (IR)
vw : very weak (IR)
w : weak (IR)
Å : angstrom
δ : chemical shift
λ : wavelength

I think the ways by which people gain knowledge

are almost as wonderful as the nature of the things themselves

Johannes Kepler

German Astronomer (1571 – 1630)

1

Introduction

1.1 Background

1.1.1 Historical development of organometallic chemistry

The first recorded organometallic compound, “Cadet’s fuming liquid”, was prepared as early as 1760 in a Parisian military pharmacy.[1] In an effort to make cobalt-based inks, cobalt minerals containing arsenic was used, and *in situ* formation of $[Me_2As]_2O$ resulted. However, as arsenic is classified as a metalloid or ‘semi-metal’, the title of the first organometallic compound may well belong to the first olefin complex, the complex $Na[PtCl_3C_2H_4]$ known as Zeise’s salt,[2] prepared by the Danish pharmacist Zeise by boiling a solution of chloroplatinic acid in ethanol, and then adding KCl.[3]

The term ‘organometallic’ was only introduced by Frankland in 1849, following his preparation of important alkylmercury compounds such as Me_2Hg.[4] After this, a wealth of main-group organometallic compounds were isolated and characterized in the late nineteenth century,[5] and industrial applications for

---

[1] Cadet de Gassicourt, L.C. *Mem. Math. Phys.* **1760**, *3*, 623.

[2] Zeise, W.C. *Pogg. Ann. Phys. Chem.* **1827**, *9*, 632.

[3] (a) Zeise, W.C. *Pogg. Ann. Phys. Chem.* **1831**, *21*, 497, (b) Zeise, W.C. *Pogg. Ann. Phys. Chem.* **1831**, *21*, 542.

[4] (a) Frankland, E. *Phil. Trans. Roy. Soc.* **1852**, *142*, 417, (b) Frankland, E. *Ann. Chem. Pharm.* **1855**, *95*, 28.

[5] (a) Krause, E.; von Grosse, A. *Die Chemie der metall-organischen Verbindungen,* Verlag Gebrüder Bornträger, Berlin, **1937**, (b) Thayer, J.S. *Adv. Organomet. Chem.* **1975**, *13*, 1.

these complexes grew exponentially. However, little was known about the true nature and structure of these complexes. For example, the first binary metal carbonyl $Ni(CO)_4$ was discovered by Mond during the commercial process for refining nickel.[6] Iron pentacarbonyl was reported almost simultaneously,[7] but the product was initially misformulated as $Fe(CO)_4$, and the nature of the compound was not elucidated.

Organometallic chemistry came to be recognized in its full right with the discovery of the first sandwich complex, ferrocene.[8] In 1951 and 1952, Pauson reported in the journals *Nature*[9] and *Journal of the Chemical Society*[10] the serendipitous preparation of "a new type of organo-iron compound". Pauson proposed a linear structural arrangement where two planar cyclopentadienyl rings linked to the iron metal as shown for resonance structure **I** in Figure 1.1. He attributed the remarkable stability of $FeC_{10}H_{10}$ to the prevalence of resonance structure **II**, where the cyclopentadienyl groups attain aromatic character with the acquisition of a negative charge.

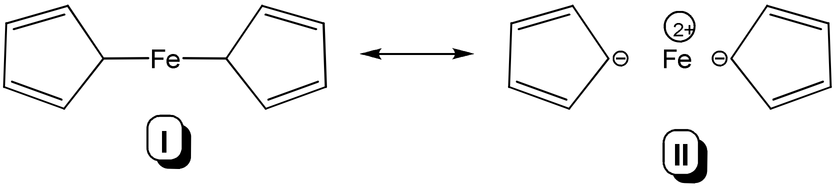

Figure 1.1 The resonance forms proposed by Pauson for ferrocene

Investigation of the structure of ferrocene by Fischer in Munich, and Wilkinson and Woodward at Harvard, lead to the proposal of a double-cone arrangement (**III** in Figure 1.2) by Fischer,[11] and an antiprismatic structure (**IV**)

---

[6] Mond, L.; Langer, C.; Quincke, F. *J. Chem. Soc.* **1890**, *57*, 749.
[7] (a) Berthelot, M. *Comt. Rend Acad. Sci.* **1891**, *112*, 1343, (b) Mond, L. ; Quincke, F. *J. Chem. Soc.* **1891**, *59,* 604.
[8] Werner, H. *Landmarks in Organo-Transition Metal Chemistry: A Personal View,* Springer Science + Business Media, New York, **2009**.
[9] Kealy, T.J.; Pauson, P.L. *Nature* **1951**, *168*, 1039.
[10] Miller, S.A.; Tebboth, J.A.; Tremaine, J.F. *J. Chem. Soc.* **1952**, 632.
[11] Fischer, E.O.; Pfab, W. *Z. Naturforsch., Part B* **1952**, *7*, 377.

by Woodward and Wilkinson.[12] Three different, independent studies confirmed the structural proposals offered by Fischer, Woodward and Wilkinson.[13] Wilkinson coined the term ‘sandwich complexes’[14] and in 1973, Fischer and Wilkinson won the Nobel Prize for Chemistry for their structural elucidation of this landmark organometallic complex. Eminent scientists such as Ron Nyholm proclaimed that they had witnessed “a renaissance of inorganic chemistry”.[15]

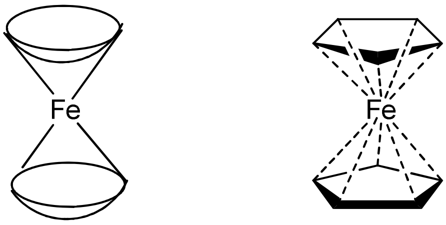

III **IV**

Figure 1.2 The structural proposals for ferrocene offered by Fischer (**III**) and Wilkinson (**IV**)

1.1.2 Early development of carbene chemistry

Approximately ten years later, King synthesized a manganese complex from the reaction of a pentacarbonyl manganate complex with 1,3-dibromopropane.[16] He correctly gave the molecular formula as $[Mn_2(CO)_{10}(CH_2)_3]$, but wrongly assigned the structure as illustrated in Figure 1.3.

---

[12] Wilkinson, G.; Rosenblum, M.; Whiting, M.C.; Woodward, R.B. *J. Am. Chem. Soc.* **1952**, *74*, 2125.

[13] (a) Fischer, E.O.; Pfab, W. *Z. Naturforsch., Part B* **1952**, *7*, 377, (b) Eiland, P.F.; Pepinsky, R. *J. Am. Chem. Soc.* **1952**, *74*, 4971, (c) Dunitz, J.D.; Orgel, L.E. *Nature* **1953**, *171*, 121.

[14] Wilkinson, G. *J. Am. Chem. Soc.* **1952**, *74*, 3458.

[15] Nyholm, R.S. *The Renaissance of Inorganic Chemistry,* Inaugural Lecture delivered at University College London, 1 March **1956**, published for the College by H.K. Lewis & Co. Ltd., London.

[16] King, R.B. *J. Am. Chem. Soc.* **1963**, *85*, 1922.

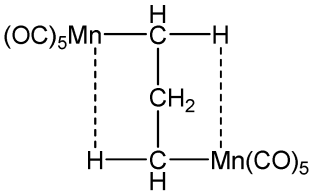

Figure 1.3 The proposed structure of King's compound

Only seven years later in 1970, did the group of Casey correctly assign the structure of King's compound as a dimanganese nonacarbonyl complex containing a cyclic carbene ligand with an oxygen atom bonded to the carbene carbon (Figure 1.4).[17] Although this was actually the first example of a Fischer carbene complex, it was never recognized as such.

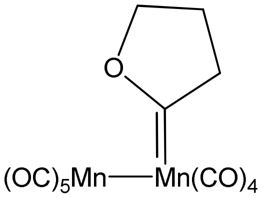

Figure 1.4 Casey's assignment of the structure of the King compound

In the meantime, E.O. Fischer continued with his pioneering work in Munich. With his graduate student Maasböl, they reacted tungsten hexacarbonyl with methyl and phenyl lithium, and after protonation of the *in situ* formed tungsten acylates, treated the corresponding hydroxycarbenes with diazomethane to afford the desired methoxy methyl- and methoxy phenyl carbene complexes,[18] demonstrated in Scheme 1.1; the first isolated and fully characterized

---

[17] (a) Casey, C.P. *J. Chem. Soc., Chem. Commun.* **1970**, 1220, (b) Casey, C.P.; Cyr, C.R.; Anderson, R.L.; Marten, D.F.; *J. Am. Chem. Soc.* **1975**, *97*, 3053, (c) Casey, C.P.; Anderson, R.L. *J. Am. Chem. Soc.* **1971**, *93,* 3554, (d) Casey, C.P.; Cyr, C.R. *J. Organomet. Chem.* **1973**, *37*, C69.

[18] Fischer, E.O.; Maasböl, A. *Angew. Chem. Int. Ed.* **1964**, *3*, 580.

complexes of this new class of metal complexes containing organic ligands coordinated by a metal-carbon double bond.

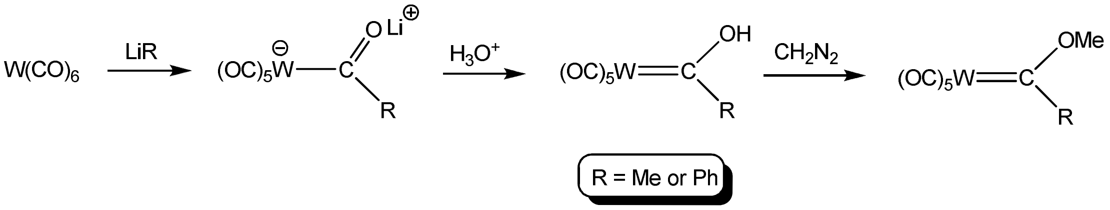

Scheme 1.1

Another important development for the chemistry of carbene complexes was achieved by R.R. Schrock, in his communication about the preparation of a stable tantalum carbene complex (Scheme 1.2) in 1974.[19] In contrast to Fischer's carbene complexes containing a heteroatom-substituted carbene ligand with an electrophilic nature, the carbene carbon of his complexes proved to be nucleophilic.

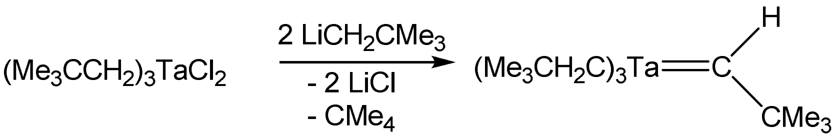

Scheme 1.2

In the years thereafter, applications for the metal-carbon double bond complexes exploded. Fischer carbene complexes have received a great deal of attention for their application as organic building blocks[20] and stabilization by bonding to a metal allowed for isolation and selective reactivity.[21] Metal carbene complexes were found to be frequent intermediates in metal

---

[19] Schrock, R.R. *J. Am. Chem. Soc.* **1974**, *96*, 6796.
[20] Dötz, K.H.; Stendel, Jr., J. *Chem. Rev.* **2009**, *109*, 3227.
[21] Dötz, K.H. *Angew. Chem., Int. Ed. Engl.* **1984**, *23*, 587.

mediated reactions[22] and were applied in the construction of multicomponent and multistep methodologies.[23] Important applications also include olefin metathesis, Fischer-Tropsch intermediates[24] and cycloaddition reactions.[25]

The work on olefin metathesis done by Schrock in the preparation of molybdenum and tungsten complexes of the general composition [M(CHR)(NAr)(OR')$_2$] and derivatives thereof,[26] Grubbs's first generation ruthenium compounds [Ru(CHR)(PCy$_3$)$_2$X$_2$] and later with sterically protected *N*-heterocyclic carbenes [Ru(CHR)(NHC)(PCy$_3$)X$_2$], and their metathesis reactions with olefins,[27] as well as the mechanism proposed by Chauvin,[28] culminated in the Nobel Prize for Chemistry in 2005 being awarded to the aforementioned three scientists.

1.1.3 Recent developments of polymetallic carbene complexes

The activation of simple organic molecules by more than one transition metal constitutes an area of research that has grown in importance.[23] The applications of carbenes as active or auxiliary ligands in organic synthesis and catalysis, however, are mostly focused on monocarbene systems. No assemblies of carbene units (carbene supramolecular chemistry) have been reported and only a few carbene complexes are known to be part of small metal organic frameworks (MOF).[29] In addition, no carbene complexes have

---

[22] (a) Barluenga, J. *Pure Appl. Chem.,* **1996,** *68,* 543 (b) de Meijere, A. *Pure Appl. Chem.,* **1996,** *68,* 61 (c) Harvey,D.F.; Sigano, D.M. *Chem. Rev.,* **1996,** *96,* 271 (d) Aumann, R.; Nienaber, H. *Adv. Organomet. Chem.,* **1997,** *41,* 163 (e) J. Barluenga, J. *Pure Appl. Chem.,* **1999,** *71,* 1385 (f) K.H. Dötz, K.H.; Tomuschat, P. *Chem. Soc. Rev.,* **1999,** *28,* 187 (g) Davies, M.W.; Johnson, C.N.; Harrity, J.P.A. *J. Org. Chem.,* **2001,** *66,* 3525 (h) Gómez-Gallego, M.; Mancheño, M.J.; Sierra, M.A. *Acc. Chem. Rev.,* **2005,** *38*, 44.

[23] Dötz, K.H.; Fischer, H.; Hofmann, P.; Kreissl, F.R.; Schubert, U.; Weiss, K. *Transition Metal Carbene Complexes,* Verlag Chemie: Weinheim, Germany, **1983**.

[24] Toomey, L.M.; Atwood, J.D. *Organometallics* **1997**, *16*, 490.

[25] Dötz, K.H. *Metal carbenes in organic synthesis,* **2004**, Springer-Verlag, Germany.

[26] Schrock, R.R. *Acc. Chem. Res.* **1986**, *19*, 342, (b) Schrock, R.R. *Angew. Chem., Int. Ed. Engl.* **2006**, *45*, 3748 (Nobel lecture).

[27] (a) Nguyen, S.T.; Johnson, L.K.; Grubbs, R.H.; Ziller, J.W. *J. Am. Chem. Soc.* **1992**, *114*, 3974, (b) Grubbs, R.H. *Angew. Chem., Int. Ed. Engl.* **2006**, *45*, 3760 (Nobel lecture).

[28] Hérrison, J.-L.; Chauvin, Y. *Makromol. Chem.* **1971**, *141*, 161.

[29] (a) Garrison, J.C.; Simons, R.S.; Tessier, C.A.; Youngs, W.J. *J. Organomet. Chem.* **2003**, *673*, 1, (b) Fernández, I.; Mancheño, M.J.; Gómez-Gallego, M.; Sierra, M.A. *Org. Lett.* **2003**, *5*, 1237.

featured in materials of note, no dendrimers with carbene functionalities have been prepared and no carbene complexes showing liquid crystalline properties have been reported. In fact very few studies on multimetal carbene complexes or cluster carbene complexes have been recorded.[30] In the field of non-linear optics, conjugated unsaturated systems with a transition metal moiety have been employed for their electron delocalisation and so-called 'push-pull' characteristics.[31]

However, the incorporation of different transition metal fragments in complexes has been widely investigated to study the role of different metal fragments on the reactivity of ligands and the chemistry of the complexes[32]. When applied in the area of Fischer carbene complexes of the type [M(CO)$_5${C(OR')R}], the carbene properties have either been modified by introducing metal-containing substituents to further activate the carbene carbon[33] or the carbene ligand is used as a connector to bridge the other transition metals.[34] The introduction of a metal fragment to the carbene oxygen offers the possibility to modulate the carbene reactivity by the electronic and steric properties of this second metal fragment.[35]

---

[30] Sierra, M.A. *Chem. Rev.* **2000**, *100*, 3591.

[31] Seed, A. *Chem. Soc. Rev.* **2007,** *36,* 2046.

[32] (a) Lotz,S.; van Rooyen, P.H.; Meyer, R. *Adv. Organomet. Chem*. **1995**, *37*, 219. (b) Bunz, U.H.F. *Angew. Chem., Int. Ed. Engl.* **1996**, *35*, 969. (c) Beck, W.; Niemer, M.; Wieser, M. *Angew. Chem., Int. Ed. Engl.* **1993**, *32*, 923. (d) Lang, H. *Angew. Chem., Int. Ed. Engl.* **1994**, *33*, 547. (e) Paul, F.; Lapinte, C. *Coord. Chem. Rev*. **1998**, *178-180*, 431.

[33] (a) Fuss, B.; Dede, M.; Weibert, B.; Fischer, H. *Organometallics* **2002**, *21*, 4425, (b) Crause, C.; Görls, H.; Lotz, S. *Dalton Trans*. **2005**, 1649, (c) Moretó, J.M.; Ricart, S.; Dötz, K.H.; Molins, E. *Organometallics* **2001**, *20*, 62.

[34] (a) Bartik, T.; Weng, W.; Ramsden, J.A.; Szafert, S.; Fallon, S.B.; Arif, A.M.; Gladysz, J.A. *J. Am. Chem. Soc*. **1998**, *120*, 11071, (b) Weng, W.; Ramsden, J.A.; Arif, A.M.; Gladysz, J.A. *J. Am. Chem. Soc*. **1993**, *115*, 3824, (c) Weng, W.; Arif, A.M.; Gladysz, J.A. *Angew. Chem., Int. Ed. Engl*. **1993**, *32*, 891. (d) Fischer, E.O.; Röll, W.; Huy, N.H.T.; Ackermann, K. *Chem. Ber*. **1982**, *115*, 2951, (e) Hartbaum, C.; Roth, G.; Fischer, H. *Chem. Ber./Recueil* **1997**, *130*, 479. (f) Hartbaum, C.; Mauz, E.; Roth, G.; Weissenbach, K.; Fischer, H. *Organometallics* **1999**, *18*, 2619, (g) Terblans, Y.M.; Roos, H.M.; Lotz, S. *J. Organomet. Chem*. **1998**, *566*, 133, (h) Landman, M.; Görls, H.; Lotz, S. *Eur. J. Inorg. Chem*. **2001**, 233, (i) Landman, M.; Görls, H.; Lotz, S. *J. Organomet. Chem*. **2001**, *617-618*, 280.

[35] Barluenga, J.; Fañanás, F.J. *Tetrahedron* **2000**, *56*, 4597 and references therein.

1.2 Aim of the study

As far as could be ascertained, no carbene complex has been reported with three different transition metal substituents that are all in electronic contact with the carbene carbon atom; a class of compounds we call carbene transition metal cluster compounds. Unlike the clusters defined by Cotton *et al.,*[36] these complexes do not contain metal-metal bonds, but rather refer to metals clustered around the carbene carbon atom.

The objective was not only to synthesize trimetallic carbene complexes of the type $[M(CO)_n\{C(OR)R'\}]$, but also to systematically study the electronic and steric effects of the different metal-containing substituents by introducing these fragments in a stepwise manner on both the R- and the R'-substituent (Scheme 1.3). The substituents chosen included aromatic (benzene) and heteroaromatic (thiophene) rings π-coordinated to a $Cr(CO)_3$-fragment, or ferrocenyl as the R' substituent, while the OR substituent would be varied systematically between an organic ethoxy group and an organometallic titanoxy group. Initially, Group VI transition metals (Cr, Mo, W) with carbonyl ligands were chosen as being representative of a class of Fischer carbene complexes that exhibit high stability.

To expand the study towards the investigation of Group VII transition metals (Mn, Re) and their character and reactivity towards the metal-substituted carbene ligands, the binary dirhenium decacarbonyl and the mononuclear $MnCp(CO)_3$ were included as precursor complexes.

---

[36] Cotton, F.A.; Wilkinson, G.; Murillo, C.A.; Bochmann, M. *Advanced Inorganic Chemistry,* 6th Ed, Wiley-Interscience, **1999**.

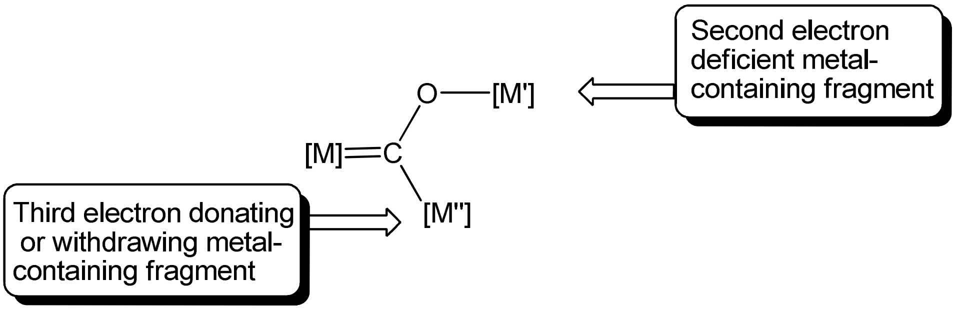

M = $Cr(CO)_5$; $Mo(CO)_5$; $W(CO)_5$; $MnCp(CO)_2$; $Re_2(CO)_9$
M' = $TiCp_2Cl$; $ZrCp_2Cl$
M'' = ferrocenyl ; η^6-$PhCr(CO)_3$; η^5-2-thienyl $Cr(CO)_3$

Scheme 1.3

The structural features and their relevance to bonding in the carbene cluster compounds of the Group VI and VII transition metals were to be investigated as they represent indicators of possible reactivity sites in multimetal carbene assemblies. Finally, the possibility of using molecular modelling calculations to quantify the effect of metal-containing substituents on the carbene ligands was proposed, as well as the correlation of the theoretical results with experimental parameters were planned to test the viability of DFT calculations as a tool for substituent effect trend prediction in carbene cluster complexes.

2

Group VI Transition Metal Carbene Cluster Complexes

2.1 Introduction

2.1.1 Background

Bi- and polymetallic transition metal complexes not containing direct metal-metal bonds, but rather different metal-containing fragments linked by bridging ligands, can be broadly divided into three classes based on the mode of coordination of the ligand. These classes are (i) σ, σ (ii) σ, π or (iii) π, π bonding of a ligand to the different metal centres. Activation of these ligands is achieved in both the σ (through inductive effects) and the π (through π-resonance effects) modes of the bridging ligand.[1] Utilizing π-conjugated bridging ligands brings the metal centres in direct electronic contact through π-resonance effects.[2]

This type of communication was illustrated in our laboratories where an unprecedented irreversible metal exchange process (Scheme 2.1) in the complex [Mn(η^1:η^5-C_4H_3S)$(CO)_5$Cr$(CO)_3$] lead to the exchange of coordination sites of the manganese and chromium metals .[3]

---

[1] Topsom, R.D. *Acc. Chem. Res.* **1983**, *16*, 292.

[2] Collman, J.P.; Hegedus, L.S.; Norton, J.R.; Finke, R.G. *Principles and Applications of Organotransition Metal Chemistry,* University Science Books, Mill Valley, Ca. **1987**

[3] (a) Waldbach, T.A.; van Rooyen, P.H.; Lotz, S. *Angew. Chem. Int. Ed. Engl.* **1993**, *32*, 710. (b) Waldbach, T.A.; van Rooyen, P.H.; Lotz, S. *Organometallics,* **1993**, *12*, 4250.

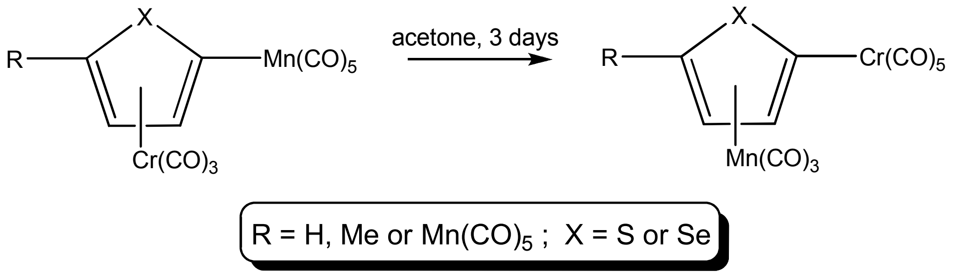

Scheme 2.1

Applying the principle of σ, π-bridging ligands to Fischer carbene complexes of the type [M(CO)$_5${C(OR')R}], π-bonded aryl or heteroaryl ligands have been used to establish electronic contact of the R-substituent or the alkoxy R'-substituent with the carbene carbon atom.[4] The first example to be synthesized was the complex [Cr(CO)$_5${C(OEt)(η^1:η^6-PhCr(CO)$_3$)] containing a π-conjugated phenyl ring[4(a)] and the series was expanded to include either tungsten or molybdenum as the pentacarbonyl metal centre.

Even before this, ferrocenyl carbene complexes of the Group VI transition metals were synthesized to study the electronic effects of the ferrocenyl substituent on the carbene ligand.[5] Thiolate, selenolate, tellurolate and [Co(CO)$_4$]$^-$ were used to modify cationic ferrocenyl carbyne complexes of manganese, constituting another example of neutral bimetallic monocarbene complexes.[6]

Increasing interest in the pseudo-aromatic five membered rings containing a heteroatom lead to the synthesis of [M(CO)$_5${C(OEt)(η^5-2-thienylCr(CO)$_3$}] complexes (M = Cr, W) in an effort to investigate the effect of π-coordination on the properties of such a carbene functionality.[7] Scheme 2.2 illustrates the expected bimetallic Fischer carbene complexes that were afforded, as well as the modified carbene complexes obtained from the incorporation of a cleaved

---

[4] (a) Fischer, E.O.; Gammel, F.J.; Neugebauer, D. *Chem. Ber.* **1980**, *113,* 1010. (b) Behrendt, U.; Pfeifer, R-M.; Wartchow, R.; Butenschön, H. *New. J. Chem.* **1999**, *23*, 891.

[5] Connor, J.A.; Jones, E.M.; Lloyd, J.P. *J. Organomet. Chem.* **1970***,* *24*, C20.

[6] Fischer, E.O. ; Wanner, J.K.R. *Chem. Ber.* **1985**, *118*, 2489.

[7] Terblans, Y.M.; Lotz, S. *J. Chem. Soc., Dalton Trans.* **1997**, 2177.

tetrahydrofuran (THF) molecule into the ethoxy substituent of the carbene ligand.

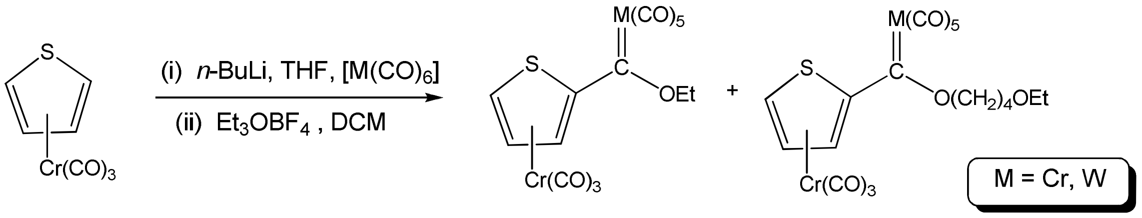

Scheme 2.2

2.1.2 Heteroatom-bonded carbene ligand substituent

The incorporation of a second metal-containing fragment, joined to the heteroatom bonded to the carbene carbon has first been explored by Fischer *et al.*[8] This involved the *O*-alkylation of an acyl chromate with titanocene dichloride to yield the corresponding metaloxycarbene complex $[Cr(CO)_5\{C(Me)OTiCp_2Cl\}]$ as well as the trimetallic bismetaloxycarbene complex $[\{\mu\text{-}O_2TiCp_2\text{-}O,O'\}\{C(Me)Cr(CO)_5\}_2]$. However, the above Fischer method is limited by the reactivity of the acyl metalate intermediate (**A** in Figure 2.1 below). The intermediate **A** requires stabilization; but if too stable, *O*-alkylation is resisted in the following step and metal alkylation can result in an acyl complex rather than the desired Fisher-type metaloxycarbene complex **B**.

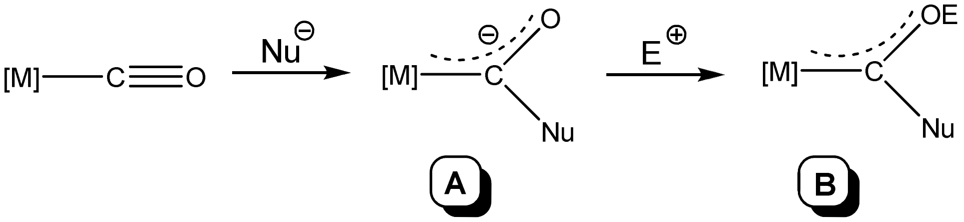

Figure 2.1 Electrophilic attack on acylmetalate **A** to form Fischer carbene complex **B**

---

[8] Fischer, E.O.; Fontana, S. *J. Organomet. Chem*. **1972**, *40*, 159.

A variety of examples of metaloxycarbene complexes has been reported,[9] including metallacyclic metaloxycarbene complexes afforded by ring-closure reactions (Scheme 2.3) of η^2-olefin complexes of titanocene, zirconocene or hafnocene or (η^4-diene) metallocenes.[10]

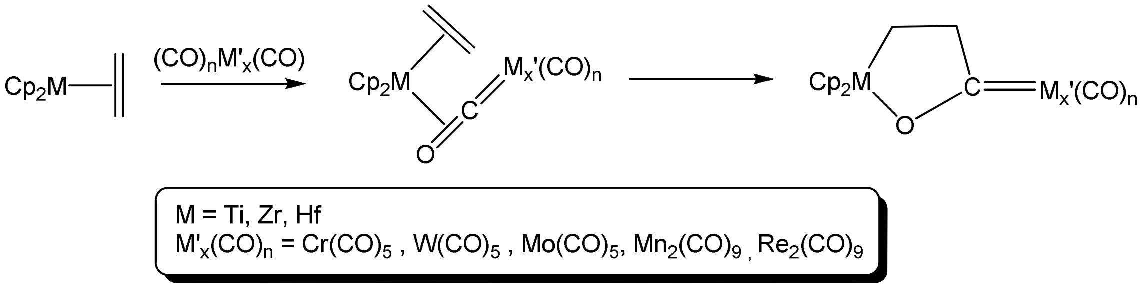

Scheme 2.3

Alkylidene titanium complexes may also be used as starting materials to prepare titanoxycarbene complexes by reaction with metal carbonyls. β,β-dimethyltitanocene metallacyclobutane, for example, reacts with metal carbonyls to yield a titanocene adduct through the intermediates formation (Scheme 2.4) of a cyclic titanoxycarbene complex.[11]

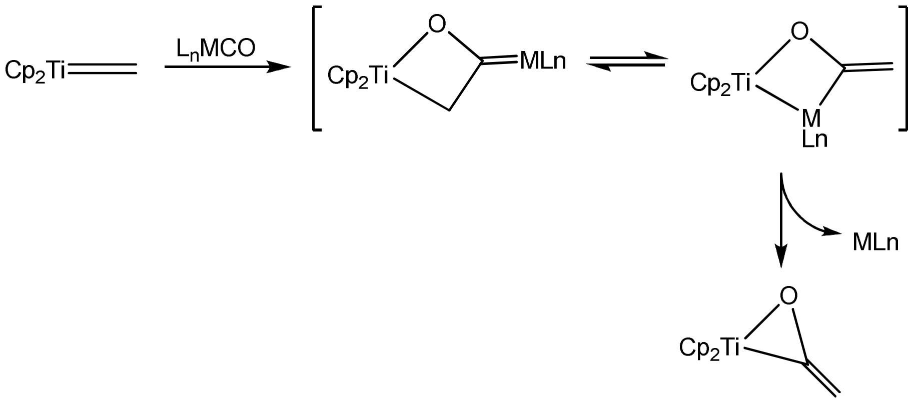

Scheme 2.4

---

[9] (a) Barluenga, J.; Fañanás, F.J. *Tetrahedron,* **2000**, *56*, 4597, (b) Sabat, M.; Gross, M.F.; Finn, M.G. *Organometallics* **1992**, *11*, 745.

[10] Erker, G. *Angew. Chem., Int. Ed. Engl.* **1989**, *28*, 397.

[11] Anslyn, E.V.; Santarsiero, B.D.; Grubbs, R.H. *Organometallics* **1988**, *7*, 2137.

Examples of metaloxycarbene complexes not containing metallocenes as carbene ligand substituents but other transition metal fragments, e.g. the rheniooxycarbene complexes of Beck,[12] are prepared by addition of the 16-electron system $Re(CO)_5^+$ (as $[Re(CO)_5BF_4]$) to acetyl pentacarbonyl chromate to form $[Cr(CO)_5\{C(ORe(CO)_5)Me\}]$.

The presence of a second metal unit, Cp_2ZrCl, leads to the activation of such carbene complexes as catalysts for the oligomerisation of 1-pentene in the presence of MAO.[13] More recently, Raubenheimer and co-workers reported an anionic Fischer-type carbene complex utilized as a bidentate ligand for complexation of a second metal, *i.e.* Cr(III), Fe(III), V(IV),[14] which can be regarded as ‘complexes of complexes’ and can form tris-, bis- or mono-chelated polymetallic compounds, as illustrated in Figure 2.2.

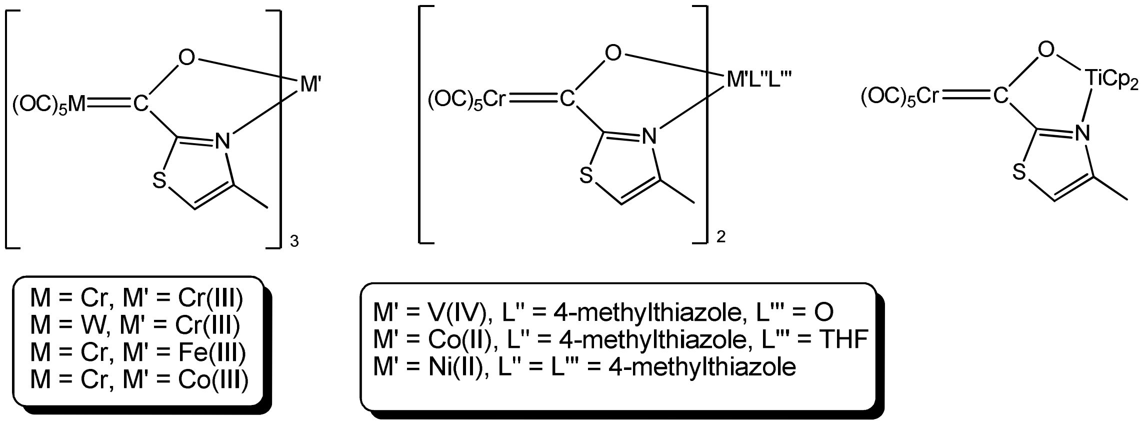

M = Cr, M' = Cr(III)
M = W, M' = Cr(III)
M = Cr, M' = Fe(III)
M = Cr, M' = Co(III)

M' = V(IV), L" = 4-methylthiazole, L'" = O
M' = Co(II), L" = 4-methylthiazole, L'" = THF
M' = Ni(II), L" = L'" = 4-methylthiazole

Figure 2.2 Anionic Fischer-type carbene complexes as bidentate (N,O) ligands

Bimetallic titanoxycarbene complexes have been widely studied as a way to use the electron deficient Lewis acid properties of the titanium to increase the electrophilicity of the carbene carbon atom. This was demonstrated by

---

[12] Fritz, P.M.; Steimann, M.; Beck, W. *Chem. Ber.* **1987**, *120*, 253.

[13] Brüll, R.; Kgosane, D.; Neveling, A.; Pasch, H.; Raubenheimer, H.G.; Sanderson, R.; Wahner, U.M. *Macromol. Symp.* **2001**, *165*, 11.

[14] Raubenheimer, H.G.; du Toit, A.; du Toit, M.; An, J. ; van Niekerk, L. ; Cronje, S.; Esterhuysen, C.; Crouch, A.M. *J. Chem. Soc., Dalton Trans.* **2004***,* 1173.

successfully reacting the titanoxycarbene complex of [MnCp(CO)$_2${C(OTiCp$_2$Cl)R}] in benzannulation reactions whereas the corresponding alkoxycarbene complexes failed to react.[15] The most direct and highest yielding method of synthesis remains the Fischer route of reacting metal carbonyls with Ti(NMe$_2$)$_4$.[16] In the context of this work the resulting acyl chromate was reacted with titanocene dichloride to afford [M(CO)$_5${C(OTiCp$_2$Cl)(heteroaryl)}] in high yields.[8, 11]

2.1.3 Carbon-bonded carbene ligand substituent

In a study performed prior to this investigation in our laboratories, mono- and dimetal substituted carbene complexes (listed as complexes **14** – **21** in Scheme 2.5) were derived from a lithiated benzothienyl substituent (2-BT) or a benzo[*b*]thienyl ring π-coordinated to Cr(CO)$_3$, (Cr(CO)$_3$(η^6-2-BT)), followed by alkylation of the acyl metalate by triethyloxonium tetrafluoroborate or metalation with titanocene dichloride.[17]

The [Cr(CO)$_3$(η^6-2-BT)]-substituent has the π-bonded chromium tricarbonyl fragment coordinated to the ring furthest away from the carbene carbon atom, leaving an unoccupied space directly beneath the thiophene bonded to the carbene carbon atom. This prompted the investigation into the possibility of replacing the benzo[*b*]thiophene fragment by a more compact, redox-active ferrocenyl substituent in order to increase the electronic communication between the π-bonded transition metal and the carbene carbon atom, as well as heteroaryl rings with the π-Cr(CO)$_3$-moiety in closer proximity to the carbene carbon atom, using the Group VI transition metals Cr, Mo and W (Figure 2.10).

---

[15] Balzer, B.L.; Cazanoue, M.; Sabat, M.; Finn, M.G. *Organometallics* **1992**, *11*, 1759.
[16] (a) Petz, W. *J. Organomet. Chem*. **1974**, *72,* 369. (b) Pebler, J.; Petz, W. *Z. Naturforsch. B* **1974**, *29*, 658.
[17] Bezuidenhout, D.I.; van der Watt, E.; Liles, D.C.; Landman, M.; Lotz, S. *Organometallics* **2008**, *27*, 2447.

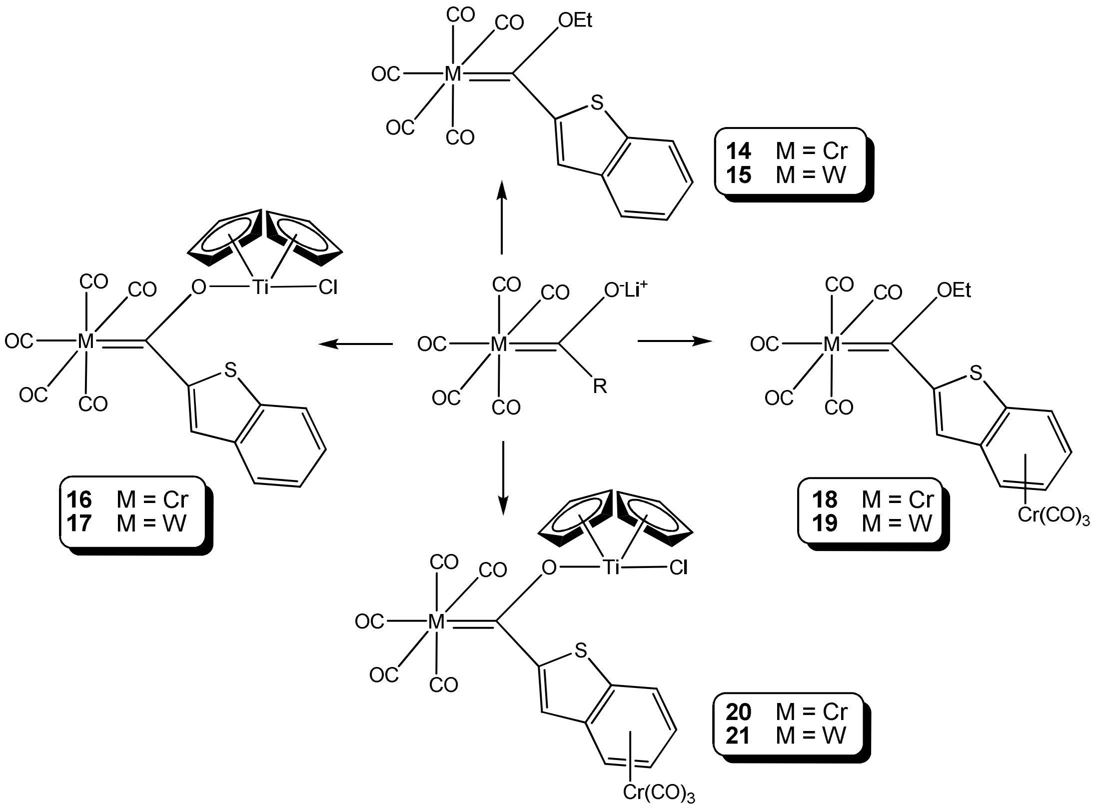

Scheme 2.5

2.1.3.1 Ferrocenyl carbene ligand substituent

Ferrocene was chosen as carbene substituent due to its wide application and the rapidly expanding field of ferrocenyl-containing ligands, where they can be used in catalytic transformations of organic compounds, especially when in contact with a second transition metal.[18] The first examples of ferrocenyl Fischer carbene complexes were synthesized by Connor *et al.*[5] as part of an investigation into the electron withdrawing nature of metal carbonyl carbene groups and comprehensively reviewed as dimetallic heteroatom stabilized Fischer carbenes.[19]

---

[18] (a) Colacot, T.J. *Chem. Rev.* **2003**, *103*, 3101. (b) Dai, L.; Tu, T.; You, S.; Deng, W.; Hou, X. *Acc. Chem. Res.* **2003**, *36*, 659.

[19] Sierra, M.A. *Chem. Rev.* **2000**, *100*, 3591.

Ferrocenes display extraordinary stabilization of adjacent electron deficient centres, comparable to amino substituents for example.[20] The electron transfer behaviour of metal carbene complexes can also be greatly influenced by the presence of additional metal centres.[21] If polyene units are introduced between the metal carbonyl carbene moiety and the ferrocenyl (Fc) substituent, both the oxidation potential and the reduction potential of these complexes decrease with increasing length of polyene,[22] illustrating the electronic communication between the above mentioned moieties and the donor-acceptor interaction of the couple.

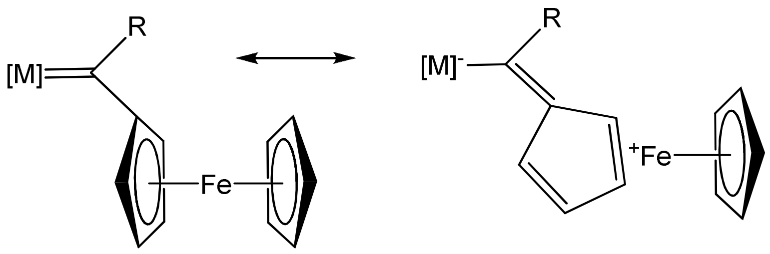

Figure 2.3 Resonance interaction between the ferrocene Cp ring and the carbene carbon atom

The electron release from the Fc group to the empty carbene carbon p_z orbital takes place via a delocalized π-system rather than through inductive effects (Figure 2.3)[23] which correlates with the findings that the normal donor strength of ferrocene is increased by interaction with strongly electrophilic centres.

The steric bulk of ferrocenyl substituents directly attached to chromium carbene complexes blocks the chromium templated benzannulation upon reaction with alkynes in favour of formation of the furan ring[24], however the reactivity patterns of other carbene complexes are followed to produce organic compounds such as cyclobutenones, ketoesters, etc.[25]

---

[20] Bildstein, B. *J. Organomet. Chem.* **2001***, 617 – 618*, 28.

[21] Sierra, M.A.; Gómez-Gallego, M.; Martínez-Álvarez, R. *Chem. Eur. J.* **2007**, *13*, 736.

[22] Jayaprakash, K.N.; Pay, P.C.; Matsuoka, I.; Bhadbhake, M.M.; Puranik, V.G.; Das, P.K.; Nishihura, H.; Sarkar, A. *Organometallics,* **1999**, *18*, 3851.

[23] Connor, J.A.; Lloyd, J.P. *J. Chem. Soc. Dalton Trans.* **1972**, 1470.

[24] Bennewits, J.; Nieger, M.; Lewall, B.; Dötz, K.H. *J. Organomet. Chem.* **2005**, *690*, 5892.

[25] Zora, M.; Güngör, E.U. *Tetrahedron Lett.* **2001**, *42*, 4733.

In the presence of two nonconjugated metal carbene moieties in homo- and heterobimetallic biscarbene complexes, these moieties behave as two independent monocarbene entities,[26] but ferrocene functions as an internal electron carrier introducing the push-pull nature of these Fc-substitued carbene complexes.

2.1.3.2 π-aryl carbene ligand substituent

Besides ferrocene, both thiophene and benzene with a chromium tricarbonyl fragment π-bonded to it were chosen as carbene substituents. The effect of π-coordination of metal fragments to different types of ring systems has been extensively studied, especially for arenes containing no heteroatoms like cyclopentadienyl and benzene. In particular, arene chromium tricarbonyls have attracted attention (Figure 2.4) as the activating substituent.

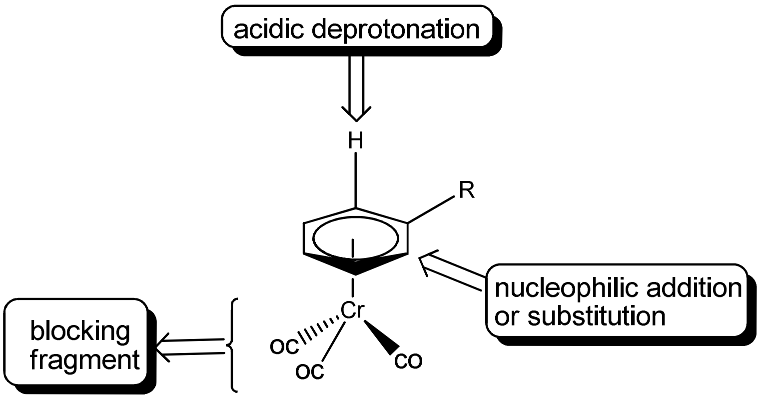

Figure 2.4 $Cr(CO)_3$ – ring activation

$Cr(CO)_3$ is symmetrically bonded to the arene ring carbons[27] and no directing effect of the $Cr(CO)_3$-substituent is observed apart from the steric crowding on one face of the arene ring therefore the substituents attached by σ-bonds to the arene ligand will have the primary influence on site selectivity.[28] X-ray analysis

---

[26] Martínez-Álvarez, R.; Gómez-Gallego, M.; Fernández, I.; Mancheño, M.J.; Sierra, M.A. *Organometallics,* **2004**, *23*, 4647.

[27] (a) Fischer, E.O.; Öfele, K. *Chem. Ber.* **1957***, 90*, 2543. (b) Natta, G.; Ercoli, R.; Calderazzo, F. *Chim. Ind.* **1958**, *40*, 287.

[28] Jackson, W.R.; Jennings, W.B.; Rennison, S.C.; Spratt, R. *J. Chem. Soc. B. Phys. Org. Chem.* **1969***,* 1214.

has, however, indicated that for an unsubstituted benzene ring in $[Cr(CO)_3(\eta^6-C_6H_6)]$, the staggered conformation of the CO ligands with regards to the ring carbons is found, rather than the eclipsed conformation[29], illustrated in Figure 2.5. In a substituted benzene complex with electron donating substituents, *ortho* and *para*-ring protons would have relatively high π-electron density, hence protons attached to these would be shielded as in the free ligand. However, π-electron density distribution will tend to orientate the tricarbonyl chromium group into an eclipsed conformation (Figure 2.5) where the three ring carbons as well as substituent R are eclipsed, in contrast to the other possible eclipsed conformation (where three ring carbons are again eclipsed, but the substituent R resides on a noneclipsed ring carbon atom), preferred for electron withdrawing substituents.[29]

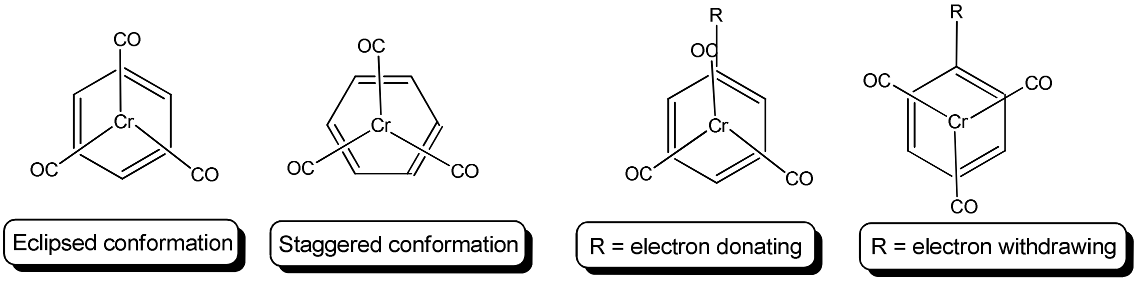

Eclipsed conformation

Staggered conformation

R = electron donating

R = electron withdrawing

Figure 2.5 Substituent directing effect on π-arene chromium tricarbonyl complexes

The π-bond of the metal to the ring carbons is known to lessen the electron delocalization of the ring, causing a decrease in the "ring current" and localizing the π-bonds.[30] Evidence indicates that the $Cr(CO)_3$ unit exerts an electron withdrawing inductive effect[31] whereby the chromium tricarbonyl fragment can be

---

[29] Muetterties, E.L. ; Bleeke, J.R. ; Wucherer, E.J. ; Albright, T.A. *Chem. Rev.* **1982**, *82*, 499.

[30] Mangini, A.; Taddei, F. *Inorg. Chim. Acta* **1968**, *2*, 8.

[31] (a) Holmes, J.D.; Jones, D.A.K.; Pettit, R. *J. Organomet. Chem.* **1965**, *4*, 324, (b) Trahanovsky, W.S. ; Wells, D.K. *J. Am. Chem. Soc.* **1969**, *91*, 5870, (c) Bly, R.S. ; Strickland, R.C. *J. Am. Chem. Soc.* **1970**, *92*, 7459, (d) Wells, D.K. ; Trahanovsky, W.S. *J. Am. Chem. Soc.* **1970**, *92*, 7461.

described as an “electron sink” disrupting the prevalent aromaticity of the benzene ring.

The σ-coordination of the abovementioned type of π-arene chromium tricarbonyls therefore causes polarization and activation of chemical bonds. The first examples of such a σ,π-bimetallic monocarbene complex to be synthesized were the Group VI transition metal complexes of Cr, Mo and W,[4(a)] which were subsequently converted to carbyne complexes after reaction with strong Lewis acids. From the initial metalation of the ring with butyllithium, it was demonstrated that the resultant negative charge is not diffused over the entire complex as believed. Instead it is very much localized on the metalated carbon and is still strong enough to act as a nucleophile and to attack a carbonyl of a metal carbonyl complex.

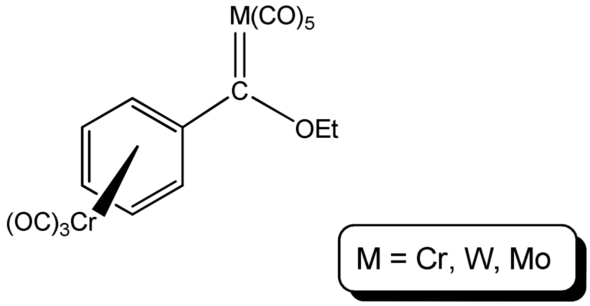

Figure 2.6 σ,π-bimetallic monocarbene complexes synthesized by Fischer *et al.*[4(a)]

The discovery of stable π-arene complexes evolved naturally into the study of related π-complexes of thiophene (TH): an electron excessive[32] aromatic ring containing sulphur as the heteroatom.[33] Compared to benzene, thiophene is more nucleophilic as indicated by the ionization potential of 8.9 eV for thiophene, in contrast to 9.3 eV for benzene,[33(a)] which would make the $Cr(\eta^5\text{-}T)(CO)_3$-fragment a weaker electron withdrawing group than $Cr(\eta^6\text{-}Ph)(CO)_3$. Coordination of thiophenes can occur either through the S-atom or through η^1,

---

[32] Albert, A. *Heterocyclic Chemistry*, Athlone Press, London, **1968**.
[33] (a) Rauchfuss, T.B. *Prog. Inorg. Chem.* **1991**, *39*, 259, (b) Angelici, R.J. *Coord. Chem. Rev.* **1990**, *105*, 61.

η^2, η^4 or η^5-binding. The first [Cr(η^5-TH)(CO)$_3$] structure was reported in 1965,[34] but the utilization of these π-heteroaryl tricarbonyl chromium complexes as carbene ligand substituents was only reported in 1997.[7]

In the case of η^5-coordination, the five *p* orbitals orthogonal to the ring give rise to five nondegenerate π-states, of which three of the π-molecular orbitals are occupied. This means that benzene would represent a better model for binding of the η^5-thiophene than for example the cyclopentadienyl anion. However, it also presents an explanation for the weaker π-coordination of the Cr(CO)$_3$-fragment to the thiophene ring than to the benzene ring, which results in the evident lability of the tricarbonyl chromium fragment as reported by Terblans *et al.* during the synthesis of the first thienyl and benzothienyl σ,π-bimetallic carbene complexes illustrated in Scheme 2.2.[7]

2.1.4 Homo- and heteronuclear polymetallic biscarbene complexes

In the field of non-linear optics, the advantages of using organometallic compounds have been described as a combination of the effect of the delocalized π-electron backbone of conjugated organic polymer systems and the incorporation of transition metals.[35] Such organometallic systems have great possibilities for redox changes and can possess metal→ligand or ligand→metal charge transfer bands in the visible spectrum.

The application employs electron transfer between two redox active termini, as illustrated by the example of biferrocenes (Figure 2.7), linked by heteroaromatic spacers in which the effect of both the length and the substitution of the oligothiophene group have been investigated.[36] Many examples exist of bimetallic complexes in which the two metal centres are connected by an acetylene bridge, $L_nM\text{-}C{\equiv}C\text{-}ML_n$ or an ethylene bridge, $L_nM\text{-}C(X){=}C(X)\text{-}ML_n$.[37]

---

[34] Bailey, M.F.; Dahl, L.F. *Inorg. Chem.* **1965**, *4*, 1306.
[35] Long, N.J. *Angew. Chem., Int. Ed. Engl.* **1995**, *34*, 21.
[36] Justin Thomas, K.R.; Lin, J.T.; Wen, Y.S. *Organometallics* **2000**, *19*, 1008.
[37] (a) Paul, F.; Lapinte, C. *Coord. Chem. Rev.* **1998**, *37*, 547, (b) Beck, W.; Niemar, B.; Wieser, M. *Angew. Chem., Int. Ed. Engl.* **1993**, *32*, 4176.

However, examples of bimetallic biscarbene complexes in which the bridging ligand is a conjugated system, $L_nM{=}CX(CR{=}CR)_nCX{=}ML_n$ are less well known. Homonuclear bimetallic carbene complexes with conjugated even-numbered carbon atoms ranging from C_4 to C_{14} and heteronuclear bimetallic carbene complexes with C_3 bridges have been reported by using reactive carbene precursors in coupling reactions.[38]

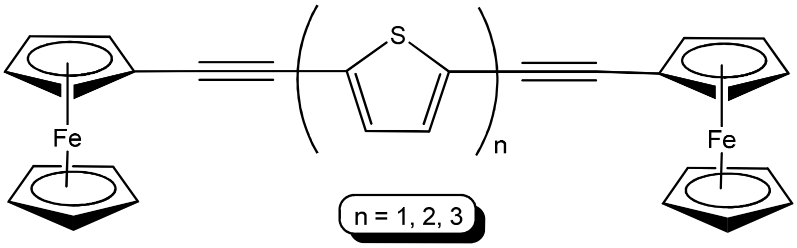

Figure 2.7 Molecular wires incorporating redox active ferrocenyl termini

2.1.4.1 Conjugated bridging biscarbene complexes

The use of aromatic rings as spacers between biscarbene units was first achieved by Fischer's group in the synthesis of dimetallic homonuclear biscarbene complexes of the Group VI transition metals with one-dimensional conjugated phenylene[39] or benzene derivatives.[40]

The reaction of *p*-phenylenedilithium with Group VI metal hexacarbonyls yielded the corresponding μ-(*p*-phenylene)bisethoxycarbene bis(pentacarbonyl metal) complexes (Scheme 2.6) while the analogous reaction of *o*-phenylenedilithium with the metal hexacarbonyls gave the mononuclear 1,4-chelated biscarbene complexes $[\overline{M(CO)_4\{C(OEt)\text{-}o\text{-}C_6H_4\text{-}C}(OEt)\}]$. Subsequent reaction of the

---

[38] (a) Weng, W.; Ramsden, J.A.; Arif, A.M.; Gladysz, J.A. *J. Am. Chem. Soc.* **1993**, *115*, 889, (b) Hartbaum, C.; Roth, G.; Fischer, H. *Chem. Ber. /Recueil* **1997**, *130,* 479, (c) Harbaum, C.; Fischer, H. *J. Organomet. Chem.* **1999**, *578*, 186, (d) Hartbaum, C.; Mauz, E.; Roth, G.; Weissenbach, K.; Fischer, H. *Organometallics* **1999**, *18*, 2619.

[39] Fischer, E.O.; Röll, W.; Huy, N.H.T.; Ackermann, K. *Chem. Ber.* **1982**, *115*, 2951.

[40] Huy, N.H.T.; Lefloch, P.; Robert, F.; Jeannin, Y. *J.Organomet. Chem.* **1987**, *327*, 211.

bimetallic bridged biscarbene complexes with borontrihalides BX_3 afforded the corresponding *trans*-halocarbyne complexes, $[X(CO)_4M{\equiv}C\text{-}p\text{-}C_6H_4\text{-}C{\equiv}M(CO)_4X]$.[39]

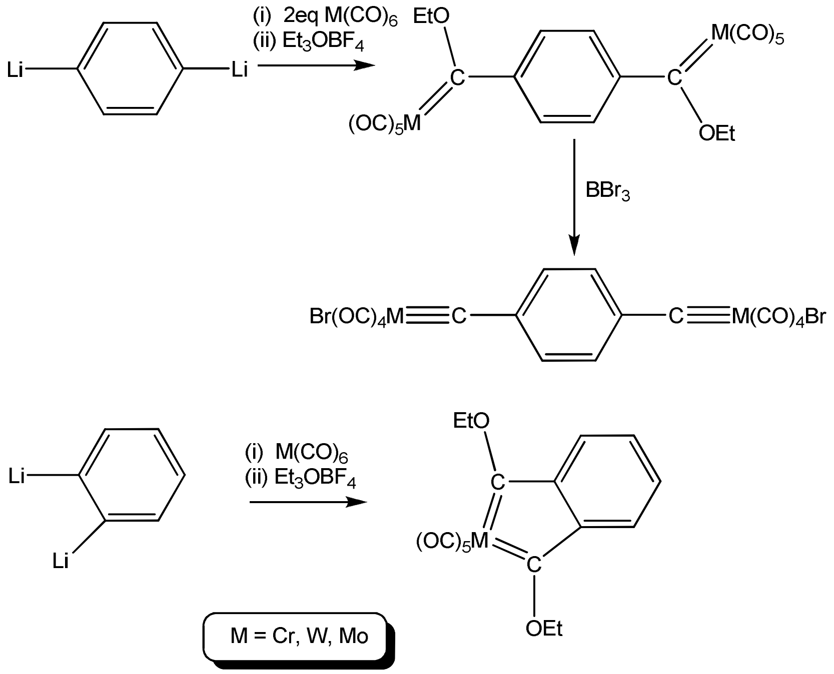

Scheme 2.6

In contrast, similar bimetallic biscarbene complexes with conjugated heteroarene moieties instead of carbon units have received less attention, but have been an important topic of research in our laboratories. Maiorana and co-workers prepared the first mixed-metal biscarbene complex of bithiophene[41] to study the interaction of the π electrons of the conjugated system and the d electrons of the transition metal atom resulting from the large overlap between the electronic systems through the carbonic link.[42] A series of homo- and heteronuclear mixed biscarbene complexes containing a variety of heteroaromatic spacers have been synthesized in our laboratory[43] and some examples are listed in Figure 2.8.

---

[41] Maiorana, S.; Papagni, A.; Licandro, E.; Persoons, A.; Clay, K.; Houbrechts, S.; Porzio, W. *Gazz. Chim. Ital.* **1995**, *125*, 377.

[42] Lancellotti, L.; Tubino, R.; Luzzati, S.; Licandro, E.; Maiorana, S.; Papagni, A. *Synth. Met.* **1998**, *93*, 27.

[43] (a) Terblans, Y.M.; Roos, H.M.; Lotz, S. *J. Organomet. Chem.* **1998**, *566,* 133, (b) Landman, M.; Görls, H.; Lotz, S. *J. Organomet. Chem.* **2001**, *617-618*, 280, (c) Landman, M.; Görls, H.

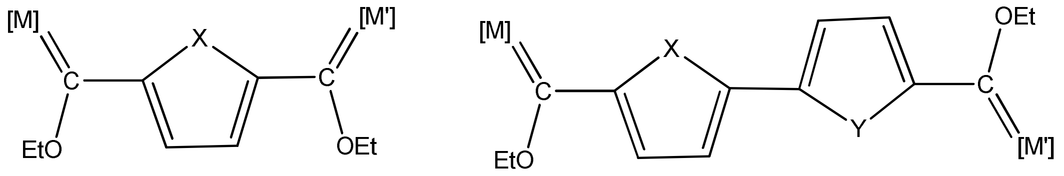

[M] = $Cr(CO)_5$; $Mo(CO)_5$; $W(CO)_5$: $MnCpMe(CO)_2$
[M'] = $Cr(CO)_5$; $Mo(CO)_5$; $W(CO)_5$: $MnCpMe(CO)_2$
X = S; O; NMe
Y = S; O; NMe

Figure 2.8 Various combinations of [M], [M'], X and Y was utilized to prepare a series of homo- and heteronuclear mixed biscarbene complexes.[43]

The role of the heteroatom in the bridging heteroarene was investigated, and known monocarbene reaction pathways for carbene modification and carbon-carbon coupling reactions was tested.[43(d)] Biscarbene complexes displayed enhanced reactivity at the carbene carbon compared to the monocarbene complexes in benzannulation reactions.[43(f)]

As far as could be ascertained, no biscarbene complexes containing a bridging ferrocen-1,1'-diyl (Fc') spacer have been reported; however the corresponding ruthenocenyl biscarbene, [μ-Ru{$C_5H_4C(OEt)Cr(CO)_5$}$_2$] has been prepared by Sierra *et al.*[44] Recently, the Sierra group has also extended the idea of conjugated biscarbene complexes by preparing homo- and heteronuclear tetrametallic macrocycles (Scheme 2.7) *via* a self-assembly route, in order to explore the electrochemical properties of the four metal centres in the cyclophanic structures.[45]

Lotz, S. *Z. Anorg. Allg. Chem.* **2002**, *628,* 2037, (d) Crause, C.; Görls, H.; Lotz, S. *J. Chem. Soc., Dalton Trans.* **2005**, 1649, (e) Lotz, S.; Crause, C.; Olivier, A.J.; Liles, D.C.; Görls, H.; Landman, M.; Bezuidenhout, D.I. *J. Chem. Soc., Dalton Trans.* **2009**, 697, (f) Landman, M.; Ramontja, J.; van Staden, M.; Bezuidenhout, D.I.; van Rooyen, P.H.; Liles, D.C.; Lotz, S. *Inorg. Chim. Acta* **2010**, *363*, 705.

[44] Lage, M.L.; Fernández, I.; Mancheño, M.J.; Gómez-Gallego, M.; Sierra, M.A. *Chem. Eur. J.* **2009**, *15*, 593.

[45] Fernández, I.; Mancheño, M.J.; Gómez-Gallego, M.; Sierra, M.A. *Org. Lett.* **2003**, *5*, 1237.

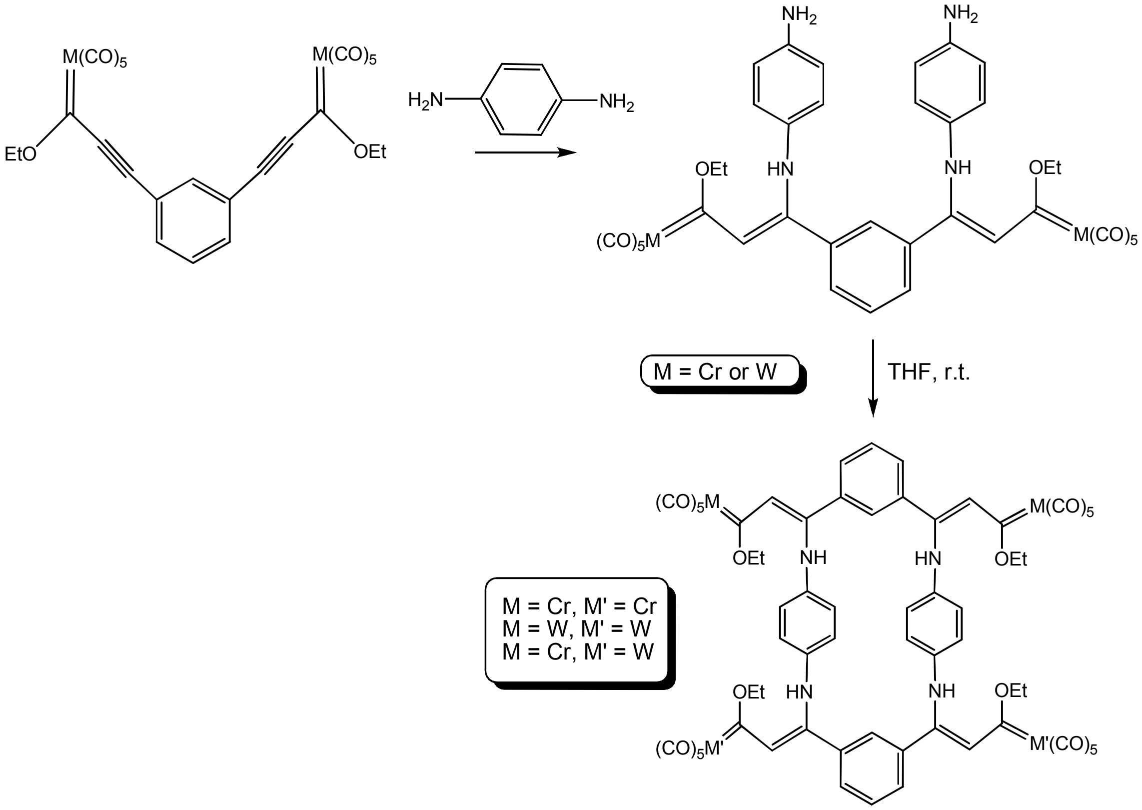

Scheme 2.7

2.1.4.2 Biscarbene complexes by connecting carbene heteroatom substituents

The principle of connecting carbene alkoxy substituents to form biscarbene complexes involves the alkylation of the oxygen where nucleophilic attack by the oxygen on a coordinated carbocationic carbon atom yields the desired product. An example[46] illustrating this is shown in Figure 2.9, where a solution of a methoxy(diethylamino)carbene complex was added to the tetramethylammonium salt of the $[(CO)_5MC(O)R]^-$ anion at low temperature. In this case, M = Cr or W and R = p-$C_6H_4CH_3$ or CH_3 and the bimetallic biscarbene complex $[Cr(CO)_5\{C(NEt_2)OC(R)\}Cr(CO)_5]$ as well as the mixed bimetallic complex $[Cr(CO)_5\{C(NEt_2)OC(R)\}W(CO)_5]$ were obtained.

---

[46] Fischer, E.O.; Kleine, W. *J.Organomet. Chem.* **1981**, *208*, C27.

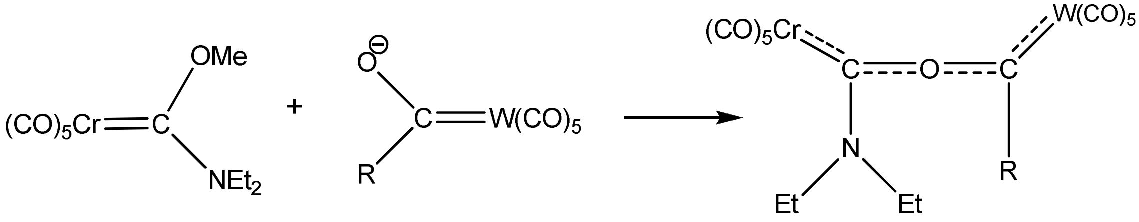

Figure 2.9 Metal acylates as nucleophiles

Another possibility to link two carbene metal moieties is to substitute the alkoxy carbene substituents in aminolysis reactions, using diamines to form amino bridged biscarbenes,[8] or to link the carbene substituents, such as alkynyl substituents, through the reaction of alkynyl alkoxycarbenes with 1,2-primary and secondary diamines as shown in Scheme 2.8.[47]

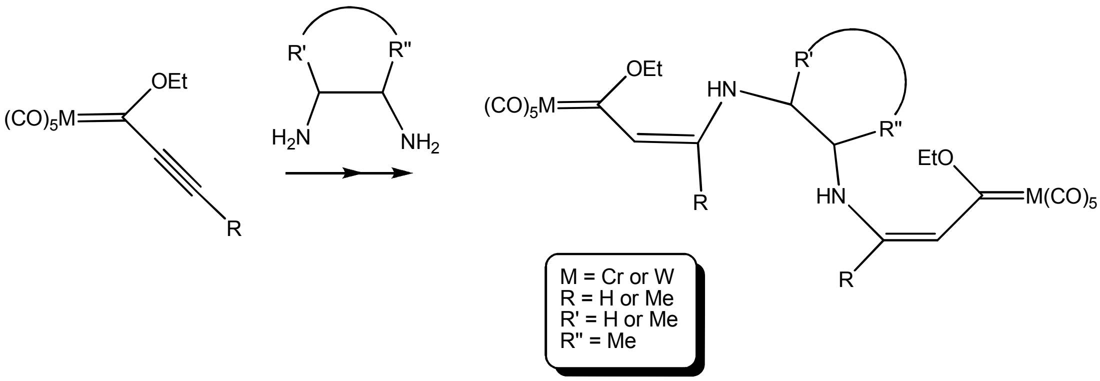

Scheme 2.8

A number of different routes exist to prepare titanoxy biscarbene complexes. The simplest method is the Fischer route in which the reaction of acyl metalate complexes, generated by the Fischer method[48] with titanocene dichloride furnishes an equimolar mixture of titanoxycarbene and biscarbene complexes.[8] Different variations of this approach have been followed, including the work of Sabat[9(b)] describing the preparation of dimeric titanium compounds, and more recently, the unusual rearrangement of these dimeric titanium complexes,

---

[47] Moretó, J.M.; Ricart, S.; Dötz, K.H.; Molins, E. *Organometallics,* **2001**, *20*, 62.
[48] Fischer, E.O.; Maasböl, A. *Angew. Chem., Int. Ed. Engl.* **1964**, *3*, 580.

(Scheme 2.9), yielding a compound where the titanium becomes coordinated by two oxycarbene units.[49]

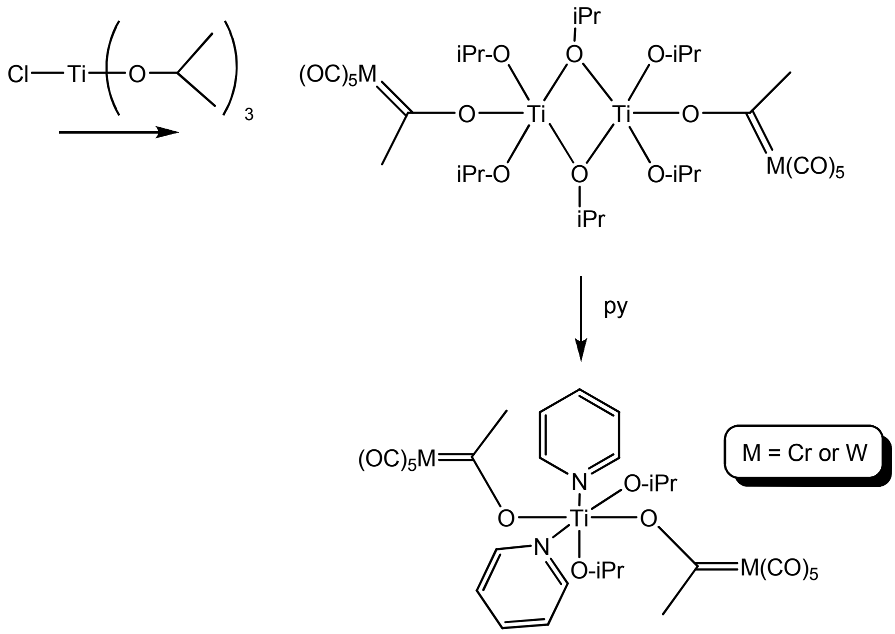

Scheme 2.9

The abovementioned method was also the approach followed in our study. However, to the best of our knowledge, no biscarbene complexes exist that are bridged both through the carbene heteroatom substituent, as well as through the α-C susbtituent bonded to the carbene carbon atom.

2.2 Results and discussion

2.2.1 Focus of this study

Expanding on the concept of σ,π-bimetallic Fischer carbene complexes, the objective was not only to synthesize trimetallic carbene complexes, but also to systematically study the electronic and steric effects of the different metal-containing substituents by introducing these fragments in a stepwise manner on both the R- and the R'-substituent. A list of the complexes synthesized is given

---

[49] Raubenheimer, H.G.; Cronje, S.; Strasser, C.E. *J. Chem. Soc., Dalton Trans.* **2009**, 8145.

in Figure 2.10. The structural features and their relevance to bonding in the carbene cluster compounds of the Group VI transition metals are discussed and represent indicators of possible reactivity sites in multimetal carbene assemblies.

In an effort to investigate the effect of different metal moieties end-capping the bridging biscarbene clusters it was attempted to synthesize the mixed heteronuclear bridging biscarbene complex **11** containing both Cr(CO)$_5$- and W(CO)$_5$-fragments on the termini.

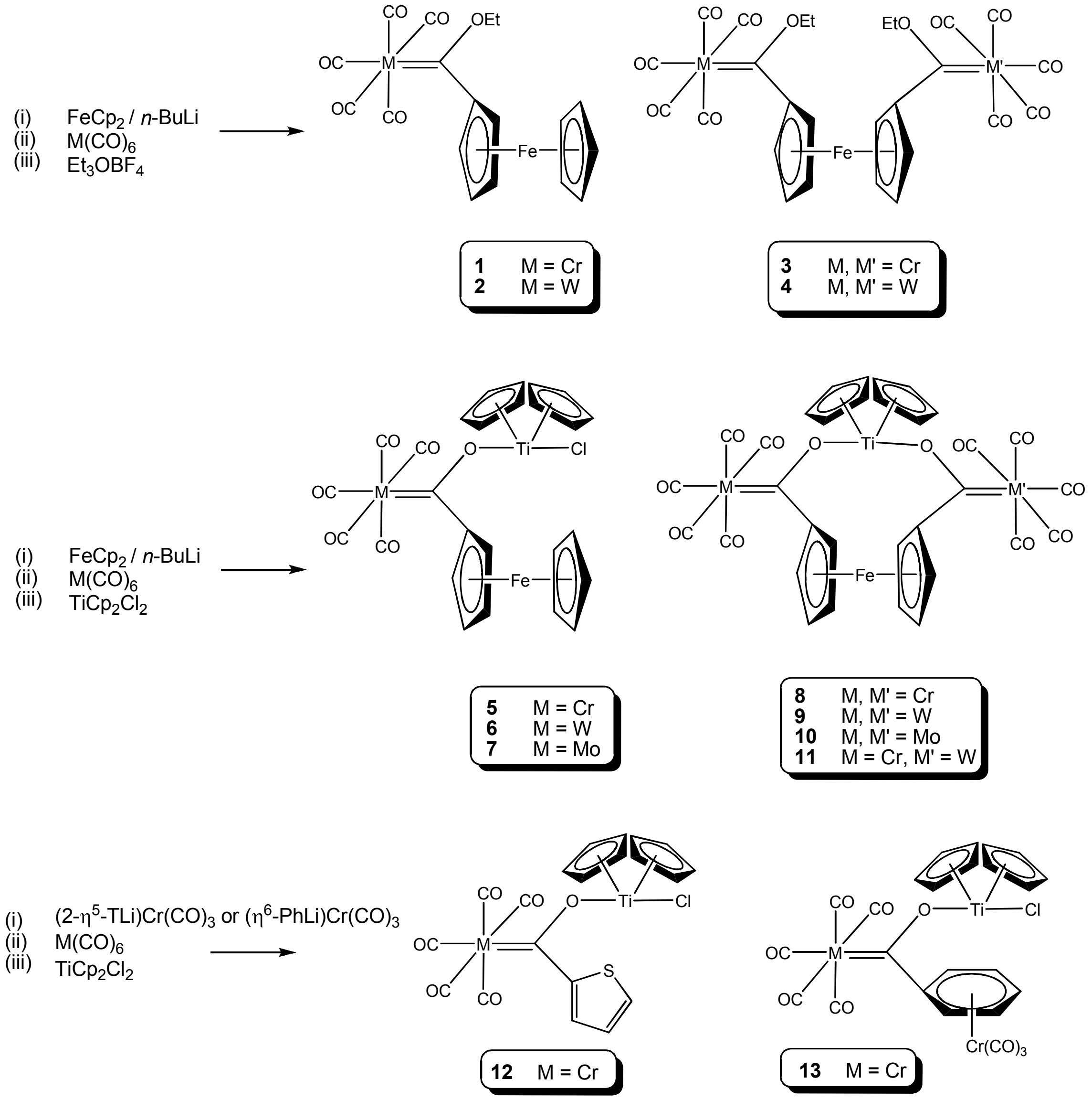

Figure 2.10 Group VI carbene complexes synthesized

2.3 Synthesis

In general, Fischer carbene complexes can be prepared following a variety of strategies.[50] These strategies include the formation of new carbene complexes from non-carbene complex precursors as well as by modification of pre-existing carbene complexes.

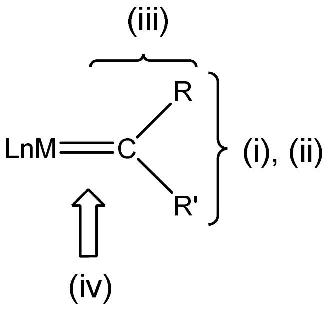

Figure 2.11 Synthetic strategies for the preparation of transition metal Fischer carbene complexes.

Specifically for Fischer carbene complexes, synthetic routes include (i) transformation of a non-carbene ligand into a carbene ligand, where the carbene carbon is already attached to the metal in the complex precursor, (ii) transfer of a pre-existing carbene ligand from one metal centre to another metal, (iii) modification of the carbene ligand and (iv) the insertion of an unsaturated organic molecule into the metal-carbene bond. The reaction sites (i) – (iv) listed above are indicated in Figure 2.11.

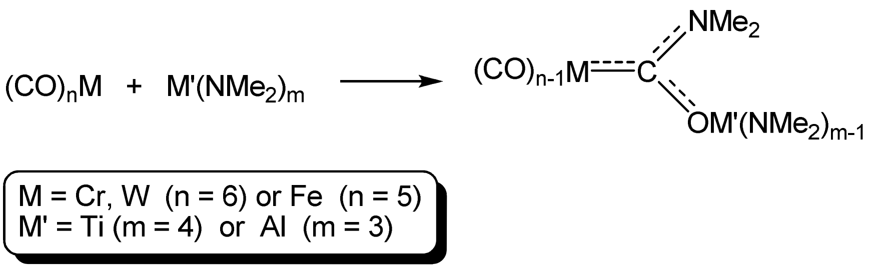

M = Cr, W (n = 6) or Fe (n = 5)
M' = Ti (m = 4) or Al (m = 3)

---

[50] Dötz, K.H.; Fischer, H.; Hofmann, P.; Kreissl, F.R.; Schubert, U.; Weiss, K. *Transition Metal Carbene Complexes,* VCH Verlag Chemie, Weinheim, **1983**, and references therein.

Scheme 2.10

Transformation of non-carbene ligand precursors into carbene ligands can be achieved, for example, in one step by employing metal amides[16(a), 51] to convert carbonyl ligands as shown in Scheme 2.10

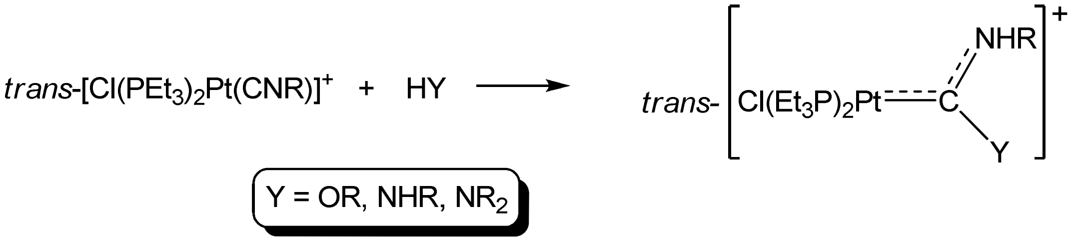

Scheme 2.11

Treatment of isonitrile complexes with nucleophilic alcohols and amines (Scheme 2.11), followed by alkylation, also yield Fischer carbenes according to the Hegedus-Semmelhack method[52] but the most useful and direct route remains the direct, two-step procedure of Fischer and Maasböl.[48]

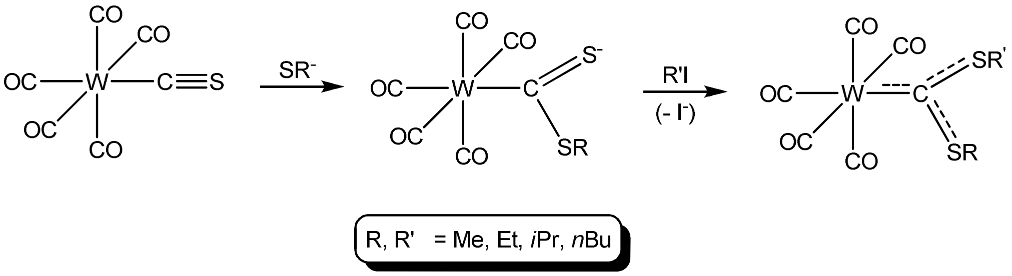

Scheme 2.12

Nucleophilic attack of the carbanion in a lithium organometallic reagent on the carbon atom of a carbonyl ligand forms an acyl metalate (Scheme 2.12) which can be alkylated with a variety of alkylating agents.[53]

---

[51] (a) Petz, W.; Schmid, G. *Angew. Chem.* **1972**, *84*, 997, (b) Petz, W.; Jonas, A. *J. Organomet. Chem.* **1973** *55,* C42.

[52] (a) Semmelhack, M.F.; Lee, G.R. *Organometallics,* **1987**, *6*, 1839, (b) Imwinkelried, R.; Hegedus, L.S. *Organometallics,* **1988**, *7*, 702.

[53] (a) Casey, C.P.; Cyr, C.R.; Boggs, R.A. *Synth. Inorg. Met.-Org. Chem.* **1973**, *3*, 249, (b) Fischer, E.O.; Gibbins, S.G.; Kellerer, W. *J. Organomet. Chem.* **1981***, 218*, C51, (c) Fischer,

2.3.1 Synthesis of ferrocenyl mono- and biscarbene Cr and Mo complexes

Monolithiation of ferrocene is best achieved by reaction of ferrocenyl bromide with *n*-BuLi in diethyl ether at -78℃.[54] Lithiation of ferrocene in this case was carried out in hexane with 1 eq. TMEDA at a temperature of 45˚C, yielding both mono- and dilithiated ferrocene. This *n*-BuLi-TMEDA chelate method[55] has the advantage of being applicable at temperatures up to 70℃, since the reagent is stable at higher temperatures. In THF, however, the solution of *n*-BuLi and TMEDA is not stable since the ethereal solvent is readily attacked at room temperature by the chelation complex, leading to the formation of lithium ethenolate and ethane.

After reacting the lithiated ferrocene with the hexacarbonyls $Cr(CO)_6$ or $Mo(CO)_6$ and quenching the metalate with titanocene dichloride, both the trimetallic carbene complexes $[Cr(CO)_5\{C(OTiCp_2Cl)Fc\}]$ (**5**) and $[Mo(CO)_5\{C(OTiCp_2Cl)Fc\}]$ (**7**) and the biscarbene complexes containing both bridging bisoxytitanocene and bridging ferrocen-1,1'-diyl substituents, $[\{\mu\text{-}TiCp_2O_2\text{-}O,O'\}\{\mu\text{-}Fe(C_5H_4)_2\text{-}C,C'\}\{CCr(CO)_5\}_2]$ (**8**) $[\{\mu\text{-}TiCp_2O_2\text{-}O,O'\}\{\mu\text{-}Fe(C_5H_4)_2\text{-}C,C'\}\{CMo(CO)_5\}_2]$ (**10**) were obtained. The general synthetic route is outlined in Scheme 2.13.

The novel complexes **8** and **10** are remarkable in that they display a bimetallacycic ring bridging two carbene carbons. In order for comparison with the bisoxytitanocene bridged biscarbene complex, the dilithiation of ferrocene was repeated, and metalation (with either $Cr(CO)_6$ or $W(CO)_6$) followed by alkylation with the Meerwein salt[56] Et_3OBF_4 afforded complex **3**, $[\mu\text{-}Fe\{C_5H_4C(OEt)Cr(CO)_5\}_2]$ and **4** $[\mu\text{-}Fe\{C_5H_4C(OEt)W(CO)_5\}_2]$ (illustrated on p. 28) in high yield. Although the monomers $[M(CO)_5\{C(OEt)Fc\}]$ (**1** (M = Cr) and **2**

E.O.; Selmayr, T.; Kreissl, F.R.; Schubert, U. *Chem. Ber.* **1977**, *110*, 2574, (d) Berke, H.; Härter, P.; Huttner, G.; von Seyerl, J. *J. Organomet. Chem.* **1981**, *219*, 317.

[54] Fish, R.W.; Rosenblum, M. *J. Org. Chem.* **1965**, *30*, 1253.

[55] Butler, I.R.; Cullen, W.R.; Ni, J.; Rettig, S.J. *Organometallics* **1985**, *4*, 2196.

[56] Meerwein, H. *Org. Synth.* **1966**, *46*, 113.

(M = W)) are known[57], the bisethoxy Fc'-bridged biscarbene (**3** and **4**) have not been synthesized before.

Unexpectedly, the chromium complexes proved more stable than the previously synthesized trimetallic carbene complexes **20** and **21** (Scheme 2.5), where a [Cr(2-η^6-BT)(CO)$_3$]-group is bonded to the carbene carbon atom. This could be ascribed to the absence of a displaceable Cr(CO)$_3$ fragment from BT (benzothienyl) in the cluster carbene complexes, the greater electron-donating character of the ferrocenyl substituent as compared to the [Cr(2-η^6-BT)(CO)$_3$]-substituent, and the prediction that a ferrocenyl group would not greatly increase the steric crowding around the carbene carbon atom.

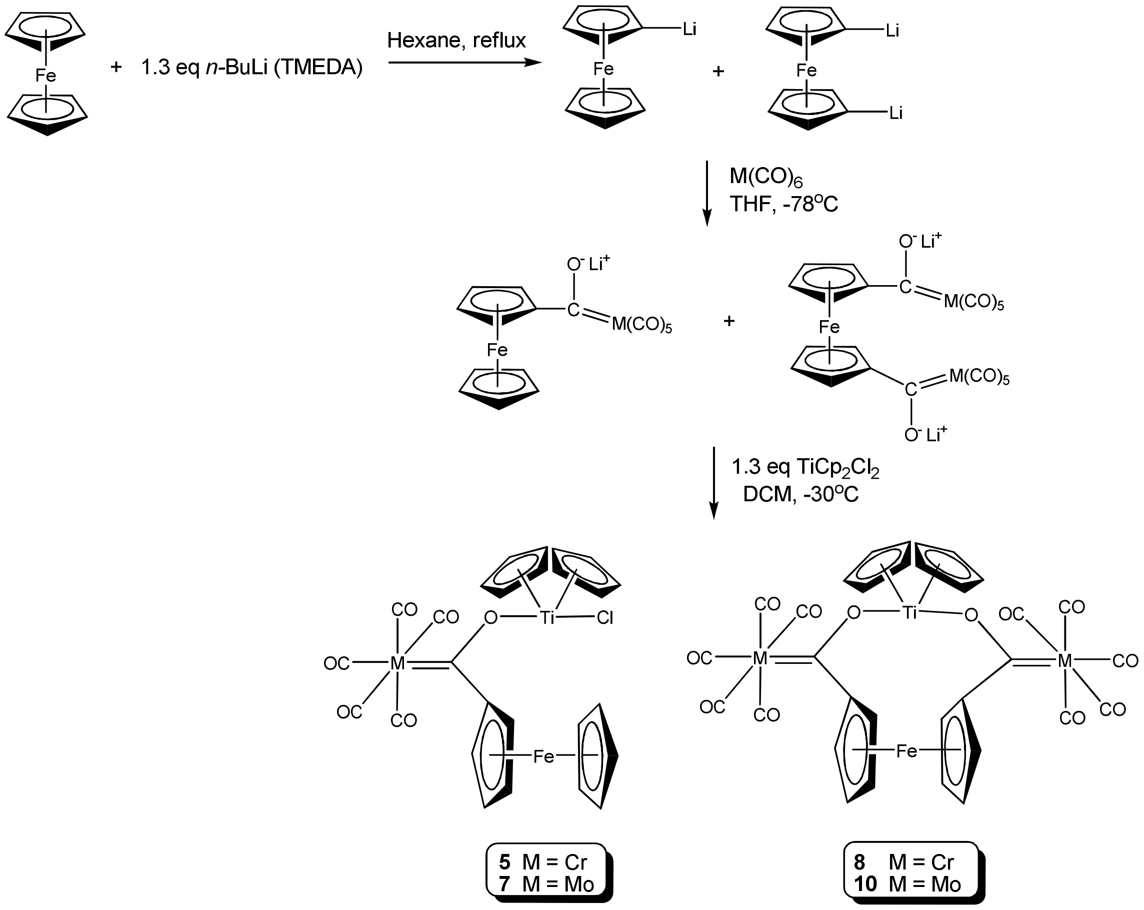

Scheme 2.13

---

[57] López-Cortés, J.G.; de la Cruz, L.F.C.; Ortega-Alfaro, M.C.; Toscano, R.A.; Alvarez-Toledano, C.; Rudler, H. *J. Organomet. Chem*. **2005**, *690*, 2229.

When comparing the monocarbene complex **5** and the biscarbene complex **8**, the absence of an activated chloro ligand on the titanium atom of **8** accounts for its greater stability. It is known that the reaction of a metal acylate with titanocene dichloride by displacement of one of the chloro ligands results in the activation of the remaining chloro ligand and can lead to the formation of two chromium carbene acylates being bridged by a titanocene fragment.[16(a)]

It should also be noted that in each of the reactions described above, unreacted *n*-butyllithium reacted with the different metal carbonyls and afforded the corresponding butylcarbene complexes $[(CO)_5M\{C(OR)(Bu)\}]$ (M = Cr, Mo, W; R = Et, $TiCp_2Cl$).[58]

2.3.2 Synthesis of tungsten carbene complexes

In the case of tungsten as central metal moiety, the above synthetic method yielded only the bridged biscarbene complex $[\{\mu\text{-}TiCp_2O_2\text{-}O,O'\}\{\mu\text{-}Fe(C_5H_4)_2\text{-}C,C'\}\{CW(CO)_5\}_2]$ (**9**) but no monocarbene could be isolated. Initially, this was ascribed to the lability of the titanium chloro ligand,[16(a)] but later proved to be the result of the low yield of the monolithiated ferrocene compared to the dilithiated ferrocene.

In an attempt to overcome this limitation, the reaction was repeated as described in Section 2.3.1 above, but after addition of the titanocene dichloride, the reaction mixture was allowed to warm to room temperature and one mole equivalent of thiophenol was added to replace the remaining chloro ligand on the titanoxy substituent (Scheme 2.14). However, none of the desired monocarbene complex $[W(CO)_5\{C(OTiCp_2SPh)Fc\}]$ was obtained. Instead, column chromatography yielded only the bright purple complex $TiCp_2(SPh)_2$[59] and the tungsten metalate remained immobile on the silica gel column.

---

[58] Hedberg, F.L.; Rosenberg, H. *Tetrahedron Lett.* **1969**, 4011.

[59] (a)Köpf, H.; Schmidt, M. *Zeitschrift für Anorganische und Allgemeine Chemie* **1965**, *340*, 139, (b) Giddings, S.A. *Inorg. Chem.* **1967**, *6*, 819, (c) Muller, E.G.; Watkins, S.F.; Dahl, L.F. *J. Organomet. Chem.* **1976**, *111*, 73.

This lead us to prepare only monolithiated ferrocene instead of the mono- and dilithiated mixture. Ferrocenyl bromide was prepared according to literature procedure.[58] Mercury acetate was added to a ferrocene solution in benzene, followed by addition of 1 mole eq LiCl to yield chloromercury ferrocene. Subsequent reaction with N-bromo succinimide gave the ferrocenyl bromide (FcBr) reagent. FcBr was lithiated using 1 mole eq of *n*-BuLi in THF, followed by addition of $W(CO)_6$ dissolved in THF. The desired monocarbene complex **6** $[W(CO)_5\{C(OTiCp_2Cl)Fc\}]$ was isolated after reaction quenching with $TiCp_2Cl_2$ in dichloromethane and purification on a silica gel column.

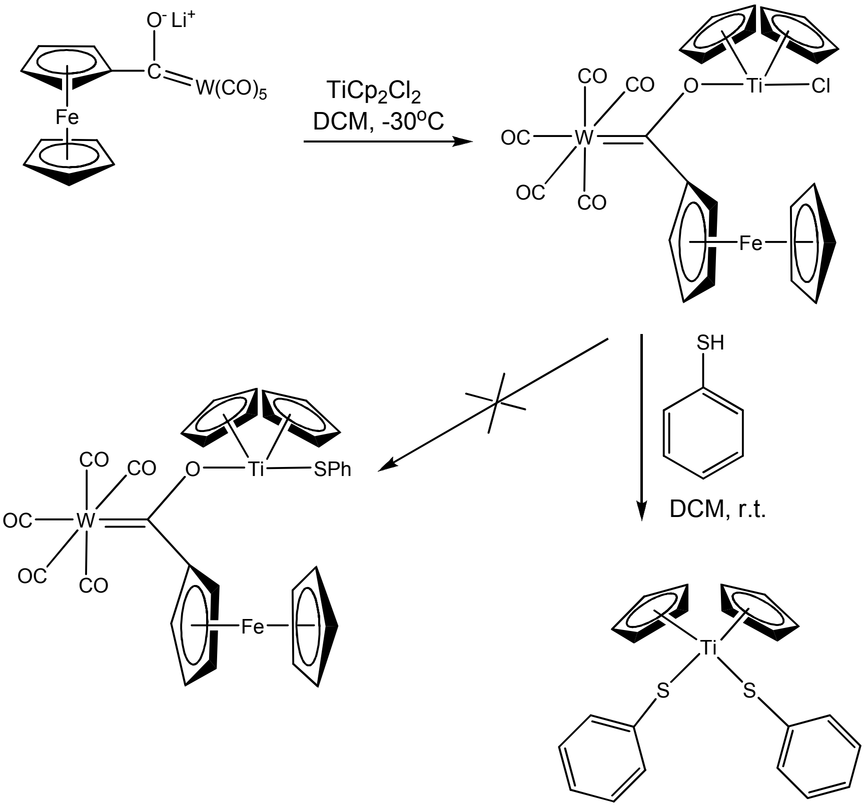

Scheme 2.14

O-metalation with $ZrCp_2Cl_2$ instead of $TiCp_2Cl_2$ was attempted but proved unsuccessful. This was ascribed to the instability of the resultant O-Zr bond in view of the greater activity of the zirconium metal compared to titanium.[9(a)]

2.3.3 Synthesis of mixed heteronuclear bridging biscarbene complexes

The investigation of mixed heteronuclear biscarbene complexes was included in the aims of this study in order to probe the possibility of enhancing the polarization across the conjugated bridge by introducing asymmetry.

The method employed by Maiorana[41] in the preparation of a heteronuclear bridging bithiophenyl biscarbene complex involved the synthesis of an anionic acyl complex of chromium, followed by metalation with *n*-BuLi and reactions with $W(CO)_6$ and Et^+ (Scheme 2.15) to yield a mixture of both the mono- and biscarbene complexes.

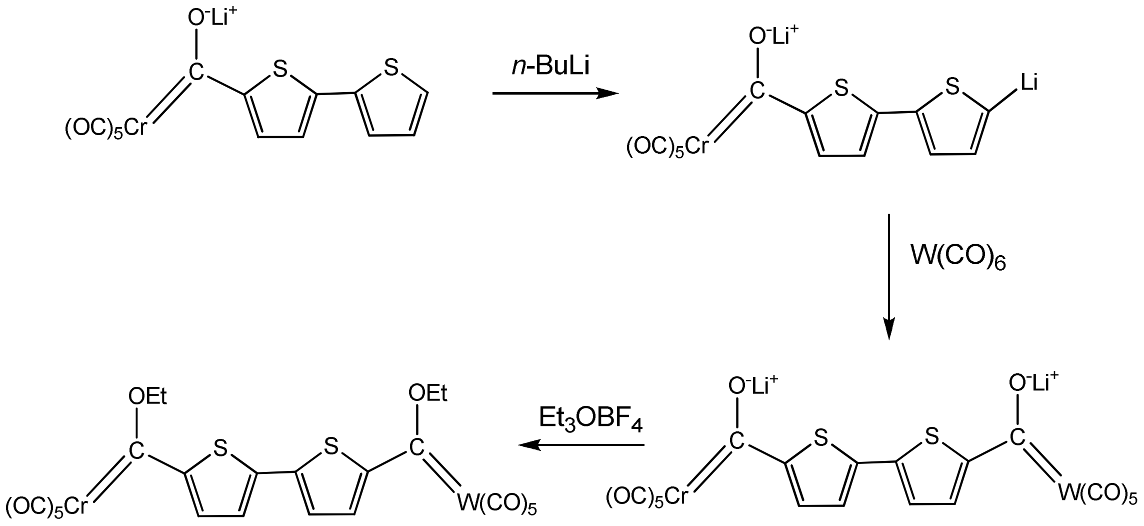

Scheme 2.15

Adaptation of the Aoki method[60] increases the yield of the heteronuclear biscarbene complexes significantly. Aoki and co-workers treated $M(CO)_6$ with a suitable lithium reagent, followed by the sequential addition of lithium diisopropyl amide (LDA), an electrophile, water and finally alkylated with an oxonium salt in a one pot reaction. This anionic protection strategy was modified in our laboratories by using a second mole equivalent of a different metal hexacarbonyl to obtain mixed metal biscarbene complexes bridged by furyl spacers.[43(d)]

---

[60] Aoki, A.; Fujimura, T.; Nakamura, E. *J. Am. Chem. Soc.* **1992**, *114*, 2985.

The method entailing sequential lithiation with first *n*-BuLi and then LDA, described above, was followed in an attempt to synthesize the heteronuclear biscarbene complex **11** $[W(CO)_5C\{\mu\text{-}TiCp_2O_2\text{-}O,O'\}\{\mu\text{-}Fe(C_5H_4)_2\text{-}C,C'\}CCr(CO)_5]$, but no product could be isolated.

In the next attempt, it was decided to employ 1,1'-dibromoferrocene as starting material for lithiation. Ferrocene was dilithiated with *n*-BuLi/TMEDA and reacted with 1,2-tetrabromoethane, which, after recrystallization, afforded 1,1'-dibromoferrocene.[61] Monolithiation was achieved by metal-halogen exchange of one of the bromo ligands with 1 mole eq of *n*-BuLi followed by metalation with $Cr(CO)_6$ at -90°C. After allowing the reaction to warm to -30°C, a second mole eq of *n*-BuLi was added. The second mole eq of metal hexacarbonyl, $W(CO)_6$, was then added. Finally $TiCp_2Cl_2$ was reacted with the resulting bis(acyl metalate). A mixture of the homonuclear dimetallic biscarbene complexes **8** and **9**, as well as heteronuclear **11** was obtained, albeit in very low yield (< 10%).

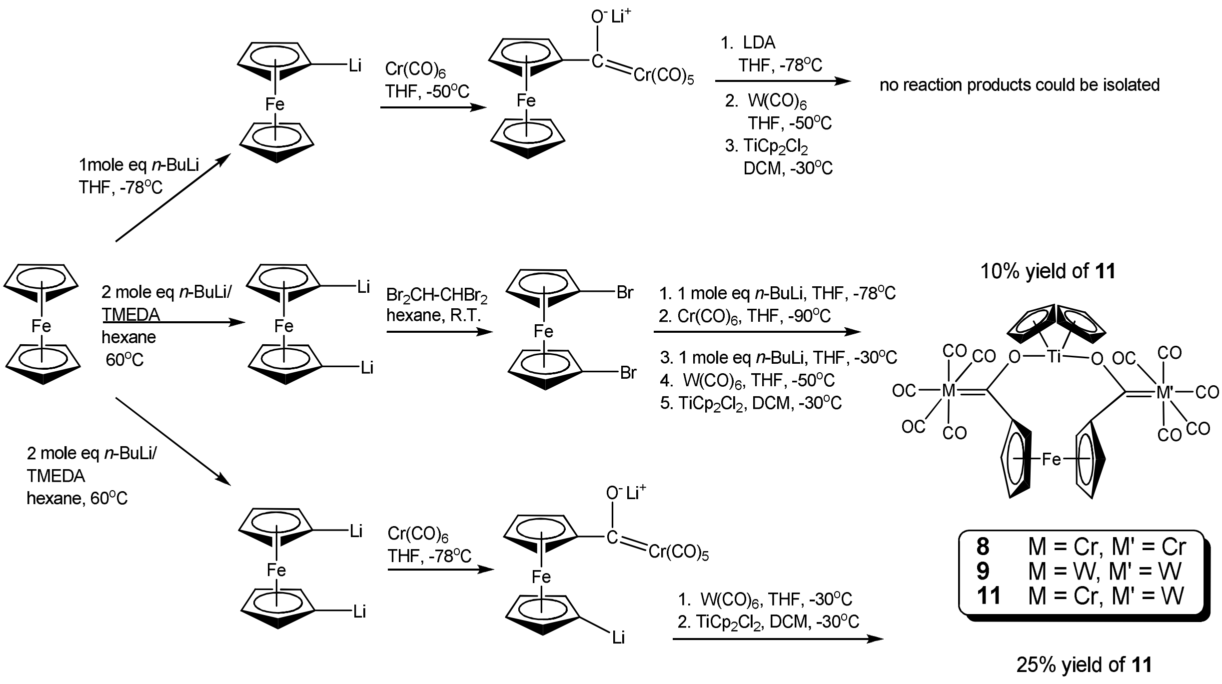

Scheme 2.16

---

[61] Kovar, R.F.; Rausch, M.D.; Rosenberg, H. *Organometallics in Chemical Synthesis* **1970**, *1*, 173.

In a final attempt to increase the yield as well as the selectivity of the preparation of the mixed metal complex, direct dilithiation of ferrocene was carried out as before. At -78℃ the first mole equivalent of $Cr(CO)_6$ was added, and the sequential addition of $W(CO)_6$ at -30℃, and quenching with titanocene dichloride gave the best result. $[W(CO)_5C\{\mu\text{-}TiCp_2O_2\text{-}O,O'\}\{\mu\text{-}Fe(C_5H_4)_2\text{-}C,C'\}CCr(CO)_5]$, complex **11**, was isolated on a silica gel column, and crystallized from a dichloromethane/hexane (1:3) solution. The single crystals obtained were analysed by X-ray diffraction.

However, the X-ray structure obtained (R factor 6.21%) showed co-crystallization of the homonuclear biscarbene complex **8** and the desired heteronuclear complex **11**, with Cr-atoms occupying 84.5(2)% of the central metal atom sites, and W occupying 15.5(2)%. The only plausible explanation of the above finding would constitute greater reactivity of the $[Cr(CO)_5\{C(OLi)Fc'Li\}]$ intermediate than of dilithiated ferrocene $Fc'Li_2$ towards $Cr(CO)_6$. The homonuclear chromium biscarbene would therefore form preferentially. Only after all of the $Cr(CO)_6$ has been consumed, the remaining $[Cr(CO)_5\{C(OLi)Fc'Li\}]$ intermediate would react with the subsequently added $W(CO)_6$ to produce heteronuclear biscarbene **11**, and the remaining dilithiated ferrocene reacts with tungsten hexacarbonyl to yield homonuclear **9**.

The synthetic strategies describing the attempted synthesis of complex **11** are given in Scheme 2.16.

2.3.4 Synthesis of π-aryl-$Cr(CO)_3$ titanoxycarbene complexes of chromium

The first example of a π-aryl chromium tricarbonyl substituted carbene complex and, incidentally, the first example of a σ,π-carbene complex was synthesized by Fischer[4(a)] *via* lithiation of $[Cr(CO)_3(\eta^6\text{-}C_6H_6)]$ with phenyl lithium. The starting material, π-benzene chromium tricarbonyl, was also originally prepared by the Fischer group in the reaction of chromium hexacarbonyl with the bis(π-arene) chromium complex $[Cr(\eta^6\text{-}C_6H_6)_2]$.[27(a)]

In this study, however, the π-benzene chromium tricarbonyl reagent was synthesized according to an improved direct reaction procedure, by heating the benzene and chromium hexacarbonyl together in dibutyl ether.[62]

Following lithiation of $[Cr(CO)_3(\eta^6\text{-}C_6H_6)]$ with *n*-BuLi and sequential metalation with $Cr(CO)_6$ and $TiCp_2Cl_2$, the dark brown-purple **13** $[Cr(CO)_5\{C(OTiCp_2Cl)(\eta^1{:}\eta^6\text{-}PhCr(CO)_3)\}]$, was formed exclusively in high yield.

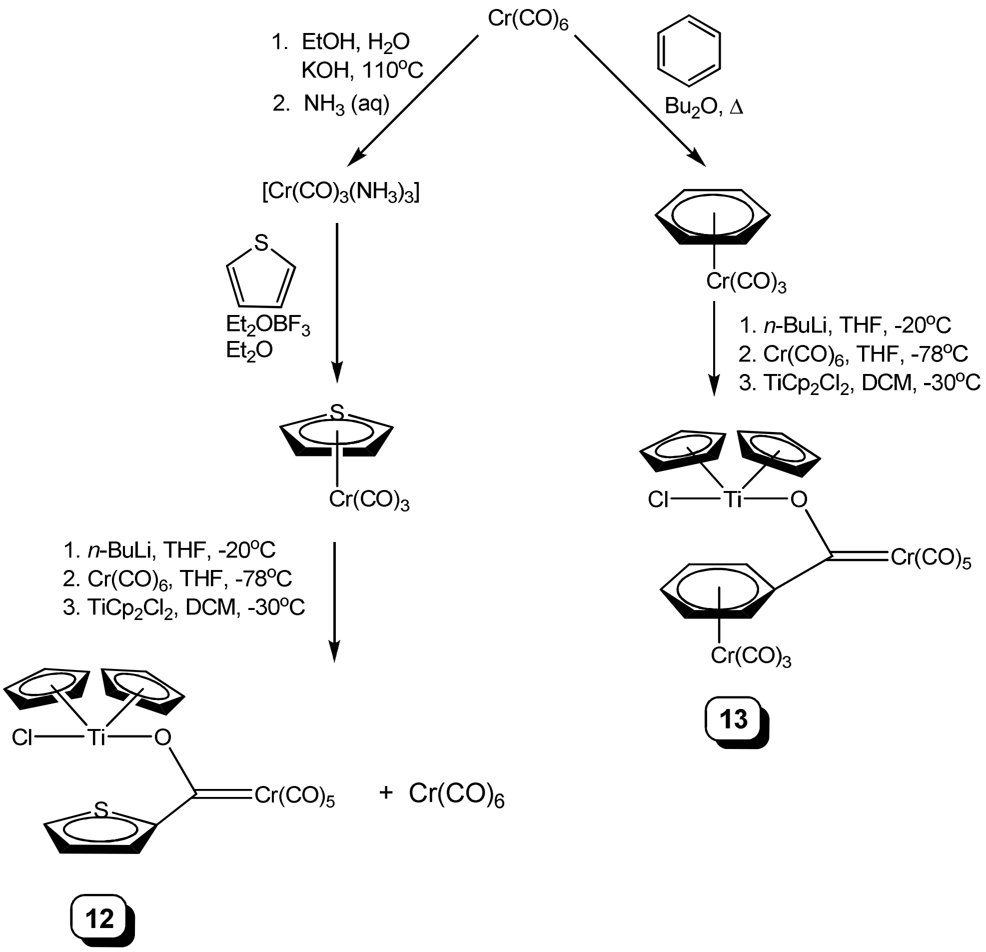

Figure 2.12 Synthesis of [Cr{π-(hetero)aryl}(CO)$_3$] chromium titanoxycarbene complexes.

As with the $[Cr(CO)_3(\eta^6\text{-}C_6H_6)]$ complex, the precursor $[Cr(CO)_3(\eta^5\text{-}SC_4H_4)]$ was prepared for the first time in a low yield by Fischer and Öfele in the thermal

---

[62] Fischer, E.O.; Goodwin, H.A.; Kreiter, C.G.; Simmons, H.D.; Sonogashira, K.; Wild, S.B. *J. Organomet. Chem.* **1968**, *14*, 359.

reaction of chromium hexacarbonyl and thiophene.[63] An increased yield was achieved by converting the $Cr(CO)_6$ to $[Cr(CO)_3(NH_3)_3]$[64] whereafter treatment with excess thiophene and 3 mole equivalents of the Lewis acid BF_3 in diethyl ether yielded $[Cr(CO)_3(\eta^5-C_4H_4S)]$.[65]

The readily achieved lithiation of $[Cr(CO)_3(\eta^5-C_4H_4S)]$ at low temperatures has been reported[66] and subsequent carbene formation and alkylation with the introduction of the third metal-containing fragment occurred as before.

During evaporation of the solvent before column chromatography, the dark red solution of desired reaction product turned orange, and thin layer chromatography indicated a large amount of $Cr(CO)_6$ present. After separation, a lighter orange complex **12** $[Cr(CO)_5\{C(OTiCp_2Cl)(C_4H_3S)\}]$, was the only other product obtained besides the $Cr(CO)_6$ and unreacted titanocene dichloride. It is known that complexes with a benzene (here, incidentally, it is a phenyl group) instead of a π-coordinated thiophene substituent are less labile, and exhibit greater stability against $Cr(CO)_3$ displacement in polar solvents. However the high yield of previously reported ethoxy analogues[7] in contrast to the high reactivity of this titanoxy equivalent would seem to indicate increased lability of the $Cr(CO)_3$-fragment as a result of overall increased lability when two transition metal fragments are bonded to the carbene carbon atom.

2.4 Spectroscopic characterization

The carbene complexes were characterized using ^1H and ^{13}C NMR spectroscopy. Chemical shift assignments were substantiated by two-dimensional HSQC-NMR experiments. Other spectroscopic characterization methods include infrared spectroscopy, mass spectrometry and single crystal X-ray diffraction where possible.

---

[63] Fischer, E.O.; Öfele, K. *Chem. Ber.* **1958**, *91*, 2385.

[64] Rausch, M.D.; Moser, G.A.; Zaiko, E.J.; Lipman, A.L. *J. Organomet. Chem.* **1970**, *23*, 185.

[65] Novi, M.; Guanti, G.; Dell'Erba, C. *J. Heterocycl. Chem.* **1975**, *12*, 1055.

[66] Nefedova, M.N.; Setkina, V.N.; Kursanov, D.N. *J. Organomet. Chem.* **1983**, *244*, C21.

2.4.1 ^{1}H NMR spectroscopy

The coordination of a metal fragment to an organic ligand markedly affects the electronic environment of the ligand protons and is reflected in the resonance frequencies of the ligand nuclei. The chemical shifts (^{1}H and ^{13}C) of the uncoordinated precursor molecules employed in this chapter are given below.

The carbene moiety, coordinated to an electropositive metal, causes draining of electron density[5] from the double bonds of the arene rings to the electrophilic carbene moiety, resulting in a downfield shift of the ring proton resonances compared to the chemical shifts of the uncoordinated arenes.

The resonance signals for the protons of the cyclopentadienyl rings on titanium uniformly occur at lower field than for ferrocene. Complex **12** contains the heteroaromatic thiophene ring bonded to the carbene carbon, while the phenyl ring of **13** has a $Cr(CO)_3$-fragment π-bonded to it. This π-coordination disrupts the aromaticity of the benzene ring and is reflected in the upfield shift of the benzene protons from 7.15 ppm in a benzene ring compared to the 4.27 ppm resonance seen for the precursor $[Cr(\eta^6\text{-}C_6H_6)(CO)_3]$.

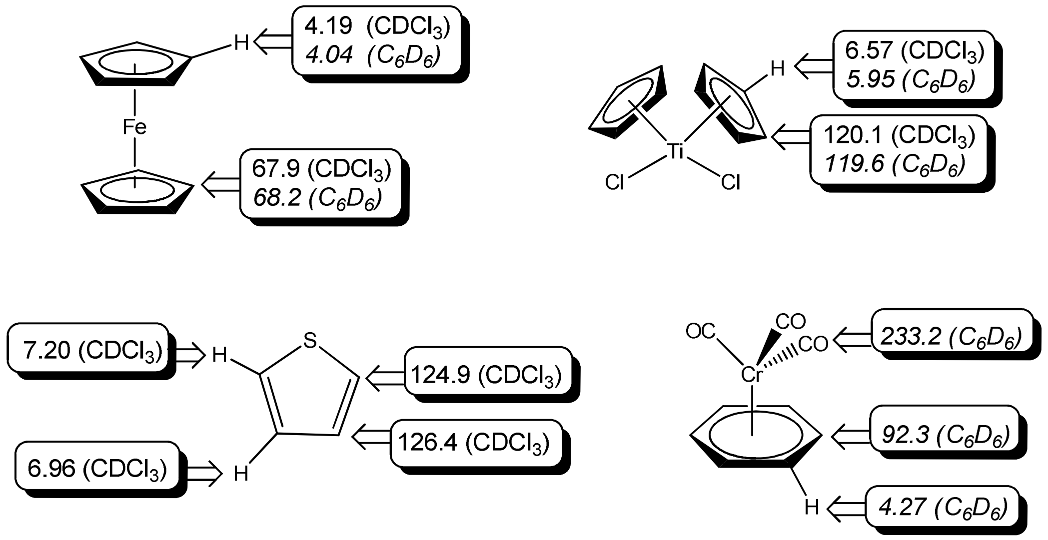

Figure 2.13 ^{1}H and ^{13}C chemical shifts (in units ppm) of precursor molecules

The NMR spectra of the chromium complexes **3**, **5**, **8** and **12**; and the tungsten complex **9**, were recorded in deuterated chloroform as solvent. Spectra of high resolution could only be obtained in d_6-benzene for the remainder and the assignments are listed in Tables 2.1 – 2.5. Slow decomposition of products with time was observed in the spectra, and broadening of the signals in the case of complex **5** was observed. The spectrum of **1** could not be determined due to decomposition, and for complexes **1** and **2** (Table 2.1) the literature values are given in brackets. In all cases, the atom numbering system employed is indicated in the relevant table.

Table 2.1 ^{1}H NMR data of ferrocenyl ethoxy monocarbene complexes

Proton Assignment	Chemical shifts (δ) and coupling constants (J)		
	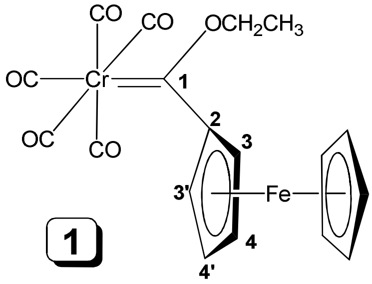 1	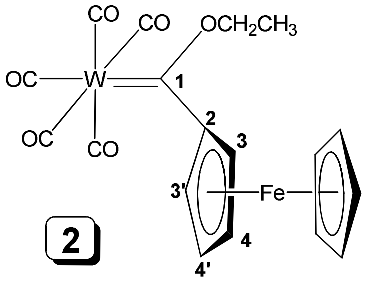 2	
	δ (*[57])	δ** (*[57])	J (Hz)**
H3, H3'	*(5.00, 4H, br, m)*	4.78, 2H, dd *(4.98, 2H, br, s)*	2.2, 1.8
H4, H4'	*(4.77, 2H, br, s)*	4.27, 2H, dd *(4.85, 4H, br, m)*	2.3, 1.7
Fe-Cp	*(4.22, 5H, s)*	3.92, 5H, s *(4.25, 5H, s)*	-
CH_2	*(5.00, 4H, br, m)*	4.49, 2H, q *(4.85, 4H, br, m)*	7.0
CH_3	*(1.60, 3H)*	0.96, 3H, t *(1.58, 3H, m)*	7.0

* Recorded in $CDCl_3$

** Recorded in C_6D_6

Different deuterated solvents were employed during NMR analysis, due to poor solubility in benzene-d_6 preventing the recording of all NMR spectra in this solvent, while the use of chlorinated solvent $CDCl_3$ caused decomposition of some of the carbene complexes. The use of different deuterated solvents during NMR analysis complicates direct comparison of the different proton resonances, as the ^1H NMR spectra of complexes recorded in $CDCl_3$ are shifted more downfield as compared to the spectra recorded in C_6D_6.

Analogous complexes containing the same ligands and substituents, with only the central metal being varied from Cr to Mo to W, afforded chemical resonances shifted more downfield for the Cr-complexes, while the W-complexes display spectra that appear to have more upfield shifts, owing to the better shielding of the protons by the larger metal nucleus.

Table 2.2 ^1H NMR data of ferrocenyl titanoxy monocarbene complexes

Proton Assignment	Chemical shifts (δ) and coupling constants (J)					
	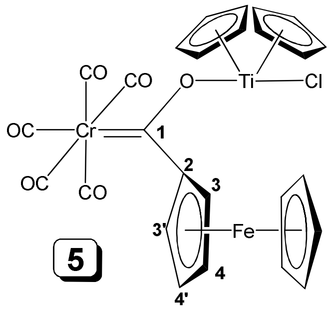 **5**		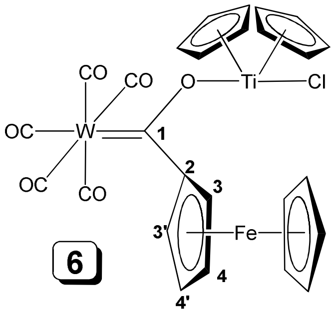 **6**		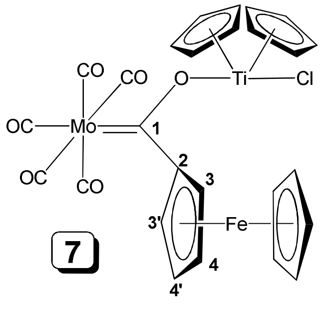 **7**	
	δ*	J (Hz)	δ*	J (Hz)	δ**	J (Hz)
Ti-Cp_2	6.52, 10H, s	-	6.46,10H, s	-	5.91, 10H, s	-
H3, H3’	4.70, 2H, br,m	-	5.04, 2H, br	-	4.89, 2H, d	2.9
H4, H4’	4.57, 2H, br,m	-	4.68, 2H, br	-	4.51, 2H, d	3.0
Fe-Cp	4.33, 5H, s	-	4.29, 5H, s	-	4.26, 5H, s	-

* Recorded in $CDCl_3$
** Recorded in C_6D_6

Relative to the Cp resonance of 4.19 ppm ($CDCl_3$) or 4.04 ppm (C_6D_6) for ferrocene, the α-proton of the attached FeCp-ring of all the ferrocenyl carbene complexes display a similar downfield shift compared to other substituted ferrocenes with an electron withdrawing group, such as $FeCp(C_5H_4(C(O)OMe))$

(δ: 4.80 H3, H3'; 4.39 H4, H4'; 4.20 Cp).[67] Since the α-proton (H3, H3') occupies the position closest to the site of the carbene carbon atom, the chemical shift of this proton is influenced most easily and is a sensitive probe for electronic ring substituent involvement with the electrophilic carbene carbon atom. Figure 2.14 demonstrates this phenomenon by considering the π-resonance effect in these compounds, as explained by Connor and Lloyd[23] (Figure 2.3). This is consistent with the finding that the donor strength of the ferrocenyl group is considerably increased by interaction with strong electrophilic centres.[68]

Table 2. 3 ^{1}H NMR data of π-aryl titanoxycarbene complexes

Proton Assignment	Chemical shifts (δ) and coupling constants (J)			
	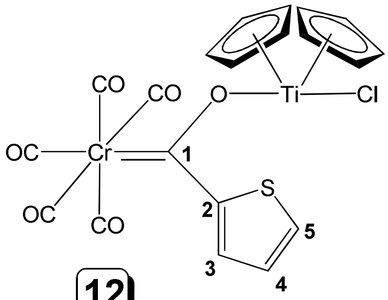 **12**		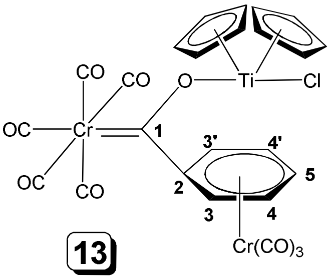 **13**	
	δ*	J (Hz)	δ**	J (Hz)
Ti-Cp$_2$	6.50, 10H, s	-	6.33, 10H, s	-
H3, H3'	8.16, 1H, br	-	4.52, 2H, dd	6.3, 3.2
H4, H4'	7.28, 1H, br	-	4.39, 2H, dd	6.3, 6.3
H5	7.72, 1H, d	4.67	4.31, 1H, br	-

* Recorded in $CDCl_3$
** Recorded in C_6D_6

The thienyl ethoxycarbene complex of Cr was first prepared by Connor and Jones[69] and the ^{1}H NMR spectrum of $[Cr(CO)_5\{C(OEt)(C_4H_3S)\}]$ reported. The large downfield shift of the methylene protons of the ethoxy group were seen as being consistent with the electron withdrawing property of $(CO)_5Cr{=}C$(2-thienyl)-

---

[67] Pickett, T.E., Richards, C.J.; *Tetrahedron Lett.* **1999**, *40*, 5251.
[68] Nesmeyanov, A.N.; Perevalova, E.G.; Gubin, S.P.; Gradberg, K.I.; Koslavsky, A.G. *Tetrahedron Lett.* **1966**, *28*, 237.
[69] Connor, J.A.; Jones, E.M. *J. Chem. Soc. A* **1971**, 1974.

group, and the assignment of H3, H4 and H5 were made according to Gronowitz:[70] H3 8.23, H4 7.20 and H5 7.68 ppm in $CDCl_3$. Likewise to the downfield shift of H3 of ferrocene, H3 of thienyl carbene complexes display a downfield shift due to π-resonance effects.

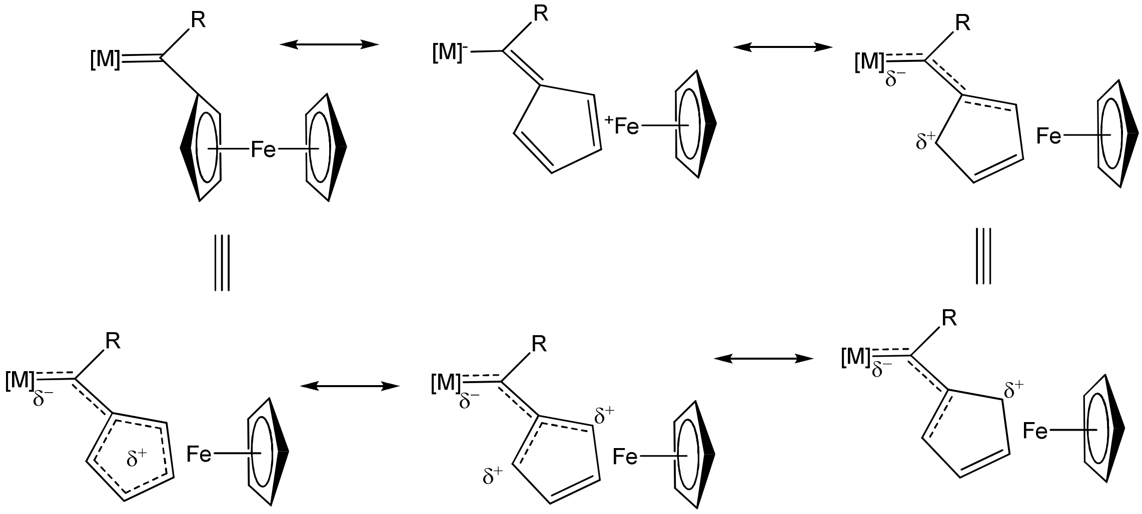

Figure 2.14 π-Resonance effects in ferrocenyl carbene complexes

Compared to the literature values obtained for $[Cr(CO)_5\{C(OEt)(C_4H_3S)\}]$, the upfield shift of H3 of complex **12** would seem to support the expectation that the titanoxy substituent leads to increased electron density on the oxygen atom. Greater interaction with the carbene carbon atom and less involvement of the thienyl substituent would result, and can be ascribed to the ionic character of the Ti-O bond. A higher contribution of the acyl resonance structure[9] illustrated in Figure 2.15 is therefore proposed. This phenomenon was also observed for the ferrocenyl complexes: compare for example $[Cr(CO)_5\{C(OEt)Fc\}]$ **1** (δ: H3,H3’ 5.00; H4, H4’ 4.77)[57] and $[Cr(CO)_5\{C(OTiCp_2Cl)Fc\}]$ **5** (δ: H3, H3’ 4.70; H4, H4’ 4.57).

---

[70] Gronowitz, S. *Adv. Heterocycl. Chem.* **1963**, *1*, 1.

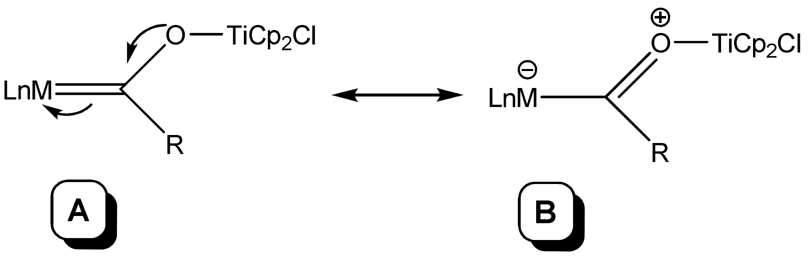

Figure 2.15 Acyl character of titanoxycarbene complexes

The same upfield shift of the π-aryl substituent is seen in the case of complex **13**. H3, H3'-values of 4.52 ppm (recorded in C_6D_6) when $-TiCp_2Cl$ is bonded to the oxygen atom, compared to a value of 5.72 ppm (recorded in acetone-d_6) with an ethoxy substituent.[4(a)]

Table 2. 4 ^{1}H NMR data of ferrocenyl ethoxy biscarbene complexes

Proton Assignment	Chemical shifts (δ) and coupling constants (J)			
	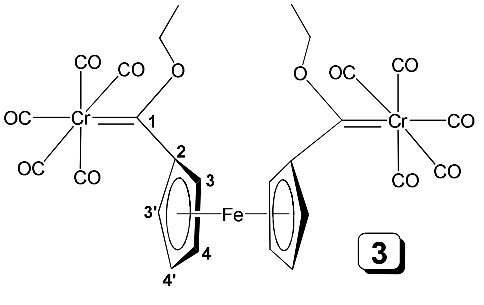		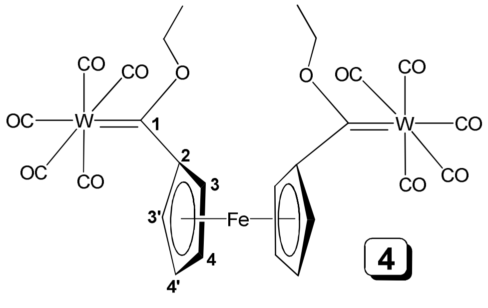	
	δ*	J (Hz)	δ**	J (Hz)
H3, H3'	5.00, 4H, dd	2.3, 1.9	4.94, 4H, dd	2.0, 1.8
H4, H4'	4.73, 4H, dd	2.3, 1.9	4.39, 4H, dd	2.0, 1.8
CH_2	5.07, 4H, q	7.1	4.55 4H, q	7.0
CH_3	1.63, 6H, t	7.1	1.06, 6H, t	7.0

* Recorded in $CDCl_3$
** Recrded in C_6D_6

When the downfield shifts of H3, H3' of the carbene complexes are compared to those of the precursor compounds, the formula $\Delta\delta = \delta_{complex} - \delta_{precursor}$ can be used to estimate the extent to which titanoxy fragments stabilize the carbene carbon atoms. The greater the downfield shift, the greater the electronic stabilization of the ring towards the carbene carbon atom, which in turn implies less stabilization of the heteroatom bonded substituent. Using the above formula for Δδ, the effect of the substituent –OEt and electron withdrawing π-(C_6H_6)Cr(CO)$_3$ *vs* electron donating Fc and –OTiCp$_2$Cl can be roughly estimated as shown in Scheme 2.17.

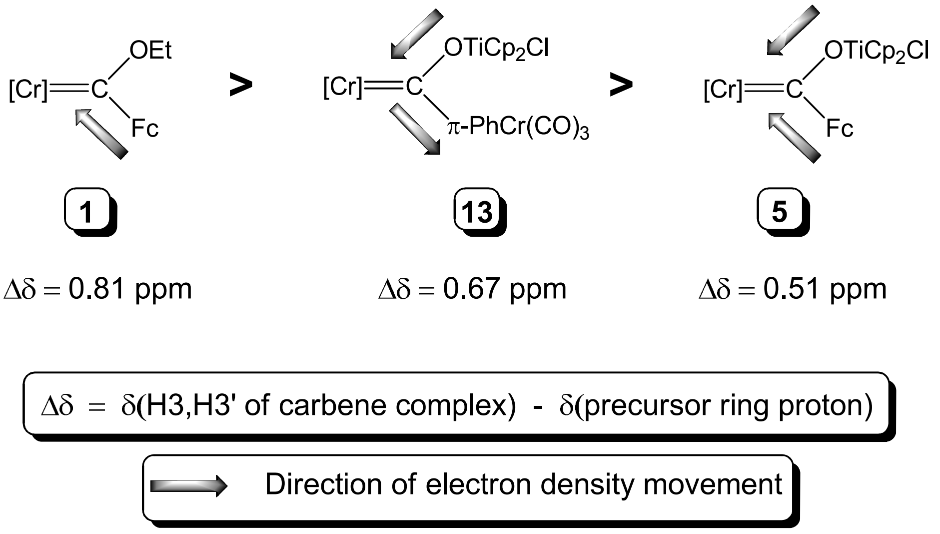

Scheme 2. 17

Ethoxy-substituted **1** shows the greatest contribution from the ferrocene towards stabilizing C1, while the titanoxy substituent of **5** results in the chemical shift resonance of H3, H3' being least affected. Complex **13** contains both an electron withdrawing carbene substituent (Cr(η^1:η^6-Ph)(CO)$_3$) and an electron donating substituent (OTiCp$_2$Cl). The titanoxy fragment in **13** compensates for the electron-draining effect of the Cr(CO)$_3$ moiety, and an intermediate Δδ value is obtained.

In the case of ethoxy biscarbene **3** and titanoxy biscarbene **8**, another direct comparison of the chemical environment of the ferrocenyl protons can be made as evidence for the increased π delocalization in the Cr-C$_{carbene}$-O-Ti unit. The

Fc chemical shifts of **3** are 5.00 and 4.73 ppm for H3 and H4 respectively, while **8** display resonances at 4.70 and 4.43 ppm. The relative contribution of the acyl resonance form **B** in Figure 2.16 is greater for a titanoxycarbene structure than for an alkoxycarbene complex, because a titanium(IV) cyclopentadienyl fragment can accommodate a positive charge more easily than an alkyl group.

Table 2. 5 ^{1}H NMR data of ferrocenyl titanoxy biscarbene complexes

Proton Assignment	Chemical shifts (δ) and coupling constants (J)					
	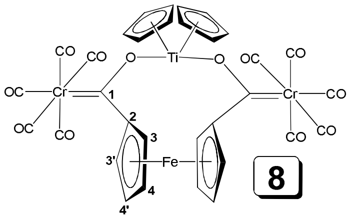 **8**		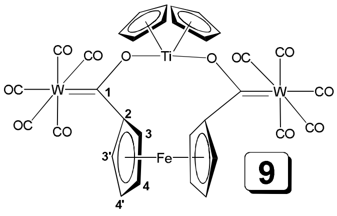 **9**		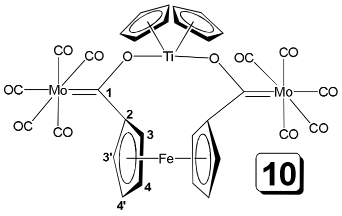 **10**	
	δ*	J (Hz)	δ*	J (Hz)	δ**	J (Hz)
Ti-Cp$_2$	6.70, 10H, s	-	6.67, 10H, s	-	5.89, 10H, s	-
H3, H3'	4.70, 4H, dd	2.0, 1.9	4.74, 4H, dd	2.2, 1.9	4.52, 4H, dd	1.5, 1.4
H4, H4'	4.43, 4H, dd	2.0, 1.9	4.58, 4H, dd	2.3, 1.9	4.06, 4H, dd	1.5, 1.4

* Recorded in $CDCl_3$
** Recorded in C_6D_6

2.4.2 ^{13}C NMR spectroscopy

The ^{13}C NMR data of complexes **1** – **13** are summarized in Tables 2.6 – 2.9, using the same atom numbering scheme as found in Tables 2.1 – 2.5. Due to long acquisition times, decomposition of complexes **7** and **12** occurred and no ^{13}C NMR spectra of these compounds could be recorded.

Fischer carbene carbon atoms are defined as being electron-deficient *sp*^{2}-hybridized carbons stabilized by dative π-bonding from the alkoxy/metaloxy substituent and from the central metal, combined with inductive release from the aromatic substituent of the carbene carbon. Spectroscopic data supports this model as metal carbene carbon shifts can be found very downfield in a broad range of 200[71] to 400 ppm.[53(c)] The carbene carbon resonances depend both on the carbene substituents and on the metal, and are more sensitive to changes in the electronic environment than carbonyl ligands.

Table 2.6 ^{13}C NMR data of ferrocenyl ethoxy monocarbene complexes

Carbon Assignment	Chemical shifts (δ)	
	1	**2**
	δ(*[57])	δ** (*[57])
C1	*(329.7)*	303.1 *(304.3)*
CO	*(223.0* (trans)*, 217.3* (cis)*)*	198.3 (*trans*), 190.8 (*cis*) *(202.5* (trans), *198.0* (cis)*)*
C2	*(93.6)*	n.o. *(95.2)*
C3, C3'	*(74.5)*	74.0 *(75.0)*
C4, C4'	*(72.3)*	71.4 *(73.3)*
Fe-Cp	*(70.6)*	68.0 *(70.8)*
CH$_2$	*(75.5)*	77.6 *(78.1)*
CH$_3$	*(15.5)*	15.3 *(15.4)*

* Recorded in CDCl$_3$
** Recorded in C$_6$D$_6$

Chemical shifts for terminal metal carbonyls lie in the range of 150 to 240 ppm[72] with shielding of the carbonyl nucleus increasing with increasing atomic number of the metal (compare analogous complexes **8** – **10** : Cr(CO)$_5$ 224.3, 218.0 ppm; Mo(CO)$_5$ 219.9, 213.1 ppm and W(CO)$_5$ 199.7, 191.1 ppm). On the other hand, carbonyl groups are fairly insensitive to changes of substituents on the other ligands present.

---

[71] Anderson, B.A.; Wulff, W.D.; Rahm, A. *J. Am. Chem. Soc.* **1993**, *115*, 4602.
[72] Mann, B.E. *Adv. Organomet. Chem.* **1974**, *12*, 135.

Table 2.7 ^{13}C NMR data of ferrocenyl titanoxy monocarbene complexes

Carbon Assignment	Chemical shifts (δ) and coupling constants (J)		
	5	**6**	**13**
	δ*	δ*	δ**
C1	n.o.	300.8	n.o.
$M(CO)_5$	223.1 (*trans*), 217.9 (*cis*)	200.4 (*trans*), 191.4 (*cis*)	223.0 (*trans*), 218.3 (*cis*)
$Cr(CO)_3$	-	-	233.2, 232.0
$Ti\text{-}Cp_2$	118.4, 117.5	119.0, 118.5	119.1
C2	n.o.	n.o.	n.o.
C3, C3’	75.7	74.3	95.7
C4, C4’	72.3	70 .2	89.7
C5	-	-	90.7

* Recorded in $CDCl_3$
** Recorded in C_6D_6

Only for complexes **2** – **4**, **6** and **8** were carbene carbon atom resonances observed. The carbene carbon resonances are shifted more downfield in biscarbene complexes but this tendency is not carried over to C2 in the ring system. For the ethoxy monocarbene tungsten complex **2** the carbene carbon resonates at 303.1 ppm. The titanoxy monocarbene tungsten complex **6** displays a carbene carbon chemical shift at 300.3 ppm, *ca.* 3 ppm upfield when the alkoxy substituent is replaced by a titanoxy substituent.

As with the proton NMR spectra and the comparison of H3 chemical shifts, this would seem to support the statement that the metaloxy fragment better stabilize the electrophilic carbene carbon atom. In broad terms, the titanoxy fragment can therefore be seen as more electron donating than the ethoxy substituent.

Table 2. 8 ^{13}C NMR data of ferrocenyl ethoxy biscarbene complexes

Carbon Assignment	Chemical shifts (δ)	
	3	**4**
	δ*	δ**
C1	306.2	303.7
CO	223.6 (*trans*), 217.1 *(cis)*	203.9, 202.7(*trans)*, 198.7 *(cis)*
C2	99.2	n.o.
C3, C3’	76.2	76.5
C4, C4’	72.7	74.2
CH_2	77.4	78.0
CH_3	15.5	14.8

* Recorded in $CDCl_3$
** Recorded in C_6D_6

Table 2. 10 ^{13}C NMR data of ferrocenyl titanoxy biscarbene complexes

Carbon Assignment	Chemical shifts (δ)		
	8	**9**	**10**
	δ*	δ**	δ**
C1	351.9	n.o.	n.o.
CO	224.3 (*trans*), 218.0 (*cis*)	199.7 (*trans)*, 191.1 (*cis*)	219.9 (*trans*), 213.1 (*cis*)
Ti-Cp_2	118.4	118.7	118.4
C2	n.o.	n.o.	n.o.
C3, C3’	76.6	72.8	70.7
C4, C4’	72.3	70.8	69.5

* Recorded in $CDCl_3$
** Recorded in C_6D_6

The titanium Cp-rings in the monocarbene complexes **12** and **13** rotate freely in solution, as is evident from a single peak for the Cp-protons and also for the carbon atoms in the NMR spectra, while the ^{13}C NMR spectrum of the ferrocenyl monocarbene complexes **5** – **7** display two signals. This observation is ascribed to restricted rotation of the C(carbene)-C(Fc) bond caused by the proximity of the bulky metal substituents. For the biscarbene complexes **8** – **10**, the symmetry of the structures precludes electronic inequivalency and only one titanium Cp-resonance is seen.

2.4.3 IR spectroscopy

The stretching vibrational frequency of terminal carbonyl ligands lies between 1820 and 2120 cm^{-1}.[73] In contrast to M-C stretching frequencies, the C-O stretching frequencies can be seen as being independent from other vibrations in the molecule. Qualitative correlation between C-O bond order can therefore be drawn from analysis of ν(CO) frequencies, as well as information about the bonding properties of ligands substituting metal carbonyl complexes. A weaker π-acceptor ligand, such as a carbene ligand, would result in more metal electron density available for backdonation towards π-acidic carbonyl ligands, resulting in absorption bands at lower wave numbers for the $[M(CO)_n(carbene)]$ complexes than for the corresponding binary $[M(CO)_{n+1}]$.

Octahedral complexes of the general formula $M(CO)_5L$ display pseudo-C_{4v} symmetry. This implies four stretching vibration modes, illustrated in Figure 2.16. The IR-active bands include the A_1^2 and the two degenerate E bands. Coupling of the A_1^1 band with the A_1^2 band can cause the A_1^1 band to also become IR active. The E band is usually the broad strongest peak, sometimes overlapping with A_1^1. For complexes where L is a good π-acceptor ligand, A_1^1 is found at higher wavenumbers than the E band, with the A_1^2 band always at the highest frequency. The B_1 mode is Raman active and IR inactive, but when L is a very bulky substituent, the equatorial plane is distorted and the stretching vibration

---

[73] Braterman, P.S. *Metal Carbonyl Spectra,* Academic Press Inc., London, **1975**, 68.

induces a change in the dipole. For sterically hindered carbene ligands, the B_1 mode can become IR active and result in a fourth band in the IR spectra.[74]

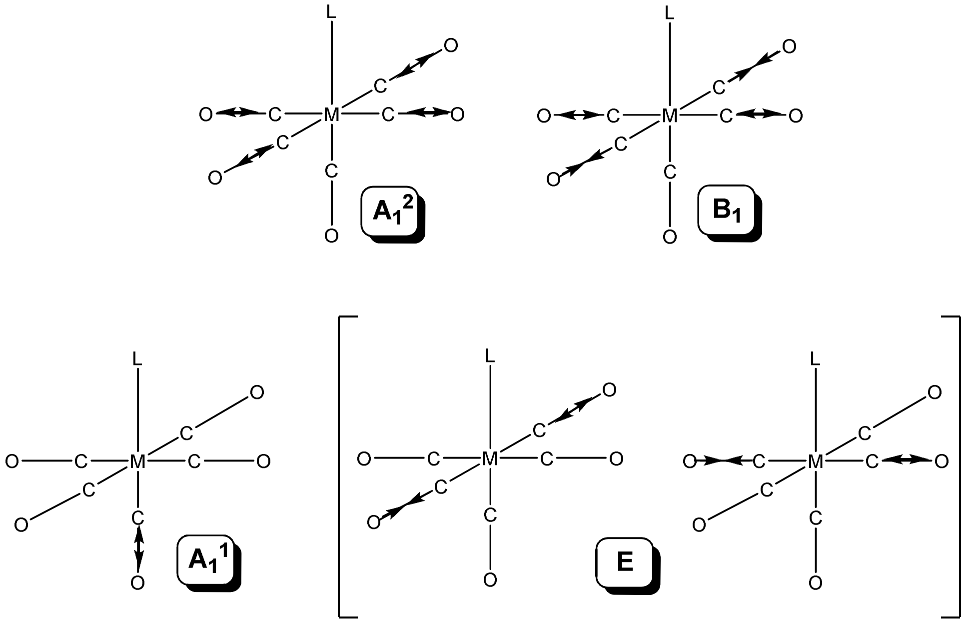

Figure 2.16 Normal modes of stretching vibrations for $M(CO)_5L$ systems

The infrared data of all the complexes **1** – **13** are summarized in Table 2.10, and representative spectra of analogous Cr, W and Mo complexes are given in Figure 2.17. The spectra were recorded in dichloromethane, due to the insolubility of the complexes in hexane. In the case of **13**, resolution of the bands could only be obtained for a spectrum recorded in the solid state in a CsI matrix.

Complex **13** contains both a $Cr(CO)_5$ and a $Cr(CO)_3$ moiety. In the case of $[M(\pi\text{-arene})(CO)_3]$ systems, the IR-active bands are one A_1 and two, degenerate E bands. The E mode is generally broader than A_1, presumably due to partial lifting of the degeneracy by asymmetric ligands.

---

[74] Adams, D.M. *Metal-Ligand and Related Vibrations,* Edward Arnold Publishers Ltd., London, **1967**, 98.

Table 2.10 Infrared data of Group VI cluster carbene complexes

Complex	$M(CO)_5$ assignment, [ν(CO), cm^{-1}]		
	A_1^2	B_1 overlapping A_1^1	E
1	2054 s	1979 m	1933 vs
2	2065 w	1975 w	1927 vs
3	2054 s	1979 sh, 1938 vs sh overlap E	1938 vs sh overlap A_1^1
4	2061 s	1927 vs overlap E	1927 vs overlap A_1^1
5	2046 w	1972 vw	1926 vs
6	2052 m	1958 m	1916 vs
7	2056 w	1984 s	1934 vs
8	2044 m	1971 sh	1929 vs
9	2055 w	1975 vs	1923 m
10	2055 m	1977 s	1934 vs
11	2050 m (W) 2028 m (Cr)	1983 w, 1936 vs overlap E (W) 1968 w, 1915 vs overlap E (Cr)	1936 vs (W) overlap A_1^1, 1915 vs (Cr) overlap A_1^2
12	2050 m	1977 w, 1933 vs overlap E	1933 vs overlap A_1^1
13* $Cr(CO)_5$	2050 s	1972 s	1929 vs
13* $Cr(CO)_3$	1990 vs (A_1)	1887 vs (E)	

* Recorded as a CsI pellet

The A_1^1 mode in the C_{4v} local symmetry represents the mode with the greatest contribution to the stretching of the C-O bond *trans* to L, and should therefore be most affected by changes in the electronic environment caused by the carbene ligand.

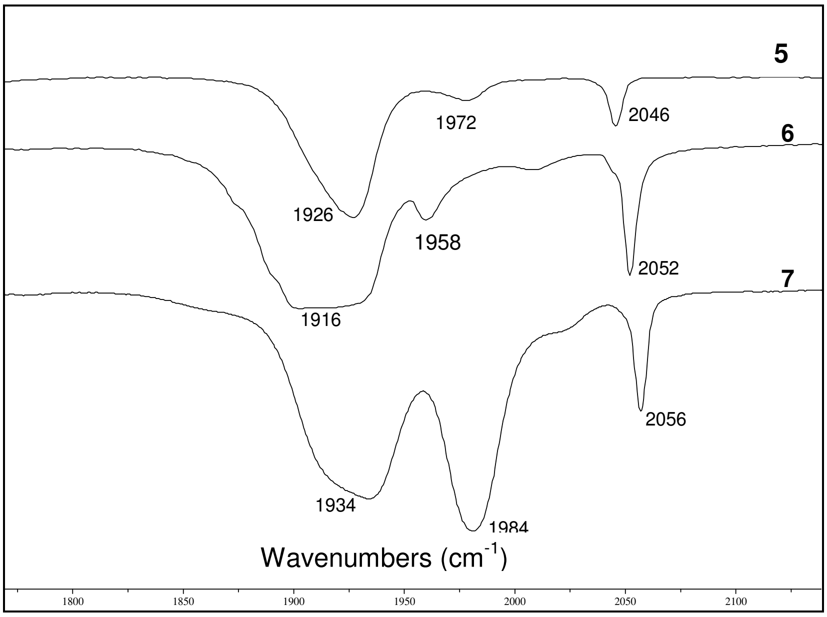

Figure 2.17 Stacked IR spectra of the carbonyl region of complexes **5**, **6** and **7**

Stabilization by carbene substituents *via* electron donation, should be reflected by ν(CO) bands of A_1^1 at higher wavenumbers. If the ethoxy (OEt), the thienyl substituent (T) and the $Cr(\pi\text{-}Ph)(CO)_3$ substituents are broadly classified as more electron withdrawing relative to the other two carbene substituents, while the titanoxy ($OTiCp_2$) and ferrocenyl (Fc) fragments are seen as electron donating, then it should be possible to observe this trend reflected in the ν(CO) values. However, due do the broadened peaks, and overlapping bands, no clear trend could be established. The A_1^2 mode defines the symmetric stretch of the CO ligands in the equatorial plane, and can therefore not be used as a direct measure of the π-acceptor ability of the carbene ligand

2.4.4 Mass spectrometry

The mass spectra of complexes **3**, **5** – **7**, **12** and **13** were recorded using fast atom bombardment (FAB) techniques. In the case of complexes **1** and **2**, no molecular ion peak (M^+) was observed. The biscarbene complexes (**4**, **8** – **11**) were not appreciably soluble in the 3-nitrobenzyl alcohol matrix employed, and the high molar masses of these compounds also contributed to the difficulty in observing an M^+ peak.

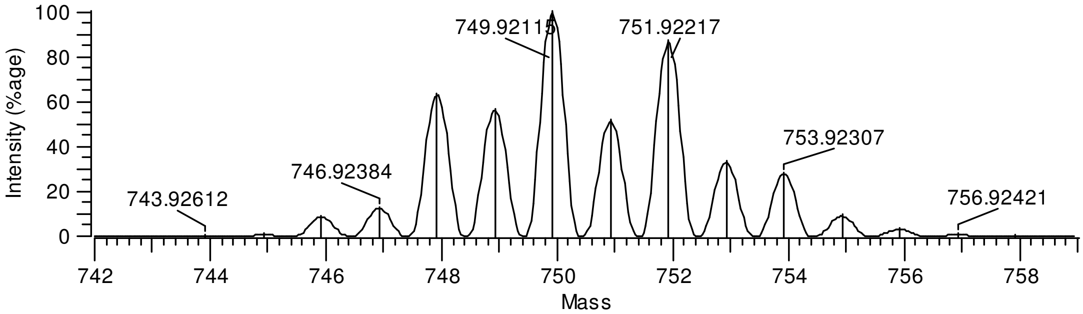

Figure 2.18 M^+ peak observed for complex **6**, with molar mass 750.45 g.mol^{-1}

The presence of an M^+ peak (illustrated in Figure 2.18) provides strong evidence of correct structure assignments, and the identified fragment ions are summarized in Table 2.11. The assignments are based on the isotopes ^{52}Cr, ^{96}Mo and ^{184}W.

Table 2.11 Mass spectral data of Group VI cluster carbene complexes

Complex	m/z	Intensity (%)	Fragment Ion
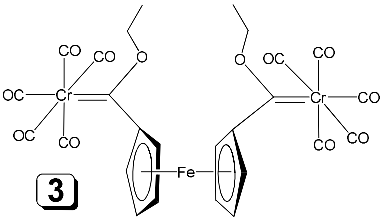 3	682	0.4	$[M]^+$
	542	0.6	$[M - 5CO]^+$
	434	3.4	$[M - Cr(CO)_5 - 2CO]^+$
	430	2.7	$[M - 9CO]^+$
	402	1.2	$[M - 10CO]^+$
	378	4.4	$[M - \{Cr(CO)_5C(OEt)\}]^+$
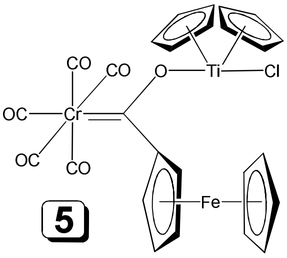 5	619	1.5	$[M]^+$
	505	2.6	$[M - 4CO]^+$
	478	1.6	$[M - 5CO]^+$
	377	0.8	$[M - TiCp_2Cl - CO]^+$
	230	3.5	$[OTiCp_2Cl]^+$

Table 2.11 ***contd.*** Mass spectral data of Group VI cluster carbene complexes

Complex	m/z	Intensity (%)	Fragment Ion
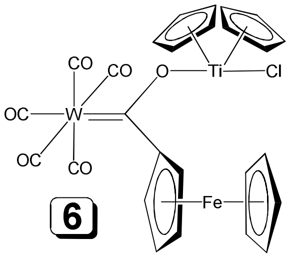 **6**	750	10	$[M]^+$
	721	0.3	$[M - CO]^+$
	694	0.7	$[M - 2CO]^+$
	635	0.6	$[M - 3CO]^+$
	601	0.8	$[M - 3CO - Cp]^+$
	537	2.4	$[M - TiCp_2Cl]^+$
	511	1.4	$[M - TiCp_2Cl - CO]^+$
	509	1.6	$[M - Fc - 2CO]^+$
	480	1.1	$[M - TiCp_2Cl - 2CO]^+$
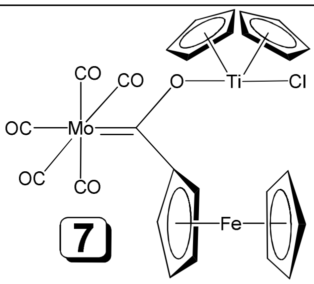 **7**	663	1.5	$[M]^+$
	605	1.7	$[M - 2CO]^+$
	578	1.3	$[M - 3CO]^+$
	551	1.4	$[M - 4CO]^+$
	523	1.9	$[M - 5CO]^+$
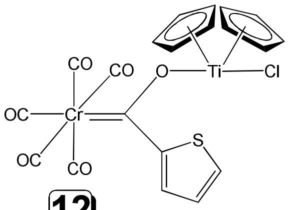 **12**	516	1.9	$[M]^+$
	460	2.0	$[M - 2CO]^+$
	433	1.8	$[M - 3CO]^+$
	404	5.5	$[M - 4CO]^+$
	376	5.4	$[M - 5CO]^+$
	370	2.0	$[M - 4CO - Cl]^+$
	304	9.0	$[M - TiCp_2Cl]^+$
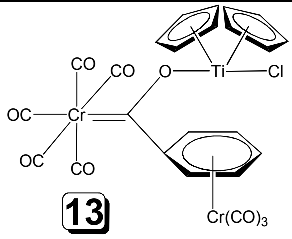 **13**	647	0.6	$[M]^+$
	511	0.8	$[M - Cr(CO)_3]^+$
	506	2.5	$[M - 5CO]^+$
	479	3.0	$[M - 6CO]^+$

All of the mass spectra demonstrate the stepwise fragmentation of the complexes with the loss of carbonyl ligands (see Figure 2.19). The higher intensities of the $[M-4CO]^+$ and $[M-5CO]^+$ ions compared to $[M-2CO]^+$ and $[M-3CO]^+$, as well as the low occurrence of $[M-CO]^+$ indicate rapid loss of the carbonyl ligands.

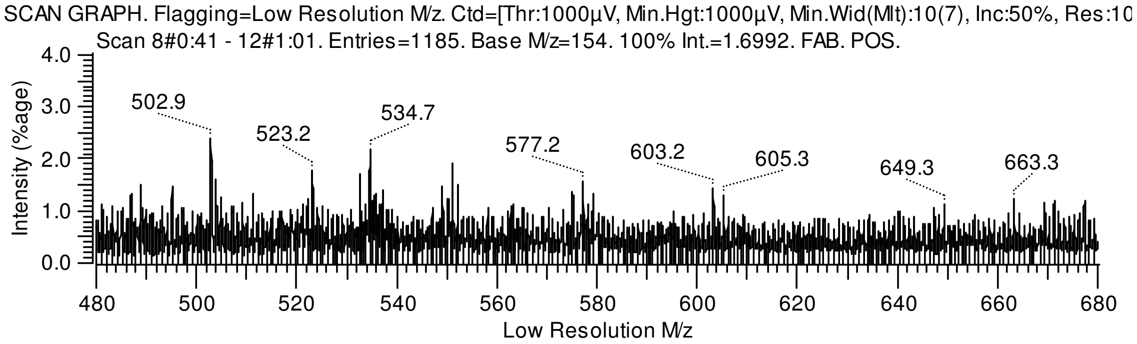

Figure 2.19 Stepwise loss of CO ligands in the mass spectrum of complex **7**

However, this is not the only possible fragmentation route. For the titanoxy monocarbene complexes, initial loss of the titanocene chloride fragment, followed by the loss of one or more carbonyl ligands constitutes another possible fragmentation pattern. Loss of the Fc-unit and the chloro ligand is also observed for complexes **6** and **12**, respectively. Complex **13** displayed the expected decomplexation of the $Cr(CO)_3$- moiety.

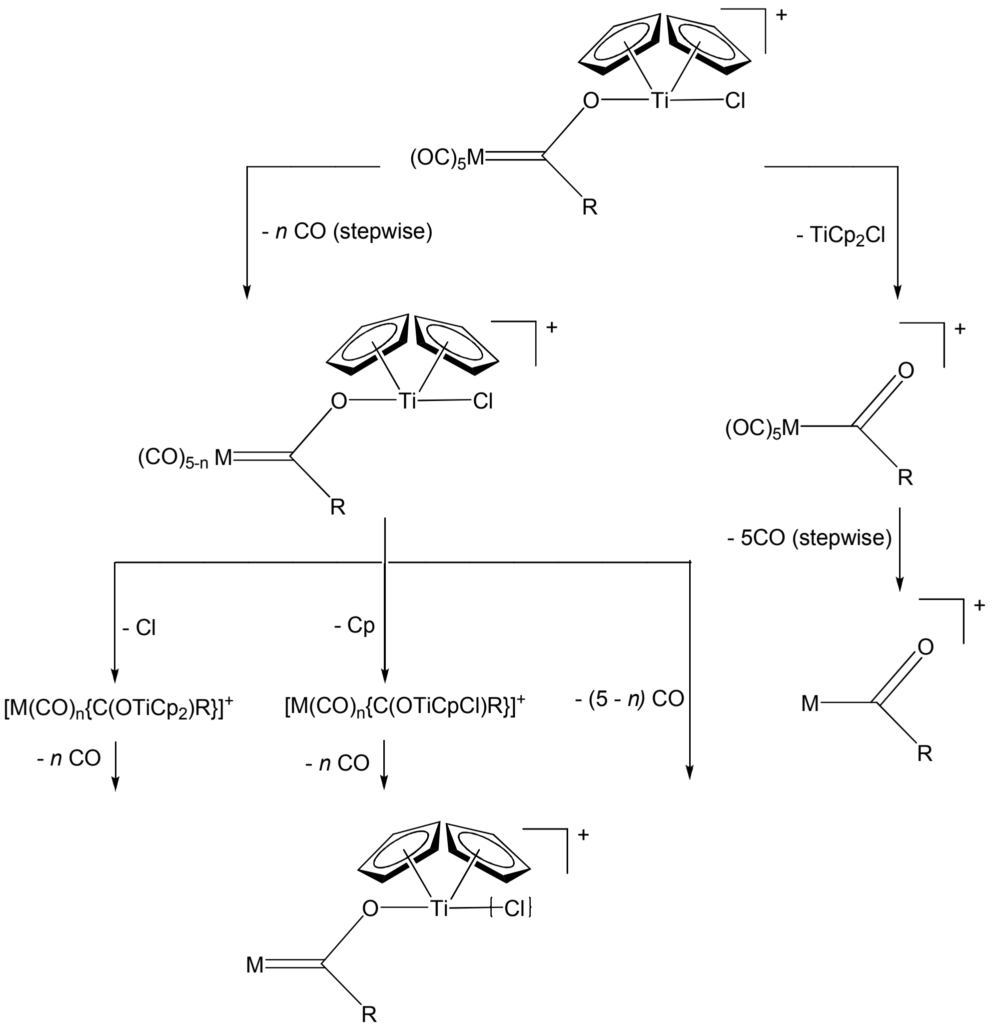

Figure 2.20 Different MS fragmentation routes observed for titanoxycarbene complexes

The mass spectral data of **3** showed fragmentation patterns containing at least one possible route unlike that of other biscarbene complexes.[75] Although the successive loss of all ten CO ligands were observed, the loss of a $Cr(CO)_5$-unit and subsequent loss of the entire carbene moiety $Cr(CO)_5\{C(OEt)\}$ were also seen. In previous studies, sequential loss of some carbonyls, then an ethyl fragment before the breakaway of the rest of the carbonyls yielded a *m/z* ion peak of the two transition metals directly bonded to the heteroaryl carbene

---

[75] (a) Crause, C. *Synthesis and application of carbene complexes with heteroaromatic substituents,* PhD Thesis, University of Pretoria, Pretoria, **2004**, 33, (b) Terblans, Y.M. *Thiophene Bimetallic Carbene Complexes,* PhD Thesis, University of Pretoria, Pretoria, **1996**, 45.

substituent. However, no loss of a pentacarbonyl metal moiety was observed before.

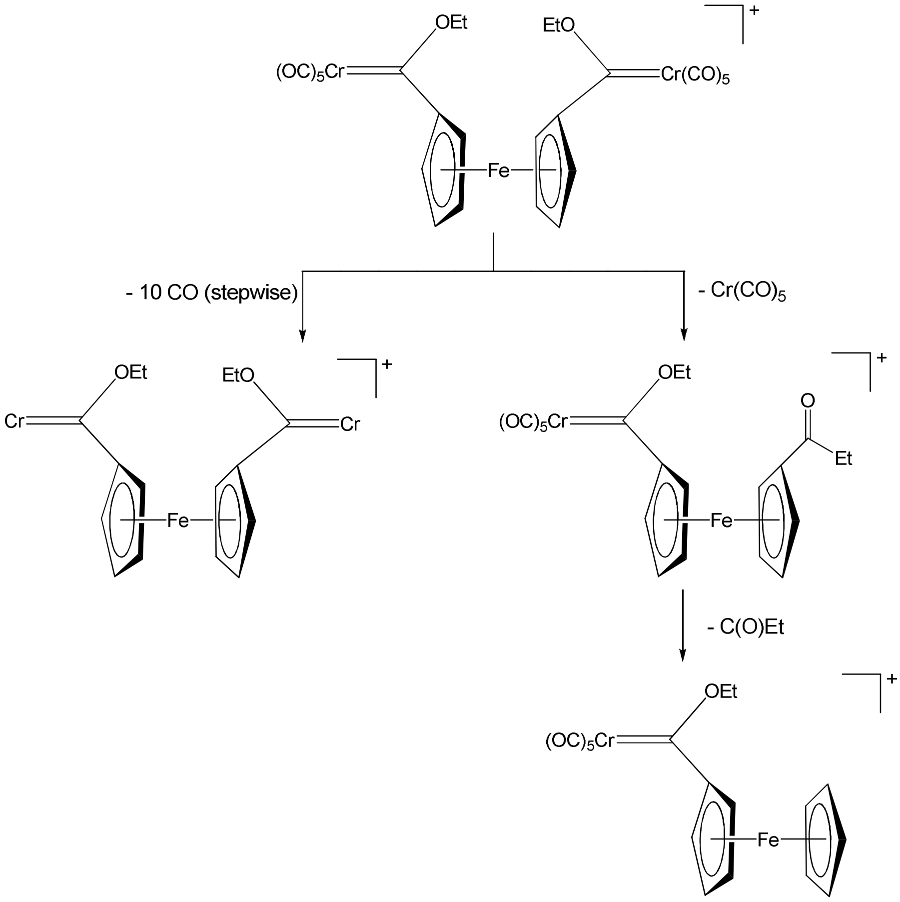

Figure 2.21 MS fragmentation routes observed for complex **3**

2.4.5 Single crystal X-ray crystallography

2.4.5.1 Molecular structures

Final confirmations of the structures of the complexes **3**, **5**, **6**, **8**, **12** and **13** were obtained from single crystal diffraction studies. The complexes crystallized from different ratios of dichloromethane/hexane solutions by layering of the solvents, yielding crystals suitable for diffraction studies. ORTEP[76] + POV-Ray[77] drawings of the molecular structures of the above listed complexes, showing the atom numbering scheme employed, are presented in Figures 2.22 – 2.27. Crystallographic data and refinement parameters are listed in the Appendices, while experimental details are given in the experimental section. Selected bond lengths, bond angles and torsion angles are given in Table 2.12 (**5**, **6**, **12** and **13**) and Table 2.13 (**3** and **8**).

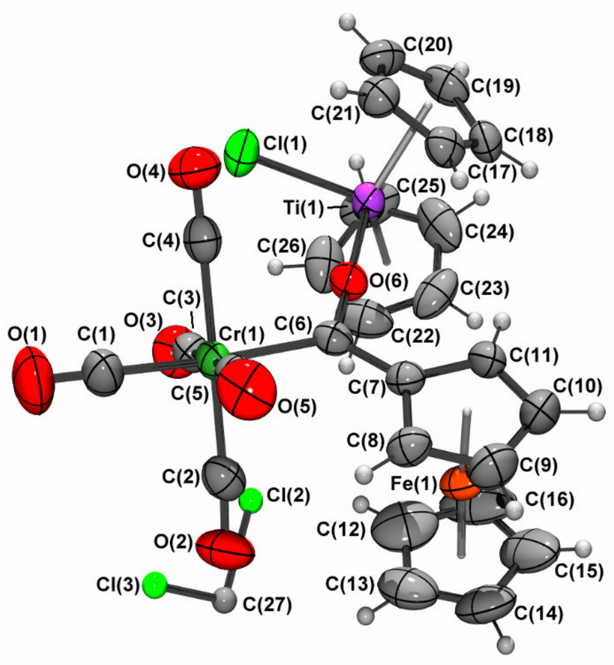

Figure 2.22 ORTEP + POV-Ray drawing of the molecular structure of **5**. Atomic displacement ellipsoids are shown at the 50% probability level.

---

[76] Farrugia, L.J. *J. Appl. Crystallogr.* **1997**, *30*, 565.

[77] The POV-Ray Team, POV-Ray 2004. URL: http://www. povray.org/download/.

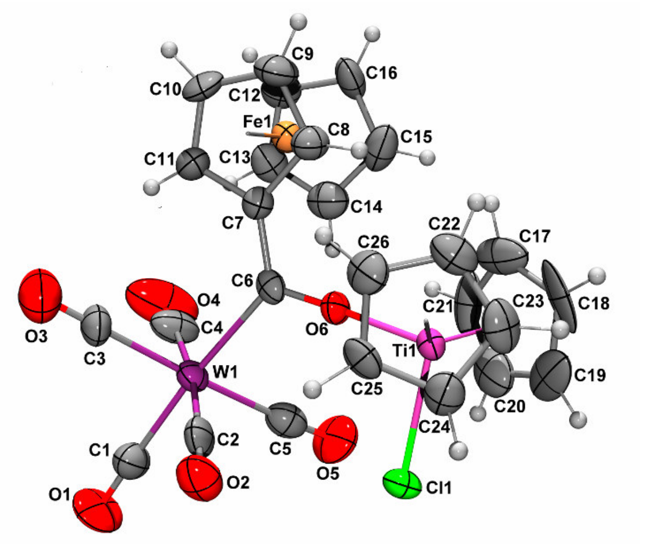

Figure 2.23 ORTEP + POV-Ray drawing of the molecular structure of **6**. Atomic displacement ellipsoids are shown at the 50% probability level.

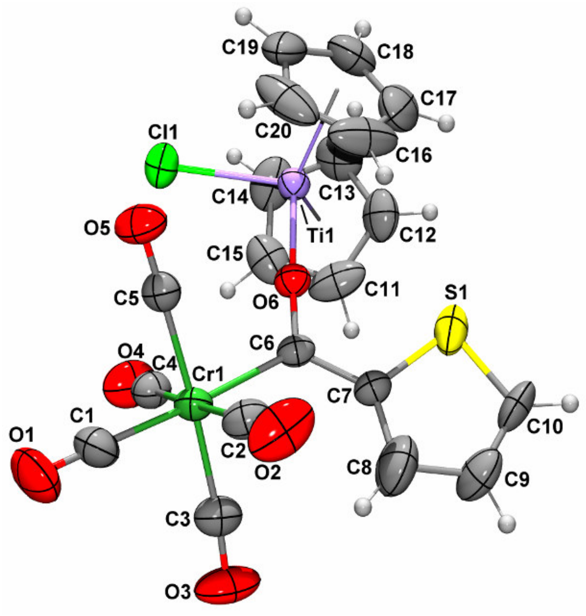

Figure 2.24 ORTEP + POV-Ray drawing of the molecular structure of **12**. Atomic displacement ellipsoids are shown at the 50% probability level.

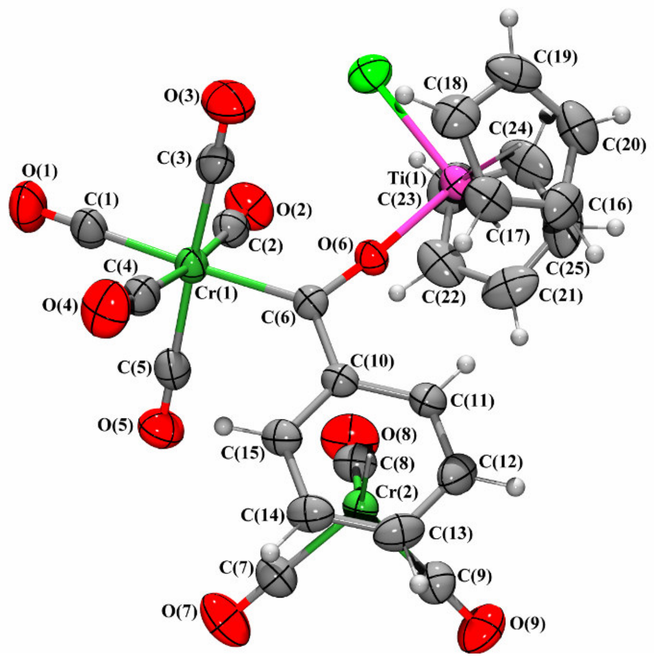

Figure 2.25 ORTEP + POV-Ray drawing of the molecular structure of **13**. Atomic displacement ellipsoids are shown at the 50% probability level.

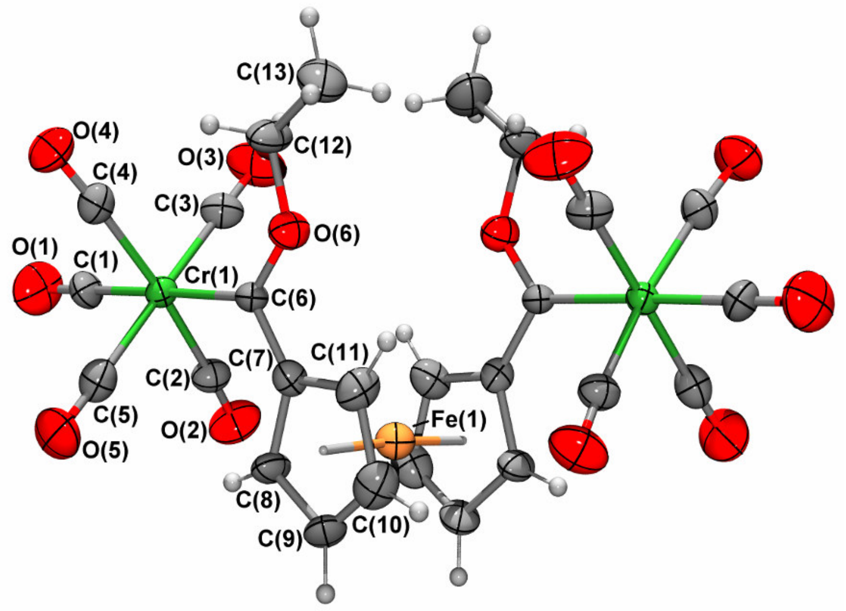

Figure 2.26 ORTEP + POV-Ray drawing of the molecular structure of **3**. Atomic displacement ellipsoids are shown at the 50% probability level.

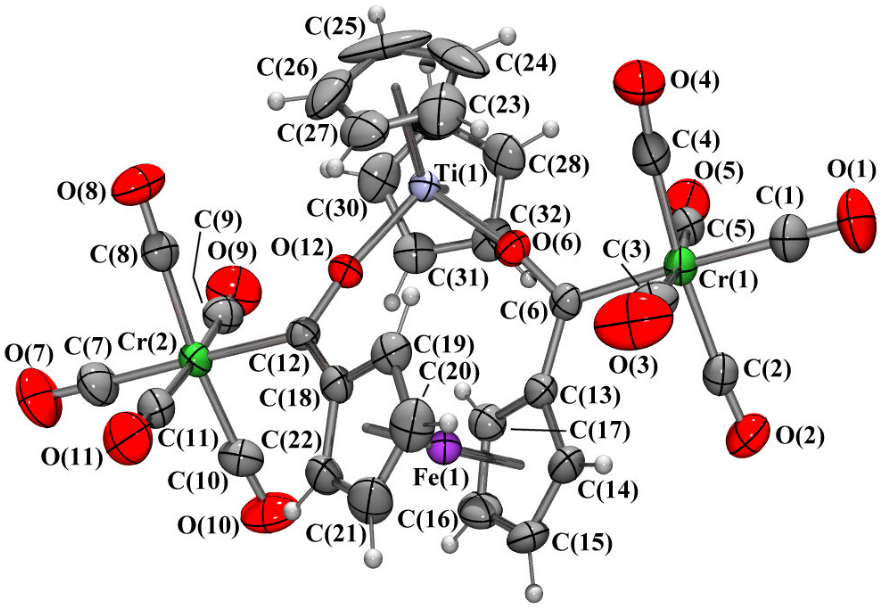

Figure 2.27 ORTEP + POV-Ray drawing of the molecular structure of **8**. Atomic displacement ellipsoids are shown at the 50% probability level.

In general, in the molecular structures of the thienyl monocarbene complexes, the sulfur atom of the thienyl ring is *cis* to the oxygen atom of the ethoxy/titanoxy substituent, indicating either restricted rotation around the C(6)-C(7) bond or a preferred packing order in the solid state.[43(e),78] Some disorder of the 2-thienyl substituent of **12** was observed: it exhibits an isomeric form with the sulfur atom in the thienyl ring *trans* to the ethoxy substituent (50.8(3)%) in addition to the *cis* isomer (49.2(3)%). The second component is rotated approximately 180° about the C(6)-C(7) bond with respect to the other component. The disorder is such that C(8A) nearly coincide with S(1) of the major component (C(7A), C(9A), C(10A) and S(1A) also nearly coincide with C(7), C(10), C(9) and C(8) respectively).

---

[78] Liles, D.C.; Lotz, S. *Acta Cryst.* **2006**, *E26*, M331.

Table 2.12 Selected bond lengths (Å), bond angles (°) and torsion angles (°) for **5**, **6**, **12** and **13**

Bond lengths	**5** (M = Cr)	**6** (M = W)	**12** (M = Cr)	**13** (M = Cr)
M(1)-C(6)	2.090(4)	2.253(9)	2.081(2)	2.067(3)
C(6)-O(6)	1.286(5)	1.273(11)	1.283(2)	1.287(4)
C(6)-C(7) / C(6)-C(7A)**/ C(6)-C(10) ‡	1.472(6)	1.465(15)	1.442(5) 1.472(5)	1.513(5)
O(6)-Ti(1)	1.905(3)	1.901(6)	1.9192(15)	1.933(2)
M(1)-C(1)	1.863(5)	2.008(13)	1.866(3)	1.879(4)
M(1)-C(2,3,4,5)*	1.893(6)	2.022(12)	1.894(2)	1.901(4)
Bond angles	**5** (M = Cr)	**6** (M = W)	**12** (M = Cr)	**13** (M = Cr)
C(1)-Cr(1)-C(6)	175.9(2)	174.2(4)	175.86(10)	175.44(14)
O(6)-C(6)-C(7) / O(6)-C(6)-C(7A)** / O(6)-C(6)-C(10) ‡	112.9(3)	114.5(8)	116.1(2) 110.3(2)**	111.5(3)
O(6)-C(6)-M(1)	119.7(3)	118.5(7)	119.92(15)	119.9(2)
C(7)-C(6)-M(1), C(7A)-C(6)-M(1)** / C(10)-C(6)-M(1) ‡	127.3(3)	127.0(7)	123.95(19) 129.6(2)**	128.5(2)
C(6)-O(6)-Ti(1)	178.5(3)	175.4(7)	174.81(16)	173.6(2)
C(6)-C(7)-C(8) / C(6)-C(7A)-C(8A)**/ C(6)-C(10)-C(15) ‡	126.2(4)	127.2(9)	129.6(2) 129.9(3)**	121.5(3)
C(6)-C(7)-C(11) / C(6)-C(7)-S(1)† / C(6)-C(7A)-S(1A)**/ C(6)-C(10)-C(11) ‡	127.4(4)	127.1(9)	129.6(3) 118.2(3)**	121.0(3)
Torsion angles	**5** (M = Cr)	**6** (M = W)	**12** (M = Cr)	**13** (M = Cr)
C(3)-M(1)-C(6)-O(6)	44.1(3)	-45.0(7)	54.76(16)	38.2(3)
O(6)-C(6)-C(7)-C(11) / O(6)-C(6)-C(7)-S(1)† / O(6)-C(6)-C(7A)-S(1A)**/ O(6)-C(6)-C(10)-C(11) ‡	-1.0(6)	179.1(9)	-5.5(8) -172.3(4)**	173.2(3)
Cr(1)-C(6)-C(7)-C(8) / Cr(1)-C(6)-C(7A)-C(8A)** / Cr(1)-C(6)-C(10)-C(15) ‡	2.7(6)	-177.5(8)	2.2(10) -170.5(5)**	-6.0(4)

* Averaged value

** Second component of **12**, with the 2-thienyl substituent rotated about C(6)-C(7) bond

† Equivalent atoms of **12** compared to **5** and **6**

‡ Equivalent atoms of **13** compared to **5** and **6**

Table 2.13 Selected bond lengths (Å), bond angles (°) and torsion angles (°) for **3** and **8**

Bond lengths*	**3**	**8**	
Cr(1)-C(6), Cr(2)-C(36)	2.083(3)	2.063(2)	2.077(2)
C(6)-O(6), C(36)-O(36)	1.305(4)	1.276(2)	1.274(2)
C(6)-C(7), C(36)-C(12)	1.464(4)	1.480(3)	1.483(3)
O(6)-C(18)	1.447	-	-
O(6)-Ti(1), O(36)-Ti(1)		1.9507(14)	1.9514(15)
Cr(1)-C(1), Cr(2)-C(31)	1.865(3)	1.882(3)	1.873(3)
Cr(1)-C(2,3,4,5)**	1.903(3)	1.892(3)	
Bond angles*	**3**	**8**	
C(1)-Cr(1)-C(6), C(31)-Cr(2)-C(36)	178.71(11)	177.32(10)	175.84(11)
O(6)-C(6)-C(7), O(36)-C(36)-C(12)	105.2(3)	113.81(18)	113.66(18)
O(6)-C(6)-Cr(1), O(36)-C(36)-Cr(2)	130.2(2)	122.91(15)	123.29(15)
C(7)-C(6)-Cr(1), C(12)-C(36)-Cr(2)	124.6(2)	123.12(14)	122.93(15)
C(6)-O(6)-C(18)	123.1(3)	-	-
C(6)-O(6)-Ti(1), C(36)-O(36)-Ti(1)	-	169.76(15)	170.10(14)
C(6)-C(7)-C(8), C(36)-C(12)-C(13)	127.6(3)	127.0(2)	126.4(2)
C(6)-C(7)-C(11), C(36)-C(12)-C(16)	126.0(3)	127.2(2)	127.7(2)
Torsion angles*	**3**	**8**	
C(3)-Cr(1)-C(6)-O(6) C(33)-Cr(2)-C(36)-O(36)	49.6(5)	24.79(19)	30.81(18)
Cr(1)-C(6)-O(6)-C(12)	2.1(9)	-	-
O(6)-C(6)-C(7)-C(11) O(36)-C(36)-C(12)-C(13)	0.6(7)	29.5(3)	25.9(3)
Cr(1)-C(6)-C(7)-C(8) Cr(2)-C(36)-C(12)-C(16)	0.7(7)	34.3(3)	31.0(3)

* The 2nd designated bond length, bond angle or torsion angle refers to geometry involving the 2nd Cr-carbene moiety in **8**. These values are tabulated in the 2nd column under **8**

** Averaged value, (Cr(1)-C(2,3,4,5) + Cr(2)-C(32,33,34,35) for **8**

In the structures of complexes **3**, **5** and **6**, the ferrocenyl cyclopentadienyl ring is approximately coplanar with the carbene moiety (Cr(1), C(6), O(6), C(7)). The torsion angles of the plane of the carbene and that of the 5-membered ring, Cr(1)-C(6)-C(7)-C(8) and O(6)-C(6)-C(7)-C(11) are all in the range 0.6(7)° to 2.7(6)° for the four complexes. However, the resonance stabilization afforded by the carbene moiety being approximately coplanar with the adjacent ring is presumably weak and may easily be overridden by the exigencies of either packing forces - as observed in complex **12** where the O-C(carbene)-C(ring)-S torsion angle 5.5(8)°, or the steric requirements of the molecule - as observed in **8** where the corresponding angles are 32.17(10)° and 28.78(9)°.

The Ti(1)-O(6/36) bonds in **5**, **6**, **8**, **12** and **13** are significantly longer (1.901(6) – 1.9514(15) Å) than those of typical terminal titanium(IV) alkoxides (1.855(2) Å in $TiCp_2(OEt)Cl$]).[79] This is indicative of O(6) → C(6) π-donation occurring at the expense of O(6) → Ti(1) π-donation and is further supported by the short C(6)-O(6) and C(36)-O(36) bond distances (1.274(2) – 1.286(5) Å) that are significantly shorter than the range of 1.305(4) – 1.324(3) Å observed for **3**, **14**, **15**, **18** and **19** (see Scheme 2.5),[17] $[Cr(CO)_5\{C(OEt)Fc\}]$[57] and $[Cr(CO)_5\{C(OMe)(C_5H_4)Fe(C_5H_4Br)\}]$.[80] Erker has also noted that an acyl resonance structure is an important contributor to the bonding of zirconoxycarbene complexes.[10]

Observing the near linear C(6/36)-O(6/36)-Ti(1) bond angles, in the range 169.76(15)° – 178.5(3)°, for all complexes except **3**, the acyl character of the carbene-oxygen bond and the very long titanium-oxygen bond, one can conclude that a significant ionic character is present in the titanium-oxygen bonds, with the electropositive Lewis acid $TiCp_2X$-fragment on the one side of the carbene oxygen atom and an electrophilic carbene carbon on the other side. This manifests in a short C(carbene)-O distance and a long Ti-O distance, the net result of strong competition between these two fragments for electron density.

---

[79] Huffman, J.C.; Moloy, K.G.; Marsella, J.A.; Caulton, K.G. *J. Am. Chem. Soc.* **1980**, *102*, 3009.

[80] Hursthouse, M.B.; Hibbs, D.E.; Butler, I.R. Private Communication **2003**, Cambridge Structural Database (Allen, F.H. *Acta Crystallogr.* **2002**, *B58*, 380), CCDC 262965.

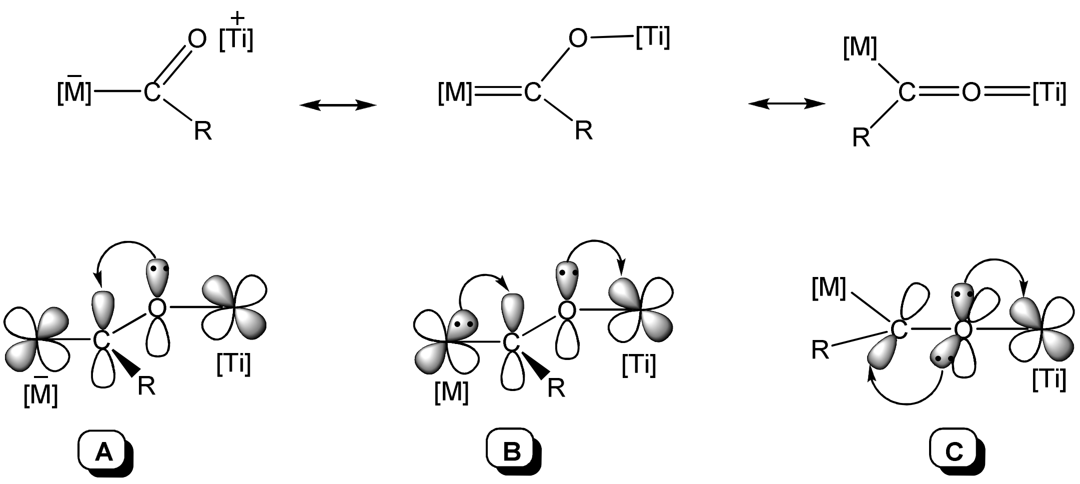

Figure 2.28 Orbital overlap for titanoxycarbene stabilization.

These experimental bond lengths support the electronic conclusions drawn from the NMR spectroscopy, and the spectroscopic observation (Figure 2.15) can therefore be extended to that shown in Figure 2.28. The resonance form **A** in the Figure below represents the most relevant structure, accounting most efficiently for the observed structural and electronic aspects.

The C(carbene)-C(Fc) distances are similar for all the complexes and fall in the range 1.464(4) – 1.483(3) Å. For **12**, C(carbene)-C(2-thienyl) bond distance is shorter (1.442(5) Å), demonstrating the heteroarene ring involvement in carbene carbon stabilization. The other extreme is **13**, where the long C(carbene)-C($PhCr(CO)_3$) bond length of 1.513(5) Å indicates less ring participation in carbene stabilization, possibly due to the presence of the π-$Cr(CO)_3$ group, pulling electron density towards itself.

The tripod described by the carbonyl ligands of the $Cr(CO)_3$-fragment in **13** adopted an eclipsed conformation with respect to the aromatic ring which correlates with an electron-donating group bonded thereto (Figure 2.5).[28] This is in direct contrast with the view that [$M(CO)_5$(carbene)]-moiety is electron withdrawing.[5] However, closer inspection of the structure reveals that steric considerations determine the $Cr(CO)_3$ conformation: the only way to accommodate the tricarbonyl group in such close proximity to the pentacarbonyl group, is to place one of the tricarbonyl CO ligands interlocked in between two pentacarbonyl equatorial CO ligands and forcing the loss of the staggered conformation.

Table 2.14 Selected bond lengths (Å) and angles (°) around the carbene carbon

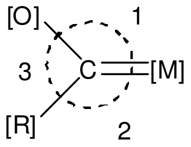

R = ferrocenyl, 2-thienyl or π-$PhCr(CO)_3$

Angle	**5**	**6**	**12**	**13**	**3**	**8**
1	119.7(3)	118.5(7)	119.92(15)	119.9(2)	130.2(2)	122.9(2) 123.3(2)
2	127.3(3)	127.0(7)	123.95(19)/129.6(2)*	128.5(2)	124.6(2)	123.1(1) 122.9(2)
3	112.9(3)	114.5(8)	116.1(2)/110.3(2)*	111.5(3)	105.2(3)	113.8(2) 113.7(2)
Bond	**5**	**6**	**12**	**13**	**3**	**8**
M-C_{carb}	2.090(4)	2.253(9)	2.081(2)	2.067(3)	2.083(3)	2.063(2) 2.077(2)
C_{carb}-O	1.286(5)	1.273(11)	1.283(2)	1.287(4)	1.305(4)	1.276(2) 1.274(2)
C_{carb}-C(R)	1.472(6)	1.465(15)	1.442(5)/1.472(5)*	1.513(5)	1.464(4)	1.480(3) 1.483(3)

* Second component of **12**, with the 2-thienyl substituent rotated about C(6)-C(7) bond

Table 2.14 summarizes the bond distances and bond angles surrounding the carbene carbon atom. The Cr-C(carbene) distances fall in the range 2.063(2) – 2.090(4) Å, which is typical for carbene complexes of $Cr(CO)_5$, while the same is true for the W-C(carbene) bond length of 2.253(9) Å and reported variations in the literature.[50]

The bond angles around the carbene carbon atom, defined as angles 1 - 3 in Table 2.14, depend on the steric requirements of the groups bonded to that carbon atom. Angle 2 (Cr-C-C) remains more or less constant for all seven complexes as the steric requirements of the cyclopentadienyl, thienyl and phenyl moieties, with respect to the carbonyl ligands *cis* to the carbene, are similar. The complexes have a ring C-H *ortho* to the carbene lying staggered with respect to two adjacent carbonyl ligands and in close contact with them leading to somewhat strained sp^2 angles in the range 122.9(2)° – 127.3(3)° for angle 2, compared to the Cr-C-C bond angle of *ca* 121° for the sterically undemanding substituted complex $[Cr(CO)_5\{C(OEt)Me\}]$.[81]

In contrast, the moiety bonded to the carbene via the oxygen atom results in marked differences in the geometry around the carbene carbon atom. In the complexes with a titanoxy substituent, the nearly linear geometry at oxygen together with the comparatively long Ti-O bonds allow the $OTiCp_2X$ moieties to be accommodated in the complexes with little or no steric strain allowing angle 1 (Cr-C-O) to adopt unstrained sp^2 values of *ca* 120° (these angles are *ca* 3° larger in **8** to accommodate both the -O-Ti-O- and the ferrocen-1,1'-diyl bridges between the two carbene ligands). Whereas in complex **3**, the ethoxy group adopts an orientation such that the methylene carbon is in a similar position relative to the second pair of carbonyl ligands *cis* to the carbene as the *ortho* carbon in the thienyl, cyclopentadienyl or phenyl ring is to the first pair of carbonyls. This observation agrees well with that of Sierra that alkoxycarbenes occur in the *anti* conformation, where the oxygen lone pairs are found *trans* to the M=C bond, even in the case of the titanoxycarbene complexes.[82] The presence of two hydrogen atoms bonded to the methylene carbon, together with shorter C-O bond distances compared with the C-C(ring) bond distances, induces even greater strain than induced by the ring C-H leading to values of *ca*

---

[81] Kruger, C.; Goddard, R.; Claus, K.H. *Z. Naturforsch., B. Chem. Sci.* **1983**, *38*, 1431.
[82] Andrada, D.M.; Zoloff Michoff, M.E.; Fernàndez, I.; Granados, A.M.; Sierra, M.A. *Organometallics,* **2007**, *26*, 5854.

130° for angle 1, similar to the Cr-C-O bond of 132.01° of the sterically unhindered [Cr(CO)$_5${C(OEt)Me}].[81]

2.4.5.2 Crystal packing

The Mercury software[83] available from the Cambridge Crystallographic Database Centre (CCDC)[84] was used to visualize the crystal structures in order to analyze the crystal packing. [Cr(CO)$_5${C(OTiCp$_2$Cl)Fc}] (**5**) crystallized with one solvent dichloromethane molecule per complex molecule. The complex molecules display π-stacking (Figure 2.29), where the ferrocenyl Cp-rings are stacked (with a slight glide) one above the other, separated by 3.584 Å.

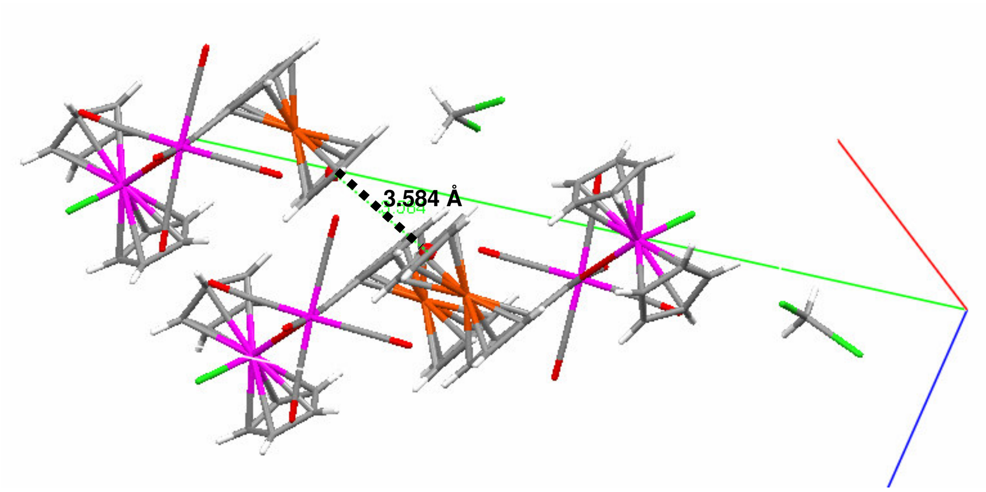

Figure 2.29 π-stacking of complex **5**

---

[83] (a) Mercury CSD 2.0 - New Features for the Visualization and Investigation of Crystal Structures, Macrae, C.F.; Bruno, I.J.; Chisholm, J.A.; Edgington, P.R.; McCabe, P.; Pidcock, E.; Rodriguez-Monge, L.; Taylor, R.; van de Streek, J.; Wood, P.A. *J. Appl. Cryst.* **2008**, *41*, 466, [DOI: 10.1107/S0021889807067908], (b) Mercury: visualization and analysis of crystal structures, Macrae, C.F.;Edgington, P.R.; McCabe, P.; Pidcock, E.; Shields, G.P.; Taylor, R.; Towler, M.; van de Streek, J. *J. Appl. Cryst.* **2006**, *39*, 453, [DOI: 10.1107/S002188980600731X]

[84] The Cambridge Structural Database: a quarter of a million crystal structures and rising Allen, F.H. *Acta Cryst.* **2002**, *B58*, [DOI: 10.1107/S0108768102003890].

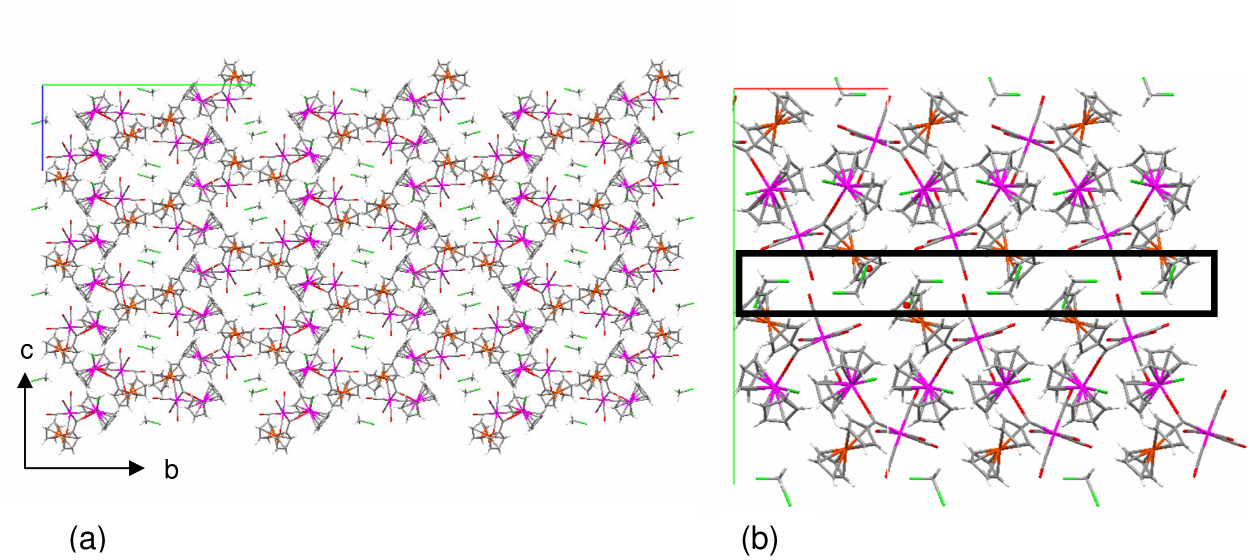

Figure 2.30 (a) Filling of channels with solvent molecules, and (b) layering of solvent molecules in crystal structure of **5**

The cell volumes of the different structures also indicate that although tungsten has a considerably larger atomic radius, the solvent inclusion increases unit cell size. For **5**, the unit cell has a volume of 2838.47 Å^3, while **6** has a unit cell volume of 2539.21 Å^3. This can be seen when looking at the crystal packing of **5** from which the solvent molecules have been deleted from the pocket, compared to the much smaller empty space/pocket of **6** in Figure 2.31.

For complexes **12** and **8**, the crystal packing seems to be the result of close-packing only, as no H-bonding, π-stacking or solvent inclusion is observed. However, the close-packing is structured and displays alternate layers of titanium fragments with chromium pentacarbonyl thienyl carbene fragment for **12**, arranged in a glided stack (Figure 2.32).

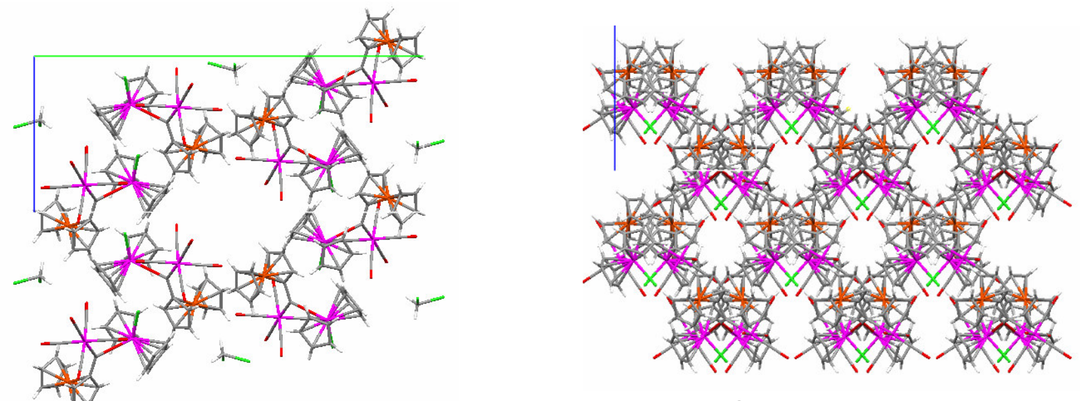

(a) Complex **5** (b) Complex **6**

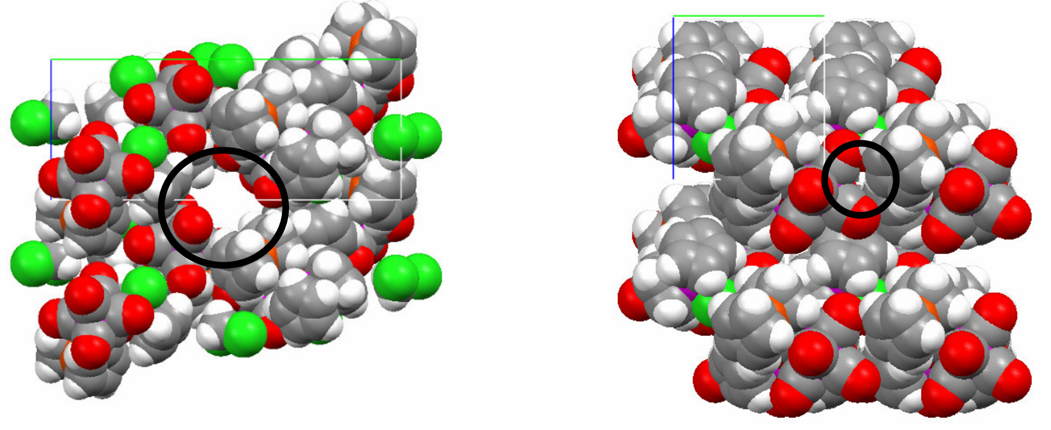

Figure 2.31 View along the a-axis to indicate presence of pocket / channel of (a) **5** (from which solvent molecules have been deleted), and (b) **6**

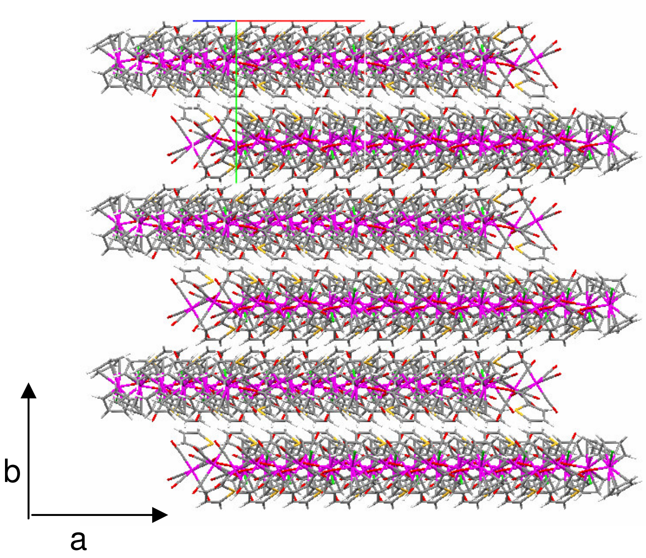

Figure 2.32 Alternate layers as viewed along the c-axis of **12**

Close contact (2.646 Å) of the titanocene Cp-protons and the chromium tricarbonyl CO-ligands of adjacent molecules are observed for **13**. This results in a zig-zag pattern (Figure 2.33) where layers are separated by the carbonyl ligands of adjacent layers.

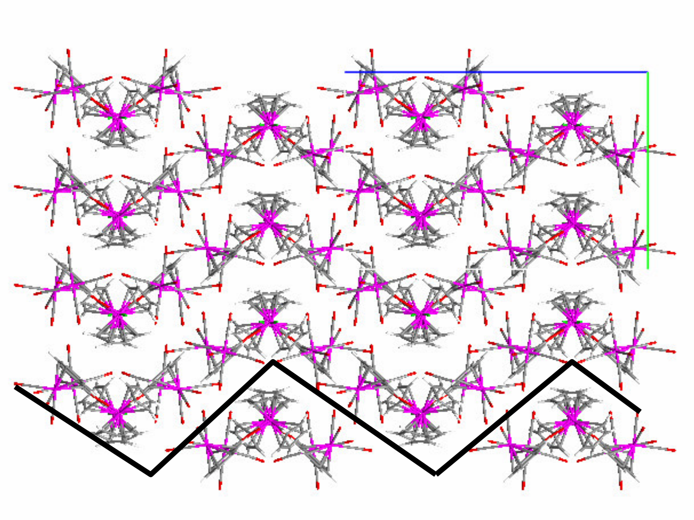

Figure 2.33 Zig-zag pattern of crystal packing of **13**

Finally, the crystallographically symmetrical ethoxy ferrocenyl biscarbene complex **3** crystallizes in such a fashion that adjacent biscarbene molecules stack one above the other so that the two ethoxy groups of one complex will eclipse the ferrocene Cp-rings of the molecule below it. This results in alternate metal (inorganic)-organic layers. This columnar packing shows a slight glide: every second row or layer is displaced by half a unit cell length along the a axis. Weak H-bonds between the methylene protons of the ethoxy groups and neighbouring molecules' carbonyl ligands are observed.

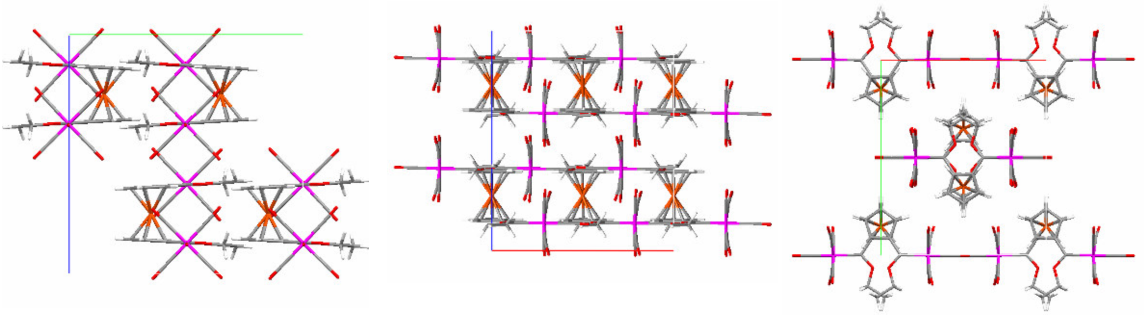

(a) (b) (c)

Figure 2.34 Ordered packing of **3**, viewed along all three axes

Intramolecular packing disorder, with interchange of the –Fc and the two –OEt sites are observed in (c) of Figure 2.34, since the size and shape of the crystal space occupied by the Fc and the two OEt moieties are very similar. Intermolecular packing disorder with the complex displayed a quarter of the cell length along the c-axis (vertical direction in (a)) so that the two $Cr(CO)_5$-moieties of the new molecule occupy the upper $Cr(CO)_5$-site of one molecule as shown, and the lower $Cr(CO)_5$-site of the molecule directly above.

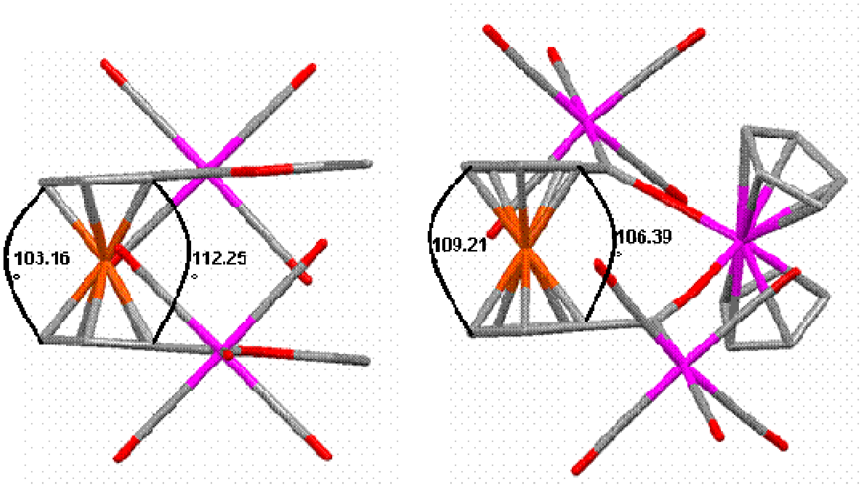

Figure 2.35 Sandwich-tilt angles of ferrocenyl substituents of **3** and **8**

A tilt-deformation of the sandwich-type ferrocenyl substituent is seen. The inner Cp-Fe-Cp angle is 112.25°, greater than the outer angle of 103.16° in **3**. This is not unexpected, as the two Cp-rings are bonded *via* the Fe but there is no bonding interaction to overcome the steric repulsion between the two OEt moieties. For **8**, the titanoxy analogue of **3**, the bridging Ti pulls the O-atom closer together.

2.5 Concluding remarks

The syntheses of di- and trimetallic cluster carbene complexes of Group VI transition metals (Cr, Mo and W) yielded monocarbene complexes containing either an ethoxy or a titanoxy substituent as the heteroatomic carbene ligand substituent, and ferrocenyl, 2-thienyl or η^6-PhCr(CO)$_3$ groups as ring substituents on the carbene carbon atom (Complexes **1** – **13**).

A direct, one-pot synthesis of both mono- and dilithiated ferrocene resulted in the formation of both titanoxy or ethoxy ferrocenyl mono- and biscarbene complexes for the chromium complexes **1**, **3**, **5** and **8**) and molybdenum complexes (complexes **7** and **10**), as well as the ethoxy tungsten carbene complexes **2** and **4**. However, no monocarbene tungsten complex could be isolated from the reaction conditions followed for the Cr- and Mo analogues; instead, the ferrocenyl biscarbene tungsten complex **9** was obtained excusively.
Various lithiation procedures were tested to obtain only monolithiated ferrocene before the titanoxy ferrocenyl monocarbene tungsten complex **6** could be successfully prepared.

Lithiation of the arenes η^5-thiophene chromium tricarbonyl and η^6-benzene chromium tricarbonyl, followed by reaction with Cr(CO)$_6$ and reaction quenching with titanocene dichloride yielded the complexes **12** and **13**, respectively. Complex **12** displayed a carbene ligand with a thienyl substituent, after decomplexation of the Cr(CO)$_3$-fragment, as the thiophene rings are less stable towards chromium decomplexation in polar solvents than the analogous benzene derivatives.

Attempts to synthesize the mixed heteronuclear biscarbene complex **11** $[W(CO)_5C\{\mu\text{-}TiCp_2O_2\text{-}O,O'\}\{\mu\text{-}Fe(C_5H_4)_2\text{-}C,C'\}CCr(CO)_5]$ were only partially successful. Monolithiation of ferrocene and metalation by $Cr(CO)_6$, followed by anionic protection of the acylate and second lithiation, and metalation by $W(CO)_6$ gave very low yields of the mixed biscarbene complex. Another attempt, whereby ferrocenes were dilithiated directly, followed by sequential metalation with the two different starting material hexacarbonyl metal complexes, gave the best results. However, the presence of mixtures of the corresponding chromium and tungsten homonuclear biscarbenes persisted, and single crystal X-ray diffraction confirmed the co-crystallization of both these homonuclear carbene complexes with the heteronuclear biscarbene complex.

The complexes synthesized were characterized by various spectroscopic techniques. The downfield shifts of the (hetero)aryl substituent chemical resonances demonstrated the electron withdrawing character of the $M(CO)_5$-fragments. NMR spectroscopy also lead to the conclusion that the titanoxy substituent resulted in increased electron density on the O-atom, due to greater interaction with the C(carbene) atom and less involvement of the ring substituents. This implies that the titanoxycarbenes show a greater relative contribution of the acyl resonance form of the carbene complexes compared to that of the ethoxycarbene complexes.

IR spectroscopy revealed that the systematic arrangement of the A_1^2 symmetric *cis*-CO stretching frequency demonstrated the stronger donating ability of the $–TiCp_2Cl$ *vs* the –OEt group. The monocarbene complexes displayed higher νCO frequencies, correlating to greater π-acceptor ability of the monocarbene ligands compared to the corresponding bridging biscarbene ligands.

The mass spectral data confirmed the expected stepwise fragmentation of the carbonyl ligands of the complexes; however, a different fragmentation route was identified where the loss of the $–TiCp_2Cl$ once again proved the ionic nature of the Ti-O bond. Ethoxy ferrocenyl biscarbene **3** displayed a unique fragmentation pattern, where loss of the $Cr(CO)_5$-unit and subsequent loss of the entire carbene $Cr(CO)_5\{C(OEt)\}$-moiety were observed.

Structural confirmation came from the crystal structures obtained by X-ray diffraction studies of complexes **3**, **5**, **6**, **8**, **12** and **13**. In all cases considered, the long Ti-O bond and short C(carbene)-O bond correlated with the acyl-like character of the titanoxycarbene ligands, and supported the conclusions drawn form the spectroscopic studies of an ionic structure.

For complex **13**, the electron withdrawing property of the π-$Cr(CO)_3$ moiety caused the lengthening of the C(carbene)-C(Ph) bond, as less ring participation in carbene stabilization is found in the presence of the ‘electron sink’ π-$Cr(CO)_3$ group. Steric considerations were seen to force interlocking of one of the tricarbonyl CO ligands in between two pentacarbonyl *eq*-CO ligands. This resulted in loss of the staggered conformation of the tricarbonyl ligands, which is the expected conformation when electron withdrawing groups such as the $Cr(CO)_5$(carbene)-fragment is bonded to the η^6-phenyl $Cr(CO)_3$.

Finally, the crystal packing of the molecules of complex **5** $[Cr(CO)_5\{C(OTiCp_2Cl)Fc\}]$ displayed π-stacking features between adjacent ferrocenyl groups. Solvent inclusion in **5** increased the unit cell size compared to the analogous tungsten complex **6**, which contains the larger W-atom. However, **6** also exhibited the presence of small, unfilled ‘pockets’ corresponding to the larger, dichloromethane-filled pockets observed for **5**.

3

Group VII Transition Metal Carbene Cluster Complexes

3.1 Introduction

3.1.1 Background

Carbene chemistry of transition metals such as chromium and tungsten is well developed and known routes exist to control and manipulate this chemistry.[1] For transition metals such as manganese and cobalt, discoveries made are still often serendipitous.

Fischer's method of *in situ* preparation of metal carbonyl carbene complexes is most successful with the Group VI transition metal carbonyl complexes.[2] However, on going from the d^6 to the d^8 transition metals, Fischer[3] and others[4] have had difficulty alkylating analogous iron acylates of the form $[Fe(CO)_4C(O)OR]^-$. Attempted methylation of $[Fe(CO)_4C(O)Ph]^-Li^+$ with $Me_3O^+BF_4^-$ lead to formation of $Fe_3(CO)_{12}$ and $Fe_2(CO)_9$ as the major reaction products. Alkylation of iron tetracarbonyl acylates by $Et_3O^+BF_4^-$ was observed

---

[1] Sierra, M.A. *Chem. Rev.* **2000**, *100*, 3591.
[2] Aumann, R.; Fischer, E.O. *Angew. Chem., Int. Ed. Engl.* **1967**, *6*, 878.
[3] Fischer, E.O.; Kiene, V. *J. Organomet. Chem.* **1970**, *23*, 215.
[4] (a) Collman, J.P. *Acc. Chem. Res.* **1975**, *8*, 342, (b) Petz, W. *Organometallics* **1983**, *2*, 1044, (c) Jiabi, C.; Guixin, L.; Weihua, X.; Xianglin, J.; Meicheng, S.; Yougi, T. *J. Organomet. Chem.* **1985**, *286*, 55, (d) Semmelhack, M.F.; Tamura, R. *J. Am. Chem. Soc.* **1983**, *105*, 4099, (e) Lotz, S.; van Rooyen, P.H.; van Dyk, M.M. *Organometallics* **1987**, *6*, 499.

only when R was a very electron withdrawing group, such as C_6F_5 or C_6Cl_5.[5] However, for complexes of the form $[FeL(CO)_3C(O)R]^-Li^+$ (L = PR_3 or $P(OR)_3$) alkylation with oxonium salts readily yields the corresponding carbene complexes $[FeL(CO)_3C(OEt)R]$.[6] The yield of the carbene complexes was found to be dependent on the electronic character of the ligand L; the less electron donating ligands promoting higher yields.

In the case of the tetracarbonyl iron acylate, metal alkylation instead of *O*-alkylation has been ascribed to the fact that these $[Fe(CO)_4C(O)OR]^-$ anions are basic, and have two possible coordination sites for Lewis acids: one at the metal and the other at the alkoxy carbonyl or the carbamoyl oxygen atom.[4(b)] In contrast, the corresponding Group VI anions $[Cr(CO)_5C(O)OR]^-$ have only one site because two electrons at the metal are replaced by a CO group to achieve noble gas configuration. Attack of an electrophile at the metal centre is therefore not expected.

An intermediate situation is expected for d^7 transition metal acylate anions. Due to the uneven number of valence electrons of Group VII transition metals, complexes of these metals require at least one X-type ligand, as classified by Green.[7] In the case of dimanganese or dirhenium nonacarbonyl carbene complexes, this implies that the $M(CO)_5$-moiety is the X-type ligand present, or in the case of η^5-cyclopentadienyl manganese dicarbonyl carbene complex, the Cp ligand constitutes an L_2X-type ligand. Compared to Group VI transition metal carbonyl complexes, more reactive intermediates are therefore possible when Group VII transition metal complexes react with nucleophiles due to the presence of both L- and X-type ligands in the precursors.

---

[5] Fischer, E.O.; Beck, H.J.; Kreiter, C.G.; Lynch, J.; Müller, J.; Winkler, E. *Chem. Ber.* **1972**, *105*, 162.

[6] Conder, H.L.; York Darensbourg, M. *Inorg. Chem.* **1974**, *13*, 3.

[7] Green, M.L.H. *J. Organomet. Chem.* **1995**, *500*, 127.

3.1.2 Monomanganese carbene complexes

The King compound [$Mn_2(CO)_9(COCH_2CH_2CH_2)$], which was initially assigned an incorrect structure without a carbene ligand [$Mn_2(CO)_{10}(CH_2)_3$],[8] sparked interest in the challenges associated with the synthesis of [$M(CO)_4$(carbene)X] (M = Mn, Re; X = halogen) complexes (Figure 3.1). Casey later employed proton NMR spectroscopy to assign the correct structure.

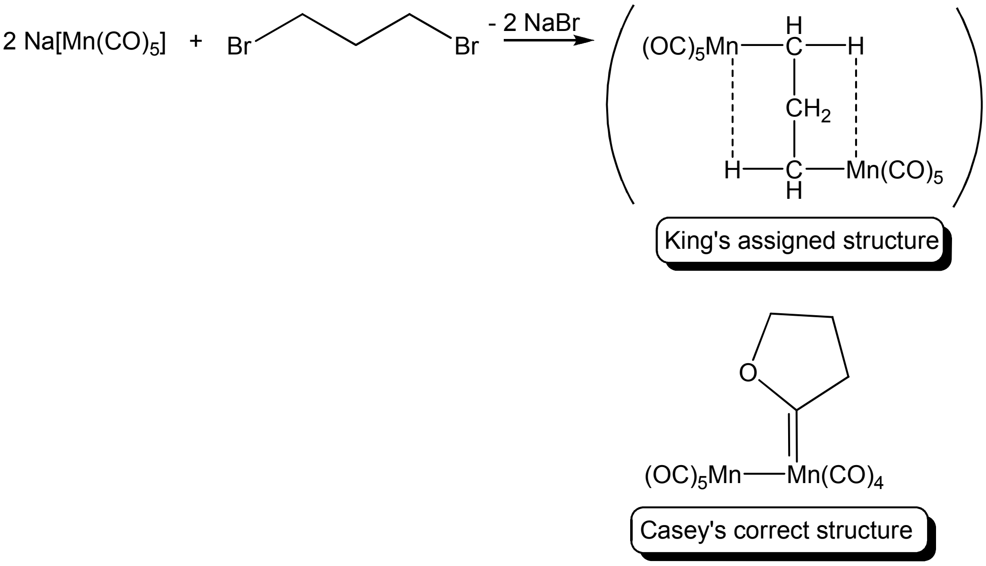

Figure 3.1 First synthesis of a manganese carbene complex

The isolation of binuclear monocarbene complexes of Group VII transition metals, [$Mn_2(CO)_9\{C(OR)R\}$], (R = alkyl) prepared from Na[$Mn(CO)_5$] and 1,3-dihaloalkanes was reinvestigated and resulted in detailed mechanistic studies of the reactions of Na[$M(CO)_5$] (M = Mn, Re) with dihaloalkanes being undertaken.[9] By using different dihaloalkanes, a number of complexes similar to the King compound all containing a cyclic carbene ligand were synthesized and

---

[8] King, R.B. *J. Am. Chem. Soc.* **1963**, *85*, 1922.

[9] (a) Casey, C.P. *J. Chem. Soc., Chem. Commun.* **1970**, 1220, (b) Casey, C.P.; Cyr, C.R.; Anderson, R.L.; Marten, D.F.; *J. Am. Chem. Soc.* **1975**, *97*, 3053, (c) Casey, C.P.; Anderson, R.L. *J. Am. Chem. Soc.* **1971**, *93,* 3554, (d) Casey, C.P.; Cyr, C.R. *J. Organomet. Chem.* **1973**, *37*, C69.

characterized (Scheme 3.1 (a)).[10] In a few instances, with more sophisticated chloro precursors, cationic mononuclear carbene complexes $[Mn(CO)_3(L)_2(carbene)]^+$ (L = phosphine or CO) could be obtained, which after subsequent treatment with halides, afforded the desired neutral halo-carbene complexes $[M(CO)_4(carbene)X]$.[11]

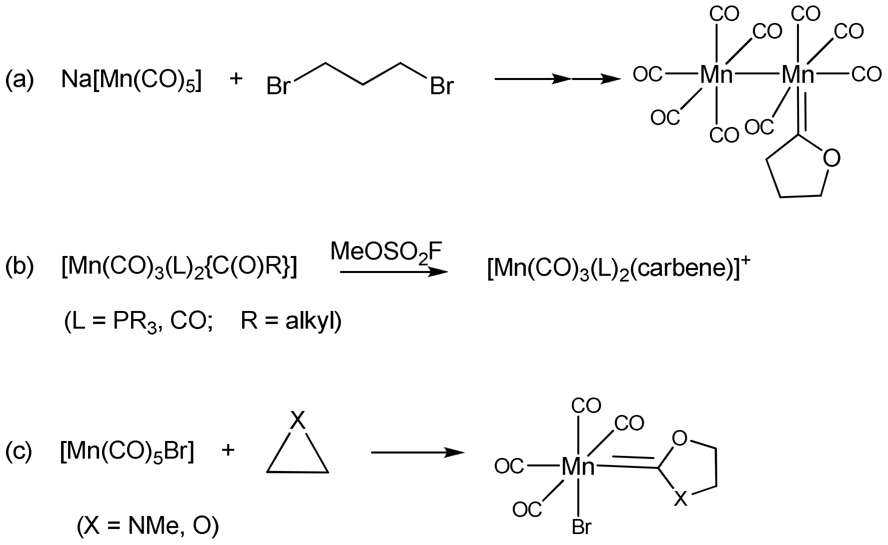

Scheme 3.1

However, the complexes $[Mn(CO)_3(L)_2(carbene)]^+$ (L = PR_3 or CO) could be prepared by employing the alkylation of $[Mn(CO)_3(L)_2\{C(O)R\}]$ with the strong alkylating agent $MeOSO_2F$[12] (Scheme 3.1, (b)). Another major contribution to the carbene chemistry of Group VII transition metals came from the group of Angelici[13] with the reaction of strained 3-membered heterocyclic substrates with $M(CO)_5X$ (M = Mn, Re; X = Br, Cl). The reactions of aziridine and oxirane with

---

[10] (a) Garner, J.-A.M.; Irving, A.; Moss, J.R. *Organometallics,* **1990***, 9,* 2836, (b) Anderson, J.-A.M.; Archer, S.J.; Moss, J.R.; Niven, M.L. *Inorg. Chim. Acta,* **1993**, *206*, 187.

[11] (a) Fraser, P.J.; Roper, W.R.; Stone, F.G.A. *J. Chem. Soc., Dalton Trans.* **1974**, 760, (b) Game, C.H.; Green, M.; Stone, F.G.A. *J. Chem. Soc., Dalton Trans.* **1975**, 2280, (c) Green, M.; Moss, J.R.; Nowell, I.W.; Stone, F.G.A. *J. Chem. Soc., Chem. Commun.* **1972**, 1339, (d) Game, C.H.; Green, M.; Moss, J.R.; Stone, F.G.A. *J. Chem. Soc., Dalton Trans.* **1974**, 351, (e) Bowen, D.H.; Green, M.; Grove, D.M.; Moss, J.R.; Stone, F.G.A. *J. Chem. Soc., Dalton Trans.* **1974**, 1189, (f) Hartshorn, A.J.; Lappert, M.F.; Turner, K. *J. Chem. Soc., Dalton Trans.* **1978**, 348.

[12] Treichel, P.M.; Wagner, K.P. *J. Organomet. Chem.* **1975**, *88*, 199.

[13] (a) Singh, M.M.; Angelici, R.J. *Inorg. Chim. Acta* **1985**, *100*, 57, (b) Miessler, G.L.; Kim, S.; Jacobson, R.A.; Angelici, R.J. *Inorg. Chem.* **1984**, *23*, 2699, (c) Singh, M.M.; Angelici, R.J. *Inorg. Chem.* **1987**, *26* 1690.

these reagents afforded 5-membered cyclic aminooxy- and dioxycarbene compounds (Scheme 3.1 (c)). The reaction could also be applied to $M_2(CO)_{10}$ (M = Mn, Re). Largely unnoticed in later work, the cleavage of the metal-metal bond of the dioxycarbene complexes by bromine was also reported.[13(a)] Nevertheless, very few examples exists where the ligand in $[M(CO)_4(carbene)X]$ (M = Mn, Re; X = halogen) is not a cyclic alkoxycarbene.

This prompted the synthesis of dimanganese monocarbene complexes $[Mn_2(CO)_9\{C(OEt)(heteroaryl)\}]$ in our laboratories following the classical Fischer method, and a range of complexes containing heteroaromatic substituents, e.g. 2,2'-bithiophene, thiophene, furan and N-methyl pyrrole, was isolated.[14] The oxidative cleaving of the metal-metal bonds in these complexes (Scheme 3.2) with halogens yielded the corresponding monometal carbene complexes.

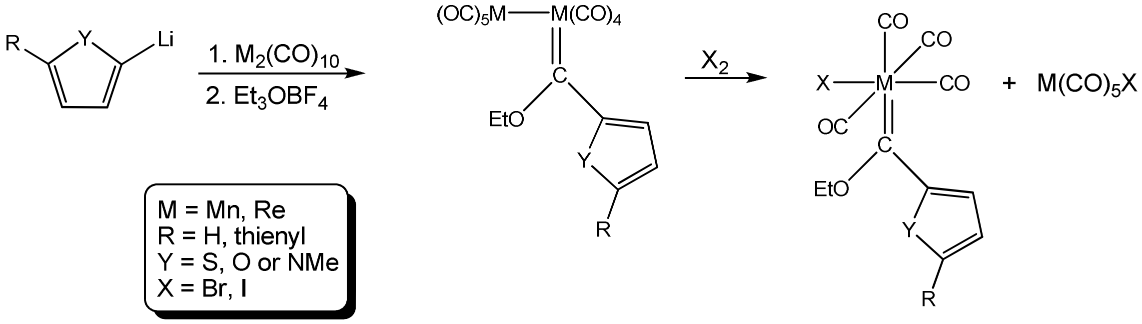

Scheme 3.2

3.1.3 π-arene substituted carbene complexes

When the structures of the Group VI complexes $[Cr(CO)_5\{C(OMe)Ph\}]$[15] and $[Cr(\eta^6\text{-}C_6H_6)(CO)_2\{C(OMe)Ph\}]$[16] (in which the carbene ligand was kept constant) were compared, it was found that increased metal-C(carbene) backbonding

---

[14] Lotz, S.; Landman, M.; Bezuidenhout, D.I.; Olivier, A.J.; Liles, D.C.; van Rooyen, P.H. *J. Organomet. Chem.* **2005**, *690*, 5929.
[15] Mills, O.S.; Redhouse, A.D. *J. Chem. Soc. (A)* **1968**, 642.
[16] Schubert, U. *J. Organomet. Chem.* **1980**, *185*, 373.

occurred for the π-arene complex. A shorter Cr-C(carbene) distance (1.935(12) Å *vs* 2.04(3) Å), and a longer C(carbene)-O distance (1.364(15) Å *vs* 1.33(2) Å) was observed for the η^6-benzene substituted complex. The observation is ascribed to the electronic nature of the π-arene ligand: these ligands induce the metal complex fragments to become better π-donors compared to the analogous $(CO)_nM$-fragments.[17] If the metal complex fragment becomes a stronger competitor for π-bonding with the carbene carbon, then the influence of the methoxy group is reduced.

A wide variety of carbene complexes has been prepared and structurally characterized in which π-bonded aromatic moieties, mainly the η^5-cyclopentadienyl (Cp) or η^5-methylcyclopentadienyl (MeCp) groups, are present as co-ligands. The first monomanganese complex of this nature to be prepared was the complex $[MnCp(CO)_2\{C(OMe)Ph\}]$.[18] After addition of PhLi to $[CpMn(CO)_3]$, the resultant acylate was protonated with a mineral acid such as H_2SO_4 and methylated with CH_2N_2 in ether.

The structural characterization[19] of $[MnCp(CO)_2\{C(OEt)Ph\}]$ revealed that, here too, the π-aromatic ligand produces efficient metal-C(carbene) back bonding. A practical consequence of this bonding situation is the presence of high Mn-C bond order. No π-donating organic substituent at the carbene carbon is therefore necessary to obtain stable complexes. Another consequence is that the presence of an oxy-substituent does not influence the Mn-C(carbene) distances significantly. The same bond lengths (1.87 – 1.89 Å) have been observed in $[MnCp(CO)_2\{C(X)Y\}]$ whether X or Y is bonded to the carbene carbon *via* an oxygen atom, or both X and Y are bonded *via* carbon atoms.

However, constant bond lengths can only be expected as long as none of the organic substituents competes effectively with the metal complex fragment. The distinct lengthening of the Mn-C(carbene) distances in the ylide-substituted

---

[17] Dötz, K.H.; Fischer, H.; Hofmann, P.; Kreissl, F.R.; Schubert, U.; Weiss, K. *Transition Metal Carbene Complexes,* VCH Verlag Chemie, Weinheim, **1983**.

[18] (a) Fischer, E.O.; Öffhaus, E.; *Chem. Ber.* **1967**, *100*, 2445, (b) Fischer, E.O.; Öffhaus, E.; Müller, J.; Nothe, D. *Chem. Ber.* **1972**, *105*, 3027.

[19] Schubert, U. *Organometallics* **1982***, 1*, 1085.

complexes [MnMeCp$(CO)_2${C(OMe)C(Me)PMe_3}][20] (1.99(1) Å) and [MnCp$(CO)_2$ {C(CO_2Me)CHPPh_3}][21] (1.985(3) Å) indicated that in these complexes, the organic substituents are better π-donors than the Mn(MeCp)$(CO)_2$-fragment.

Following the synthesis of heterodimetallic Group VI carbene complexes by the addition of ferrocenyl lithium (FcLi) to $M(CO)_6$ (M = Cr, W) and alkylation with either Me_3OBF_4 or Et_3OBF_4,[22] the preparation of the complexes [CpV$(CO)_3${C(OR)Fc}] and [CpCo(CO){C(OR)Fc}] in the same manner was attempted. This proved unsuccessful, and in each case, only unreacted starting material and ferrocene were recovered. Repeating the reaction with (CpMe)Mn$(CO)_3$ yielded the desired product [(MeCp)Mn$(CO)_2${C(OMe)Fc}] as the first example of a ferrocenyl CpMn-carbene complex.

3.1.4 Dirhenium carbene complexes

To determine whether binuclear metal carbonyl complexes can accommodate carbene ligands, Fischer and Öffhaus[23] successfully synthesized the binuclear [$M_2(CO)_9${C(OR')R}] complexes (M = Mn, Tc, Re; R = alkyl or aryl; R' = alkyl). Following the first paper reporting the preparation of the alkoxycarbene complexes [$Mn_2(CO)_9${C(OEt)Me}] and [$Mn_2(CO)_9${C(OEt)Ph}], there was some uncertainty as to whether the carbene ligand was in an equatorial or axial position. From the IR spectrum, nine carbonyl stretching bands were observed for [$Mn_2(CO)_9${C(OEt)Me}], corresponding to the C_s symmetry of an equatorial [$Mn_2(CO)_9$L] complex. However, for [$Mn_2(CO)_9${C(OEt)Ph}], five ν_{CO} bands, corresponding to C_{4v} symmetry of an axial [$Mn_2(CO)_9$L] complex were seen in the IR spectrum. Shortly after this, Huttner and Regler[24] reported the crystal structure of [$Mn_2(CO)_9${C(OEt)Ph}] and found the carbene ligand to be in an equatorial position, with the ethyl group in the *syn* configuration with respect to

---

[20] (a) Malisch, W.; Blau, H.; Schubert, U.; *Angew. Chem.* **1980**, *92*, 1065, (b) Malisch, W.; Blau, H.; Schubert, U. *Chem. Ber.* **1983**, *116*, 690.

[21] Kolobova, N.E.; Ivanov, L.L.; Zhvanko, O.S.; Chechulina, I.N.; Batsanov, A.S.; Struchkov, Y.T. *J. Organomet. Chem.* **1982**, *238*, 223.

[22] Connor, J.A.; Lloyd, J.P. *J. Chem. Soc., Dalton Trans.* **1972**, 1470.

[23] Fischer, E.O.; Öffhaus, E.; *Chem. Ber.* **1969**, *102*, 2449.

[24] Huttner, G.; Regler, D. *Chem. Ber.* **1972***, 105,* 1230.

the phenyl group about the C-O bond, in contrast to the *anti* configuration found in the X-ray crystal structure of $[Cr(CO)_5\{C(OMe)Ph\}]$.[24]

This result was ascribed to the fact that an equatorial carbene ligand would be too sterically hindered to accommodate the substituents on the carbene ligand in the *anti* configuration, and they explained the appearance of five IR bands instead of nine as the result of degeneracy and band overlap.

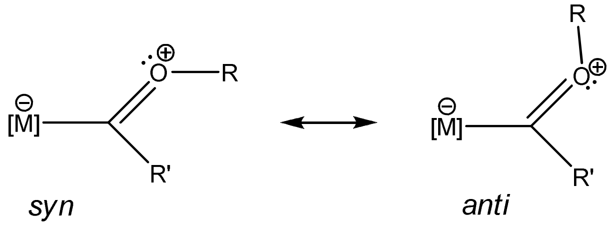

Figure 3.2 *Syn-* and *anti* configurations around the C-O bond

3.1.5 Axial or equatorial carbene ligands of nonacarbonyl dimetal complexes

For complexes of the type $[M_2(CO)_9(\text{carbene})]$ (M = Mn, Tc, Re), the preferred substitution site for the carbene ligand is the electronically favoured equatorial position, where the weaker π-acceptor carbene ligand lies *trans* to a stronger π-acid carbonyl, rather than *trans* to the X-ligand, the $M(CO)_5$-moiety.

However, it was found that for dimetal nonacarbonyl carbene complexes, the site for carbene substitution can be manipulated by the steric bulk of the carbene ligand substituents.[25] During the aminolysis reaction of the unusual *ax*-$[Mn_2(CO)_9\{C(OEt)(2\text{-}C_4H_3Y)\}]$ (Y = S; O) with *n*-propylamine (*n*-Pr), *ax*-$[Mn_2(CO)_9\{C(NH\textit{n}\text{-}Pr)(2\text{-}C_4H_3Y)\}]$ was obtained. Repeating the reaction with the less bulky NH_3(g) resulted in the rearrangement of the carbene ligand to yield *eq*-$[Mn_2(CO)_9\{C(NH_2)(2\text{-}C_4H_3Y)\}]$ (Scheme 3.3). The same rearrangement is not

---

[25] Bezuidenhout, D.I.; Liles, D.C.; van Rooyen, P.H.; Lotz, S. *J. Organomet. Chem.* **2007**, *692*, 774.

observed for the analogous rhenium complexes; due to the increased atomic radius of a Re atom compared to the Mn atom, the Re-Re bond length is considerably longer than that of the corresponding Mn-Mn compound. The steric hindrance of the M(CO)$_5$-fragment is therefore much more pronounced in the case of manganese.

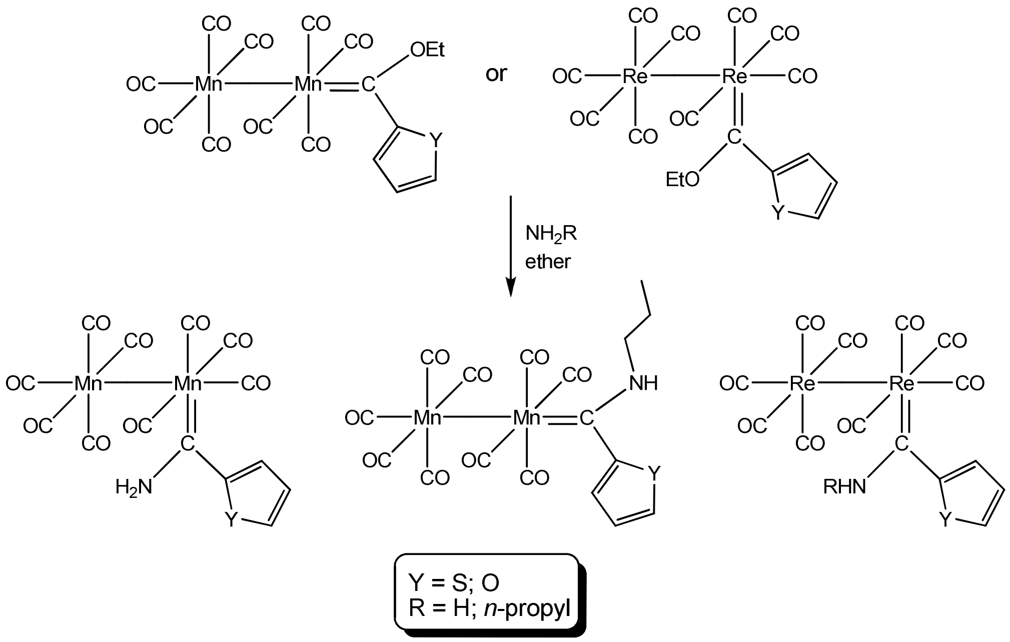

Scheme 3.3

Besides the above two examples, only one other axially substituted dimanganese nonacarbonyl monocarbene complex has been structurally characterized.[26] This complex has the unusual carbene ligand, $C(NMe_2)OAl_2(NMe_2)_5$.

In the case of rhenium, extremely bulky triphenylsilyl groups have been employed to force axial substitution as illustrated in Scheme 3.4.[27] When the study was expanded[28] to include the steric and electronic influences on bond lengths and angles at the carbene carbon, biscarbene complexes containing an axial carbene ligand on one Re(CO)$_4$-fragment, and an equatorial carbene ligand on the adjacent Re(CO)$_4$-fragment were isolated. The equatorial Re-

---

[26] Janik, J.Fr.; Duesler, E.N.; Paine, R.T. *J. Organomet. Chem.* **1987**, *323*, 149.
[27] Fischer, E.O.; Rustemeyer, P. *J. Organomet. Chem.* **1982**, *225*, 265.
[28] Schubert, U.; Ackermann, K.; Rustemeyer, P. *J. Organomet. Chem.* **1982**, *231*, 323.

C(carbene) bond length was found to be significantly longer (2.08(3) Å) than the axial Re-C(carbene) bond length (1.85(3) Å) when a weaker π-acceptor ligand is bonded *trans* thereto.

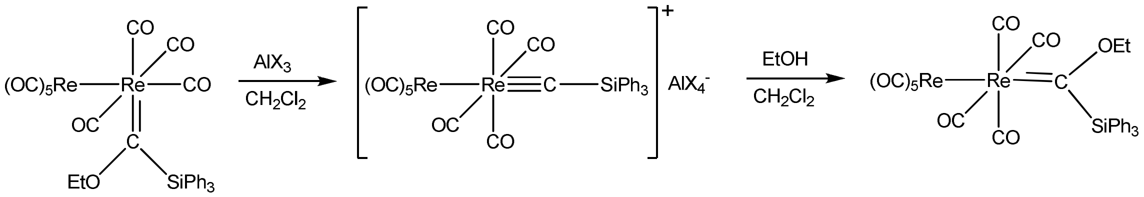

Scheme 3.4

3.1.6 Different reactivities of manganese and rhenium complexes

Previous studies in our laboratories, have shown that the reaction of lithiated [$Cr(CO)_3(\eta^5$-thiophene)] with [$Mn(CO)_5Br$] involves attack either directly on the metal centre or on a carbonyl ligand with elimination of bromide, as shown in Scheme 3.5.[29] This yields the binuclear complexes [$Mn(CO)_5(\eta^1:\eta^5$-T)$Cr(CO)_3$] (T = thienyl) and [$Mn(CO)_5\{C(O)$-$\eta^1:\eta^5$-T)$Cr(CO)_3$ }].[30]

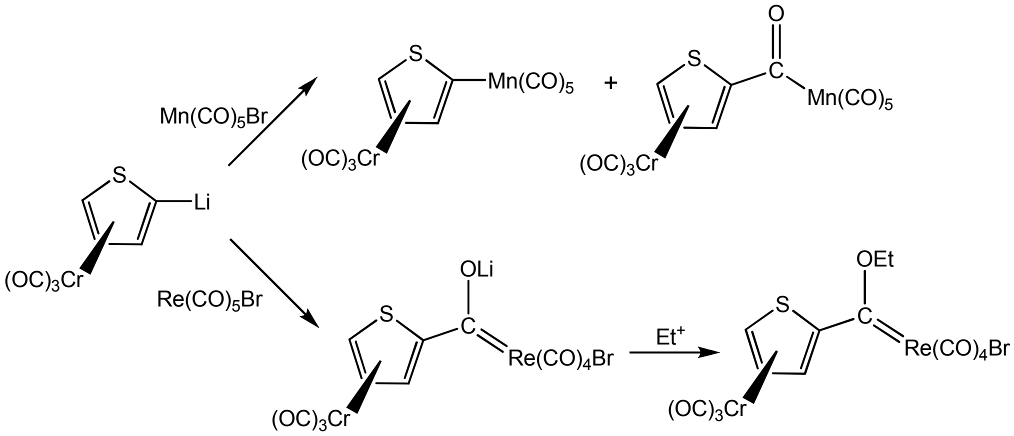

Scheme 3.5

---

[29] (a) Lotz, S.; Schindehutte, M.; van Rooyen, P.H. *Organometallics* **1992**, *11*, 629, (b) van Rooyen, P.H.; Schindehutte, M.; Lotz, S. *Inorg. Chim. Acta* **1993**, *208*, 207.

[30] (a) Waldbach, T.A.; van Rooyen, P.H.; Lotz, S. *Angew. Chem., Int. Ed. Engl.* **1993**, *32*, 710, (b) Waldbach, T.A.; van Eldik, R.; van Rooyen, P.H.; Lotz, S. *Organometallics* **1997**, *16*, 4056, (c) Waldbach, T.A.; van Rooyen, P.H.; Lotz, S. *Organometallics* **1993**, *12*, 4250.

In contrast (Scheme 3.5), the corresponding reaction with [$Re(CO)_5Br$] involved attack on a carbonyl ligand without the elimination of bromide. Subsequent alkylation of the latter with Et_3OBF_4 yielded the carbene complex [$Re(CO)_4Br\{C(OEt)(\eta^1:\eta^5\text{-T})Cr(CO)_3\}$].

The latter result prompted the investigation of the reaction of [$Re(CO)_5Br$] with lithiated thiophene to assess the role, if any, of the $Cr(CO)_3$-fragment. Although not reacting smoothly, the monocarbene dirhenium nonacarbonyl complex, [$Re_2(CO)_9\{C(OEt)(2\text{-T})\}$] was isolated and characterized after alkylation with an oxonium salt.[31] This reaction (Scheme 3.6) shows that it is possible to eliminate a bromide from [$Re(CO)_5X$] during a Fischer carbene synthesis procedure (Li-thienyl/Et_3OBF_4) and replace it with the isolobal fragment $Re(CO)_5$ to give [$Re_2(CO)_9\{C(OEt)(2\text{-T})\}$]. In contrast, reactions of lithiated thiophene with [$Mn(CO)_5Br$] afford a number of unstable compounds that could not be characterized unambiguously.

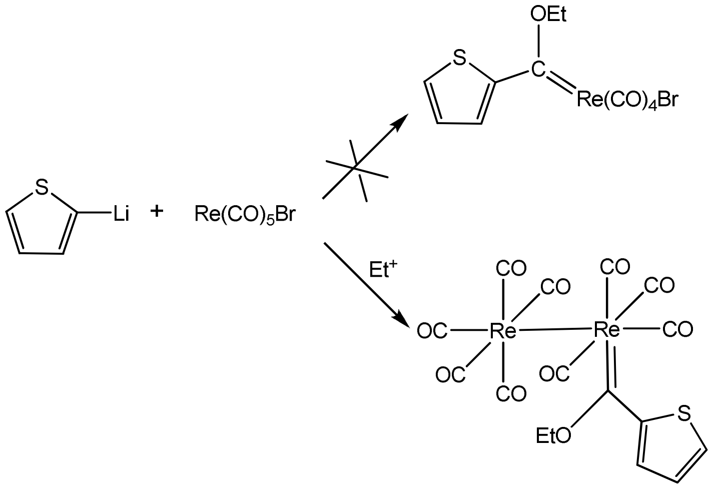

Scheme 3.6

The postulated mechanism of the above reaction involves the breaking of the Re-Br bond, and nucleophilic attack of the *in situ* generated [$Re(CO)_5$]$^-$ on the coordinatively unsaturated acyl complex, Figure 3.3, probably in a concerted

---

[31] Olivier, A.J. *Modification of Rhenium carbonyls with thienyl nucleophiles,* PhD. Thesis, University of Pretoria, Pretoria, **2009**.

mechanism. The mechanism parallels the findings of Norton[32] where rhenium acyl complexes only react with metal hydrides after decarbonylation (Figure 3.4). A vacant coordination site must become available on the rhenium atom bearing the acyl ligand, before the acyl complex can be attacked by [Re(CO)$_5$H].

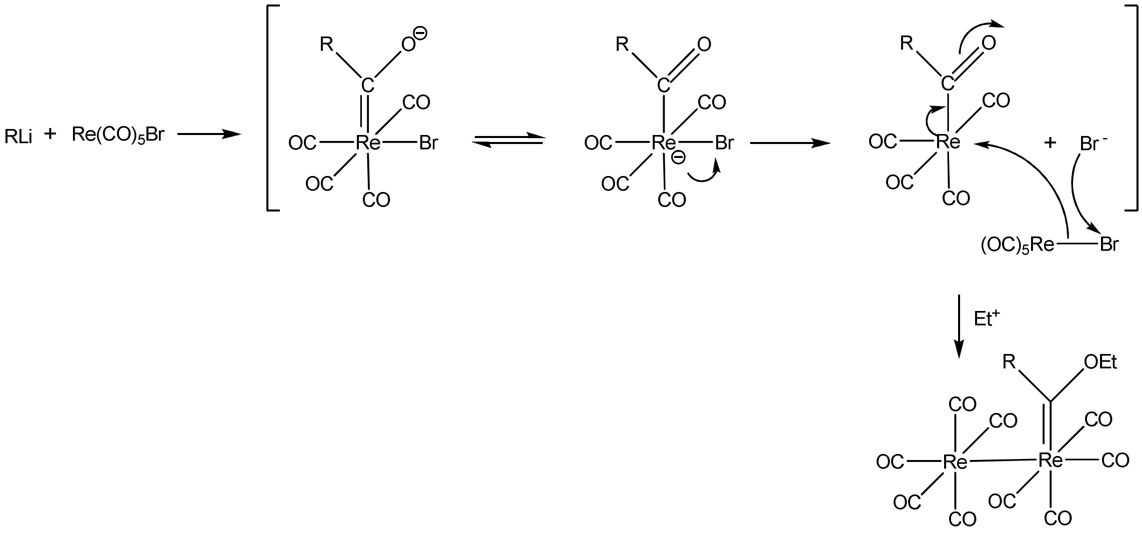

Figure 3.3 Proposed reaction mechanism for dirhenium monocarbene formation from a rhenium pentacarbonyl bromide precursor

The rhenium acyl complex undergoes nucleophilic attack at the rhenium atom by the pair of electrons in the Re-H bond, forming a species with a 3-centre, 2-electron bond. Reductive elimination yields the product aldehyde and the dinuclear rhenium complex. Neutral metal formyl complexes have also been found to transfer hydrides to metal carbonyl cations.[33]

Other kinetic studies have been conducted to investigate the reaction pathways of the Group VII metal hydrides [M(CO)$_5$H] with Group VII metal acyls [M(CO)$_5$C(O)R] (M = Mn, Re). In contrast to the proposed hydrido-acyl

---

[32] (a) Martin, B.D.; Warner, K.E.; Norton, J.R. *J. Am. Chem. Soc.* **1986**, *108*, 33, (b) Warner, K.E.; Norton, J.R. *Organometallics* **1985**, *4*, 2150, (c) Jones, W.D.; Bergman, R.G. *J. Am. Chem. Soc.* **1979**, *101*, 5447.

[33] Lin, G.-Y.; Tam, W.; Gladysz, J. *Organometallics* **1982**, *1*, 525.

intermediate found for the rhenium complexes, Halpern[34] has found that manganese reacts according to a radical mechanism.

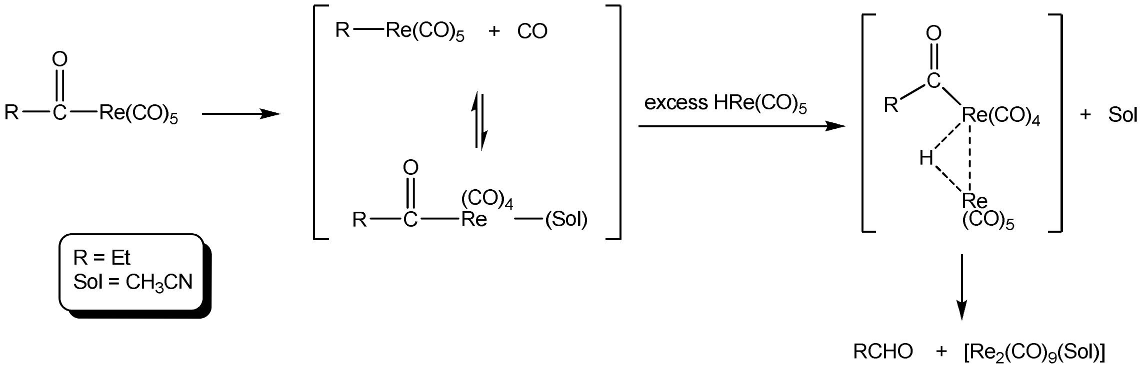

Figure 3.4 Hydrogen transfer to acyl rhenium complexes proposed by Norton[32]

3.1.7 Hydrido-acyl and hydroxycarbene transition metal complexes

As mentioned earlier, the site of alkylation or protonation of transition metal acylates determines the reaction pathway and composition of products and can be divided into two classes of reaction products. *O*-alkylation/protonation will leads to the formation of electrophilic carbene complexes (as seen for Group VI transition metals),[1,35] whereas metal alkylation/protonation generally favours the formation of organic products (Group VIII transition metals).[3, 4] The formation of alkyl- or hydrido-acyl transition metal complexes resulting from oxygen protonation or metal alkylation, and the subsequent elimination of these ligands affords the corresponding ketones or aldehydes.[2(c), 18(a), 36] The site of alkylation of the lithium salt of the metal acylates can be controlled or influenced by a

---

[34] (a) Nappa, M.J.; Santi, R.; Halpern, J. *Organometallics* **1985**, *4*, 34, (b) Sweany, R.C.; Halpern, J. *J. Am. Chem. Soc.* **1977**, *99*, 8335.

[35] (a) Fischer, E.O. *Angew. Chem.* **1974**, *86*, 651, (b) Strassner, T. *Top. Organomet. Chem.* **2004**, *13*, 4.

[36] (a) Alper, H.; Fabre, J.-L. *Organometallics* **1982**, *1*, 1037, (b) Goldberg, K.I.; Bergman, R.C. *J. Am. Chem. Soc.* **1989**, *111*, 1285, (c) Bergamo, M.; Beringhelli, T.; D'Alfonso, G.; Maggioni, D.; Mercandelli, P.; Sironi, A. *Inorg. Chim. Acta* **2003**, *350*, 475.

variety of factors such as the properties of the alkylating agent, the solvent and the electronic and steric properties of intermediates.[4(d), 36(b), 37]

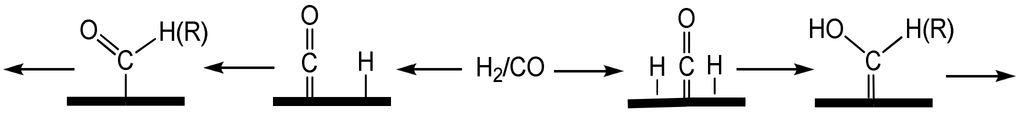

Figure 3.5 Acyl/formyl and hydroxycarbene units as potential building blocks in the Fischer-Tropsch process

Acyl/formyl and hydroxycarbene complexes (Figure 3.5) are thought to be important intermediates in CO reductions, such as found in the Fischer-Tropsch process.[38] Calculations have suggested that hydroxycarbene intermediates could also in some instances be key intermediates in hydroformylation and aldehyde decarbonylation reactions.[39]

The first transition metal hydroxycarbene complex, [ReCp$(CO)_2${C(OH)Me}] was synthesized by Fischer in 1968 by protonation of the metal acylate.[40] In view of the high reactivity of acyl alkyl or acyl hydride complexes, such species have featured as undetected intermediates in ketone and aldehyde forming reactions.[41] Examples of isolable acyl hydride complexes have been reported[42] and hydroxycarbene complexes stabilized by hydrogen bonding in the solid state have also been documented.[43] Casey *et al.* observed, during the course of

---

[37] Dötz, K.H.; Wenicker, U.; Müller, G.; Alt, H.G.; Seyferth, D. *Organometallics* **1986**, *5*, 2570.

[38] (a) Cornils, B.; Herrmann, W.A. Eds. *Applied Homogeneous Catalysis with Organometallic Compounds* VCH Weinheim, **1996**, (b) Muetterties, E.L.; Stein, J. *Chem. Rev.* **1979**, *79*, 479, (c) Herrmann, W.A. *Angew. Chem., Int. Ed. Engl.* **1982**, *21*, 117.

[39] Sola, M.; Ziegler, T. *Organometallics* **1996**, *15*, 2611.

[40] Fischer, E.O.; Riedel, A. *Chem. Ber.* **1968***, 101*, 156.

[41] Milstein, D. *Acc. Chem. Res.* **1984**, *17*, 221.

[42] (a) Garralda, M. A. *Dalton Trans*. **2009**, 3635, (b) Milstein, D. *Organometallics* **1982**, *1*, 1549, (c) Landvatter, E. F.; Rauchfuss, T. B. *Organometallics* **1982**, *1*, 506, (d) (e) Wang, K.; Emge, T. J.; Goldman, A. S.; Li, C.; Nolan, S. P. *Organometallics* **1995**, *14*, 4929, (f) Brockaart, G.; El Mail, R.; Garralda, M. A.; Hernández, R.; Ibarlicea, L.; Santos, J. I. *Inorg.Chim. Acta* **2002**, *338*, 249.

[43] (a) Fischer, E. O.; Kreis, G.; Kreissl, F. R. *J. Organomet. Chem*. **1973**, 56, C37, (b) Moss, J. R.; Green, M.; Stone, F. A. G. *J. Chem. Soc., Dalton Trans*. **1973**, 975, (c) Darst, K. P.; Lukehart, C. M. *J. Organomet. Chem.* **1979**, *171*, 65, (d) Chatt, J.; Leigh, G. J.; Pickett, C. J.; Stanley, D. R. *J. Organomet. Chem*. **1980**, *184*, C64, (e) Klingler, R. J.; Huffman, J. C.; Kochi, J. K. *Inorg. Chem*. **1981**, *20*, 34, (f) Casey, C. P.; Sakaba, H.; Underiner, T. L. *J. Am. Chem. Soc.*

synthesizing a rotationally restricted rhenium carbene complex having a 2-carbon link between the Cp-ligand and C(carbene) atom, an equilibrium between a hydroxycarbene complex and the isomeric metal acyl hydride complex.[44]

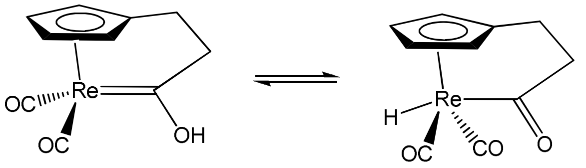

Figure 3.6 Interconversion between the Casey's[44] hydroxycarbene and acyl hydride tautomers

Although metal acyl hydrides and hydroxycarbene complexes are tautomers, no one before Casey had previously reported an observed equilibrium between the two isomers. The tautomers illustrated in Figure 3.6 are the organometallic version of the keto-enol tautomers found in organic chemistry. It was also observed that this mixture of tautomers decomposed under thermal conditions in benzene to give aldehydes.

Reactivity studies on bimetallic μ-malonyl rhenium complexes demonstrated novel carbon-carbon coupling reactions, and after cleavage and alkylation, both neutral and cationic hydroxycarbene complexes were isolated (Scheme 3.7).[45]

1991, *113*, 6673, (g) Steinborn, D.; Gerisch, M.; Bruhn, C.; Davies, J. A. *Inorg. Chem.* **1999**, *38*, 680, (h) Esterhuysen, M. W.; Raubenheimer, H. G. *Eur. J. Inorg. Chem.* **2003**, 3861.

[44] (a) Casey, C.P.; Czerwinski, C.J.; Hagashi, R.K. *J. Am. Chem. Soc.* **1995**, *117*, 4189, (b) Casey, C.P.; Czerwinski, C.J.; Fusie, K.A.; Hagashi, R.K. *J. Am. Chem. Soc.* **1997**, *119*, 3971, (c) Casey, C.P.; Czerwinski, C.J.; Powell, D.R.; Hagashi, R.K. *J. Am. Chem. Soc.* **1997**, *119*, 5750, (d) Casey, C.P.; Nagashima, H. *J. Am. Chem. Soc.* **1989**, *111,* 2352, (e) Casey, C.P.; Vosejpka, P.C.; Askham, F.R. *J. Am. Chem. Soc.* **1990**, *112*, 3713.

[45] O'Connor, J.M.; Uhrhammer, R.; Chadha, R.K.; Tsu, B.; Rheingold, A.L. *J. Organomet. Chem.* **1993**, *455*, 143.

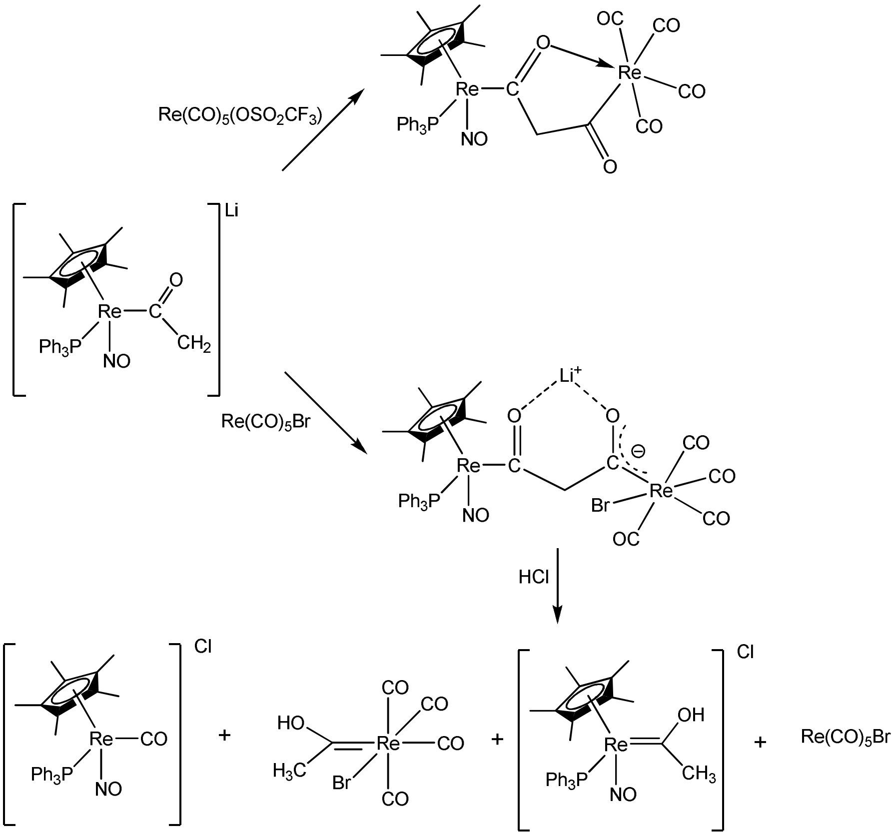

Scheme 3.7

The co-existence of a hydroxycarbene and an acyl ligand in the same monorhenium complex [Re(CO)$_4${C(O)Me}{C(OH)Me}] was reported and exploited by Lukehart and Zeile demonstrating the stabilization of a hydroxycarbene ligand through hydrogen bonding by an acyl ligand.[46] The hydroxycarbene in this complex represents the metallo-enol analogue of acetylacetone (*acac*). The deprotonated form of the metallo-organic ligand displayed coordination properties to other metal ions (Scheme 3.8).[47] Steinborn and co-workers studied similar β-diketones of platinum.[48]

---

[46] Lukehart, C. M.; Zeile, J. V. *J. Am. Chem. Soc.* **1976**, *98*, 2365.

[47] (a) Lukehart, C. M.; Torrence, G. P.; Zeile, J. V. *J. Am. Chem. Soc.* **1975**, *97* 6903, (b) Lukehart, C. M.; Torrence, G. P.; Zeile, J. V. *Inorg. Chem.* **1976**, *15,* 2393, (c) Lukehart, C. M.; Zeile, J. V. *J. Am. Chem. Soc.* **1977**, *99*, 4368.

[48] (a) Steinborn, D. *Dalton Trans.* **2005**, 2664, (b) Steinborn, D.; Schwieger, S. *Chem. Eur. J.* **2007**, *13*, 9668.

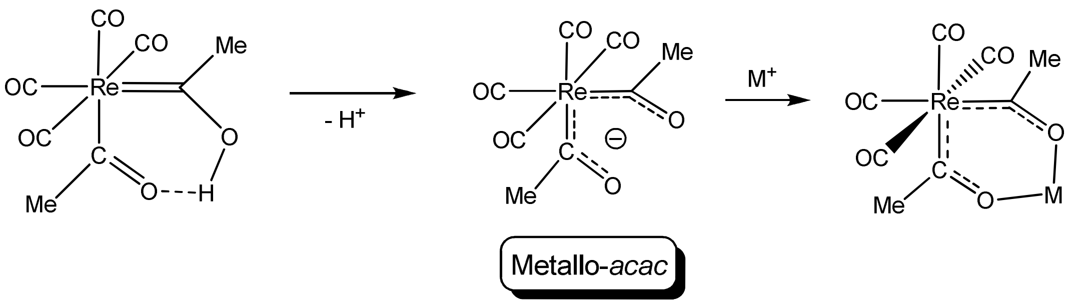

Scheme 3.8

More recently, Olivier[31] isolated and structurally characterized a hydroxycarbene-acyl complex formed from the reaction of rhenium pentacarbonyl bromide and lithiated thiophene, followed by protonation.

The complex was seen as consisting of two fragment complexes held together by a proton and a hydride, and the proposed reaction route is described in Scheme 3.9. The resemblance of this hydride acyl hydroxycarbene complex to the ruthenium Shvo catalyst[49] was emphasized: both complexes feature pendant oxygen atoms with a protonic hydrogen between them, as well as a bridging hydride.

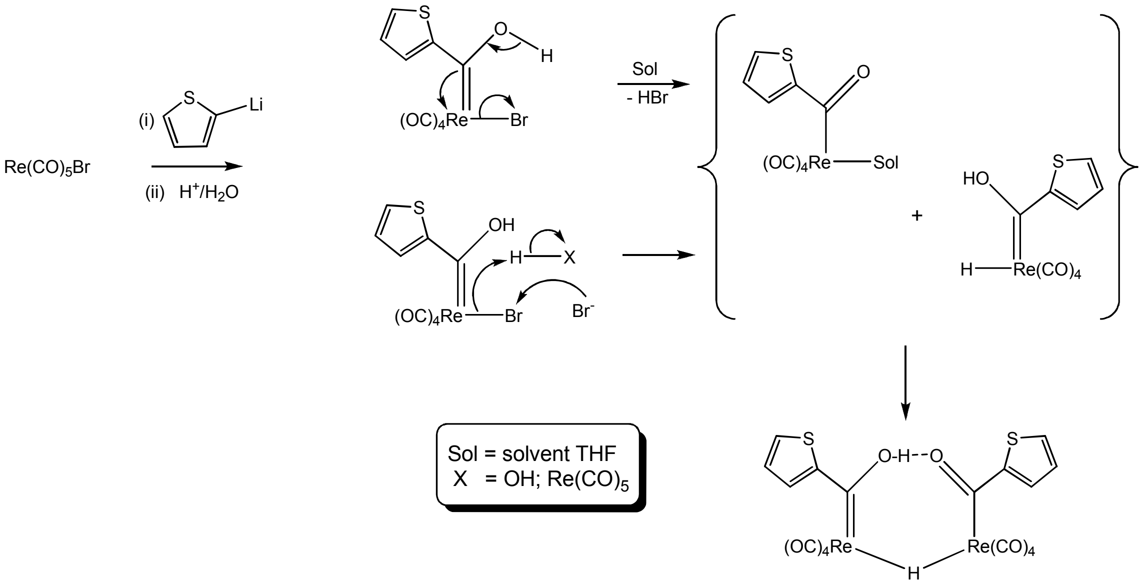

Scheme 3.9

---

[49] (a) Shvo, Y.; Czarkie, D.; Rahamim, Y. *J. Am. Chem. Soc.* **1986**, *108*, 7400, (b) Casey, C.P.; Powell, D.R.; Hayashi, R.K.; Kavana, M. *J. Am. Chem. Soc.* **2001**, *123,* 1090, (c) Bullock, R.M. *Chem. Eur. J.* **2004**, *10*, 2366.

The Shvo catalyst (Figure 3.7) dissociates into a 16 electron Ru(0) and an 18 electron Ru(II) species and has found application in redox reactions, hydrogenation reactions and racemisation reaction. It contains both an hydridic hydrogen bonded to the metal, and a protonic hydrogen bonded to the ligand, and was the first ligand-metal bifunctional hydrogenation catalyst to be developed. However, only the hydride mononuclear species can be obtained if the Shvo catalyst is reacted with H_2 or formic acid.[50] Therefore inefficient use of the ruthenium metal is made, because much of it is present as the diruthenium species which is not active in reduction.[51]

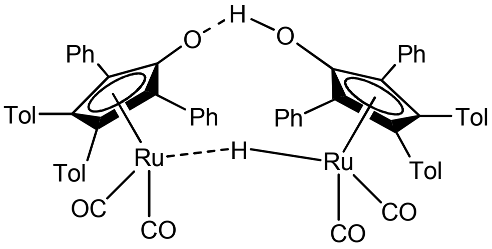

Figure 3.7 The Shvo catalyst

3.2 Results and discussion

3.2.1 Focus of this study

The range of Group VI cluster carbene complexes synthesized in Chapter 2 was extended by making use of mononuclear manganese (in the form of cyclopentadienyl dicarbonyl manganese) as the central metal, and the carbene substituents employed were ferrocene (bonded directly to the carbene carbon atom) as well as ethyl or titanocene chloride (bonded to the carbene oxygen atom). As before, both the mono- and the corresponding biscarbene complexes were synthesized, and are illustrated in Figure 3.8.

---

[50] Casey, C.P.; Singer, S.W.; Powell, D.R. *Can. J. Chem.* **2001**, *79*, 1002.
[51] Casey, C.P.; Beetner, S.E.; Johnson, J.B. *J. Am. Chem. Soc.* **2008**, *130*, 2285.

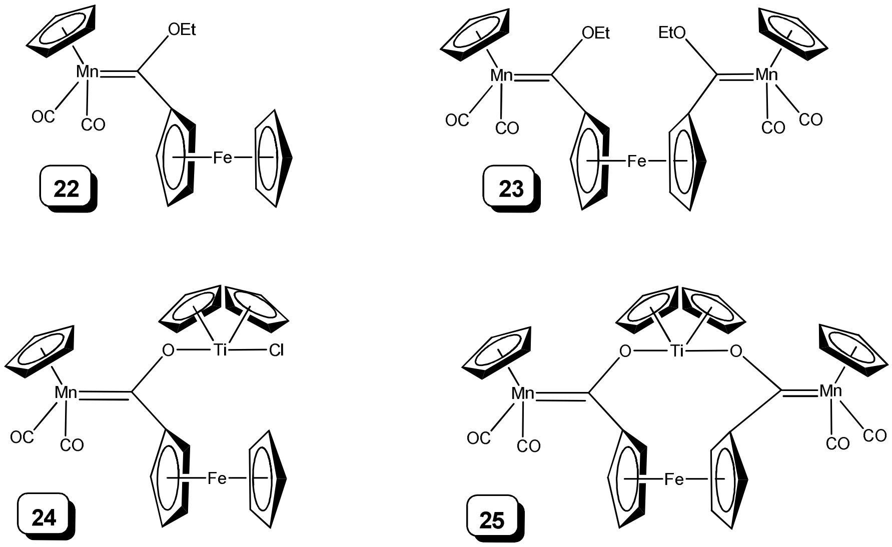

Figure 3.8 Manganese carbene complexes synthesized

Next, the possibility of increasing the number of metal fragments in the cluster complexes was investigated by employing the dinuclear Group VII binary metal carbonyl, $Re_2(CO)_{10}$ as precursor central metal. A variety of products consisting of both mono- and dirhenium complexes indicated a mixture of the dirhenium acylate precursor and other species resulting from Re-Re bond cleavage during this stage of the reaction. Depending on the site of alkylation/metalation/protonation, a range of di- and monorhenium Fischer carbene complexes and other products could be isolated. The acyl and hydrido intermediates formed, as well as hydroxycarbene complexes are precursors to aldehyde formation. Figure 3.9 lists all the rhenium metal-containing product complexes isolated from the rhenium synthesis reactions in this chapter.

26

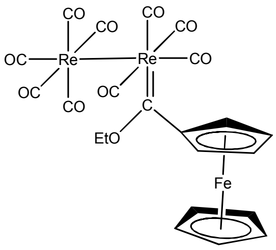

27

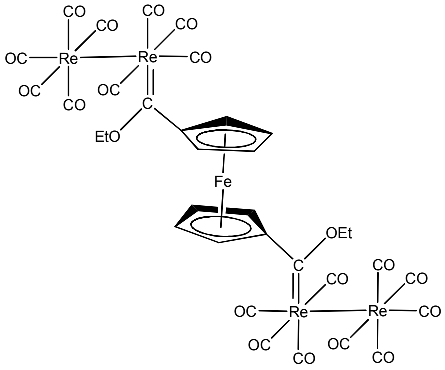

28

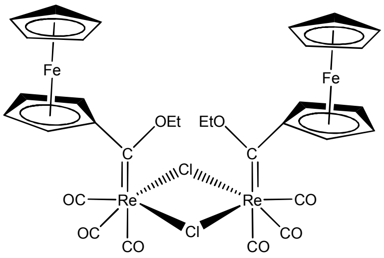

29

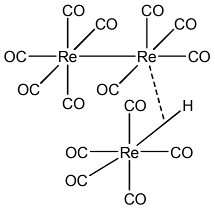

30

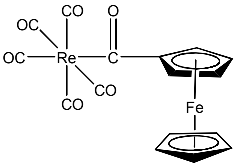

31

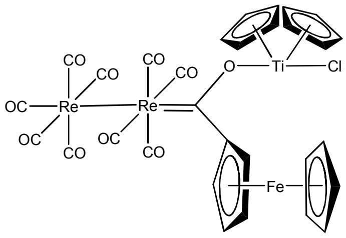

32

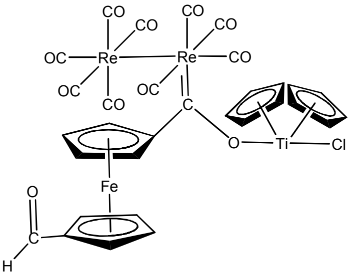

33

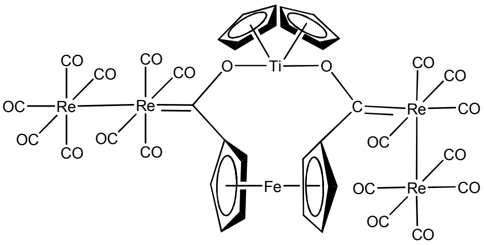

34

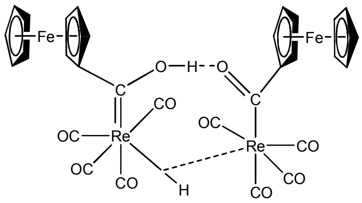

Figure 3.9 Complexes obtained from rhenium reactions

3.3 Synthesis

3.3.1 Synthesis of cyclopentadienyl manganese carbene complexes

For Group VII transition metals, carbene complexes with cyclopentadienyl as an auxiliary ligand, are readily accessible.[52] The corresponding biscarbene complexes can also be obtained by intermolecular oxidative coupling in the presence of anhydrous $FeCl_3$,[52(a)] as shown in Scheme 3.10.

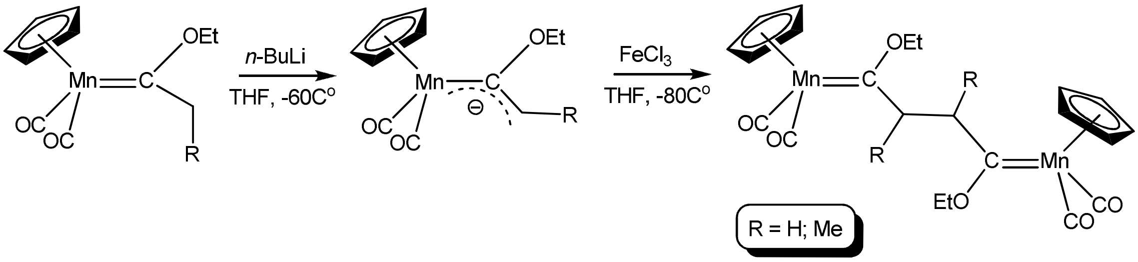

Scheme 3.10

As with the Group VI transition metals Cr and W, the monocarbene complex of methylcyclopentadienyl manganese with ferrocenyl and ethoxy substituents on the carbene ligand has been synthesized before.[22] The analogous complex $[MnCp(CO)_2\{C(OEt)Fc\}]$ (**22**) was synthesized in this study for the purpose of comparison. The general procedure followed involved reaction of *n*-BuLi with ferrocene to yield both the mono- and dilithiated precursors, followed by the addition of $[MnCp(CO)_3]$ in THF at low temperatures. Alkylation with Et_3OBF_4 in dichloromethane yielded complex **22** and the novel biscarbene complex **23** $[\mu\text{-}Fe\{C_5H_4C(OEt)MnCp(CO)_2\}_2]$. Alternatively, metalation with titanocene dichloride yielded, the monocarbene complex **24** $[MnCp(CO)_2\{C(OTiCp_2Cl)Fc\}]$ and the bridging bisoxy titanocene and bridging ferrocen-1,1'-diyl complex **25** [{μ-

---

[52] (a) Rabier, A.; Lugan, N.; Mathieu, R. *J. Organomet. Chem.* **2001**, *617 - 618*, 681, (b) Casey, C.P.; Kraft, S. ; Powell, D.R. ; Kavana, M. *J. Organomet. Chem.* **2001**, *617 – 618*, 723.

$TiCp_2O_2$-O,O'}{μ-$Fe(C_5H_4)_2$-C,C'}[$CMnCp(CO)_2\}_2$]. The Fischer procedure for the preparation of the above complexes is summarized in Scheme 3.11.

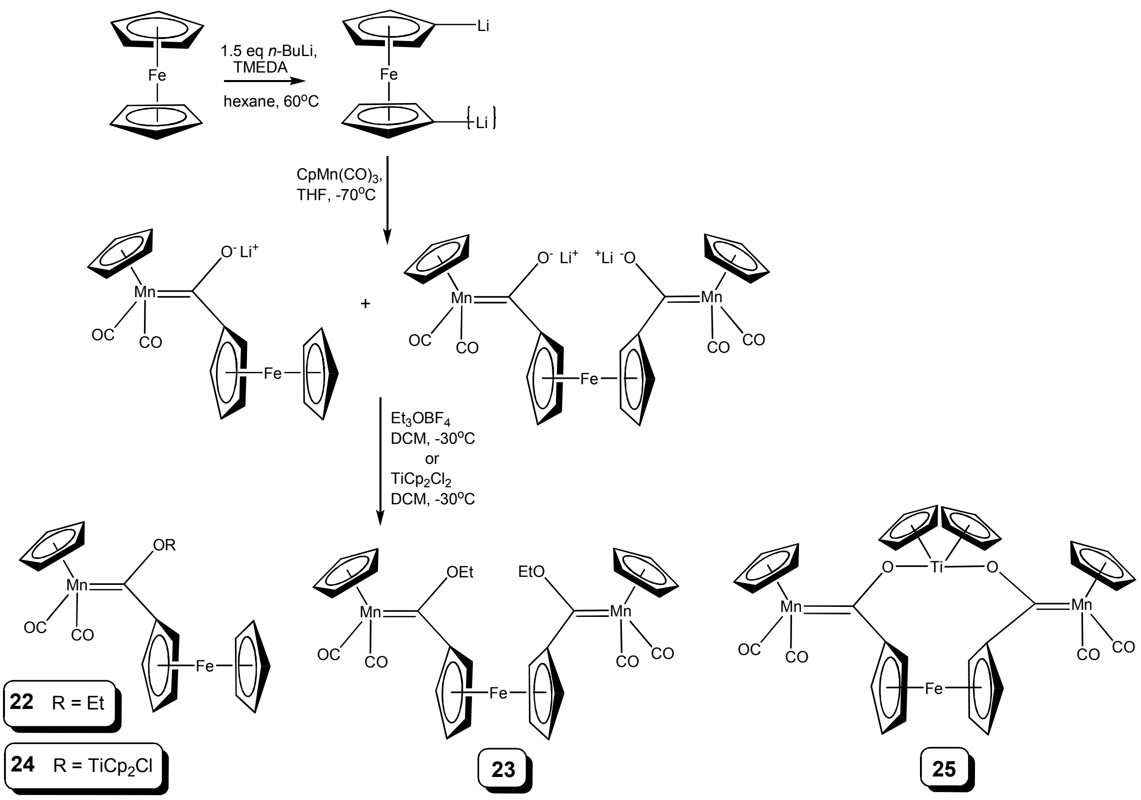

Scheme 3.11

3.3.2 Synthesis of dirhenium ethoxycarbene complexes

Lithioferrocene can be prepared either by direct abstraction of a proton from ferrocene by butyllithium[53] or by an exchange reaction between chloromercuriferrocene and butyllithium.[54] The former route leads to a mixture of mono- and dilithiated ferrocene, usually with a low yield of FcLi. The latter route is complicated by the possibility of the formation of both alkylated and mercury-

---

[53] (a) Benkeser, R.A.; Goggin, D.; Schroll, G.A. *J. Am. Chem. Soc.* **1954**, *76*, 4025, (b) Mayo, D.W.; Shaw, R.D.; Rausch, M. *Chem. Ind.* London, **1957**, 1388.

[54] (a) Helling, J.F.; Seyferth, D. *Chem. Ind.* London, **1961**, 1568, (b) Seyferth, D.; Hoffman, H.P.; Burton, R.; Helling, J.F. *Inorg. Chem.* **1962**, *1*, 227, (c) Hedberg, F.L.; Rosenberg, H. *Tetrahedron Lett.* **1969**, *46*, 4011.

containing derivatives of ferrocene as undesired side products. After the former method was employed in our laboratory with no appreciable yield of FcLi, it was decided to use halogen-metal exchange of iodoferrocene and *n*-BuLi to afford the monolithiated product in high yield. Fish and Rosenblum's method[55] was followed to prepare FcI, and the exchange reaction of a stoichiometric amount of *n*-butyllithium in ether at -70℃ resulted in a high yield of FcLi with no concurrent dilithiation. Subsequent metalation with $Re_2(CO)_{10}$ in THF at -50℃, followed by alkylation with Et_3OBF_4 in dichloromethane yielded the dark red complex $[Re_2(CO)_9\{C(OEt)Fc\}]$ (**26**). Unreacted $Re_2(CO)_{10}$ and ferrocene were separated from the reaction mixture by column chromatography. Only one dark red band was isolated besides the unreacted starting materials. However, NMR spectroscopy revealed duplication of all the ^1H and ^{13}C chemical shifts. The IR spectrum also displayed more carbonyl stretching vibration bands than expected, many of the bands overlapping. From this information, we concluded that a mixture of the equatorial and the axial isomers were present in solution, as the steric bulk of the ferrocenyl substituent could force the electronically unfavoured axial substitution. Unfortunately, the two different isomers could not be separated and purified, possibly due to the fact that the isomers are in equilibrium in solution.

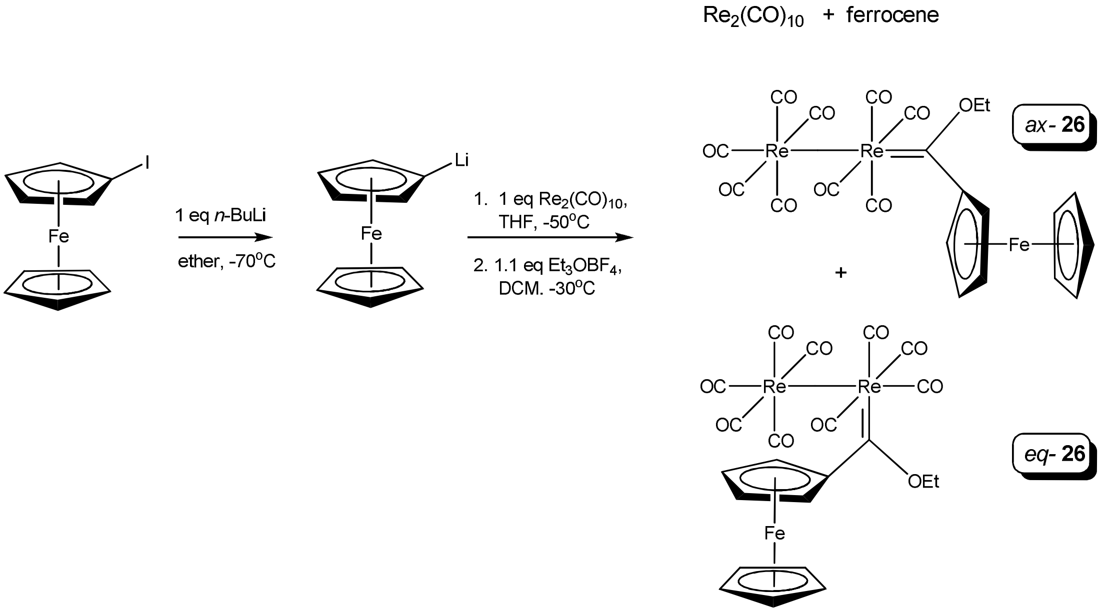

Figure 3.10 Synthesis of *ax*- and *eq*-$[Re_2(CO)_9\{C(OEt)Fc\}]$

---

[55] Fish, R.W.; Rosenblum, M. *J. Org. Chem.* **1965,** *30,*1253.

For the preparation of **27**, the corresponding biscarbene complex to **26**, ferrocene was readily dilithiated with *n*-BuLi and TMEDA in hexane at 45°C. The dilithiated species precipitate out of the solution as an orange solid and the yield relative to the monolithiated species could be increased (> 80%) by removal of the solution *via* canula. After solvent evaporation and cooling to -50°C, 2 mole eq of dirhenium decacarbonyl was added in THF, and alkylation with 2 mole eq of alkylating agent yielded, besides unreacted rhenium carbonyl, three fractions identified by thin layer chromatography. The two products eventually obtained by column chromatography are illustrated in Scheme 3.12.

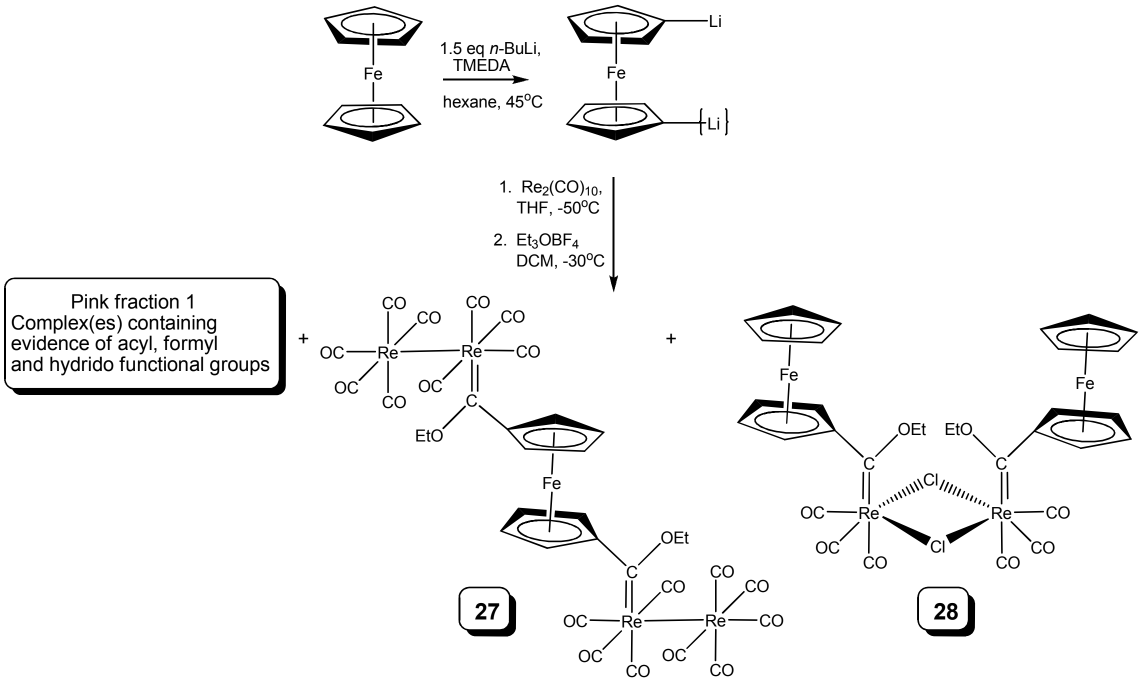

Scheme 3.12

The first pink fraction to be eluted from column chromatography on silica gel could not be successfully characterized before decomposition. The IR spectrum of the compound therein showed four υ(CO) bands at 2102 (m), 2038 (s), 1994 (vs) and 1939 (s) cm^{-1}, but over time, new bands appeared (overlapping with the previous bands) at 2087 and 1968 cm^{-1}. From the ^{13}C NMR spectrum, a carbene signal of strong intensity could be assigned at 308.1 ppm. However, more than the expected number of ferrocenyl resonances (in the range of 72 -78 ppm), ethoxy resonances and carbonyl resonances (186 – 199 ppm) were observed. In addition, two acyl-like chemical shifts at δ = 286.5 and 274.9 were seen, but the corresponding C-O stretches (that would appear in the range of 1500-1700 cm^{-1} of the infrared spectrum) were not observed. Furthermore, the proton NMR spectrum displayed a very downfield shift at 9.20 ppm, usually associated with an aldehyde functional group, as well as a very highfield chemical shift at -13.70 ppm. For most monorhenium complexes the hydride signal is seen in the range -4 to -10 ppm[44(a), 56] and for the dirhenium complexes or rhenium clusters with a bridging hydride, the signal commonly seen is in the range of -14 to -20 ppm.[57] Although thin layer chromatography revealed the presence of only one compound, the possibility of more than one complex present could not be ruled out. Decomposition of the formed products with loss of the metal carbonyl moiety to yield compounds such as FcCHO is, however, the most probable event.

The contents of the next band was collected as a bright red compound, which was identified by single crystal X-ray crystallography as being *fac*-$[(\mu\text{-Cl})_2\text{-}(Re(CO)_3\{C(OEt)Fc\})_2]$ (**28**). Finally, the expected product, dark brown complex *eq*,*eq*-$[\mu\text{-Fe}\{C_5H_4C(OEt)Re_2(CO)_9\}_2]$ (**27**), was eluted as the third fraction in a yield of 38%. Unlike the monocarbene analogue, no evidence of an axial isomer was observed.

Complex **28** displays some similarities to the acyl-hydrido hydroxycarbene dirhenium complex:[31] in both cases, cleavage of the Re-Re bond of the precursor $Re_2(CO)_{10}$ has occurred. The complex can be seen as made up of two coordinatively unsaturated $[Re(CO)_3\{C(OEt)Fc\}Cl]$-fragments. If employing the same approach as demonstrated in Scheme 3.9, a possible reaction route can be proposed as in Scheme 3.13.

---

[56] Krumper, J.R.; Martin, R.L.; Hay, P.J.; Yung, C.M.; Veltheer, J.; Bergman, R.G. *J. Am. Chem. Soc.* **2004**, *126*, 14804.

[57] (a) Adams, R.D.; Captain, B.; Hollandsworth, C.B.; Johansson, M.; Smith, Jr., J.L. *Organometallics* **2006**, *25*, 3848, (b) Adams, R.D.; Kwon, O.-S.; Perrin, J.L. *J. Organomet. Chem.* **2000**, *596*, 102.

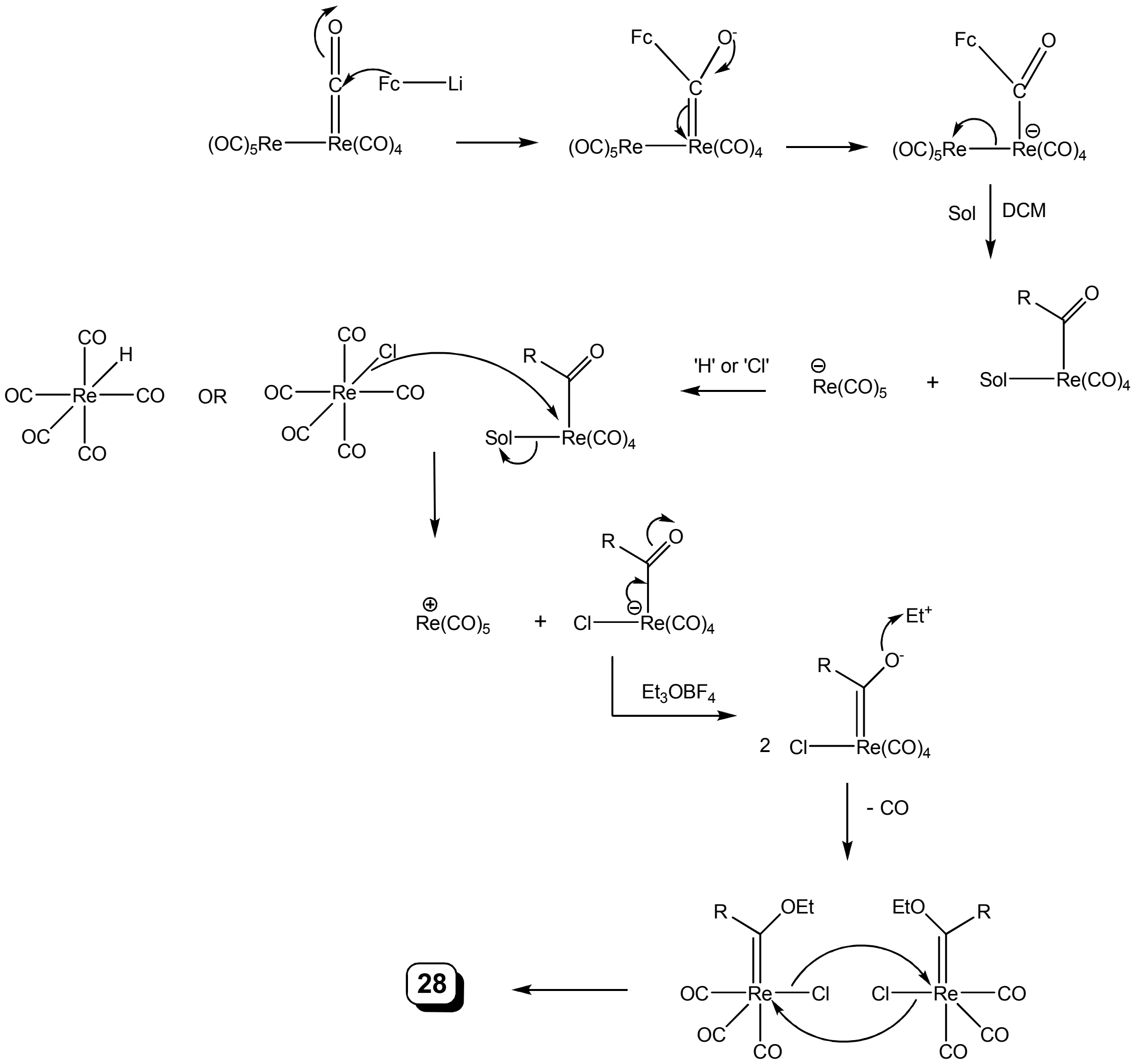

Scheme 3.13

1,1'-dilithioferrocene attacks on a carbonyl ligand of [$Re_2(CO)_{10}$] and imparts a negative charge to the complex, stabilized by resonance as the metal acylate. The formation of this anionic intermediate facilitates the loss of the $Re(CO)_5$-fragment and the Re-Re bond breaks heterolytically, and a solvent (THF) molecule coordinates to the vacant site.[32] The other fragment, the $[Re(CO)_5]^-$ anion, abstracts a chlorine atom from solvent dichloromethane, as this is the only chlorine source available. Evidence of chlorine abstraction from dichloromethane in a radical mechanism by a tetrahedrane cluster [$RCCo_2Mo(\eta^5$-indenyl)$(CO)_8$] (R = H; Ph), after breaking of the Mo-Co and Co-

Co bond, has recently been published by Watson *et al.*[58] Reaction of a ruthenium carbonyl complex [$Ru_2(CO)_2(\mu\text{-}CO)H(\mu\text{-}CCPh)(\mu\text{-}dppm)_2$] with chlorinated solvent CH_2Cl_2 also resulted in ligand substitution by a solvent chlorine atom to give [$Ru_2(CO)_2(\mu\text{-}CO)Cl(\mu\text{-}CCPh)(\mu\text{-}dppm)_2$].[59]

From literature, Mn-X bond dissociation energies can be ordered as follows:[60] $(CO)_5Mn\text{-}X$ [Δ(Mn-X), $kJ.mol^{-1}$] X = Br (280) > H (250) > Ph (sp^2-C) (205) > CH_3 (sp^3-C) (185) > $C(O)CH_3$ (165) > $Mn(CO)_5$ (160). Re-X bonds are approximately 20% stronger and according to the above approximate values, a Re-Cl bond would be much stronger than a Re-Re bond. The chloro ligand is therefore transferred to the [(Sol)-$Re(CO)_4${C(O)Fc}] complex, and after alkylation and decarbonylation, two of the resultant coordinatively unsaturated *fac*-[$Re(CO)_3${C(OEt)Fc}Cl]-fragments form chloro-bridges to yield complex **28**.

It is possible, too, that the rhenium pentacarbonyl anion can abstract a hydrogen atom by the same mechanism, yielding the rhenium pentacarbonyl hydride complex, another byproduct identified along with the rhenium pentacarbonyl chloride complex.

3.3.3 Synthesis of dirhenium carbene cluster complexes

The same procedure as described in Section 3.3.2 above was employed to synthesize the titanoxycarbene complexes, the only difference being metalation of the acyl metalate with titanocene dichloride in dichloromethane, instead of alkylation with an oxonium salt.

Before alkylation/metalation, the lithiated salt can be represented as either a rhenium acylate (**A**) that can be converted to the rhenium carbonyl anion (**B**) and an acyl rhenium complex (**C**), respectively (Figure 3.11).

---

[58] Watson, W.H.; Poola, B.; Richmond, M.G. *J. Organomet. Chem.* **2006**, *691*, 5567.

[59] Kuncheria, J.; Mirza, H.A.; Vittal, J.J.; Puddepatt, R.J. *J. Organomet. Chem.* **2000**, *593 – 594*, 77.

[60] (a) Connor, J.A. *Top. Curr. Chem.* **1977**, *71*, 71, (b) Collman, J.P.; Hegedus, L.S.; Norton, J.R.; Finke, R.G. *Principles and Application of Organotransition Metal Chemistry,* Oxford University Press, Mill Valley, CA, **1987**.

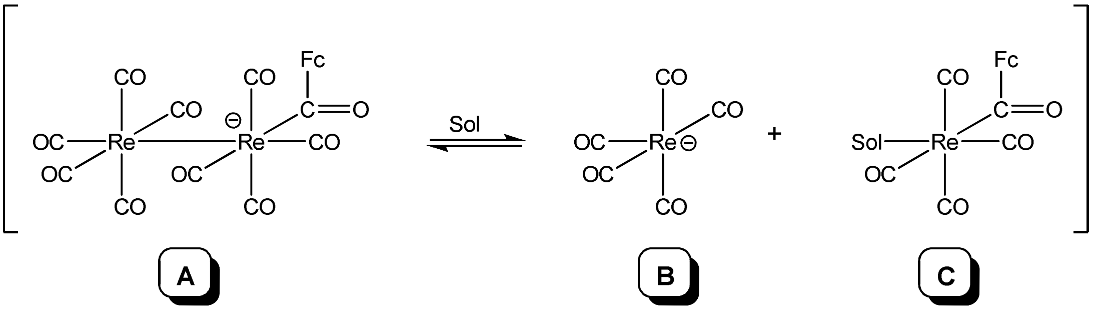

Figure 3.11 Re-acylate (**A**), $Re(CO)_5^-$ (**B**) and Re-acyl (**C**) intermediates

Thin layer chromatography, after complexation with $TiCp_2Cl$, revealed the presence of nine different compounds, and these were separated and purified on an alumina column, and will be discussed in the order of elution from the column. The formation of the minor byproducts isolated from the reaction mixture can mostly be ascribed to the transfer of a proton by two possible mechanisms, either ionic or radical. Firstly, transfer of a proton from dichloromethane or other proton source *via* a radical mechanism, or the protonation of the rhenium pentacarbonyl anion, $[Re(CO)_5]^-$ (**B**) to give $[Re(CO)_5H]$. Hydrolysis of the rhenium complexes occurs both in reaction mixture solvent THF or dichloromethane, as well as on the silica gel columns during chromatography if trace amounts of water are present. The *in situ* formation of $[Re(CO)_5H]$ was noted in NMR studies and the secondary product, the trirhenium hydride $[Re_3(CO)_{14}H]$ (**29**) was isolated. More important was the subsequent hydrogen transfer reaction of $[Re(CO)_5H]$ with the corresponding neutral ferrocene-acyl complex of rhenium. The products also contained some ferrocenyl aldehydes or acyl complexes.

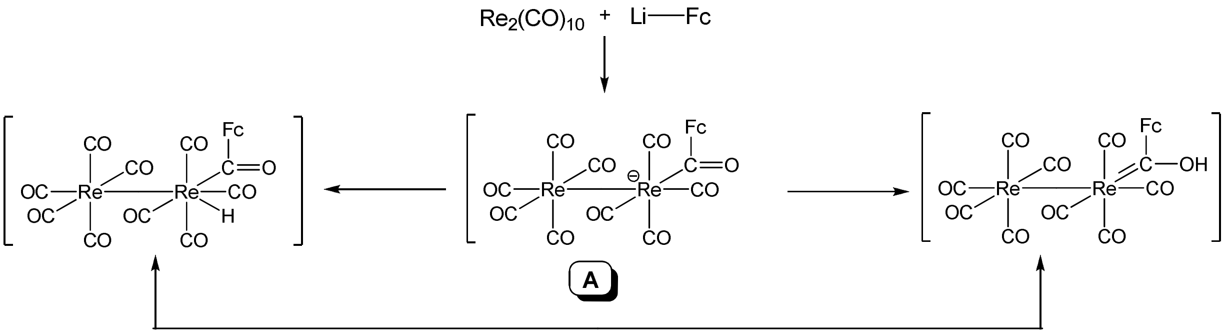

Scheme 3.14

The first band eluted contained the colourless starting material $Re_2(CO)_{10}$. After this followed the second fraction, pink in colour. IR spectroscopy clearly displayed carbonyl stretches in the expected range, and the presence of the unique hydroxycarbene-acyl complex $[(\mu\text{-H})_2\text{-}(Re(CO)_4\{C(O)Fc\})_2]$ (**34**), identified as the molecular ion peak in a mass spectrum, indicated a similar mechanism as was discussed by Olivier.[31] The postulated reaction pathway for the formation of **34** is shown in Figure 3.11 and Schemes 3.14 and 3.15.

The formation of **34** is interesting and can be seen as originating from **B** and **C** (Scheme 3.15) by a hydrogen transfer process from $[Re(CO)_5H]$ to the acyl fragment after metal alkylation. This is then comparable to a similar process studied kinetically by Norton.[32] An intramolecular transfer of the hydrogen atom from the rhenium to the oxygen will result in the formation of an acyl-hydride that is in equilibrium with the hydroxycarbene ligand. Cleavage of the $Re(CO)_5$-fragments form the building blocks of **34**.

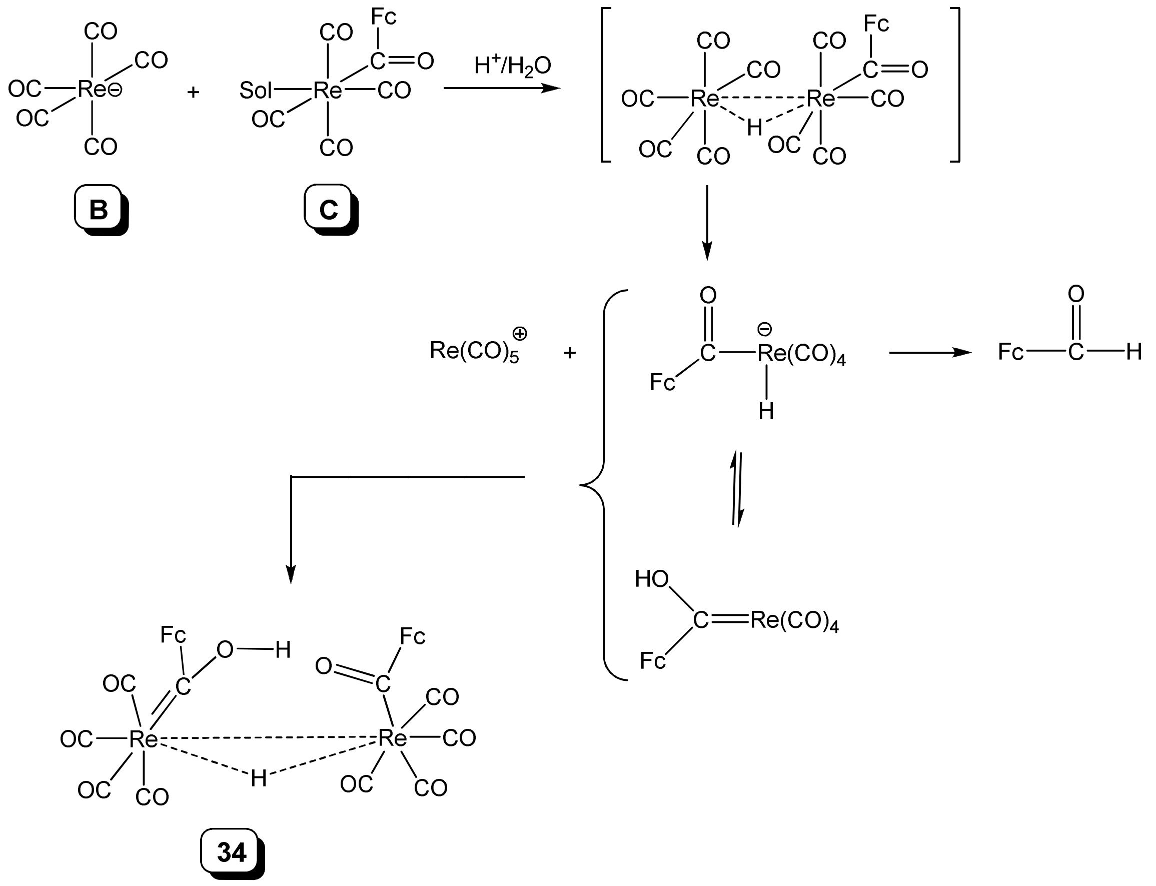

Scheme 3.15

This H-transfer is, however, only one mechanistic possibility for the formation of **34**. Protonation of the initial rhenium acylate, for example after alkylation with Et_3OBF_4 or metalation with $TiCp_2Cl_2$, subsequent hydrolysis reaction during column chromatography can also result in the obtained product. As mentioned before, the equilibrium between the hydroxycarbene and hydrido-acyl intermediates for rhenium cyclopentadienyl complexes has been previously studied and reported by Casey.[44] Unlike in the Casey studies, no monorhenium hydroxycarbene or hydrido-acyl complexes could be isolated and it was assumed that the equilibrium whereby the hydroxycarbene was converted into the acyl-hydride intermediate was favoured.

Complex **34** decomposed in the course of a few days, and subsequent NMR spectroscopy and X-ray diffraction identified one of the decomposition products as biferrocene.[61] The formation of this dimeric byproduct can be rationalized by the ionic nature of the titanoxy substituent, which would favour the rhenium acylate form of the intermediate (Figure 3.11) because of enhanced backbonding from the anionic oxygen to the electrophilic carbene carbon. The ionic nature of titanoxycarbene complexes is supported by structural studies (Chapter 2) and in this study, by the ease of acyl decomplexation. Thus the titanoxycarbene complex acts as an acyl synthon similarly to the situation observed by Barluenga and co-workers for $[Mo(CO)_5\{C(OBX_2)R]$,[62] illustrated in Figure 3.12.

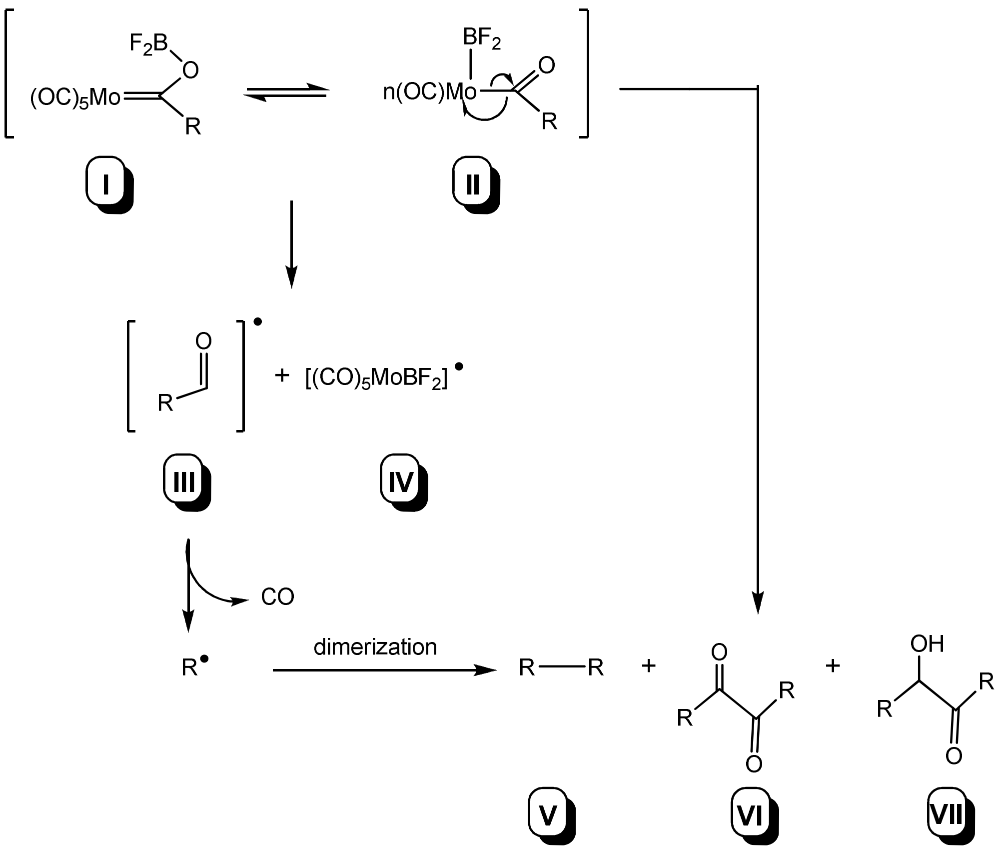

Figure 3.12 Mechanism for the formation of dimerization product **V**

---

[61] (a) Rausch, M.D.; Vogel, M.; Rosenberg, H. *J. Org. Chem.* **1957**, *22*, 900, (b) Rausch, M.D. *J. Am. Chem. Soc.* **1960**, *82*, 2080.

[62] Barluenga, J.; Rodríguez, F.; Fañanás, F.J. *Chem. Eur. J.* **2000**, *6*, 1930.

Homolytic scission of the carbon-metal bond of **II** leads to the acyl radical **III** and the radical species **IV**. Formation of the dimer **V** can be understood as the result of the decarbonylation[63] of **III** and dimerization of the radical species thus obtained.

The third fraction (orange) was spectroscopically characterized as containing formylferrocene (FcCHO), both by its NMR spectra as well as the characteristic C=O vibration in the IR spectrum at 1681 cm^{-1}.[64] Once again, the two possible routes towards formation of FcCHO involves either hydrogen transfer (as illustrated in Scheme 3.13) to the rhenium acylate intermediate (**C**) in Figure 3.11, which can be inferred to yield the product aldehyde after reductive elimination of this ligand. The other possibility involves hydrolysis of the carbene ligand, after which the hydroxycarbene intermediate is converted to the acyl hydride intermediate, as shown in Scheme 3.16. Acyl-hydride elimination is initiated by the reaction of trace amounts of water during chromatography.

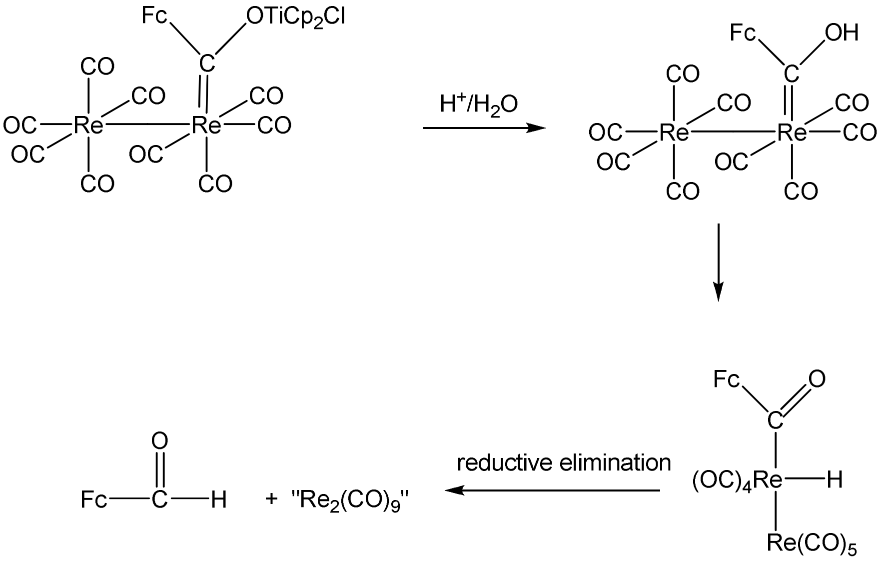

Scheme 3.16

---

[63] (a) Ryu, I.; Sonoda, N. *Angew. Chem., Int. Ed. Engl.* **1996**, *35*, 1050, (b) Chatgilialoglu, C.; Crich, D.; Komatsu, M. ; Ryu, I. *Chem. Rev.* **1999**, *99*, 1991.

[64] (a) Rosenblum, M. *Chem. Ind.* **1957**, *3*, 72, (b) Kamezawa, N. *Journal of Magnetic Resonance* **1973**, *11*, 88.

The fourth band eluted was light yellow in colour. Initially, no ^1H NMR signals could be detected for this compound. However, the IR spectrum revealed the existence of many carbonyl stretches. Final confirmation of the structure of this compound (**29**) was obtained by X-ray crystallography, and the complex was identified as the Fellman-Kaesz complex $[Re_3(CO)_{14}H]$.[65] Re-investigation of the proton NMR spectrum then yielded the expected extreme upfield hydride shift (Table 3.4) at δ: -15.41.

The complex **29** has also been obtained previously in approximately 50% yield from the photochemical reaction of dirhenium decacarbonyl and triphenylsilane[66] or thiophene.[67] The complex can be viewed as a $Re(CO)_5$- and a $Re_2(CO)_9$-fragment bridged by a hydrido ligand. Byers and Brown have suggested a radical mechanism for the formation of this complex, either from $Re_2(CO)_9H$- and $Re(CO)_5$-radicals, or from $Re_2(CO)_9$ and $Re(CO)_5H$. This would support the finding of dimerization to yield biferrocene as discussed before. The transfer of a proton from dichloromethane (solvent) to the reactive rhenium carbonyl anion was indicated by a control NMR spectrum of the reaction mixture immediately before alkylation, and the proposed reaction pathway for the formation of **29** from intermediate **B** (Figure 3.11) is shown in Scheme 3.17.

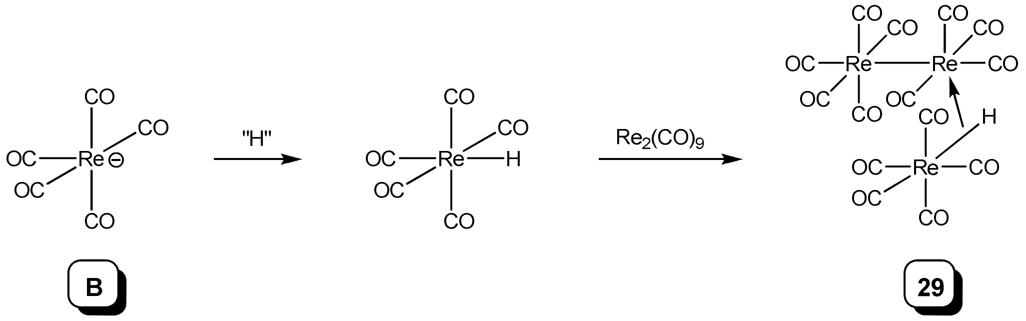

Scheme 3.17

---

[65] Fellman, W.; Kaesz, H.D. *Inorg. Nucl. Chem. Lett.* **1966**, *2*, 63.
[66] Hoyano, J.K.; Graham, W.A.G. *Inorg. Chem.* **1972**, *11*, 1265.
[67] Yang, C.S.; Cheng, C.P.; Guo, L.W.; Wang, Y. *J. Chin. Chem. Soc.* **1985**, *32*, 17.

The fifth fraction obtained was light yellow in colour, and contained $[Re(CO)_5Cl]$. Once again, isolation of this product provides evidence in support of the formation of the $[Re(CO)_5]^-$ anion (ionic mechanism) or the $Re(CO)_5$ radical. Chlorine atom abstraction from solvent dichloromethane[58] or hydride substitution by chlorine[59] would afford the obtained rhenium pentacarbonyl chloro complex. Alternatively, labile chloride ions lost from the titanocene dichloride metalating agent could offer another source of the chlorine atom.

Fraction six yielded an orange coloured solid after separation and purification on the alumina column. Complex **30** was identified as the acyl compound $[Re(CO)_5\{C(O)Fc\}]$. The prevalence of the acyl intermediate **C** proposed earlier in Figure 3.11 is confirmed if one assumes the formation of **30** as being the product of acyl complex **C** and complexation of a carbonyl ligand. This acyl complex has previously been synthesized by Beck *et al.*[68] by reaction of $[CpFe(\eta^5\text{-}C_5H_4C(O)Cl]$ and $[Re(CO)_5]^-$ and structurally characterized. As before, cleaving of the Re-Re bond is observed. The Re-Re bond energy is far less than that of a Re-C(O) or Re-C(OEt)R bond, which again is lower than that of a Re-halide or Re-H bond.[60, 69] This can account for the ease of cleavage and formation of Re-Re bonds during reactions.

The target hexametallic biscarbene complex **33** *ax*, *eq*-$[\{\mu\text{-}TiCp_2O_2\text{-}O,O'\}\{\mu\text{-}Fe(C_5H_4)_2\text{-}C,C'\}\{CRe_2(CO)_9\}_2]$ was eluted as a dark brown-red fraction, displaying a bridging ferrocene and titandioxy substituent between the two carbene ligands. X-ray diffraction studies elucidated the interesting variation in the substitution site of the bridging carbene ligand: on one end, axial substitution of the bridging carbene ligand on a $Re_2(CO)_9$-fragment, on the other, equatorial substitution. Steric constraints are assumed to be responsible for this unique substitution pattern, as the electronically favourable substitution site remains the equatorial site. As for the complexes synthesized in Chapter 2, the remaining chloro ligand of the titanoxy substituent displays enhanced activation and reacts with a second acylate oxygen to form **33**.

---

[68] Breimair, J.; Wieser, M.; Wagner, B.; Polborn, K.; Beck, W. *J. Organomet. Chem.* **1991**, *421*, 55.

[69] Elschenbroich, Ch.; Salzer, A. *Organometallics. An concise introduction* VCH Verlag, Weinheim, **1992**.

The eighth fraction was also deep red in colour. Although a very low yield (<5%) was obtained, the characterization of this complex could be achieved by NMR and IR spectroscopy, as well as mass spectrometry. Complex **32** *eq*-[$Re_2(CO)_9\{C(OTiCp_2Cl)(Fc'CHO)\}$] was identified, formed from a dilithiated ferrocene precursor, with reductive elimination of the $Re_2(CO)_9$-moiety only occurring on one side of the ferrocene, the other retaining its [$Re_2(CO)_9\{C(OTiCp_2Cl)$] metal carbene fragment. The same mechanism as proposed for the formation of FcCHO seems plausible in this case as well. Equatorial substitution of the carbene ligand was assigned from the IR spectrum of this compound. As has been observed from **31** and **33**, both equatorial (electronically favoured) and axial substitution (sterically favoured) are possible.

Finally, product nine was found to be the red monocarbene target complex **31**, *ax*-[$Re_2(CO)_9\{C(OTiCp_2Cl)Fc\}$]. The assignment of an axial carbene ligand substitution was based purely on the infrared data obtained. This complex proved to be the least stable of the Fischer carbene metal cluster complexes. A summary of all the products obtained from this reaction is given in Figure 3.13.

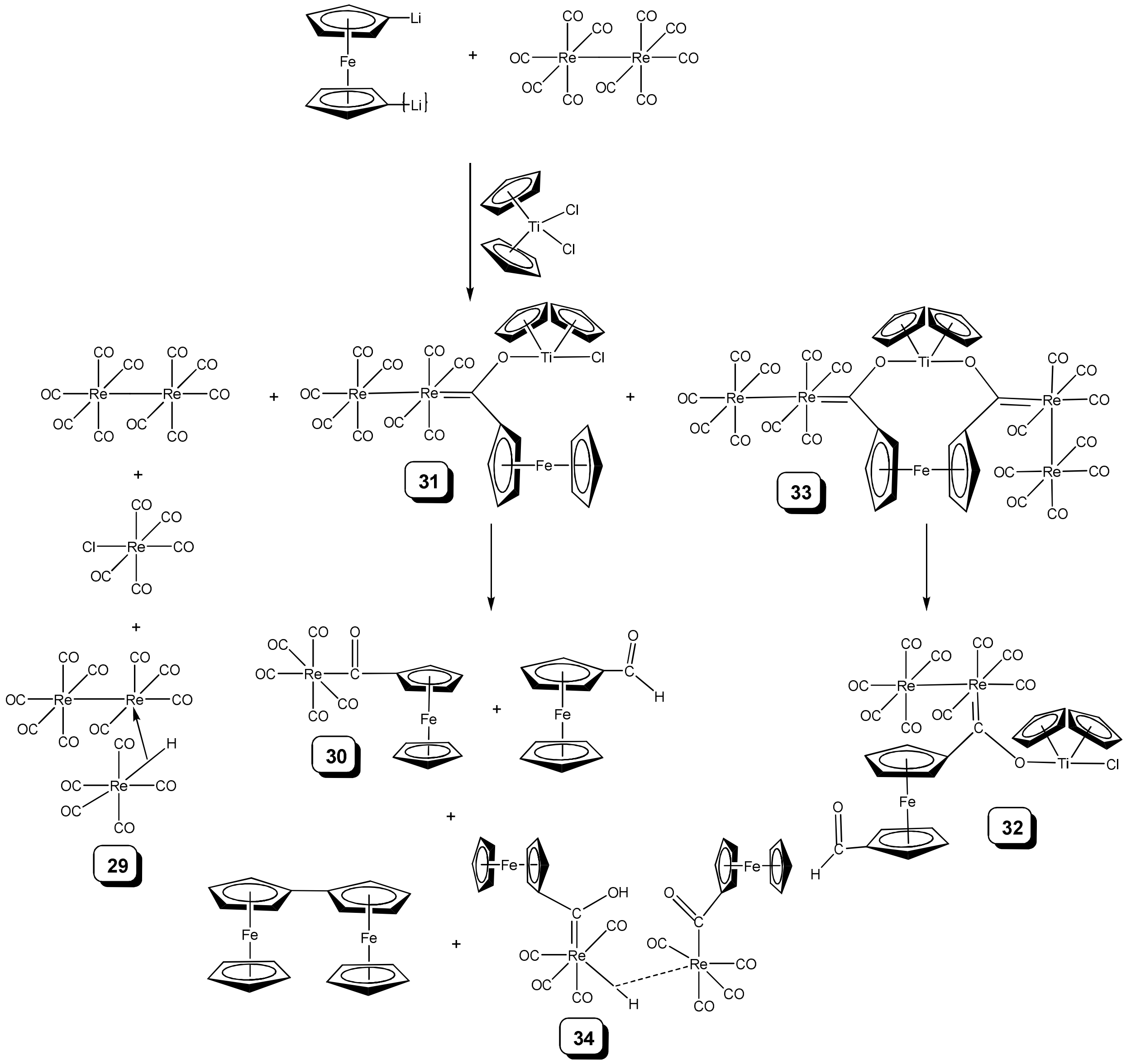

Figure 3.13 Fischer carbene transition metal complexes

3.4 Spectroscopic characterization

The product compounds were characterized using ^{1}H and ^{13}C NMR and IR spectroscopy as well as mass spectrometry and the data confirmed the assigned structures. Further support of the molecular structures was found in solid state crystal structure determinations.

3.4.1 ^{1}H NMR spectroscopy

The proton NMR data of the manganese and rhenium complexes are listed in Tables 3.1 – 3.6, and the relevant numbering scheme employed are illustrated in each table respectively. The spectra of all the manganese carbene complexes were recorded in deuterated benzene as solvent, while chloroform-d[1] was employed for the rhenium complexes, with the exception of **30**. A spectrum of high quality could only be obtained in C_6D_6. Broadening of the signals of the manganese complexes **22** – **24** was observed. In the case of the rhenium complexes, slow decomposition of the products over time was observed.

Table 3. 1 ^{1}H NMR data of ethoxycarbene complexes of manganese

Proton Assignment	Chemical shifts (δ) and coupling constants (J)		
	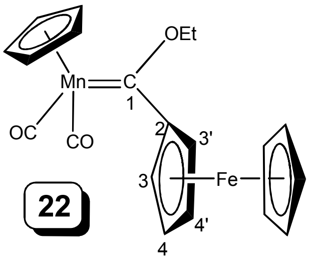 **22**	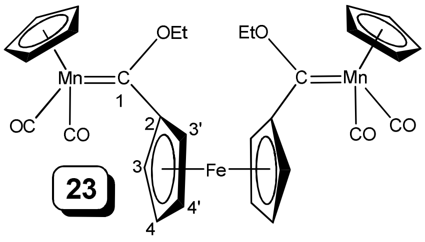 **23**	
	δ*	δ*	J (Hz)
Mn-Cp	4.16, 5H, s	4.12, 10H, s	-
H3, H3'	4.83, 2H, br	4.92, 4H, dd	1.8, 1.8
H4, H4'	4.58, 2H, br	4.57, 4H, dd	2.0, 1.8
Fe-Cp	4.12, 5H, s	-	-
CH_2	4.80, 2H, br	4.82, 4H, q	7.0
CH_3	1.24, 3H, br	1.29, 6H, t	7.0

* Recorded in C_6D_6

For the cyclopentadienyl manganese ferrocenyl carbene complexes, the biscarbene complexes show resonances consistently more downfield than that of the corresponding monocarbene complexes.

As seen for the Group VI transition metal carbene clusters, the H3, H3’ α-proton of the ferrocenyl substituent gives a good indication of the electronic ring substituent involvement with the electrophilic carbene carbon atom, due both to its close proximity and the π-resonance effect, illustrated in Figure 2.15. Downfield shifts are observed in all cases, indicating the electron withdrawing effect of the metal carbonyl fragment bonded to the carbene ligand, as well as the π-delocalization of the ferrocene ring towards stabilizing the electrophilic carbene carbon atom.

Table 3.2 ^{1}H NMR data of titanoxycarbene complexes of manganese

Proton Assignment	Chemical shifts (δ) and coupling constants (J)		
	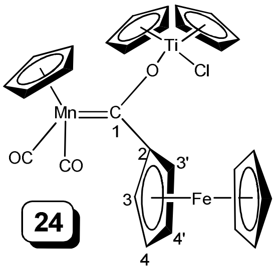 **24**	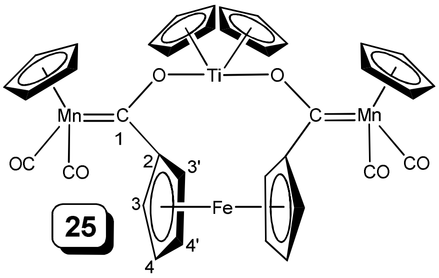 **25**	
	δ*	δ*	J (Hz)
Ti-Cp$_2$	6.20, 10H, s	6.37, 10H, s	-
Mn-Cp	4.03, 5H, s	4.38, 10H, s	-
H3, H3’	4.22, 2H, br	4.28, 4H, dd	1.7, 1.7
H4, H4’	3.87, 2H, br	3.99, 4H, dd	1.7, 1.7
Fe-Cp	4.19, 5H, s	-	-

* Recorded in C$_6$D$_6$

If one employs the formula: Δδ = δ(H3, H3’ of carbene complex) – δ(precursor ring proton), then a direct comparison can be made between carbene complexes containing the same [M(CO)$_n${C(Fc)}]-fragment to determine the effect of the heteroatom carbene substituent (that is, the ethoxy substituent *vs* the titanoxy substituent on the carbene of the same metal). Alternatively, if the carbene ligand is kept constant, either {C(OEt)Fc} or {C(OTiCp$_2$Cl)Fc}, the effect of the central metal moiety on the electrophilic carbene carbon can be estimated (even if spectra were recorded in different deuterated solvents).

Table 3.3 ^{1}H NMR data of ethoxycarbene complexes of rhenium

Proton Assignment	Chemical shifts (δ) and coupling constants (J)				
	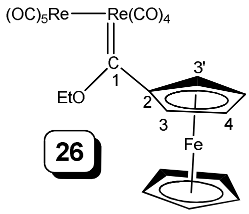 **26**		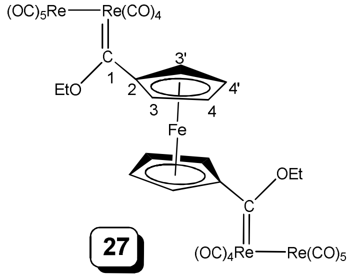 **27**		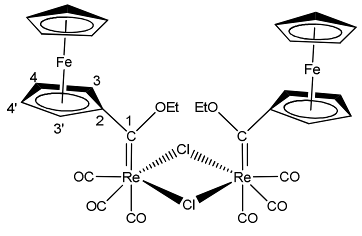 **28**
	δ*†	J (Hz)	δ*	J (Hz)	δ*
H3$_{a,b}$, H3$_{a,b}$’	4.92, 2H, dd *4.91, 2H, dd*	2.2, 1.8 2.2, 2.0	4.88, 4H, dd	3.9, 2.0	4.78, 4H, br
H4$_{eq}$, H4$_{eq}$’ *H4$_{ax}$, H4$_{ax}$’*	4.75, 2H, dd *4.66, 2H, dd*	2.2, 2.2 *1.9, 1.9*	4.63, 4H, dd	3.9, 2.0	4.68, 4H, br
Fe-Cp$_{eq}$ *Fe-Cp$_{ax}$*	4.24, 5H, s *4.27, 5H, s*	-	-	-	4.39, 10H, s
CH$_{2eq}$ ***CH***$_{2ax}$	4.67, 2H, q *4.55, 2H, q*	6.7 *7.2*	4.50, 4H, q	7.1	4.29, 4H, br
CH$_{3ax, eq}$	1.64, 6H, t (overlap)	6.9	1.69, 6H, t	6.9	1.53, 6H, br

* Recorded in CDCl$_3$

† Signal duplication is ascribed to the presence of both axial and equatorial isomers in solution

As seen from Tables 3.1 and 3.2, when the ethoxy substituent of the cyclopentadienyl manganese ethoxycarbene complexes is replaced by a titanoxy substituent, the chemical shift of the H3,3’ proton is shifted upfield (compare for example **22,** Δδ = 0.79 while the titanoxy analogue **24** has Δδ =

0.18, and **23** has Δδ = 0.88 while Δδ = 0.24 for **25**). As for the Group VI ferrocenyl carbene, this indicates the greater electron donating power, or at least stabilization towards carbene carbon atom, of the titanoxy substituent compared to the ethoxy group. This is rationalized by the predominant acyl character of the C-O bond, and the ionic nature of the Ti-O bond, as shown previously in Figure 2.16.

Table 3. 4 ^{1}H NMR data of byproduct rhenium complexes

Proton Assignment	Chemical shifts (δ) and coupling constants (J)		
	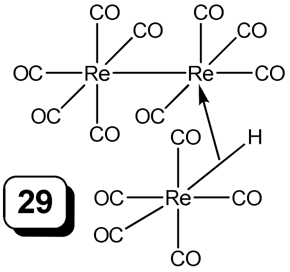 **29**	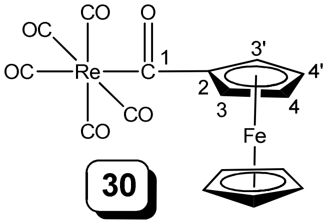 **30**	
	δ*	δ**	J (Hz)
H3, H3'	-	4.49, 2H, dd	2.7, 2.4
H4, H4'	-	4.04, 2H, dd	2.7, 2.8
Fe-Cp	-	3.85, 5H, s	-
Re-H	-15.41, 1H, s	-	-

* Recorded in $CDCl_3$
** Recorded in C_6D_6

Duplication of all the chemical shifts is observed for complex **26** (Figure 3.14). In solution, both the axial and equatorial isomers are present in a ratio of approximately 1:1. Two-dimensional NMR experiments were used to distinguish between the two sets of signals, as listed in Table 3.3. It is anticipated that the carbene in the axial position will have the Re-atom more involved in π-backbonding because of poor π-interaction with the second Re-metal (Re-Re bond). As a result, less electron donation is expected from the Fc ligand and upfield resonances for H3 and H4, compared to the equatorial isomer, is expected. The remote ethoxy CH_3-group is hardly influenced, and only one triplet is observed; however integration of the signal confirmed the resonance as that of six hydrogens, therefore two CH$_3$-groups.

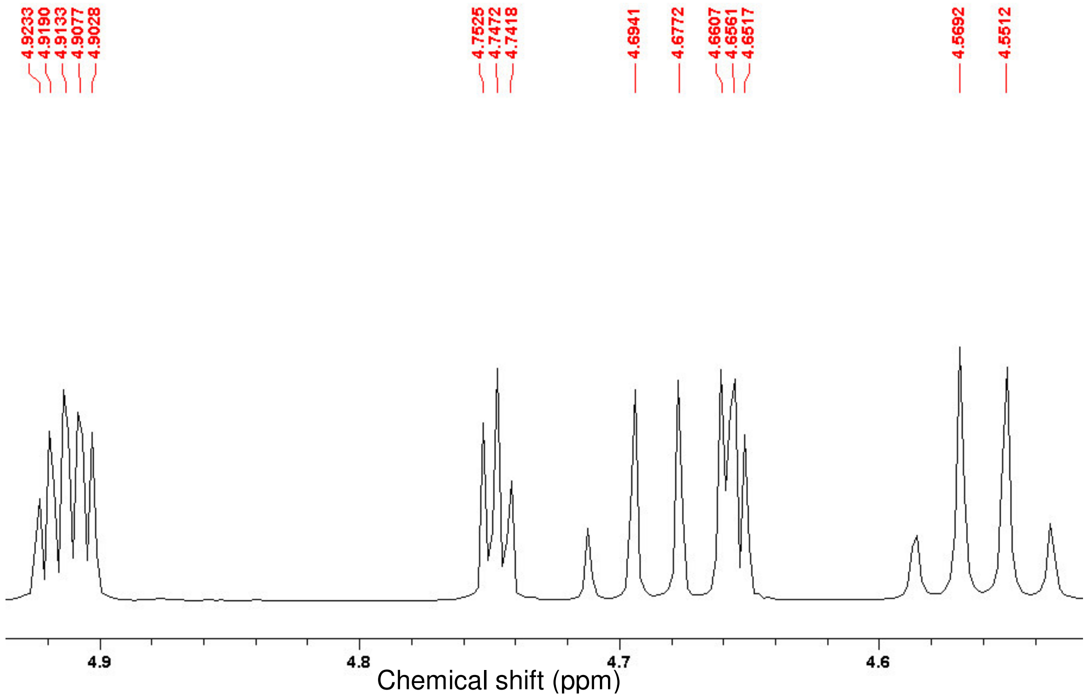

Figure 3.14 Excerpt of the ^{1}H NMR spectrum of **26** displaying presence of both equatorial and axial isomers in solution

Table 3.5 ^{1}H NMR data of titanoxycarbene complexes of rhenium

Proton Assignment	Chemical shifts (δ) and coupling constants (J)	
	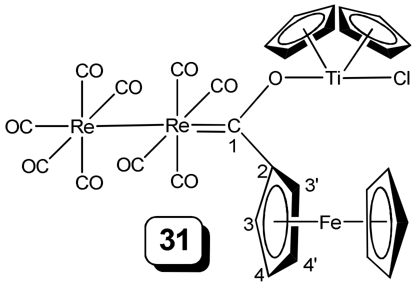 **31**	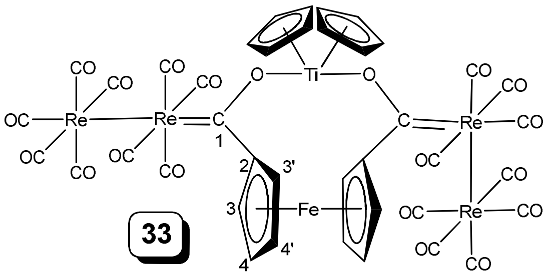 **33**
	δ*	δ*
Ti-Cp$_2$	6.57, 10H, s	6.71, 10H, s
H3, H3’	4.98, 2H, br	4.97, 4H, br
H4, H4’	4.71, 2H, br	4.76, 4H, br
Fe-Cp	4.39, 5H, s	-

* Recorded in $CDCl_3$

Table 3. 6 ^1H NMR data of byproduct rhenium carbene complexes

Proton Assignment	Chemical shifts (δ) and coupling constants (J)	
	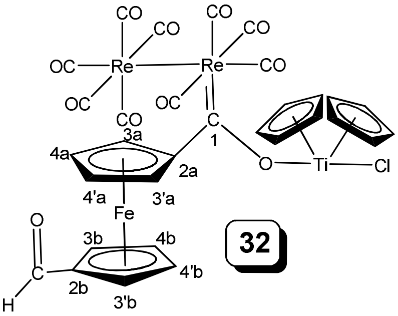 **32**	**34** 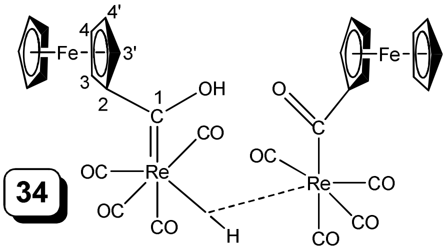
	δ*	δ*
CH**O**	9.97, 1H, s	-
C(O**H**)	-	9.93, 1H, s
Ti-Cp_2	6.56, 10H, s	-
$H3_a$, $H3_a$' *$H3_b$, $H3_b$'*	4.91, 2H, br *4.78, 2H, br*	5.03, 4H, br
$H4_a$, $H4_a$' *$H4_b$, $H4_b$'*	4.71, 2H, br *4.60, 2H, br*	4.98, 4H, br
Fe-Cp		4.70, 10H, br
Re-H		-15.59, 1H, s

* Recorded in $CDCl_3$

For the two ferrocenyl ethoxycarbene rhenium complexes (*mono*-**26** and *bis*-**27**, the chemical resonances of the H3,3' protons are very similar, resulting in close values for Δδ: 0.72 and 0.69 ppm respectively. However, the bridged bischloro ferrocenyl biscarbene **28** contains an X-μ-L type ligand[7] for each metal centre, resulting in greater electron density available on the metal centres for backdonation towards the carbene carbon atom. This cascade effect results in less involvement of the ferrrocenyl rings towards carbene stabilization, and a resultant higher field chemical shift of the α-prontons.

If the carbene ligand is kept constant for comparison, all of the different metal moieties can be listed in order of electron donating power,[22] as illustrated in Figure 3.15. The cyclopentadienyl manganese group is proven to have the greatest π-electron donor strength, while the dirhenium nonacarbonyl fragment is the strongest electron withdrawing group.

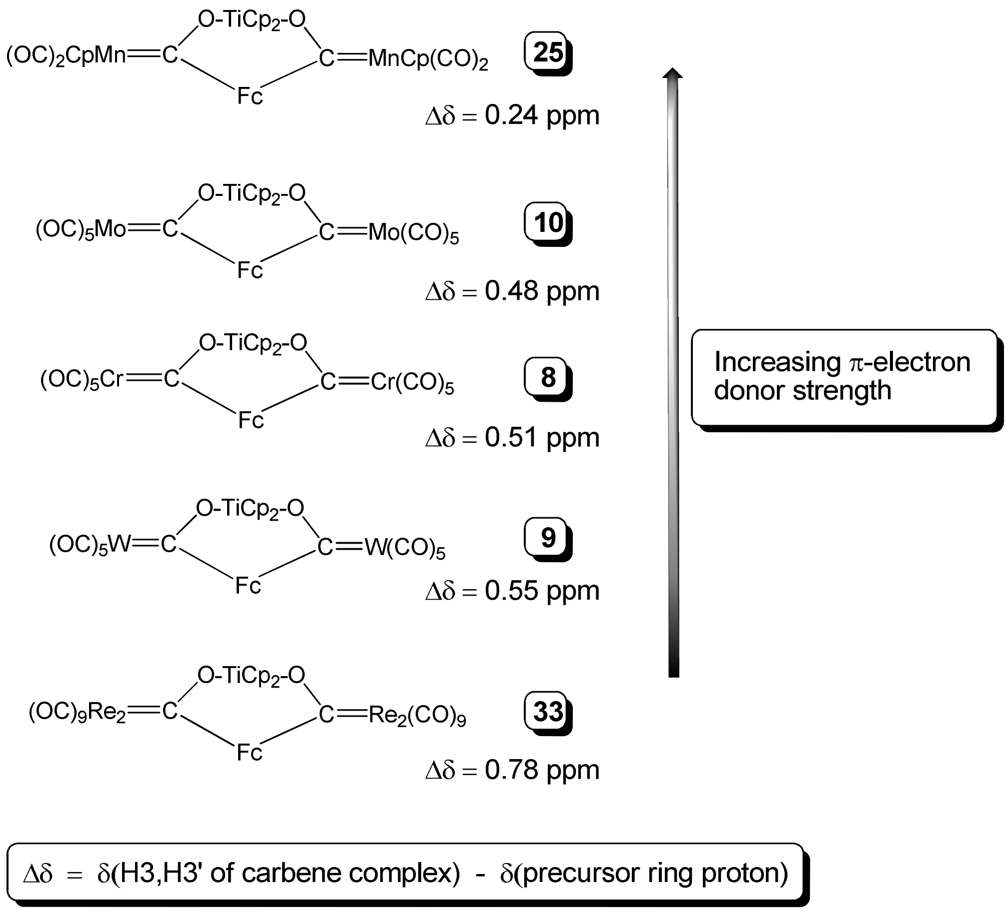

Figure 3.15 Central metal moiety effect on the carbene ligand

Table 3.6 lists the data of the two modified rhenium carbene complexes, **32** and **34**. In both cases, greater downfield shifts of H3,3’ are observed than in any other case. Specifically for the acyl-hydrido hydroxycarbene complex **34**, the carbene heteroatom substituent cannot contribute towards π-stabilization of the carbene, therefore much greater influence is felt on the ferrocenyl ring, and a Δδ-value of 0.99 is calculated for this complex.

Complex **34** is unusual in that it exhibits a hydroxycarbene trapped in a dinuclear acyl-hydroxycarbene, and also displays a bridging rhenium hydride. The two most significant signals in the spectrum are the highfield and lowfield signals that correspond to the hydridic and the protonic hydrogen atoms of the complex. The peak at 9.93 ppm is assigned to the protonic hydrogen. This hydrogen atom is, however, not as deshielded as that of the analogous thienyl acyl-hydrido/hydroxycarbene prepared by Olivier.[31] For the thienyl acyl hydroxycarbene, a singlet at δ: 21.5 was assigned to the protonic hydrogen. In the case of the Shvo catalyst (Figure 3.7), better agreement was found with the value obtained in this study, where the Shvo proton displays a chemical shift of around 8 ppm[49] compared to the value of 9.93 ppm found for the ferrocenyl acyl-hydrido hydroxycarbene. This could indicate that the protonic hydrogen of **34** is not O-H-O bridging, possibly due to steric reasons, so that a conformation of **34** where the acyl fragment is twisted to the opposite side of the hydroxycarbene ligand is found. As speculated in Scheme 3.18, the resulting weaker link between the two Re-fragments, and the orientation of the bridging hydride and acyl would assist in aldehyde elimination/decomposition. The bridging hydride value of -15.59 ppm is also in good agreement with the values obtained for the corresponding thienyl complex (δ: -15.7) and the Shvo catalyst (δ: -17.9).

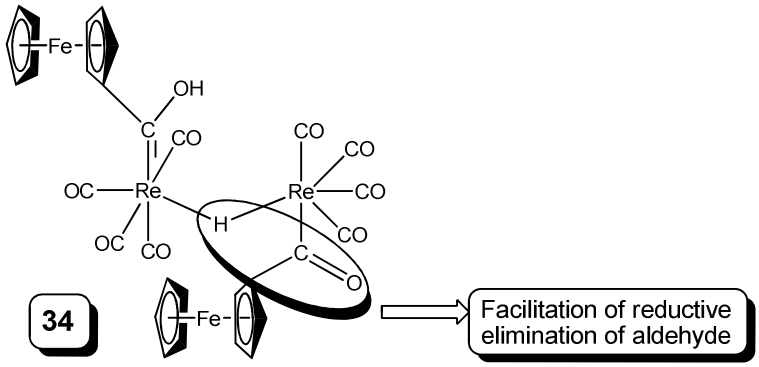

Scheme 3.18

It is interesting to note that complex **34** appears to have a symmetrical structure at room temperature in solution, as the signals for the two ferrocenyl ligands coincide. Therefore the two constituent parts lose their individual identity, and two resonance structures can be drawn to support this statement as the extended double bond character of the Re-C(carbene) and C(carbene)-O bonds in Scheme 3.19 demonstrates. However, this factor disputes the speculation on the opposite orientation of the hydroxycarbene and acyl ligands.

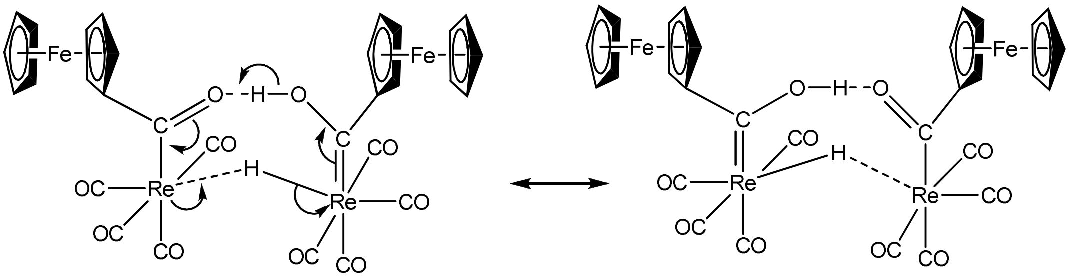

Scheme 3.19

3.4.2 ^{13}C NMR spectroscopy

The ^{13}C NMR data for the manganese complexes are summarized in Tables 3.7 and 3.8, while the data of the rhenium complexes are listed in Tables 3.9 – 3.12. The same atom numbering scheme is used as for the ^{1}H NMR spectra in Section 3.4.1.

Table 3.7 ^{13}C NMR data of ethoxycarbene complexes of manganese

Carbon Assignment	Chemical shifts (δ)	
	22	**23**
	δ*	δ*
C1	328.5	336.5
Mn-CO	232.0, 230.4	231.9
C2	95.9	96.5
Mn-Cp	83.8	84.0
C3, C3’	73.6	73.9
C4, C4’	72.3	72.3
Fe-Cp	71.3	-
CH_2	73.7	74.7
CH_3	14.8	15.3

* Recorded in C_6D_6

Table 3.8 ^{13}C NMR data of titanoxycarbene complexes of manganese

Carbon Assignment	Chemical shifts (δ)	
	24	**25**
	δ*	δ*
C1	321.8	338.4
Mn-CO	n.o.	233.7
Ti-Cp_2	118.2	117.7
C2	n.o.	n.o.
Mn-Cp	82.7	85.7
C3, C3’	71.3	69.3
C4, C4’	70.1	68.2
Fe-Cp	64.2	-

* Recorded in C_6D_6

The carbene carbon resonances of the cyclopentadienyl manganese complexes fall well within the range expected for CpMn-carbene complexes.[70]

As in the proton NMR spectra, the biscarbene complexes' chemical resonances are consistently lower field than the corresponding monocarbene complexes. Especially prominent are the carbene carbon chemical shifts, which show differences of 8 – 17 ppm. This downfield shift of the biscarbene carbon resonance compared to the monocarbene resonance is not observed for the rhenium complexes.

Table 3.9 ^{13}C NMR data of ethoxycarbene complexes of rhenium

Carbon Assignment	Chemical shifts (δ) and coupling constants (J)		
	26	**27**	**28**
	$\delta^{*\dagger}$	δ^{*}	δ *
C1$_{eq}$ *C1*$_{ax}$	306.3 275.6	307.7	n.o.
Re-CO$_{eq,\ ax}$ *(overlap)*	199.2, 199.1, 194.9, 193.1, 189.7	198.8, 194.6, 192.3, 189.2	199.2, 191.9
C2$_{eq}$ *C2*$_{ax}$	98.8 *96.1*	102.0	n.o.
C3$_{eq}$ *C3*$_{ax}$'	n.o. (overlap solvent signal)	74.7	74.0
C4$_{eq}$ *C4*$_{ax}$'	73.2 *72.6*	72.8	71.8
Fe-Cp$_{eq}$ *Fe-Cp*$_{ax}$'	70.7 70.4	-	70.7
CH$_{2eq}$ *CH*$_{2ax}$	*76.3* *74.0*	77.8	76.3
CH$_{3eq,\ ax}$ *(overlap)*	14.8	14.8	14.8

* Recorded in CDCl$_3$

† Signal duplication is ascribed to the presence of both axial and equatorial isomers in solution

---

[70] Mann, B.E. *Adv. Organomet. Chem.* **1974**, *12*, 135.

The titanium Cp-rings in the manganese monocarbene complex **24** rotate freely in solution, as is evident from a single peak for the Cp-protons as well as carbon atoms in the NMR spectra, while the ^{13}C NMR spectrum of the ferrocenyl monocarbene rhenium complexes **31** and **32** display two signals. This observation is ascribed to restricted rotation of the C(carbene)-C(Fc) bond caused by the proximity of the bulky metal substituents. For the biscarbene complexes **25** and **33**, the symmetry of the structures precludes electronic inequivalency and only one titanium Cp-resonance is seen.

Table 3.10 ^{13}C NMR data of byproduct rhenium complexes

Carbon Assignment	Chemical shifts (δ)	
	29	**30**
	δ*	δ*
C1	-	234.8
Re-CO	196.1, 190.6 (*ax*-$(CO)_9$) 186.5, 186.3, 178.9 (*eq*-$(CO)_9$) 183.6 (*cis*-$(CO)_5$) 176.8 (*trans*-$(CO)_5$)	191.9, 183.9, 181.6
C2	-	n.o.
C3, C3’	-	80.4
C4, C4’	-	72.7
Fe-Cp	-	69.7

* Recorded in $CDCl_3$

Well-resolved carbonyl signals were observed for **29**. The downfield resonances are assigned to the less shielded $Re_2(CO)_9$-fragment, while the $Re(CO)_4H$-fragment display two resonances more upfield. The carbonyl *trans* to the hydride ligand receives more π-electron backdonation from the metal, and is therefore assigned the highest field signal, while competition between two π-accepting CO ligands *trans* to each other leads to less shielding, and a downfield shift of the *cis*-CO ligands of the $Re(CO)_4$-group.

When comparing the carbene carbon resonances of the ethoxycarbene complexes (**26**, **27**) with those of the titanoxycarbene carbons (**32**, **33**), a clear upfield shift of the titanoxy analogues would seem to support the finding that the titanoxy fragment better stabilizes the carbene carbon atom than an ethoxy group (similarly to the results obtained form proton NMR spectra and the comparison of the H3,3' chemical shifts).

Table 3.11 ^{13}C NMR data of titanoxycarbene complexes of rhenium

Carbon Assignment	Chemical shifts (δ)	
	31	**33**
	δ*	δ*
C1	n.o.	272.6
Re-CO	178.9, 176.9	199.8, 193.8, 192.5, 186.9, 186.3, 186.2
Ti-Cp_2	120.1, 118.9	125.8
C2	85.1	95.5
C3, C3'	76.3	74.1
C4, C4'	71.5	72.2
Fe-Cp	70.5	-

* Recorded in $CDCl_3$

The ^{13}C NMR spectrum of **26** displays duplication of the signals similar to that observed in the ^{1}H NMR spectrum (Figure 3.14). Similarly to the proton spectrum, a tentative assignment of the axial and equatorial isomers can be made. For the equatorially substituted complex, the carbene ligand would be *trans* to the greater π-acceptor group, a carbonyl ligand, and would therefore be less shielded and the carbene carbon would resonate more downfield. For an axially substituted carbene complex, the group *trans* to the carbene ligand would be the $Re(CO)_5$-fragment, an X-type ligand. The isomer with carbene carbon δ:

306.3, can therefore be assumed to be the equatorial carbene complex, and the other isomer (carbene carbon δ: 275.6) as the axial isomer.

Complex **30** contains an acyl functionality, where the C=O chemical shift occurs at 234.8 ppm. In contrast, the most downfield carbene carbon atom resonance, 307.7 ppm, is that of complex **27**, the bisethoxycarbene complex. An intermediate value of 272.6 ppm is observed for the titanoxy biscarbene complex **33**. For the acyl-hydrido hydroxycarbene complex **34**, both the acyl (δ: 231.5) and the extremely downfield hydroxycarbene signal (δ: 346.2) are observed. The observation of these separate resonances would indicate that doubt about the presence of the bridging O-H-O hydrogen bond in solution is justified, and supports the speculated arrangement given in Scheme 3.18. In contrast, the ferrocenyl and carbonyl signals coincide as for a symmetrical system (observed in the ^{1}H NMR system, as well as for the acyl hydroxycarbene of Olivier[31]).

Table 3.12 ^{13}C NMR data of byproduct carbene complexes of rhenium

Carbon Assignment	Chemical shifts (δ)	
	32	**34**
	δ*	δ*
C1	287.0	346.2, 231.5
Re-CO	200.9, 195.7	185.9
CHO	178.9	
Ti-Cp_2	120.2, 119.2	-
C2	n.o.	n.o.
$C3_{a,b}$, $C3'_{a,b}$	74.5, 73.2	76.0
$C4_{a,b}$, $C4'_{a,b}$	71.3, 69.6	74.0
Fe-Cp	-	70.8

* Recorded in $CDCl_3$

3.4.3 IR spectroscopy

The number and intensities of carbonyl stretching frequencies are dependent on the local symmetry of the carbonyl ligands around the central atom. The IR spectra of the carbonyl vibration of cyclopentadienyl manganese mono- and biscarbene complexes show two bands: the IR-active υ(CO) A_1 and B_1 band. The A_1 band occurs at higher frequency, but the bands have roughly equal intensity.[71]

The infrared data (recorded in dichloromethane) of the manganese complexes are summarized in Table 3.13. Complex **24** decomposed during measurement, and no resolved spectrum of this compound could be obtained.

As expected, the ethoxycarbene complexes displayed carbonyl stretching vibrations at higher frequencies, implying stronger Mn-C(carbene) backbonding compared to the titanoxycarbene **25**.

Table 3.13 Infrared data of manganese cluster carbene complexes

Complex	$MCp(CO)_2$ assignment, [ν(CO), cm^{-1}]*	
	A_1	B_1
22	1938 vs	1862 s
23	1927 vs	1858 s
25	1922 vs	1849 s

* Spectra recorded in CH_2Cl_2

The carbonyl stretching modes of equatorially and axially substituted bimetal nonacarbonyl complexes were summarized by Ziegler *et al.*[72] The *eq*-$[M_2(CO)_9L]$ displays a nine band pattern in the IR spectrum, corresponding to C_s symmetry (Figure 3.16). These bands include six A' bands and three degenerate A'' bands. On the other hands, the IR spectrum of *ax*-$[M_2(CO)_9L]$ is observed to

---

[71] Adams, D.M. *Metal-Ligand and Related Vibrations,* Edward Arnold Publishers Ltd., London, **1967**, 98.

[72] Ziegler, M.L.; Haas, H.; Sheline, R.K. *Chem. Ber.* **1965**, *98,* 2454.

have only five bands: three A' bands and two E bands, according to C_{4v} symmetry (Figure 3.17).

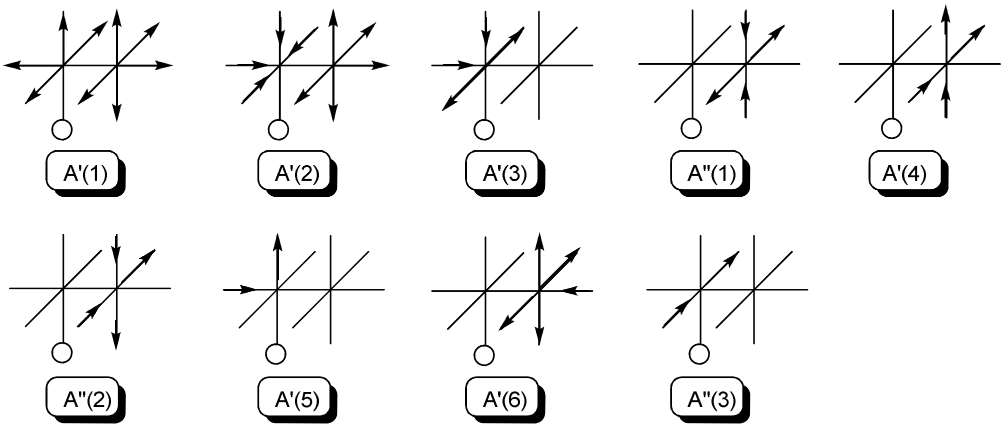

Figure 3.16 IR-active normal modes observed for *eq*-[$M_2(CO)_9L$]

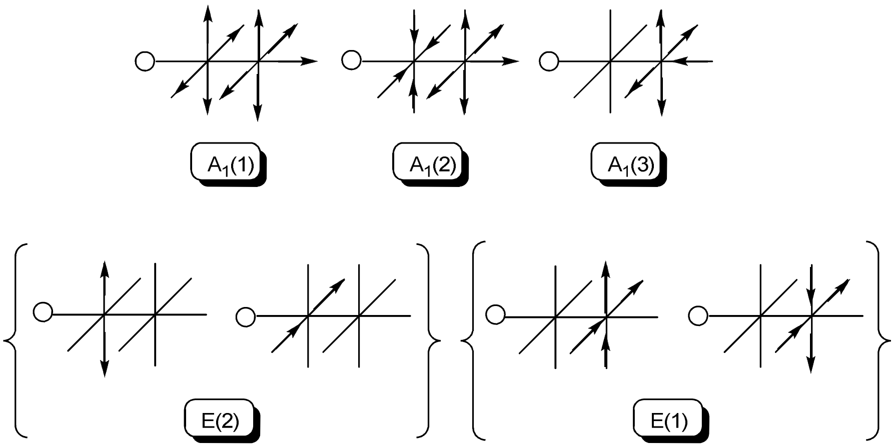

Figure 3.17 IR-active normal modes observed for *ax*-[$M_2(CO)_9L$]

Due to the low solubility of the rhenium complexes in the nonpolar solvent hexane, the IR spectra of all complexes were recorded in dichloromethane. Dichloromethane does not have the same resolution power as hexane, and results in both lifting of band degeneracy in DCM, and a great extent of band overlap. Assignment of the carbonyl bands were therefore considerably complicated, and no clear distinction between the equatorial and axial isomers could be made. Instead, the observed bands are listed in Table 3.14.

Table 3.14 Infrared data of octahedral dirhenium nonacarbonyl complexes

Complex	Carbonyl stretching frequencies (cm^{-1})*
26	Mixture: *eq*-$M_2(CO)_9$ and *ax*-$M_2(CO)_9$ Overlapping bands: 2101 w, 2039 m, 1996 vs, 1970 m, 1938 m
27	*eq*-$M_2(CO)_9$ Overlapping bands: 2102 m, 2038 m, 1995 vs, 1968 sh, 1940 m
28	*fac*-$M(CO)_3$, from precursor *cis*-$M(CO)_4$ 2101 m (A_1^1), 2036 m (A_1^2), 1991 s (B_1), 1936 m (B_2)
29	Combination: *eq*-$M_2(CO)_9$ and $M(CO)_5$ Overlapping bands: 2147 w, 2101 s, 2046 vs, 2016 m, 1989 vs, 1922 m
30	$M(CO)_5$ 2140 m (A_1^2), 2038 m (B_1), 2010 s (A_1^1), 1975 vs (E), 1565 m (acyl)
31	*ax*-$M_2(CO)_9$ 2156 w (A_1^1), 2064 w (A_1^2), 2046 vs(E_1), 1985 s (A_1^3), 1929 m (E_2)
32	*eq*-$M_2(CO)_9$ Overlapping bands: 2099 w, 2046 m, 2023 m, 1988 vs, 1953 m, 1917 s, 1883 w, 1684 w (CHO)
33	Combination: *eq*-$M_2(CO)_9$ and *ax*-$M_2(CO)_9$ Overlapping bands: 2098 m, 2084 w, 2046 vw, 2027 m, 2005 s, 1991 vs, 1958 m, 1933 m, 1919 m
34	Two different systems of *cis*-$M(CO)_4$ 2083 w(A_1^2, 2069 w (A_1^2, 2012 vs (B_1), 1985 sh (B_1) 1971 m (A_1^1), 1955 m (A_1^1), 1926 w (overlap, B_2), 1610 w (acyl)

* Spectra recorded in CH_2Cl_2

For **26** (a mixture of equatorial and axial $M_2(CO)_9$-systems), **27** (*eq*-$M_2(CO)_9$), **29** (a combination of an *eq*-$M_2(CO)_9$ and an $M(CO)_5$-system), **32** (*eq*-$M_2(CO)_9$) and **33** (a combination of an *eq*-$M_2(CO)_9$ and an *ax*-$M_2(CO)_9$-system), band overlap prevented band assignment. The facially substituted, octahedral $M(CO)_3$-system of complex **28** resulted in four νCO bands. For a *fac*-$M(CO)_3L_3$ octahedral complex, two IR active bands are expected, namely the A_1 band (at higher frequency) and the E band, roughly twice the intensity of the A_1 band as well as broader, due to partial lifting of the degeneracy by asymmetric ligands.[71] This pattern was not obtained. Instead, the four bands displayed the pattern expected for a *cis*-$M(CO)_4L_2$ system, containing two A_1 bands, a B_1 and a B_2 band that are IR active. This was ascribed to the precursor *cis*-[Re(CO)$_4${C(OEt)Fc}Cl] that is present during the formation of **28**, as depicted in Scheme 3.13.

For complex **30**, the expected $M(CO)_5L$-pattern of four bands for pseudo-C_{4v} symmetry is obtained, in good agreement with literature values.[68] However, literature records the presence of two acyl bands at 1572 and 1543 cm^{-1}, while only one band at 1565 cm^{-1} was observed in this study.
The five νCO bands corresponding to *ax*-$M_2(CO)_9L$ was observed for **31**.

Acyl hydrido hydroxycarbene **34** displayed a duplication of signals, similarly to that of **28**. A *cis*-$M(CO)_4L$ system should display four IR active bands; two A_1 bands, a B_1 and a B_2 band. The signal duplication would seem to support the finding of a non-symmetrical structure of **34**, precluding the presence of an O-H-O bridge. Further support of this comes from the presence of the distinct acyl C-O stretching frequency at 1610 cm^{-1}, therefore the speculated arrangement of **34** in Scheme 3.18, rather than the orientation suggested in Scheme 3.19, seems more plausible.

3.4.4 Mass spectrometry

FAB-MS methods in a 3-nitrobenzyl alcohol matrix were employed to record the mass spectra of the manganese carbene complexes **23** – **25**, and the mass spectral data are summarized in Table 3.15. No molecular ion peak (M^+), nor any other m/z peak could be identified for **22**.

Limited information could be obtained from the mass spectral data listed below. The molecular ion peak was identified in all three cases, as well as the peak representing the fragment ion after loss of two carbonyl ligands, evidence of correct structure assignment. For both **23** and **24**, loss of the heteroatom carbene substituent was observed as well. Connor *et al.* reported a novel metal-extrusion process for the $[Mn(MeCp)(CO)_2\{C(OMe)Fc\}]$ complex where the ion $[Mn(MeCp)Fc]^+$ lost manganese to give $[MeCpFc]^+$ as well as the dimerisation product olefin, $[Fc\{C(OEt)\}]_2$.[22] None of these peaks could be identified during this study.

Table 3.15 Mass spectral data of manganese carbene complexes

Complex	m/z	Intensity (%)	Fragment Ion
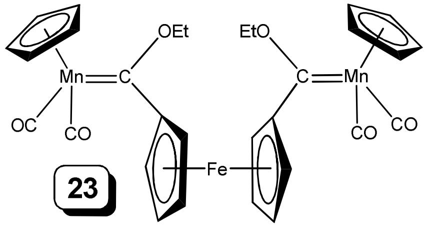 **23**	650 594 577	3.5 4.2 2.8	$[M]^+$ $[M-2CO]^+$ $[M-CO-OEt]^+$
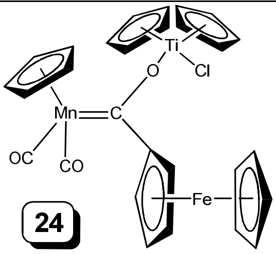 **24**	603 511 389	1.5 2.0 15.0	$[M]^+$ $[M-2CO-Cl]^+$ or $[M-CO-Cp]^+$ $[M-TiCp_2Cl]^+$
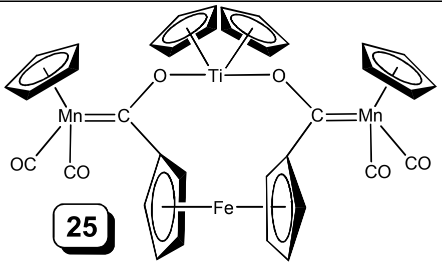 **25**	770 714	1.1 0.8	$[M]^+$ $[M-2CO]^+$

No mass spectrum could be obtained for complex **30**, and no M^+ molecular ion peaks were observed for complexes **28** and **33**. The mass spectral data of all rhenium complexes barring that of **30** are listed in Table 3.16.

Stepwise fragmentation of the carbonyl ligands, followed by loss of the terminal $Re(CO)_5$-fragments were observed consistently for all of the rhenium complexes (Figure 3.18). For the ethoxycarbene complexes, loss of the carbene substituents (either the ferrocenyl or ethoxy substituents) did not feature in the fragmentation pattern, although the bridged dichloro biscarbene complex **28** did display loss of the bridging chloro ligands.

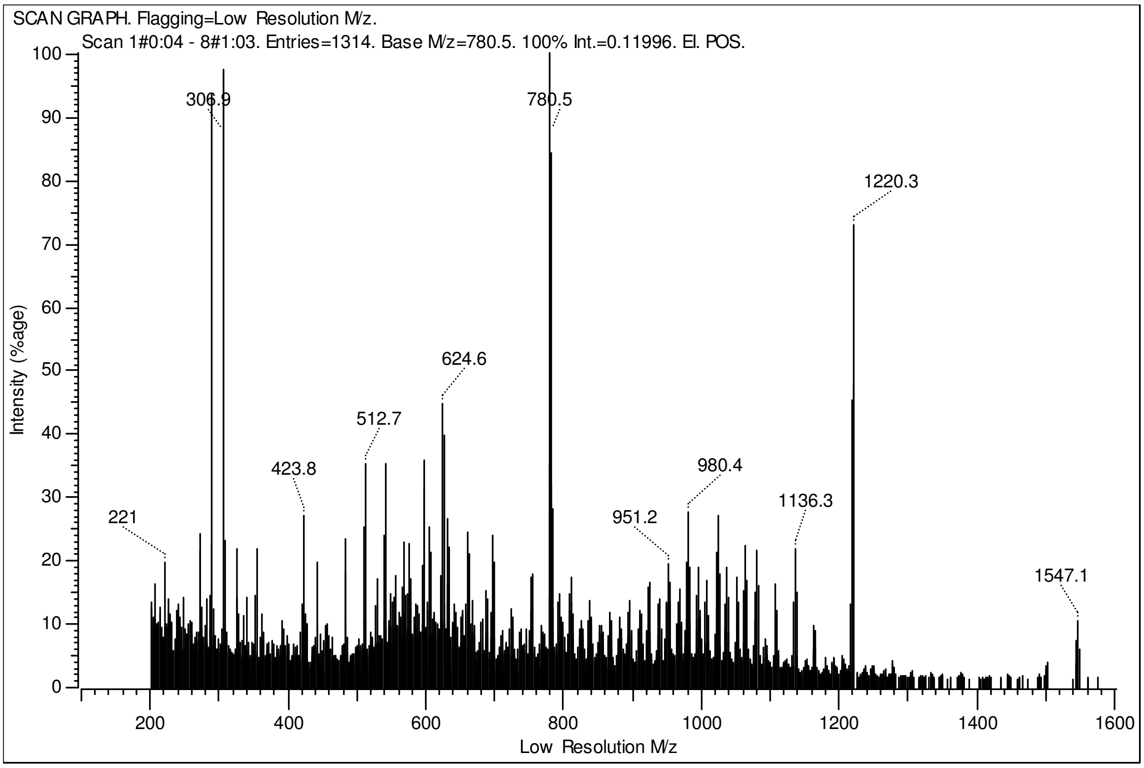

Figure 3.18 Stepwise loss of CO ligands, followed by subsequent loss of $Re(CO)_5$-units in the mass spectrum of complex **27**

In contrast, the mass spectra of the titanoxycarbene rhenium complexes show loss of both titanocene (chloride) and ferrocenyl, to yield the corresponding acyl complexes. In some cases, loss of the entire carbene ligand was observed. The decomposition aldehyde (FcCHO) and dimerization product biferrocene were observed in the mass spectra of compounds **32** and **34** respectively, and re-formation of the precursor dirhenium decacarbonyl was seen for **34**.

Table 3.16 Mass spectral data of rhenium complexes

Complex	m/z	Intensity (%)	Fragment Ion
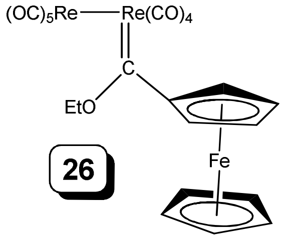 **26**	867	1.7	$[M]^+$
	782	0.5	$[M - 3CO]^+$
	541	8.1	$[M - Re(CO)_5]^+$
	513	6.5	$[M - Re(CO)_5 - CO]^+$
	484	7.2	$[M - Re(CO)_5 - 2CO]^+$
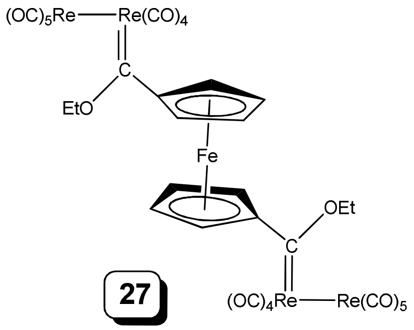 **27**	1547	11	$[M]^+$
	1502	40	$[M - OEt]^+$
	1491	20	$[M - 2CO]^+$
	1220	75	$[M - Re(CO)_5]^+$
	1164	11	$[M - Re(CO)_5 - 2CO]^+$
	1136	22	$[M - Re(CO)_5 - 3CO]^+$
	1108	16	$[M - Re(CO)_5 - 4CO]^+$
	1080	22	$[M - Re(CO)_5 - 5CO]^+$
	1052	17	$[M - Re(CO)_5 - 6CO]^+$
	1024	27	$[M - Re(CO)_5 - 7CO]^+$
	980	28	$[M - 2Re(CO)_5]^+$
	952	19	$[M - 2Re(CO)_5 - CO]^+$
	867	14	$[M - 2Re(CO)_5 - 2CO]^+$
	811	13	$[M - 2Re(CO)_5 - 3CO]^+$
	781	10	$[M - 2Re(CO)_5 - 4\ CO]^+$
	755	19	$[M - 2Re(CO)_5 - 5CO]^+$
	699	21	$[M - 2Re(CO)_5 - 7CO]^+$

Table 3.16 *contd. 2* Mass spectral data of rhenium complexes

Complex	m/z	Intensity (%)	Fragment Ion
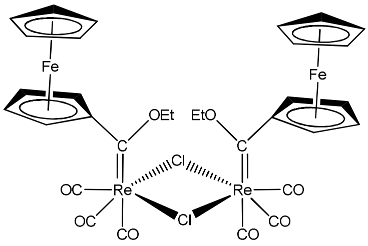 **28**	541	48	$[M - Re(CO)_3Cl\{C(OEt)\} - Cl]^+$
	513	32	$[M - Re(CO)_3Cl\{C(OEt)\} - Cl - CO]^+$
	485	42	$[M - Re(CO)_3Cl\{C(OEt)\} - Cl - 2CO]^+$
	457	12	$[M - Re(CO)_3Cl\{C(OEt)\} - Cl - 3CO]^+$
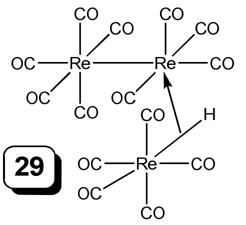 **29**	952	48	$[M]^+$
	811	7.5	$[M - 5CO]^+$
	783	6	$[M - 6CO - H]^+$
	625	100	$[Re_2(CO)_9]^+$
	598	62	$[M - Re(CO)_5H - CO]^+$
	569	16	$[M - Re(CO)_5H - 2CO]^+$
	542	5	$[M - Re(CO)_5H - 3CO]^+$
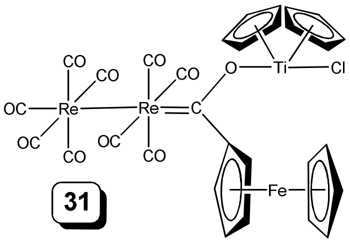 **31**	1052	0.7	$[M]^+$
	1015	0.5	$[M - Cl]^+$
	995	0.3	$[M - 2CO]^+$
	725	8.0	$[M - Re(CO)_5]^+$
	690	2.4	$[M - Re(CO)_5 - Cl]^+$
	653	2.4	$[M - TiCp_2Cl - Fc]^+$
	625	2.1	$[M - \{C(OTiCp_2Cl)Fc\}]^+$
	597	1.9	$[M - \{C(OTiCp_2Cl)Fc\} - CO]^+$
	512	6.0	$[M - \{C(OTiCp_2Cl)Fc\} - 4CO]^+$
	484	6.2	$[M - \{C(OTiCp_2Cl)Fc\} - 4CO]^+$

Table 3.16 *contd. 3* Mass spectral data of rhenium complexes

Complex	m/z	Intensity (%)	Fragment Ion
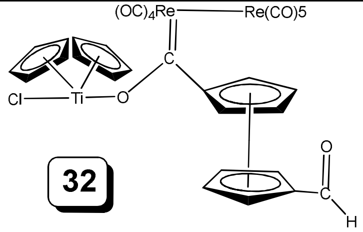 **32**	1079	0.5	$[M]^+$
	753	39	$[M - Re(CO)_5]^+$
	540	4	$[M - Re(CO)_5 - TiCp_2Cl]^+$
	214	21	$[FcCHO]^+$
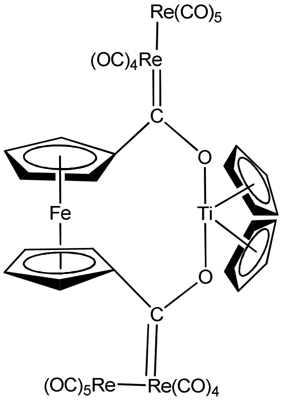 **33**	1014	1.9	$[M - 2Re(CO)_5]^+$
	986	2.1	$[M - 2Re(CO)_5 - CO]^+$
	930	1.9	$[M - 2Re(CO)_5 - 3CO]^+$
	904	1.2	$[M - 2Re(CO)_5 - 4CO]^+$
	874	1.2	$[M - 2Re(CO)_5 - 5CO]^+$
	838	2.8	$[Re_2(CO)_9\{C(O)Fc\}]^+$
	810	3.2	$[Re_2(CO)_9\{C(O)Fc\} - CO]^+$
	782	4.8	$[Re_2(CO)_9\{C(O)Fc\} - 2CO]^+$
	754	2.0	$[Re_2(CO)_9\{C(O)Fc\} - 3CO]^+$
	726	3.2	$[Re_2(CO)_9\{C(O)Fc\} - 4CO]^+$
	698	2.0	$[Re_2(CO)_9\{C(O)Fc\} - 5CO]^+$
	689	2.6	$[Re(CO)_4\{C(OTiCp_2)Fc\}]^+$
	653	15.7	$[Re_2(CO)_{10}]^+$
	625	10.4	$[Re_2(CO)_9]^+$
	597	10.6	$[Re_2(CO)_8]^+$
	569	3.8	$[Re_2(CO)_7]^+$
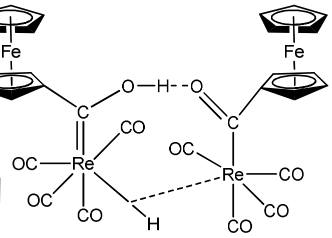 **34**	1022	0.8	$[M]^+$
	994	0.4	$[M - CO]^+$
	910	0.5	$[M - 4CO]^+$
	810	3.5	$[M - \{C(OH)Fc\}]^+$
	782	3.0	$[M - \{C(OH)Fc\} - CO]^+$
	726	1.2	$[M - \{C(OH)Fc\} - 3CO]^+$
	698	0.5	$[M - \{C(OH)Fc\} - 4CO]^+$
	370	95	$[Fc\text{-}Fc]^+$

The presence of a high intensity peak of the [M – Re(CO)$_5$]$^+$ fragment in all compounds containing a Re$_2$(CO)$_9$-moiety indicates the low bond strength of the Re-Re bond, as mentioned previously in the text.

3.4.5 Single crystal X-ray crystallography

Single crystals of suitable quality were obtained for complexes **23**, **27**, **28** and **33** and X-ray diffraction confirmed the molecular structures of these compounds. Layering of different ratios of dichloromethane/hexane was used as solvent from which the complexes crystallized. In the case of **28**, solvent inclusion during crystallization occurred, and equimolar amounts of dichloromethane co-crystallized with the complex molecules. ORTEP[73] + POV-Ray[74] drawings of the molecular structures are presented in Figures 3.19, 3.21 – 3.23, indicating the relevant atom numbering system employed. Experimental details are given in the experimental section and crystallographic data and refinement parameters are listed in the Appendices. Selected bond lengths, bond angles and torsion angles are given in Table 3.17 for the manganese biscarbene complex **23**, and the rhenium biscarbene complexes (**27**, **28** and **33**) in Tables 3.18 and 3.19.

3.4.5.1 Molecular structures

In the crystal structure of **23** (Figure 3.19), the space occupied by the two ethoxy groups, which lie one above the other, is similar to that occupied by the ferrocenyl group. Thus one enantiomer of the complex can occupy the crystal space of the other enantiomer with three carbon atoms of each Cp ring nearly coinciding with the non-hydrogen atom positions of the two ethyl groups. Therefore the crystal structure is disordered with 8(2)% of the other enantiomer occupying the site of each molecule. The minor position occupied by the iron

---

[73] Farrugia, L.J. *J. Appl. Crystallogr.* **1997**, *30*, 565.
[74] The POV-Ray Team, POV-Ray 2004. URL: http://www. povray.org/download/.

atom and the four carbon atom positions needed to complete the two Cp rings are shown as small spheres in Figure 3.19.

The molecule has approximate C_2 symmetry and thus the corresponding bond lengths, bond angles, and torsion angles surrounding the two carbene carbon atoms are approximately equivalent, therefore discussion of the structure will focus on only the Mn(1)-terminal half of the molecule.

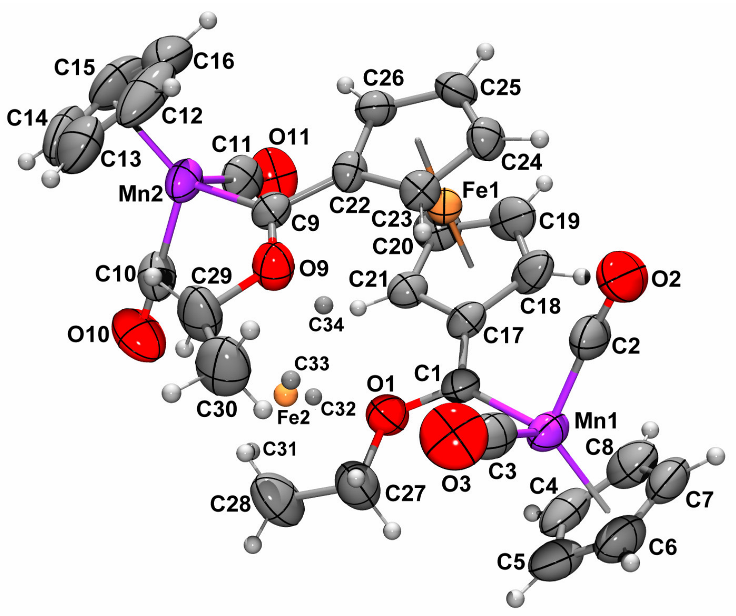

Figure 3.19 ORTEP + POV-Ray drawing of the molecular structure of **23**. Atomic displacement ellipsoids are shown at the 50% probability level.

In [MnCp(CO)$_2${C(OR)Y}] complexes, with two different organic substituents R and Y (Y = planar ring substituent), there are three possible conformations (**I**, **II** and **III** in Figure 3.20) as far as the mutual orientation of the carbene plane and the MnCp(CO)$_2$-moiety is concerned. In **I**, the carbene plane is perpendicular to the mirror plane of the MnCp(CO)$_2$ fragment with C_s symmetry. In both **II** and **III**, the carbene plane coincides with the mirror plane, but different positions of the organic substituents are assumed.

Table 3.17 Selected bond lengths (Å), bond angles (°) and torsion angles (°) for **23**

Bond lengths		Bond angles	
Mn(1)-C(1)	1.924(5)	Mn(1)-C(1)-O(1)	127.1(3)
Mn(2)-C(9)	1.916(5)	Mn(2)-C(9)-O(9)	128.7(3)
C(1)-O(1)	1.340(5)	Mn(1)-C(9)-C(17)	126.3(3)
C(9)-O(9)	1.338(5)	Mn(2)-C(9)-C(22)	126.4(3)
C(1)-C(17)	1.447(6)	O(1)-C(1)-C(17)	106.3(4)
C(9)-C(22)	1.446(6)	O(9)-C(9)-C(22)	104.4(4)
O(1)-C(27)	1.439(5)	C(1)-O(1)—C(27)	123.1(4)
O(9)-C(29)	1.450(6)	C(9)-O(9)-C(29)	122.1(4)
Mn(1)-C(2, 3)*	1.759(6)	C(1)-C(17)-C(18)	127.1(4)
Mn(2)-(C10, 11)*	1.763(6)	C(9)-C(22)-C(23)	128.2(4)
C(2, 3)-O(2, 3)*	1.170(6)	C(1)-C(17)-C(21)	127.7(4)
C(10, 11)-O(10, 11)*	1.157(7)	C(9)-C(22)-C(26)	127.0(4)

Torsion angles	
C(2)-Mn(1)-C(1)-O(1)	-144.7(4)
C(10)-Mn(2)-C(9)-O(9)	-50.1(4)
Mn(1)-C(1)-C(17)-C(18)	-5.0(6)
Mn(2)-C(9)-C(22)-C(26)	-5.2(6)
O(1)-C(1)-C(17)-C(21)	4.7(6)
O(9)-C(9)-C(22)-C(23)	5.1(6)

* Averaged value

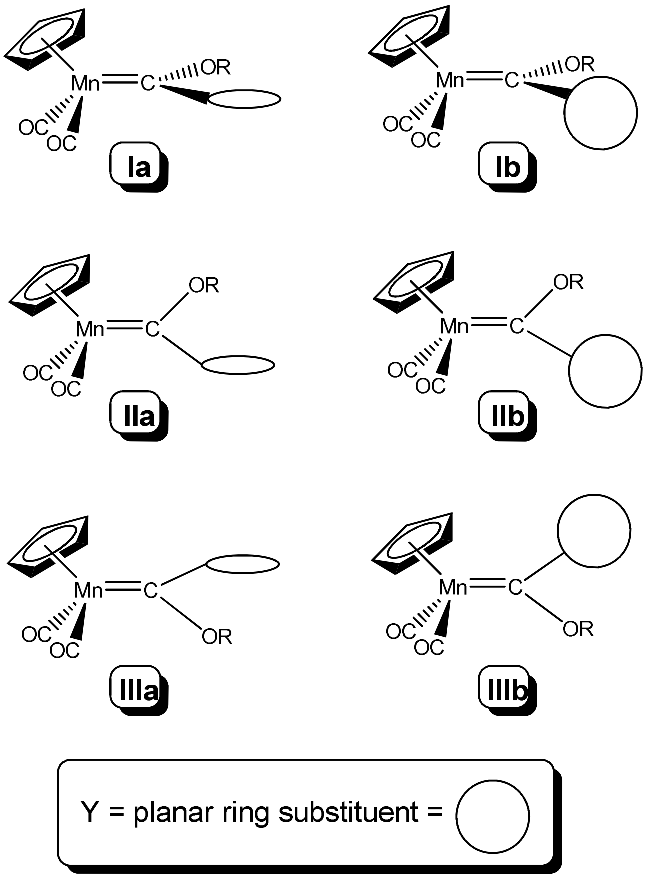

Figure 3.20 Possible conformations/geometric isomers of carbene complexes $[MnCp(CO)_2\{C(OR)Y\}]$

Kostić and Fenske[75] have calculated the relative energies of the isomers/conformations **I** – **III** and found **IIb** to be the most stable where the ring substituent is approximately co-planar to the carbene plane. **I** was found to be the least stable, with a barrier for the rotation of the carbene ligand about the Mn-C(carbene) axis. Comparison of known structures of $[MnCp(CO)_2(carbene)]$ complexes[19,20,76] shows that, as predicted by theory, the orientation of the carbene plane approximately in the mirror plane of the $MnCp(CO)_2$-fragment (**II** and **III** in Figure 3.20) is more favourable than the orientation perpendicular to it (conformer **I**). In the case of complex **23**, however, it was found that the

---

[75] Kostić, N.M.; Fenske, R.F. *Organometallics* **1982**, *1*, 974.

[76] (a) Fischer, E.O.; Kleine, W.; Shambeck, W.; Schubert, U. *Z. Naturforsch., B.: Anorg. Chem. Org. Chem.* **1981**, *36B*, 1575, (b) Friedrich, P.; Besl, G.; Fischer, E.O.; Huttner, G. *J. Organomet. Chem.* **1977**, *139*, C68, (c) Herrmann, W.A.; Weidenhammer, K.; Ziegler, M.L. *Z. Anorg. Allg. Chem.* **1980**, *460*, 200, (d) Fontana, S.; Schubert, U.; Fischer, E.O. *J. Organomet. Chem.* **1978**,*146*, 39.

carbene plane is twisted about 85° relative to the mirror plane, giving it the conformation of **Ia** as illustrated above. This also means that the ring substituent is perpendicular to the carbene plane. Only two other structures exhibit conformation **I** : [MnCp(CO)$_2${C(OMe)menthyl}][76(d)] and [Mn((MeCp)(CO)$_2${C(OMe)PMe$_3$}].[20] In all of these complexes, the carbene carbon carries bulky substituents, forcing the carbene plane to orient in a less favourable way with respect to the MnCp(CO)$_2$-fragment. Also in the case of biscarbene complexes[52] was conformation **I** not observed.

MnCp(CO)$_2$-moieties exhibit high backbonding ability and supply sufficient electron density to the carbene carbon so that π-donating organic substituents at the carbene carbon are not essential to stabilize of these types of complexes. A structural consequence of the above statement is the longer C(carbene)-O bond distance (1.340(5) Ǻ) than for Group VI alkoxycarbene complexes in which alkoxy groups serve as π-donating substituents.[19] The ethoxy group poorly competes with the MnCp(CO)$_2$-moiety for π-bonding with the carbene carbon. This is also true for most other [MnCp(CO)$_2$(carbene)] complexes, however, a significantly longer Mn-C(carbene) bond length is found for **23** than for other reported cyclopentadienyl manganese carbene complexes.[19,76] In most cases, the Mn-C(carbene) bond distance was reported as being (1.85-1.87 Ǻ), not significantly influenced by the nature of the organic substituents. For the ferrocenyl-substituted **23**, Mn-C(carbene) distances of 1.924(5) and 1.916(5) Ǻ were observed, thereby the π-donating ability of the ferrocenyl substituent considerably can be inferred as less backdonation of the MnCp(CO)$_2$-fragment is required.

For complexes of the type [Re$_2$(CO)$_9$(carbene)], the favoured electronic position for the carbene ligand is *cis* to the rhenium-rhenium bond. Neutral rhenium carbonyl complexes require one X-type ligand, which is a bulky Re(CO)$_5$-fragment for the complexes **27** and **33**. Thus the carbene ligand should lie in the equatorial plane and be in a staggered conformation with respect to the carbonyl ligands of the equatorial plane of the other Re(CO)$_5$ group. This is true for **27** but not for **33**.

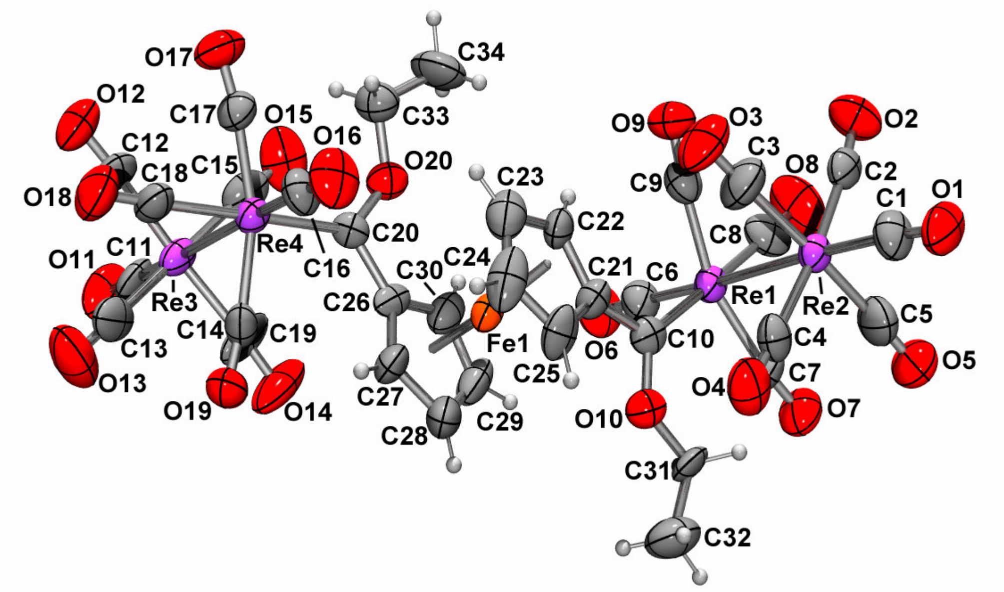

Figure 3.21 ORTEP + POV-Ray drawing of the molecular structure of **27**. Atomic displacement ellipsoids are shown at the 50% probability level.

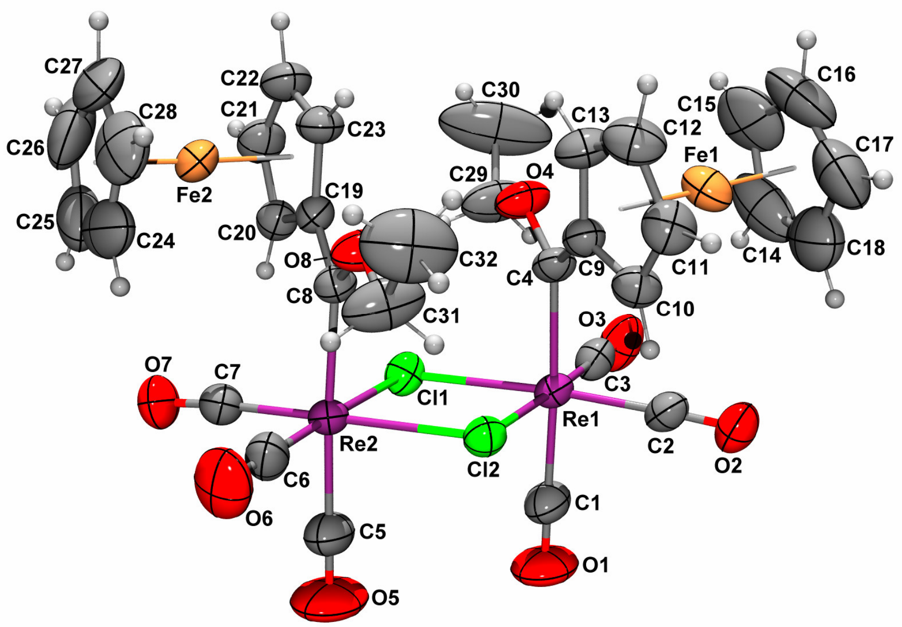

Figure 3.22 ORTEP + POV-Ray drawing of the molecular structure of **28**. Atomic displacement ellipsoids are shown at the 50% probability level.

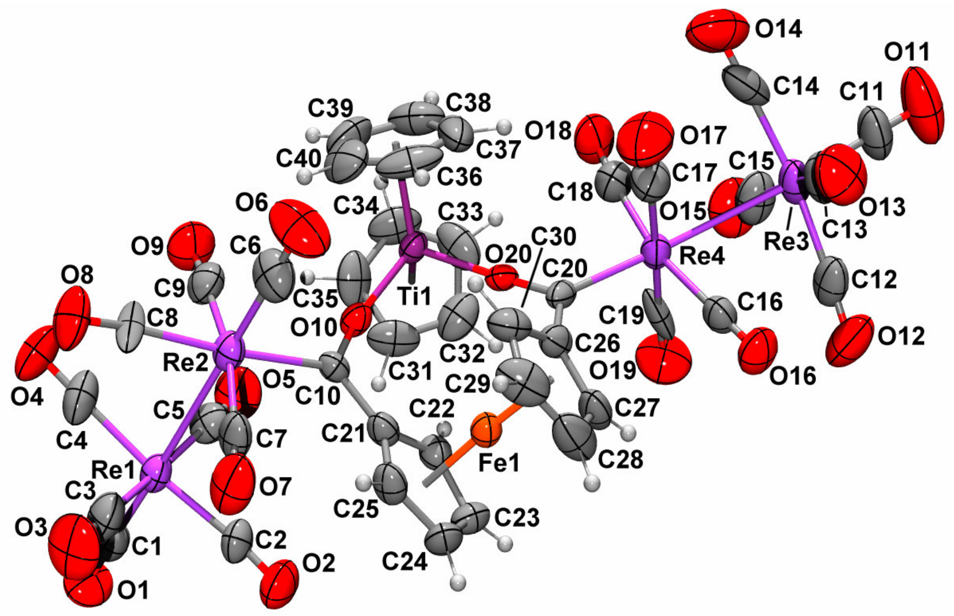

Figure 3.23 ORTEP + POV-Ray drawing of the molecular structure of **33**. Atomic displacement ellipsoids are shown at the 50% probability level.

The geometries of the two rhenium-carbene carbon termini in the biscarbene complexes **27** and **28** are approximately equivalent, but complex **33** is exceptional in that one of the carbene ligands has sacrificed the electronic favoured equatorial position for an axial position. This is one of the rare examples for dirhenium nonacarbonyl complexes to deviate from equatorially coordinated ligands. Fischer and Rustemeyer[27, 28] reported a rhenium octacarbonyl complex containing two carbene ligands and found one of the carbene ligands in an equatorial and the other in an axial position, *eq*,*ax*-$[\{Re(CO)_4\{C(OEt)SiPh_3\}\}_2]$.

In **28**, there are only two monorhenium fragments but the orientations are nevertheless retained through the two bridging chloro ligands. The Re-Re distance is *ca*. 0.8 Ǻ longer because of these bridging ligands.

Table 3.18 Selected bond lengths (Å) of ferrocenyl rhenium biscarbene complexes **27**, **28** and **33**

Bond lengths	**27**	Bond lengths	**28**	Bond lengths	**33**
Re(1)-Re(2) Re(3)-Re(4)	3.0974(9) 3.0632(9)	Re(1)---Re(2)	3.9046(4)	Re(1)-Re(2) Re(3)-Re(4)	3.0712(8) 3.0569(8)
Re(2)-C(1) Re(3)-C(11)	1.924(19) 1.93(2)	Re(2)-C(1) Re(2)-C(5)	1.953(7) 1.959(8)	Re(1)-C(1) Re(3)-C(11)	1.912(17) 1.912(18)
Re(1)-C(10) Re(4)-C(20)	2.111(15) 2.108(14)	Re(1)-C(4) Re(2)-C(8)	2.171(6) 2.166(6)	Re(2)-C(10) Re(4)-C(20)	2.178(11) 2.059(13)
C(10)-O(10) C(20)-O(20)	1.355(17) 1.327(16)	C(4)-O(4) C(8)-O(8)	1.321(7) 1.324(7)	C(10)-O(10) C(20)-O(20)	1.286(14) 1.272(14)
C(10)-C(21) C(20)-C(26)	1.460(19) 1.493(19)	C(4)-C(9) C(8)-C(19)	1.437(9) 1.441(8)	C(10)-C(21) C(20)-C(26)	1.448(17) 1.481(18)
O(10)-C(31) O(20)-C(33)	1.449(16) 1.444(18)	O(4)-C(29) O(8)-C(31)	1.451(9) 1.457(9)	O(10)-Ti(3\1) O(20)-Ti(1)	1.968(9) 1.929(8)
Re(1)-C(6,7,8,9)* Re(4)-C(16,17,18,19)*	1.958(19) 1.952(18)	Re(1)-C(2,3)* Re(2)-C(6,7)*	1.888(7) 1.890(8)	Re(2)-C(6,7,8,9)* Re(4)-C(16,17,18,19)*	1.949(16) 1.936(18)
-	-	Re(1)-Cl(1) Re(1)-Cl(2) Re(2)-Cl(1) Re(2)-Cl(2)	2.5252(15) 2.5289(15) 2.5249(15) 2.5351(15)	-	-

* Averaged value

The rhenium-carbene distances listed above display double bond character with an *sp*^{2}-hybridized carbene carbon atom and defines a carbene plane (Re-C-(O(X))-C(Fc)). A second plane is that of the ferrocenyl Cp-rings, and ideally, because of π-conjugation, will be coplanar with the carbene plane. This plane is twisted approximately 16° for **27** (torsion angles Re(1)-C(10)-C(21)-C(25) and Re(4)-C(20)-C(28)-C(30) are -164.0(12) and 163.3(11)°, respectively) due to steric effects (Table 3.19).

Table 3.19 Selected bond angles (°) and torsion angles (°) of ferrocenyl rhenium biscarbene complexes **27**, **28** and **33**

Bond angles	**27**	Bond angles	**28**	Bond angles	**33**
Re(2)-Re(1)-C(10) Re(3)-Re(4)-C(20)	84.2(4) 90.7(4)	-	-	Re(1)-Re(2)-C(10) Re(3)-Re(4)-C(20)	95.0(3) 175.1(3)
Re(1)-C(10)-O(10) Re(4)-C(20)-O(20)	129.2(10) 128.7(10)	Re(1)-C(4)-O(4) Re(2)-C(8)-O(8)	127.07(4) 127.29(4)	Re(2)-C(10)-O(10) Re(4)-C(20)-O(20)	120.6(8) 125.7(10)
Re(1)-C(10)-C(21) Re(4)-C(20)-C(26)	125.9(12) 126.4(11)	Re(1)-C(4)-C(9) Re(2)-C(8)-C(19)	125.35(5) 125.02(5)	Re(2)-C(10)-C(21) Re(4)-C(20)-C(26)	126.4(8) 120.6(8)
C(10)-O(10)-C(31) C(20)-O(20)-C(33)	122.0(12) 125.5(12)	C(4)-O(4)-C(29) C(8)-O(8)-C(31)	123.81(6) 124.38(6)	C(10)-O(10)-Ti(1) C(20)-O(20)-Ti(1)	161.3(8) 176.2(8)
C(10)-Re(1)-C(6) C(20)-Re(4)-C(16)	89.0(7) 90.1(6)	C(4)-Re(1)-C(3) C(8)-Re(2)-C(7)	93.7(3) 93.9(2)	C(10)-Re(2)-C(6) C(20)-Re(4)-C(16)	87.6(5) 97.4(5)
C(10)-Re(1)-C(8) C(20)-Re(4)-C(18)	177.1(6) 175.3(7)	C(1)-Re(1)-C(4) C(5)-Re(2)-C(8)	175.9(3) 176.6(3)	C(10)-Re(2)-C(8)	172.2(8)
O(10)-C(10)-C(21) O(20)-C(20)-C(26)	104.8(13) 104.9(12)	O(4)-C(4)-C(9) O(8)-C(8)-C(19)	107.4(5) 107.6(5)	O(10)-C(10)-C(21) O(20)-C(20)-C(26)	113.0(10) 112.8(11)
-	-	Re(1)-Cl(1)-Re(2) Re(1)-Cl(2)-Re(2)	101.28(5) 100.90(5)	-	-
Torsion angles	**27**	Torsion angles	**28**	Torsion angles	**33**
C(6)-Re(1)-C(10)-O(10) C(16)-Re(4)-C(20)-O(20)	91.6(14) -91.56(1)	C(3)-Re(1)-C(4)-O(4) C(6)-Re(2)-C(8)-O(8)	50.7(6) 45.6(6)	C(6)-Re(2)-C(10)-O(10) C(16)-Re(4)-C(20)-O(20)	103.8(9) -175.57(1)
Re(1)-C(10)-C(21)-C(22) Re(4)-C(20)-C(26)-C(27)	17(2) -23(2)	Re(1)-C(4)-C(9)-C(10) Re(2)-C(8)-C(19)-C(20)	14.35(1) 10.2(9)	Re(2)-C(10)-C(21)-C(22) Re(4)-C(20)-C(26)-C(27)	156.8(10) -56.0(17)
Re(1)-C(10)-C(21)-C(25) Re(4)-C(20)-C(28)-C(30)	-164.0(12) 163.3(11)	Re(1)-C(4)-C(9)-C(13) Re(2)-C(8)-C(19)-C(23)	-179.23(5) -179.5(5)	Re(2)-C(10)-C(21)-C(25) Re(4)-C(20)-C(26)-C(30)	-21.6(19) -48.6(17)
Re(1)-C(10)-O(10)-C(31) Re(4)-C(20)-O(20)-C(33)	-1.36(2) 13.72(2)	Re(1)-C(4)-O(4)-C(29) Re(2)-C(8)-O(8)-C(31)	-10.67(9) -6.93(9)	Re(2)-C(10)-O(10)-Ti(1) Re(4)-C(20)-O(20)-Ti(1)	121.43(2) -89.54(12)

The longer Re-Re distance observed in **28**, however, allows for the two carbene ligands to lie on the same side of the Re_2Cl_2-plane, with the ethoxy group of one carbene ligand stacked across the Fe-Cp ring of the other, and the ferrocenyl Cp-rings co-planar with the defined carbene plane (Re(1)-C(4)-C(9)-C(19) -179.2(5)°, Re(2)-C(8)-C(19)-C(23) -179.5(5)). The sterically hindered metallacycle formed by the bridging biscarbene ligand of **33** results in a large twist in the carbene and ferrocenyl planes and the corresponding torsion angles, Re(2)-C(10)-C(21)-C(25) and Re(4)-C(20)-C(26)-C(30), are -21.6(19) and -48.6(17)° respectively.

Table 3.20 Selected bond lengths (Å) and angles (°) around the carbene carbon atoms, specified as equatorial, axial or *cis*-substituted carbenes

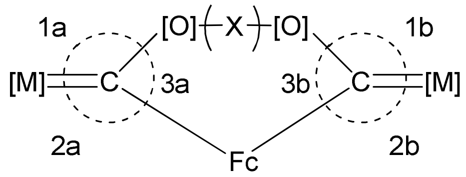

a: *eq*-**27**; b: *eq*-**27**
a: *cis*-**28**; b: *cis*-**28**
a: *eq*-**33**; b: *ax*-**33**

Angle	**27**		**28**		**33**	
	(a: *eq*)	(b: *eq*)	(a: *cis*)	(b: *cis*)	(a: *eq*)	(b: *ax*)
1	129.2(10)	128.7(10)	127.07(4)	127.29(4)	120.6(8)	125.7(10)
2	125.9(12)	126.4(11)	125.35(5)	125.02(5)	126.4(8)	120.6(8)
3	104.8(13)	104.9(12)	107.4(5)	107.6(5)	113.0(10)	112.8(11)
Bond	**27**		**28**		**33**	
	(a: *eq*)	(b: *eq*)	(a: *cis*)	(b: *cis*)	(a: *eq*)	(b: *ax*)
M-C_{carb}	2.111(15)	2.108(14)	2.171(6)	2.166(6)	2.178(11)	2.059(13)
C_{carb}-O	1.355(17)	1.327(16)	1.321(7)	1.324(7)	1.286(14)	1.272(14)
C_{carb}-C(Fc)	1.460(19)	1.493(19)	1.437(9)	1.441(8)	1.448(17)	1.481(18)

The two complexes **27** and **28** both have ethoxy substituents adopting an orientation with their methylene carbon atoms towards the metal carbonyl ligands, which is electronically favoured.[77]

The carbene substituent bond lengths and angles around each carbene carbon atom of the biscarbene ligands are summarized in Table 3.20. Complex **33** has both the longest and the shortest Re-C(carbene) bond lengths. The axial substitution of the one carbene places the ligand *trans* to the Re(CO)$_5$-fragment, where negligible competition for π-backdonation from the Re-atom is expected. A shorter bond length (2.059(13) Å) and higher bond order than the mean value reported for terminal alkoxycarbenes (2.098 Å)[78] is observed. In contrast, a significantly longer equatorial Re-C(carbene) bond distance of 2.178(11) Å corroborates the findings of the previous chapter: the acyl resonance structure contributes predominantly to the carbene complex's structure (Figure 2.29). Even stronger support of this supposition is the fact that for both the equatorial and axial carbene ligands, the C(carbene)-O bond length is found to be 0.035 – 0.08 Å shorter than those of the corresponding ethoxycarbene complexes, irrespective of substitution site, as well as the near linear C(carbene)-O-Ti angles (161.3(8), 176.2(8)°). For the O-C(carbene)-C(ring) bond angle, **33** shows a significantly larger angle for both the equatorial and the axial carbene ligands (113.0(10)° and 112.8(11)°) compared to the smaller angles for **27** and **28** (104.8(13)°, 104.9(12)° and 107.4(5)°, 107.6(5)°, respectively). This observation seems to indicate that the loss in electronic stability of the equatorial position is compensated for by the sterically more favourable axial coordination.

3.4.5.2 Crystal packing

Packing of the manganese and rhenium crystal structures obtained seemed to be mostly governed by closest-packing, although a few interesting features were

---

[77] Fernández, I.; Cossío, F.P.; Arrieta, A.; Lecea, B.; Mancheño, M.J.; Sierra, M.A. *Organometallics* **2004**, *23*, 1065.
[78] Orpen, A.G.; Brammer, L.; Allen, F.H.; Kennard, O.; Watson, D.G.; Taylor, R. *J. Chem. Soc., Dalton Trans.* **1989**, S1.

observed. The Mercury software[79] available from the CCDC[80] was employed to determine the presence of H-bonds or other short-contact bonds in the crystal lattices.

Complex **23** displayed a pattern of metal carbonyl layers, alternated by an 'organic' layer made up of ferrocenyl and ethoxy groups, as shown in Figure 3.24.

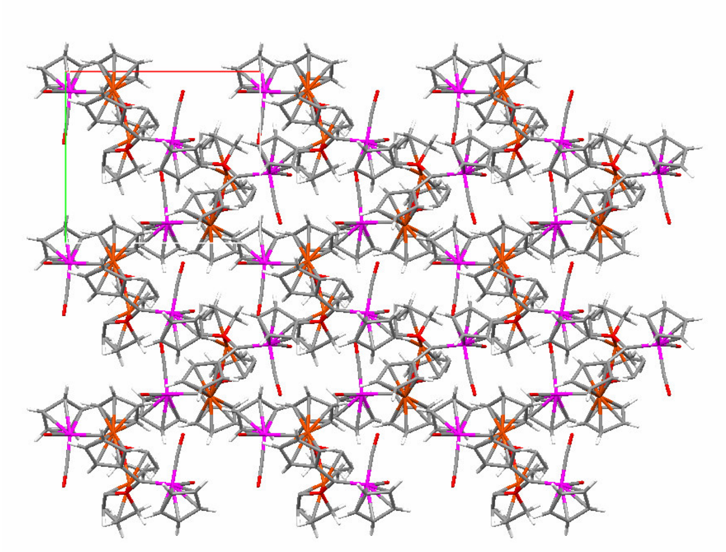

Figure 3.24 View along the *c*-axis of **23**

Complex **27** exhibits another variation of this layered packing, in that the metal carbonyl groups (Figure 3.25) cluster together in a staggered two-layered fashion.

---

[79] (a) Mercury CSD 2.0 - New Features for the Visualization and Investigation of Crystal Structures, Macrae, C.F.; Bruno, I.J.; Chisholm, J.A.; Edgington, P.R.; McCabe, P.; Pidcock, E.; Rodriguez-Monge, L.; Taylor, R.; van de Streek, J.; Wood, P.A. *J. Appl. Cryst.* **2008**, *41*, 466, [DOI: 10.1107/S0021889807067908], (b) Mercury: visualization and analysis of crystal structures, Macrae, C.F.;Edgington, P.R.; McCabe, P.; Pidcock, E.; Shields, G.P.; Taylor, R.; Towler, M.; van de Streek, J. *J. Appl. Cryst.* **2006**, *39*, 453, [DOI: 10.1107/S002188980600731X].

[80] The Cambridge Structural Database: a quarter of a million crystal structures and rising Allen, F.H. *Acta Cryst.* **2002**, *B58*, [DOI: 10.1107/S0108768102003890].

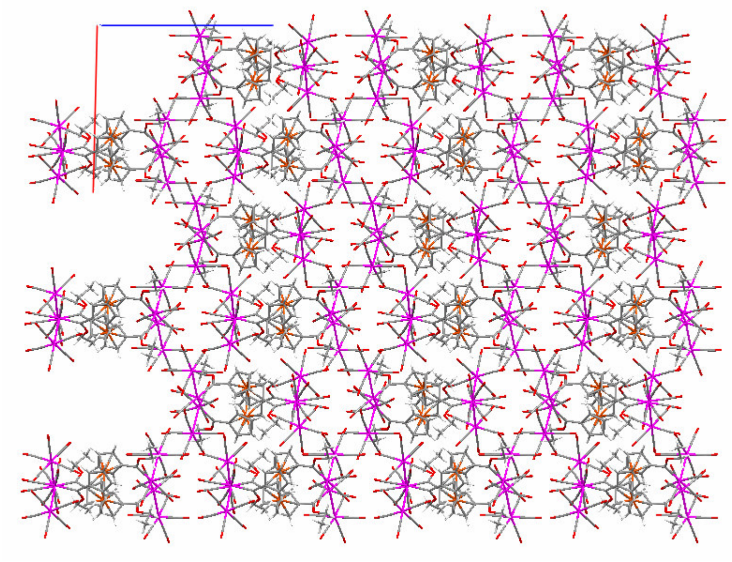

Figure 3.25 View along the *b*-axis of **27**

Layered packing was not observed for the titanoxy analogue **33** of **27**, instead, discrete clusters of the complexes formed channels bordered by the carbonyl-O atoms.

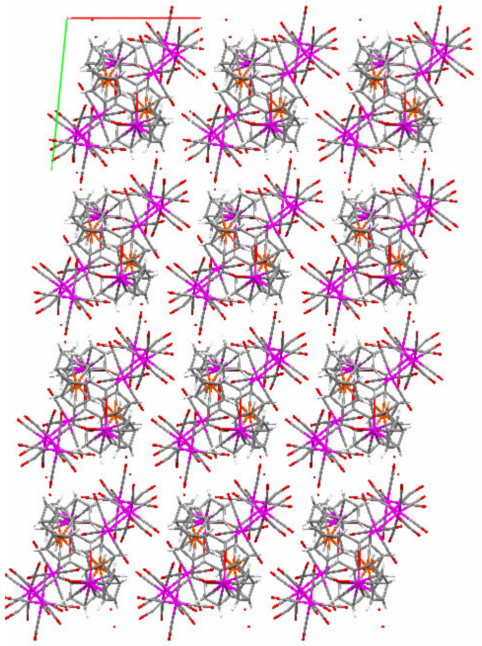

Figure 3.26 View along the *c*-axis of **33**

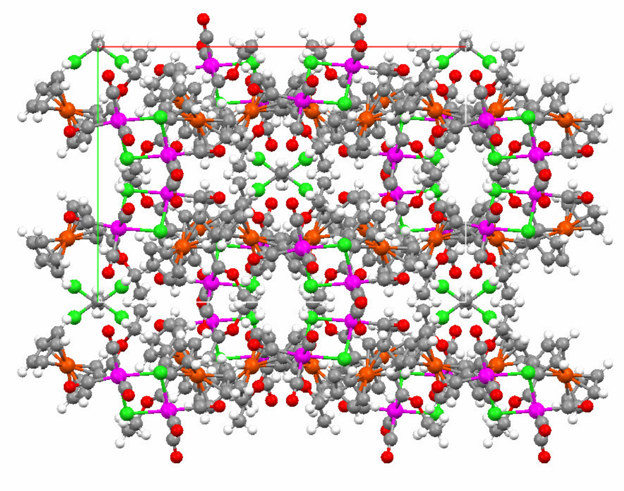

Figure 3.27 View along the *c*-axis of **28**

In the case of complex **28**, channels filled by inclusion solvent dichloromethane molecules were observed similar to the structure of the ferrocenyl titanoxycarbene complex of chromium (**5**). Besides ordered close-packing, no other inter- or intramolecular forces determining crystal packing could be identified.

3.5 Concluding remarks

Group VII transition metal cluster carbene complexes were synthesized from mononuclear [MnCp(CO)$_3$] and binary dinuclear [Re$_2$(CO)$_{10}$] starting materials. After alkylation with an oxonium salt, the known complex [MnCp(CO)$_2${C(OEt)Fc}] **22** and the novel biscarbene complex **23** [μ-Fe{C$_5$H$_4$C(OEt)MnCp(CO)$_2$}$_2$] were isolated. Reaction quenching with titanocene dichloride instead of alkylation lead to the formation of the cluster carbene complexes **24** [MnCp(CO)$_2${C(OTiCp$_2$Cl)Fc}] and the corresponding biscarbene complex **25** [{μ-TiCp$_2$O$_2$-O,O'}{μ-Fe(C$_5$H$_4$)$_2$-C,C'}[CMnCp(CO)$_2$}$_2$]. This complex also displays the unique bimetallacyclic bridging carbene ligand as first prepared in Chapter 2.

From the crystal structure of **23** it was seen that the complex displays an unusual conformation, where the carbene plane is approximately perpendicular to the mirror plane of the $MnCp(CO)_2$-fragment, and the ferrocenyl substituent is again perpendicular to the carbene plane. From literature, this conformation is described as the least stable.[75]

After preparation of the monolithiated ferrocene from iodoferrocene, the well known Fischer-method of carbene synthesis was employed to synthesize the monocarbene complex **26** $[Re_2(CO)_9\{C(OEt)Fc\}]$. Evidence of both axial and equatorial isomers was seen in the spectroscopic data, but the two isomers could not be separated. This lead to the supposition that an equilibrium exists between the two isomers, as the one conformation is electronically more stable (equatorial) and the other is less sterically hindered (axial isomer).

During the synthesis of the biscarbene complex **27**, *eq*,*eq*-$[\mu\text{-}Fe\{C_5H_4C(OEt)Re_2(CO)_9\}_2]$, another biscarbene complex was obtained. Complex **28** *fac*-$[(\mu\text{-}Cl)_2\text{-}(Re(CO)_3\{C(OEt)Fc\})_2]$ exhibited a cleaved Re-Re bond, and the proposed reaction mechanism for the complex formation requires abstraction of a chlorine atom from the solvent dichloromethane, the only possible chlorine source. It is anticipated that this compound originated from the tetracarbonyl precursor, $[Re(CO)_4\{C(OEt)Fc\}Cl]$.

Dilithiation of ferrocene, followed by subsequent metalation with dirhenium carbonyl and titanocene dichloride yielded the target monocarbene complex **31** *ax*-$[Re_2(CO)_9\{C(OTiCp_2Cl)Fc\}]$ and biscarbene **33** *ax*,*eq*-$[\{\mu\text{-}TiCp_2O_2\text{-}O,O'\}\{\mu\text{-}Fe(C_5H_4)_2\text{-}C,C'\}\{CRe_2(CO)_9\}_2]$, both displaying the unusual axial substitution of the carbene ligand (although in the biscarbene complex, one axial and one equatorial ligand was observed). A range of other products was also isolated form the reaction mixture. Products such as $[Re(CO)_5Cl]$, $[Re_3(CO)_{14}H]$ (**29**), $[Re(CO)_5\{C(O)Fc\}]$ (**30**), FcCHO and Fc-Fc, $[(\mu\text{-}H)_2\text{-}(Re(CO)_4\{C(O)Fc\})_2]$ (**34**) and *eq*-$[Re_2(CO)_9\{C(OTiCp_2Cl)(Fc'CHO)\}]$ (**32**) were characterized.

Two possible reaction mechanisms for the formation of these products were proposed; one involving proton transfer form solvents *via* a radical mechanism involving hidrido intermediates such as [Re(CO)$_5$H]. This mechanism is supported by the finding of the dimerization decomposition product diferrocene. The other mechanism involves acyl hydrido intermediates from ionic hydrolysis reaction with trace amounts of water present. Reductive elimination then yields the decomposition product formylferrocene (FcCHO), as well as the FcCHO-substituted carbene ligand in complex **32**. In both cases, the weak Re-Re bond is broken, as shown by the ease of metal-metal bond breaking in the mass spectrometric data.

Complex **34** is the ferrocenyl analogue of the acyl hydrido thienyl hydroxycarbene complexe synthesized previously in our laboratories, showing the same bridging hydride and bridging hydroxyl-acyl ligands as the Shvo catalyst. However, some doubt exists about the existence of the O-H-O bridge in complex **34**, as evidenced by NMR and IR spectroscopy.

NMR spectroscopy was used to determine a trend in π-electron donor strength of the central metal moieties of the complexes synthesized in both Chapter 2 and 3. The donor abilities of the metal fragments could be arranged in increasing order as $Re_2(CO)_9 < W(CO)_5 < Cr(CO)_5 < Mo(CO)_5 < MnCp(CO)_2$.

4

Investigation of substituent effect on carbene ligands

4.1 Introduction

4.1.1 Background

After the initial recognition and first full characterization of a transition metal carbene complex by Fischer in 1964,[1] interest in divalent carbon as part of a metal system expanded quickly. Four years later the first of the so-called N-heterocyclic carbene (NHC) complexes were synthesized by Wanzlick,[2] followed shortly by the publication of another stable diaminocarbene metal complex by Öfele.[3] In an effort to prepare a homoleptic tantalum(V) alkyl complex, the first nucleophilic carbene metal complex was reported by Schrock six years later.[4]

Classification of the types of carbene complexes (Figure 4.1) was based on their unique characteristics. The carbene carbon atom of Fischer carbene complexes was found to be electrophilic, in contrast to Schrock carbene complexes. On the other hand, NHC's were initially seen as being a specific type of Fischer carbene, however significant differences qualified these types of complexes as a separate subclass of carbene complexes. As an example, the metal-carbon bond in Fischer and Schrock carbenes display double bond character while the

---

[1] Fischer, E.O.; Maasböl, A. *Angew. Chem., Int. Ed. Engl.* **1964**, *3*, 580.
[2] Wanzlick, H.W.; Schoenherr, H.J. *Angew. Chem., Int. Ed. Engl.* **1968**, *7*, 141.
[3] Öfele, K. *J. Organomet. Chem.* **1968**, *12*, 42.
[4] Schrock, R.R. *J. Am. Chem. Soc.* **1974**, *96*, 6796.

longer M-C bond lengths of NHC's (of the corresponding central metals), are classified as single bonds.[5]

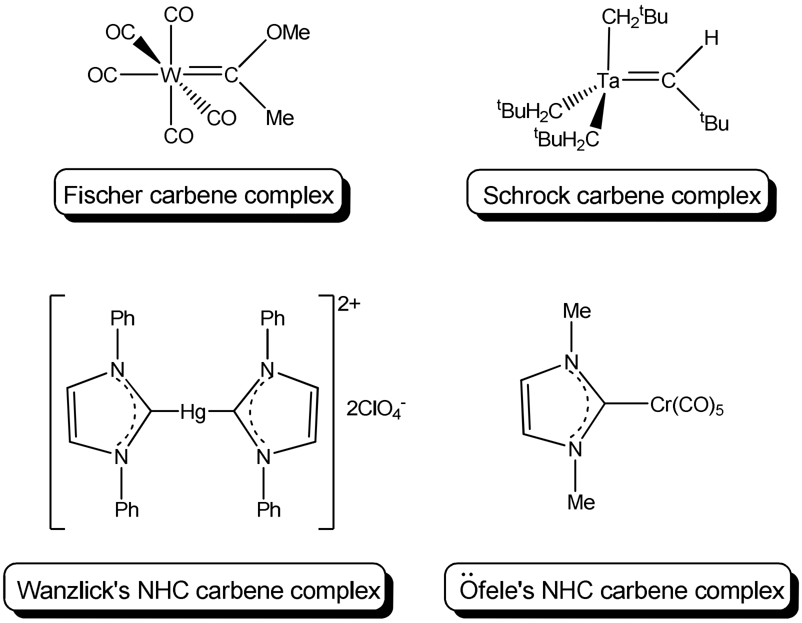

Figure 4.1 The first carbene complex to be synthesized in each of the three classes

General characteristics for carbene carbon atoms were found to be approximate sp^2 hybridization and trigonal planar geometry around the carbon atom.[6] However, Schrock carbene complexes are usually characterized by an early transition metal in high oxidation state as the central metal, with strong donor and weak π-acceptor ligands,[7] while the electrophilic Fischer carbene complexes contain predominantly low valent Group VI – VIII transition metals stabilized by π-acceptor ligands.[8]

---

[5] Herrmann, W.A. *Angew. Chem., Int. Ed. Engl.* **2002**, *41*, 1290.

[6] Elschenbroich, Ch.; Salzer, A. *Organometallics: a concise introduction 2nd edition,* **1992**, Verlagsgesellschaft, New York.

[7] (a) Schwab, P.; France, M.B.; Ziller, J.W.; Grubbs, R.H. *Angew. Chem., Int. Ed. Engl.* **1995**, *34*, 2039, (b) Scwab, P.; Grubbs, R.H.; Ziller, J.W. *J. Am. Chem. Soc.* **1996**, *118*, 100.

[8] Dötz, K.H.; Fischer, H.; Hofmann, P.; Kreissl, F.R.; Schubert, U.; Weiss, K. *Transition Metal Carbene Complexes,* VCH Verlag Chemie, Weinheim, **1983**.

The main speciation of the different types of carbene complexes are made by the nature of the metal-carbon bond, which in turn is influenced by the types of substituents bonded to the carbene carbon atom. Fischer carbene complexes contain at least one heteroatom bonded directly to the carbene carbon atom and NHC's have two N-atoms as α-substituents on the carbene carbon. Metal alkylidene, or Schrock carbene complexes, on the other hand, typically have alkyl- or H-atoms as carbene carbon atom substituents.

4.1.2 Theoretical bonding model of carbene ligands

The generally accepted bonding model employs the singlet and triplet states of the ground state spin multiplicities of the fragments CR_2 and L_nM as building blocks for carbene complexes.[9] For Fischer carbene complexes, the model describes the metal-to-carbon bond in terms of 'donor-acceptor interactions' between a ($^1A_1$) singlet carbene and a singlet metal fragment.[10] Carbene ligands with π-donor groups and a singlet ground state will preferentially engage in donor-acceptor interactions with singlet metal fragments.[11] In particular, dihalocarbenes, which have singlet ground states and large singlet to triplet excitation energies, are considered to be donor-accepting bonding and thus 'Fischer-type'. The resulting electrophilic carbene carbon can be considered as a neutral 2-electron ligand (LZ-type as described by Green's ligand classification method[12]). Applying the Dewar-Chatt-Duncanson (DCD) model[13] to describe the synergic interaction of the Fischer carbene bond, the primary interaction can be seen as the σ-donation from the sp^2 orbital of the carbene carbon atom to the metal σ-hybrid orbital, and π-backdonation from the metal *d*-orbital to the empty *p*-orbital of the carbene carbon atom.

---

[9] Bourissou, D.; Geurret, O.; Gabbaï, F.P.; Bertrand, G. *Chem. Rev.* **2000**, *100*, 39.

[10] Dötz, K.H. *Metal carbenes in organic synthesis*, Springer-Verlag, Germany, **2004**.

[11] Marquez, A.; Sanz, J.F. *J. Am. Chem. Soc.* **1992**, *114*, 2903.

[12] Green, M.L.H. *J. Organomet. Chem.* **1995**, *500*, 127.

[13] (a) Casey, C.P.; Boggs, R.A.; Anderson, R.L. *J. Am. Chem. Soc.* **1972**, *94,* 8947, (b) Weiss, K.; Fischer, E.O. *Chem. Ber.* **1973**, *106*, 1277.

Bonding in Schrock complexes are described as a covalent bond between a $^3B_1$ triplet carbene and a triplet metal fragment,[14] implying that the electronic ground state of a carbene ligand can be used to predict binding interactions with a transition metal.

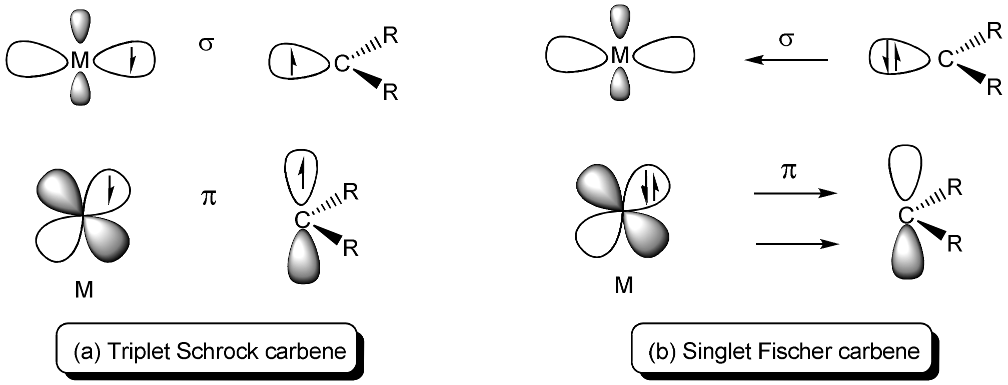

Figure 4.2 Orbital interactions of (a) Schrock and (b) Fischer carbene ligands

The neutral description of the Schrock carbene (Figure 4.2) can also be rewritten as the nucleophilic form L_nM^+-CR_2^- to explain the experimental observations that the Schrock carbene compounds react mostly as nucleophiles. A partial negative charge resides on the carbene carbon atom as a result of polarization of shared electrons between an electropositive metal and a more electronegative carbene carbon atom, as no heteroatom resides in the α-position for stabilization. The carbene ligand is therefore formally considered as an X_2-type ligand, resulting in electron sharing in a metal-carbon σ- and π-bond.

In Fischer and Schrock carbene complexes the *p*-orbital of the carbene is used for backbonding to the metal but in NHC's this *p*-orbital is used for backbonding from the adjacent nitrogen atoms.[15] Thus, only the σ-component is present in

---

[14] Cundari, T.R.; Gordon, M.S. *J. Am. Chem. Soc.* **1991**, *113*, 5231.

[15] Tafipolsky, M.; Scherer, W.; Öfele, K.; Artus, G.R.J.; Herrmann, W.A.; McGrady, G.S. *J. Am. Chem. Soc.* **2002**, *124*, 5865.

the M-C bond in NHCs and the negligible π-backbonding[16] is confirmed and verified with recent charge-density studies. As a result of this, NHC's can rotate around the M-C axis.

4.2 Molecular modelling

Molecular modelling is used to assist with prediction and confirmation of many aspects of experimental chemistry. The goal of the interpretative theoretical research is to present models which can help to qualitatively understand and predict the structures and reactivities of molecules. If the theory is an acceptable description of the system of interest, considerable information can be obtained theoretically. The model should also form a bridge between the chemical behaviour of a molecule and the underlying physical laws.

4.2.1 The theoretical method

Two main methods are used in molecular modelling: molecular mechanics (MM), which is based on the laws of classical physics, and the electronic structure method, which is based on quantum mechanics.[17] The latter can be divided into semi-empirical, *ab initio* and density functional theory (DFT). The DFT method is the most widely used, taking the effects of electron correlation into account. Although the DFT method is very similar to the *ab initio* Hartree-Fock (HF) method, the electron in the latter method is assumed to interact with an averaged electron density.[17] In the DFT method, the electronic energy can be seen as a summation of the electrons' kinetic energy, the potential energy of the nuclear electron interaction, the electron-electron repulsion energy and an exchange correlation term that describes the rest of the electron-electron interactions. The exchange correlation term is a functional of the electron

---

[16] Frenking, G.; Solà, M.; Vyboischchikov, S.F. *J. Organomet. Chem.* **2005**, *690*, 6178.
[17] Foresman, J.B.; Frisch, Æ. *Exploring Chemistry with Electronic structure methods,* 2nd Ed., Gaussian Inc., Pittsburgh, **1996**.

density function, and can be separated into the exchange and correlation functionals.

A pure DFT functional is usually defined by pairing an exchange functional with a correlation functional as in the case of the B3LYP functional where a Becke (B) defined functional is combined with a Lee-Yang-Parr (LYP) functional.[18]
For a theoretical calculation it is also necessary to describe mathematically the orbitals that combine to approximate the total electronic wavefunction of the system under investigation. Better orbital description implies larger basis sets, which leads to longer calculation times being required.

4.2.2 Molecular modelling of transition metal complexes

The progress in quantum chemical methods for the calculation of electronic structure has given insight into the nature of the chemical bond in transition metal carbene complexes. The paper published by Frenking and Frölich gave a comprehensive overview of the methods and approaches of computational chemistry as applied to the bonding in transition metal compounds.[19] Due to the advances in modern and well-defined quantum chemical charge and energy partitioning methods, it is now possible to study complex organometallic systems. Methods include atoms in molecules (AIM),[20] charge decompostition analysis (CDA),[21] energy decomposition analysis (EDA)[22] and natural bond orbital analysis (NBO).[23] The methods provide quantitative answers to questions regarding the bonding situation in terms of simple bonding models. Specifically, the NBO method gives a quantitative interpretation of the electronic structure of

---

[18] Becke, A.D. *Phys. Rev.* **1988**, *A38,* 3098.

[19] Frenking, G.; Fröhlich, N. *Chem. Rev.* **2000**, *100*, 717.

[20] Bader, R.F.W. *Atoms in Molecules: A Quantum Theory,* Oxford University Press, **1990**.

[21] (a) Dapprich, S.; Frenking, G. CDA 2.1, Marburg, **1994**, (b) Dapprich, S.; Frenking, G. *J. Phys. Chem.* **1995**, *99*, 9352.

[22] (a) Ziegler, T.; Rauk, A.; *Inorg. Chem.* **1979**, *18*, 1755, (b) Bickelhaupt, F.M.; Nibbering, N.M.M.; van Wezenbeek, E.M.; Baerends, E.J. *J. Phys. Chem.* **1992**, *96*, 4864, (c) Ziegler, T.; Rauk, A. *Inorg. Chem.* **1979**, *18*, 1558, (d) Ziegler, T.; Rauk, A. *Theor. Chim. Acta* **1977**, *46*, 1 (e) Kitaura, K.; Morokuma, K. *Int. J. Quantum Chem.* **1976**, *10*, 325.

[23] (a) Foster, J.P.; Weinhold, F. *J. Am. Chem. Soc.* **1980**, *102*, 7211, (b) Reed, A.E.; Weinhold, F.J. *J. Chem. Phys.* **1985**, *83*, 1736, (c) Reed, A.E.; Weinstock, R.B.; Weinhold, F. *J. Chem. Phys.* **1985**, *83*, 735, (d) Reed, A.E.; Curtiss, L.A.; Weinhold, F. *Chem. Rev.* **1988**, *88,* 899.

a molecule in terms of Lewis structures. Since Lewis structures are popular representations, the NBO method is frequently chosen. NBO analysis also has the advantage that results are quite robust against changing the basis set.[19]

The EDA method of bonding analysis focuses on the instantaneous interaction energy of the bond, which is the energy difference between the molecule and the fragments in the frozen geometry of the compound.[22] Dapprich and Frenking's CDA method[21] can be seen as a quantitative expression of the Dewar-Chatt-Duncanson (DCD) model[24] of the synergistic metal-ligand bonding, which considers the ligand→metal σ-donation and ligand←metal π-backdonation as the dominant factors of the metal-ligand bond.

4.2.3 Modelling of Fischer carbene complexes

Recently, various aspects of reactivities and properties of Fischer carbene complexes have been theoretically investigated by means of DFT calculations.[25] For example, the nature of the bonding of the metal-carbon bond in complexes was investigated by Frenking *et al.*[25(c)] Charge and energy decomposition analyses were carried out for 16 valence electron (VE) compounds $[Ru(PMe_3)_2Cl_2(C)]$ and $[Fe(PMe_3)_2Cl_2(C)]$; and 18VE compounds $[M(PMe_3)_2(CO)_2(C)]$ and $[M(CO)_4(C)]$ (M = Ru; Fe). The bonding analysis showed that 16 VE carbon complexes were much more stabilized by metal-carbon σ-interaction than 18 VE complexes. EDA calculations illustrated that the nature of the transition metal – carbon and the transition metal–carbonyl binding interactions resemble each other, and that the π-bonding contribution to the orbital energies in the 18 VE carbon complexes is always stronger than σ-

---

[24] (a) Dewar, M.J.S. *Bull. Soc. Chim. Fr.* **1951**,*18*, C79, (b) Chatt, J.; Duncanson, L.A. *J. Chem. Soc.* **1984**, *106*, 1576.

[25] (a) Cases, M.; Frenking, G.; Duran, M.; Sol, M.; *Organometallics* **2002**, *21*, 4182, (b) Krapp, A.; Frenking, G.; *J. Am. Chem. Soc.* **2008**, *130*, 16646, (c) Krapp, A.; Pandey, K.K.; Frenking,G. *J. Am. Chem. Soc.* **2007**, *129*, 7596, (d) Frenking, G.; Sola, M.; Vyboishchikov, S.F. *J. Organomet. Chem.* **2005**, *690*, 6178, (e) Sierra, M.A.; Fernández, I.; Cossío, F.P. *Chem. Commun.* **2008**, 4761, (f) Lage, M.L.; Fernández, I.; Mancheño, M.J.; Sierra, M.A. *Inorg. Chem.* **2008**, *47*, 5253, (g) Andrada, D.M.; Zoloff Michoff, M.E.; Fernández, I. Granados, A.M.; Sierra, M.A. *Organometallics* **2007**, *26*, 5854.

bonding. The properties of carbon complexes as donor ligands, and the nature of the donor-acceptor interactions with Lewis acids were also studied.[25(b)]

Studies of the steric and electronic effects of the heteroatom (S and O) on free carbenes and their metal complexes were carried out by the group of Sierra.[26] Carbenes can exist in two conformations, either *syn* or *anti* (Figure 4.3), and a clear bias for the *anti*-isomer of the free alkoxycarbenes were found.

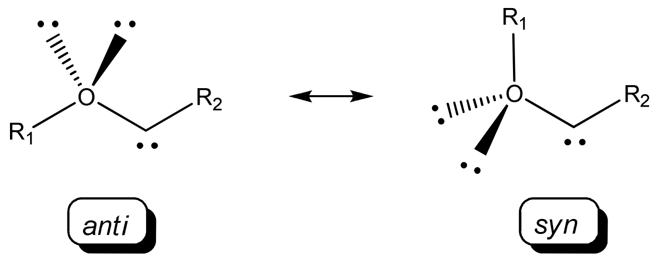

Figure 4.3 Possible conformations of carbene carbon heteroatom subsitituent

This was ascribed to the unfavourable steric repulsion between the substituent directly bonded to the heteroatom and the carbene carbon substituent of the *syn*-isomer, as well as the electronic repulsive interaction between the carbene electron pair and the two nonbonding electron pairs of the oxygen. For metal-complexed Fischer carbene ligands, only steric effects needed to be considered in the absence of the free carbene electron pair. Validation of the model was obtained in the observation of decreased differences of energies between the preferred *anti*- and *syn*-isomer.

Extensive studies, including molecular modelling, on reactivity and reaction mechanisms of thermal and photochemical transformations of Fischer carbene complexes have also been carried out by the aforementioned research

---

[26] Fernández, I.; Cossío, F.P.; Arrieta, A.; Lecea, B.; Mancheño, M.J.; Sierra, M.A. *Organometallics* **2004**, *23*, 1065.

group.[25(e), 27] It was found that the isolobal analogy[28] between Group VI Fischer carbene complexes and organic esters or amides holds for reactions occurring outside the participation of the metal. However, when the metal is directly involved in the reaction, the isolobal analogy should be excluded.

Other properties calculated include dipole moments, where recently it was found that the incorporation of two different metal fragments at the termini of a heteronuclear biscarbene complex, created a polarization effect comparable to that of a monocarbene complex, as illustrated in Figure 4.4.[29]

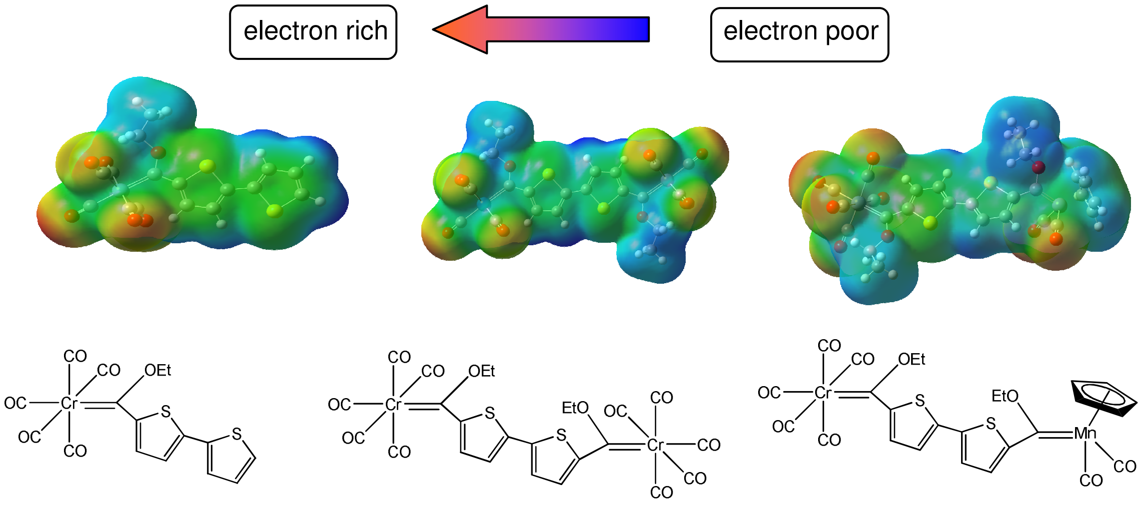

Figure 4.4 Electrostatic surface potentials mapped with total density of the molecule[29]

---

[27] (a) Fernández, I.; Sierra, M.A.; Mancheño, M.J.; Gómez-Gallego, M.; Cossío, F.P. *J. Am. Chem. Soc.* **2008**, *130*, 13892, (b) Fernández, I.; Sierra, M.A.; Mancheño, M.J.; Gómez-Gallego, M.; Cossío, F.P. *Eur. J. Chem.* **2008**, 2454, (c) Fernández, I.; Sierra, M.A.; Gómez-Gallego, M.; Mancheño, M.J.; Cossío, F.P. *Chem. Eur. J.* **2005**, *11*, 5988, (d) Arrieta, A.; Cossío, F.P.; Fernández, I.; Gómez-Gallego, M.; Lecea, B.; Mancheño, M.J.; Sierra, M.A. *J. Am. Chem. Soc.* **2000**, *122*, 11509.

[28] (a) Hoffmann, R. *Science* **1981**, *211*, 995, (b) Hoffmann, R. *Angew. Chem., Int. Ed. Engl.* **1982**, *21*, 711.

[29] Landman, M.; Ramontja, J.; van Staden, M.; Bezuidenhout, D.I.; van Rooyen, P.H.; Liles, D.C.; Lotz, S. *Inorg. Chim. Acta* **2010**, *363*, 705.

4.2.4 Substituent effect

Besides the above properties, quite a few theoretical investigations have focused on the effect of substituents on the carbene ligand. Several studies have shown that the chemical reactivity of the Fischer-type Cr-carbene complexes $[Cr(CO)_5\{C(X)R\}]$ depends mainly on the electronic characteristics of the carbene substituents X and R, which seem to have remarkable control on the electrophilicity of the complex.[30] Specifically, it has been proposed that the π-bond character of a metal carbene can be better represented by a M-C-X 3-centre, 4-electron bond.[31] For complexes where substituent X is a heteroatomic substituent (ethoxy, amino or thiophenol) and R a heteroaromatic substituent (furyl, thienyl and *N*-methylpyrryl), spectroscopic studies including IR, UV and NMR spectroscopy were directed at the investigation of the electronic properties of these complexes, specifically the donation of electron density from X and R into the empty *p* orbital on the carbene carbon.[32] It was concluded that stabilization occurs by conjugative release of electrons from the heteroarene substituent R rather than specific $\pi \rightarrow p$ donation, and that the electronic character of the carbene carbon atom is more strongly influenced by the X group than either the metal or the R group.

Poater *et al.* similarly found that donation from the carbene ligand is stronger than backdonation from the $Cr(CO)_5$-fragment.[33] However, they found that it is backdonation rather than σ-donation that correlates with most geometrical and electronic parameters of the complexes. Charge backdonation values and π-orbital interaction energies are more scattered over a large range of values, while charge donation values and σ-orbital interaction energies are more constant. Additionally, it was found that the smaller the π-donor character of X,

---

[30] (a) Dötz, K.H. *Angew. Chem., Int. Ed. Engl.* **1975**, *14*, 644, (b) Bernasconi, C.F.; Ali, M.; Lu, F. *J. Am. Chem. Soc.* **2000**, *122*, 2183.

[31] (a) Wang, C.-C.; Wang, Y.; Liu, H.-J.; Lin, K.-J.; Chou, L.-K.; Chan, K.-S. *J. Phys. Chem. A* **1997**, *101*, 8887, (b) Block, T.F.; Fenske, R.F. *J. Am. Chem. Soc.* **1977**, *99*, 4321.

[32] (a) Connor, J.A.; Jones, E.M. *J. Chem. Soc. A, Inorg. Phys. Theor.* **1971**, *12*, 1974, (b) Connor, J.A.; Jones, E.M.; Randall, E.W.; Rosenburg, E. *J. Chem. Soc., Dalton Trans.* **1972**, *22*, 2419.

[33] Poater, J.; Cases, M.; Fradera, X.; Duran, M.; Solà, M. *Chem. Phys.* **2003**, *294*, 129.

the larger the backdonation from the metal. In general, it was found that backdonation, as defined in the CDA[21] and EDA[22] methods, is proportional to the Cr-CO_{trans} distance, and inversely proportional to the Cr-C(carbene) and C-O(*trans*) distances. Therefore, the π-donor character of the X-substituent has the largest impact on the electron delocalization between the Cr, C(carbene) and X atoms. Substituents with a high π-donor character will lead to a decrease in electron sharing between C(carbene) and X.

Other properties of carbene complexes have also been used as a gauge of substituent effect on molecular structure and bonding. The groups of Frenking[34] and Goldman[35] have found that when comparing the carbonyl stretching frequencies of $[M(CO)_nL]$ systems, higher or lower values of ν(CO) does not necessarily indicate stronger or weaker π-acceptance of L. σ-bonding and charge interactions also have a significant influence, therefore a more legitimate correlation between the bonding situation and the force constants, rather than the vibrational frequencies, can be made.

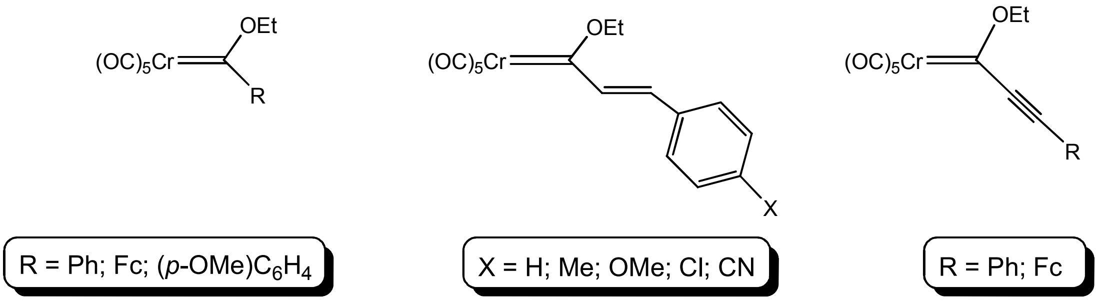

Figure 4.5 Alkoxycarbene chromium(0) complexes studied by TD-DFT[25(f)]

A computational time-dependent density functional theory (TD-DFT) experimental study of UV-visible spectroscopy of alkoxycarbene chromium(0) complexes (Figure 4.5) has been carried out to accurately assign the vertical transitions responsible for observed spectra.[25(f)] Ferrocene was included as a

---

[34] Lupinett, A.J.; Fau, S.; Frenking, G.; Strauss, S.H. *J. Phys. Chem. A* **1997**, *101*, 9551.

[35] Goldman, A.S.; Krogh-Jesperson, K. *J. Am. Chem. Soc.* **1996**, *118*, 12159.

substituent to investigate the effect of an additional metal atom on the electronic properties of Fischer carbenes.

Both the ligand field (LF) and metal-to-ligand charge transfer (MLCT) bands were seen to exhibit remarkable π-π* character, demonstrated by the strong dependence of the absorptions on the donor/acceptor nature of the carbene carbon substituent. The substituent effect was also found to be related to the equilibrium geometry of the complexes and the occupation of the *p*-atomic orbital of the carbene carbon atom. For example, for styryl-substituted Fischer carbene complexes, π-donor styryl substituents were seen to populate the resonance structure **B** (Scheme 4.1) and therefore shorten the C(carbene)=C bond with concomitant lengthening of the Cr=C bond. Strong acceptor substituents like a cyano group have the opposite effect in the bond distances because the resonance form **B** in Scheme 4.1 cannot be populated. Finally, the ferrocenyl moiety was found to behave as a π-donor group in chromium Fischer carbene complexes. Poorer relations between the bond lengths and the position of absorption maxima of MLCT bands were found than for LF bands. This observation supported the statement that the LF transition displayed higher sensitivity with the π-conjugation compared to the MLCT band.

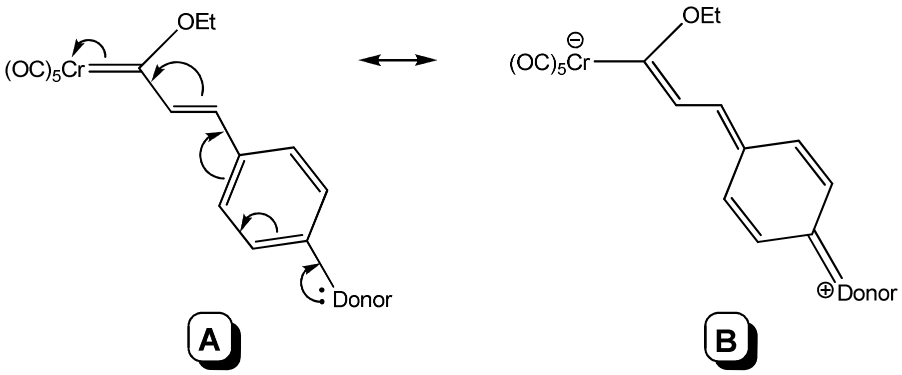

Scheme 4.1

The results of the study changed the interpretation of the UV-vis spectroscopy of Fischer carbene complexes. Earlier results, based on molecular orbital (MO) calculations,[36] assigned the MLCT band to the promotion of an electron from the nonbonding metal-centred orbital HOMO (highest occupied molecular orbital) to the carbene carbon *p*-orbital-centred LUMO (lowest unoccupied molecular orbital), whereas the LF band was attributed to the more energetic population of the metal-centred LUMO+1. In this study, the TD-DFT calculations assigned the LF band to the HOMO-3 → LUMO transition, and the MLCT was ascribed to the HOMO-1 → LUMO transition.

For the ferrocenyl substituted complexes, slight blue shifts of the MLCT band, and a more pronounced red shift in the LF band correlated with that of the other π-donor substituents. The origin of this donation was found with the help of second-order perturbation theory of the NBO method.[23] A stabilizing two-electron interaction, illustrated in Figure 4.6, between the occupied *d* orbital of the iron atom and the *p* orbital of the carbene carbon atom was found. The associated second-order perturbation energy ($\Delta E^{(2)}$) = -0.60 kcal/mol was determined. This effect was seen as the likely cause for the higher computed *p*-occupation in $[Cr(CO)_5\{C(OEt)Fc\}]$ than in $[Cr(CO)_5\{C(OEt)Ph\}]$.

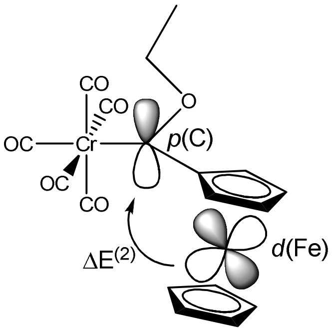

Figure 4.6 Two-electron donation from the iron atom to the carbene carbon atom[25(f)]

---

[36] (a) Block, T.J.; Fenske, R.F.; Casey, C.P. *J. Am. Chem. Soc.* **1976**, *98*, 441, (b) Nakatsuji, H.; Uskio, J.; Yonezawa, T. *J. Am. Chem. Soc.* **1983**, *105*, 426, (c) Foley, H.C.; Strubinger, L.M.; Targos, T.S.; Geoffroy, G.L. *J. Am. Chem. Soc.* **1983**, *105*, 3064.

4.3 Electrochemical approach

The redox potentials of coordination compounds have been correlated to many other properties along the years, namely the HOMO energy, the gas-phase ionization potential, the ligand field stabilization energy, the energy of charge transfer bands, infrared stretching frequencies, X-ray photoelectron spectroscopy binding energies, NMR parameters and ligand structural parameters, apart from solvent and supporting electrolyte effects.[37] These features are often dependent on the electronic and/or structural properties of the ligands and their coordination metal centers, suggesting that one could define suitable electrochemical parameters, based on the redox potential, for measuring such ligand and metal site properties. The research has often been directed towards the establishment of simple additive ligand effects on the redox potential. This has long been recognized for the series of closely related 18VE octahedral carbonyl/isocyanide complexes $[Mn(CO)_{6-x}(CNR)_x]^+$ ($x = 1 - 6$).[37(j)] A single electron reversible oxidation associated with an oxidation potential that correlates linearly with the HOMO energy was obtained, where a higher value of the former corresponded to a greater stability of the latter, as expected for an electron removal from the orbital. A linear relationship was developed, containing terms that include a constant that is metal-, solvent- and reference electrode dependent, and the term $[dE^{\circ}/dx)_L$, i.e. the shift of the oxidation potential per each CO replacement by L as a measure of the effect of the L ligand.

---

[37] (a) Pombeiro, A.J.L.; Amatore, C. (Eds.) *Trends in Molecular Electrochemistry,* Marcel Dekker/Fontis Media, New York/Lausanne, **2004**, (b) Pombeiro, A.J.L.; McCleverty, J. (Eds.) *Molecular Electrochemistry of Inorganic, Bioinorganic and Organometallic Compounds,* NATO ASI Series, Kluwer, Dordrecht, **1993**, (c) Zanello, P. *Inorganic Electrochemistry: Theory, Practice and Application,* Royal Society of Chemistry, Cambridge, **2003**, (d) Astruc, D. *Electron Transfer and Radical Processes in Transition Metal Chemistry,* VCH, New York, **1995**, (e) Pombeiro, A.J.L. *New J. Chem.* **1997**, *21*, 649, (f) Pombeiro, A.J.L. *Portugaliae Electrochim. Acta* **1983**, *1*, 19, (g) Silva, M.E.N.P.R.A.; Pombeiro, A.J.L.; Fraústo da Silva, J.J.R.; Herrmann, R.; Deus, M.; Bozak, R.E. *J. Organomet. Chem.* **1994**, *480*, 81, (h) Silva, M.E.N.P.R.A.; Pombeiro, A.J.L.; Fraústo da Silva, J.J.R.; Herrmann, R.; Deus, M.; Castilho, T.J.; Silva, M.F.C.G. *J. Organomet. Chem.* **1991**, *421*, 75, (i) Vlcëk, A. *Chemtracts – Inorg. Chem.* **1993**, *5*, 1, (j) Sarapu, A.C.; Fenske, R.F. *Inorg. Chem.* **1975**, *14*, 247, (k) Pickett, C.J.; Pletcher, D. *J. Organomet. Chem.* **1975**, *102*, 327.

Using this approach of the concept that electrochemical potentials are additive with respect to ligand substitution for substituted metal carbonyls as a common basis, electrochemical parameters were defined: the Pickett ligand parameter P_L[37(k), 38] and the Lever ligand parameter E_L.[39] Pickett's and Lever's models of systematic approach have been applied to numerous ligands with electron donor and π-electron acceptor characters, binding various types of metal centers. Pombeiro extended this study to report the estimated electrochemical parameters for carbyne, carbene, vinylidene, allenylidene and alkynyl ligands from the reported values of the redox potentials of their complexes found in the literature.[40] It was found that the net electron acceptance of Group VI transition metal Fischer carbene complexes were sensitive to the nature of the groups attached to the carbene carbon, as a wide range of estimated P_L and E_L values were obtained. The strongest π-electron acceptors, namely diphenyl carbene,[41] displayed an extended conjugated π-system.

4.3.1 Anodic electrochemical behaviour of Fischer carbene complexes

The ferrocenyl carbene complexes[42] with the central metals $M(CO)_5$ (M = Cr, W), systematically exhibit lower oxidation potentials than the related carbene complexes with an alkyl or aryl group instead of ferrocenyl. This behaviour, observed for ferrocenyl alkoxycarbenes, aminocarbenes and anionic oxocarbenes, suggests that the ferrocenyl carbenes are stronger electron donors that the corresponding alkyl or aryl carbenes, on account of an effective π-electron donor ability as ferrocenyl moieties have the known ability to enter

---

[38] Chatt, J.; Kan, C.T.; Leigh, G.J.; Pickett, C.J.; Stanley, D.R. *J. Chem. Soc., Dalton Trans.* **1980**, 2052.

[39] (a) Lever, A.B.P. *Inorg. Chem.* **1990**, *29*, 1271, (b) Lever, A.B.P. *Inorg. Chem.* **1991**, *30,* 1980.

[40] Pombeiro, A.J.L. *J. Organomet. Chem.* **2005**, *690*, 6021.

[41] Guedes da Silva, M.F.C.; Lemos, M.A.N.D.A.; Fraústo da Silva, J.J.R.; Pombeiro, A.J.L.; Pellinghelli, M.A.; Tiripicchio, A. *J. Chem. Soc., Dalton Trans.* **2000**, 373.

[42] Lloyd, M.K.; McCleverty, J.A.; Orchard, D.G.; Connor, J.A.; Hall, M.B.; Hillier, I.H.; Jones, E.M.; McEwen, G.K. *J. Chem. Soc., Dalton Trans.* **1973**, 1743.

into conjugation with a neighbouring centre by π-donation.[37(g), 43] However, Pombeiro cautioned that the electrochemical parameters of $[M(CO)_5\{C(X)Fc\}]$ complexes encompass both the redox M^0 and Fe^{2+} centers, as the HOMO is not simply localized at the former.[40]

Another electrochemical study of ferrocenyl carbenes involved the reaction of ferrocene amides $(Ph_2P)Fc'C(O)NR_2$ (complex **I** as shown in Scheme 4.2) with $[Cr(CO)_5]^{2-}$ in the presence of Me_3SiCl to give the respective P-chelated carbene complex $[Cr(CO)_4\{(Ph_2P)Fc'C(NR_2)\text{-}\mu_2\text{-}C,P\}]$ (**II**) and a phosphine complex (**III**).[44]

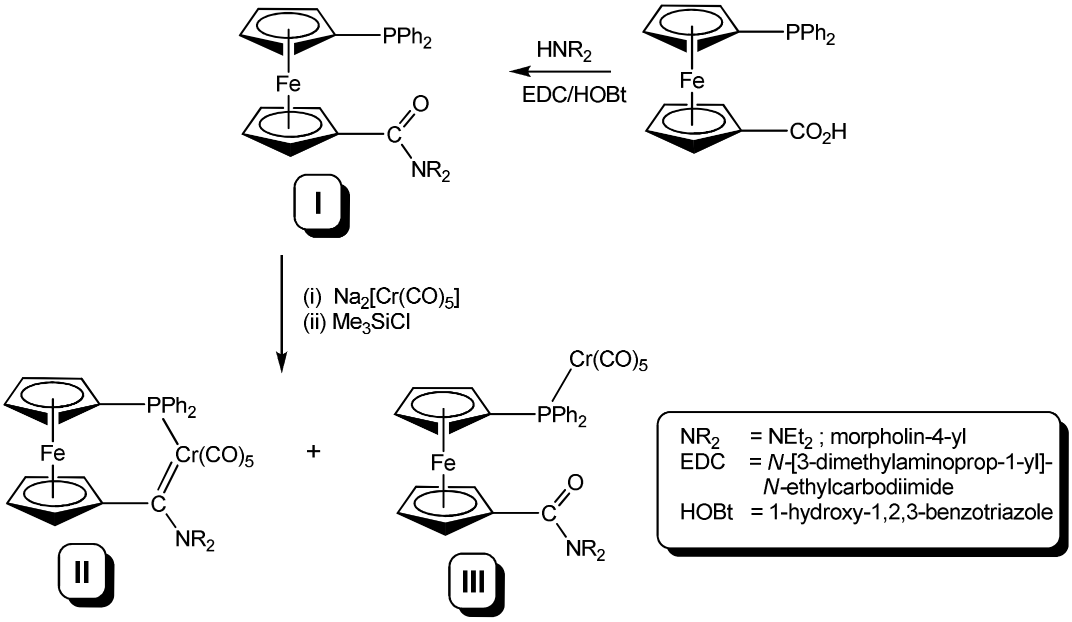

Scheme 4.2

An electrochemical analysis showed that where compounds **I** and **III** behave as a simple ferrocene system (**I**) and two localized redox systems (**III**) (ferrocene and chromium), respectively, carbene **II** is an electronically delocalized system, where the redox change probably occurs in the whole molecule.

---

[43] Gubin, S.P.; Lubovich, A.A. *J. Organomet. Chem.* **1970**, *22*, 183.

[44] Meca, L.; Dvořák, D.; Ludvík, J.; Císařová, I.; Štěpnička, P. *Organometallics* **2004**, *23*, 2541.

Unlike the [$Cr(CO)_5\{C(Y)Fc\}$] carbene complexes, which display a single one-electron wave ascribed to the removal of an electron from a molecular orbital which encompasses both metal centres,[42] the type **II** carbene complexes exhibit two one-electron redox processes. The first oxidation is reversible, shifted to markedly lower potentials than in the other compounds. The negative shift of the first oxidation wave in **II** was accounted for by the cooperative influence of the higher electron donating ability of NR_2 as compared to the OR group, and an electron density increase resulting from a replacement of one CO ligand with a phosphine, which makes the oxidation easier. This indicated that carbenes **II** are an example of the cooperative effect of the metal centre, enhanced by a conjugated bridge.

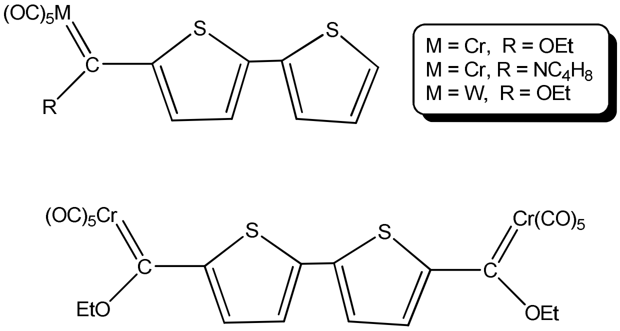

Scheme 4.3

Limberg *et al.* investigated the electrochemical behaviour of mono- and biscarbene complexes of chromium and tungsten by cyclic voltammetry (CV) and controlled potential electrolysis (CPE).[45] The complexes, illustrated in Scheme 4.3, all showed a single anodic wave. For the chromium compounds, this wave presented a partially reversible character, whereas the oxidation wave of the tungsten compound was irreversible.

The cyclic voltammograms displayed several cathodic waves. For the ethoxy substituted complexes, the first reduction waves were reversible, and found in

---

[45] Limberg, A.; Lemos, M.A.N.D.A.; Pombeiro, A.J.C.; Maiorana, S.; Papagni, A.; Licandro, E. *Portugaliae Electrochim. Acta* **1995**, *13*, 319.

the range -0.70 V to -1.02 V. However, the aminocarbene complex showed an irreversible cathodic wave at a remarkably more negative potential (-1.68 V). This large potential shift was seen as being due to the electron donating character of the amino group, and a possible indication that the energy of the LUMO is much influenced by carbene substituents, as expected for a significant contribution of the carbene carbon to that orbital as observed for related carbene complexes.[46]

Expanding on the cyclic voltammetry study of Group VI transition metal Fischer carbene complexes and focusing on the modulating effects of both the carbene metal and substituent, the group of Maiorana studied complexes of the type [M(CO)$_5${C(XR)R'}] (M = Cr; Mo; W and X = O; S; NR'').[47] It was found that the first oxidation step of the chromium compounds were significantly easier that that of the tungsten counterparts. This was correlated to the first ionization potentials of the two metals in gas phase (652.9 kL.mol^{-1} for Cr and 770 kJ.mol^{-1} for W),[48] indicating that the oxidation step is centred on the carbene metal.
The tungsten complexes featured chemically irreversible oxidation peaks, while the chemically reversible and monoelectronic peak of the chromium complexes implies that a chemically stable product forms. The potentials were also found to be widely modulable by changing both the XR and R' substituents.

4.3.2 Cathodic behaviour of Fischer carbene complexes

Fischer carbene complexes contain the electron withdrawing M(CO)$_5$-moieties, which make the carbene carbon atoms very electrophilic; hence, the carbene carbons are good electron acceptors. From DFT calculations, it can be seen that the LUMO is centred on the carbene carbon while the HOMO is metal-centred.[49] Therefore, the capture of one electron should succeed in a much more localized

---

[46] Casey, C.P.; Albin, L.D.; Saeman, M.C.; Evans, D.H. *J. Organomet. Chem.* **1978**, *155*, C37.
[47] Baldoli, Cl; Cerea, P.; Falciola, L.; Giannini, C.; Licandro, E.; Maiorana, S. ; Mussini, P. ; Perdicchia, D. *J. Organomet. Chem.* **2005**, *690*, 5777.
[48] Center for X-ray Optics and Advanced Light Source, X-ray Data Booklet **2001**, Lawrence Berkeley National Laboratory, University of California.
[49] Sierra, M.A.; Gòmez-Gallego, M.; Martínez-Álvarez, R. *Chem. Eur. J.* **2007**, *13*, 736.

site of the molecule, while the negative charge will be centred on the metal, and stabilized species may arise from the capture of one electron.

The single electron transfer (SET) of Group VI Fischer carbene complexes was investigated by chemical reagents (such as C_8K and SmI_2), as well as electrospray ionization (ESI) by Sierra *et al.*[49] The results obtained indicate that depending on the stability of the radical ion formed, the electrophile present in the reaction medium and the nature of the metal, different reaction products could be observed, from CO_2 trapping, to addition to electron poor olefins, CO insertions and dimerizations.

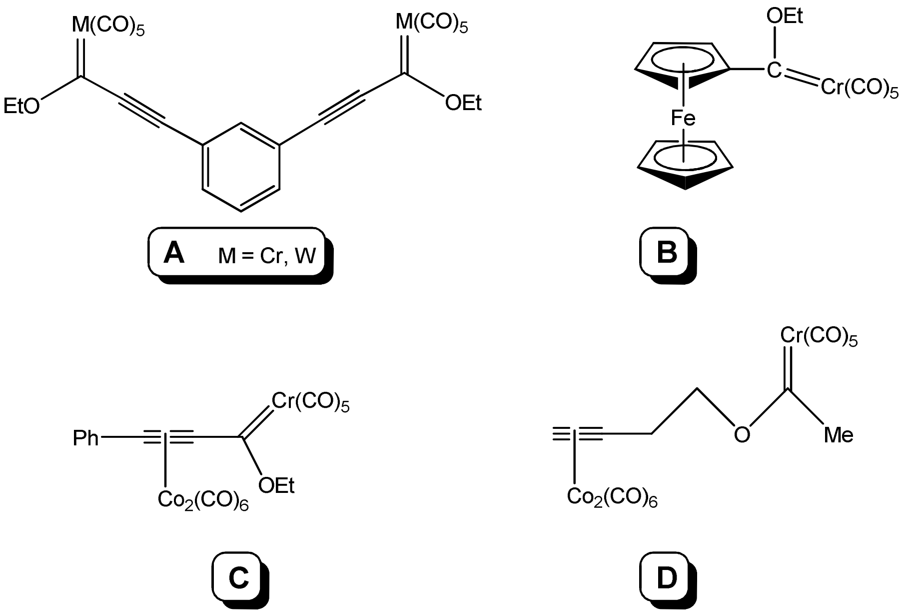

Scheme 4.4

The ESI-ET behaviour of metal carbene complexes could also be influenced by the presence of additional metal centres. Thus, the presence of two nonconjugated metal carbene moieties in homo- and heterobimetallic biscarbene complexes (**A** in Scheme 4.4) did not alter the general reactivity, and behaved in a similar fashion as the corresponding monocarbene complex $[Cr(CO)_5\{C(OEt)C{\equiv}CPh\}]$ in the presence of electron carrier additives such as tetrathiafulvalene (TTF) or hydroquinone (HQ). In electrochemical studies, the biscarbene complexes have also been found to behave as two independent monocarbene entities.[50]

The presence of a conjugated ferrocene moiety in the structure of the Fischer carbene comlexes, however, has a noticeable effect in the course of the ESI ionization.

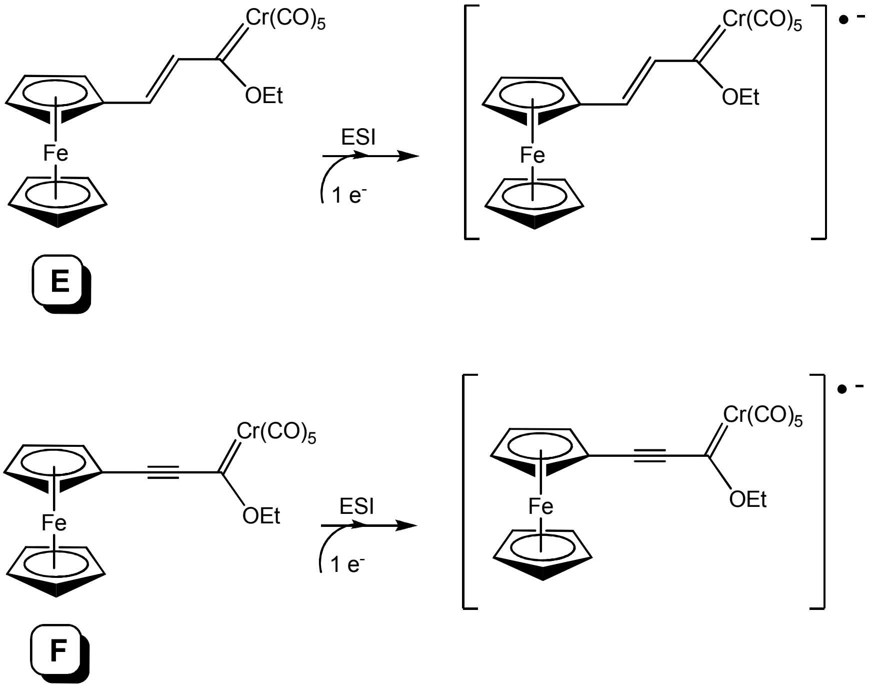

Figure 4.7 The ferrocenyl moiety acting as internal electron carrier in conjugated bimetallic carbene complexes

Ferrocenyl complexes **E** and **F** in Figure 4.7, ionize under ESI conditions even in the absence of the additives TTF and HQ, leading to radical anions. The experimental results could be understood considering the push-pull nature of these complexes. The ferrocenyl moiety is an electron donor and the $Cr(CO)_5$-group behaves like a large electron depleted group, since the five CO ligands are strong π-acceptors. Ferrocene can therefore be considered as an internal electron carrier that facilitates the direct formation of the carbene radical anion.

---

[50] Martínez-Álvarez, R.; Gòmez-Gallego, M.; Fernández, I.; Mancheño, M.J.; Sierra, M.A. *Organometallics* **2004**, *23*, 4647.

However, for complex **B** in Scheme 4.4, there is no π-tether linking the iron nucleus to the chromium, and no direct electrospray ionization could take place.

The presence of cobalt clusters exercised a radical effect in the ESI of the Group VI Fischer carbene complexes. When the $Co_2(CO)_6$-moiety was included in the structure of the complexes (**C** and **D** in Scheme 4.4), the electron transfer process from the additives was hampered. The ablility of $[Co_2(CO)_8]$ towards reduction is well known[51] and therefore the bimetallic cluster is seen as behaving as an electron sink inhibiting the ionization process.

4.4 Results and discussion

4.4.1 Focus of this study

The paper published by Cundari and Gordon[52] focused on the effect of ligand and substituent modification on the transition metal-alkylidene bond. They found that the intrinsic nature of the metal-carbon double bond could typically be changed within limits by modification of the electronegativities of the two carbene ligand substituents. Significant changes could be effected in three other ways: (i) variation of the central metal, (ii) use of π-donor substituents at the carbene group, and (iii) introduction of highly electropositive substituents like Li.

In this study, the aim was to investigate the effect of substituents on the carbene ligand of Group VI transition metal complexes of the type $[M(CO)_5\{C(OR)Y\}]$. The substituents included in this study ranged from the usual organic substituents (R = Et and Y = 2-benzothienyl or 2-thienyl); or metal-containing fragments that could either act as π-donors (Y = Fc), an electron sink (Y = $[Cr(CO)_3(2\text{-}\eta^6\text{-benzo}[b]\text{thienyl})]$ or $[Cr(CO)_3(\eta^6\text{-phenyl})]$) where a $Cr(CO)_3$-moiety is π-bonded to a (hetero)arene ring, or an electropositive titanoxy group (R =

---

[51] (a) Sweany, R.L. *Comprehensive Organometallic Chemistry II,* (Eds. Abel, E.W.; Stone, F.G.; Wilkinson, G.), Pergamon, Oxford, **1995**, *8*, (b) Gibson, D.H.; Ahmed, F.U.; Philips, K.R. *J. Organomet. Chem.* **1981**, *218*, 325.

[52] Cundari, T.R.; Gordon, M.S. *J. Am. Chem. Soc.* **1992**, *114*, 539.

TiCp$_2$Cl), as listed in Figure 4.8, in order to effect marked modulation of the carbene ligands, as stipulated by Cundari and Gordon.[52]

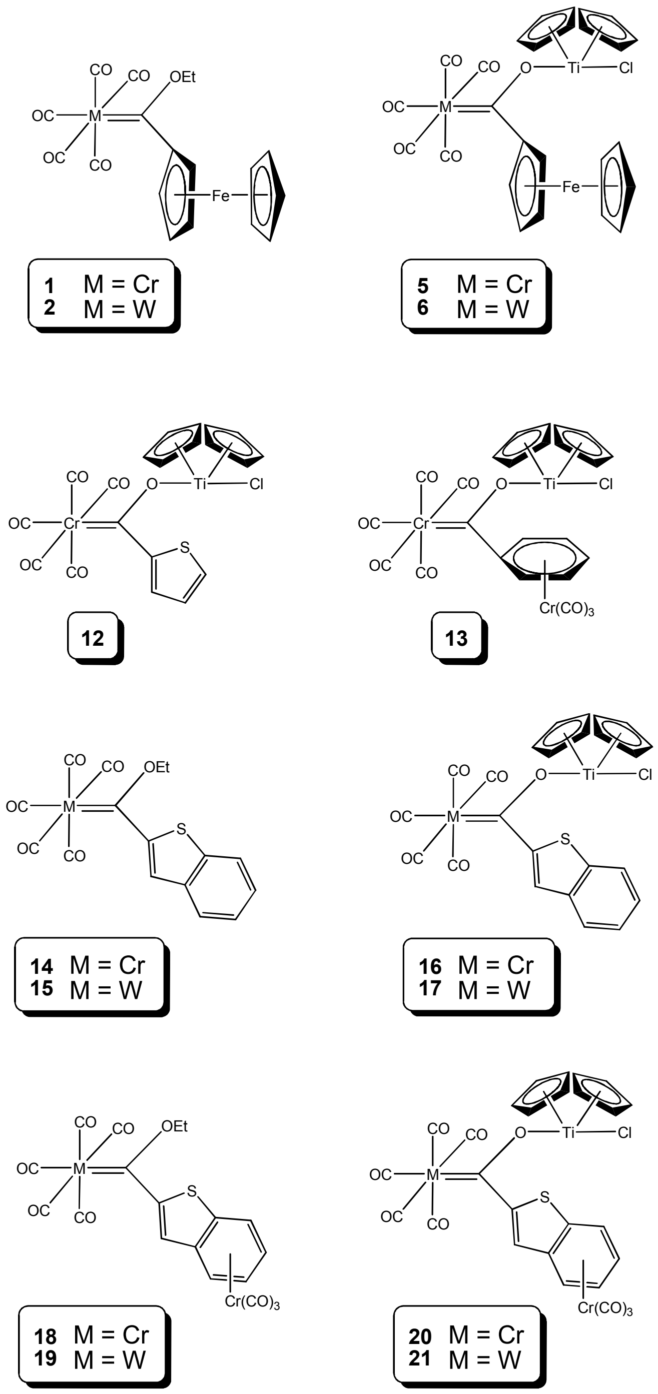

Figure 4.8 Monocarbene complexes studied by theoretical and electrochemical means

The synthesis and X-ray structural elucidation of the benzothienyl carbene complexes **14** – **21** have been previously published by our research group,[53] but were included for purposes of comparison in this study. Both theoretical and electrochemical methods were employed during this study. The possibility of using DFT calculations as a viable tool for pre-evaluation of cluster carbene complexes was also investigated.

4.5 Theoretical investigation of substituent effect

4.5.1 Computational details

The calculations reported in this chapter were obtained with the GAUSSIAN 03 suite of programmes.[54] Each complex was treated as an open-shell system using spin restricted DFT wavefunctions (RB3LYP)[55] i.e. the Becke three-parameter exchange functional in combination with the LYP correlation functional of Lee, Yang and Parr, with effective core potentials basis set LANL2DZ for the metal atoms. This method was specifically chosen as it allows increased accuracy of the model, with a small increase in the computation time; the increased accuracy arising from the inclusion of electron correlation effects where electrons interact with other electrons, not just an averaged electron cloud.[17] This is a quantum mechanical model, making use of the wavefunction of

---

[53] (a) Bezuidenhout, D.I.; van der Watt, E.; Liles, D.C.; Landman, M.; Lotz, S. *Organometallics* **2008**, *27*, 2447, (b) Van der Watt, E. *Fischer carbene complexes with metal-containing substituents,* MSc. Dissertation, University of Pretoria, Pretoria, **2006**.

[54] Frisch, M.J.; Trucks, G.W.; Schlegel, H.B.; Scuseria, G.E.; Robb, M.A.; Cheeseman, J.R.; Montgomery Jr, J.A.; Vreven, T.; Kudin, K.N.; Burant, J.C.; Millam, J.M.; Iyengar, S.S.; Tomasi, J.; Barone, V.; Mennucci, B.; Cossi, M.; Scalmani, G.; Rega, N.; Petersson, G.A.; Nakatsuji, H.; Hada, M.; Ehara, M.; Toyota, K.; Fukuda, R.; Hasegawa, J.; Ishida, M.; Nakajima, T.; Honda, Y.; Kitao, O.; Nakai, H.; Klene, M.; Li, X.; Knox, J.E.; Hratchian, H.P.; Cross, J.B.; Bakken, V.; Adamo, C.; Jaramillo, J.; Gomperts, R.; Stratmann, R.E.; Yazyev, O.; Austin, A.J.; Cammi, R.; Pomelli, C.; Ochterski, J.W.; Ayala, P.Y.; Morokuma, K.; Voth, G.A.; Salvador, P.; Dannenberg, J.J.; Zakrzewski, V.; Dapprich, S.; Daniels, A.D.; Strain, M.C.; Farkas, O.; Malick, D.K.; Rabuck, A.D.; Raghavachari, K.; Foresman, J.B.; Ortiz, J.V.; Cui, Q.; Baboul, A.G.; Clifford, S.; Cioslowski, J.; Stefanov, B.B.; Liu, G.; Liashenko, A.; Piskorz, P.; Komaromi, I.; Martin, R.L.; Fox, D.J.; Keith, T.; Al-Laham, M.A.; Peng, C.Y.; Nanayakkara, A.; Challacombe, M.; Gill, P.M.W.; Johnson, B.; Chen, W.; Wong, M.W.; Gonzalez, C.; Pople, J.A. *Gaussian 03*, revision C.02; Gaussian, Inc.: Wallingford, CT, **2004**.

[55] (a) Becke, A.D. *J. Chem. Phys.* **1993**, *98*, 5648, (b) Lee, C.; Yang, W.; Parr, R.G. *Phys. Rev. B* **1998**, *37*, 785, (c) Vosko, S.H.; Wilk, L.; Nusair, M. *Can. J. Phys.* **1980**, *58*, 1200.

the electrons, rather than the Newtonian-like molecular mechanics. The basis set LANL2DZ was chosen as it includes relativistic effects, which become important for the heavy atoms like W in the complexes. No symmetry constraints were applied and only the default convergence criteria were used during the geometric optimizations. The complexes were all modelled in the singlet spin state with S = ½ and the optimized structures were confirmed to be minima energy conformations as the vibrational frequency analysis[56] yielded no imaginary frequencies.

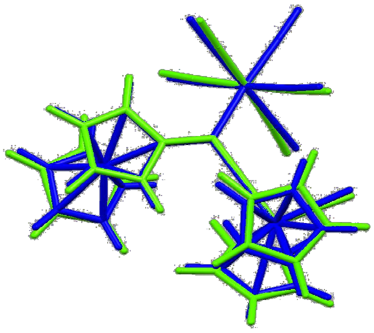

Figure 4.9 Representative overlay of experimental crystal structure and DFT optimised structure of complex **5**

The accuracy of the computational method was evaluated by comparing the root-mean-square deviations (RMSD's) between the optimized molecular structure and the crystal structure using the non-hydrogen atoms in the molecule. RMSD values were calculated using the 'RMS Compare Structures' utility in CHEMCRAFT Version 1.5.[57] Good agreement between experimental and theoretical structures was obtained as illustrated in Figure 4.9, and reflected by root-mean-square deviation (RMSD's) values in the range of 0.10 – 0.16 Å for the chromium complexes, and 0.06 – 0.19 Å for the tungsten complexes.

---

[56] McIver, J.W.; Komornicki, A.K. *J. Am. Chem. Soc.* **1972**, *94,* 2625.
[57] Zhurko, G.A.; Zhurko, D.A. *Chemcraft*, Version 1.5 (build 282), **2007**.

4.5.2 Theoretical results

Initially it was attempted to correlate the donor properties of the various carbene ligands in the complexes listed in Figure 4.8, with both the C≡O stretching frequencies and bond lengths with the aid of DFT calculations, as illustrated by Gusev.[58] The A_1^1 band, the mode associated with the stretching of the C-O bond *trans* to the carbene ligand was chosen as probe, as it is expected to be most affected by the electronic environment.

It is well known that (i) the assumption of an harmonic force field, (ii) the neglect or inadequate treatment of electron correlation effects and (iii) basis set deficiencies are sources of error in quantum mechanically computed vibrational frequencies.[59] Therefore it is common to multiply computed vibrational frequencies by a scale factor developed to minimize the RMS error from experiment. For organometallic complexes, it has been found that almost invariably, computed frequencies are greater than experiment.[60] For organometallic complexes, the CO vibrational frequencies determined at the B3LYP level with the relativistic core potential LANL2DZ, delivered reliable results from an optimized scale factor of 0.9521. The results obtained from this study gave a reasonable estimation of the carbonyl IR frequencies when compared to the experimental data of the solution IR spectra (reported in Chapter 2, as well as in previous studies[53] for the complexes **14** – **21**). However, the modelled data displayed consistent underestimations of the A_1^1 band frequencies calculated, the absolute deviations ranging from 10 – 60 cm^{-1}. The experimental solution IR data were therefore corrected by applying a scale factor of 1.02 to the modelled data. As the experimental data includes solution IR data recorded in either solvent hexane or dichloromethane, the scaled frequencies calculated by DFT methods were used to eliminate solvent effects.

---

[58] Gusev, D.G.; *Organometallics* **2009**, *28*, 763.

[59] Scott, A.P.; Radom, L. *J. Phys. Chem.* **1996**, *100*, 16502.

[60] Yu, L.; Srinivas, G.N.; Schwartz, M. *J. Mol. Struct. (Theochem)* **2003**, *625*, 215, and references therein.

The calculated frequencies for the A_1^1 band are tabulated in Tables 4.1 and 4.2 in order of decreasing wavenumbers, and should provide an indication of the π-acceptor ability of the relevant carbene ligand: the lower the wavenumber of the ν(CO), the weaker the *trans*-C-O bond, implying increased bond strength of the *trans*-OC-M bond and resultant decreased bond strength of the M=C(carbene). Tables 4.1 and 4.2 therefore also include the experimental bond lengths of the crystal structures. Not only the M=C(carbene) and *trans*-OC-M bond lengths were included, but also the *trans*-C-O, the C(carbene)-O and the C(carbene)-C((hetero)arene substituent) in order to determine if a trend could be established towards substituent involvement towards carbene stabilization.

For the sake of clarity, each complex [M(CO)$_5${C(OR)(hetero)aryl}] will be denoted by its central metal, eg. Cr(CO)$_5$-group represented by Cr; the (hetero)aryl ring substuent indicated as BT for 2-benzothienyl, T = 2-thienyl, Fc = ferrocenyl, BTCr = [Cr(CO)$_3$(η^6-2-benzo[*b*]thienyl)] and PhCr = [Cr(CO)$_3$(η^6-phenyl)], and R = Et (ethyl) or Ti (titanocene chloride). Therefore, complex **5** [Cr(CO)$_5${C(OTiCp$_2$Cl)Fc}] for example, will be represented by the abbreviation CrFcTi, and so on. The tables are colour coded, with red indicating the greatest value, and the smallest value coloured blue.

In general, the A_1^1 frequencies seem to correlate well with the M=C(carbene) bond lengths, for both the chromium and tungsten complexes, with the shortest bond distances obtained for the MBTCrET complexes **18** and **19**, respectively, corresponding to the highest ν(CO) wavenumbers. The weakest M=C bonds are the MFcTi, MFcET and MBTTi complexes (**5** and **6**; **1** and **2**; **16** and **17** respectively, M = Cr or W), which correspond to the lowest ν(CO) wavenumbers.

Table 4.1 Scaled, calculated A_1^{1} frequencies (cm^{-1}) and associated experimental bond lengths (Å) of selected chromium carbene complexes

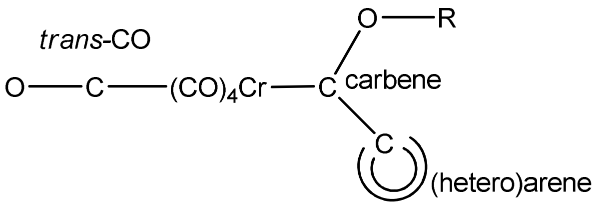

Complex	A_1^{1} ν(CO)*	Bond lengths				
		trans-C-O	Cr-CO*trans*	Cr-$C_{carbene}$	$C_{carbene}$-O	$C_{carbene}$-$C_{(hetero)arene}$
18 CrBTCrEt	1971	1.139(3)	1.884(3)	2.050(2)	1.324(3)	1.472(3)
13 CrPhCrTi	1968	1.146(5)	1.879(4)	2.067(3)	1.287(4)	1.513(5)
20 CrBTCrTi	1967	1.159(7)	1.859(6)	2.077(4)	1.285(5)	1.463(6)
14 CrBTEt	1964	1.143(3)	1.875(3)	2.067(3)	1.319(3)	1.462(3)
12 CrTTi	1961	1.150(3)	1.866(3)	2.081(2)	1.283(2)	1.442(5)
16 CrBTTi	1960	1.073(5)	1.926(9)	2.104(7)	1.275(9)	1.461(13)
1 CrFcEt	1959	1.135(3)	1.876(3)	2.084(2)	1.317(2)	1.452(3)
5 CrFcTi	1957	1.151(6)	1.863(5)	2.090(4)	1.286(5)	1.472(6)

* Corrected by a scale factor of 1.02

🟥 🟧 🟧 🟨 🟩 🟩 🟦 🟦

Decreasing values →

Table 4.2 Scaled, calculated A_1^1 frequencies (cm^{-1}) and associated experimental bond lengths (Å) of selected tungsten carbene complexes

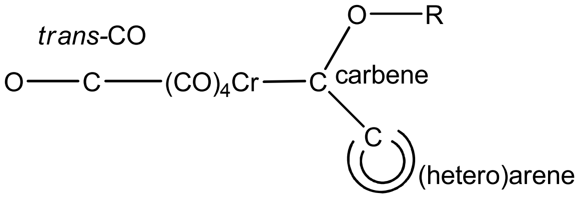

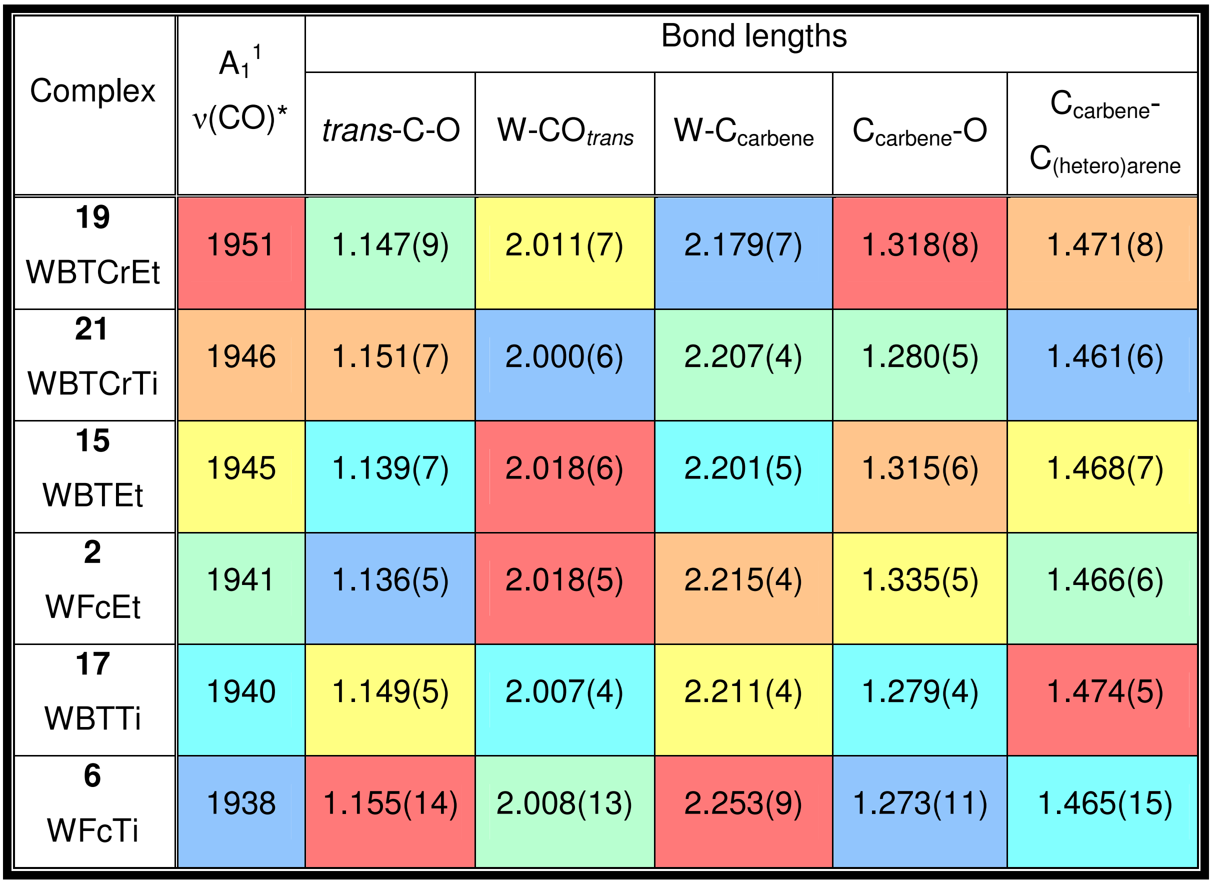

Complex	A_1^1 ν(CO)*	Bond lengths				
		trans-C-O	W-CO*trans*	W-Ccarbene	Ccarbene-O	Ccarbene-C(hetero)arene
19 WBTCrEt	1951	1.147(9)	2.011(7)	2.179(7)	1.318(8)	1.471(8)
21 WBTCrTi	1946	1.151(7)	2.000(6)	2.207(4)	1.280(5)	1.461(6)
15 WBTEt	1945	1.139(7)	2.018(6)	2.201(5)	1.315(6)	1.468(7)
2 WFcEt	1941	1.136(5)	2.018(5)	2.215(4)	1.335(5)	1.466(6)
17 WBTTi	1940	1.149(5)	2.007(4)	2.211(4)	1.279(4)	1.474(5)
6 WFcTi	1938	1.155(14)	2.008(13)	2.253(9)	1.273(11)	1.465(15)

* Corrected by a scale factor of 1.02

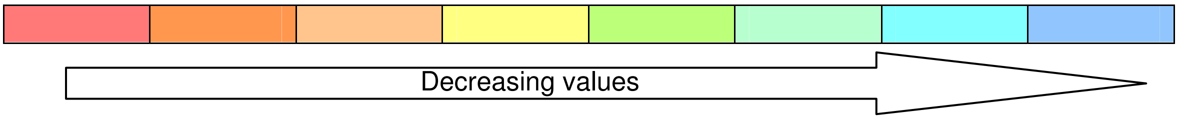

For both cases Cr and W as central method, a marked increase in C(carbene)-O bond length is observed for the ethoxycarbenes compared to the titanoxycarbene complexes. However, from the data in Table 4.2 a further distinction can be made: for either ethoxy- or titanoxycarbenes, the C(carbene)-

O bond distances increase in the substituent order Fc < BT < BTCr. Assuming that greater *O*-heteroatom stabilization towards the carbene carbon is necessary for ferrocenyl *vs* benzothienyl substituents is however not justified, as the C(carbene)-C(ring) bond lengths should then follow the inverse trend to demonstrate ring-involvement towards stabilization. For example, CrPhCrTi (**13**) exhibits long C(carbene)-O and C(carbene)-C(ring) bond distances, and a short Cr=C(carbene) bond length corresponding to a weak Cr-(CO)$_{trans}$ bond and high A_1' frequency. However, CrBTTi (**16**) shows the weakest Cr=C(carbene) bond, as well as the weakest Cr-(CO)$_{trans}$ bond. The shortest C(carbene)-O bond is also observed for this complex, which would seem to indicate most stabilization from the acyl-like titanoxy group. However, steric factors were not included in these arguments, which complicates identification of a clear trend from this data.

4.5.3 Vibrational spectroscopy results

To exclude solvent effects, solid, crystalline samples of complexes **5** and **6** (MFcTi); **18** and **19** (MBTCrEt); and **20** and **21** (MBTCrTi) (M = Cr, W) were obtained and solid state infrared spectra measured. The Raman spectra of the same complexes were also measured, using the 647.1 nm (red) line of a Krypton-ion laser. The IR data displayed clearly resolved spectra, with the expected localized C_{4v} pattern[61] of the IR-active A_1^2, A_1^1 and E-modes. Although all four modes (A_1^2, A_1^1, B_1 and E) are Raman-active, only the A_1^1 and A_1^2 bands were observed in the Raman spectra. In addition, the A_1^1 band (specifically, the vibrational ν(*trans*-C-O) frequency of interest) was not observed in the presence of titanoxycarbene substituents due to distortional effects, as illustrated in Figure 4.10. From the crystal structures of these complexes, it can be seen that the Cl-atom of the titanoxy substituent protrudes in between two *cis*-CO ligands (Figure 4.11). This distortion of the C_{4v} symmetry can lead to loss or reduction of symmetry, resulting in either C_s or C_{2v} symmetry which explains the disappearance of some Raman active vibrational modes.

---

[61] Adams, D.M. *Metal-Ligand and Related Vibrations,* Edward Arnold Publishers Ltd., London, **1967**, 98.

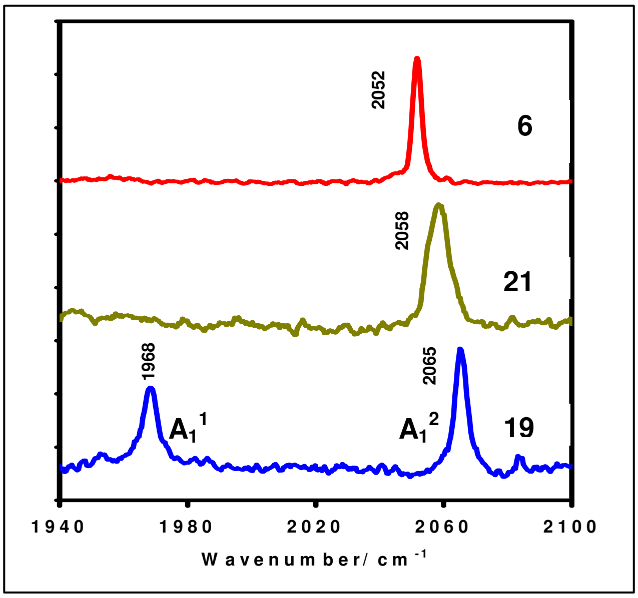

Figure 4.10 ν(CO) region of the Raman spectra of complexes **6, 19** and **21,** showing the disappearance of the A_1^1 band due to distortion effect of –TiCp$_2$Cl substituent

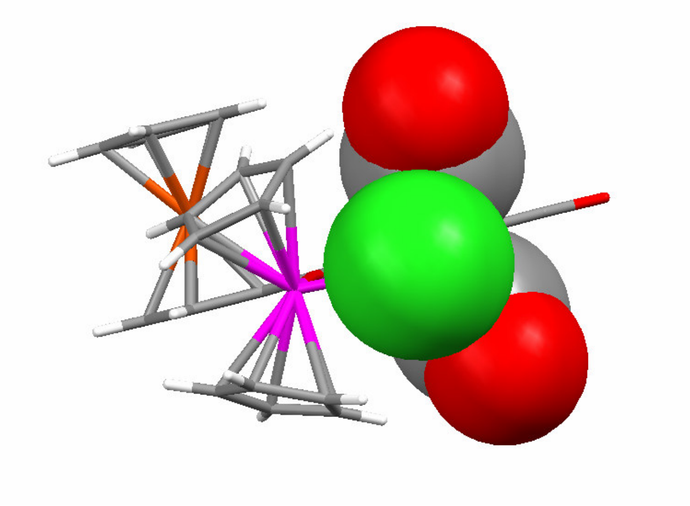

Figure 4.11 Space-filled representation of the Cl-atom (green) protruding between two *cis*-CO ligands of complex **6**

The above observation meant that the A_1^1 band could therefore not be used as a probe for substituent effect. Not only is the A_1^1 band absent in the Raman spectra of the titanoxy complexes, but DFT calculations also indicated significant contribution from the π-bonded $Cr(CO)_3$-fragment, where present. Therefore, other substituent influenced vibrational bands had to be employed in this investigation.

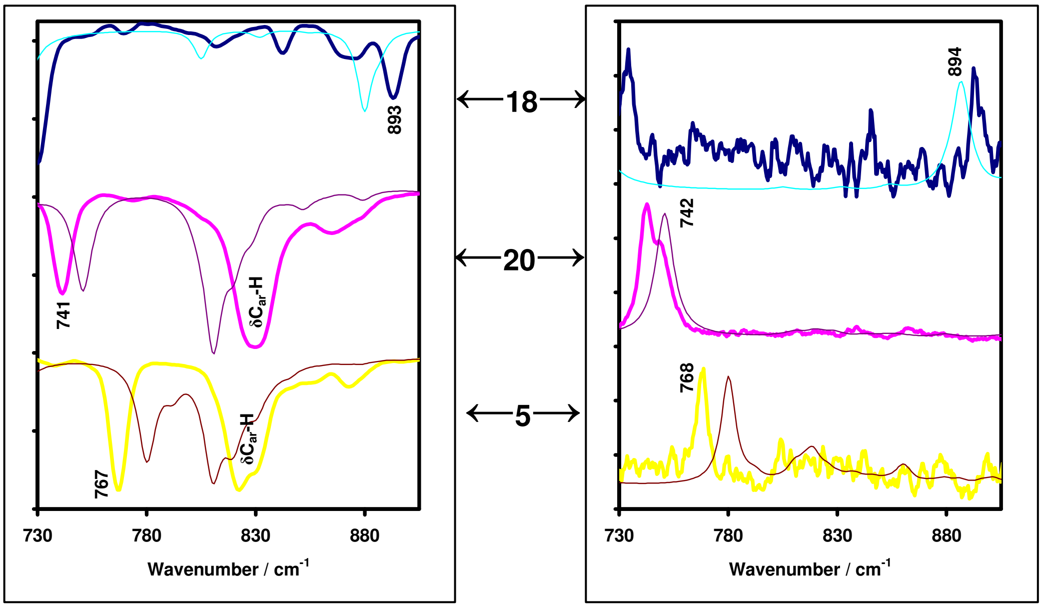

Figure 4.12 Comparative experimental (bold) and unscaled calculated (thin line) IR (left) and Raman (right) spectra of the $\delta CC_{carbene}O$ scissor mode for the chromium complexes

For $M(CO)_5L$ molecules, three IR active $\nu(M\text{-}C_{carbonyl})$ vibrations occur ($2\ A_1 + E$) in the far-infrared region, usually in the range of 380 – 500 cm^{-1}.[62] These metal-carbon stretching vibrations fall within range of the chromium tricarbonyl-fragment $M\text{-}C_{carbonyl}$ and other M-L vibrations, eg. Ti-Cl etc. DFT calculations were therefore employed to assist in the assignment of a $M\text{-}C_{carbene}$ stretching frequency. As far as could be ascertained, no such vibrational bands have been reported to date. However, the modelled data indicated that no pure $\nu(M\text{-}C_{carbene})$

---

[62] Darensbourg, M.Y.; Darensbourg, D.J. *Inorg. Chem.* **1970**, *9*, 32.

mode exists. Instead, a bending vibration or scissor mode could be identified from the calculations. A representative overlay of the measured experimental IR and Raman spectra and the calculated spectra used for assignment is demonstrated in Figure 4.12. The IR spectra illustrated in Figure 4.12 also display the ring-C-H deformation ($\delta C_{aromatic}$-H) modes. The $\delta(CC_{carbene}O)$ scissor mode consists of a stretching vibration of the carbene carbon atom towards the central metal atom, with contribution from the carbene carbon substituents, as depicted in Figure 4.13. This carbene ligand associated band was observed at higher wavenumbers than the $\nu(M\text{-}C_{carbonyl})$ bands in both the solid state IR and Raman spectra, and assignment of the scissor mode-related band, as well as the other substituent-influenced band, the A_1^1 $\nu(CO)$ mode, are done in Table 4.3.

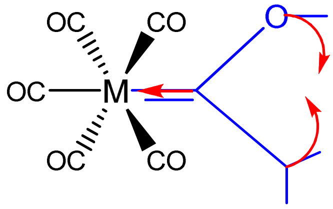

Figure 4.13 A schematic representation of the $\delta CC_{carbene}O$ scissor mode

Table 4.3 Experimental IR and Raman data of substituent influenced vibrational bands (cm^{-1})

Assignment	**18** CrBTCrEt		**20** CrBTCrTi		**5** CrFcTi	
	IR	Raman	IR	Raman	IR	Raman
$\nu(CO)$ A_1^1	1963	1968	1934	-	1921	-
$\delta CC_{carbene}O$	893	894	741	742	767	768
Assignment	**19** WBTCrET		**21** WBTCrTi		**6** WFcTi	
	IR	Raman	IR	Raman	IR	Raman
$\nu(CO)$ A_1^1	1960	1968	1913	-	1928	-
$\delta CC_{carbene}O$	895	895	746	748	774	774

The carbene ligand associated δCCO band displayed the highest energy for the η^6-2-benzo[*b*]thienyl chromium tricarbonyl ethoxy-substituted carbene complexes, corresponding to the shortest M=C(carbene) bond lengths tabulated in Tables 4.1 and 4.2. This supports the supposition that greater backdonation from the metal is necessary for a ring substituent π-bonded to a $Cr(CO)_3$-fragment that acts as an electron sink, minimizing ring-involvement towards carbene stabilization. The acyl character of the carbene oxygen atom of the titanoxy substituents (as discussed in previous chapters) could also be assumed to require less metal donation to the carbene carbon *p* orbital as it is a better π-donor, compared to that of the ethoxycarbenes. However, when the titanoxy substituent is kept constant and the effect of the η^6-2-benzo[*b*]thienyl chromium tricarbonyl *vs* the ferrocenyl substituent is compared, lower δCCO frequencies are obtained for the [$Cr(CO)_3$(η^6-2-benzo[*b*]thienyl)]-complexes even though Fc is the better π-donor. This could be ascribed to the greater bulk of the aforementioned substituent compared to that of Fc, contributing to the moment of inertia of the scissor mode. This result therefore does not preclude the spectroscopic data as a viable tool for substituent effect investigation, but both steric and electronic effects should be taken into account before any conclusions can be drawn. The calculated force constants of the vibrations were also considered, but followed the same order of magnitude trends as the actual vibrational frequencies.

4.5.4 Molecular orbital analysis

Comparison of the charges of the atoms calculated *via* Mulliken population analysis[63] cannot be done by considering the absolute values, as the chromium complexes display negatively charged Cr atoms compared to the positive W atoms. Instead the absolute differences between central metal atom and carbene carbon atom; carbene oxygen and carbene carbon atoms; and carbene

---

[63] Mulliken, R.S. *J. Chem. Phys.* **1955**, *23*, 1833.

carbon and arene substituent carbon atoms are used in the analysis of the atomic charges. The values are listed in Table 4.4.

Table 4.4 Calculated Mulliken charge differences of relevant atoms in carbene complexes

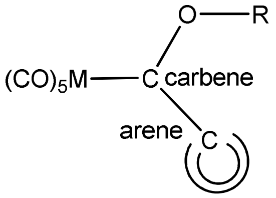

Complex	$\lvert Cr - C_{carbene} \rvert$	$\lvert O - C_{carbene} \rvert$	$\lvert C_{arene} - C_{carbene} \rvert$
1 CrFcEt	0.726	0.496	0.002
5 CrFcTi	0.597	0.720	0.020
12 CrTTi	0.711	0.876	0.544
13 CrPhCrTi	0.581	0.714	0.156
14 CrBTEt	0.846	0.662	0.565
16 CrBTTi	0.688	0.854	0.509
18 CrBTCrEt	0.821	0.641	0.554
20 CrBTCrTi	0.673	0.844	0.638
Complex	$\lvert W - C_{carbene} \rvert$	$\lvert O - C_{carbene} \rvert$	$\lvert C_{arene} - C_{carbene} \rvert$
2 WFcEt	0.592	0.258	0.236
6 WFcTi	0.746	0.507	0.145
15 WBTEt	0.338	0.501	0.423
17 WBTTi	0.549	0.708	0.394
19 WBTCrEt	0.370	0.478	0.424
21 WBTCrTi	0.543	0.698	0.529

The blue and red coded cells in the table indicate heteroatom substituent effect: for ethoxy substituted complexes, a larger charge difference (blue) between the

Cr atom and carbene carbon is observed, as the titanoxy substituent is expected to better stabilize the carbene carbon atom, due to the greater electron density present on the titanoxy-O atom (red) compared to that of the ethoxy-O atom. For the tungsten complexes, the W atom is originally assigned a positive charge in contrast to the negative charge of the Cr atom. The inverse trend observed (blue) therefore indicates agreement of the results obtained for the chromium complexes.

The charge differences between carbene carbon atom and (hetero)arene carbon should indicate to what extent the π-ring is involved towards stabilization of the carbene, as aromaticity is disrupted. In the case of the η^6-phenyl chromium tricarbonyl substituted complex **13** (yellow), the small difference value can be ascribed to the ‘electron sink’ capability of the $Cr(CO)_3$-fragment, drawing electron density towards itself. For the η^6-2-benzo[*b*]thienyl chromium tricarbonyl complexes, the $Cr(CO)_3$-moiety is not bonded to the thienyl ring which is directly bonded to the carbene carbon atom, and therefore does not display such a marked effect. On the other hand, the small difference values obtained for the ferrocenyl complexes can be explained by the stabilization effect of ferrocenes that takes place through π-delocalization rather than through inductive effects.[64]

The importance of the LUMO of Fischer carbene complexes in the nucleophilic attack of carbene carbons were explained by Block *et al.*[36(a)] Calculated atomic charges indicated that the carbene carbon atom is less positive than the carbonyl carbons, in agreement with the X-ray photoelectron spectroscopic data of Perry.[65] Nevertheless, the carbene carbon was found to be the preferred site for nucleophilic attack and charge did not determine reactivities.

However, frontier orbital control,[66] which emphasizes the importance of a compound’s HOMO or LUMO in determining which sites in the molecule will be most susceptible to attack by an electrophile or nucleophile could explain the reactivities. A striking result of the MO calculations on the carbene complexes

---

[64] Connor, J.A.; Lloyd, J.P. *J. Chem. Soc., Dalton Trans.* **1972**, 1470.

[65] Perry, W.B.; Schaaf, T.F.; Jolly, W.L.; Todd, L.J.; Cronin, D.L. *Inorg. Chem.* **1973**, *13*, 2038.

[66] (a) Fukui, K.; Fujimoto, H. *Bull. Chem. Soc. Jpn.* **1969**, *42*, 3399, (b) Klopman, G.; Hudson, R.F. *Theor. Chim. Acta* **1967**, *8*, 165.

was the marked separation of the LUMO from all of the other molecular orbitals. The carbene complex LUMO was found to lie 4.6 eV below the next lowest unoccupied MO, and 6.6 eV above the HOMO. The LUMO is localized on the carbene carbon: the LUMO's major component is the carbene carbon $2p_x$ orbital, which constitutes 60% of the level. The preference for nucleophilic attack at the carbene carbon could therefore be explained as a result of the spatial localization and energetic isolation of the LUMO of the complex.

In order to investigate the so-called electrophilicity of the carbene complexes with the different substituents, as described above, the molecular orbitals were calculated and the spatial localization of the chromium complex MO's are given in Figures 4.14 and 4.15. The tungsten complexes displayed similar orbitals.

For the monometallic complexes (**14**, **15**), as well as the bimetallic complexes of which the second metal was the titanium in the titanoxy substituent (**16**, **17**), the HOMO's are localized on the $M(CO)_5$-moiety, while the LUMO's are distributed across the *trans*-CO ligand, the carbene ligand as well as the delocalized ring-substituents. For complexes **18** – **21**, containing a $Cr(CO)_3$-fragment π-bonded, the $M(CO)_5$ contribution towards the HOMO's is considerably decreased, with the HOMO mostly localized on the $Cr(CO)_3$-group, although the LUMO's of these complexes exhibited the same site positions as those of the monometallic complexes.

An interesting deviation was observed for the ferrocenyl complexes (**1**, **2**) and (**5**, **6**): while the ferrocenyl ethoxycarbenes (**1**, **2**) have HOMO's distributed across both the $M(CO)_5$-moiety and the ferrocenyl group, the corresponding titanoxycarbenes (**5**, **6**) have HOMO's located almost exclusively on the $M(CO)_5$-group. This finding is in direct contrast to that of Pombeiro,[40] where the HOMO's of ferrocenyl carbene complexes encompassed both the M^0 as well as the Fe^{2+} centers. The ethoxy analogues showed a small contribution from the $M(CO)_5$-moiety with most of the HOMO situated on the ferrocenyl substituent. On the other hand, the ethoxy analogues diplayed LUMO's of the same shape as those of the aforementioned complexes, but the ferrocenyl titanoxycarbene complexes **5** and **6** are the only complexes where the LUMO is located only on the titanoxy- and carbene atoms, with no contribution from the *trans*-carbonyl ligand or the arene substituent.

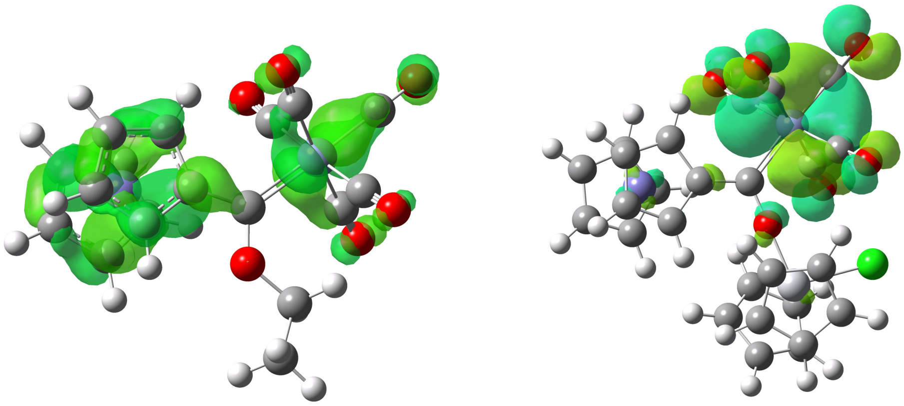

(a) **1** CrFcEt
Energy = -6.2221 eV

(b) **5** CrFcTi
Energy = -6.1070 eV

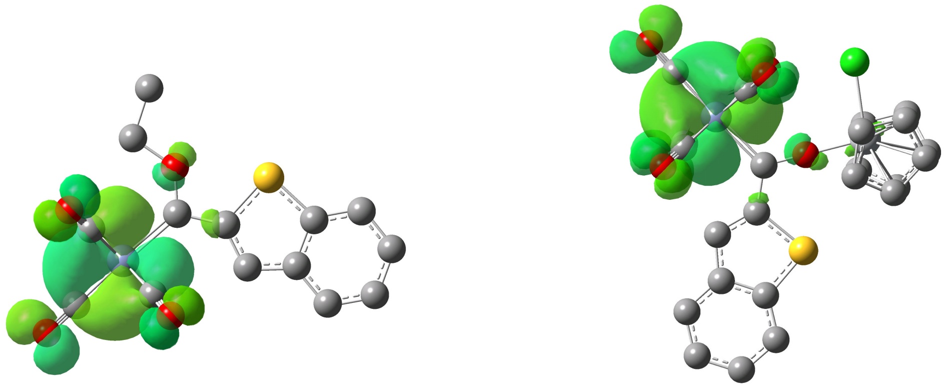

(c) **14** CrBTEt
Energy = -6.5277 eV

(d) **16** CrBTTi
Energy = -6.1903 eV

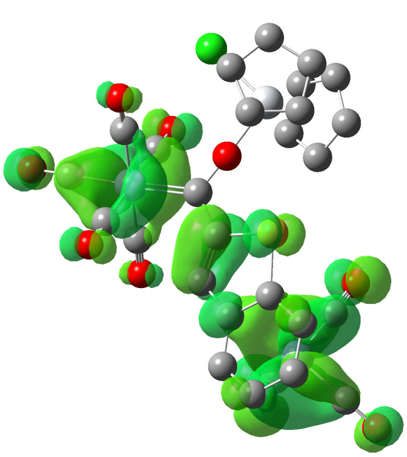

(e) **18** CrBTCrEt
Energy = -6.2420 eV

(f) **20** CrBTCrTi
Energy = -6.2918 eV

Figure 4.14 Selected HOMO representations and associated energies

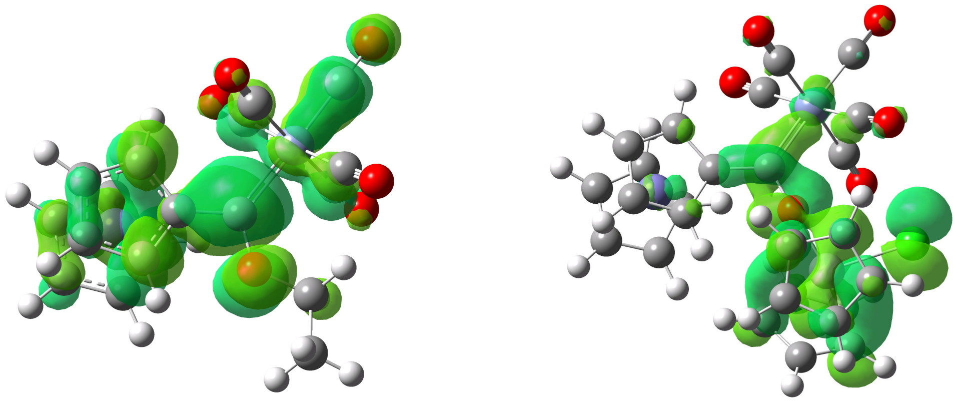

(a) **1** CrFcEt
Energy = -2.529 eV

(b) **5** CrFcTi
Energy = -2.8818 eV

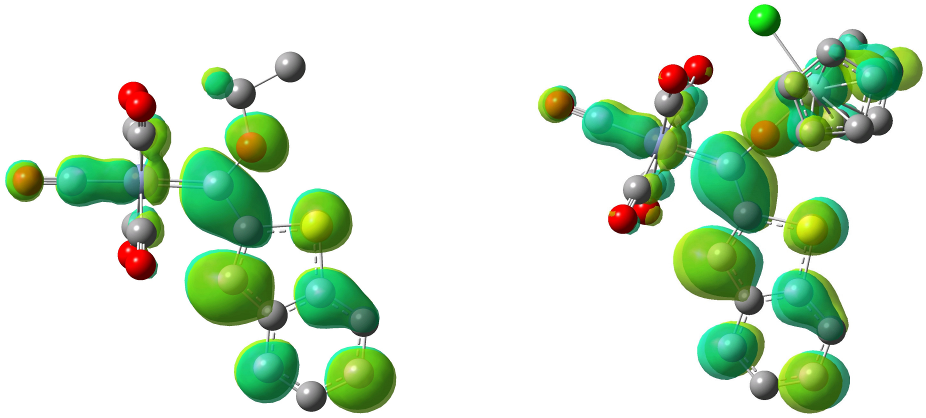

(c) **14** CrBTEt
Energy = -3.1645 eV

(d) **16** CrBTTi
Energy = -3.2489 eV

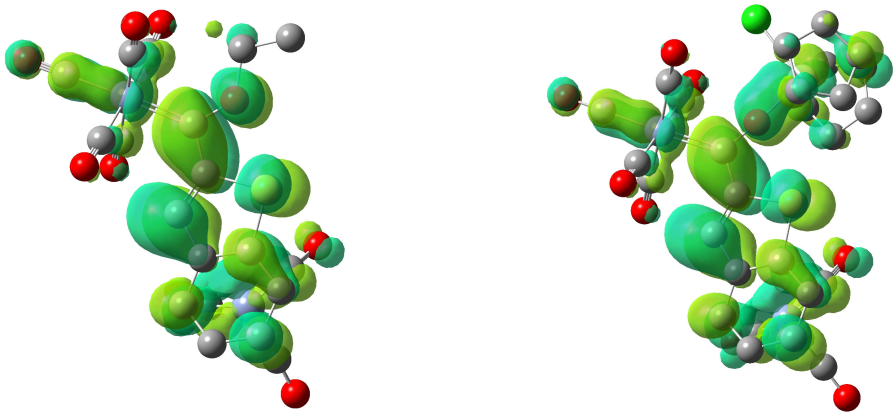

(e) **18** CrBTCrEt
Energy = -3.6244 eV

(f) **20** CrBTCrTi
Energy = -3.5833 eV

Figure 4.15 Selected LUMO representations and associated energies

As the LUMO determines the site of nucleophilic attack, [66] it seems reasonable to assume that the titanoxy *vs* ethoxy substituent will therefore greatly influence this reactivity.

To determine if the same isolation of the LUMO energy level from the other molecular orbitals calculated for a molecule also determined carbene ligand electrophilicity as observed by Block[36(a)] the energy differences between the LUMO's and the next-closest lying molecular orbitals were calculated, and are listed in Table 4.5.

Table 4.5 Molecular orbital energy differences (eV) calculated for the complexes analyzed

Complex	LUMO - HOMO	LUMO+1 - LUMO	Complex	LUMO - HOMO	LUMO+1 - LUMO
1 CrFcEt	3.6932	1.0198	**2** WFcEt	3.4818	0.6356
5 CrFcTi	3.2253	0.0460	**6** WFcTi	3.0320	0.0506
14 CrBTEt	3.3632	1.5374	**15** WBTEt	3.1335	1.0941
16 CrBTTi	2.9414	0.3320	**17** WBTTi	2.7278	0.3744
18 CrBTCrEt	2.6176	1.7387	**19** WBTCrEt	2.5308	1.3118
20 CrBTCrTi	2.7085	0.4827	**21** WBTCrTi	2.5466	0.5989

In most cases, the greatest energy separation of the LUMO from either the HOMO or the LUMO+1 energy levels were for ethoxy substituted complexes, as indicated by the blue cell in the table, while the green cells indicate differences larger than the average. For both the chromium and tungsten ferrocenyl titanoxycarbene complexes (**5** and **6**) , the calculated energy difference between the HOMO and LUMO is larger than expected, however, a very small energy difference between the LUMO and the next lowest unoccupied molecular orbital is observed, therefore not demarcating these complexes as potentially more electrophilic than the other titanoxycarbene complexes. However, this energy difference of the HOMO and LUMO orbital energies are defined not to determine electrophilicity, but chemical hardness as defined by Pearson.[67]

Formally, as a result of the σ-donation being larger than backdonation in Fischer carbene complexes, these complexes have a $[(CO)_5Cr^{\delta-}\leftarrow C^{\delta+}]$ charge separation, which indicates lack of charge on the carbene carbon atom and also supports the electrophilic reactivity of the carbene site. Another way to evaluate the electrophilicty of these complexes is to calculate the electrophilicity index, ω, for each complex measured according to Parr, Szentpály and Liu,[68] using the expression

$$\omega \equiv \mu^2 / \eta$$

In the above equation, μ is the chemical potential[69] (the negative of the electronegativity) and η is the hardness.[67] These values are related to the molecular orbital energies, and the chemical potential and hardness can be calculated from the HOMO and LUMO orbital energies using the following approximate expressions:

$$\mu = (E_{\mathrm{LUMO}} + E_{\mathrm{HOMO}}) / 2$$

$$\eta = E_{\mathrm{LUMO}} - E_{\mathrm{HOMO}}$$

Table 4.6 Electrophilicity index of the complexes analyzed

Complex	ω (eV)	Complex	ω (eV)
1 CrFcEt	2.5919	**2** WFcEt	2.8401
5 CrFcTi	3.1315	**6** WFcTi	3.2709
14 CrBTEt	3.4915	**15** WBTEt	3.7613
16 CrBTTi	3.7864	**17** WBTTi	3.9969
18 CrBTCrEt	4.6486	**19** WBTCrEt	4.8946
20 CrBTCrTi	4.5005	**21** WBTCrTi	4.7390

---

[67] Pearson, R.G. *Chemical Hardness*, Wiley-VCH, Oxford, **1997**.

[68] Parr, R.G.; v. Szentpály, L.; Liu, S. *J. Am. Chem. Soc.* **1999**, *121*, 1922.

[69] Parr, R.G.; Yang, W. *Density-Functional Theory of Atoms and Molecules*, Oxford University Press, New York, **1989**.

When electrophilic indices were calculated by Frenking *et al.*[25(a)] for Fischer carbene complexes, it was found that π-donor substituents reduce the electrophilicity of the complexes, as a result of the acceptor orbital in the carbene becoming occupied by π-donation. The values listed in Table 4.6 clearly adhere to above statement. Thus for every fixed [M(CO)$_5${C(OX)(arene)}] (X = Et or TiCp$_2$Cl), the electrophilicity increases following the order Fc < 2-benzothienyl < 2-η^6-benzo[*b*]thienyl chromium tricarbonyl, demonstrating the donating properties of the ferrocenyl group, and the largest electrophilicities of the π-bonded Cr(CO)$_3$-substituted carbene complexes in line with the acceptor character of these substituents. Due to the greatly differing nature of these substituents, a greater impact on the carbene electrophilicity is effected by these ring-substituents, compared to the results of Connor[32] where the nature of the heteroatom substituent, rather than the arene-substituent or the metal, more strongly influenced the electronic nature of the carbene carbon atom.

No clear trend could be identified for the *O*-substituents. In the case of the ferrocenyl and benzothienyl complexes, higher electrophilicity indices were calculated for the titanoxy analogues. For the [Cr(CO)$_3$(2-η^6-BT)]-substituted complexes, higher ω-values were obtained for the ethoxycarbene complexes, as expected from previous results where the donating character of the acyl-like oxygen of the titanoxycarbenes were proven.

4.5.5 Correlation between UV/Vis spectroscopy and MO analysis

The UV/vis spectra of complexes **5**, **6** and **18** – **21** were measured in benzene, as decomposition in chlorinated solvents, and limited solubility in hexane precluded use of these solvents. Poorly resolved spectra were obtained, thus the peak-fitting utility of the OriginPro 7.5© software programme was employed to aid in the deconvolution of the three observed absorbance peaks. Representative spectra are illustrated in Figure 4.18.

The UV-spectra of Fischer carbene complexes are known to display three well-defined absorptions: a spin-forbidden MLCT absorption at approximately 500 nm, a spin-allowed and moderately intense LF absorption in the range of 350 – 450 nm, and one additional LF transition in the range of 300 – 350 nm.[70] Strong ligand-based absorption bands occur in the range 200 – 250 nm, but were not measured during this study. The LF absorptions occurring in the 300 – 500 nm range are the π-π* transitions, where coordination to metal fragments can shift these bands to higher wavelengths. Interaction of the metal carbene π-system with that of the (hetero)aryl substituent are thus indicated by reduced energies of the π-π* transitions. The UV-visible data of the selected complexes are listed in Table 4.7, and includes energy values of the MLCT transitions in units of electron volt.

The lower energy absorption MLCT band is a metal-*d* to carbene-*p* orbital transition,[71] where the metal donates electrons to the empty *p*-orbital of the carbene carbon in the excited state, whilst the heteroatom bonded to the carbene carbon atom acts as π-donor towards the metal in the ground state (Figure 4.17). The colour of each complex is characteristic to the number of metal moieties coordinated to the ligand, and corresponds to the MLCT transition: shorter wavelength absorptions observed for the complexes displaying increasingly red colour.

Table 4.7 UV/vis data of selected complexes*

Complex	Colour	LF π-π* transition (λ, nm)	MLCT transition (λ, nm)	MLCT transition (E, eV)
5 CrFcTi	Red-brown	293, 436	504	2.460
18 CrBTCrEt	Purple	314, 471	577	2.149
20 CrBTCrTi	Dark purple	287, 509	599	2.070
6 WFcTi	Dark red	285, 427	521	2.380
19 WBTCrEt	Dark brown	323, 448	581	2.134
21 WBTCrTi	Purple	315, 480	572	2.168

* Recorded in solvent benzene

---

[70] Hegedus, L.S. *Tetrahedron* **1997**, *53*, 4105.
[71] Shriver, D.F.; Atkins, P.W. *Inorganic Chemistry,* 3rd Ed. Oxford University Press, Oxford, **1999**.

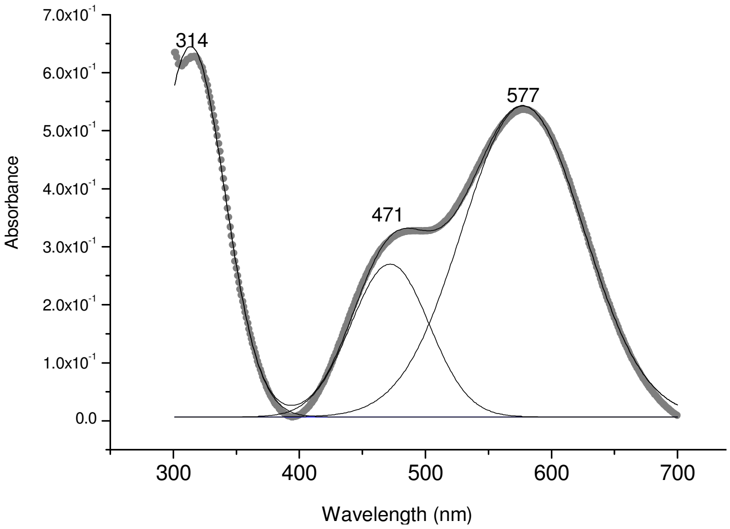

(a)

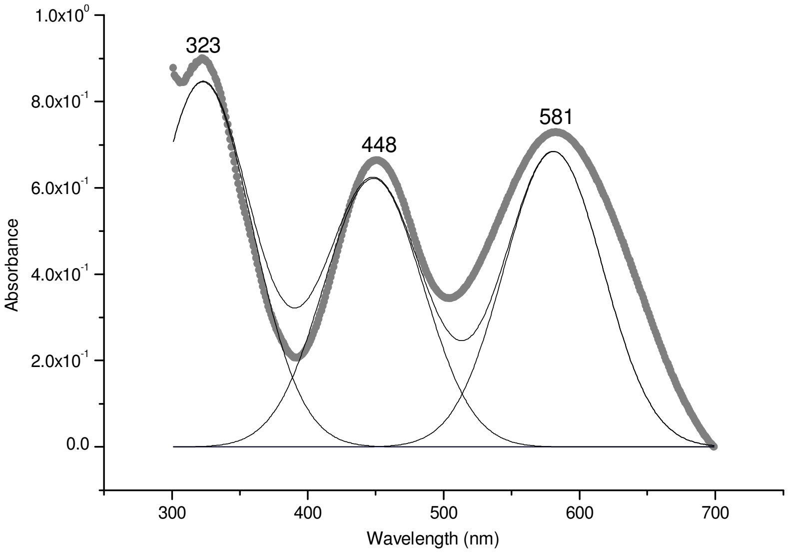

(b)

Figure 4.16 UV/vis spectra of complexes (a) **18** and (b) **19**, illustrating peak deconvolution

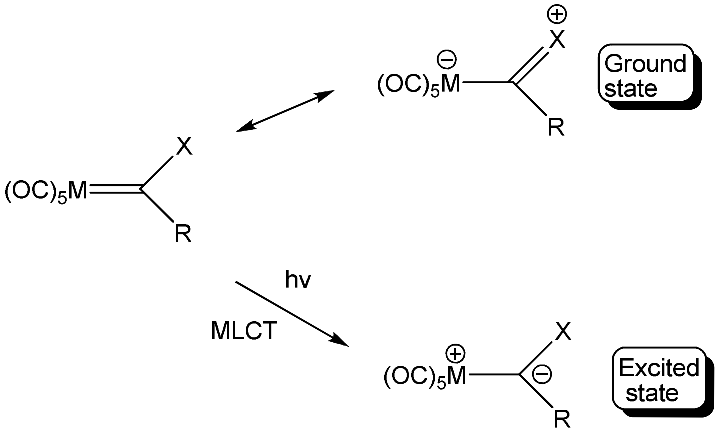

Figure 4.17 Ground and excited states in Fischer carbene complexes

The magnitude of the energies of the MLCT transitions seems to correlate more with a HOMO → LUMO transition (compare Tables 4.5 and 4.7), as described in earlier work,[36] than with the results obtained by Sierra[25(f)] where the transition was attributed to the promotion of one electron from the HOMO-1 to the LUMO. However, the UV/vis experimental work has not been corroborated by DFT calculations in this case. The size of the HOMO-LUMO energy gap can be arranged in the order CrFcTi **5** > CrBTCrEt **18** > CrBTCrTi **20**, corresponding to the inverse order of the wavelengths of the MLCT band: CrBTCrTi **20** > CrBTCrEt **18** > CrFcTi **5**. Similarly for the tungsten complexes: the HOMO-LUMO gap (eV): WFcTi **6** > WBTCrEt **19** ~ WBTCrTi **21**, and the MLCT λ (nm): WBTCrEt **19** ~ WBTCrTi **21** > WFcTi **6**.

The effect of π-accepting or donating aryl-substituents on the LF band could not be established as the arene substituents themselves varied (Fc *vs* 2-BTCr(CO)$_3$). The effect of the greater donating ability of the titanoxy fragment compared to the ethoxy group was seen in the blue shift of the π-π* transition of the ethoxycarbenes **18** and **19** (471 and 448 nm, respectively) in relation to the titanoxycarbenes **20** and **21** (509 and 480 nm, respectively).

4.5.6 Natural bond orbital analysis

The atomic orbital occupations and donor-acceptor interactions of the chromium complexes **1**, **5**, **14**, **16**, **18** and **20** were computed using the NBO method.[23] The atomic charges and orbital occupations of the relevant atoms, as indicated in Figure 4.18, participating in the metal-carbene bonding interaction, are listed in Tables 4.8 and 4.9, respectively.

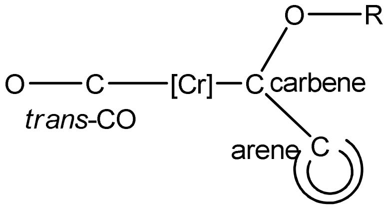

Figure 4.18 Relevant atoms and bonds (M-CO$_{trans}$, M-C$_{carbene}$, C$_{carbene}$-C$_{arene}$, and C$_{carbene}$-O) analyzed by the NBO method

Table 4.8 Calculated atomic charges of selected complexes by NBO analysis

Complexes	Atomic charges			
	Cr	C(carbene)	O	C(arene)
1 CrFcEt	-1.408	+0.429	-0.555	-0.198
5 CrFcTi	-1.394	+0.453	-0.597	-0.198
14 CrBTEt	-1.401	+0.405	-0.549	-0.249
16 CrBTTi	-1.388	+0.425	-0.600	-0.243
18 CrBTCrEt	-1.400	+0.407	-0.549	-0.227
20 CrBTCrTi	-1.383	+0.427	-0.602	-0.214

The data listed in Table 4.8 only show significant variations in atomic charges on exchanging an ethoxy substituent for a titanoxy substituent, while no great effect is observed on changing the ring-substituent, unlike the Mulliken charges listed in Table 4.4. In each case, the titanoxycarbene complex display a decreased negative charge on the chromium atom, an increased positive charge on the carbene carbon atom and an increased negative charge on the oxygen atom, demonstrating the increased ionic nature of the C(carbene)-Ti bond, so that resonance structure **I** in Figure 4.19 probably shows a greater contribution to the structure of the titanoxycarbenes, compared to their ethoxy analogues.

Table 4.9 Comparison of calculated NBO occupation of the relevant carbene ligand-associated orbitals

Calculated NBO	**1** CrFcEt	**5** CrFcTi	**14** CrBTEt	**16** CrBTTi	**18** CrBTCrEt	**20** CrBTCrTi
Cr-$C_{carbene}$ BD	-	-	1.605	1.605	1.879 1.613	1.609
Cr-$C_{carbene}$ BD*	-	-	0.486	0.500	0.646 0.472	0.486
Cr-C_{trans} BD	1.890	1.895	1.937	1.941	1.739	1.941
Cr-C_{trans} BD*	0.466	0.463	0.600	0.594	0.477	0.599
$(C\text{-}O)_{trans}$ BD	1.998 1.996 1.994	1.998 1.995 1.993	1.998 1.995 1.994	1.998 1.995 1.994	1.995 1.995	1.998 1.994 1.995
$(C\text{-}O)_{trans}$ BD*	0.189 0.170 0.016	0.189 0.170 0.016	0.187 0.167 0.016	0.188 0.168 0.016	0.050 0.149	0.184 0.016 0.163

† BD denotes a bonding orbital, BD* an antibonding orbital. Successive values denote the presence of successive bonding orbitals, therefore the presence of two BD occupation indicates a double bond.

‡ LP denotes a lone pair orbital

Table 4.9 *contd.* Comparison of calculated NBO occupation of the relevant carbene ligand-associated orbitals

Calculated NBO	**1** CrFcEt	**5** CrFcTi	**14** CrBTEt	**16** CrBTTi	**18** CrBTCrEt	**20** CrBTCrTi
$C_{carbene}$-O BD	1.987 1.974	1.987 1.932	1.988	1.987	1.987	1.987
$C_{carbene}$-O BD*	0.058 0.339	0.036 0.329	0.056	0.036	0.037	0.036
$C_{carbene}$-C_{ring} BD	1.967	1.969	1.970	1.987	1.969	1.973
$C_{carbene}$-C_{ring} BD*	0.032	0.044	0.027	0.039	0.027	0.040
O-R BD (R= Et or Ti)	1.987	1.986 1.964	1.987	-	1.987	-
O-R BD* (R= Et or Ti)	0.039	0.272 0.272	0.041	-	0.041	-
O_{trans} LP	1.973	1.974	1.974	1.974	1.974 1.546	1.974
C_{trans} LP	-	-	-	-	1.400	-
$C_{carbene}$ LP	1.403	1.376	1.406	1.378	-	1.379
O LP	1.957	-	1.953 1.717	1.745 1.644	1.952 1.714	1.780 1.757 1.637

† BD denotes a bonding orbital, BD* an antibonding orbital. Successive values denote the presence of successive bonding orbitals, therefore the presence of two BD occupation indicates a double bond.

‡ LP denotes a lone pair orbital

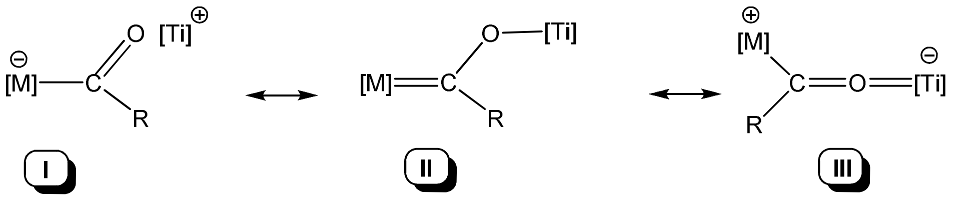

Figure 4.19 Contribution of resonance structures to the titanoxycarbene complexes

Complex **18** CrBTCrET displays the lowest electron occupation for the Cr-CO$_{trans}$ bond, and is also the only complex exhibiting a formal Cr=C(carbene) bond with bond order of two. As seen from the experimental bond length (Table 4.1), the complex also has the shortest experimental Cr-C(carbene) bond distance. This can be ascribed to the combined electron withdrawing properties of the 2-η^6-benzo[*b*]thienyl chromium tricarbonyl substituent, and the ethoxy group which is less donating than the titanoxy group. The carbene carbon *p*-orbital also has the highest occupation, due to the greater π-donation of the central chromium towards stabilization of this electrophilic carbene carbon, thereby explaining the decreased C-O bond order of the *trans*-carbonyl ligand and its decreased electron occupation. Correspondingly, the calculated electrophilicity index ω is the highest for this complex (Table 4.6).

The ferrocenyl complexes **1** and **5** both show no formal Cr-C(carbene) bond; instead, a lone pair orbital localized on the carbene carbon atom, as well as a double bond between the C(carbene)-O atoms are obtained from NBO analysis. This correlates with the longer Cr-C(carbene) bond distances found, as the π-donor substituent ferrocenyl populates the resonance structure **B** (Scheme 4.5), shortening the C=C bond with concomitant lengthening of the Cr=C bond (Table 4.1).

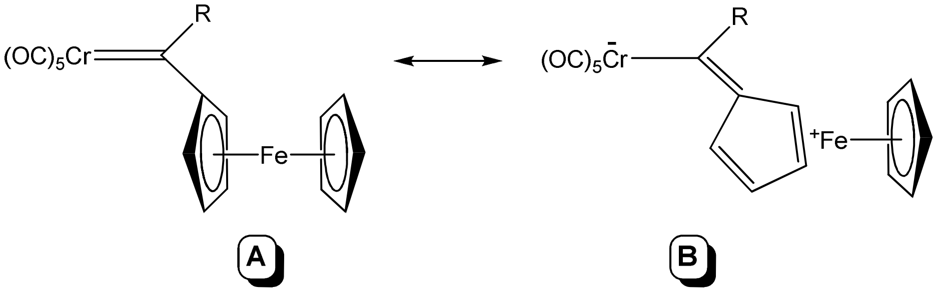

Scheme 4.5

However, no direct comparative trend for the –OEt *vs* the –OTiCp$_2$Cl substituents can be made for a complex where the aryl-substituent is kept constant: similar occupations of the C(carbene) *p*-orbital, the Cr-C(carbene) bonding orbital and the Cr-CO$_{trans}$ are found. Therefore, systematic prediction of the effect of different combinations of electron withdrawing and accepting substituents cannot be done. Only the results obtained for the extreme cases of accepting/least donating groups (complex **18** CrBTCrEt) or donating/donating (complex **5** CrFcTi) do correlate with the experimentally observed parameters.

4.6 Electrochemical investigation of substituent effect

Organometallic compounds that undergo rapid chemically reversible oxidation or reduction may be able to function as effective redox switches that can be turned on or off by electron transfer.[72] The chemical reactivity of the molecular system to which the redox active switch is attached can be modulated, either by electrostatic effects with the inclusion of an additional redox active metal, or by controlling the coordination environment (and reactivity) of the metal.[73]

In order to correlate the redox properties of the carbene complexes listed in Figure 4.8 with the electron donor/acceptor ability of the carbene ligands, an

---

[72] Yeung, L.K.; Kim, J.E.; Chung, Y.K.; Rieger, P.H.; Sweigart, D.A. *Organometallics* **1996**, *15*, 3891.

[73] Singewald, E.T.; Mirkin, C.A.; Stern, C.L. *Angew. Chem., Int. Ed. Engl.* **1995**, *34*, 1624.

investigation of the electrochemical (specifically the anodic oxidation) behaviour of these complexes were undertaken.

In a similar study of carbene and Lewis base complexes [M(CO)$_5$L] or [M(CO)$_4$L$_2$] (M = Cr, Mo or W; L = carbene ligand C(X)Y or Lewis base), it was found that the primary oxidation of these complexes corresponded to a one electron transfer.[42] In neutral compounds, the redox potential $E_{½}$ values were found to be higher when ligand L was a better π-acceptor. Increased π-conjugation within a ligand system lead to a decrease in the ease of oxidation, and increased $E_{½}$ values. In addition, for complexes [Cr(CO)$_5$C(X)Y] the value of $E_{½}$ was not greatly influenced by Y for a specific X-group, provided that Y was an organic fragment. But if Y = Fc, redox potentials decreased by more than 200 mV. Therefore, as Y substituent became more electron donating, $E_{½}$ values decreased. Similary for decreasing donor strength of X into C(carbene) *p* orbital, increased redox potentials were observed.

4.6.1 Cyclic voltammetric studies

From the above information, it was attempted to establish a qualitative contribution of the different combinations of accepting/accepting, accepting/donating, donating/accepting and donating/donating substituents of the carbene ligands, if the substituents could be classified (for the X and Y carbene substituents, respectively) as follows: X = OTiCp$_2$Cl (donating), X = OEt (less donating), and Y = 2-η^6-benzo[*b*]thienyl chromium tricarbonyl (accepting), Y = ferrocenyl (donating) and Y = 2-benzothienyl (less donating).

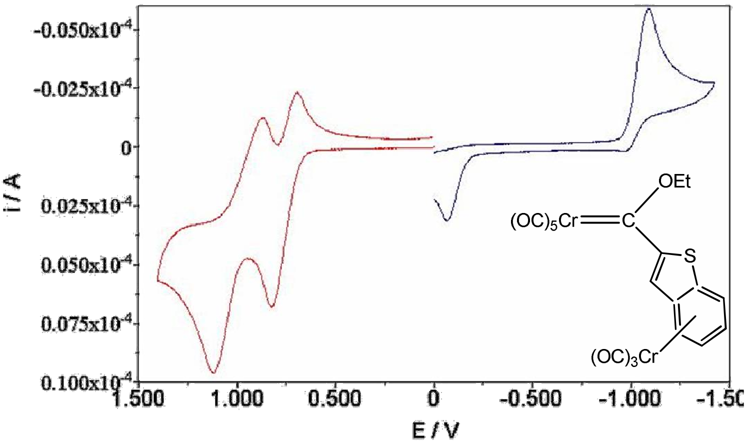

Figure 4.20 CV of 1.0 mM [Cr(CO)$_5${C(OEt)(2- η^6-benzo[*b*]thienyl-Cr(CO)$_3$)}] in CH_2Cl_2/0.10 M Bu_4NPF_6 under N_2 (g) at -75℃. The working electrode was a 1.0 mm diameter platinum disk, and the scan rate was 0.50 V.s^{-1}. A ferrocene internal standard had $E_{½}$ = +0.52 V

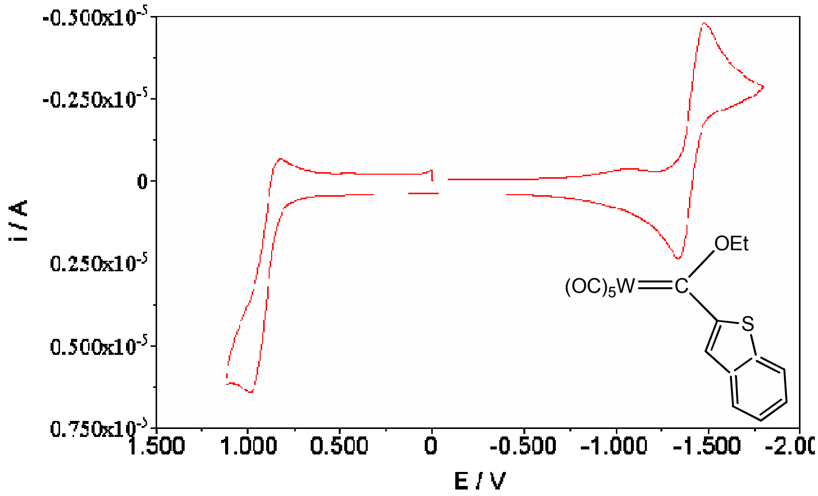

Figure 4.21 CV of 1.0 mM [W(CO)$_5${C(OEt)(2-benzothienyl)}] in CH_2Cl_2/0.10 M Bu_4NPF_6 under N_2 (g) at -75℃. The working electrode was a 1.0 mm diameter platinum disk, and the scan rate was 0.50 V.s^{-1}. A ferrocene internal standard had $E_{½}$ = +0.52 V

Figures 4.20 and 4.21 show typical cyclic voltammograms (CV) obtained for the complex **18** CrBTCrEt and **19** WBTEt, respectively, in CH_2Cl_2 solvent at low temperature (-75℃), and the electrochemical data is listed in Table 4.10. Full experimental details are given in the experimental section, Chapter 5.

For the chromium complexes, all reductions observed were irreversible, whereas the first reduction wave of the tungsten compounds was reversible or partially reversible. For both the chromium and tungsten complexes, the ethoxy substituted complexes only showed one cathodic wave, while the cyclic voltammograms of the titanoxycarbene complexes displayed several waves. The peak potentials of reductions are listed in Table 4.10, and are ascribed to carbene ligand-centred reductions. The titanoxycarbene complexes **16** and **20** showed irreversible cathodic waves at remarkably less negative potential (-0.95 V and -0.88 V, respectively) than the analogous ethoxycarbenes **14** and **18** with E_p = -1.21 V and -1.09 V respectively. This large potential shift can be seen as a result of the polarization of the Ti-O bond, leaving greater electron density on the oxygen atom for donating towards carbene carbon. It also serves as a possible indication of the influence of the carbene substituents on the energy of the LUMO,[46] as the LUMO's of the titanoxycarbene complexes are consistently at lower energy levels than their ethoxy counterparts observed in the molecular orbital analysis of this study.

For monometallic chromium complexes only one reversible anodic wave, corresponding to oxidation of the pentacarbonyl metal centre, is observed. The same is true for the tungsten complexes, although the oxidation waves are irreversible.

Table 4.10 Voltammetric data* and MO energies obtained for Group VI carbene complexes

Complex	Oxidation $E_{½}$ (V)	HOMO (eV)	Reduction E_c** (V)	LUMO (eV)
5 CrFcTi	+0.84 +0.62	-2.529	-1.05	-6.222
14 CrBTEt	+0.97	-3.165	-1.21	-6.528
16 CrBTTi	+0.74	-3.249	-0.95	-6.190
18 CrBTCrEt	+1.00 +0.75	-3.624	-1.09	-6.242
20 CrBTCrTi	+0.93 +0.74	-3.383	-0.88	-6.292
15 WBTEt	+1.19 †	-3.288	-1.03	-6.422
17 WBTTi	+1.03 †	-3.306	-1.05	-6.034
21 WBTCrTi	+1.11 † +0.89 †	-3.640	-1.10 -0.71	-6.186

* 1.0 mM [carbene complex] in CH_2Cl_2/0.10 M Bu_4NPF_6 under N_2 (g) at -75℃. The working electrode was a 1.0 mm diameter platinum disk, and the scan rate was 0.50 V.s^{-1}. A ferrocene internal standard had $E_{½}$ = +0.52 V

** E_c = peak potential of irreversible cathodic waves, or first reduction wave of reversible waves

† These values correspond to the irreversible anodic wave peak potential E_a of the tungsten complexes

For the complexes containing a second metal moiety, either Fc or 2-BTCr(CO)$_3$, another oxidation wave is observed at lower potential, showing that the two metal moieties in each complex function as separate, localized redox centres, in contrast to results obtained previously for ferrocenyl carbene complexes.[44] This implies that a direct comparison of substituent effects on the pentacarbonyl metal can be made, as it is not an electronically delocalized system. A more positive potential for CrBTCrEt **18** is obtained than for CrBTEt **14**, due to the electron withdrawing effect of the Cr(CO)$_3$-fragment in **18**, decreasing the ease of oxidation. This was also found to be valid for complex CrBTCrTi **20** *vs* CrBTTi **16**.

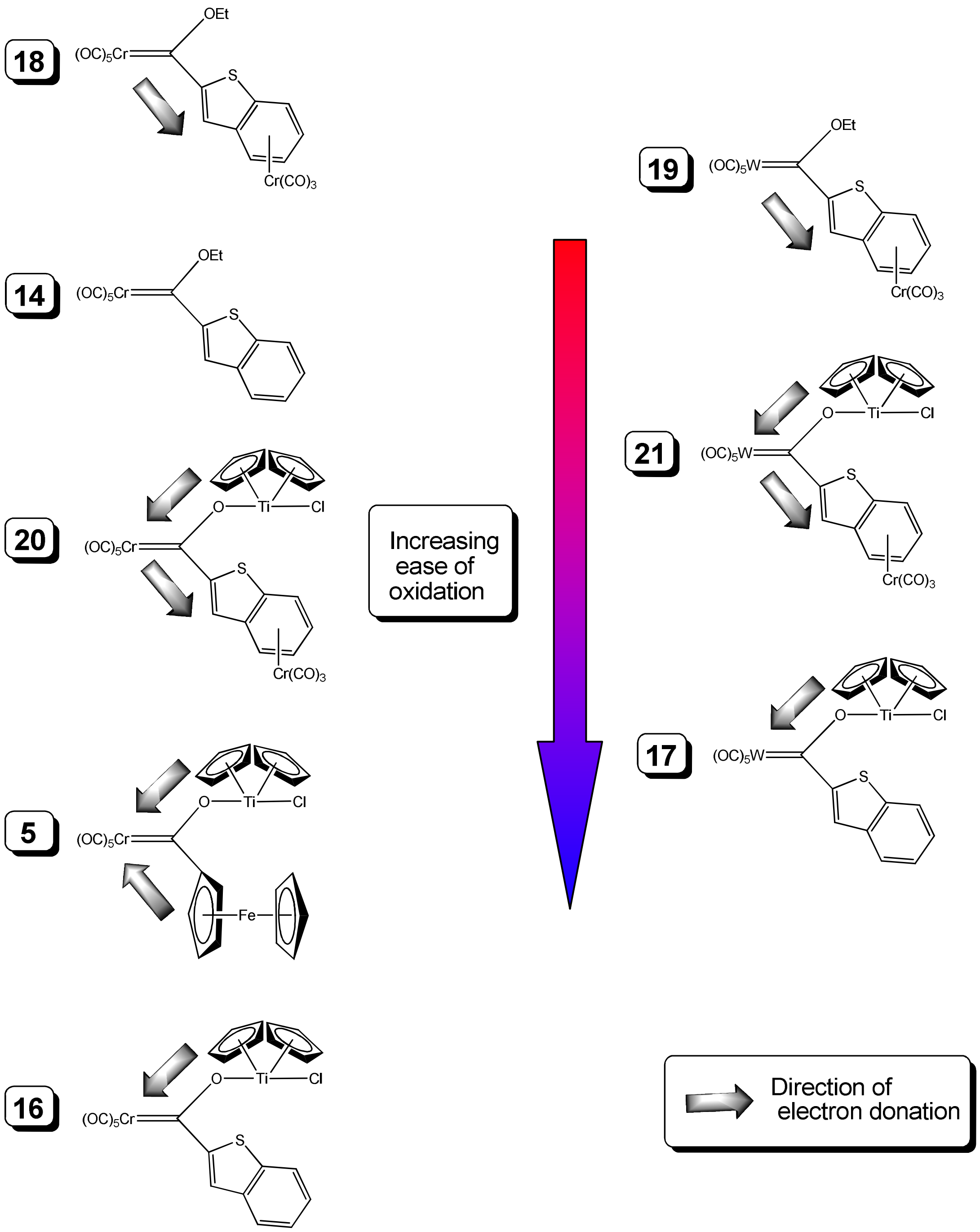

Scheme 4.6

In turn, when the –OEt *vs* –OTiCp$_2$Cl fragments are compared, the increased donating character of the titanoxy fragment reflects in the lower oxidation potentials obtained for these complexes **16** and **20** in relation to their ethoxy counterparts **14** and **18**. The CrFcTi complex **5** shows oxidation of the Cr-atom at a slightly higher potential (+0.84 V) than expected compared to CrBTTi **16** (+0.74 V), as the ferrocenyl group is a stronger π-donor than the benzothienyl substituent. However, this can be rationalized by electrostatic effects: ferrocenyl complex is already oxidized at a potential of +0.62 V, localized at the iron atom. It is therefore increasingly difficult to remove a second electron from an already positively charged complex, reflecting in the higher than expected potential. The information available for the tungsten complexes reflects the same trends, and a summary of the substituent effect on oxidation potential is given in Scheme 4.6.

It is thus possible to gauge the effect of both the heteroatom substituent as well as the (hetero)arene substituent, and in addition, different combinations of the above. To combine these experimental results with the theoretical results obtained, the energies of the highest occupied molecular orbitals can be compared (Table 4.10). Except for the outlier value of the CrBTEt **14** HOMO energy, the rest of the complexes display a trend of increasing oxidation potentials corresponding to greater stability of the HOMO, as expected for a single, reversible electron removal.[45]

4.7 Concluding remarks

4.7.1 Summary

Previous studies have shown that the νCO frequencies of the carbonyl ligand *trans* to ligand L in [M(CO)$_5$L] system does not necessarily indicate stronger or weaker π-acceptance of L, instead, correlations of π-acceptor ability with the force constants of the related carbonyl stretching frequency have been found. In this vibrational study, both νCO and calculated force constants only reflected the influence of the –OEt and –OTiCp$_2$Cl substituents. The A$_1^1$ band of the carbonyl IR spectra correlated with the weakest (CrFcTi **5** and CrBTTi **16**) and strongest (CrBTCrEt **18**) M=C(carbene) bonds, but the intermediate values of the A$_1$' band frequencies displayed some deviations from the experimental bond lengths.

In order to remove solvent effect, solid state IR and Raman spectra were also measured. A novel $\delta CC_{carbene}O$ scissor mode was identified to directly predict the strength of the M-C(carbene) bond, and excellent correlation between the theoretically predicted frequency and observed experimental frequency was obtained. However, the inertia effects of the heavier substituents complicated assignment of the donor/acceptor properties of the carbene ligands.

Calculated electrophilicity indices ω (related to the energies of the HOMO's and LUMO's of the complexes), gave an indication of the (hetero)aromatic substituent effect, however, no conclusion about the heteroatomic substituent effect could be made. The experimental results from the UV/vis spectral data, specifically the MLCT band maxima could also be related to the magnitude of the HOMO-LUMO gap.

NBO analysis of the chromium complexes confirmed predictions about the substituent effects of the extreme cases: for the acceptor/acceptor substituted CrBTCrEt **18**, the largest bond order between the Cr-C(carbene) atoms were found, as expected for the experimentally determined shortest bond length, due to greater backdonation from the chromium towards the carbene carbon *p*-orbital. This was also reflected in the highest electron occupation of this orbital for this complex. The inverse was found for the donor/donor substituted CrFcTi **5** complex, but for the other variations of the acceptor/donor combination substituted complexes, similar occupations of the carbene carbon *p*-orbital were calculated.

The best results were obtained from the cyclic voltammetric studies, where the localized central metal redox centre's oxidation potential correlated to both the calculated HOMO energy, and the effect of both the heteroatom substituent as well as the (hetero)arene substituent, as well as different combinations of the above. Unlike the conclusion from previous studies that the electronic character of the carbene carbon atom is more strongly influenced by the X-group than either the metal or the R-group in $[M(CO)_5\{C(X)R\}]$ systems, the introduction of a third metal moiety in the R-group markedly changes the carbene character.

Carbene ligand modulation can therefore be effected by either the ring- or the heteroaromatic substituent if metal fragments are incorporated that introduces properties not available from pure organic fragments.

The substituents could be arranged in order of increasing electron withdrawing ability: ferrocenyl < 2-benzothienyl < 2-η^6-benzo[*b*]thienyl chromium tricarbonyl. The heteroatom substituents, ethoxy and titanoxy, in turn, can be arranged in order of an increasing donating effect; ethoxy < titanoxy. The arrangement of various combinations of the above (hetero)aryl and *O*-substituents (from the electrochemical analysis and HOMO energies resulted in the following trend, in order of increasing acceptor ability:

Fc, $OTiCp_2Cl$ < BT, $OTiCp_2Cl$ < $BTCr(CO)_3$, $OTiCp_2Cl$ < BT, OEt < $BTCr(CO)_3$, OEt

4.7.2 Future work

A more quantitative method of substituent analysis can be carried out by employing energy and charge decomposition analysis, where both the σ-donation between the carbene-metal bond and the π-backdonation between the metal-carbene bond and the respective contributions from these factors to the overall metal-ligand bonding situation may be established.

5

Experimental

5.1 Standard operating procedure

All operations were carried out under an inert atmosphere of nitrogen or argon gas using standard Schlenk techniques. Solvents were dried and distilled under an atmosphere of nitrogen. Diethyl ether, hexane and THF were distilled from sodium metal, with benzophenone as indicator for the ethereal solvents. Dichloromethane was distilled from phosphorous pentoxide. Most chemicals were used without prior purification, unless stated otherwise. Column chromatography, using Kieselgel 60 (particle size 0.0063 - 0.200mm) or neutral aluminium oxide 90 was used as resin for all separations.

5.2 Characterization techniques

5.2.1 Nuclear magnetic resonance spectroscopy

NMR spectra were recorded on a Bruker ARX-300 spectrometer and on an AVANCE 500 spectrometer with the help of Mr E.R. Palmer at the University of Pretoria. ^{1}H NMR spectra were recorded at 300.135 and 500.139 MHz and ^{13}C NMR spectra at 75.469 and 125.75 MHz respectively. The signal of the deuterated solvent was used as reference: ^{1}H $CDCl_3$ 7.24 ppm, benzene-d_6

7.15 ppm and ^{13}C $CDCl_3$ 77.00 ppm, benzene-d_6 128.00 ppm. For resolution enhancement of the manganese and rhenium complexes, longer acquisition times were achieved by manual shimming and manipulation of the sweep width.

5.2.2 Infrared spectroscopy

Solution IR spectra were recorded on a Perkin-Elmer Spectrum RXI FT-IR spectrophotometer with a NaCl cell. All spectra were recorded using either dicloromethane or hexane as solvent. The vibrational stretching bands in the carbonyl region (*ca*. 1500 - 2200 cm^{-1}) were recorded for all complexes.

Solid state Fourier Transform infrared (FTIR) spectra were obtained under vacuum as a 1% w/w CsI disk using a Bruker IFS 113 spectrometer over the region 125 – 4000 cm^{-1} with a spectral resolution of 4 cm^{-1}. OPUS 5.5 software was used for data processing.

5.2.3 Raman spectroscopy

Experimental solid-state Raman spectra were obtained with the help of Dr W. Barnard (University of Pretoria) using a dispersive Raman spectrometer. All dispersive spectra were obtained by exciting the samples with the 647.1 nm (red) line of a Spectraphysics 5012 Krypton-ion laser. For the solid-state spectra, an Olympus confocal microscope with a 50X objective was used to focus the laser light on the sample. The scattered light was dispersed and recorded by means of a Dilor XY multichannel Raman spectrometer equipped with a liquid nitrogen-cooled Wright Generation 1 CCD detector. A Linkam RMS 90 cell was employed to obtain the solid-state Raman spectrum for all the complexes measured at non-ambient conditions of -196 ºC, as degradation of the samples were seen at room temperature. All Raman spectra were obtained from the same samples as used for solid state FTIR; as

CsI pellets, in order for heat dissipation by the CsI matrix. The spectral resolution was 3 cm^{-1}, while laser output power at the source (300 – 500 mW) and integration times (30 – 120 seconds) were varied to obtain the best possible spectra. Three to four spectral accumulations were averaged, and the software used for data processing was Labspec 3.03.

5.2.4 Fast atom bombardment mass spectrometry

FAB-MS spectra were recorded on a VG 70SEQ Mass Spectrometer, with the resolution for FAB = 1000 in a field of 8 kV. Nitrobenzyl alcohol was used as solvent and internal standard. All FAB-MS spectra were recorded at the University of the Witwatersrand.

5.2.5 X-ray crystallography

Data collection and structure determinations were done by Mr D.C. Liles, University of Pretoria. X-ray crystal structure analysis was done from data collected at 20℃ on a Siemens P4 Bruker 1K CCK detector and SMART control software using graphite-monochromated, Mo-Kα radiation by means of a combination of ϕ and ω scans. Data were corrected for Lorenz polarization effects and data reduction was performed using SAINT+[1] and the intensities were corrected for absorption using SADABS.[1] The structures were solved by direct methods using SHELXTS[1] and refined by full-matrix least squares using SHELXTL[1] and SHELXL-97.[2] In the structure refinements all hydrogen atoms were added in calculated positions and treated as riding on the atom to which they are attached. All non-hydrogen atoms (except those refined as rigid groups) were refined with anisotropic displacement parameters, all isotropic displacement parameters for hydrogen atoms were calculated as $X \times U_{eq}$ of

---

[1] SMART (Version 5.054), SAINT (Version 6.45), SADABS (Version 2.10) and SHELXTS/SHELXTL (Version 6.12). Bruker AXS Inc., Madison, Wisconsin, USA, **2001**.
[2] SHELXS-97 and SHELXL-97. Sheldrick, GM University of Göttingen, Germany, **1997**.

the atom to which they are attached, *X* = 1.5 for the methyl hydrogens and 1.2 for all other hydrogens. In structures **3**, **12** and **23** some disorder was observed. The parameters for the major orientations were refined freely. The minor orientations were refined as rigid bodies with geometries derived from those of the major orientations. Site occupation factors for the major and minor orientations were refined but constrained to sum to 1.0.

5.2.6 UV/Visible spectroscopy

All the complexes were referenced to benzene and spectra measured in a range of 200.0 - 800.0 nm in a quartz sample cell. A Hewlett-Packard 8452A Diode Array spectrophotometer and a Shimadzu UV-2101 PC UV-Vis scanning spectrophotometer were used.

5.3 Electrochemistry

Electrochemical experiments were conducted under the supervision of Prof D.A. Sweigart, Brown University, USA. Voltammetric experiments were done under a blanket of nitrogen that was saturated with solvent. The electrolyte was 0.10 M Bu_4NPF_6, which was synthesized by metathesis of Bu_4Br and HPF_6, recrystallized from dichloromethane/hexane, and dried under vacuum. HPLC grade dichloromethane was the solvent employed in all experiments. Once opened, the solvent was kept under argon and contact with the atmosphere was minimized. Additional purification was not deemed necessary or desirable. Cyclic voltammetry was done with EG&G 173/175/179 potentiostatic instrumentation. The working electrode was a 1 mm diameter platinum disk, and the counter electrode was a platinum wire. The reference was a Metrohm Ag/AgCl electrode filled with dichloromethane/Bu_4NPF_6 and saturated with LiCl; this was separated from the test solution by a salt bridge containing 0.10 M Bu_4NPF_6 in CH_2Cl_2.

5.4 Preparation of compounds

5.4.1 Preparation of starting material compounds

5.4.1.1 Triethyl oxonium tetrafluoroborate[3]

Epichlorohydrin (140.0 g, 119 mL, 1.51 mol) was added dropwise to a solution of sodium-dried ether (500 mL) and freshly distilled boron fluoride etherate (284.0 g, 252 mL, 2.00 mol) at a rate sufficient to maintain vigorous boiling (about 1 hour is needed). The mixture was refluxed and allowed to stand at RT overnight. Supernatant ether was withdrawn from the crystalline mass of triethyloxonium tetrafluoroborate under an inert N_2 atmosphere. Crystals were washed with ether; yield 244 - 272 g (85 - 95%).

5.4.1.2 Chloromercury ferrocene[4]

At room temperature (RT) 4.91 g (15.4 mmol) mercury acetate was mixed with 90 mL methanol and dropped into a solution of 2.80 g (15.05 mmol) ferrocene and 25 mol benzene. The solution was left to stir over night at RT. 0.66 g LiCl (15.6 mmol) was mixed with a 5 mL solution of ethanol and water (1:1) and then dropped into the ferrocene solution. The mixture was stirred for 2 hours at RT and then refluxed for 1 hour at 80 °C. The solvent was removed under reduced pressure and collected for Soxhlet extraction with DCM. The extract was washed with water and dried over $MgSO_4$. The solution was filtered and dried under reduced pressure to give an orange product, with a yield of 4.38 g (68 %).

---

[3] Meerwein, H. *Org. Synth.* **1966**, *46*, *113*.
[4] Fish, R.W.; Rosenblum, M. *J. Org. Chem.* **1965**, *30*, 1253.

5.4.1.3 Bromoferrocene[4]

0.80 g (4.5 mmol) *N*-bromosuccinimide was dissolved in 70 mL dimethylformamide and added to a solution of 1.48 g (3.5 mmol) chloromercury ferrocene in dimethylformamide. The solution was stirred at 0°C for 3 hours. 150 mL of a 10% sodium sulphate solution was added, and the resulting reaction solution was extracted with diethyl ether. The combined organic extracts were washed with water and dried over magnesium sulphate. The solution was filtered and the solvent removed under reduced pressure. Further purification was done with column chromatography on silica gel with hexane. The yellow product bromoferrocene was collected with a yield of 0.35 g (37.5%).

5.4.1.4 Iodoferrocene[4]

A solution of *N*-iodosuccinimide (1.2 g, 5.1 mmol) in 100 mL dichloromethane was added dropwise to a stirred suspension of chloromercury ferrocene (2.10 g, 5.0 mmol) in dichloromethane at 0°C. After allowing the reaction to continue for 12 hours, 50 mL of an aqueous 10% sodium bisulphite solution was added, followed by and equal volume of a 10% sodium carbonate solution. The organic layer was separated and extracted with dichloromethane, followed by successive washings with 10% sodium carbonate solution and water. After drying over water, the solvent from the combined extracts were removed under vacuum, and column chromatography yielded the product iodoferrocene in 77% (1.20 g).

5.4.1.5 Trisammine tricarbonyl chromium[5]

Chromium hexacarbonyl (3.40 g, 16.4 mmol) was added to a solution of 95 mL ethanol, 5 mL degassed water and KOH (5.90 g, 104.6 mmol) in a

---

[5] Rausch, M.D.; Moser, G.A.; Zaiko, E.J.; Lipman, A.L. *J. Organomet. Chem.* **1970**, *23*, 185.

pressure flask. Nitrogen gas was bubbled through the solution for 10 minutes, after which the pressure flask was sealed and heated to 110 °C for 6 hours. The container was then removed from the heat source and allowed to cool in an ice bath. To the bright orange solution was added a degassed solution of concentrated NH_3 (aq) (115 mL, 6.10 mol), and reaction was continued for 2 hours with continuous stirring. Thereafter the solution was filtered and the residue washed with ethanol to remove excess ammonia, and the yellow product $[Cr(CO)_3(NH_3)_3]$ was isolated with a yield of 90 % (2.76 g).

5.4.1.6 η^5-thiophene chromium tricarbonyl[6]

2.5 g (29.4 mmol) thiophene and freshly distilled Et_2OBF_3 (6.26 g. 44.1 mmol) was added to a solution of $[Cr(CO)_3(NH_3)_3]$ (2.76 g, 14.7 mmol) in 100 mL diethyl ether. The reaction mixture was left overnight, and a dark red suspension formed. 50 mL of degassed water was added to the reaction mixture and the solution was stirred vigorously while being saturated with nitrogen gas. Two layers were then allowed to separate. The top organic layer was removed *via* canula under pressure, and the aqueous phase washed with successive portions of ether. After combining the extracts and the red organic layer, the solvent was removed and column chromatography was used to isolate the orange product, which was recrystallized from dichloromethane and hexane to yield 2.42 g, 74% $[Cr(CO)_3(\eta^5\text{-thiophene})]$.

5.4.1.7 η^6- benzene chromium tricarbonyl[7]

To 55 mL of dibutyl ether was added $Cr(CO)_6$ (1.76 g, 8 mmol) and excess benzene (~ 30 mmol). The reaction mixture was refluxed overnight, whereafter the solvent was removed under pressure. Column chromatography

---

[6] Novi, M.; Guanti, G.; Dell'Erba, C. *J. Heterocycl. Chem.* **1975**, *12*, 1055.

[7] Fischer, E.O.; Goodwin, H.A.; Kreiter, C.G.; Simmons, H.D.; Sonogashira, K.; Wild, S.B.; *J. Organomet. Chem.* **1968**, *14*, 359.

in benzene/hexane eluent, followed by recrystallization of the yellow product [$Cr(CO)_3(\eta^6$-benzene)] (1.11 g, 65%).

5.4.2 Preparation of organometallic complexes

5.4.2.1 General carbene preparation with direct lithiation of ferrocene in the presence of TMEDA[8]

Synthesis of complexes **1** – **4**, **22**, **23**, **27** *and* **28**

To a solution of ferrocene (1.86 g, 10.0 mmol) in hexane was added a mixture of 1.3 mole eq of 1.5 M *n*-BuLi in hexane (13 mmol, 8.66 mL) and 1.3 mole eq TMEDA (13 mmol, 1.96 mL) in the case of the syntheis of Group VI carbene complexes, and 1.5 mole eq *n*-BuLi (15 mmol, 10 mL) with 1.5 mole eq TMEDA (15 mmol, 2.27 mL) for the Group VII carbene synthesis, at RT under an inert N_2 atmosphere. The reaction mixture was refluxed for two hours, after which the hexane was removed under reduced pressure. The reaction mixture was cooled to -78 °C and redissolved in a minimum of THF, after which the starting material metal carbonyl complex was added (10 mmol). After continuous stirring for 2 hours at low temperature, the reaction mixture was allowed to warm to room temperature, after which the solvent THF was evaporated. Dichloromethane was added at -30°C and a slight excess (10 -15 mmol) of the oxonium salt Et_3OBF_4 or titanocene dichloride was added. After complete alkylation or metalation, followed by thin layer chromatography, the solution was filtered through a short silica gel filter to remove lithium salts, followed by column chromatography with gradient elution with hexane and dichloromethane. Crystallization was achieved from layered dichloromethane/hexane mixtures. The complexes obtained from this reaction method and their yields, are listed in Table 5.1.

---

[8] (a) Fischer, E.O.; Öffhaus, E. *Chem. Ber.* **1969**, *102*, 2449, (b) Fischer, E.O.; Rustemeyer, P. *J. Organomet. Chem.* **1982**, *225*, 265, (c) Schubert, U.; Ackermann, K.; Rustemeyer, P. *J. Organomet. Chem.* **1982**, *231*, 323.

Table 5.1 Carbene complexes synthesized from direct lithitation of ferrocene

Starting material metal carbonyl complex (10 mmol)	Product obtained					
	Complex	Colour	Molar mass (g/mol)	Mass (g)	mmol	Yield (%)
$[Cr(CO)_6]$ 2.20 g	**1**	Red	434.14	1.36	3.13	31
	3	Dark red	682.26	3.96	5.80	58
$[W(CO)_6]$ 3.52 g	**2**	Red	565.98	1.13	1.99	20
	4	Dark red	945.95	3.99	4.22	42
$[Cr(CO)_6]$ 2.20 g	**5**	Red brown	618.61	1.85	2.99	30
	8	Dark brown	802.20	3.08	3.84	38
$[Mo(CO)_6]$ 2.64 g	**7**	Brown	662.55	0.68	1.02	10
	10	Dark brown	890.09	3.04	3.41	34
$[W(CO)_6]$ 3.52 g	**9**	Purple brown	1065.89	7.19	6.75	68
$[MnCp(CO)_3]$ 2.04 g	**22**	Red	418.15	1.57	3.76	38
	23	Red	650.30	2.96	4.55	46
$[MnCp(CO)_3]$ 2.04 g	**24**	Red	602.61	1.48	2.45	25
	25	Brown	770.21	4.06	5.27	53
$[Re_2(CO)_{10}]$ 6.52 g	**27**	Dark brown	1547.14	5.07	3.28	33
	28	Red	1095.54	2.21	2.02	20
$[Re_2(CO)_{10}]$ 6.52 g	**29**	Light yellow	951.78	0.761	0.80	8
	30	Orange	539.30	0.30	0.55	6
	31	Red	1051.07	2.24	2.13	21
	32	Dark red	1079.08	0.41	0.38	4
	33	Dark brown-red	1667.11	4.47	2.68	27
	34	Pink red	1024.59	0.46	0.45	5

5.4.2.2 General carbene complex preparation with aryl lithiation at low temperatures[8]

Synthesis of complexes **6**, **12, 13**, *and* **26**

The arene (5 mmol) was stirred while adding *n*-BuLi (5.5 mmol, 1.5 M, 3.66 mL) in 40 mL THF at -20℃ under an inert N_2 atmosphere. Stirring was continued for 2 hours. The binary metal carbonyl complex (5 mmol) was added to the reaction mixture at -78℃, resulting in a change of the reaction mixture to a darker colour while stirring for 1 hour. Stirring was then continued for an additional 30 min at RT. THF solvent was evaporated under reduced pressure. Et_3OBF_4 (6 mmol, 1.15 g) or $TiCp_2Cl_2$ (6 mmol, 1.49 g) in dichloromethane was added to the reaction mixture at -30℃ and stirred until reaction completion. $LiBF_4$ salts were removed by filtering and reaction products were purified via column chromatography using hexane/dichloromethane (4:1) as eluent. Recrystallization of products was done by solvent layering of hexane/dichloromethane (1:1). Actual amounts of arene precursors and yields of complexes obtained are given in Table 5.2.

5.4.2.3 Preparation of mixed heteronuclear carbene complex[9]

Synthesis of complex **11**

A mixture of *n*-BuLi (2.2 mmol, 1.5 M, 1.47 mL) and TMEDA (2.2 mmol, 0.33 mL) in hexane was added slowly to a solution of ferrocene (2 mmol, 0.37 g) in hexane under inert conditions, and refluxed for 2 hours. Solvent hexane was evaporated after the reaction mixture was cooled down, and a minimum amount of THF was added to dissolve the dilithiated ferrocene. After cooling the reaction mixture down to -78℃, 1mole eq of $Cr(CO)_6$ was added (2 mmol, 0.44 g) and stirred for 1 hour. The reaction mixture was allowed to warm to -

---

[9] Aoki, A.; Fujimura, T.; Nakamura, E. *J. Am. Chem. Soc.* **1992**, *114*, 2985.

30°C and 1 mole eq of $W(CO)_6$ (2 mmol, 0.70 g) was added, and stirred for a further 30 minutes in the cold. After warming the reaction mixture to room temperature, the THF was removed under reduced pressure, and the dimetal bisacylate redissolved in dichloromethane at -30°C. Reaction quenching was accomplished by the addition of $TiCp_2Cl_2$ (2.2 mmol, 0.55 g), after which the byproduct lithium salts were removed by filtration. Separation of the heteronuclear complex **11** from homonuclear biscarbene complexes **8** and **9** was achieved by gradient elution column chromatography on silica gel with hexane and dichloromethane, after which **11** was crystallized from a dichloromethane/hexane (1:3) solution to yield the dark brown product **11** (MW = 934.04 g.mol^{-1}) (0.50 mmol, 0.47 g, 25 % yield).

Table 5.2 Carbene complexes synthesized from low temperature lithitation of arenes

Starting material metal carbonyl complex (5 mmol)	Starting material arene (5 mmol)	Product obtained					
		Complex	Colour	Molar mass (g/mol)	Mass (g)	mmol	Yield (%)
$[W(CO)_6]$ 1.76 g	FcBr 1.32 g	**6**	Dark brown	750.45	2.34	3.12	62
$[Cr(CO)_6]$ 1.10 g	$[Cr(CO)_3(\eta^5\text{-}C_4H_3S)]$ 1.10 g	**12**	Dark red	516.70	0.86	1.67	33
$[Cr(CO)_6]$ 1.10 g	$[Cr(CO)_3(\eta^6\text{-}C_6H_6)]$ 1.07 g	**13**	Dark purple brown	646.72	1.61	2.49	50
$[Re_2(CO)_{10}]$ 3.26 g	FcI 1.56 g	**26**	Red	866.61	2.08	2.40	48

5.5 Analytical data

Melting points could not be recorded as complexes decomposed during heating. The elemental analyses done for the carbon and hydrogen atoms of the complexes are listed in Table 5.3. The C and H elemental analyses were performed by the analytical laboratories of ARC·LNR Institute for Soil, Climate and Water. Elemental analysis was not performed for complexes **1** – **4**, **11**, **29**, **32** and **34**.

Table 5.3 Analytical data of synthesized carbene complexes

Complex	Molecular formula	Calculated (%)		Found (%)	
		C	H	C	H
5	$CrFeTiC_{26}O_6H_{19}Cl$	50.48	3.10	51.10	3.09
6	$WFeTiC_{26}O_6H_{19}Cl$	41.61	2.55	41.65	2.48
7	$MoFeTiC_{26}O_6H_{19}Cl$	47.13	2.89	47.88	2.87
8	$Cr_2FeTiC_{32}O_{12}H_{18}$	47.91	2.26	48.23	2.30
9	$W_2FeTiC_{32}O_{12}H_{18}$	36.06	1.70	36.52	1.72
10	$Mo_2FeTiC_{32}O_{12}H_{18}$	43.18	2.04	43.76	2.12
12	$CrTiC_{20}O_6H_{13}SCl$	46.49	2.54	46.97	2.47
13	$Cr_2TiC_{25}O_9H_{15}Cl$	46.43	2.34	46.97	2.26
22	$MnFeC_{20}O_3H_{19}$	57.45	4.58	57.61	4.34
23	$Mn_2FeC_{30}O_6H_{28}$	55.41	4.34	56.02	4.19
24	$MnFeTiC_{28}O_3H_{24}Cl$	55.81	4.01	56.32	3.99
25	$Mn_2FeTiC_{36}O_6H_{28}$	56.14	3.66	56.83	3.57
26	$Re_2FeC_{22}O_{10}H_{14}$	30.49	1.63	30.86	1.58
27	$Re_4FeC_{34}O_{20}H_{18}$	26.40	1.17	26.34	1.35
28	$Re_2Fe_2C_{30}O_8H_{28}Cl_2$	32.89	2.58	33.23	2.76
30	$ReFeC_{16}O_6H_9$	35.63	1.68	36.22	1.59
31	$Re_2FeTiC_{30}O_{10}H_{19}Cl$	34.28	1.82	34.66	1.79
33	$Re_4FeTiC_{40}O_{20}H_{18}$	28.82	1.09	29.20	1.01

Table of Contents

Appendix 1

Crystallographic data of Complex 3

Table 1. Crystal data and structure refinement for Complex **3**.

Identification code	kgc2l_ac2c	
Empirical formula	$C_{26} H_{18} Cr_2 Fe O_{12}$	
Formula weight	682.25	
Temperature	293(2) K	
Wavelength	0.71073 Å	
Crystal system	Monoclinic	
Space group	C 2/c	
Unit cell dimensions	a = 12.3910(15) Å	a= 90°.
	b = 14.6211(17) Å	b= 90.047(2)°.
	c = 14.9681(18) Å	g = 90°.
Volume	2711.8(6) Å^3	
Z	4	
Density (calculated)	1.671 Mg/m^3	
Absorption coefficient	1.379 mm^{-1}	
F(000)	1376	
Crystal size	0.34 x 0.08 x 0.06 mm^3	
Theta range for data collection	2.55 to 26.43°.	
Index ranges	-14<=h<=12, -17<=k<=14, -11<=l<=18	
Reflections collected	7163	
Independent reflections	2537 [R(int) = 0.0273]	
Completeness to θ = 25.00°	99.5 %	
Absorption correction	Semi-empirical from equivalents	
Max. and min. transmission	0.921 and 0.769	
Refinement method	Full-matrix least-squares on F^2	
Data / restraints / parameters	2537 / 0 / 201	
Goodness-of-fit on F^2	1.076	
Final R indices [I>2σ(I)]	R1 = 0.0374, wR2 = 0.1075	
R indices (all data)	R1 = 0.0408, wR2 = 0.1122	
Extinction coefficient	0	
Largest diff. peak and hole	0.512 and -0.317 e.Å^{-3}	

Table 2. Atomic coordinates (x 10^4) and equivalent isotropic displacement parameters (Å^{2}x 10^3) for Complex **3**. U(eq) is defined as one third of the trace of the orthogonalized U^{ij} tensor.

	x	y	z	U(eq)
Cr(1)	2869(1)	10030(1)	6259(1)	32(1)
Fe(1)	0	8513(1)	7500	29(1)
C(1)	4375(3)	10037(2)	6248(5)	45(1)
O(1)	5301(2)	10028(2)	6201(5)	76(1)
C(2)	3006(4)	9106(2)	7146(2)	42(1)
O(2)	3201(3)	8573(2)	7666(3)	69(1)
C(3)	2881(4)	10912(2)	7192(2)	45(1)
O(3)	2930(4)	11427(2)	7746(2)	79(1)
C(4)	2961(4)	10952(2)	5361(2)	42(1)
O(4)	3126(3)	11492(2)	4839(2)	66(1)
C(5)	2864(4)	9119(3)	5343(2)	48(1)
O(5)	2898(5)	8585(2)	4795(3)	83(1)
C(6)	1189(2)	9996(2)	6282(4)	33(1)
O(6)	497(2)	10682(2)	6262(3)	48(1)
C(7)	539(3)	9178(2)	6330(3)	36(1)
C(8)	922(3)	8240(3)	6363(3)	47(1)
C(9)	-3(4)	7651(2)	6398(2)	54(1)
C(10)	-909(3)	8176(3)	6399(3)	35(1)
C(11)	-619(4)	9100(3)	6353(4)	34(1)
C(18)	805(3)	11634(2)	6176(4)	56(1)
C(19)	-183(4)	12184(3)	6159(3)	71(1)
Fe(1A)	0	11463(4)	7500	29(1)
Fe(1B)	-40(12)	11477(3)	5013(2)	24(1)
C(10A)	-937(18)	11798(16)	6316(19)	69(5)
C(11A)	-630(20)	10862(17)	6230(30)	84(6)

Table 3. Bond lengths [Å] and angles [°] for Complex **3**.

Cr(1)-C(1)	1.866(4)	Fe(1B)-C(10A)	2.29(3)
Cr(1)-C(3)	1.901(3)	C(10A)-C(11A)	1.42(3)
Cr(1)-C(2)	1.902(3)		
Cr(1)-C(4)	1.908(3)	C(1)-Cr(1)-C(3)	89.7(2)
Cr(1)-C(5)	1.910(4)	C(1)-Cr(1)-C(2)	85.5(2)
Cr(1)-C(6)	2.083(3)	C(3)-Cr(1)-C(2)	88.17(18)
Fe(1)-C(10)	2.056(4)	C(1)-Cr(1)-C(4)	86.0(2)
Fe(1)-C(11)	2.067(5)	C(3)-Cr(1)-C(4)	92.17(14)
Fe(1)-C(9)	2.076(3)	C(2)-Cr(1)-C(4)	171.42(13)
Fe(1)-C(8)	2.089(5)	C(1)-Cr(1)-C(5)	90.0(2)
Fe(1)-C(7)	2.112(4)	C(3)-Cr(1)-C(5)	178.52(16)
C(1)-O(1)	1.151(5)	C(2)-Cr(1)-C(5)	90.35(15)
C(2)-O(2)	1.128(5)	C(4)-Cr(1)-C(5)	89.27(17)
C(3)-O(3)	1.121(4)	C(1)-Cr(1)-C(6)	178.87(16)
C(4)-O(4)	1.130(4)	C(3)-Cr(1)-C(6)	90.7(2)
C(5)-O(5)	1.134(5)	C(2)-Cr(1)-C(6)	93.48(19)
C(6)-O(6)	1.320(3)	C(4)-Cr(1)-C(6)	95.09(19)
C(6)-C(7)	1.443(4)	C(5)-Cr(1)-C(6)	89.6(2)
O(6)-C(18)	1.449(4)	C(10)-Fe(1)-C(10)#1	152.2(3)
C(7)-C(11)	1.439(4)	C(10)-Fe(1)-C(11)#1	165.60(18)
C(7)-C(8)	1.452(5)	C(10)-Fe(1)-C(11)	39.72(17)
C(8)-C(9)	1.434(6)	C(11)#1-Fe(1)-C(11)	130.9(2)
C(8)-H(8)	0.9300	C(10)-Fe(1)-C(9)	38.4(2)
C(9)-C(10)	1.360(7)	C(11)-Fe(1)-C(9)	65.88(17)
C(9)-H(9)	0.9300	C(10)-Fe(1)-C(9)#1	119.45(19)
C(10)-C(11)	1.401(6)	C(11)-Fe(1)-C(9)#1	155.9(2)
C(10)-H(10)	0.9300	C(9)-Fe(1)-C(9)#1	105.23(18)
C(11)-H(11)	0.9300	C(10)-Fe(1)-C(8)	66.48(12)
C(18)-C(19)	1.465(5)	C(11)-Fe(1)-C(8)	66.76(18)
C(18)-H(18A)	0.9700	C(9)-Fe(1)-C(8)	40.29(16)
C(18)-H(18B)	0.9700	C(10)-Fe(1)-C(8)#1	107.89(12)
C(19)-H(19A)	0.9600	C(11)-Fe(1)-C(8)#1	123.61(18)
C(19)-H(19B)	0.9600	C(9)-Fe(1)-C(8)#1	122.04(17)
C(19)-H(19C)	0.9600	C(8)-Fe(1)-C(8)#1	157.9(2)
Fe(1A)-C(10A)	2.17(3)	C(10)-Fe(1)-C(7)	67.61(16)
Fe(1A)-C(11A)	2.23(4)	C(11)-Fe(1)-C(7)	40.27(12)
Fe(1B)-C(11A)	2.17(3)	C(9)-Fe(1)-C(7)	67.71(13)

C(8)-Fe(1)-C(7)	40.45(14)
C(10)-Fe(1)-C(7)#1	127.01(17)
C(11)-Fe(1)-C(7)#1	112.39(11)
C(9)-Fe(1)-C(7)#1	159.74(18)
C(8)-Fe(1)-C(7)#1	159.57(15)
C(7)-Fe(1)-C(7)#1	125.21(19)
O(1)-C(1)-Cr(1)	176.8(9)
O(2)-C(2)-Cr(1)	172.8(4)
O(3)-C(3)-Cr(1)	177.3(5)
O(4)-C(4)-Cr(1)	173.0(4)
O(5)-C(5)-Cr(1)	177.6(5)
O(6)-C(6)-C(7)	105.6(3)
O(6)-C(6)-Cr(1)	129.10(19)
C(7)-C(6)-Cr(1)	125.3(2)
C(6)-O(6)-C(18)	124.1(3)
C(6)-C(7)-C(11)	128.5(3)
C(6)-C(7)-C(8)	127.0(3)
C(11)-C(7)-C(8)	104.5(3)
C(6)-C(7)-Fe(1)	126.8(4)
C(11)-C(7)-Fe(1)	68.2(3)
C(8)-C(7)-Fe(1)	68.9(3)
C(9)-C(8)-C(7)	107.9(3)
C(9)-C(8)-Fe(1)	69.4(2)
C(7)-C(8)-Fe(1)	70.6(2)
C(9)-C(8)-H(8)	126.1
C(7)-C(8)-H(8)	126.1
Fe(1)-C(8)-H(8)	125.5
C(10)-C(9)-C(8)	108.8(2)
C(10)-C(9)-Fe(1)	70.0(2)
C(8)-C(9)-Fe(1)	70.3(2)
C(10)-C(9)-H(9)	125.6
C(8)-C(9)-H(9)	125.6
Fe(1)-C(9)-H(9)	125.7
C(9)-C(10)-C(11)	109.4(3)
C(9)-C(10)-Fe(1)	71.6(2)
C(11)-C(10)-Fe(1)	70.6(3)
C(9)-C(10)-H(10)	125.3
C(11)-C(10)-H(10)	125.3
Fe(1)-C(10)-H(10)	124.1
C(10)-C(11)-C(7)	109.5(3)
C(10)-C(11)-Fe(1)	69.7(3)
C(7)-C(11)-Fe(1)	71.6(3)
C(10)-C(11)-H(11)	125.2
C(7)-C(11)-H(11)	125.2
Fe(1)-C(11)-H(11)	125.1
O(6)-C(18)-C(19)	107.9(3)
O(6)-C(18)-H(18A)	110.1
C(19)-C(18)-H(18A)	110.1
O(6)-C(18)-H(18B)	110.1
C(19)-C(18)-H(18B)	110.1
H(18A)-C(18)-H(18B)	108.4
C(18)-C(19)-H(19A)	109.5
C(18)-C(19)-H(19B)	109.5
H(19A)-C(19)-H(19B)	109.5
C(18)-C(19)-H(19C)	109.5
H(19A)-C(19)-H(19C)	109.5
H(19B)-C(19)-H(19C)	109.5
C(10A)-Fe(1A)-C(10A)#1	154.0(13)
C(10A)-Fe(1A)-C(11A)	37.7(9)
C(10A)-Fe(1A)-C(11A)#1	165.6(10)
C(11A)-Fe(1A)-C(11A)#1	133.6(14)
C(11A)-Fe(1B)-C(10A)	37.1(8)
C(11A)-C(10A)-Fe(1A)	73.3(18)
C(11A)-C(10A)-Fe(1B)	66.6(17)
C(10A)-C(11A)-Fe(1B)	76.3(18)
C(10A)-C(11A)-Fe(1A)	69.0(17)

Symmetry transformations used to generate equivalent atoms:

#1 -x,y,-z+3/2

Table 4. Anisotropic displacement parameters (Å^{2}x 10^{3})for Complex **3**. The anisotropic displacement factor exponent takes the form: $-2p^{2}[\ h^{2}a^{*2}U^{11} + ... + 2\ h\ k\ a^{*}\ b^{*}\ U^{12}\ ]$

	U^{11}	U^{22}	U^{33}	U^{23}	U^{13}	U^{12}
Cr(1)	31(1)	32(1)	33(1)	1(1)	0(1)	-1(1)
Fe(1)	31(1)	23(1)	31(1)	0	0(1)	0
C(1)	43(2)	44(2)	49(2)	2(1)	12(3)	3(1)
O(1)	36(2)	86(2)	106(3)	3(2)	-6(3)	0(1)
C(2)	40(2)	41(2)	46(2)	2(1)	-5(2)	1(2)
O(2)	79(2)	60(2)	67(3)	24(2)	-12(2)	1(1)
C(3)	48(2)	43(2)	44(2)	-1(1)	-7(2)	-6(2)
O(3)	110(3)	65(2)	61(2)	-23(2)	-21(2)	0(2)
C(4)	40(2)	42(2)	44(2)	3(1)	0(2)	3(2)
O(4)	77(3)	61(2)	59(2)	22(2)	15(2)	6(2)
C(5)	50(2)	50(2)	42(2)	4(2)	3(2)	-9(2)
O(5)	117(3)	71(2)	59(2)	-27(2)	12(2)	-19(2)
C(6)	37(1)	25(1)	37(2)	2(1)	1(2)	2(1)
O(6)	40(1)	39(1)	65(1)	4(1)	0(1)	3(1)
C(7)	34(2)	36(2)	38(2)	-4(2)	-3(2)	-4(1)
C(8)	44(2)	33(2)	63(3)	-8(2)	3(2)	-6(1)
C(9)	58(2)	39(1)	66(2)	-9(1)	-3(3)	-17(2)
C(10)	34(2)	37(2)	34(3)	2(2)	-7(2)	-13(2)
C(11)	28(2)	33(2)	41(3)	2(2)	-8(2)	2(2)
C(18)	46(2)	32(2)	91(3)	7(2)	1(2)	6(1)
C(19)	66(3)	55(2)	93(3)	13(2)	7(3)	24(2)

Table 5. Hydrogen coordinates (x 10^4) and isotropic displacement parameters (Å^{2}x 10^3) for Complex **3**.

	x	y	z	U(eq)
H(8)	1640	8054	6363	56
H(9)	15	7015	6416	65
H(10)	-1612	7955	6426	42
H(11)	-1099	9588	6339	41
H(18A)	1212	11726	5630	67
H(18B)	1255	11814	6677	67
H(19A)	2	12821	6121	107
H(19B)	-588	12077	6695	107
H(19C)	-610	12016	5650	107

Table 6. Torsion angles [°] for Complex **3**.

C(3)-Cr(1)-C(6)-O(6)	49.8(6)
C(2)-Cr(1)-C(6)-O(6)	138.0(5)
C(4)-Cr(1)-C(6)-O(6)	-42.5(6)
C(5)-Cr(1)-C(6)-O(6)	-131.7(6)
C(3)-Cr(1)-C(6)-C(7)	-129.9(5)
C(2)-Cr(1)-C(6)-C(7)	-41.6(5)
C(4)-Cr(1)-C(6)-C(7)	137.9(5)
C(5)-Cr(1)-C(6)-C(7)	48.7(5)
C(7)-C(6)-O(6)-C(18)	-177.4(4)
Cr(1)-C(6)-O(6)-C(18)	2.9(8)
O(6)-C(6)-C(7)-C(11)	0.0(10)
Cr(1)-C(6)-C(7)-C(11)	179.7(6)
O(6)-C(6)-C(7)-C(8)	179.8(4)
Cr(1)-C(6)-C(7)-C(8)	-0.5(8)
O(6)-C(6)-C(7)-Fe(1)	-90.1(5)
Cr(1)-C(6)-C(7)-Fe(1)	89.5(5)
C(6)-C(7)-C(8)-C(9)	-179.4(5)
C(11)-C(7)-C(8)-C(9)	0.4(6)
C(7)-C(8)-C(9)-C(10)	-0.8(4)
C(8)-C(9)-C(10)-C(11)	0.9(5)
C(9)-C(10)-C(11)-C(7)	-0.6(7)
C(6)-O(6)-C(18)-C(19)	178.7(5)

Appendix 2

Crystallographic data of Complex 5

Table 1. Crystal data and structure refinement for Complex **5**.

Identification code	db52bc2_abs	
Empirical formula	$C_{27} H_{21} Cl_3 Cr Fe O_6 Ti$	
Formula weight	703.54	
Temperature	293(2) K	
Wavelength	0.71073 Å	
Crystal system	Monoclinic	
Space group	$P 2_1/n$	
Unit cell dimensions	a = 10.2230(7) Å	a= 90°.
	b = 26.2984(19) Å	b= 90.7190(10)°.
	c = 10.5587(8) Å	g = 90°.
Volume	2838.5(4) Å^3	
Z	4	
Density (calculated)	1.646 Mg/m^3	
Absorption coefficient	1.477 mm^{-1}	
F(000)	1416	
Crystal size	0.44 x 0.40 x 0.08 mm^3	
Theta range for data collection	2.47 to 26.38°.	
Index ranges	-5<=h<=12, -32<=k<=32, -10<=l<=12	
Reflections collected	14859	
Independent reflections	5143 [R(int) = 0.0414]	
Completeness to theta = 25.00°	97.9 %	
Absorption correction	Semi-empirical from equivalents	
Max. and min. transmission	0.889 and 0.544	
Refinement method	Full-matrix least-squares on F^2	
Data / restraints / parameters	5143 / 0 / 352	
Goodness-of-fit on F^2	1.035	
Final R indices [I>2sigma(I)]	R1 = 0.0488, wR2 = 0.1224	
R indices (all data)	R1 = 0.0798, wR2 = 0.1423	
Extinction coefficient	0	
Largest diff. peak and hole	0.590 and -0.623 e.Å^{-3}	

Table 2. Atomic coordinates (x 10^4) and equivalent isotropic displacement parameters (Å^{2}x 10^3) for Complex **5**. U(eq) is defined as one third of the trace of the orthogonalized U^{ij} tensor.

	x	y	z	U(eq)
Cr(1)	-802(1)	1296(1)	8269(1)	42(1)
C(1)	-2270(5)	1083(2)	7349(5)	62(1)
O(1)	-3194(4)	951(2)	6809(5)	99(2)
C(2)	-199(5)	623(2)	8399(5)	55(1)
O(2)	101(4)	205(1)	8440(4)	84(1)
C(3)	167(5)	1345(2)	6749(5)	50(1)
O(3)	729(4)	1346(2)	5826(4)	73(1)
C(4)	-1464(4)	1977(2)	8170(4)	49(1)
O(4)	-1918(4)	2368(1)	8159(4)	67(1)
C(5)	-1759(4)	1204(2)	9754(5)	49(1)
O(5)	-2371(3)	1132(2)	10633(4)	72(1)
C(6)	826(4)	1587(2)	9244(4)	37(1)
O(6)	1451(3)	1967(1)	8784(3)	43(1)
Fe(1)	2733(1)	894(1)	10901(1)	53(1)
C(7)	1330(4)	1429(2)	10496(4)	40(1)
C(8)	817(4)	1025(2)	11267(4)	47(1)
C(9)	1541(5)	1012(2)	12406(5)	63(1)
C(10)	2514(6)	1392(2)	12370(5)	67(2)
C(11)	2416(4)	1647(2)	11202(5)	49(1)
C(12)	3430(8)	561(3)	9289(8)	97(2)
C(13)	2889(6)	194(2)	10063(7)	83(2)
C(14)	3547(6)	200(2)	11200(8)	86(2)
C(15)	4536(6)	573(3)	11148(9)	103(3)
C(16)	4443(7)	796(3)	9952(10)	109(3)
Ti(1)	2339(1)	2535(1)	8077(1)	36(1)
Cl(1)	819(1)	2667(1)	6374(1)	58(1)
C(17)	1723(4)	2869(2)	10081(4)	47(1)
C(18)	3011(5)	3018(2)	9839(4)	51(1)
C(19)	2961(5)	3355(2)	8797(5)	57(1)
C(20)	1680(5)	3397(2)	8390(5)	56(1)
C(21)	906(4)	3089(2)	9180(4)	49(1)
C(22)	3620(6)	1831(2)	7346(7)	72(2)

C(23)	4333(5)	2082(3)	8250(5)	70(2)
C(24)	4634(5)	2554(3)	7799(7)	77(2)
C(25)	4030(5)	2602(2)	6605(6)	75(2)
C(26)	3420(5)	2143(3)	6351(5)	71(2)
Cl(2)	3635(5)	509(2)	5445(5)	264(2)
Cl(3)	1491(11)	-148(3)	5542(11)	472(7)
C(27)	2930(20)	-153(6)	5890(30)	380(20)

Table 3. Bond lengths [Å] and angles [°] for Complex **5**.

Cr(1)-C(1)	1.863(5)	C(12)-C(16)	1.388(10)
Cr(1)-C(5)	1.875(5)	C(12)-H(12)	0.9300
Cr(1)-C(2)	1.880(6)	C(13)-C(14)	1.369(9)
Cr(1)-C(3)	1.900(5)	C(13)-H(13)	0.9300
Cr(1)-C(4)	1.917(5)	C(14)-C(15)	1.411(9)
Cr(1)-C(6)	2.090(4)	C(14)-H(14)	0.9300
C(1)-O(1)	1.151(6)	C(15)-C(16)	1.394(11)
C(2)-O(2)	1.141(6)	C(15)-H(15)	0.9300
C(3)-O(3)	1.137(6)	C(16)-H(16)	0.9300
C(4)-O(4)	1.128(5)	Ti(1)-C(25)	2.345(5)
C(5)-O(5)	1.141(6)	Ti(1)-C(18)	2.348(4)
C(6)-O(6)	1.286(5)	Ti(1)-C(23)	2.367(5)
C(6)-C(7)	1.472(6)	Ti(1)-C(24)	2.368(5)
O(6)-Ti(1)	1.905(3)	Ti(1)-C(19)	2.372(5)
Fe(1)-C(14)	2.029(5)	Ti(1)-C(26)	2.378(5)
Fe(1)-C(8)	2.031(4)	Ti(1)-C(21)	2.381(4)
Fe(1)-C(11)	2.032(4)	Ti(1)-C(17)	2.384(4)
Fe(1)-C(9)	2.038(5)	Ti(1)-Cl(1)	2.3870(13)
Fe(1)-C(15)	2.040(6)	Ti(1)-C(20)	2.390(5)
Fe(1)-C(16)	2.042(7)	Ti(1)-C(22)	2.400(5)
Fe(1)-C(10)	2.044(6)	C(17)-C(21)	1.384(6)
Fe(1)-C(13)	2.049(6)	C(17)-C(18)	1.400(6)
Fe(1)-C(12)	2.049(7)	C(17)-H(17)	0.9300
Fe(1)-C(7)	2.050(4)	C(18)-C(19)	1.413(7)
C(7)-C(8)	1.440(6)	C(18)-H(18)	0.9300
C(7)-C(11)	1.449(6)	C(19)-C(20)	1.377(7)
C(8)-C(9)	1.405(7)	C(19)-H(19)	0.9300
C(8)-H(8)	0.9300	C(20)-C(21)	1.413(7)
C(9)-C(10)	1.411(7)	C(20)-H(20)	0.9300
C(9)-H(9)	0.9300	C(21)-H(21)	0.9300
C(10)-C(11)	1.405(7)	C(22)-C(26)	1.346(8)
C(10)-H(10)	0.9300	C(22)-C(23)	1.364(8)
C(11)-H(11)	0.9300	C(22)-H(22)	0.9300
C(12)-C(13)	1.384(9)	C(23)-C(24)	1.365(8)

C(23)-H(23)	0.9300
C(24)-C(25)	1.402(9)
C(24)-H(24)	0.9300
C(25)-C(26)	1.384(8)
C(25)-H(25)	0.9300
C(26)-H(26)	0.9300
Cl(2)-C(27)	1.94(2)
Cl(3)-C(27)	1.516(17)
C(27)-H(27A)	0.9700
C(27)-H(27B)	0.9700

C(1)-Cr(1)-C(5)	88.4(2)
C(1)-Cr(1)-C(2)	90.9(2)
C(5)-Cr(1)-C(2)	89.5(2)
C(1)-Cr(1)-C(3)	90.3(2)
C(5)-Cr(1)-C(3)	176.4(2)
C(2)-Cr(1)-C(3)	87.2(2)
C(1)-Cr(1)-C(4)	88.3(2)
C(5)-Cr(1)-C(4)	88.74(19)
C(2)-Cr(1)-C(4)	178.1(2)
C(3)-Cr(1)-C(4)	94.5(2)
C(1)-Cr(1)-C(6)	175.9(2)
C(5)-Cr(1)-C(6)	93.18(18)
C(2)-Cr(1)-C(6)	92.88(19)
C(3)-Cr(1)-C(6)	88.36(18)
C(4)-Cr(1)-C(6)	87.92(17)
O(1)-C(1)-Cr(1)	178.3(5)
O(2)-C(2)-Cr(1)	176.0(5)
O(3)-C(3)-Cr(1)	176.1(4)
O(4)-C(4)-Cr(1)	175.6(4)
O(5)-C(5)-Cr(1)	177.1(4)
O(6)-C(6)-C(7)	112.9(3)
O(6)-C(6)-Cr(1)	119.7(3)
C(7)-C(6)-Cr(1)	127.3(3)
C(6)-O(6)-Ti(1)	178.5(3)
C(14)-Fe(1)-C(8)	121.2(2)
C(14)-Fe(1)-C(11)	156.7(3)
C(8)-Fe(1)-C(11)	69.40(19)
C(14)-Fe(1)-C(9)	105.3(3)
C(8)-Fe(1)-C(9)	40.39(19)
C(11)-Fe(1)-C(9)	68.4(2)
C(14)-Fe(1)-C(15)	40.6(2)
C(8)-Fe(1)-C(15)	156.6(3)
C(11)-Fe(1)-C(15)	121.9(2)
C(9)-Fe(1)-C(15)	120.7(3)
C(14)-Fe(1)-C(16)	67.1(3)
C(8)-Fe(1)-C(16)	161.5(3)
C(11)-Fe(1)-C(16)	109.8(2)
C(9)-Fe(1)-C(16)	157.8(3)
C(15)-Fe(1)-C(16)	39.9(3)
C(14)-Fe(1)-C(10)	120.5(3)
C(8)-Fe(1)-C(10)	68.4(2)
C(11)-Fe(1)-C(10)	40.3(2)
C(9)-Fe(1)-C(10)	40.5(2)
C(15)-Fe(1)-C(10)	106.0(3)
C(16)-Fe(1)-C(10)	123.8(3)
C(14)-Fe(1)-C(13)	39.2(3)
C(8)-Fe(1)-C(13)	108.4(2)
C(11)-Fe(1)-C(13)	163.0(3)
C(9)-Fe(1)-C(13)	121.6(2)
C(15)-Fe(1)-C(13)	67.0(3)
C(16)-Fe(1)-C(13)	66.6(3)
C(10)-Fe(1)-C(13)	155.9(3)
C(14)-Fe(1)-C(12)	66.4(3)
C(8)-Fe(1)-C(12)	125.2(3)
C(11)-Fe(1)-C(12)	127.2(3)
C(9)-Fe(1)-C(12)	158.4(3)
C(15)-Fe(1)-C(12)	66.8(3)
C(16)-Fe(1)-C(12)	39.6(3)
C(10)-Fe(1)-C(12)	161.1(3)
C(13)-Fe(1)-C(12)	39.5(3)
C(14)-Fe(1)-C(7)	159.0(2)

C(8)-Fe(1)-C(7)	41.31(16)
C(11)-Fe(1)-C(7)	41.57(17)
C(9)-Fe(1)-C(7)	68.59(19)
C(15)-Fe(1)-C(7)	159.8(2)
C(16)-Fe(1)-C(7)	125.8(3)
C(10)-Fe(1)-C(7)	68.65(19)
C(13)-Fe(1)-C(7)	125.7(2)
C(12)-Fe(1)-C(7)	111.7(2)
C(8)-C(7)-C(11)	106.4(4)
C(8)-C(7)-C(6)	126.2(4)
C(11)-C(7)-C(6)	127.4(4)
C(8)-C(7)-Fe(1)	68.6(2)
C(11)-C(7)-Fe(1)	68.5(2)
C(6)-C(7)-Fe(1)	128.1(3)
C(9)-C(8)-C(7)	108.2(4)
C(9)-C(8)-Fe(1)	70.1(3)
C(7)-C(8)-Fe(1)	70.1(2)
C(9)-C(8)-H(8)	125.9
C(7)-C(8)-H(8)	125.9
Fe(1)-C(8)-H(8)	125.5
C(8)-C(9)-C(10)	108.8(4)
C(8)-C(9)-Fe(1)	69.5(3)
C(10)-C(9)-Fe(1)	70.0(3)
C(8)-C(9)-H(9)	125.6
C(10)-C(9)-H(9)	125.6
Fe(1)-C(9)-H(9)	126.5
C(11)-C(10)-C(9)	108.6(5)
C(11)-C(10)-Fe(1)	69.4(3)
C(9)-C(10)-Fe(1)	69.5(3)
C(11)-C(10)-H(10)	125.7
C(9)-C(10)-H(10)	125.7
Fe(1)-C(10)-H(10)	127.0
C(10)-C(11)-C(7)	108.0(4)
C(10)-C(11)-Fe(1)	70.3(3)
C(7)-C(11)-Fe(1)	69.9(2)
C(10)-C(11)-H(11)	126.0
C(7)-C(11)-H(11)	126.0
Fe(1)-C(11)-H(11)	125.4
C(13)-C(12)-C(16)	108.3(7)
C(13)-C(12)-Fe(1)	70.3(4)
C(16)-C(12)-Fe(1)	69.9(4)
C(13)-C(12)-H(12)	125.9
C(16)-C(12)-H(12)	125.9
Fe(1)-C(12)-H(12)	125.6
C(14)-C(13)-C(12)	108.4(7)
C(14)-C(13)-Fe(1)	69.6(4)
C(12)-C(13)-Fe(1)	70.3(4)
C(14)-C(13)-H(13)	125.8
C(12)-C(13)-H(13)	125.8
Fe(1)-C(13)-H(13)	125.9
C(13)-C(14)-C(15)	108.5(7)
C(13)-C(14)-Fe(1)	71.2(3)
C(15)-C(14)-Fe(1)	70.2(3)
C(13)-C(14)-H(14)	125.7
C(15)-C(14)-H(14)	125.7
Fe(1)-C(14)-H(14)	124.5
C(16)-C(15)-C(14)	106.7(7)
C(16)-C(15)-Fe(1)	70.1(3)
C(14)-C(15)-Fe(1)	69.3(3)
C(16)-C(15)-H(15)	126.7
C(14)-C(15)-H(15)	126.7
Fe(1)-C(15)-H(15)	125.5
C(12)-C(16)-C(15)	108.2(7)
C(12)-C(16)-Fe(1)	70.5(4)
C(15)-C(16)-Fe(1)	70.0(4)
C(12)-C(16)-H(16)	125.9
C(15)-C(16)-H(16)	125.9
Fe(1)-C(16)-H(16)	125.3
O(6)-Ti(1)-C(25)	132.63(18)
O(6)-Ti(1)-C(18)	104.46(15)
C(25)-Ti(1)-C(18)	105.9(2)
O(6)-Ti(1)-C(23)	89.38(19)

C(25)-Ti(1)-C(23)	56.5(2)
C(18)-Ti(1)-C(23)	88.2(2)
O(6)-Ti(1)-C(24)	122.8(2)
C(25)-Ti(1)-C(24)	34.6(2)
C(18)-Ti(1)-C(24)	78.86(19)
C(23)-Ti(1)-C(24)	33.5(2)
O(6)-Ti(1)-C(19)	135.61(15)
C(25)-Ti(1)-C(19)	87.0(2)
C(18)-Ti(1)-C(19)	34.84(17)
C(23)-Ti(1)-C(19)	101.9(2)
C(24)-Ti(1)-C(19)	76.07(19)
O(6)-Ti(1)-C(26)	100.9(2)
C(25)-Ti(1)-C(26)	34.1(2)
C(18)-Ti(1)-C(26)	135.03(18)
C(23)-Ti(1)-C(26)	55.4(2)
C(24)-Ti(1)-C(26)	56.2(2)
C(19)-Ti(1)-C(26)	121.0(2)
O(6)-Ti(1)-C(21)	89.37(15)
C(25)-Ti(1)-C(21)	137.84(19)
C(18)-Ti(1)-C(21)	57.10(16)
C(23)-Ti(1)-C(21)	143.61(19)
C(24)-Ti(1)-C(21)	131.65(19)
C(19)-Ti(1)-C(21)	56.66(16)
C(26)-Ti(1)-C(21)	159.23(19)
O(6)-Ti(1)-C(17)	78.97(14)
C(25)-Ti(1)-C(17)	140.0(2)
C(18)-Ti(1)-C(17)	34.41(15)
C(23)-Ti(1)-C(17)	110.73(18)
C(24)-Ti(1)-C(17)	112.06(19)
C(19)-Ti(1)-C(17)	56.80(16)
C(26)-Ti(1)-C(17)	166.09(18)
C(21)-Ti(1)-C(17)	33.78(15)
O(6)-Ti(1)-Cl(1)	95.74(10)
C(25)-Ti(1)-Cl(1)	88.18(17)
C(18)-Ti(1)-Cl(1)	134.39(13)
C(23)-Ti(1)-Cl(1)	133.10(15)
C(24)-Ti(1)-Cl(1)	122.70(19)
C(19)-Ti(1)-Cl(1)	106.20(14)
C(26)-Ti(1)-Cl(1)	77.89(14)
C(21)-Ti(1)-Cl(1)	83.18(12)
C(17)-Ti(1)-Cl(1)	116.02(12)
O(6)-Ti(1)-C(20)	123.59(15)
C(25)-Ti(1)-C(20)	103.40(19)
C(18)-Ti(1)-C(20)	57.11(17)
C(23)-Ti(1)-C(20)	135.3(2)
C(24)-Ti(1)-C(20)	106.2(2)
C(19)-Ti(1)-C(20)	33.61(17)
C(26)-Ti(1)-C(20)	130.7(2)
C(21)-Ti(1)-C(20)	34.45(16)
C(17)-Ti(1)-C(20)	56.56(16)
Cl(1)-Ti(1)-C(20)	77.58(13)
O(6)-Ti(1)-C(22)	77.63(16)
C(25)-Ti(1)-C(22)	55.6(2)
C(18)-Ti(1)-C(22)	121.1(2)
C(23)-Ti(1)-C(22)	33.3(2)
C(24)-Ti(1)-C(22)	55.3(2)
C(19)-Ti(1)-C(22)	131.28(19)
C(26)-Ti(1)-C(22)	32.7(2)
C(21)-Ti(1)-C(22)	166.08(19)
C(17)-Ti(1)-C(22)	136.1(2)
Cl(1)-Ti(1)-C(22)	102.83(18)
C(20)-Ti(1)-C(22)	158.77(19)
C(21)-C(17)-C(18)	108.5(4)
C(21)-C(17)-Ti(1)	73.0(3)
C(18)-C(17)-Ti(1)	71.4(3)
C(21)-C(17)-H(17)	125.7
C(18)-C(17)-H(17)	125.7
Ti(1)-C(17)-H(17)	121.6
C(17)-C(18)-C(19)	107.0(4)
C(17)-C(18)-Ti(1)	74.2(3)
C(19)-C(18)-Ti(1)	73.5(3)
C(17)-C(18)-H(18)	126.5

C(19)-C(18)-H(18)	126.5
Ti(1)-C(18)-H(18)	117.9
C(20)-C(19)-C(18)	108.6(4)
C(20)-C(19)-Ti(1)	73.9(3)
C(18)-C(19)-Ti(1)	71.7(3)
C(20)-C(19)-H(19)	125.7
C(18)-C(19)-H(19)	125.7
Ti(1)-C(19)-H(19)	120.4
C(19)-C(20)-C(21)	107.9(4)
C(19)-C(20)-Ti(1)	72.4(3)
C(21)-C(20)-Ti(1)	72.4(3)
C(19)-C(20)-H(20)	126.1
C(21)-C(20)-H(20)	126.1
Ti(1)-C(20)-H(20)	120.8
C(17)-C(21)-C(20)	107.9(4)
C(17)-C(21)-Ti(1)	73.2(3)
C(20)-C(21)-Ti(1)	73.1(3)
C(17)-C(21)-H(21)	126.0
C(20)-C(21)-H(21)	126.0
Ti(1)-C(21)-H(21)	119.5
C(26)-C(22)-C(23)	109.0(5)
C(26)-C(22)-Ti(1)	72.7(3)
C(23)-C(22)-Ti(1)	72.0(3)
C(26)-C(22)-H(22)	125.5
C(23)-C(22)-H(22)	125.5
Ti(1)-C(22)-H(22)	121.4
C(22)-C(23)-C(24)	108.4(5)
C(22)-C(23)-Ti(1)	74.7(3)
C(24)-C(23)-Ti(1)	73.3(3)
C(22)-C(23)-H(23)	125.8
C(24)-C(23)-H(23)	125.8
Ti(1)-C(23)-H(23)	118.1
C(23)-C(24)-C(25)	107.3(5)
C(23)-C(24)-Ti(1)	73.2(3)
C(25)-C(24)-Ti(1)	71.8(3)
C(23)-C(24)-H(24)	126.3
C(25)-C(24)-H(24)	126.3
Ti(1)-C(24)-H(24)	120.5
C(26)-C(25)-C(24)	106.7(5)
C(26)-C(25)-Ti(1)	74.3(3)
C(24)-C(25)-Ti(1)	73.6(3)
C(26)-C(25)-H(25)	126.7
C(24)-C(25)-H(25)	126.7
Ti(1)-C(25)-H(25)	117.6
C(22)-C(26)-C(25)	108.5(5)
C(22)-C(26)-Ti(1)	74.6(3)
C(25)-C(26)-Ti(1)	71.7(3)
C(22)-C(26)-H(26)	125.8
C(25)-C(26)-H(26)	125.8
Ti(1)-C(26)-H(26)	119.8
Cl(3)-C(27)-Cl(2)	107.1(11)
Cl(3)-C(27)-H(27A)	110.3
Cl(2)-C(27)-H(27A)	110.3
Cl(3)-C(27)-H(27B)	110.3
Cl(2)-C(27)-H(27B)	110.3
H(27A)-C(27)-H(27B)	108.5

Table 4. Anisotropic displacement parameters (Å^{2}x 10^3)for Complex **5**. The anisotropic displacement factor exponent takes the form: -2p^2[h^{2}a*^{2}U^{11} + ... + 2 h k a* b* U^{12}]

	U^{11}	U^{22}	U^{33}	U^{23}	U^{13}	U^{12}
Cr(1)	40(1)	39(1)	47(1)	-3(1)	0(1)	-6(1)
C(1)	63(3)	57(3)	65(3)	7(3)	-12(3)	-11(3)
O(1)	86(3)	108(4)	103(3)	5(3)	-36(3)	-36(3)
C(2)	60(3)	50(3)	54(3)	-1(2)	5(2)	-10(2)
O(2)	105(3)	40(2)	108(3)	-1(2)	2(3)	2(2)
C(3)	55(3)	44(3)	50(3)	-5(2)	-3(2)	-1(2)
O(3)	78(3)	82(3)	58(2)	-3(2)	15(2)	1(2)
C(4)	38(2)	57(3)	51(3)	-1(2)	1(2)	-9(2)
O(4)	68(2)	51(2)	82(3)	4(2)	2(2)	11(2)
C(5)	37(2)	46(3)	64(3)	-4(2)	0(2)	-2(2)
O(5)	59(2)	80(3)	77(3)	-3(2)	26(2)	-6(2)
C(6)	36(2)	33(2)	44(2)	-4(2)	9(2)	1(2)
O(6)	42(2)	40(2)	47(2)	5(1)	3(1)	-8(1)
Fe(1)	41(1)	37(1)	80(1)	8(1)	-4(1)	4(1)
C(7)	38(2)	33(2)	49(3)	2(2)	3(2)	4(2)
C(8)	42(2)	44(3)	56(3)	10(2)	5(2)	1(2)
C(9)	73(3)	60(3)	56(3)	16(3)	1(3)	2(3)
C(10)	81(4)	53(3)	65(3)	5(3)	-28(3)	2(3)
C(11)	51(3)	35(2)	61(3)	0(2)	-12(2)	-1(2)
C(12)	92(5)	85(5)	116(6)	-1(4)	36(5)	42(4)
C(13)	71(4)	48(3)	129(6)	-9(4)	17(4)	12(3)
C(14)	78(4)	54(4)	125(6)	25(4)	-1(4)	22(3)
C(15)	56(4)	62(4)	189(8)	11(5)	-26(4)	19(3)
C(16)	58(4)	61(4)	210(10)	30(5)	41(5)	20(3)
Ti(1)	32(1)	39(1)	38(1)	4(1)	3(1)	-4(1)
Cl(1)	51(1)	71(1)	53(1)	7(1)	-12(1)	-2(1)
C(17)	56(3)	46(3)	39(2)	-3(2)	6(2)	-1(2)
C(18)	51(3)	51(3)	51(3)	-12(2)	-11(2)	-2(2)
C(19)	55(3)	44(3)	72(3)	-7(3)	13(2)	-14(2)
C(20)	73(3)	42(3)	52(3)	8(2)	6(2)	8(2)
C(21)	43(2)	51(3)	54(3)	-3(2)	5(2)	5(2)
C(22)	68(3)	49(3)	100(5)	-8(3)	35(3)	3(3)

C(23)	54(3)	97(5)	59(3)	10(3)	7(3)	35(3)
C(24)	35(3)	89(5)	107(5)	-37(4)	12(3)	-9(3)
C(25)	60(3)	79(4)	86(4)	33(3)	44(3)	21(3)
C(26)	55(3)	109(5)	48(3)	-18(3)	7(2)	10(3)
Cl(2)	272(5)	262(5)	256(5)	-81(4)	-28(4)	83(4)
Cl(3)	547(14)	264(7)	614(16)	-73(9)	362(13)	-11(9)
C(27)	370(30)	143(13)	620(40)	-190(20)	-330(30)	112(17)

Table 5. Hydrogen coordinates (x 10^4) and isotropic displacement parameters ($Å^2$x 10^3) for Complex **5**.

	x	y	z	U(eq)
H(8)	127	811	11049	57
H(9)	1402	789	13074	76
H(10)	3120	1462	13011	80
H(11)	2954	1909	10932	59
H(12)	3160	637	8466	117
H(13)	2198	-20	9847	99
H(14)	3371	-7	11891	103
H(15)	5133	655	11787	123
H(16)	4970	1056	9650	131
H(17)	1461	2658	10737	56
H(18)	3758	2915	10279	61
H(19)	3673	3521	8446	68
H(20)	1379	3594	7715	67
H(21)	7	3042	9108	59
H(22)	3319	1498	7407	86
H(23)	4575	1953	9039	84
H(24)	5144	2798	8208	92
H(25)	4038	2888	6085	89
H(26)	2952	2063	5617	85
H(27A)	3381	-419	5433	460
H(27B)	3048	-214	6793	460

Table 6. Torsion angles [°] for Complex **5**

C(5)-Cr(1)-C(6)-O(6)	-139.1(3)
C(2)-Cr(1)-C(6)-O(6)	131.2(3)
C(3)-Cr(1)-C(6)-O(6)	44.1(3)
C(4)-Cr(1)-C(6)-O(6)	-50.5(3)
C(5)-Cr(1)-C(6)-C(7)	36.2(4)
C(2)-Cr(1)-C(6)-C(7)	-53.5(4)
C(3)-Cr(1)-C(6)-C(7)	-140.6(4)
C(4)-Cr(1)-C(6)-C(7)	124.8(4)
O(6)-C(6)-C(7)-C(8)	178.3(4)
Cr(1)-C(6)-C(7)-C(8)	2.7(6)
O(6)-C(6)-C(7)-C(11)	-1.0(6)
Cr(1)-C(6)-C(7)-C(11)	-176.5(3)
C(11)-C(7)-C(8)-C(9)	1.6(5)
C(6)-C(7)-C(8)-C(9)	-177.7(4)
C(7)-C(8)-C(9)-C(10)	-0.8(6)
C(8)-C(9)-C(10)-C(11)	-0.3(6)
C(9)-C(10)-C(11)-C(7)	1.4(6)
C(8)-C(7)-C(11)-C(10)	-1.8(5)
C(6)-C(7)-C(11)-C(10)	177.5(4)
C(12)-C(13)-C(14)-C(15)	-0.7(7)
C(13)-C(14)-C(15)-C(16)	0.7(7)
C(13)-C(12)-C(16)-C(15)	0.0(7)
C(21)-C(17)-C(18)-C(19)	2.7(5)
C(17)-C(18)-C(19)-C(20)	-1.9(5)
C(18)-C(19)-C(20)-C(21)	0.4(6)
C(18)-C(17)-C(21)-C(20)	-2.4(5)
C(19)-C(20)-C(21)-C(17)	1.2(5)
C(26)-C(22)-C(23)-C(24)	-2.4(6)
C(22)-C(23)-C(24)-C(25)	2.9(6)
C(23)-C(24)-C(25)-C(26)	-2.4(6)
C(23)-C(22)-C(26)-C(25)	0.8(6)
C(24)-C(25)-C(26)-C(22)	1.0(6)

Symmetry transformations used to generate equivalent atoms:

Table 7. Selected least-squares planes and deviations from the planes (Åx10^3) for Complex **5**

Plane 1 $-6.199(7)x + 17.075(36)y + 4.927(18)z = 6.777(11)$

Atoms *	Cr(1)	C(6)	O(6)	C(7)		rms	[Ti(1)]
Deviations	7(1)	-26(3)	10(1)	9(1)		15	[81(6)]

Plane 2 $-6.507(20)x + 17.165(50)y + 4.423(24) z = 6.219(28)$

Atoms *	C(7)	C(8)	C(9)	C(10)	C(11)	rms	[Fe(1)]
Deviations	10(3)	-7(3)	2(3)	5(3)	-9(3)	7	[-1642(2)]

Plane 3 $-6.603(24)x + 17.832(59)y + 3.789(31)z = 2.254(36)$

Atoms *	C(12)	C(13)	C(14)	C(15)	C(16)	rms	[Fe(1)]
Deviations	1(4)	-3(4)	4(4)	-3(4)	1(4)	3	[1665(3)]

Plane 4 $-1.356(23)x + 20.460(39)y + 6.501(20)z = 12.176(11)$

Atoms *	C(17)	C(18)	C(19)	C(20)	C(21)	rms	[Ti(1)]
Deviations	15(3)	-13(3)	7(3)	2(3)	-10(3)	10	[-2056(2)]

Plane 5 $-8.588(14)x + 9.142(64)y + 4.507(24)z = 1.885(27)$

Atoms *	C(22)	C(23)	C(24)	C(25)	C(26)	rms	[Ti(1)]
Deviations	-9(3)	15(3)	-15(3)	10(3)	-1(3)	11	[2064(2)]

Dihedral angles between planes (º):

Planes 1 and 2:	3.26(33)	Planes 4 and 5:	50.39(23)
Planes 2 and 3:	17.14(17)		

* rms = root mean square deviation from the plane;
atoms not involved in calculating the plane are shown in brackets [ ].

Appendix 3

Crystallographic data of Complex 6

Table 1. Crystal data and structure refinement for Complex **6**.

Identification code	bvdw01_pna21	
Empirical formula	C_{26} H_{19} Cl Fe O_6 Ti W	
Formula weight	750.46	
Temperature	293(2) K	
Wavelength	0.71073 Å	
Crystal system	Orthorhombic	
Space group	Pna2_1	
Unit cell dimensions	a = 23.220(3) Å	a= 90°.
	b = 10.0663(14) Å	b= 90°.
	c = 10.8634(15) Å	g = 90°.
Volume	2539.2(6) Å^3	
Z	4	
Density (calculated)	1.963 Mg/m^3	
Absorption coefficient	5.535 mm^{-1}	
F(000)	1448	
Crystal size	0.22 x 0.18 x 0.01 mm^3	
Theta range for data collection	2.57 to 26.43°.	
Index ranges	-28<=h<=13, -11<=k<=12, -12<=l<=11	
Reflections collected	12791	
Independent reflections	4518 [R(int) = 0.0616]	
Completeness to theta = 25.00°	99.9 %	
Absorption correction	Semi-empirical from equivalents	
Max. and min. transmission	0.946 and 0.328	
Refinement method	Full-matrix least-squares on F^2	
Data / restraints / parameters	4518 / 1 / 325	
Goodness-of-fit on F^2	1.034	
Final R indices [I>2σ(I)]	R1 = 0.0413, wR2 = 0.0885	
R indices (all data)	R1 = 0.0667, wR2 = 0.0996	
Absolute structure parameter	0.027(14)	
Extinction coefficient	0	
Largest diff. peak and hole	0.977 and -2.287 e.Å^{-3}	

Table 2. Atomic coordinates (x 10^4) and equivalent isotropic displacement parameters (Å^{2}x 10^3) for Complex **6**. U(eq) is defined as one third of the trace of the orthogonalized U^{ij} tensor.

	x	y	z	U(eq)
W(1)	1151(1)	9655(1)	10737(1)	36(1)
C(1)	939(5)	11270(13)	11722(12)	52(3)
O(1)	837(5)	12207(10)	12297(10)	89(3)
C(2)	1981(4)	10294(9)	10785(19)	46(2)
O(2)	2438(3)	10740(7)	10844(12)	61(2)
C(3)	1043(5)	10684(12)	9171(12)	47(3)
O(3)	946(5)	11256(10)	8323(11)	83(3)
C(4)	311(4)	9255(11)	10687(18)	59(3)
O(4)	-186(4)	9095(11)	10684(18)	123(5)
C(5)	1190(5)	8544(13)	12321(12)	51(3)
O(5)	1153(4)	7884(12)	13190(9)	83(4)
C(6)	1469(4)	7829(9)	9749(9)	32(2)
O(6)	1886(3)	7180(7)	10218(6)	36(2)
Fe(1)	587(1)	5952(2)	8470(1)	38(1)
C(7)	1249(4)	7279(11)	8592(10)	35(3)
C(8)	1437(5)	6093(11)	7984(9)	43(3)
C(9)	1093(5)	5896(14)	6933(11)	55(3)
C(10)	689(5)	6970(13)	6866(9)	54(3)
C(11)	778(5)	7785(11)	7858(9)	46(3)
C(12)	-237(5)	5211(13)	8419(13)	55(3)
C(13)	-179(5)	6052(13)	9438(11)	54(3)
C(14)	264(5)	5586(13)	10190(12)	58(3)
C(15)	471(5)	4373(13)	9645(14)	64(4)
C(16)	170(5)	4152(12)	8528(14)	56(3)
Ti(1)	2547(1)	6325(2)	10877(2)	31(1)
Cl(1)	2705(1)	7881(3)	12518(2)	44(1)
C(17)	2087(7)	4239(11)	10772(18)	70(4)
C(18)	2623(6)	3996(11)	11284(18)	83(6)
C(19)	2626(8)	4698(14)	12421(17)	87(6)
C(20)	2076(8)	5227(13)	12543(14)	69(4)
C(21)	1775(6)	4931(14)	11557(17)	70(5)
C(22)	3071(5)	5677(12)	9146(11)	52(3)

C(23)	3464(4)	5724(11)	10106(12)	51(3)
C(24)	3518(4)	7043(11)	10487(11)	47(3)
C(25)	3138(4)	7778(11)	9736(10)	44(3)
C(26)	2870(5)	6958(12)	8883(10)	49(3)

Table 3. Bond lengths [Å] and angles [°] for Complex **6**.

W(1)-C(4)	1.993(10)	C(12)-C(16)	1.430(17)
W(1)-C(3)	2.008(13)	C(12)-H(12)	0.9300
W(1)-C(1)	2.008(13)	C(13)-C(14)	1.395(16)
W(1)-C(2)	2.033(10)	C(13)-H(13)	0.9300
W(1)-C(5)	2.053(14)	C(14)-C(15)	1.440(18)
W(1)-C(6)	2.253(9)	C(14)-H(14)	0.9300
C(1)-O(1)	1.155(14)	C(15)-C(16)	1.419(18)
C(2)-O(2)	1.154(11)	C(15)-H(15)	0.9300
C(3)-O(3)	1.109(14)	C(16)-H(16)	0.9300
C(4)-O(4)	1.163(12)	Ti(1)-C(22)	2.332(11)
C(5)-O(5)	1.158(15)	Ti(1)-C(19)	2.351(13)
C(6)-O(6)	1.273(11)	Ti(1)-C(25)	2.358(10)
C(6)-C(7)	1.465(15)	Ti(1)-C(17)	2.359(10)
O(6)-Ti(1)	1.901(6)	Ti(1)-C(23)	2.366(10)
Fe(1)-C(11)	2.011(11)	Ti(1)-C(26)	2.380(11)
Fe(1)-C(10)	2.036(11)	Ti(1)-C(20)	2.386(13)
Fe(1)-C(7)	2.042(11)	Ti(1)-C(18)	2.392(11)
Fe(1)-C(9)	2.042(12)	Ti(1)-C(21)	2.393(13)
Fe(1)-C(8)	2.047(11)	Ti(1)-Cl(1)	2.402(3)
Fe(1)-C(14)	2.047(12)	Ti(1)-C(24)	2.404(10)
Fe(1)-C(12)	2.054(12)	C(17)-C(21)	1.32(2)
Fe(1)-C(16)	2.055(12)	C(17)-C(18)	1.387(19)
Fe(1)-C(15)	2.056(13)	C(17)-H(17)	0.9300
Fe(1)-C(13)	2.069(11)	C(18)-C(19)	1.42(2)
C(7)-C(8)	1.432(14)	C(18)-H(18)	0.9300
C(7)-C(11)	1.447(14)	C(19)-C(20)	1.39(2)
C(8)-C(9)	1.407(15)	C(19)-H(19)	0.9300
C(8)-H(8)	0.9300	C(20)-C(21)	1.31(2)
C(9)-C(10)	1.433(17)	C(20)-H(20)	0.9300
C(9)-H(9)	0.9300	C(21)-H(21)	0.9300
C(10)-C(11)	1.370(15)	C(22)-C(23)	1.386(16)
C(10)-H(10)	0.9300	C(22)-C(26)	1.401(16)
C(11)-H(11)	0.9300	C(22)-H(22)	0.9300
C(12)-C(13)	1.400(17)	C(23)-C(24)	1.396(14)

C(23)-H(23)	0.9300
C(24)-C(25)	1.411(14)
C(24)-H(24)	0.9300
C(25)-C(26)	1.389(15)
C(25)-H(25)	0.9300
C(26)-H(26)	0.9300

C(4)-W(1)-C(3)	87.6(7)
C(4)-W(1)-C(1)	86.5(5)
C(3)-W(1)-C(1)	90.2(6)
C(4)-W(1)-C(2)	173.2(4)
C(3)-W(1)-C(2)	88.7(6)
C(1)-W(1)-C(2)	87.8(5)
C(4)-W(1)-C(5)	87.5(6)
C(3)-W(1)-C(5)	175.1(5)
C(1)-W(1)-C(5)	90.3(5)
C(2)-W(1)-C(5)	96.2(6)
C(4)-W(1)-C(6)	98.3(4)
C(3)-W(1)-C(6)	93.3(4)
C(1)-W(1)-C(6)	174.2(4)
C(2)-W(1)-C(6)	87.7(4)
C(5)-W(1)-C(6)	86.6(4)
O(1)-C(1)-W(1)	177.7(11)
O(2)-C(2)-W(1)	175.2(10)
O(3)-C(3)-W(1)	175.5(12)
O(4)-C(4)-W(1)	176.1(10)
O(5)-C(5)-W(1)	172.8(10)
O(6)-C(6)-C(7)	114.5(8)
O(6)-C(6)-W(1)	118.5(7)
C(7)-C(6)-W(1)	127.0(7)
C(6)-O(6)-Ti(1)	175.4(7)
C(11)-Fe(1)-C(10)	39.6(4)
C(11)-Fe(1)-C(7)	41.8(4)
C(10)-Fe(1)-C(7)	68.8(5)
C(11)-Fe(1)-C(9)	68.2(5)
C(10)-Fe(1)-C(9)	41.2(5)
C(7)-Fe(1)-C(9)	68.8(5)
C(11)-Fe(1)-C(8)	68.8(5)
C(10)-Fe(1)-C(8)	68.4(5)
C(7)-Fe(1)-C(8)	41.0(4)
C(9)-Fe(1)-C(8)	40.3(4)
C(11)-Fe(1)-C(14)	123.2(5)
C(10)-Fe(1)-C(14)	156.1(5)
C(7)-Fe(1)-C(14)	109.6(5)
C(9)-Fe(1)-C(14)	162.3(5)
C(8)-Fe(1)-C(14)	127.0(5)
C(11)-Fe(1)-C(12)	121.9(5)
C(10)-Fe(1)-C(12)	105.5(5)
C(7)-Fe(1)-C(12)	160.2(5)
C(9)-Fe(1)-C(12)	120.2(5)
C(8)-Fe(1)-C(12)	156.3(5)
C(14)-Fe(1)-C(12)	67.5(5)
C(11)-Fe(1)-C(16)	157.3(5)
C(10)-Fe(1)-C(16)	121.6(5)
C(7)-Fe(1)-C(16)	158.4(4)
C(9)-Fe(1)-C(16)	105.8(6)
C(8)-Fe(1)-C(16)	121.6(5)
C(14)-Fe(1)-C(16)	69.0(6)
C(12)-Fe(1)-C(16)	40.7(5)
C(11)-Fe(1)-C(15)	160.6(5)
C(10)-Fe(1)-C(15)	159.4(5)
C(7)-Fe(1)-C(15)	124.4(5)
C(9)-Fe(1)-C(15)	124.2(6)
C(8)-Fe(1)-C(15)	109.9(5)
C(14)-Fe(1)-C(15)	41.1(5)
C(12)-Fe(1)-C(15)	67.3(5)
C(16)-Fe(1)-C(15)	40.4(5)
C(11)-Fe(1)-C(13)	108.2(5)
C(10)-Fe(1)-C(13)	120.6(5)
C(7)-Fe(1)-C(13)	125.6(5)
C(9)-Fe(1)-C(13)	155.7(5)
C(8)-Fe(1)-C(13)	163.0(4)

C(14)-Fe(1)-C(13)	39.6(5)
C(12)-Fe(1)-C(13)	39.7(5)
C(16)-Fe(1)-C(13)	67.8(5)
C(15)-Fe(1)-C(13)	67.0(5)
C(8)-C(7)-C(11)	105.6(9)
C(8)-C(7)-C(6)	127.2(9)
C(11)-C(7)-C(6)	127.1(9)
C(8)-C(7)-Fe(1)	69.7(6)
C(11)-C(7)-Fe(1)	68.0(6)
C(6)-C(7)-Fe(1)	124.4(7)
C(9)-C(8)-C(7)	108.6(10)
C(9)-C(8)-Fe(1)	69.7(7)
C(7)-C(8)-Fe(1)	69.3(6)
C(9)-C(8)-H(8)	125.7
C(7)-C(8)-H(8)	125.7
Fe(1)-C(8)-H(8)	126.9
C(8)-C(9)-C(10)	107.9(10)
C(8)-C(9)-Fe(1)	70.0(7)
C(10)-C(9)-Fe(1)	69.2(6)
C(8)-C(9)-H(9)	126.1
C(10)-C(9)-H(9)	126.1
Fe(1)-C(9)-H(9)	126.2
C(11)-C(10)-C(9)	108.2(10)
C(11)-C(10)-Fe(1)	69.2(6)
C(9)-C(10)-Fe(1)	69.6(7)
C(11)-C(10)-H(10)	125.9
C(9)-C(10)-H(10)	125.9
Fe(1)-C(10)-H(10)	126.8
C(10)-C(11)-C(7)	109.7(10)
C(10)-C(11)-Fe(1)	71.2(7)
C(7)-C(11)-Fe(1)	70.2(6)
C(10)-C(11)-H(11)	125.1
C(7)-C(11)-H(11)	125.1
Fe(1)-C(11)-H(11)	125.0
C(13)-C(12)-C(16)	108.8(11)
C(13)-C(12)-Fe(1)	70.7(7)
C(16)-C(12)-Fe(1)	69.7(7)
C(13)-C(12)-H(12)	125.6
C(16)-C(12)-H(12)	125.6
Fe(1)-C(12)-H(12)	125.6
C(14)-C(13)-C(12)	109.3(12)
C(14)-C(13)-Fe(1)	69.3(7)
C(12)-C(13)-Fe(1)	69.6(7)
C(14)-C(13)-H(13)	125.3
C(12)-C(13)-H(13)	125.3
Fe(1)-C(13)-H(13)	127.3
C(13)-C(14)-C(15)	106.9(11)
C(13)-C(14)-Fe(1)	71.0(7)
C(15)-C(14)-Fe(1)	69.8(7)
C(13)-C(14)-H(14)	126.5
C(15)-C(14)-H(14)	126.5
Fe(1)-C(14)-H(14)	124.3
C(16)-C(15)-C(14)	108.7(11)
C(16)-C(15)-Fe(1)	69.8(7)
C(14)-C(15)-Fe(1)	69.1(7)
C(16)-C(15)-H(15)	125.7
C(14)-C(15)-H(15)	125.7
Fe(1)-C(15)-H(15)	127.0
C(15)-C(16)-C(12)	106.2(12)
C(15)-C(16)-Fe(1)	69.8(7)
C(12)-C(16)-Fe(1)	69.6(8)
C(15)-C(16)-H(16)	126.9
C(12)-C(16)-H(16)	126.9
Fe(1)-C(16)-H(16)	125.3
O(6)-Ti(1)-C(22)	104.2(4)
O(6)-Ti(1)-C(19)	130.3(5)
C(22)-Ti(1)-C(19)	109.9(6)
O(6)-Ti(1)-C(25)	89.5(4)
C(22)-Ti(1)-C(25)	56.4(4)
C(19)-Ti(1)-C(25)	139.7(5)
O(6)-Ti(1)-C(17)	91.1(5)
C(22)-Ti(1)-C(17)	87.1(6)

C(19)-Ti(1)-C(17)	56.6(5)
C(25)-Ti(1)-C(17)	142.3(6)
O(6)-Ti(1)-C(23)	135.2(4)
C(22)-Ti(1)-C(23)	34.3(4)
C(19)-Ti(1)-C(23)	90.3(6)
C(25)-Ti(1)-C(23)	56.6(4)
C(17)-Ti(1)-C(23)	99.4(5)
O(6)-Ti(1)-C(26)	77.9(4)
C(22)-Ti(1)-C(26)	34.6(4)
C(19)-Ti(1)-C(26)	144.3(6)
C(25)-Ti(1)-C(26)	34.1(4)
C(17)-Ti(1)-C(26)	109.7(6)
C(23)-Ti(1)-C(26)	57.5(4)
O(6)-Ti(1)-C(20)	97.2(5)
C(22)-Ti(1)-C(20)	136.2(5)
C(19)-Ti(1)-C(20)	34.1(6)
C(25)-Ti(1)-C(20)	162.3(5)
C(17)-Ti(1)-C(20)	54.3(6)
C(23)-Ti(1)-C(20)	124.3(5)
C(26)-Ti(1)-C(20)	163.6(5)
O(6)-Ti(1)-C(18)	125.0(5)
C(22)-Ti(1)-C(18)	80.6(5)
C(19)-Ti(1)-C(18)	34.9(6)
C(25)-Ti(1)-C(18)	131.5(4)
C(17)-Ti(1)-C(18)	33.9(5)
C(23)-Ti(1)-C(18)	75.4(4)
C(26)-Ti(1)-C(18)	114.1(5)
C(20)-Ti(1)-C(18)	55.9(5)
O(6)-Ti(1)-C(21)	77.1(4)
C(22)-Ti(1)-C(21)	118.4(6)
C(19)-Ti(1)-C(21)	55.2(5)
C(25)-Ti(1)-C(21)	164.1(5)
C(17)-Ti(1)-C(21)	32.2(5)
C(23)-Ti(1)-C(21)	129.3(5)
C(26)-Ti(1)-C(21)	132.4(6)
C(20)-Ti(1)-C(21)	31.9(5)
C(18)-Ti(1)-C(21)	54.8(4)
O(6)-Ti(1)-Cl(1)	96.1(2)
C(22)-Ti(1)-Cl(1)	134.5(3)
C(19)-Ti(1)-Cl(1)	85.0(5)
C(25)-Ti(1)-Cl(1)	84.1(3)
C(17)-Ti(1)-Cl(1)	133.3(5)
C(23)-Ti(1)-Cl(1)	107.0(3)
C(26)-Ti(1)-Cl(1)	116.9(3)
C(20)-Ti(1)-Cl(1)	79.0(4)
C(18)-Ti(1)-Cl(1)	119.4(5)
C(21)-Ti(1)-Cl(1)	105.5(5)
O(6)-Ti(1)-C(24)	123.7(3)
C(22)-Ti(1)-C(24)	56.8(4)
C(19)-Ti(1)-C(24)	105.2(5)
C(25)-Ti(1)-C(24)	34.4(3)
C(17)-Ti(1)-C(24)	133.2(5)
C(23)-Ti(1)-C(24)	34.0(3)
C(26)-Ti(1)-C(24)	57.6(4)
C(20)-Ti(1)-C(24)	134.7(5)
C(18)-Ti(1)-C(24)	105.0(4)
C(21)-Ti(1)-C(24)	158.9(4)
Cl(1)-Ti(1)-C(24)	78.0(3)
C(21)-C(17)-C(18)	109.1(16)
C(21)-C(17)-Ti(1)	75.4(8)
C(18)-C(17)-Ti(1)	74.3(6)
C(21)-C(17)-H(17)	125.5
C(18)-C(17)-H(17)	125.5
Ti(1)-C(17)-H(17)	116.8
C(17)-C(18)-C(19)	105.3(13)
C(17)-C(18)-Ti(1)	71.7(6)
C(19)-C(18)-Ti(1)	71.0(7)
C(17)-C(18)-H(18)	127.3
C(19)-C(18)-H(18)	127.3
Ti(1)-C(18)-H(18)	121.8
C(20)-C(19)-C(18)	105.6(13)
C(20)-C(19)-Ti(1)	74.3(8)

C(18)-C(19)-Ti(1)	74.1(8)	C(22)-C(23)-Ti(1)	71.5(6)
C(20)-C(19)-H(19)	127.2	C(24)-C(23)-Ti(1)	74.5(6)
C(18)-C(19)-H(19)	127.2	C(22)-C(23)-H(23)	125.8
Ti(1)-C(19)-H(19)	116.7	C(24)-C(23)-H(23)	125.8
C(21)-C(20)-C(19)	108.9(14)	Ti(1)-C(23)-H(23)	119.9
C(21)-C(20)-Ti(1)	74.3(8)	C(23)-C(24)-C(25)	105.8(10)
C(19)-C(20)-Ti(1)	71.6(8)	C(23)-C(24)-Ti(1)	71.5(6)
C(21)-C(20)-H(20)	125.6	C(25)-C(24)-Ti(1)	71.0(6)
C(19)-C(20)-H(20)	125.6	C(23)-C(24)-H(24)	127.1
Ti(1)-C(20)-H(20)	120.2	C(25)-C(24)-H(24)	127.1
C(20)-C(21)-C(17)	110.9(14)	Ti(1)-C(24)-H(24)	122.2
C(20)-C(21)-Ti(1)	73.8(9)	C(26)-C(25)-C(24)	110.7(10)
C(17)-C(21)-Ti(1)	72.5(7)	C(26)-C(25)-Ti(1)	73.8(6)
C(20)-C(21)-H(21)	124.5	C(24)-C(25)-Ti(1)	74.6(6)
C(17)-C(21)-H(21)	124.5	C(26)-C(25)-H(25)	124.6
Ti(1)-C(21)-H(21)	120.8	C(24)-C(25)-H(25)	124.6
C(23)-C(22)-C(26)	110.0(11)	Ti(1)-C(25)-H(25)	118.6
C(23)-C(22)-Ti(1)	74.2(7)	C(25)-C(26)-C(22)	105.2(11)
C(26)-C(22)-Ti(1)	74.6(6)	C(25)-C(26)-Ti(1)	72.1(6)
C(23)-C(22)-H(22)	125.0	C(22)-C(26)-Ti(1)	70.9(6)
C(26)-C(22)-H(22)	125.0	C(25)-C(26)-H(26)	127.4
Ti(1)-C(22)-H(22)	118.0	C(22)-C(26)-H(26)	127.4
C(22)-C(23)-C(24)	108.3(10)	Ti(1)-C(26)-H(26)	121.5

Symmetry transformations used to generate equivalent atoms:

Table 4. Anisotropic displacement parameters ($Å^2$x 10^3)for Complex **6**. The anisotropic displacement factor exponent takes the form: $-2p^2[h^2a^{*2}U^{11} + ... + 2 h k a^* b^* U^{12}]$

	U^{11}	U^{22}	U^{33}	U^{23}	U^{13}	U^{12}
W(1)	37(1)	31(1)	42(1)	-6(1)	-1(1)	4(1)
C(1)	50(7)	50(8)	56(8)	-6(7)	-10(6)	7(6)
O(1)	105(8)	65(7)	98(8)	-46(6)	-5(6)	42(6)
C(2)	45(5)	32(5)	61(7)	1(8)	-8(10)	13(4)
O(2)	45(4)	49(4)	90(6)	-4(6)	-8(6)	-9(3)
C(3)	58(8)	37(7)	46(7)	11(6)	1(6)	5(5)
O(3)	100(8)	66(7)	84(8)	13(6)	-1(6)	9(6)
C(4)	38(5)	66(7)	71(7)	-32(12)	3(9)	2(5)
O(4)	47(5)	134(10)	188(12)	-80(14)	5(10)	-9(5)
C(5)	44(7)	49(8)	61(8)	-11(7)	2(6)	-6(5)
O(5)	121(10)	83(9)	44(6)	26(6)	2(5)	-12(6)
C(6)	39(6)	25(5)	33(5)	6(4)	9(4)	-3(5)
O(6)	33(4)	31(4)	42(4)	-3(3)	-7(3)	7(3)
Fe(1)	42(1)	32(1)	41(1)	-1(1)	-7(1)	0(1)
C(7)	37(6)	34(6)	34(6)	2(5)	-1(4)	1(4)
C(8)	42(6)	47(7)	39(6)	-5(5)	-1(5)	2(5)
C(9)	66(8)	53(7)	45(7)	-18(6)	-1(6)	1(6)
C(10)	75(9)	66(9)	21(6)	0(5)	-9(5)	4(7)
C(11)	55(7)	40(7)	41(7)	0(5)	-14(5)	1(5)
C(12)	47(7)	53(8)	66(9)	-1(7)	-12(6)	-15(6)
C(13)	43(7)	48(8)	71(8)	-3(7)	1(6)	-1(6)
C(14)	68(8)	56(8)	51(7)	2(6)	4(6)	-14(6)
C(15)	56(8)	57(9)	80(10)	26(7)	-24(7)	-13(6)
C(16)	52(7)	26(6)	90(10)	-2(7)	-15(7)	2(5)
Ti(1)	35(1)	24(1)	35(1)	1(1)	-3(1)	2(1)
Cl(1)	57(2)	35(2)	40(1)	-11(1)	-6(1)	-3(1)
C(17)	113(11)	47(7)	50(7)	7(11)	-5(13)	-44(7)
C(18)	72(9)	12(5)	165(19)	26(8)	44(10)	7(6)
C(19)	113(14)	38(8)	110(14)	42(9)	-53(11)	-43(9)
C(20)	106(12)	47(8)	53(8)	18(7)	13(9)	-2(8)
C(21)	48(8)	59(9)	102(12)	56(9)	15(8)	10(6)
C(22)	49(7)	46(7)	60(8)	-12(6)	11(6)	-3(5)

C(23)	28(5)	45(7)	79(8)	9(6)	9(5)	5(5)
C(24)	41(5)	44(6)	56(9)	8(6)	-5(5)	-9(4)
C(25)	50(6)	24(6)	57(7)	0(5)	4(5)	-10(5)
C(26)	61(7)	47(7)	40(6)	10(6)	9(5)	-5(6)

Table 5. Hydrogen coordinates (x 10^4) and isotropic displacement parameters ($Å^2$x 10^3) for Complex **6**.

	x	y	z	U(eq)
H(8)	1736	5544	8241	51
H(9)	1122	5194	6381	66
H(10)	414	7093	6254	65
H(11)	567	8547	8033	55
H(12)	-497	5323	7776	66
H(13)	-401	6804	9589	65
H(14)	399	5983	10907	70
H(15)	755	3826	9972	77
H(16)	226	3458	7976	67
H(17)	1966	3959	9998	84
H(18)	2919	3483	10955	99
H(19)	2931	4784	12968	105
H(20)	1943	5712	13214	83
H(21)	1394	5176	11430	84
H(22)	2958	4909	8738	62
H(23)	3658	5001	10439	61
H(24)	3755	7369	11107	56
H(25)	3076	8688	9804	52
H(26)	2613	7206	8268	59

Table 6. Torsion angles [°] for Complex **6**.

C(4)-W(1)-C(6)-O(6)	-132.0(9)
C(3)-W(1)-C(6)-O(6)	139.9(8)
C(2)-W(1)-C(6)-O(6)	51.4(9)
C(5)-W(1)-C(6)-O(6)	-45.0(7)
C(4)-W(1)-C(6)-C(7)	48.1(10)
C(3)-W(1)-C(6)-C(7)	-39.9(9)
C(2)-W(1)-C(6)-C(7)	-128.5(10)
C(5)-W(1)-C(6)-C(7)	135.1(9)
O(6)-C(6)-C(7)-C(8)	2.6(15)
W(1)-C(6)-C(7)-C(8)	-177.5(8)
O(6)-C(6)-C(7)-C(11)	179.1(9)
W(1)-C(6)-C(7)-C(11)	-1.0(15)
C(11)-C(7)-C(8)-C(9)	0.0(12)
C(6)-C(7)-C(8)-C(9)	177.1(10)
C(7)-C(8)-C(9)-C(10)	0.6(13)
C(8)-C(9)-C(10)-C(11)	-1.0(14)
C(9)-C(10)-C(11)-C(7)	1.0(14)
C(8)-C(7)-C(11)-C(10)	-0.6(12)
C(6)-C(7)-C(11)-C(10)	-177.7(10)
C(16)-C(12)-C(13)-C(14)	1.4(15)
C(12)-C(13)-C(14)-C(15)	-2.7(14)
C(13)-C(14)-C(15)-C(16)	3.0(15)
C(14)-C(15)-C(16)-C(12)	-2.1(16)
C(21)-C(17)-C(18)-C(19)	-4.5(14)
C(17)-C(18)-C(19)-C(20)	4.2(13)
C(18)-C(19)-C(20)-C(21)	-2.5(15)
C(19)-C(20)-C(21)-C(17)	-0.3(16)
C(18)-C(17)-C(21)-C(20)	3.1(16)
C(26)-C(22)-C(23)-C(24)	0.6(13)
C(22)-C(23)-C(24)-C(25)	0.9(12)
C(23)-C(24)-C(25)-C(26)	-2.1(12)
C(24)-C(25)-C(26)-C(22)	2.5(12)
C(23)-C(22)-C(26)-C(25)	-1.9(13)

Appendix 4

Crystallographic data of Complex 8

Table 1. Crystal data and structure refinement for Complex **8**.

Identification code	db52a3n_abs	
Empirical formula	$C_{32} H_{18} Cr_2 Fe O_{12} Ti$	
Formula weight	802.21	
Temperature	293(2) K	
Wavelength	0.71073 Å	
Crystal system	Monoclinic	
Space group	$P\ 2_1/c$	
Unit cell dimensions	a = 9.9813(4) Å	a= 90°.
	b = 15.8650(7) Å	b= 101.723(1)°.
	c = 20.1457(9) Å	g = 90°.
Volume	3123.6(2) $Å^3$	
Z	4	
Density (calculated)	1.706 Mg/m^3	
Absorption coefficient	1.444 mm^{-1}	
F(000)	1608	
Crystal size	0.42 x 0.12 x 0.12 mm^3	
Theta range for data collection	2.43 to 26.53°.	
Index ranges	-4<=h<=12, -17<=k<=19, -24<=l<=25	
Reflections collected	16699	
Independent reflections	5958 [R(int) = 0.0290]	
Completeness to theta = 25.00°	99.8 %	
Absorption correction	Semi-empirical from equivalents	
Max. and min. transmission	0.841 and 0.725	
Refinement method	Full-matrix least-squares on F^2	
Data / restraints / parameters	5958 / 0 / 433	
Goodness-of-fit on F^2	1.076	
Final R indices [$I>2\sigma(I)$]	R1 = 0.0314, wR2 = 0.0824	
R indices (all data)	R1 = 0.0409, wR2 = 0.0911	
Extinction coefficient	0	
Largest diff. peak and hole	0.407 and -0.286 e.$Å^{-3}$	

Table 2. Atomic coordinates (x 10^4) and equivalent isotropic displacement parameters (Å^{2}x 10^3) for Complex **8**. U(eq) is defined as one third of the trace of the orthogonalized U^{ij} tensor.

	x	y	z	U(eq)
Cr(1)	-244(1)	5514(1)	3626(1)	39(1)
C(1)	-1290(3)	6024(2)	4194(1)	58(1)
O(1)	-1921(2)	6339(2)	4539(1)	91(1)
C(2)	-1865(2)	5526(1)	2939(1)	42(1)
O(2)	-2876(2)	5529(1)	2559(1)	56(1)
C(3)	411(3)	6552(2)	3369(1)	55(1)
O(3)	877(3)	7165(2)	3229(1)	96(1)
C(4)	1247(3)	5528(2)	4366(1)	55(1)
O(4)	2093(2)	5566(2)	4841(1)	91(1)
C(5)	-607(2)	4393(2)	3862(1)	47(1)
O(5)	-759(2)	3706(1)	3994(1)	68(1)
C(6)	826(2)	4957(1)	2967(1)	35(1)
O(6)	1881(1)	4499(1)	3166(1)	39(1)
Cr(2)	5224(1)	3626(1)	1256(1)	37(1)
C(7)	6273(3)	3115(2)	695(1)	57(1)
O(7)	6929(3)	2805(2)	362(1)	93(1)
C(8)	6753(2)	3639(2)	1986(1)	45(1)
O(8)	7667(2)	3607(1)	2427(1)	69(1)
C(9)	4813(3)	2546(2)	1543(1)	49(1)
O(9)	4616(3)	1868(1)	1683(1)	79(1)
C(10)	3575(3)	3535(2)	607(1)	50(1)
O(10)	2553(2)	3441(2)	239(1)	79(1)
C(11)	5754(2)	4678(2)	924(1)	47(1)
O(11)	6116(2)	5281(1)	714(1)	72(1)
C(12)	4119(2)	4276(1)	1862(1)	35(1)
O(12)	3952(1)	4006(1)	2435(1)	39(1)
Fe(1)	1515(1)	5426(1)	1565(1)	38(1)
C(13)	378(2)	4998(2)	2221(1)	39(1)
C(14)	-312(2)	5688(2)	1828(1)	49(1)
C(15)	-548(3)	5475(2)	1139(1)	58(1)
C(16)	-29(3)	4657(2)	1078(1)	56(1)
C(17)	544(2)	4362(2)	1739(1)	44(1)

C(18)	3529(2)	5124(1)	1687(1)	39(1)
C(19)	3308(2)	5768(1)	2158(1)	43(1)
C(20)	2711(3)	6479(2)	1785(2)	56(1)
C(21)	2538(3)	6290(2)	1088(2)	59(1)
C(22)	3036(2)	5472(2)	1020(1)	51(1)
Ti(1)	3454(1)	3743(1)	3300(1)	31(1)
C(23)	4393(3)	4893(2)	4005(2)	68(1)
C(24)	4335(4)	4198(3)	4403(1)	97(2)
C(25)	5289(5)	3611(3)	4236(3)	120(2)
C(26)	5816(3)	3980(3)	3726(2)	83(1)
C(27)	5269(3)	4751(2)	3613(2)	64(1)
C(28)	2063(3)	2720(2)	3711(1)	58(1)
C(29)	3337(3)	2353(2)	3749(2)	65(1)
C(30)	3610(3)	2287(2)	3100(2)	59(1)
C(31)	2435(3)	2576(2)	2644(1)	49(1)
C(32)	1492(2)	2834(2)	3022(1)	50(1)

Table 3. Bond lengths [Å] and angles [°] for Complex **8**.

Cr(1)-C(4)	1.881(3)	Fe(1)-C(20)	2.049(3)
Cr(1)-C(1)	1.882(3)	Fe(1)-C(16)	2.052(3)
Cr(1)-C(3)	1.883(3)	Fe(1)-C(21)	2.059(2)
Cr(1)-C(5)	1.895(3)	Fe(1)-C(15)	2.065(2)
Cr(1)-C(2)	1.904(2)	C(13)-C(17)	1.432(3)
Cr(1)-C(6)	2.063(2)	C(13)-C(14)	1.443(3)
C(1)-O(1)	1.144(3)	C(14)-C(15)	1.400(4)
C(2)-O(2)	1.136(3)	C(14)-H(14)	0.9300
C(3)-O(3)	1.137(3)	C(15)-C(16)	1.411(4)
C(4)-O(4)	1.141(3)	C(15)-H(15)	0.9300
C(5)-O(5)	1.139(3)	C(16)-C(17)	1.417(3)
C(6)-O(6)	1.276(2)	C(16)-H(16)	0.9300
C(6)-C(13)	1.480(3)	C(17)-H(17)	0.9300
O(6)-Ti(1)	1.9507(14)	C(18)-C(19)	1.442(3)
Cr(2)-C(7)	1.873(3)	C(18)-C(22)	1.444(3)
Cr(2)-C(9)	1.880(3)	C(19)-C(20)	1.419(3)
Cr(2)-C(10)	1.888(3)	C(19)-H(19)	0.9300
Cr(2)-C(8)	1.893(2)	C(20)-C(21)	1.411(4)
Cr(2)-C(11)	1.912(3)	C(20)-H(20)	0.9300
Cr(2)-C(12)	2.077(2)	C(21)-C(22)	1.406(4)
C(7)-O(7)	1.141(3)	C(21)-H(21)	0.9300
C(8)-O(8)	1.137(3)	C(22)-H(22)	0.9300
C(9)-O(9)	1.139(3)	Ti(1)-C(24)	2.330(3)
C(10)-O(10)	1.143(3)	Ti(1)-C(25)	2.355(3)
C(11)-O(11)	1.135(3)	Ti(1)-C(30)	2.356(2)
C(12)-O(12)	1.274(2)	Ti(1)-C(26)	2.369(3)
C(12)-C(18)	1.483(3)	Ti(1)-C(31)	2.380(2)
O(12)-Ti(1)	1.9514(15)	Ti(1)-C(23)	2.383(3)
Fe(1)-C(17)	2.014(2)	Ti(1)-C(28)	2.390(2)
Fe(1)-C(19)	2.014(2)	Ti(1)-C(29)	2.396(3)
Fe(1)-C(13)	2.027(2)	Ti(1)-C(27)	2.403(3)
Fe(1)-C(18)	2.032(2)	Ti(1)-C(32)	2.405(2)
Fe(1)-C(14)	2.043(2)	C(23)-C(27)	1.311(4)
Fe(1)-C(22)	2.047(2)	C(23)-C(24)	1.372(5)

C(23)-H(23)	0.9300
C(24)-C(25)	1.421(6)
C(24)-H(24)	0.9300
C(25)-C(26)	1.376(6)
C(25)-H(25)	0.9300
C(26)-C(27)	1.341(5)
C(26)-H(26)	0.9300
C(27)-H(27)	0.9300
C(28)-C(29)	1.387(4)
C(28)-C(32)	1.400(4)
C(28)-H(28)	0.9300
C(29)-C(30)	1.393(4)
C(29)-H(29)	0.9300
C(30)-C(31)	1.411(4)
C(30)-H(30)	0.9300
C(31)-C(32)	1.388(4)
C(31)-H(31)	0.9300
C(32)-H(32)	0.9300
C(4)-Cr(1)-C(1)	87.70(12)
C(4)-Cr(1)-C(3)	86.81(12)
C(1)-Cr(1)-C(3)	93.27(13)
C(4)-Cr(1)-C(5)	88.48(12)
C(1)-Cr(1)-C(5)	95.34(12)
C(3)-Cr(1)-C(5)	170.01(11)
C(4)-Cr(1)-C(2)	174.26(10)
C(1)-Cr(1)-C(2)	86.69(11)
C(3)-Cr(1)-C(2)	94.75(10)
C(5)-Cr(1)-C(2)	90.80(10)
C(4)-Cr(1)-C(6)	94.97(10)
C(1)-Cr(1)-C(6)	177.32(10)
C(3)-Cr(1)-C(6)	86.78(11)
C(5)-Cr(1)-C(6)	84.86(9)
C(2)-Cr(1)-C(6)	90.63(9)
O(1)-C(1)-Cr(1)	179.5(3)
O(2)-C(2)-Cr(1)	175.9(2)

O(3)-C(3)-Cr(1)	176.3(3)
O(4)-C(4)-Cr(1)	175.2(2)
O(5)-C(5)-Cr(1)	176.2(2)
O(6)-C(6)-C(13)	113.81(18)
O(6)-C(6)-Cr(1)	122.91(15)
C(13)-C(6)-Cr(1)	123.12(14)
C(6)-O(6)-Ti(1)	169.76(15)
C(7)-Cr(2)-C(9)	88.55(12)
C(7)-Cr(2)-C(10)	93.72(12)
C(9)-Cr(2)-C(10)	85.97(11)
C(7)-Cr(2)-C(8)	90.70(11)
C(9)-Cr(2)-C(8)	87.89(10)
C(10)-Cr(2)-C(8)	172.34(11)
C(7)-Cr(2)-C(11)	86.44(12)
C(9)-Cr(2)-C(11)	174.94(11)
C(10)-Cr(2)-C(11)	95.05(10)
C(8)-Cr(2)-C(11)	91.47(10)
C(7)-Cr(2)-C(12)	175.84(11)
C(9)-Cr(2)-C(12)	95.55(10)
C(10)-Cr(2)-C(12)	87.28(10)
C(8)-Cr(2)-C(12)	88.75(9)
C(11)-Cr(2)-C(12)	89.45(9)
O(7)-C(7)-Cr(2)	178.9(3)
O(8)-C(8)-Cr(2)	176.7(2)
O(9)-C(9)-Cr(2)	175.0(2)
O(10)-C(10)-Cr(2)	175.7(2)
O(11)-C(11)-Cr(2)	176.6(2)
O(12)-C(12)-C(18)	113.66(18)
O(12)-C(12)-Cr(2)	123.29(15)
C(18)-C(12)-Cr(2)	122.93(15)
C(12)-O(12)-Ti(1)	170.09(14)
C(17)-Fe(1)-C(19)	121.56(9)
C(17)-Fe(1)-C(13)	41.52(9)
C(19)-Fe(1)-C(13)	104.52(9)
C(17)-Fe(1)-C(18)	106.29(9)
C(19)-Fe(1)-C(18)	41.76(9)

C(13)-Fe(1)-C(18)	120.86(9)	C(22)-Fe(1)-C(15)	124.20(11)
C(17)-Fe(1)-C(14)	68.81(10)	C(20)-Fe(1)-C(15)	123.18(11)
C(19)-Fe(1)-C(14)	121.55(10)	C(16)-Fe(1)-C(15)	40.08(11)
C(13)-Fe(1)-C(14)	41.52(9)	C(21)-Fe(1)-C(15)	109.20(11)
C(18)-Fe(1)-C(14)	158.40(9)	C(17)-C(13)-C(14)	105.8(2)
C(17)-Fe(1)-C(22)	124.01(10)	C(17)-C(13)-C(6)	127.2(2)
C(19)-Fe(1)-C(22)	69.07(10)	C(14)-C(13)-C(6)	127.0(2)
C(13)-Fe(1)-C(22)	159.41(9)	C(17)-C(13)-Fe(1)	68.76(13)
C(18)-Fe(1)-C(22)	41.46(9)	C(14)-C(13)-Fe(1)	69.86(13)
C(14)-Fe(1)-C(22)	158.46(9)	C(6)-C(13)-Fe(1)	125.68(15)
C(17)-Fe(1)-C(20)	157.84(11)	C(15)-C(14)-C(13)	109.0(2)
C(19)-Fe(1)-C(20)	40.86(10)	C(15)-C(14)-Fe(1)	70.94(14)
C(13)-Fe(1)-C(20)	120.74(11)	C(13)-C(14)-Fe(1)	68.62(12)
C(18)-Fe(1)-C(20)	69.38(10)	C(15)-C(14)-H(14)	125.5
C(14)-Fe(1)-C(20)	106.80(11)	C(13)-C(14)-H(14)	125.5
C(22)-Fe(1)-C(20)	67.93(11)	Fe(1)-C(14)-H(14)	126.5
C(17)-Fe(1)-C(16)	40.79(10)	C(14)-C(15)-C(16)	108.5(2)
C(19)-Fe(1)-C(16)	159.10(10)	C(14)-C(15)-Fe(1)	69.22(14)
C(13)-Fe(1)-C(16)	69.24(10)	C(16)-C(15)-Fe(1)	69.44(14)
C(18)-Fe(1)-C(16)	123.13(11)	C(14)-C(15)-H(15)	125.7
C(14)-Fe(1)-C(16)	67.72(11)	C(16)-C(15)-H(15)	125.7
C(22)-Fe(1)-C(16)	109.43(11)	Fe(1)-C(15)-H(15)	127.2
C(20)-Fe(1)-C(16)	159.44(11)	C(15)-C(16)-C(17)	107.9(2)
C(17)-Fe(1)-C(21)	160.31(11)	C(15)-C(16)-Fe(1)	70.48(15)
C(19)-Fe(1)-C(21)	68.47(11)	C(17)-C(16)-Fe(1)	68.16(13)
C(13)-Fe(1)-C(21)	157.48(11)	C(15)-C(16)-H(16)	126.0
C(18)-Fe(1)-C(21)	69.01(10)	C(17)-C(16)-H(16)	126.0
C(14)-Fe(1)-C(21)	122.59(10)	Fe(1)-C(16)-H(16)	126.9
C(22)-Fe(1)-C(21)	40.05(10)	C(16)-C(17)-C(13)	108.8(2)
C(20)-Fe(1)-C(21)	40.19(11)	C(16)-C(17)-Fe(1)	71.05(15)
C(16)-Fe(1)-C(21)	124.66(12)	C(13)-C(17)-Fe(1)	69.72(13)
C(17)-Fe(1)-C(15)	68.20(11)	C(16)-C(17)-H(17)	125.6
C(19)-Fe(1)-C(15)	157.97(11)	C(13)-C(17)-H(17)	125.6
C(13)-Fe(1)-C(15)	68.86(10)	Fe(1)-C(17)-H(17)	125.2
C(18)-Fe(1)-C(15)	159.68(11)	C(19)-C(18)-C(22)	105.9(2)
C(14)-Fe(1)-C(15)	39.84(10)	C(19)-C(18)-C(12)	126.4(2)

C(22)-C(18)-C(12)	127.7(2)
C(19)-C(18)-Fe(1)	68.47(12)
C(22)-C(18)-Fe(1)	69.85(13)
C(12)-C(18)-Fe(1)	125.33(15)
C(20)-C(19)-C(18)	108.6(2)
C(20)-C(19)-Fe(1)	70.89(15)
C(18)-C(19)-Fe(1)	69.78(13)
C(20)-C(19)-H(19)	125.7
C(18)-C(19)-H(19)	125.7
Fe(1)-C(19)-H(19)	125.2
C(21)-C(20)-C(19)	108.1(2)
C(21)-C(20)-Fe(1)	70.27(16)
C(19)-C(20)-Fe(1)	68.25(14)
C(21)-C(20)-H(20)	125.9
C(19)-C(20)-H(20)	125.9
Fe(1)-C(20)-H(20)	127.1
C(22)-C(21)-C(20)	108.6(2)
C(22)-C(21)-Fe(1)	69.54(14)
C(20)-C(21)-Fe(1)	69.54(14)
C(22)-C(21)-H(21)	125.7
C(20)-C(21)-H(21)	125.7
Fe(1)-C(21)-H(21)	126.8
C(21)-C(22)-C(18)	108.8(2)
C(21)-C(22)-Fe(1)	70.40(14)
C(18)-C(22)-Fe(1)	68.69(13)
C(21)-C(22)-H(22)	125.6
C(18)-C(22)-H(22)	125.6
Fe(1)-C(22)-H(22)	126.9
O(6)-Ti(1)-O(12)	95.07(6)
O(6)-Ti(1)-C(24)	94.54(14)
O(12)-Ti(1)-C(24)	132.04(10)
O(6)-Ti(1)-C(25)	129.73(17)
O(12)-Ti(1)-C(25)	115.83(18)
C(24)-Ti(1)-C(25)	35.29(16)
O(6)-Ti(1)-C(30)	131.19(8)
O(12)-Ti(1)-C(30)	91.09(9)
C(24)-Ti(1)-C(30)	116.19(16)
C(25)-Ti(1)-C(30)	88.96(13)
O(6)-Ti(1)-C(26)	131.79(11)
O(12)-Ti(1)-C(26)	82.78(12)
C(24)-Ti(1)-C(26)	56.70(13)
C(25)-Ti(1)-C(26)	33.86(15)
C(30)-Ti(1)-C(26)	97.02(12)
O(6)-Ti(1)-C(31)	99.22(8)
O(12)-Ti(1)-C(31)	80.08(8)
C(24)-Ti(1)-C(31)	143.70(13)
C(25)-Ti(1)-C(31)	123.37(12)
C(30)-Ti(1)-C(31)	34.67(9)
C(26)-Ti(1)-C(31)	127.31(11)
O(6)-Ti(1)-C(23)	79.63(9)
O(12)-Ti(1)-C(23)	103.15(10)
C(24)-Ti(1)-C(23)	33.82(13)
C(25)-Ti(1)-C(23)	56.23(14)
C(30)-Ti(1)-C(23)	145.19(11)
C(26)-Ti(1)-C(23)	54.62(12)
C(31)-Ti(1)-C(23)	176.63(10)
O(6)-Ti(1)-C(28)	87.58(8)
O(12)-Ti(1)-C(28)	136.47(9)
C(24)-Ti(1)-C(28)	90.78(11)
C(25)-Ti(1)-C(28)	94.29(14)
C(30)-Ti(1)-C(28)	57.07(10)
C(26)-Ti(1)-C(28)	126.01(13)
C(31)-Ti(1)-C(28)	56.71(10)
C(23)-Ti(1)-C(28)	119.98(11)
O(6)-Ti(1)-C(29)	121.27(9)
O(12)-Ti(1)-C(29)	125.06(9)
C(24)-Ti(1)-C(29)	87.88(15)
C(25)-Ti(1)-C(29)	72.87(12)
C(30)-Ti(1)-C(29)	34.07(11)
C(26)-Ti(1)-C(29)	97.51(14)
C(31)-Ti(1)-C(29)	56.31(10)
C(23)-Ti(1)-C(29)	121.57(12)

C(28)-Ti(1)-C(29)	33.69(10)	C(24)-C(25)-Ti(1)	71.39(17)
O(6)-Ti(1)-C(27)	99.76(9)	C(26)-C(25)-H(25)	127.1
O(12)-Ti(1)-C(27)	77.10(9)	C(24)-C(25)-H(25)	127.1
C(24)-Ti(1)-C(27)	54.97(11)	Ti(1)-C(25)-H(25)	119.9
C(25)-Ti(1)-C(27)	55.07(13)	C(27)-C(26)-C(25)	108.2(4)
C(30)-Ti(1)-C(27)	128.71(11)	C(27)-C(26)-Ti(1)	75.07(15)
C(26)-Ti(1)-C(27)	32.63(12)	C(25)-C(26)-Ti(1)	72.51(19)
C(31)-Ti(1)-C(27)	151.39(10)	C(27)-C(26)-H(26)	125.9
C(23)-Ti(1)-C(27)	31.79(10)	C(25)-C(26)-H(26)	125.9
C(28)-Ti(1)-C(27)	145.24(10)	Ti(1)-C(26)-H(26)	118.4
C(29)-Ti(1)-C(27)	127.31(11)	C(23)-C(27)-C(26)	110.6(3)
O(6)-Ti(1)-C(32)	75.04(8)	C(23)-C(27)-Ti(1)	73.29(16)
O(12)-Ti(1)-C(32)	105.25(8)	C(26)-C(27)-Ti(1)	72.30(17)
C(24)-Ti(1)-C(32)	122.62(10)	C(23)-C(27)-H(27)	124.7
C(25)-Ti(1)-C(32)	126.66(13)	C(26)-C(27)-H(27)	124.7
C(30)-Ti(1)-C(32)	56.70(9)	Ti(1)-C(27)-H(27)	121.3
C(26)-Ti(1)-C(32)	152.00(13)	C(29)-C(28)-C(32)	107.1(3)
C(31)-Ti(1)-C(32)	33.72(9)	C(29)-C(28)-Ti(1)	73.37(15)
C(23)-Ti(1)-C(32)	143.20(10)	C(32)-C(28)-Ti(1)	73.60(14)
C(28)-Ti(1)-C(32)	33.95(9)	C(29)-C(28)-H(28)	126.5
C(29)-Ti(1)-C(32)	55.67(9)	C(32)-C(28)-H(28)	126.5
C(27)-Ti(1)-C(32)	174.37(10)	Ti(1)-C(28)-H(28)	118.6
C(27)-C(23)-C(24)	109.1(3)	C(28)-C(29)-C(30)	109.3(3)
C(27)-C(23)-Ti(1)	74.92(17)	C(28)-C(29)-Ti(1)	72.94(15)
C(24)-C(23)-Ti(1)	70.96(17)	C(30)-C(29)-Ti(1)	71.41(14)
C(27)-C(23)-H(23)	125.5	C(28)-C(29)-H(29)	125.3
C(24)-C(23)-H(23)	125.5	C(30)-C(29)-H(29)	125.3
Ti(1)-C(23)-H(23)	120.3	Ti(1)-C(29)-H(29)	122.0
C(23)-C(24)-C(25)	106.2(3)	C(29)-C(30)-C(31)	107.0(3)
C(23)-C(24)-Ti(1)	75.22(17)	C(29)-C(30)-Ti(1)	74.52(15)
C(25)-C(24)-Ti(1)	73.31(19)	C(31)-C(30)-Ti(1)	73.58(14)
C(23)-C(24)-H(24)	126.9	C(29)-C(30)-H(30)	126.5
C(25)-C(24)-H(24)	126.9	C(31)-C(30)-H(30)	126.5
Ti(1)-C(24)-H(24)	116.8	Ti(1)-C(30)-H(30)	117.5
C(26)-C(25)-C(24)	105.9(3)	C(32)-C(31)-C(30)	107.8(2)
C(26)-C(25)-Ti(1)	73.63(17)	C(32)-C(31)-Ti(1)	74.13(14)

C(30)-C(31)-Ti(1)	71.75(14)	C(31)-C(32)-Ti(1)	72.14(13)
C(32)-C(31)-H(31)	126.1	C(28)-C(32)-Ti(1)	72.45(14)
C(30)-C(31)-H(31)	126.1	C(31)-C(32)-H(32)	125.7
Ti(1)-C(31)-H(31)	119.8	C(28)-C(32)-H(32)	125.7
C(31)-C(32)-C(28)	108.7(2)	Ti(1)-C(32)-H(32)	121.4

Symmetry transformations used to generate equivalent atoms:

Table 4. Anisotropic displacement parameters ($Å^2$x 10^3)for Complex **8**. The anisotropic displacement factor exponent takes the form: $-2p^2[h^2a^{*2}U^{11} + ... + 2 h k a^* b^* U^{12}]$

	U^{11}	U^{22}	U^{33}	U^{23}	U^{13}	U^{12}
Cr(1)	36(1)	44(1)	39(1)	-1(1)	11(1)	2(1)
C(1)	56(2)	67(2)	53(2)	-3(1)	16(1)	9(1)
O(1)	90(2)	109(2)	83(2)	-17(1)	43(1)	30(1)
C(2)	40(1)	39(1)	49(1)	2(1)	16(1)	2(1)
O(2)	42(1)	57(1)	65(1)	8(1)	3(1)	2(1)
C(3)	52(1)	50(2)	58(2)	1(1)	1(1)	-5(1)
O(3)	102(2)	71(2)	101(2)	21(1)	-15(2)	-35(1)
C(4)	48(1)	74(2)	45(2)	-7(1)	15(1)	3(1)
O(4)	62(1)	153(2)	51(1)	-16(1)	-3(1)	1(1)
C(5)	40(1)	59(2)	44(1)	4(1)	14(1)	4(1)
O(5)	70(1)	59(1)	77(1)	17(1)	23(1)	1(1)
C(6)	30(1)	34(1)	40(1)	3(1)	9(1)	-2(1)
O(6)	34(1)	42(1)	41(1)	6(1)	7(1)	4(1)
Cr(2)	40(1)	41(1)	31(1)	-1(1)	8(1)	1(1)
C(7)	67(2)	62(2)	45(1)	-8(1)	17(1)	4(1)
O(7)	108(2)	110(2)	73(2)	-24(1)	47(1)	18(2)
C(8)	47(1)	42(1)	45(1)	-6(1)	11(1)	5(1)
O(8)	62(1)	69(1)	63(1)	-9(1)	-16(1)	11(1)
C(9)	54(1)	47(2)	43(1)	-2(1)	7(1)	3(1)
O(9)	104(2)	45(1)	86(2)	9(1)	16(1)	-2(1)
C(10)	62(2)	48(1)	38(1)	5(1)	4(1)	-2(1)
O(10)	73(1)	84(2)	64(1)	6(1)	-21(1)	-15(1)
C(11)	42(1)	54(2)	45(1)	4(1)	11(1)	1(1)
O(11)	66(1)	70(1)	81(2)	23(1)	21(1)	-12(1)
C(12)	30(1)	41(1)	31(1)	2(1)	4(1)	-5(1)
O(12)	39(1)	45(1)	33(1)	7(1)	10(1)	3(1)
Fe(1)	37(1)	42(1)	34(1)	8(1)	8(1)	6(1)
C(13)	31(1)	47(1)	38(1)	6(1)	8(1)	3(1)
C(14)	40(1)	61(2)	48(1)	13(1)	12(1)	16(1)
C(15)	42(1)	81(2)	46(2)	16(1)	0(1)	14(1)
C(16)	48(1)	76(2)	39(1)	-3(1)	-2(1)	-7(1)
C(17)	42(1)	47(1)	40(1)	0(1)	5(1)	-5(1)

C(18)	36(1)	43(1)	41(1)	7(1)	14(1)	1(1)
C(19)	40(1)	39(1)	49(1)	2(1)	8(1)	-4(1)
C(20)	60(2)	35(1)	77(2)	7(1)	22(1)	0(1)
C(21)	64(2)	53(2)	65(2)	30(1)	25(1)	9(1)
C(22)	52(1)	61(2)	44(1)	17(1)	19(1)	10(1)
Ti(1)	31(1)	34(1)	28(1)	3(1)	5(1)	1(1)
C(23)	54(2)	75(2)	73(2)	-31(2)	7(1)	-16(1)
C(24)	89(2)	173(4)	26(1)	-14(2)	6(2)	-70(3)
C(25)	129(4)	77(3)	106(3)	36(2)	-87(3)	-26(2)
C(26)	35(1)	117(3)	86(2)	-32(2)	-14(2)	9(2)
C(27)	42(1)	83(2)	61(2)	-2(2)	-3(1)	-23(1)
C(28)	65(2)	53(2)	59(2)	13(1)	22(1)	-12(1)
C(29)	77(2)	46(2)	66(2)	25(1)	0(2)	-4(1)
C(30)	59(2)	33(1)	83(2)	0(1)	14(1)	6(1)
C(31)	56(1)	35(1)	53(2)	-5(1)	7(1)	-8(1)
C(32)	44(1)	41(1)	65(2)	2(1)	8(1)	-12(1)

Table 5. Hydrogen coordinates (x 10^4) and isotropic displacement parameters ($Å^2$x 10^3) for Complex **8**.

	x	y	z	U(eq)
H(14)	-560	6194	2003	59
H(15)	-976	5814	782	69
H(16)	-58	4364	676	67
H(17)	959	3840	1843	52
H(19)	3521	5724	2628	52
H(20)	2475	6983	1967	67
H(21)	2157	6646	733	71
H(22)	3047	5200	612	61
H(23)	3892	5386	4012	82
H(24)	3782	4125	4718	116
H(25)	5512	3084	4431	144
H(26)	6443	3737	3500	100
H(27)	5482	5133	3300	77
H(28)	1663	2864	4074	69
H(29)	3919	2178	4146	78
H(30)	4413	2089	2988	70
H(31)	2315	2591	2174	59
H(32)	624	3048	2847	60

Table 6. Torsion angles [°] for Complex **8**.

C(4)-Cr(1)-C(6)-O(6)	24.79(19)	C(19)-C(20)-C(21)-C(22)	-0.8(3)
C(3)-Cr(1)-C(6)-O(6)	111.30(18)	C(20)-C(21)-C(22)-C(18)	0.6(3)
C(5)-Cr(1)-C(6)-O(6)	-63.23(18)	C(19)-C(18)-C(22)-C(21)	-0.2(3)
C(2)-Cr(1)-C(6)-O(6)	-153.98(18)	C(12)-C(18)-C(22)-C(21)	178.8(2)
C(4)-Cr(1)-C(6)-C(13)	-160.13(18)	C(27)-C(23)-C(24)-C(25)	1.5(3)
C(3)-Cr(1)-C(6)-C(13)	-73.62(18)	C(23)-C(24)-C(25)-C(26)	-2.5(3)
C(5)-Cr(1)-C(6)-C(13)	111.85(18)	C(24)-C(25)-C(26)-C(27)	2.6(4)
C(2)-Cr(1)-C(6)-C(13)	21.10(18)	C(24)-C(23)-C(27)-C(26)	0.1(3)
C(9)-Cr(2)-C(12)-O(12)	30.81(18)	C(25)-C(26)-C(27)-C(23)	-1.8(3)
C(10)-Cr(2)-C(12)-O(12)	116.49(18)	C(32)-C(28)-C(29)-C(30)	3.9(3)
C(8)-Cr(2)-C(12)-O(12)	-56.94(18)	C(28)-C(29)-C(30)-C(31)	-3.5(3)
C(11)-Cr(2)-C(12)-O(12)	-148.42(17)	C(29)-C(30)-C(31)-C(32)	1.7(3)
C(9)-Cr(2)-C(12)-C(18)	-153.40(17)	C(30)-C(31)-C(32)-C(28)	0.7(3)
C(10)-Cr(2)-C(12)-C(18)	-67.72(18)	C(29)-C(28)-C(32)-C(31)	-2.8(3)
C(8)-Cr(2)-C(12)-C(18)	118.84(18)		
C(11)-Cr(2)-C(12)-C(18)	27.36(18)		
O(6)-C(6)-C(13)-C(17)	29.5(3)		
Cr(1)-C(6)-C(13)-C(17)	-145.97(19)		
O(6)-C(6)-C(13)-C(14)	-150.2(2)		
Cr(1)-C(6)-C(13)-C(14)	34.3(3)		
C(17)-C(13)-C(14)-C(15)	-0.1(3)		
C(6)-C(13)-C(14)-C(15)	179.7(2)		
C(13)-C(14)-C(15)-C(16)	0.2(3)		
C(14)-C(15)-C(16)-C(17)	-0.3(3)		
C(15)-C(16)-C(17)-C(13)	0.3(3)		
C(14)-C(13)-C(17)-C(16)	-0.1(3)		
C(6)-C(13)-C(17)-C(16)	-179.9(2)		
O(12)-C(12)-C(18)-C(19)	25.9(3)		
Cr(2)-C(12)-C(18)-C(19)	-150.22(18)		
O(12)-C(12)-C(18)-C(22)	-152.8(2)		
Cr(2)-C(12)-C(18)-C(22)	31.0(3)		
C(22)-C(18)-C(19)-C(20)	-0.3(3)		
C(12)-C(18)-C(19)-C(20)	-179.3(2)		
C(18)-C(19)-C(20)-C(21)	0.7(3)		

Table 7. Selected least-squares planes and deviations from the planes (Åx10^4) for Complex **8**.

Plane 1 $5.711(6)\ x + 13.012(7)\ y - 2.240(19)\ z = 6.230(5)$

Atoms forming the Plane*	Cr(1)	C(6)	O(6)	C(13)	rms	[Ti(1)]
Deviations	-72(4)	270(16)	-106(6)	-92(6)	156	[-1265(29)]

Plane 2 $7.670\ (3)\ x + 6.946(15)\ y + 6.060(14)\ z = 7.280\ (3)$

Atoms forming the Plane*	Cr(2)	C(12)	O(12)	C(18)	rms	[Ti(1)]
Deviations	61(4)	-231(16)	92(6)	78(5)	134	[-309(29)]

Plane 3 $9.151\ (5)\ x + 6.243\ (20)\ y - 5.085(34)\ z = 2.336\ (14)$

Atoms forming the Plane*	C(13)	C(14)	C(15)	C(16)	C(17)	rms	[C(6)]
Deviations	4(17)	-2(9)	-2(9)	2(11)	-2(11)	3	[55(46)]

Plane 4 $9.267(5)\ x + 5.893\ (18)\ y - 3.786(25)\ z = 5.651(10)$

Atoms forming the Plane*	C(18)	C(19)	C(20)	C(21)	C(22)	rms	[C(12)]
Deviations	6(14)	-31(15)	45(16)	-41(16)	21(16)	32	[-189(37)]

Plane 5 $6.034\ (11)\ x + 6.159\ (22)\ y + 11.245\ (25)\ z = 10.164(6)$

Atoms forming the Plane*	C(23)	C(24)	C(25)	C(26)	C(27)	rms
Deviations	46(17)	-118(18)	148(19)	-127(19)	52(17)	106

Plane 6 $3.899(12)\ x + 14.573(8)\ y - 0.340(26)\ z = 4.601(8)$

Atoms forming the Plane*	C(28)	C(29)	C(30)	C(31)	C(32)	rms
Deviations	189(16)	-210(17)	147(16)	-30(15)	-97(15)	150

Dihedral angles between planes (º):

Planes 1 and 2: 36.76(9)
Planes 1 and 3: 32.12(11)
Planes 2 and 4: 28.78(9)
Planes 3 and 4: 4.21(12)
Planes 5 and 6: 50.58(13)

* rms = root mean square deviation from the plane;
atoms not involved in calculating the plane are shown in brackets [ ].

Appendix 5

Crystallographic data of Complex 12

Table 1. Crystal data and structure refinement for Complex **12**.

Identification code	db100f2_abs	
Empirical formula	$C_{20} H_{13} Cl Cr O_6 S Ti$	
Formula weight	516.71	
Temperature	293(2) K	
Wavelength	0.71073 Å	
Crystal system	Monoclinic	
Space group	$P 2_1/c$	
Unit cell dimensions	a = 10.7477(5) Å	a= 90°.
	b = 13.5857(7) Å	b= 104.0110(10)°.
	c = 14.9790(7) Å	g = 90°.
Volume	2122.09(18) Å^3	
Z	4	
Density (calculated)	1.617 Mg/m^3	
Absorption coefficient	1.147 mm^{-1}	
F(000)	1040	
Crystal size	0.32 x 0.22 x 0.20 mm^3	
Theta range for data collection	2.46 to 26.46°.	
Index ranges	-11<=h<=13, -15<=k<=16, -18<=l<=6	
Reflections collected	11215	
Independent reflections	4000 [R(int) = 0.0286]	
Completeness to θ = 25.00°	99.6 %	
Absorption correction	Semi-empirical from equivalents	
Max. and min. transmission	0.795 and 0.685	
Refinement method	Full-matrix least-squares on F^2	
Data / restraints / parameters	4000 / 0 / 293	
Goodness-of-fit on F^2	1.057	
Final R indices [I>2σ(I)]	R1 = 0.0351, wR2 = 0.0930	
R indices (all data)	R1 = 0.0399, wR2 = 0.0990	
Extinction coefficient	0	
Largest diff. peak and hole	0.365 and -0.276 e.Å^{-3}	

Table 2. Atomic coordinates (x 10^4) and equivalent isotropic displacement parameters ($Å^2$x 10^3) for Complex **12**. U(eq) is defined as one third of the trace of the orthogonalized U^{ij} tensor.

	x	y	z	U(eq)
Cr(1)	5107(1)	2680(1)	10332(1)	36(1)
C(1)	6353(2)	3333(2)	11220(2)	54(1)
O(1)	7140(2)	3736(2)	11750(2)	84(1)
C(2)	5950(2)	3047(2)	9424(2)	49(1)
O(2)	6472(2)	3262(2)	8872(2)	83(1)
C(3)	6141(2)	1545(2)	10596(2)	51(1)
O(3)	6845(2)	912(2)	10802(2)	83(1)
C(4)	4185(2)	2234(2)	11197(2)	47(1)
O(4)	3650(2)	1933(2)	11701(1)	74(1)
C(5)	4158(2)	3875(2)	10125(2)	41(1)
O(5)	3634(2)	4609(1)	10000(1)	59(1)
C(6)	3671(2)	2052(2)	9304(1)	34(1)
O(6)	2496(1)	2293(1)	9229(1)	39(1)
C(7)	3908(4)	1373(7)	8624(4)	38(1)
C(8)	5072(3)	980(7)	8520(6)	84(6)
C(9)	4862(5)	400(10)	7723(8)	64(2)
C(10)	3605(5)	355(9)	7208(7)	57(3)
S(1)	2615(3)	1032(3)	7714(2)	60(1)
C(7A)	3777(4)	1382(6)	8554(5)	38(1)
C(8A)	2832(3)	1059(7)	7790(5)	67(5)
C(9A)	3365(5)	405(9)	7261(6)	49(2)
C(10A)	4655(5)	198(8)	7598(5)	48(2)
S(1A)	5272(3)	835(3)	8596(2)	62(1)
Ti(1)	698(1)	2530(1)	9090(1)	34(1)
Cl(1)	932(1)	3485(1)	10449(1)	53(1)
C(11)	860(3)	796(2)	9347(3)	69(1)
C(12)	-211(3)	978(2)	8614(2)	63(1)
C(13)	-1105(3)	1475(2)	8958(2)	66(1)
C(14)	-611(3)	1631(2)	9874(2)	67(1)
C(15)	605(3)	1225(2)	10131(2)	63(1)
C(16)	1068(3)	3326(3)	7764(2)	87(1)
C(17)	-73(4)	2837(3)	7503(2)	70(1)

C(18)	-916(3)	3264(3)	7916(2)	66(1)
C(19)	-340(3)	4009(2)	8463(2)	71(1)
C(20)	925(4)	4067(2)	8392(3)	87(1)

Table 3. Bond lengths [Å] and angles [°] for Complex **12**.

Cr(1)-C(1)	1.866(3)	Ti(1)-C(20)	2.374(3)
Cr(1)-C(2)	1.876(2)	Ti(1)-Cl(1)	2.3753(7)
Cr(1)-C(3)	1.885(2)	Ti(1)-C(15)	2.378(2)
Cr(1)-C(5)	1.902(2)	Ti(1)-C(14)	2.378(2)
Cr(1)-C(4)	1.911(2)	Ti(1)-C(16)	2.378(3)
Cr(1)-C(6)	2.081(2)	Ti(1)-C(19)	2.379(3)
C(1)-O(1)	1.150(3)	Ti(1)-C(13)	2.380(3)
C(2)-O(2)	1.143(3)	Ti(1)-C(11)	2.386(2)
C(3)-O(3)	1.139(3)	C(11)-C(15)	1.396(4)
C(4)-O(4)	1.130(3)	C(11)-C(12)	1.406(4)
C(5)-O(5)	1.138(3)	C(11)-H(11)	0.9300
C(6)-O(6)	1.283(2)	C(12)-C(13)	1.373(4)
C(6)-C(7)	1.442(5)	C(12)-H(12)	0.9300
C(6)-C(7A)	1.472(5)	C(13)-C(14)	1.362(4)
O(6)-Ti(1)	1.9192(15)	C(13)-H(13)	0.9300
C(7)-C(8)	1.4034	C(14)-C(15)	1.384(4)
C(7)-S(1)	1.7571	C(14)-H(14)	0.9300
C(8)-C(9)	1.4021	C(15)-H(15)	0.9300
C(8)-H(8)	0.9300	C(16)-C(17)	1.366(5)
C(9)-C(10)	1.3852	C(16)-C(20)	1.411(5)
C(9)-H(9)	0.9300	C(16)-H(16)	0.9300
C(10)-S(1)	1.7155	C(17)-C(18)	1.346(4)
C(10)-H(10)	0.9300	C(17)-H(17)	0.9300
C(7A)-C(8A)	1.4034	C(18)-C(19)	1.354(5)
C(7A)-S(1A)	1.7571	C(18)-H(18)	0.9300
C(8A)-C(9A)	1.4021	C(19)-C(20)	1.392(5)
C(8A)-H(8A)	0.9300	C(19)-H(19)	0.9300
C(9A)-C(10A)	1.3852	C(20)-H(20)	0.9300
C(9A)-H(9A)	0.9300		
C(10A)-S(1A)	1.7155	C(1)-Cr(1)-C(2)	90.10(12)
C(10A)-H(10A)	0.9300	C(1)-Cr(1)-C(3)	87.39(12)
Ti(1)-C(17)	2.359(3)	C(2)-Cr(1)-C(3)	90.33(10)
Ti(1)-C(12)	2.361(3)	C(1)-Cr(1)-C(5)	88.57(10)
Ti(1)-C(18)	2.371(3)	C(2)-Cr(1)-C(5)	89.38(10)

C(3)-Cr(1)-C(5)	175.95(11)
C(1)-Cr(1)-C(4)	93.90(11)
C(2)-Cr(1)-C(4)	175.79(11)
C(3)-Cr(1)-C(4)	88.51(10)
C(5)-Cr(1)-C(4)	92.06(10)
C(1)-Cr(1)-C(6)	175.86(10)
C(2)-Cr(1)-C(6)	88.52(10)
C(3)-Cr(1)-C(6)	96.52(10)
C(5)-Cr(1)-C(6)	87.51(9)
C(4)-Cr(1)-C(6)	87.59(9)
O(1)-C(1)-Cr(1)	178.2(3)
O(2)-C(2)-Cr(1)	179.3(2)
O(3)-C(3)-Cr(1)	174.0(3)
O(4)-C(4)-Cr(1)	177.3(2)
O(5)-C(5)-Cr(1)	177.28(19)
O(6)-C(6)-C(7)	116.1(2)
O(6)-C(6)-C(7A)	110.3(2)
O(6)-C(6)-Cr(1)	119.92(15)
C(7)-C(6)-Cr(1)	123.95(19)
C(7A)-C(6)-Cr(1)	129.6(2)
C(6)-O(6)-Ti(1)	174.81(14)
C(8)-C(7)-C(6)	129.6(3)
C(8)-C(7)-S(1)	111.8
C(6)-C(7)-S(1)	118.4(3)
C(9)-C(8)-C(7)	110.2
C(9)-C(8)-H(8)	124.9
C(7)-C(8)-H(8)	124.9
C(10)-C(9)-C(8)	115.6
C(10)-C(9)-H(9)	122.2
C(8)-C(9)-H(9)	122.2
C(9)-C(10)-S(1)	110.9
C(9)-C(10)-H(10)	124.6
S(1)-C(10)-H(10)	124.6
C(10)-S(1)-C(7)	91.4
C(8A)-C(7A)-C(6)	129.9(3)
C(8A)-C(7A)-S(1A)	111.8
C(6)-C(7A)-S(1A)	118.2(3)
C(9A)-C(8A)-C(7A)	110.2
C(9A)-C(8A)-H(8A)	124.9
C(7A)-C(8A)-H(8A)	124.9
C(10A)-C(9A)-C(8A)	115.6
C(10A)-C(9A)-H(9A)	122.2
C(8A)-C(9A)-H(9A)	122.2
C(9A)-C(10A)-S(1A)	110.9
C(9A)-C(10A)-H(10A)	124.6
S(1A)-C(10A)-H(10A)	124.6
C(10A)-S(1A)-C(7A)	91.4
O(6)-Ti(1)-C(17)	103.76(10)
O(6)-Ti(1)-C(12)	102.40(9)
C(17)-Ti(1)-C(12)	80.50(12)
O(6)-Ti(1)-C(18)	133.42(9)
C(17)-Ti(1)-C(18)	33.06(11)
C(12)-Ti(1)-C(18)	88.68(11)
O(6)-Ti(1)-C(20)	89.28(11)
C(17)-Ti(1)-C(20)	56.53(12)
C(12)-Ti(1)-C(20)	137.02(11)
C(18)-Ti(1)-C(20)	55.78(11)
O(6)-Ti(1)-Cl(1)	95.98(5)
C(17)-Ti(1)-Cl(1)	134.89(9)
C(12)-Ti(1)-Cl(1)	134.18(7)
C(18)-Ti(1)-Cl(1)	108.21(9)
C(20)-Ti(1)-Cl(1)	84.06(11)
O(6)-Ti(1)-C(15)	90.29(9)
C(17)-Ti(1)-C(15)	137.08(12)
C(12)-Ti(1)-C(15)	56.77(10)
C(18)-Ti(1)-C(15)	131.32(11)
C(20)-Ti(1)-C(15)	165.77(12)
Cl(1)-Ti(1)-C(15)	81.84(8)
O(6)-Ti(1)-C(14)	124.12(10)
C(17)-Ti(1)-C(14)	118.90(13)
C(12)-Ti(1)-C(14)	55.88(10)
C(18)-Ti(1)-C(14)	99.69(12)

C(20)-Ti(1)-C(14)	143.67(14)
Cl(1)-Ti(1)-C(14)	79.03(8)
C(15)-Ti(1)-C(14)	33.84(11)
O(6)-Ti(1)-C(16)	78.44(9)
C(17)-Ti(1)-C(16)	33.51(13)
C(12)-Ti(1)-C(16)	107.12(14)
C(18)-Ti(1)-C(16)	55.17(11)
C(20)-Ti(1)-C(16)	34.54(13)
Cl(1)-Ti(1)-C(16)	117.59(13)
C(15)-Ti(1)-C(16)	158.18(13)
C(14)-Ti(1)-C(16)	152.22(14)
O(6)-Ti(1)-C(19)	123.25(10)
C(17)-Ti(1)-C(19)	55.63(11)
C(12)-Ti(1)-C(19)	121.01(12)
C(18)-Ti(1)-C(19)	33.13(11)
C(20)-Ti(1)-C(19)	34.05(13)
Cl(1)-Ti(1)-C(19)	79.57(8)
C(15)-Ti(1)-C(19)	142.94(12)
C(14)-Ti(1)-C(19)	110.59(12)
C(16)-Ti(1)-C(19)	56.17(11)
O(6)-Ti(1)-C(13)	133.30(9)
C(17)-Ti(1)-C(13)	86.70(12)
C(12)-Ti(1)-C(13)	33.67(10)
C(18)-Ti(1)-C(13)	75.94(11)
C(20)-Ti(1)-C(13)	131.41(11)
Cl(1)-Ti(1)-C(13)	108.37(8)
C(15)-Ti(1)-C(13)	56.13(10)
C(14)-Ti(1)-C(13)	33.28(10)
C(16)-Ti(1)-C(13)	120.11(14)
C(19)-Ti(1)-C(13)	100.44(12)
O(6)-Ti(1)-C(11)	77.57(8)
C(17)-Ti(1)-C(11)	109.36(13)
C(12)-Ti(1)-C(11)	34.46(11)
C(18)-Ti(1)-C(11)	123.13(12)
C(20)-Ti(1)-C(11)	158.11(15)
Cl(1)-Ti(1)-C(11)	114.36(9)
C(15)-Ti(1)-C(11)	34.07(11)
C(14)-Ti(1)-C(11)	56.07(10)
C(16)-Ti(1)-C(11)	124.28(14)
C(19)-Ti(1)-C(11)	155.02(12)
C(13)-Ti(1)-C(11)	56.27(10)
C(15)-C(11)-C(12)	107.0(3)
C(15)-C(11)-Ti(1)	72.64(15)
C(12)-C(11)-Ti(1)	71.77(15)
C(15)-C(11)-H(11)	126.5
C(12)-C(11)-H(11)	126.5
Ti(1)-C(11)-H(11)	120.9
C(13)-C(12)-C(11)	107.9(3)
C(13)-C(12)-Ti(1)	73.93(16)
C(11)-C(12)-Ti(1)	73.77(15)
C(13)-C(12)-H(12)	126.0
C(11)-C(12)-H(12)	126.0
Ti(1)-C(12)-H(12)	118.2
C(14)-C(13)-C(12)	108.5(3)
C(14)-C(13)-Ti(1)	73.27(15)
C(12)-C(13)-Ti(1)	72.40(15)
C(14)-C(13)-H(13)	125.7
C(12)-C(13)-H(13)	125.7
Ti(1)-C(13)-H(13)	120.3
C(13)-C(14)-C(15)	109.2(3)
C(13)-C(14)-Ti(1)	73.44(15)
C(15)-C(14)-Ti(1)	73.10(14)
C(13)-C(14)-H(14)	125.4
C(15)-C(14)-H(14)	125.4
Ti(1)-C(14)-H(14)	119.8
C(14)-C(15)-C(11)	107.3(3)
C(14)-C(15)-Ti(1)	73.06(15)
C(11)-C(15)-Ti(1)	73.29(14)
C(14)-C(15)-H(15)	126.3
C(11)-C(15)-H(15)	126.3
Ti(1)-C(15)-H(15)	119.2
C(17)-C(16)-C(20)	107.6(3)

C(17)-C(16)-Ti(1)	72.45(16)	C(19)-C(18)-H(18)	125.0
C(20)-C(16)-Ti(1)	72.55(16)	Ti(1)-C(18)-H(18)	119.9
C(17)-C(16)-H(16)	126.2	C(18)-C(19)-C(20)	107.9(3)
C(20)-C(16)-H(16)	126.2	C(18)-C(19)-Ti(1)	73.11(17)
Ti(1)-C(16)-H(16)	120.6	C(20)-C(19)-Ti(1)	72.77(16)
C(18)-C(17)-C(16)	108.4(3)	C(18)-C(19)-H(19)	126.1
C(18)-C(17)-Ti(1)	73.98(16)	C(20)-C(19)-H(19)	126.1
C(16)-C(17)-Ti(1)	74.04(17)	Ti(1)-C(19)-H(19)	119.9
C(18)-C(17)-H(17)	125.8	C(19)-C(20)-C(16)	106.1(3)
C(16)-C(17)-H(17)	125.8	C(19)-C(20)-Ti(1)	73.18(17)
Ti(1)-C(17)-H(17)	118.1	C(16)-C(20)-Ti(1)	72.91(16)
C(17)-C(18)-C(19)	110.0(3)	C(19)-C(20)-H(20)	126.9
C(17)-C(18)-Ti(1)	72.97(16)	C(16)-C(20)-H(20)	126.9
C(19)-C(18)-Ti(1)	73.76(15)	Ti(1)-C(20)-H(20)	119.0
C(17)-C(18)-H(18)	125.0		

Table 4. Anisotropic displacement parameters (Å^{2}x 10^3)for Complex **12**. The anisotropic displacement factor exponent takes the form: -2p^2[h^{2}a*^{2}U^{11} + ... + 2 h k a* b* U^{12}]

	U^{11}	U^{22}	U^{33}	U^{23}	U^{13}	U^{12}
Cr(1)	30(1)	35(1)	43(1)	5(1)	8(1)	1(1)
C(1)	45(1)	57(2)	55(1)	6(1)	1(1)	4(1)
O(1)	62(1)	90(2)	82(1)	-10(1)	-20(1)	-11(1)
C(2)	45(1)	37(1)	67(2)	7(1)	20(1)	3(1)
O(2)	99(2)	63(1)	110(2)	19(1)	71(2)	3(1)
C(3)	46(1)	51(1)	59(1)	14(1)	21(1)	5(1)
O(3)	78(1)	70(1)	108(2)	40(1)	38(1)	40(1)
C(4)	47(1)	46(1)	48(1)	6(1)	14(1)	7(1)
O(4)	77(1)	82(1)	76(1)	22(1)	43(1)	12(1)
C(5)	36(1)	39(1)	49(1)	0(1)	10(1)	-5(1)
O(5)	50(1)	38(1)	88(1)	5(1)	14(1)	5(1)
C(6)	33(1)	29(1)	43(1)	7(1)	13(1)	2(1)
O(6)	31(1)	39(1)	46(1)	-1(1)	10(1)	2(1)
C(7)	36(1)	35(1)	44(1)	2(1)	14(1)	2(1)
C(8)	115(12)	60(7)	80(8)	-24(5)	29(7)	0(6)
C(9)	70(5)	43(6)	89(6)	-20(4)	39(4)	-8(4)
C(10)	80(6)	45(4)	60(5)	-15(4)	42(5)	4(5)
S(1)	75(1)	61(2)	45(1)	-15(1)	19(1)	0(1)
C(7A)	36(1)	35(1)	44(1)	2(1)	14(1)	2(1)
C(8A)	104(9)	52(7)	50(7)	11(5)	27(5)	5(6)
C(9A)	51(3)	59(5)	43(4)	-5(3)	18(3)	-7(3)
C(10A)	54(4)	36(5)	58(4)	-21(3)	24(3)	-9(3)
S(1A)	48(1)	64(1)	79(2)	-23(1)	24(1)	5(1)
Ti(1)	29(1)	37(1)	35(1)	1(1)	8(1)	0(1)
Cl(1)	61(1)	53(1)	47(1)	-11(1)	16(1)	-2(1)
C(11)	62(2)	31(1)	126(3)	14(1)	44(2)	0(1)
C(12)	79(2)	51(2)	59(2)	-12(1)	17(1)	-24(1)
C(13)	41(1)	70(2)	85(2)	-1(2)	11(1)	-19(1)
C(14)	67(2)	69(2)	78(2)	-7(2)	43(2)	-24(2)
C(15)	73(2)	56(2)	55(1)	15(1)	9(1)	-23(1)
C(16)	72(2)	117(3)	87(2)	70(2)	49(2)	43(2)
C(17)	95(2)	75(2)	39(1)	9(1)	12(1)	16(2)

C(18)	46(1)	86(2)	59(2)	17(2)	-1(1)	9(1)
C(19)	85(2)	67(2)	56(2)	10(1)	5(1)	40(2)
C(20)	84(2)	61(2)	90(2)	45(2)	-30(2)	-26(2)

Table 5. Hydrogen coordinates (x 10^4) and isotropic displacement parameters (Å^{2}x 10^3) for Complex **12**.

	x	y	z	U(eq)
H(8)	5867	1088	8921	101
H(9)	5524	68	7551	77
H(10)	3335	6	6662	69
H(8A)	1976	1252	7654	81
H(9A)	2883	128	6720	59
H(10A)	5125	-229	7321	57
H(11)	1598	455	9316	83
H(12)	-298	793	8004	75
H(13)	-1911	1672	8623	79
H(14)	-1026	1958	10265	80
H(15)	1151	1237	10716	75
H(16)	1805	3194	7564	104
H(17)	-240	2301	7106	84
H(18)	-1767	3076	7837	79
H(19)	-722	4411	8823	85
H(20)	1550	4504	8696	104

Table 6. Torsion angles [°] for Complex **12**.

C(2)-Cr(1)-C(6)-O(6)	-126.85(17)
C(3)-Cr(1)-C(6)-O(6)	142.99(16)
C(5)-Cr(1)-C(6)-O(6)	-37.40(16)
C(4)-Cr(1)-C(6)-O(6)	54.76(16)
C(2)-Cr(1)-C(6)-C(7)	50.5(5)
C(3)-Cr(1)-C(6)-C(7)	-39.7(5)
C(5)-Cr(1)-C(6)-C(7)	139.9(5)
C(4)-Cr(1)-C(6)-C(7)	-127.9(5)
C(2)-Cr(1)-C(6)-C(7A)	48.1(5)
C(3)-Cr(1)-C(6)-C(7A)	-42.0(5)
C(5)-Cr(1)-C(6)-C(7A)	137.6(5)
C(4)-Cr(1)-C(6)-C(7A)	-130.3(5)
O(6)-C(6)-C(7)-C(8)	179.6(6)
Cr(1)-C(6)-C(7)-C(8)	2.2(10)
O(6)-C(6)-C(7)-S(1)	5.5(8)
Cr(1)-C(6)-C(7)-S(1)	-171.9(3)
C(6)-C(7)-C(8)-C(9)	-175.9(12)
S(1)-C(7)-C(8)-C(9)	-1.5
C(7)-C(8)-C(9)-C(10)	1.5
C(8)-C(9)-C(10)-S(1)	-0.9
C(9)-C(10)-S(1)-C(7)	0.0
C(8)-C(7)-S(1)-C(10)	0.9
C(6)-C(7)-S(1)-C(10)	176.0(10)
O(6)-C(6)-C(7A)-C(8A)	4.8(8)
C(7)-C(6)-C(7A)-C(8A)	171(8)
Cr(1)-C(6)-C(7A)-C(8A)	-170.5(5)
O(6)-C(6)-C(7A)-S(1A)	-172.3(4)
C(7)-C(6)-C(7A)-S(1A)	-7(7)
Cr(1)-C(6)-C(7A)-S(1A)	12.4(9)
C(6)-C(7A)-C(8A)-C(9A)	-178.8(11)
S(1A)-C(7A)-C(8A)-C(9A)	-1.5
C(7A)-C(8A)-C(9A)-C(10A)	1.5
C(8A)-C(9A)-C(10A)-S(1A)	-0.9
C(9A)-C(10A)-S(1A)-C(7A)	0.0
C(8A)-C(7A)-S(1A)-C(10A)	0.9
C(6)-C(7A)-S(1A)-C(10A)	178.5(9)
C(15)-C(11)-C(12)-C(13)	-2.0(3)
C(11)-C(12)-C(13)-C(14)	1.6(3)
C(12)-C(13)-C(14)-C(15)	-0.6(3)
C(13)-C(14)-C(15)-C(11)	-0.7(3)
C(12)-C(11)-C(15)-C(14)	1.7(3)
C(20)-C(16)-C(17)-C(18)	2.0(3)
C(16)-C(17)-C(18)-C(19)	-1.6(3)
C(17)-C(18)-C(19)-C(20)	0.5(3)
C(18)-C(19)-C(20)-C(16)	0.8(3)
C(17)-C(16)-C(20)-C(19)	-1.7(3)

Appendix 6

Crystallographic data of Complex 13

Table 1. Crystal data and structure refinement for Complex **13**.

Identification code	db76a_abs	
Empirical formula	C_{25} H_{15} Cl Cr_2 O_9 Ti	
Formula weight	646.72	
Temperature	293(2) K	
Wavelength	0.71073 Å	
Crystal system	Orthorhombic	
Space group	P b c a	
Unit cell dimensions	a = 14.9820(8) Å	a= 90°.
	b = 15.3296(8) Å	b= 90°.
	c = 21.8203(12) Å	g = 90°.
Volume	5011.4(5) $Å^3$	
Z	8	
Density (calculated)	1.714 Mg/m^3	
Absorption coefficient	1.323 mm^{-1}	
F(000)	2592	
Crystal size	0.28 x 0.20 x 0.10 mm^3	
Theta range for data collection	2.66 to 26.53°.	
Index ranges	-18<=h<=18, -5<=k<=18, -27<=l<=26	
Reflections collected	21839	
Independent reflections	4680 [R(int) = 0.0404]	
Completeness to θ = 25.00°	98.9 %	
Absorption correction	Semi-empirical from equivalents	
Max. and min. transmission	0.876 and 0.688	
Refinement method	Full-matrix least-squares on F^2	
Data / restraints / parameters	4680 / 0 / 343	
Goodness-of-fit on F^2	1.136	
Final R indices [I>2σ(I)]	R1 = 0.0388, wR2 = 0.0946	
R indices (all data)	R1 = 0.0616, wR2 = 0.1180	
Extinction coefficient	0	
Largest diff. peak and hole	0.570 and -0.475 e.$Å^{-3}$	

Table 2. Atomic coordinates (x 10^4) and equivalent isotropic displacement parameters (Å^{2}x 10^3) for Complex **13**. U(eq) is defined as one third of the trace of the orthogonalized U^{ij} tensor.

	x	y	z	U(eq)
Cr(1)	5488(1)	837(1)	6040(1)	36(1)
C(1)	4322(3)	722(2)	5732(2)	48(1)
O(1)	3612(2)	674(2)	5541(2)	70(1)
C(2)	5205(3)	2032(2)	6170(2)	44(1)
O(2)	4990(2)	2740(2)	6237(1)	64(1)
C(3)	5134(3)	511(2)	6837(2)	47(1)
O(3)	4935(2)	261(2)	7309(1)	73(1)
C(4)	5643(2)	-382(2)	5926(2)	44(1)
O(4)	5680(2)	-1123(2)	5882(2)	66(1)
C(5)	5931(3)	1114(2)	5239(2)	44(1)
O(5)	6188(2)	1277(2)	4766(1)	58(1)
C(6)	6745(2)	1066(2)	6396(1)	32(1)
O(6)	6841(2)	1587(1)	6854(1)	35(1)
Cr(2)	8568(1)	1089(1)	5460(1)	33(1)
C(7)	8349(3)	920(2)	4639(2)	46(1)
O(7)	8226(3)	802(2)	4128(1)	74(1)
C(8)	7985(3)	2155(2)	5393(2)	47(1)
O(8)	7618(2)	2801(2)	5338(2)	74(1)
C(9)	9631(3)	1637(2)	5264(2)	47(1)
O(9)	10300(2)	1952(2)	5151(2)	69(1)
C(10)	7629(2)	684(2)	6195(1)	33(1)
C(11)	8448(2)	968(2)	6464(2)	38(1)
C(12)	9257(3)	610(2)	6284(2)	45(1)
C(13)	9287(3)	-52(2)	5837(2)	46(1)
C(14)	8500(3)	-339(2)	5569(2)	42(1)
C(15)	7676(2)	25(2)	5742(2)	37(1)
Ti(1)	6907(1)	2276(1)	7594(1)	31(1)
Cl(1)	5340(1)	2333(1)	7780(1)	52(1)
C(16)	8135(3)	1665(3)	8098(2)	51(1)
C(17)	7626(3)	961(2)	7903(2)	46(1)
C(18)	6804(3)	985(2)	8203(2)	51(1)
C(19)	6822(3)	1690(3)	8610(2)	60(1)
C(20)	7637(3)	2110(3)	8544(2)	59(1)
C(21)	7903(3)	3215(2)	7062(2)	65(1)
C(22)	7061(4)	3358(2)	6809(2)	60(1)
C(23)	6530(3)	3709(2)	7263(2)	63(1)

C(24)	7034(4)	3772(2)	7796(2)	70(1)
C(25)	7888(4)	3488(3)	7658(3)	72(1)

Table 3. Bond lengths [Å] and angles [°] for Complex **13**.

Cr(1)-C(1)	1.879(4)	Ti(1)-C(24)	2.342(4)
Cr(1)-C(3)	1.886(4)	Ti(1)-C(20)	2.357(4)
Cr(1)-C(4)	1.900(4)	Ti(1)-C(25)	2.373(4)
Cr(1)-C(2)	1.901(4)	Ti(1)-C(21)	2.376(4)
Cr(1)-C(5)	1.916(4)	Ti(1)-C(23)	2.381(4)
Cr(1)-C(6)	2.067(3)	Ti(1)-C(17)	2.383(3)
C(1)-O(1)	1.146(5)	Ti(1)-Cl(1)	2.3833(11)
C(2)-O(2)	1.141(4)	Ti(1)-C(18)	2.389(3)
C(3)-O(3)	1.139(5)	Ti(1)-C(19)	2.394(4)
C(4)-O(4)	1.141(4)	Ti(1)-C(22)	2.396(4)
C(5)-O(5)	1.130(4)	C(16)-C(17)	1.389(5)
C(6)-O(6)	1.287(4)	C(16)-C(20)	1.405(6)
C(6)-C(10)	1.513(5)	C(16)-H(16)	0.9300
O(6)-Ti(1)	1.933(2)	C(17)-C(18)	1.395(6)
Cr(2)-C(7)	1.840(4)	C(17)-H(17)	0.9300
Cr(2)-C(9)	1.852(4)	C(18)-C(19)	1.399(6)
Cr(2)-C(8)	1.859(4)	C(18)-H(18)	0.9300
Cr(2)-C(15)	2.197(3)	C(19)-C(20)	1.388(6)
Cr(2)-C(12)	2.198(3)	C(19)-H(19)	0.9300
Cr(2)-C(14)	2.204(3)	C(20)-H(20)	0.9300
Cr(2)-C(11)	2.206(3)	C(21)-C(25)	1.365(7)
Cr(2)-C(13)	2.213(3)	C(21)-C(22)	1.394(7)
Cr(2)-C(10)	2.221(3)	C(21)-H(21)	0.9300
C(7)-O(7)	1.144(4)	C(22)-C(23)	1.380(6)
C(8)-O(8)	1.139(4)	C(22)-H(22)	0.9300
C(9)-O(9)	1.140(5)	C(23)-C(24)	1.390(7)
C(10)-C(15)	1.416(4)	C(23)-H(23)	0.9300
C(10)-C(11)	1.428(5)	C(24)-C(25)	1.384(7)
C(11)-C(12)	1.387(5)	C(24)-H(24)	0.9300
C(11)-H(11)	0.9300	C(25)-H(25)	0.9300
C(12)-C(13)	1.409(5)		
C(12)-H(12)	0.9300	C(1)-Cr(1)-C(3)	92.49(17)
C(13)-C(14)	1.388(5)	C(1)-Cr(1)-C(4)	88.52(16)
C(13)-H(13)	0.9300	C(3)-Cr(1)-C(4)	83.90(16)
C(14)-C(15)	1.408(5)	C(1)-Cr(1)-C(2)	86.44(16)
C(14)-H(14)	0.9300	C(3)-Cr(1)-C(2)	93.16(16)
C(15)-H(15)	0.9300	C(4)-Cr(1)-C(2)	174.05(16)
Ti(1)-C(16)	2.339(4)	C(1)-Cr(1)-C(5)	91.00(17)

C(3)-Cr(1)-C(5)	175.39(17)
C(4)-Cr(1)-C(5)	93.19(15)
C(2)-Cr(1)-C(5)	90.06(15)
C(1)-Cr(1)-C(6)	175.44(14)
C(3)-Cr(1)-C(6)	87.37(15)
C(4)-Cr(1)-C(6)	96.00(14)
C(2)-Cr(1)-C(6)	89.01(14)
C(5)-Cr(1)-C(6)	89.39(14)
O(1)-C(1)-Cr(1)	178.2(4)
O(2)-C(2)-Cr(1)	176.3(4)
O(3)-C(3)-Cr(1)	175.7(3)
O(4)-C(4)-Cr(1)	174.9(4)
O(5)-C(5)-Cr(1)	179.7(4)
O(6)-C(6)-C(10)	111.5(3)
O(6)-C(6)-Cr(1)	119.9(2)
C(10)-C(6)-Cr(1)	128.5(2)
C(6)-O(6)-Ti(1)	173.6(2)
C(7)-Cr(2)-C(9)	89.55(18)
C(7)-Cr(2)-C(8)	87.87(16)
C(9)-Cr(2)-C(8)	89.22(17)
C(7)-Cr(2)-C(15)	93.45(15)
C(9)-Cr(2)-C(15)	157.72(15)
C(8)-Cr(2)-C(15)	112.93(15)
C(7)-Cr(2)-C(12)	146.41(16)
C(9)-Cr(2)-C(12)	86.34(16)
C(8)-Cr(2)-C(12)	125.33(16)
C(15)-Cr(2)-C(12)	78.99(14)
C(7)-Cr(2)-C(14)	87.54(15)
C(9)-Cr(2)-C(14)	120.99(15)
C(8)-Cr(2)-C(14)	149.38(16)
C(15)-Cr(2)-C(14)	37.32(13)
C(12)-Cr(2)-C(14)	66.57(14)
C(7)-Cr(2)-C(11)	160.22(16)
C(9)-Cr(2)-C(11)	109.73(15)
C(8)-Cr(2)-C(11)	96.54(15)
C(15)-Cr(2)-C(11)	67.05(13)
C(12)-Cr(2)-C(11)	36.72(13)
C(14)-Cr(2)-C(11)	78.84(13)
C(7)-Cr(2)-C(13)	109.73(15)
C(9)-Cr(2)-C(13)	91.44(15)
C(8)-Cr(2)-C(13)	162.39(16)
C(15)-Cr(2)-C(13)	66.77(14)
C(12)-Cr(2)-C(13)	37.25(14)
C(14)-Cr(2)-C(13)	36.62(14)
C(11)-Cr(2)-C(13)	66.71(13)
C(7)-Cr(2)-C(10)	123.43(16)
C(9)-Cr(2)-C(10)	146.98(15)
C(8)-Cr(2)-C(10)	90.29(14)
C(15)-Cr(2)-C(10)	37.37(12)
C(12)-Cr(2)-C(10)	67.31(13)
C(14)-Cr(2)-C(10)	67.45(12)
C(11)-Cr(2)-C(10)	37.65(12)
C(13)-Cr(2)-C(10)	79.64(13)
O(7)-C(7)-Cr(2)	178.5(4)
O(8)-C(8)-Cr(2)	178.2(4)
O(9)-C(9)-Cr(2)	177.8(4)
C(15)-C(10)-C(11)	117.5(3)
C(15)-C(10)-C(6)	121.5(3)
C(11)-C(10)-C(6)	121.0(3)
C(15)-C(10)-Cr(2)	70.38(18)
C(11)-C(10)-Cr(2)	70.60(19)
C(6)-C(10)-Cr(2)	131.0(2)
C(12)-C(11)-C(10)	120.9(3)
C(12)-C(11)-Cr(2)	71.3(2)
C(10)-C(11)-Cr(2)	71.76(18)
C(12)-C(11)-H(11)	119.6
C(10)-C(11)-H(11)	119.6
Cr(2)-C(11)-H(11)	129.9
C(11)-C(12)-C(13)	120.7(4)
C(11)-C(12)-Cr(2)	71.9(2)
C(13)-C(12)-Cr(2)	71.9(2)
C(11)-C(12)-H(12)	119.7
C(13)-C(12)-H(12)	119.7
Cr(2)-C(12)-H(12)	128.8
C(14)-C(13)-C(12)	119.5(3)
C(14)-C(13)-Cr(2)	71.4(2)
C(12)-C(13)-Cr(2)	70.8(2)
C(14)-C(13)-H(13)	120.2

C(12)-C(13)-H(13)	120.2
Cr(2)-C(13)-H(13)	130.1
C(13)-C(14)-C(15)	120.4(3)
C(13)-C(14)-Cr(2)	72.0(2)
C(15)-C(14)-Cr(2)	71.05(18)
C(13)-C(14)-H(14)	119.8
C(15)-C(14)-H(14)	119.8
Cr(2)-C(14)-H(14)	129.6
C(14)-C(15)-C(10)	121.0(3)
C(14)-C(15)-Cr(2)	71.63(19)
C(10)-C(15)-Cr(2)	72.25(18)
C(14)-C(15)-H(15)	119.5
C(10)-C(15)-H(15)	119.5
Cr(2)-C(15)-H(15)	129.0
O(6)-Ti(1)-C(16)	102.34(12)
O(6)-Ti(1)-C(24)	134.12(14)
C(16)-Ti(1)-C(24)	103.88(18)
O(6)-Ti(1)-C(20)	134.39(13)
C(16)-Ti(1)-C(20)	34.81(15)
C(24)-Ti(1)-C(20)	84.43(17)
O(6)-Ti(1)-C(25)	120.58(16)
C(16)-Ti(1)-C(25)	78.40(16)
C(24)-Ti(1)-C(25)	34.12(18)
C(20)-Ti(1)-C(25)	75.28(16)
O(6)-Ti(1)-C(21)	87.43(14)
C(16)-Ti(1)-C(21)	88.74(16)
C(24)-Ti(1)-C(21)	56.46(17)
C(20)-Ti(1)-C(21)	101.76(18)
C(25)-Ti(1)-C(21)	33.42(16)
O(6)-Ti(1)-C(23)	103.82(14)
C(16)-Ti(1)-C(23)	134.34(16)
C(24)-Ti(1)-C(23)	34.21(17)
C(20)-Ti(1)-C(23)	118.46(16)
C(25)-Ti(1)-C(23)	56.10(17)
C(21)-Ti(1)-C(23)	56.07(16)
O(6)-Ti(1)-C(17)	78.27(11)
C(16)-Ti(1)-C(17)	34.19(13)
C(24)-Ti(1)-C(17)	137.59(17)
C(20)-Ti(1)-C(17)	56.67(14)
C(25)-Ti(1)-C(17)	111.47(17)
C(21)-Ti(1)-C(17)	111.53(15)
C(23)-Ti(1)-C(17)	166.87(16)
O(6)-Ti(1)-Cl(1)	96.41(7)
C(16)-Ti(1)-Cl(1)	135.20(11)
C(24)-Ti(1)-Cl(1)	90.72(15)
C(20)-Ti(1)-Cl(1)	108.13(13)
C(25)-Ti(1)-Cl(1)	124.84(15)
C(21)-Ti(1)-Cl(1)	132.79(12)
C(23)-Ti(1)-Cl(1)	77.53(12)
C(17)-Ti(1)-Cl(1)	115.33(10)
O(6)-Ti(1)-C(18)	90.49(12)
C(16)-Ti(1)-C(18)	57.16(14)
C(24)-Ti(1)-C(18)	135.39(16)
C(20)-Ti(1)-C(18)	56.72(15)
C(25)-Ti(1)-C(18)	131.00(16)
C(21)-Ti(1)-C(18)	144.51(16)
C(23)-Ti(1)-C(18)	156.64(16)
C(17)-Ti(1)-C(18)	34.00(14)
Cl(1)-Ti(1)-C(18)	82.66(11)
O(6)-Ti(1)-C(19)	124.44(13)
C(16)-Ti(1)-C(19)	57.12(15)
C(24)-Ti(1)-C(19)	101.41(16)
C(20)-Ti(1)-C(19)	33.95(16)
C(25)-Ti(1)-C(19)	105.82(18)
C(21)-Ti(1)-C(19)	135.46(19)
C(23)-Ti(1)-C(19)	127.90(16)
C(17)-Ti(1)-C(19)	56.30(14)
Cl(1)-Ti(1)-C(19)	78.69(12)
C(18)-Ti(1)-C(19)	34.01(14)
O(6)-Ti(1)-C(22)	77.64(12)
C(16)-Ti(1)-C(22)	122.50(16)
C(24)-Ti(1)-C(22)	56.54(15)
C(20)-Ti(1)-C(22)	131.21(16)
C(25)-Ti(1)-C(22)	55.95(16)
C(21)-Ti(1)-C(22)	33.97(16)
C(23)-Ti(1)-C(22)	33.59(16)
C(17)-Ti(1)-C(22)	138.11(15)
Cl(1)-Ti(1)-C(22)	101.02(13)

C(18)-Ti(1)-C(22)	167.85(14)	Ti(1)-C(20)-H(20)	119.6
C(19)-Ti(1)-C(22)	157.91(15)	C(25)-C(21)-C(22)	108.3(4)
C(17)-C(16)-C(20)	107.3(4)	C(25)-C(21)-Ti(1)	73.2(3)
C(17)-C(16)-Ti(1)	74.6(2)	C(22)-C(21)-Ti(1)	73.8(2)
C(20)-C(16)-Ti(1)	73.3(2)	C(25)-C(21)-H(21)	125.8
C(17)-C(16)-H(16)	126.3	C(22)-C(21)-H(21)	125.8
C(20)-C(16)-H(16)	126.3	Ti(1)-C(21)-H(21)	119.1
Ti(1)-C(16)-H(16)	117.8	C(23)-C(22)-C(21)	107.4(4)
C(16)-C(17)-C(18)	108.7(3)	C(23)-C(22)-Ti(1)	72.6(2)
C(16)-C(17)-Ti(1)	71.16(19)	C(21)-C(22)-Ti(1)	72.2(2)
C(18)-C(17)-Ti(1)	73.2(2)	C(23)-C(22)-H(22)	126.3
C(16)-C(17)-H(17)	125.6	C(21)-C(22)-H(22)	126.3
C(18)-C(17)-H(17)	125.6	Ti(1)-C(22)-H(22)	120.7
Ti(1)-C(17)-H(17)	121.6	C(22)-C(23)-C(24)	108.2(4)
C(17)-C(18)-C(19)	107.6(4)	C(22)-C(23)-Ti(1)	73.8(2)
C(17)-C(18)-Ti(1)	72.78(19)	C(24)-C(23)-Ti(1)	71.4(2)
C(19)-C(18)-Ti(1)	73.2(2)	C(22)-C(23)-H(23)	125.9
C(17)-C(18)-H(18)	126.2	C(24)-C(23)-H(23)	125.9
C(19)-C(18)-H(18)	126.2	Ti(1)-C(23)-H(23)	120.7
Ti(1)-C(18)-H(18)	119.7	C(25)-C(24)-C(23)	107.4(4)
C(20)-C(19)-C(18)	108.1(4)	C(25)-C(24)-Ti(1)	74.2(2)
C(20)-C(19)-Ti(1)	71.6(2)	C(23)-C(24)-Ti(1)	74.4(2)
C(18)-C(19)-Ti(1)	72.8(2)	C(25)-C(24)-H(24)	126.3
C(20)-C(19)-H(19)	126.0	C(23)-C(24)-H(24)	126.3
C(18)-C(19)-H(19)	126.0	Ti(1)-C(24)-H(24)	117.2
Ti(1)-C(19)-H(19)	121.4	C(21)-C(25)-C(24)	108.6(5)
C(19)-C(20)-C(16)	108.3(4)	C(21)-C(25)-Ti(1)	73.4(2)
C(19)-C(20)-Ti(1)	74.5(2)	C(24)-C(25)-Ti(1)	71.7(2)
C(16)-C(20)-Ti(1)	71.9(2)	C(21)-C(25)-H(25)	125.7
C(19)-C(20)-H(20)	125.8	C(24)-C(25)-H(25)	125.7
C(16)-C(20)-H(20)	125.8	Ti(1)-C(25)-H(25)	120.9

Symmetry transformations used to generate equivalent atoms:

Table 4. Anisotropic displacement parameters ($Å^2 x 10^3$)for Complex **13**. The anisotropic displacement factor exponent takes the form: $-2p^2[h^2a^{*2}U^{11} + ... + 2 h k a^* b^* U^{12}]$

	U^{11}	U^{22}	U^{33}	U^{23}	U^{13}	U^{12}
Cr(1)	34(1)	35(1)	39(1)	-6(1)	-2(1)	1(1)
C(1)	44(2)	48(2)	51(2)	-17(2)	-2(2)	4(2)
O(1)	44(2)	86(2)	79(2)	-29(2)	-17(2)	9(2)
C(2)	43(2)	46(2)	41(2)	-2(2)	-4(2)	3(2)
O(2)	83(2)	45(2)	65(2)	-4(1)	-4(2)	18(2)
C(3)	44(2)	44(2)	52(2)	-6(2)	4(2)	-9(2)
O(3)	92(3)	73(2)	55(2)	1(2)	19(2)	-27(2)
C(4)	37(2)	47(2)	49(2)	-5(2)	-1(2)	0(2)
O(4)	69(2)	37(2)	92(2)	-9(1)	-6(2)	1(1)
C(5)	43(2)	42(2)	48(2)	-8(2)	-8(2)	6(2)
O(5)	62(2)	68(2)	43(2)	3(1)	3(1)	5(2)
C(6)	38(2)	26(1)	32(2)	3(1)	0(1)	-2(1)
O(6)	38(1)	33(1)	35(1)	-6(1)	-1(1)	1(1)
Cr(2)	36(1)	28(1)	34(1)	0(1)	2(1)	1(1)
C(7)	56(2)	41(2)	41(2)	0(2)	-3(2)	4(2)
O(7)	108(3)	72(2)	40(2)	-2(1)	-14(2)	7(2)
C(8)	53(2)	39(2)	48(2)	3(2)	7(2)	1(2)
O(8)	91(3)	41(2)	91(2)	7(1)	6(2)	23(2)
C(9)	51(2)	39(2)	49(2)	4(2)	0(2)	-5(2)
O(9)	53(2)	73(2)	82(2)	14(2)	7(2)	-20(2)
C(10)	38(2)	29(1)	31(2)	3(1)	2(1)	0(1)
C(11)	39(2)	45(2)	31(2)	-1(1)	2(2)	0(2)
C(12)	37(2)	57(2)	39(2)	11(2)	-4(2)	2(2)
C(13)	41(2)	44(2)	52(2)	11(2)	9(2)	15(2)
C(14)	48(2)	28(2)	49(2)	0(1)	11(2)	5(2)
C(15)	43(2)	28(1)	40(2)	-1(1)	6(2)	-1(1)
Ti(1)	37(1)	24(1)	33(1)	-2(1)	-1(1)	1(1)
Cl(1)	42(1)	54(1)	59(1)	-2(1)	7(1)	6(1)
C(16)	45(2)	56(2)	53(2)	18(2)	-10(2)	5(2)
C(17)	59(3)	34(2)	46(2)	7(2)	-3(2)	14(2)
C(18)	59(3)	41(2)	51(2)	19(2)	2(2)	-4(2)
C(19)	75(3)	67(3)	37(2)	11(2)	10(2)	21(2)
C(20)	80(3)	52(2)	46(2)	0(2)	-18(2)	1(2)
C(21)	65(3)	34(2)	94(4)	16(2)	25(3)	-3(2)
C(22)	99(4)	34(2)	48(2)	14(2)	-4(2)	-7(2)
C(23)	67(3)	28(2)	95(4)	16(2)	-1(3)	7(2)

C(24)	119(5)	26(2)	64(3)	-10(2)	10(3)	-9(2)
C(25)	85(4)	42(2)	89(4)	13(2)	-28(3)	-26(2)

Table 5. Hydrogen coordinates (x 10^4) and isotropic displacement parameters ($Å^2$x 10^3) for Complex **13**.

	x	y	z	U(eq)
H(11)	8439	1398	6765	46
H(12)	9784	809	6460	53
H(13)	9831	-295	5722	55
H(14)	8518	-775	5272	50
H(15)	7154	-171	5557	44
H(16)	8702	1814	7958	61
H(17)	7803	542	7619	55
H(18)	6330	602	8144	61
H(19)	6367	1850	8877	71
H(20)	7821	2602	8759	71
H(21)	8391	2975	6860	77
H(22)	6889	3239	6408	72
H(23)	5936	3876	7220	76
H(24)	6835	3968	8175	83
H(25)	8370	3484	7926	86

Table 6. Torsion angles [°] for Complex **13**.

C(3)-Cr(1)-C(6)-O(6)	-55.0(3)	Cr(2)-C(10)-C(11)-C(12)	-53.9(3)
C(4)-Cr(1)-C(6)-O(6)	-138.5(2)	C(15)-C(10)-C(11)-Cr(2)	54.2(3)
C(2)-Cr(1)-C(6)-O(6)	38.2(3)	C(6)-C(10)-C(11)-Cr(2)	-126.8(3)
C(5)-Cr(1)-C(6)-O(6)	128.3(2)	C(7)-Cr(2)-C(11)-C(12)	112.9(5)
C(3)-Cr(1)-C(6)-C(10)	124.2(3)	C(9)-Cr(2)-C(11)-C(12)	-53.6(3)
C(4)-Cr(1)-C(6)-C(10)	40.6(3)	C(8)-Cr(2)-C(11)-C(12)	-145.1(2)
C(2)-Cr(1)-C(6)-C(10)	-142.6(3)	C(15)-Cr(2)-C(11)-C(12)	102.8(2)
C(5)-Cr(1)-C(6)-C(10)	-52.5(3)	C(14)-Cr(2)-C(11)-C(12)	65.6(2)
O(6)-C(6)-C(10)-C(15)	173.2(3)	C(13)-Cr(2)-C(11)-C(12)	29.3(2)
Cr(1)-C(6)-C(10)-C(15)	-6.0(4)	C(10)-Cr(2)-C(11)-C(12)	133.0(3)
O(6)-C(6)-C(10)-C(11)	-5.7(4)	C(7)-Cr(2)-C(11)-C(10)	-20.1(5)
Cr(1)-C(6)-C(10)-C(11)	175.1(2)	C(9)-Cr(2)-C(11)-C(10)	173.5(2)
O(6)-C(6)-C(10)-Cr(2)	-96.2(3)	C(8)-Cr(2)-C(11)-C(10)	81.9(2)
Cr(1)-C(6)-C(10)-Cr(2)	84.6(3)	C(15)-Cr(2)-C(11)-C(10)	-30.24(18)
C(7)-Cr(2)-C(10)-C(15)	41.8(3)	C(12)-Cr(2)-C(11)-C(10)	-133.0(3)
C(9)-Cr(2)-C(10)-C(15)	-141.5(3)	C(14)-Cr(2)-C(11)-C(10)	-67.4(2)
C(8)-Cr(2)-C(10)-C(15)	129.4(2)	C(13)-Cr(2)-C(11)-C(10)	-103.7(2)
C(12)-Cr(2)-C(10)-C(15)	-101.9(2)	C(10)-C(11)-C(12)-C(13)	-1.0(5)
C(14)-Cr(2)-C(10)-C(15)	-28.9(2)	Cr(2)-C(11)-C(12)-C(13)	-55.1(3)
C(11)-Cr(2)-C(10)-C(15)	-130.2(3)	C(10)-C(11)-C(12)-Cr(2)	54.1(3)
C(13)-Cr(2)-C(10)-C(15)	-65.1(2)	C(7)-Cr(2)-C(12)-C(11)	-145.7(3)
C(7)-Cr(2)-C(10)-C(11)	172.0(2)	C(9)-Cr(2)-C(12)-C(11)	130.6(2)
C(9)-Cr(2)-C(10)-C(11)	-11.4(3)	C(8)-Cr(2)-C(12)-C(11)	44.2(3)
C(8)-Cr(2)-C(10)-C(11)	-100.4(2)	C(15)-Cr(2)-C(12)-C(11)	-66.2(2)
C(15)-Cr(2)-C(10)-C(11)	130.2(3)	C(14)-Cr(2)-C(12)-C(11)	-103.2(2)
C(12)-Cr(2)-C(10)-C(11)	28.3(2)	C(13)-Cr(2)-C(12)-C(11)	-132.1(3)
C(14)-Cr(2)-C(10)-C(11)	101.2(2)	C(10)-Cr(2)-C(12)-C(11)	-29.0(2)
C(13)-Cr(2)-C(10)-C(11)	65.1(2)	C(7)-Cr(2)-C(12)-C(13)	-13.6(4)
C(7)-Cr(2)-C(10)-C(6)	-73.3(3)	C(9)-Cr(2)-C(12)-C(13)	-97.2(2)
C(9)-Cr(2)-C(10)-C(6)	103.3(4)	C(8)-Cr(2)-C(12)-C(13)	176.3(2)
C(8)-Cr(2)-C(10)-C(6)	14.3(3)	C(15)-Cr(2)-C(12)-C(13)	65.9(2)
C(15)-Cr(2)-C(10)-C(6)	-115.1(4)	C(14)-Cr(2)-C(12)-C(13)	28.9(2)
C(12)-Cr(2)-C(10)-C(6)	143.0(3)	C(11)-Cr(2)-C(12)-C(13)	132.1(3)
C(14)-Cr(2)-C(10)-C(6)	-144.1(3)	C(10)-Cr(2)-C(12)-C(13)	103.2(2)
C(11)-Cr(2)-C(10)-C(6)	114.7(4)	C(11)-C(12)-C(13)-C(14)	0.9(5)
C(13)-Cr(2)-C(10)-C(6)	179.8(3)	Cr(2)-C(12)-C(13)-C(14)	-54.1(3)
C(15)-C(10)-C(11)-C(12)	0.4(5)	C(11)-C(12)-C(13)-Cr(2)	55.1(3)
C(6)-C(10)-C(11)-C(12)	179.3(3)	C(7)-Cr(2)-C(13)-C(14)	-56.0(3)

C(9)-Cr(2)-C(13)-C(14)	-146.1(2)
C(8)-Cr(2)-C(13)-C(14)	122.0(5)
C(15)-Cr(2)-C(13)-C(14)	29.1(2)
C(12)-Cr(2)-C(13)-C(14)	131.9(3)
C(11)-Cr(2)-C(13)-C(14)	103.0(2)
C(10)-Cr(2)-C(13)-C(14)	65.9(2)
C(7)-Cr(2)-C(13)-C(12)	172.1(2)
C(9)-Cr(2)-C(13)-C(12)	82.0(2)
C(8)-Cr(2)-C(13)-C(12)	-9.9(6)
C(15)-Cr(2)-C(13)-C(12)	-102.8(2)
C(14)-Cr(2)-C(13)-C(12)	-131.9(3)
C(11)-Cr(2)-C(13)-C(12)	-28.9(2)
C(10)-Cr(2)-C(13)-C(12)	-66.0(2)
C(12)-C(13)-C(14)-C(15)	-0.2(5)
Cr(2)-C(13)-C(14)-C(15)	-54.1(3)
C(12)-C(13)-C(14)-Cr(2)	53.9(3)
C(7)-Cr(2)-C(14)-C(13)	128.6(2)
C(9)-Cr(2)-C(14)-C(13)	40.6(3)
C(8)-Cr(2)-C(14)-C(13)	-149.7(3)
C(15)-Cr(2)-C(14)-C(13)	-132.4(3)
C(12)-Cr(2)-C(14)-C(13)	-29.4(2)
C(11)-Cr(2)-C(14)-C(13)	-65.8(2)
C(10)-Cr(2)-C(14)-C(13)	-103.4(2)
C(7)-Cr(2)-C(14)-C(15)	-99.0(2)
C(9)-Cr(2)-C(14)-C(15)	173.0(2)
C(8)-Cr(2)-C(14)-C(15)	-17.3(4)
C(12)-Cr(2)-C(14)-C(15)	103.0(2)
C(11)-Cr(2)-C(14)-C(15)	66.6(2)
C(13)-Cr(2)-C(14)-C(15)	132.4(3)
C(10)-Cr(2)-C(14)-C(15)	29.0(2)
C(13)-C(14)-C(15)-C(10)	-0.4(5)
Cr(2)-C(14)-C(15)-C(10)	-55.0(3)
C(13)-C(14)-C(15)-Cr(2)	54.5(3)
C(11)-C(10)-C(15)-C(14)	0.4(5)
C(6)-C(10)-C(15)-C(14)	-178.6(3)
Cr(2)-C(10)-C(15)-C(14)	54.7(3)
C(11)-C(10)-C(15)-Cr(2)	-54.3(3)
C(6)-C(10)-C(15)-Cr(2)	126.7(3)
C(7)-Cr(2)-C(15)-C(14)	81.4(2)
C(9)-Cr(2)-C(15)-C(14)	-15.9(5)
C(8)-Cr(2)-C(15)-C(14)	170.5(2)
C(12)-Cr(2)-C(15)-C(14)	-65.6(2)
C(11)-Cr(2)-C(15)-C(14)	-102.0(2)
C(13)-Cr(2)-C(15)-C(14)	-28.6(2)
C(10)-Cr(2)-C(15)-C(14)	-132.5(3)
C(7)-Cr(2)-C(15)-C(10)	-146.1(2)
C(9)-Cr(2)-C(15)-C(10)	116.6(4)
C(8)-Cr(2)-C(15)-C(10)	-57.0(2)
C(12)-Cr(2)-C(15)-C(10)	66.9(2)
C(14)-Cr(2)-C(15)-C(10)	132.5(3)
C(11)-Cr(2)-C(15)-C(10)	30.44(19)
C(13)-Cr(2)-C(15)-C(10)	103.9(2)
O(6)-Ti(1)-C(16)-C(17)	-46.2(2)
C(24)-Ti(1)-C(16)-C(17)	171.8(2)
C(20)-Ti(1)-C(16)-C(17)	113.9(4)
C(25)-Ti(1)-C(16)-C(17)	-165.3(3)
C(21)-Ti(1)-C(16)-C(17)	-133.3(3)
C(23)-Ti(1)-C(16)-C(17)	-169.9(3)
Cl(1)-Ti(1)-C(16)-C(17)	66.3(3)
C(18)-Ti(1)-C(16)-C(17)	36.3(2)
C(19)-Ti(1)-C(16)-C(17)	77.0(3)
C(22)-Ti(1)-C(16)-C(17)	-129.3(2)
O(6)-Ti(1)-C(16)-C(20)	-160.0(2)
C(24)-Ti(1)-C(16)-C(20)	58.0(3)
C(25)-Ti(1)-C(16)-C(20)	80.8(3)
C(21)-Ti(1)-C(16)-C(20)	112.9(3)
C(23)-Ti(1)-C(16)-C(20)	76.2(3)
C(17)-Ti(1)-C(16)-C(20)	-113.9(4)
Cl(1)-Ti(1)-C(16)-C(20)	-47.5(3)
C(18)-Ti(1)-C(16)-C(20)	-77.5(3)
C(19)-Ti(1)-C(16)-C(20)	-36.8(2)
C(22)-Ti(1)-C(16)-C(20)	116.9(3)
C(20)-C(16)-C(17)-C(18)	2.5(4)
Ti(1)-C(16)-C(17)-C(18)	-64.1(3)
C(20)-C(16)-C(17)-Ti(1)	66.6(3)
O(6)-Ti(1)-C(17)-C(16)	134.0(2)
C(24)-Ti(1)-C(17)-C(16)	-11.8(4)
C(20)-Ti(1)-C(17)-C(16)	-38.7(2)

C(25)-Ti(1)-C(17)-C(16)	15.5(3)
C(21)-Ti(1)-C(17)-C(16)	51.5(3)
C(23)-Ti(1)-C(17)-C(16)	33.4(8)
Cl(1)-Ti(1)-C(17)-C(16)	-134.5(2)
C(18)-Ti(1)-C(17)-C(16)	-117.2(3)
C(19)-Ti(1)-C(17)-C(16)	-79.7(3)
C(22)-Ti(1)-C(17)-C(16)	77.9(3)
O(6)-Ti(1)-C(17)-C(18)	-108.9(2)
C(16)-Ti(1)-C(17)-C(18)	117.2(3)
C(24)-Ti(1)-C(17)-C(18)	105.3(3)
C(20)-Ti(1)-C(17)-C(18)	78.5(3)
C(25)-Ti(1)-C(17)-C(18)	132.7(3)
C(21)-Ti(1)-C(17)-C(18)	168.7(3)
C(23)-Ti(1)-C(17)-C(18)	150.5(7)
Cl(1)-Ti(1)-C(17)-C(18)	-17.3(3)
C(19)-Ti(1)-C(17)-C(18)	37.5(2)
C(22)-Ti(1)-C(17)-C(18)	-164.9(3)
C(16)-C(17)-C(18)-C(19)	-2.7(4)
Ti(1)-C(17)-C(18)-C(19)	-65.4(3)
C(16)-C(17)-C(18)-Ti(1)	62.7(2)
O(6)-Ti(1)-C(18)-C(17)	67.9(2)
C(16)-Ti(1)-C(18)-C(17)	-36.5(2)
C(24)-Ti(1)-C(18)-C(17)	-112.2(3)
C(20)-Ti(1)-C(18)-C(17)	-78.3(3)
C(25)-Ti(1)-C(18)-C(17)	-65.1(3)
C(21)-Ti(1)-C(18)-C(17)	-18.4(4)
C(23)-Ti(1)-C(18)-C(17)	-163.6(4)
Cl(1)-Ti(1)-C(18)-C(17)	164.3(2)
C(19)-Ti(1)-C(18)-C(17)	-115.1(4)
C(22)-Ti(1)-C(18)-C(17)	55.8(9)
O(6)-Ti(1)-C(18)-C(19)	-177.0(3)
C(16)-Ti(1)-C(18)-C(19)	78.5(3)
C(24)-Ti(1)-C(18)-C(19)	2.9(4)
C(20)-Ti(1)-C(18)-C(19)	36.7(3)
C(25)-Ti(1)-C(18)-C(19)	50.0(4)
C(21)-Ti(1)-C(18)-C(19)	96.7(4)
C(23)-Ti(1)-C(18)-C(19)	-48.6(5)
C(17)-Ti(1)-C(18)-C(19)	115.1(4)
Cl(1)-Ti(1)-C(18)-C(19)	-80.6(3)
C(22)-Ti(1)-C(18)-C(19)	170.9(7)
C(17)-C(18)-C(19)-C(20)	1.8(4)
Ti(1)-C(18)-C(19)-C(20)	-63.3(3)
C(17)-C(18)-C(19)-Ti(1)	65.2(2)
O(6)-Ti(1)-C(19)-C(20)	120.0(3)
C(16)-Ti(1)-C(19)-C(20)	37.8(2)
C(24)-Ti(1)-C(19)-C(20)	-61.5(3)
C(25)-Ti(1)-C(19)-C(20)	-26.6(3)
C(21)-Ti(1)-C(19)-C(20)	-8.3(4)
C(23)-Ti(1)-C(19)-C(20)	-85.7(3)
C(17)-Ti(1)-C(19)-C(20)	78.9(3)
Cl(1)-Ti(1)-C(19)-C(20)	-149.9(3)
C(18)-Ti(1)-C(19)-C(20)	116.4(4)
C(22)-Ti(1)-C(19)-C(20)	-58.5(5)
O(6)-Ti(1)-C(19)-C(18)	3.6(3)
C(16)-Ti(1)-C(19)-C(18)	-78.7(3)
C(24)-Ti(1)-C(19)-C(18)	-177.9(3)
C(20)-Ti(1)-C(19)-C(18)	-116.4(4)
C(25)-Ti(1)-C(19)-C(18)	-143.1(3)
C(21)-Ti(1)-C(19)-C(18)	-124.7(3)
C(23)-Ti(1)-C(19)-C(18)	157.9(3)
C(17)-Ti(1)-C(19)-C(18)	-37.5(2)
Cl(1)-Ti(1)-C(19)-C(18)	93.6(3)
C(22)-Ti(1)-C(19)-C(18)	-174.9(4)
C(18)-C(19)-C(20)-C(16)	-0.3(4)
Ti(1)-C(19)-C(20)-C(16)	-64.4(3)
C(18)-C(19)-C(20)-Ti(1)	64.1(3)
C(17)-C(16)-C(20)-C(19)	-1.4(4)
Ti(1)-C(16)-C(20)-C(19)	66.1(3)
C(17)-C(16)-C(20)-Ti(1)	-67.5(2)
O(6)-Ti(1)-C(20)-C(19)	-87.9(3)
C(16)-Ti(1)-C(20)-C(19)	-115.7(4)
C(24)-Ti(1)-C(20)-C(19)	120.1(3)
C(25)-Ti(1)-C(20)-C(19)	153.5(3)
C(21)-Ti(1)-C(20)-C(19)	174.1(3)
C(23)-Ti(1)-C(20)-C(19)	116.5(3)
C(17)-Ti(1)-C(20)-C(19)	-77.8(3)
Cl(1)-Ti(1)-C(20)-C(19)	31.1(3)
C(18)-Ti(1)-C(20)-C(19)	-36.8(2)

C(22)-Ti(1)-C(20)-C(19)	154.8(3)
O(6)-Ti(1)-C(20)-C(16)	27.8(3)
C(24)-Ti(1)-C(20)-C(16)	-124.2(3)
C(25)-Ti(1)-C(20)-C(16)	-90.8(3)
C(21)-Ti(1)-C(20)-C(16)	-70.2(3)
C(23)-Ti(1)-C(20)-C(16)	-127.8(3)
C(17)-Ti(1)-C(20)-C(16)	38.0(2)
Cl(1)-Ti(1)-C(20)-C(16)	146.8(2)
C(18)-Ti(1)-C(20)-C(16)	78.9(3)
C(19)-Ti(1)-C(20)-C(16)	115.7(4)
C(22)-Ti(1)-C(20)-C(16)	-89.5(3)
O(6)-Ti(1)-C(21)-C(25)	-173.0(3)
C(16)-Ti(1)-C(21)-C(25)	-70.6(3)
C(24)-Ti(1)-C(21)-C(25)	37.0(3)
C(20)-Ti(1)-C(21)-C(25)	-38.1(3)
C(23)-Ti(1)-C(21)-C(25)	78.4(3)
C(17)-Ti(1)-C(21)-C(25)	-96.7(3)
Cl(1)-Ti(1)-C(21)-C(25)	90.6(3)
C(18)-Ti(1)-C(21)-C(25)	-85.8(4)
C(19)-Ti(1)-C(21)-C(25)	-33.4(4)
C(22)-Ti(1)-C(21)-C(25)	115.5(4)
O(6)-Ti(1)-C(21)-C(22)	71.5(3)
C(16)-Ti(1)-C(21)-C(22)	173.9(3)
C(24)-Ti(1)-C(21)-C(22)	-78.5(3)
C(20)-Ti(1)-C(21)-C(22)	-153.6(3)
C(25)-Ti(1)-C(21)-C(22)	-115.5(4)
C(23)-Ti(1)-C(21)-C(22)	-37.0(3)
C(17)-Ti(1)-C(21)-C(22)	147.8(2)
Cl(1)-Ti(1)-C(21)-C(22)	-24.8(3)
C(18)-Ti(1)-C(21)-C(22)	158.8(3)
C(19)-Ti(1)-C(21)-C(22)	-148.9(3)
C(25)-C(21)-C(22)-C(23)	-1.0(4)
Ti(1)-C(21)-C(22)-C(23)	64.6(3)
C(25)-C(21)-C(22)-Ti(1)	-65.6(3)
O(6)-Ti(1)-C(22)-C(23)	140.5(3)
C(16)-Ti(1)-C(22)-C(23)	-122.6(3)
C(24)-Ti(1)-C(22)-C(23)	-37.2(3)
C(20)-Ti(1)-C(22)-C(23)	-80.0(4)
C(25)-Ti(1)-C(22)-C(23)	-78.5(3)
C(21)-Ti(1)-C(22)-C(23)	-115.4(4)
C(17)-Ti(1)-C(22)-C(23)	-163.3(3)
Cl(1)-Ti(1)-C(22)-C(23)	46.3(3)
C(18)-Ti(1)-C(22)-C(23)	152.9(7)
C(19)-Ti(1)-C(22)-C(23)	-40.8(6)
O(6)-Ti(1)-C(22)-C(21)	-104.1(3)
C(16)-Ti(1)-C(22)-C(21)	-7.2(3)
C(24)-Ti(1)-C(22)-C(21)	78.2(3)
C(20)-Ti(1)-C(22)-C(21)	35.4(4)
C(25)-Ti(1)-C(22)-C(21)	36.9(3)
C(23)-Ti(1)-C(22)-C(21)	115.4(4)
C(17)-Ti(1)-C(22)-C(21)	-47.9(3)
Cl(1)-Ti(1)-C(22)-C(21)	161.7(2)
C(18)-Ti(1)-C(22)-C(21)	-91.7(8)
C(19)-Ti(1)-C(22)-C(21)	74.6(5)
C(21)-C(22)-C(23)-C(24)	-0.8(4)
Ti(1)-C(22)-C(23)-C(24)	63.5(3)
C(21)-C(22)-C(23)-Ti(1)	-64.3(3)
O(6)-Ti(1)-C(23)-C(22)	-39.8(3)
C(16)-Ti(1)-C(23)-C(22)	83.5(4)
C(24)-Ti(1)-C(23)-C(22)	116.2(4)
C(20)-Ti(1)-C(23)-C(22)	122.6(3)
C(25)-Ti(1)-C(23)-C(22)	78.0(3)
C(21)-Ti(1)-C(23)-C(22)	37.5(3)
C(17)-Ti(1)-C(23)-C(22)	57.9(8)
Cl(1)-Ti(1)-C(23)-C(22)	-133.4(3)
C(18)-Ti(1)-C(23)-C(22)	-166.0(4)
C(19)-Ti(1)-C(23)-C(22)	161.9(3)
O(6)-Ti(1)-C(23)-C(24)	-156.0(3)
C(16)-Ti(1)-C(23)-C(24)	-32.8(4)
C(20)-Ti(1)-C(23)-C(24)	6.3(4)
C(25)-Ti(1)-C(23)-C(24)	-38.2(3)
C(21)-Ti(1)-C(23)-C(24)	-78.8(3)
C(17)-Ti(1)-C(23)-C(24)	-58.4(8)
Cl(1)-Ti(1)-C(23)-C(24)	110.4(3)
C(18)-Ti(1)-C(23)-C(24)	77.7(5)
C(19)-Ti(1)-C(23)-C(24)	45.6(4)
C(22)-Ti(1)-C(23)-C(24)	-116.2(4)
C(22)-C(23)-C(24)-C(25)	2.3(4)

Ti(1)-C(23)-C(24)-C(25)	67.4(3)
C(22)-C(23)-C(24)-Ti(1)	-65.1(3)
O(6)-Ti(1)-C(24)-C(25)	-80.3(4)
C(16)-Ti(1)-C(24)-C(25)	42.8(3)
C(20)-Ti(1)-C(24)-C(25)	71.9(3)
C(21)-Ti(1)-C(24)-C(25)	-36.2(3)
C(23)-Ti(1)-C(24)-C(25)	-113.7(4)
C(17)-Ti(1)-C(24)-C(25)	49.6(4)
Cl(1)-Ti(1)-C(24)-C(25)	-180.0(3)
C(18)-Ti(1)-C(24)-C(25)	99.8(3)
C(19)-Ti(1)-C(24)-C(25)	101.4(3)
C(22)-Ti(1)-C(24)-C(25)	-77.2(3)
O(6)-Ti(1)-C(24)-C(23)	33.4(4)
C(16)-Ti(1)-C(24)-C(23)	156.5(3)
C(20)-Ti(1)-C(24)-C(23)	-174.4(3)
C(25)-Ti(1)-C(24)-C(23)	113.7(4)
C(21)-Ti(1)-C(24)-C(23)	77.5(3)
C(17)-Ti(1)-C(24)-C(23)	163.3(3)
Cl(1)-Ti(1)-C(24)-C(23)	-66.3(3)
C(18)-Ti(1)-C(24)-C(23)	-146.5(3)
C(19)-Ti(1)-C(24)-C(23)	-144.9(3)
C(22)-Ti(1)-C(24)-C(23)	36.5(3)
C(22)-C(21)-C(25)-C(24)	2.4(5)
Ti(1)-C(21)-C(25)-C(24)	-63.6(3)
C(22)-C(21)-C(25)-Ti(1)	66.0(3)
C(23)-C(24)-C(25)-C(21)	-2.9(5)
Ti(1)-C(24)-C(25)-C(21)	64.7(3)
C(23)-C(24)-C(25)-Ti(1)	-67.6(3)
O(6)-Ti(1)-C(25)-C(21)	8.1(4)
C(16)-Ti(1)-C(25)-C(21)	105.7(3)
C(24)-Ti(1)-C(25)-C(21)	-116.6(4)
C(20)-Ti(1)-C(25)-C(21)	141.3(3)
C(23)-Ti(1)-C(25)-C(21)	-78.3(3)
C(17)-Ti(1)-C(25)-C(21)	96.9(3)
Cl(1)-Ti(1)-C(25)-C(21)	-116.6(3)
C(18)-Ti(1)-C(25)-C(21)	129.9(3)
C(19)-Ti(1)-C(25)-C(21)	156.3(3)
C(22)-Ti(1)-C(25)-C(21)	-37.5(3)
O(6)-Ti(1)-C(25)-C(24)	124.7(3)
C(16)-Ti(1)-C(25)-C(24)	-137.7(3)
C(20)-Ti(1)-C(25)-C(24)	-102.1(3)
C(21)-Ti(1)-C(25)-C(24)	116.6(4)
C(23)-Ti(1)-C(25)-C(24)	38.3(3)
C(17)-Ti(1)-C(25)-C(24)	-146.5(3)
Cl(1)-Ti(1)-C(25)-C(24)	0.0(4)
C(18)-Ti(1)-C(25)-C(24)	-113.5(3)
C(19)-Ti(1)-C(25)-C(24)	-87.0(3)
C(22)-Ti(1)-C(25)-C(24)	79.1(3)

Appendix 7

Crystallographic data of Complex 23

Table 1. Crystal data and structure refinement for Complex **23**.

Identification code	db78a1_pn	
Empirical formula	C_{30} H_{28} Fe Mn_2 O_6	
Formula weight	650.25	
Temperature	293(2) K	
Wavelength	0.71073 Å	
Crystal system	Monoclinic	
Space group	P n	
Unit cell dimensions	a = 11.9498(11) Å	a= 90°.
	b = 9.7620(9) Å	b= 115.7030(10)°.
	c = 12.9245(12) Å	g = 90°.
Volume	1358.5(2) $Å^3$	
Z	2	
Density (calculated)	1.590 Mg/m^3	
Absorption coefficient	1.485 mm^{-1}	
F(000)	664	
Crystal size	0.36 x 0.30 x 0.015 mm^3	
Theta range for data collection	2.72 to 26.44°.	
Index ranges	-14<=h<=12, -11<=k<=12, -15<=l<=12	
Reflections collected	6873	
Independent reflections	3294 [R(int) = 0.0264]	
Completeness to theta = 25.00°	99.2 %	
Absorption correction	Semi-empirical from equivalents	
Max. and min. transmission	0.978 and 0.590	
Refinement method	Full-matrix least-squares on F^2	
Data / restraints / parameters	3294 / 2 / 371	
Goodness-of-fit on F^2	1.066	
Final R indices [I>2σ(I)]	R1 = 0.0317, wR2 = 0.0779	
R indices (all data)	R1 = 0.0384, wR2 = 0.0829	
Absolute structure parameter	0.53(3)	
Extinction coefficient	0	
Largest diff. peak and hole	0.295 and -0.303 e.$Å^{-3}$	

Table 2. Atomic coordinates (x 10^4) and equivalent isotropic displacement parameters (Å^{2}x 10^3) for Complex **23**. U(eq) is defined as one third of the trace of the orthogonalized U^{ij} tensor.

	x	y	z	U(eq)
Mn(1)	5227(1)	8821(1)	5965(1)	53(1)
C(1)	6903(4)	8781(4)	6121(4)	45(1)
O(1)	7873(3)	8115(3)	6922(3)	61(1)
C(2)	4513(5)	8856(6)	4465(5)	66(1)
O(2)	3938(4)	8823(5)	3462(4)	96(2)
C(3)	5063(5)	7017(6)	5903(5)	68(1)
O(3)	4902(5)	5838(4)	5804(5)	96(1)
C(4)	5826(5)	10283(6)	7336(5)	75(2)
C(5)	5260(7)	9185(6)	7634(6)	76(2)
C(6)	4051(6)	9127(6)	6791(6)	75(2)
C(7)	3837(5)	10146(6)	5995(5)	73(2)
C(8)	4954(7)	10898(6)	6326(6)	79(2)
Mn(2)	10481(1)	5899(1)	4946(1)	53(1)
C(9)	8777(4)	6120(4)	4655(4)	44(1)
O(9)	8129(3)	5430(3)	5109(3)	59(1)
C(10)	11087(5)	5953(4)	6457(5)	60(1)
O(10)	11548(5)	6037(4)	7441(4)	90(1)
C(11)	10750(4)	7673(5)	4961(5)	59(1)
O(11)	11027(4)	8823(4)	5005(4)	83(1)
C(12)	9906(6)	4317(10)	3685(8)	106(3)
C(13)	10814(8)	3777(7)	4697(8)	94(2)
C(14)	11893(6)	4527(8)	4960(7)	96(2)
C(15)	11654(7)	5499(9)	4120(8)	100(2)
C(16)	10435(8)	5373(9)	3333(6)	96(2)
Fe(1)	7442(1)	8953(1)	3976(1)	39(1)
C(17)	7391(4)	9586(4)	5469(4)	46(1)
C(18)	6708(5)	10490(4)	4527(5)	61(1)
C(19)	7521(7)	11047(5)	4124(6)	69(2)
C(20)	8694(5)	10494(5)	4754(5)	59(1)
C(21)	8636(5)	9600(5)	5580(4)	47(1)
C(22)	7860(4)	6956(4)	3767(4)	41(1)
C(23)	6575(4)	7113(4)	3497(4)	41(1)

C(24)	6014(4)	8063(5)	2588(4)	48(1)
C(25)	6939(5)	8517(6)	2281(4)	55(1)
C(26)	8066(4)	7870(4)	2984(3)	48(1)
C(27)	7767(5)	7230(6)	7766(5)	74(2)
C(28)	9007(6)	6717(7)	8505(5)	87(2)
C(29)	8679(6)	4346(6)	5944(6)	75(2)
C(30)	7646(7)	3737(6)	6144(7)	83(2)
Fe(2)	8285(6)	5994(5)	6802(5)	25(1)
C(31)	9720(40)	6870(40)	8200(30)	25(1)
C(32)	9190(40)	7810(40)	7260(30)	25(1)
C(33)	6940(40)	4480(40)	6010(30)	25(1)
C(34)	7030(40)	5340(40)	5140(30)	25(1)

Table 3. Bond lengths [Å] and angles [°] for Complex **23**.

Mn(1)-C(2)	1.747(5)	C(9)-C(22)	1.446(6)
Mn(1)-C(3)	1.770(6)	O(9)-C(34)	1.33(4)
Mn(1)-C(1)	1.924(5)	O(9)-C(29)	1.450(6)
Mn(1)-C(7)	2.118(5)	O(9)-Fe(2)	2.184(7)
Mn(1)-C(6)	2.122(5)	C(10)-O(10)	1.149(7)
Mn(1)-C(8)	2.137(5)	C(11)-O(11)	1.164(6)
Mn(1)-C(4)	2.142(5)	C(12)-C(16)	1.386(11)
Mn(1)-C(5)	2.170(6)	C(12)-C(13)	1.391(12)
C(1)-O(1)	1.340(5)	C(12)-H(12)	0.9300
C(1)-C(17)	1.447(6)	C(13)-C(14)	1.390(10)
O(1)-C(27)	1.439(5)	C(13)-H(13)	0.9300
O(1)-C(32)	1.46(4)	C(14)-C(15)	1.375(10)
O(1)-Fe(2)	2.149(6)	C(14)-H(14)	0.9300
C(2)-O(2)	1.175(7)	C(15)-C(16)	1.374(10)
C(3)-O(3)	1.165(6)	C(15)-H(15)	0.9300
C(4)-C(8)	1.403(9)	C(16)-H(16)	0.9300
C(4)-C(5)	1.407(8)	Fe(1)-C(18)	2.018(4)
C(4)-H(4)	0.9300	Fe(1)-C(23)	2.031(4)
C(5)-C(6)	1.383(9)	Fe(1)-C(26)	2.037(4)
C(5)-H(5)	0.9300	Fe(1)-C(21)	2.041(5)
C(6)-C(7)	1.373(8)	Fe(1)-C(25)	2.049(5)
C(6)-H(6)	0.9300	Fe(1)-C(20)	2.052(5)
C(7)-C(8)	1.417(8)	Fe(1)-C(19)	2.052(5)
C(7)-H(7)	0.9300	Fe(1)-C(17)	2.052(4)
C(8)-H(8)	0.9300	Fe(1)-C(24)	2.057(5)
Mn(2)-C(11)	1.761(5)	Fe(1)-C(22)	2.059(4)
Mn(2)-C(10)	1.764(6)	C(17)-C(21)	1.432(6)
Mn(2)-C(9)	1.916(5)	C(17)-C(18)	1.437(7)
Mn(2)-C(16)	2.125(6)	C(18)-C(19)	1.396(8)
Mn(2)-C(12)	2.131(6)	C(18)-H(18)	0.9300
Mn(2)-C(15)	2.134(6)	C(19)-C(20)	1.389(9)
Mn(2)-C(14)	2.149(6)	C(19)-H(19)	0.9300
Mn(2)-C(13)	2.159(6)	C(20)-C(21)	1.403(7)
C(9)-O(9)	1.338(5)	C(20)-H(20)	0.9300

C(21)-H(21)	0.9300
C(22)-C(23)	1.427(6)
C(22)-C(26)	1.449(6)
C(23)-C(24)	1.416(6)
C(23)-H(23)	0.9300
C(24)-C(25)	1.399(7)
C(24)-H(24)	0.9300
C(25)-C(26)	1.406(6)
C(25)-H(25)	0.9300
C(26)-H(26)	0.9300
C(27)-C(28)	1.460(8)
C(27)-H(27A)	0.9700
C(27)-H(27B)	0.9700
C(28)-H(28A)	0.9600
C(28)-H(28B)	0.9600
C(28)-H(28C)	0.9600
C(29)-C(30)	1.489(8)
C(29)-H(29A)	0.9700
C(29)-H(29B)	0.9700
C(30)-H(30A)	0.9600
C(30)-H(30B)	0.9600
C(30)-H(30C)	0.9600
Fe(2)-C(32)	2.03(4)
Fe(2)-C(31)	2.06(4)
Fe(2)-C(33)	2.09(4)
Fe(2)-C(34)	2.11(4)
C(31)-C(32)	1.43(5)
C(33)-C(34)	1.44(5)

C(2)-Mn(1)-C(3)	88.8(3)
C(2)-Mn(1)-C(1)	95.8(2)
C(3)-Mn(1)-C(1)	94.2(2)
C(2)-Mn(1)-C(7)	90.0(2)
C(3)-Mn(1)-C(7)	122.4(3)
C(1)-Mn(1)-C(7)	143.0(2)
C(2)-Mn(1)-C(6)	116.4(3)
C(3)-Mn(1)-C(6)	94.5(3)
C(1)-Mn(1)-C(6)	146.7(2)
C(7)-Mn(1)-C(6)	37.8(2)
C(2)-Mn(1)-C(8)	100.2(3)
C(3)-Mn(1)-C(8)	158.3(3)
C(1)-Mn(1)-C(8)	104.3(2)
C(7)-Mn(1)-C(8)	38.9(2)
C(6)-Mn(1)-C(8)	63.9(2)
C(2)-Mn(1)-C(4)	137.1(3)
C(3)-Mn(1)-C(4)	133.7(3)
C(1)-Mn(1)-C(4)	88.15(19)
C(7)-Mn(1)-C(4)	64.0(2)
C(6)-Mn(1)-C(4)	63.1(2)
C(8)-Mn(1)-C(4)	38.3(2)
C(2)-Mn(1)-C(5)	152.9(3)
C(3)-Mn(1)-C(5)	99.3(3)
C(1)-Mn(1)-C(5)	109.2(2)
C(7)-Mn(1)-C(5)	63.8(2)
C(6)-Mn(1)-C(5)	37.6(2)
C(8)-Mn(1)-C(5)	64.3(2)
C(4)-Mn(1)-C(5)	38.1(2)
O(1)-C(1)-C(17)	106.3(4)
O(1)-C(1)-Mn(1)	127.1(3)
C(17)-C(1)-Mn(1)	126.3(3)
C(1)-O(1)-C(27)	123.1(4)
C(1)-O(1)-C(32)	141.8(14)
C(27)-O(1)-C(32)	94.8(14)
C(1)-O(1)-Fe(2)	124.0(3)
C(27)-O(1)-Fe(2)	64.8(3)
C(32)-O(1)-Fe(2)	65.1(14)
O(2)-C(2)-Mn(1)	173.6(5)
O(3)-C(3)-Mn(1)	176.3(6)
C(8)-C(4)-C(5)	109.3(6)
C(8)-C(4)-Mn(1)	70.7(3)
C(5)-C(4)-Mn(1)	72.0(3)
C(8)-C(4)-H(4)	125.4

C(5)-C(4)-H(4)	125.4
Mn(1)-C(4)-H(4)	123.5
C(6)-C(5)-C(4)	106.1(6)
C(6)-C(5)-Mn(1)	69.3(3)
C(4)-C(5)-Mn(1)	69.9(3)
C(6)-C(5)-H(5)	127.0
C(4)-C(5)-H(5)	127.0
Mn(1)-C(5)-H(5)	125.4
C(7)-C(6)-C(5)	110.6(6)
C(7)-C(6)-Mn(1)	71.0(3)
C(5)-C(6)-Mn(1)	73.1(3)
C(7)-C(6)-H(6)	124.7
C(5)-C(6)-H(6)	124.7
Mn(1)-C(6)-H(6)	122.8
C(6)-C(7)-C(8)	107.7(6)
C(6)-C(7)-Mn(1)	71.3(3)
C(8)-C(7)-Mn(1)	71.3(3)
C(6)-C(7)-H(7)	126.2
C(8)-C(7)-H(7)	126.2
Mn(1)-C(7)-H(7)	123.0
C(4)-C(8)-C(7)	106.4(6)
C(4)-C(8)-Mn(1)	71.1(3)
C(7)-C(8)-Mn(1)	69.9(3)
C(4)-C(8)-H(8)	126.8
C(7)-C(8)-H(8)	126.8
Mn(1)-C(8)-H(8)	123.9
C(11)-Mn(2)-C(10)	88.5(2)
C(11)-Mn(2)-C(9)	93.73(19)
C(10)-Mn(2)-C(9)	96.0(2)
C(11)-Mn(2)-C(16)	100.1(3)
C(10)-Mn(2)-C(16)	156.4(3)
C(9)-Mn(2)-C(16)	105.2(3)
C(11)-Mn(2)-C(12)	135.9(4)
C(10)-Mn(2)-C(12)	135.2(4)
C(9)-Mn(2)-C(12)	88.2(2)
C(16)-Mn(2)-C(12)	38.0(3)
C(11)-Mn(2)-C(15)	91.6(3)
C(10)-Mn(2)-C(15)	121.0(3)
C(9)-Mn(2)-C(15)	142.7(3)
C(16)-Mn(2)-C(15)	37.6(3)
C(12)-Mn(2)-C(15)	63.2(3)
C(11)-Mn(2)-C(14)	118.3(3)
C(10)-Mn(2)-C(14)	93.7(3)
C(9)-Mn(2)-C(14)	146.7(3)
C(16)-Mn(2)-C(14)	62.8(3)
C(12)-Mn(2)-C(14)	63.0(3)
C(15)-Mn(2)-C(14)	37.5(3)
C(11)-Mn(2)-C(13)	154.2(3)
C(10)-Mn(2)-C(13)	100.3(3)
C(9)-Mn(2)-C(13)	109.2(3)
C(16)-Mn(2)-C(13)	63.3(3)
C(12)-Mn(2)-C(13)	37.8(3)
C(15)-Mn(2)-C(13)	63.0(3)
C(14)-Mn(2)-C(13)	37.6(3)
O(9)-C(9)-C(22)	104.4(4)
O(9)-C(9)-Mn(2)	128.7(3)
C(22)-C(9)-Mn(2)	126.4(3)
C(34)-O(9)-C(9)	144.1(16)
C(34)-O(9)-C(29)	93.7(16)
C(9)-O(9)-C(29)	122.1(4)
C(34)-O(9)-Fe(2)	69.0(16)
C(9)-O(9)-Fe(2)	119.9(3)
C(29)-O(9)-Fe(2)	67.9(3)
O(10)-C(10)-Mn(2)	175.4(6)
O(11)-C(11)-Mn(2)	174.7(4)
C(16)-C(12)-C(13)	108.0(7)
C(16)-C(12)-Mn(2)	70.8(4)
C(13)-C(12)-Mn(2)	72.2(4)
C(16)-C(12)-H(12)	126.0
C(13)-C(12)-H(12)	126.0
Mn(2)-C(12)-H(12)	122.7
C(14)-C(13)-C(12)	107.0(8)

C(14)-C(13)-Mn(2)	70.8(4)
C(12)-C(13)-Mn(2)	70.0(4)
C(14)-C(13)-H(13)	126.5
C(12)-C(13)-H(13)	126.5
Mn(2)-C(13)-H(13)	124.4
C(15)-C(14)-C(13)	108.5(7)
C(15)-C(14)-Mn(2)	70.7(4)
C(13)-C(14)-Mn(2)	71.6(4)
C(15)-C(14)-H(14)	125.7
C(13)-C(14)-H(14)	125.7
Mn(2)-C(14)-H(14)	123.6
C(16)-C(15)-C(14)	108.3(7)
C(16)-C(15)-Mn(2)	70.8(3)
C(14)-C(15)-Mn(2)	71.8(4)
C(16)-C(15)-H(15)	125.9
C(14)-C(15)-H(15)	125.9
Mn(2)-C(15)-H(15)	123.1
C(15)-C(16)-C(12)	108.1(7)
C(15)-C(16)-Mn(2)	71.6(4)
C(12)-C(16)-Mn(2)	71.2(4)
C(15)-C(16)-H(16)	125.9
C(12)-C(16)-H(16)	125.9
Mn(2)-C(16)-H(16)	123.0
C(18)-Fe(1)-C(23)	121.5(2)
C(18)-Fe(1)-C(26)	160.45(18)
C(23)-Fe(1)-C(26)	68.08(17)
C(18)-Fe(1)-C(21)	68.3(2)
C(23)-Fe(1)-C(21)	128.54(19)
C(26)-Fe(1)-C(21)	120.96(18)
C(18)-Fe(1)-C(25)	124.1(2)
C(23)-Fe(1)-C(25)	67.4(2)
C(26)-Fe(1)-C(25)	40.25(18)
C(21)-Fe(1)-C(25)	154.36(19)
C(18)-Fe(1)-C(20)	67.5(2)
C(23)-Fe(1)-C(20)	164.8(2)
C(26)-Fe(1)-C(20)	107.5(2)
C(21)-Fe(1)-C(20)	40.1(2)
C(25)-Fe(1)-C(20)	119.3(2)
C(18)-Fe(1)-C(19)	40.1(2)
C(23)-Fe(1)-C(19)	155.0(2)
C(26)-Fe(1)-C(19)	124.1(2)
C(21)-Fe(1)-C(19)	67.2(2)
C(25)-Fe(1)-C(19)	106.7(2)
C(20)-Fe(1)-C(19)	39.6(3)
C(18)-Fe(1)-C(17)	41.34(19)
C(23)-Fe(1)-C(17)	109.52(17)
C(26)-Fe(1)-C(17)	156.46(18)
C(21)-Fe(1)-C(17)	40.95(17)
C(25)-Fe(1)-C(17)	162.4(2)
C(20)-Fe(1)-C(17)	68.3(2)
C(19)-Fe(1)-C(17)	68.3(2)
C(18)-Fe(1)-C(24)	107.4(2)
C(23)-Fe(1)-C(24)	40.53(18)
C(26)-Fe(1)-C(24)	67.87(18)
C(21)-Fe(1)-C(24)	165.19(19)
C(25)-Fe(1)-C(24)	39.8(2)
C(20)-Fe(1)-C(24)	152.9(2)
C(19)-Fe(1)-C(24)	119.3(3)
C(17)-Fe(1)-C(24)	126.57(19)
C(18)-Fe(1)-C(22)	156.61(18)
C(23)-Fe(1)-C(22)	40.85(16)
C(26)-Fe(1)-C(22)	41.42(16)
C(21)-Fe(1)-C(22)	108.89(18)
C(25)-Fe(1)-C(22)	68.81(19)
C(20)-Fe(1)-C(22)	126.3(2)
C(19)-Fe(1)-C(22)	162.1(2)
C(17)-Fe(1)-C(22)	121.09(18)
C(24)-Fe(1)-C(22)	69.04(18)
C(21)-C(17)-C(18)	105.2(4)
C(21)-C(17)-C(1)	127.7(4)
C(18)-C(17)-C(1)	127.1(4)
C(21)-C(17)-Fe(1)	69.1(2)

C(18)-C(17)-Fe(1)	68.0(2)
C(1)-C(17)-Fe(1)	124.6(3)
C(19)-C(18)-C(17)	108.9(5)
C(19)-C(18)-Fe(1)	71.3(3)
C(17)-C(18)-Fe(1)	70.6(2)
C(19)-C(18)-H(18)	125.5
C(17)-C(18)-H(18)	125.5
Fe(1)-C(18)-H(18)	124.2
C(20)-C(19)-C(18)	108.6(5)
C(20)-C(19)-Fe(1)	70.2(3)
C(18)-C(19)-Fe(1)	68.6(3)
C(20)-C(19)-H(19)	125.7
C(18)-C(19)-H(19)	125.7
Fe(1)-C(19)-H(19)	127.0
C(19)-C(20)-C(21)	108.5(5)
C(19)-C(20)-Fe(1)	70.2(3)
C(21)-C(20)-Fe(1)	69.5(3)
C(19)-C(20)-H(20)	125.8
C(21)-C(20)-H(20)	125.8
Fe(1)-C(20)-H(20)	126.1
C(20)-C(21)-C(17)	108.8(5)
C(20)-C(21)-Fe(1)	70.4(3)
C(17)-C(21)-Fe(1)	69.9(3)
C(20)-C(21)-H(21)	125.6
C(17)-C(21)-H(21)	125.6
Fe(1)-C(21)-H(21)	125.7
C(23)-C(22)-C(9)	128.2(4)
C(23)-C(22)-C(26)	104.7(4)
C(9)-C(22)-C(26)	127.0(4)
C(23)-C(22)-Fe(1)	68.5(2)
C(9)-C(22)-Fe(1)	125.0(3)
C(26)-C(22)-Fe(1)	68.5(2)
C(24)-C(23)-C(22)	110.2(4)
C(24)-C(23)-Fe(1)	70.7(3)
C(22)-C(23)-Fe(1)	70.6(2)
C(24)-C(23)-H(23)	124.9
C(22)-C(23)-H(23)	124.9
Fe(1)-C(23)-H(23)	125.4
C(25)-C(24)-C(23)	107.1(4)
C(25)-C(24)-Fe(1)	69.8(3)
C(23)-C(24)-Fe(1)	68.8(3)
C(25)-C(24)-H(24)	126.4
C(23)-C(24)-H(24)	126.4
Fe(1)-C(24)-H(24)	126.5
C(24)-C(25)-C(26)	109.1(4)
C(24)-C(25)-Fe(1)	70.4(3)
C(26)-C(25)-Fe(1)	69.4(2)
C(24)-C(25)-H(25)	125.4
C(26)-C(25)-H(25)	125.4
Fe(1)-C(25)-H(25)	126.4
C(25)-C(26)-C(22)	108.8(4)
C(25)-C(26)-Fe(1)	70.3(2)
C(22)-C(26)-Fe(1)	70.1(2)
C(25)-C(26)-H(26)	125.6
C(22)-C(26)-H(26)	125.6
Fe(1)-C(26)-H(26)	125.5
O(1)-C(27)-C(28)	107.7(5)
O(1)-C(27)-H(27A)	110.2
C(28)-C(27)-H(27A)	110.2
O(1)-C(27)-H(27B)	110.2
C(28)-C(27)-H(27B)	110.2
H(27A)-C(27)-H(27B)	108.5
C(27)-C(28)-H(28A)	109.5
C(27)-C(28)-H(28B)	109.5
H(28A)-C(28)-H(28B)	109.5
C(27)-C(28)-H(28C)	109.5
H(28A)-C(28)-H(28C)	109.5
H(28B)-C(28)-H(28C)	109.5
O(9)-C(29)-C(30)	106.1(5)
O(9)-C(29)-H(29A)	110.5
C(30)-C(29)-H(29A)	110.5
C(34)-C(29)-H(29A)	119.5

O(9)-C(29)-H(29B)	110.5
C(30)-C(29)-H(29B)	110.5
H(29A)-C(29)-H(29B)	108.7
C(29)-C(30)-H(30A)	109.5
C(29)-C(30)-H(30B)	109.5
H(30A)-C(30)-H(30B)	109.5
C(29)-C(30)-H(30C)	109.5
H(30A)-C(30)-H(30C)	109.5
H(30B)-C(30)-H(30C)	109.5

Symmetry transformations used to generate equivalent atoms:

Table 4. Anisotropic displacement parameters ($Å^2$x 10^3)for Complex **23**. The anisotropic displacement factor exponent takes the form: -2p^2[$h^2a^{*2}U^{11}$ + ... + 2 h k a* b* U^{12}]

	U^{11}	U^{22}	U^{33}	U^{23}	U^{13}	U^{12}
Mn(1)	40(1)	71(1)	50(1)	-11(1)	22(1)	0(1)
C(1)	47(3)	50(2)	40(2)	-4(2)	22(2)	3(2)
O(1)	48(2)	80(2)	58(2)	11(2)	27(2)	4(2)
C(2)	43(3)	95(4)	55(3)	-8(3)	18(3)	14(2)
O(2)	56(3)	160(5)	59(3)	-5(2)	12(2)	18(2)
C(3)	53(3)	92(4)	61(3)	-12(3)	26(2)	-6(3)
O(3)	97(4)	79(3)	99(3)	-21(2)	31(3)	-25(2)
C(4)	58(3)	99(4)	78(4)	-41(3)	38(3)	-7(3)
C(5)	82(5)	95(4)	69(4)	-12(3)	49(4)	-1(3)
C(6)	59(4)	100(4)	81(4)	-8(3)	44(3)	0(3)
C(7)	55(3)	100(4)	70(4)	-13(3)	34(3)	15(3)
C(8)	89(5)	74(4)	95(5)	-10(3)	59(4)	7(3)
Mn(2)	38(1)	60(1)	57(1)	-8(1)	17(1)	5(1)
C(9)	48(3)	40(2)	47(2)	-8(2)	23(2)	-2(2)
O(9)	55(2)	54(2)	72(2)	13(2)	32(2)	5(2)
C(10)	50(3)	50(3)	64(4)	-6(2)	12(3)	4(2)
O(10)	91(3)	85(3)	61(3)	-1(2)	4(2)	-7(2)
C(11)	35(3)	70(3)	64(3)	-5(3)	14(2)	-5(2)
O(11)	60(3)	73(2)	104(3)	3(2)	23(3)	-17(2)
C(12)	62(4)	122(6)	123(6)	-81(5)	30(4)	-3(4)
C(13)	106(6)	75(4)	111(6)	-12(4)	58(5)	22(4)
C(14)	55(4)	117(5)	102(5)	-24(5)	22(3)	32(4)
C(15)	81(5)	123(6)	123(6)	-24(5)	69(5)	6(4)
C(16)	106(6)	124(6)	64(4)	-12(4)	41(4)	37(5)
Fe(1)	39(1)	38(1)	41(1)	2(1)	19(1)	-1(1)
C(17)	47(3)	42(2)	54(3)	-10(2)	27(2)	-4(2)
C(18)	76(3)	43(2)	84(4)	5(2)	53(3)	10(2)
C(19)	99(5)	42(2)	79(4)	8(2)	52(4)	5(3)
C(20)	62(3)	49(3)	69(3)	-8(2)	33(3)	-21(3)
C(21)	49(3)	47(2)	46(2)	-9(2)	21(2)	-5(2)
C(22)	33(2)	39(2)	46(2)	-7(2)	13(2)	-1(2)
C(23)	39(2)	39(2)	46(2)	-3(2)	18(2)	-7(2)

C(24)	36(2)	54(3)	48(3)	-1(2)	12(2)	0(2)
C(25)	52(3)	74(3)	34(2)	7(2)	15(2)	5(2)
C(26)	48(3)	57(2)	41(2)	-2(2)	22(2)	-2(2)
C(27)	61(3)	86(4)	73(3)	27(3)	28(3)	10(3)
C(28)	64(4)	106(5)	71(4)	23(3)	12(3)	-3(3)
C(29)	74(4)	63(3)	91(4)	30(3)	38(3)	13(3)
C(30)	88(5)	65(3)	105(5)	22(3)	51(4)	0(3)

Table 5. Hydrogen coordinates (x 10^4) and isotropic displacement parameters ($Å^2$x 10^3) for Complex **23**.

	x	y	z	U(eq)
H(4)	6647	10558	7743	90
H(5)	5626	8614	8270	91
H(6)	3464	8486	6766	90
H(7)	3093	10313	5353	87
H(8)	5084	11649	5950	95
H(12)	9087	4021	3311	127
H(13)	10718	3052	5119	112
H(14)	12649	4393	5596	115
H(15)	12221	6133	4091	120
H(16)	10034	5905	2677	115
H(18)	5863	10674	4234	74
H(19)	7312	11682	3533	83
H(20)	9399	10684	4647	70
H(21)	9298	9099	6111	56
H(23)	6165	6657	3864	50
H(24)	5186	8334	2258	58
H(25)	6827	9146	1704	66
H(26)	8820	8006	2951	57
H(27A)	7213	6473	7391	88
H(27B)	7434	7733	8217	88
H(28A)	8953	6057	9032	130
H(28B)	9526	7465	8926	130
H(28C)	9357	6292	8042	130
H(29A)	9313	4712	6654	91
H(29B)	9054	3660	5650	91
H(30A)	7927	2907	6579	125
H(30B)	6960	3537	5419	125
H(30C)	7386	4375	6562	125

Table 6. Torsion angles [°] for Complex **23**.

C(2)-Mn(1)-C(1)-O(1)	-144.7(4)	C(2)-Mn(1)-C(4)-C(8)	19.5(5)
C(3)-Mn(1)-C(1)-O(1)	-55.5(4)	C(3)-Mn(1)-C(4)-C(8)	-149.8(4)
C(7)-Mn(1)-C(1)-O(1)	117.6(4)	C(1)-Mn(1)-C(4)-C(8)	116.1(4)
C(6)-Mn(1)-C(1)-O(1)	49.3(6)	C(7)-Mn(1)-C(4)-C(8)	-38.8(4)
C(8)-Mn(1)-C(1)-O(1)	113.2(4)	C(6)-Mn(1)-C(4)-C(8)	-81.2(4)
C(4)-Mn(1)-C(1)-O(1)	78.2(4)	C(5)-Mn(1)-C(4)-C(8)	-118.8(5)
C(5)-Mn(1)-C(1)-O(1)	45.9(4)	C(2)-Mn(1)-C(4)-C(5)	138.3(4)
C(2)-Mn(1)-C(1)-C(17)	42.6(4)	C(3)-Mn(1)-C(4)-C(5)	-31.0(5)
C(3)-Mn(1)-C(1)-C(17)	131.8(4)	C(1)-Mn(1)-C(4)-C(5)	-125.1(4)
C(7)-Mn(1)-C(1)-C(17)	-55.2(5)	C(7)-Mn(1)-C(4)-C(5)	80.0(4)
C(6)-Mn(1)-C(1)-C(17)	-123.4(4)	C(6)-Mn(1)-C(4)-C(5)	37.6(4)
C(8)-Mn(1)-C(1)-C(17)	-59.5(4)	C(8)-Mn(1)-C(4)-C(5)	118.8(5)
C(4)-Mn(1)-C(1)-C(17)	-94.6(4)	C(8)-C(4)-C(5)-C(6)	0.9(6)
C(5)-Mn(1)-C(1)-C(17)	-126.9(4)	Mn(1)-C(4)-C(5)-C(6)	-60.2(4)
C(17)-C(1)-O(1)-C(27)	178.3(4)	C(8)-C(4)-C(5)-Mn(1)	61.2(4)
Mn(1)-C(1)-O(1)-C(27)	4.4(6)	C(2)-Mn(1)-C(5)-C(6)	20.5(7)
C(17)-C(1)-O(1)-C(32)	-10(2)	C(3)-Mn(1)-C(5)-C(6)	-85.3(4)
Mn(1)-C(1)-O(1)-C(32)	176(2)	C(1)-Mn(1)-C(5)-C(6)	176.9(4)
C(17)-C(1)-O(1)-Fe(2)	-101.7(4)	C(7)-Mn(1)-C(5)-C(6)	36.4(4)
Mn(1)-C(1)-O(1)-Fe(2)	84.4(4)	C(8)-Mn(1)-C(5)-C(6)	79.9(4)
C(3)-Mn(1)-C(2)-O(2)	60(4)	C(4)-Mn(1)-C(5)-C(6)	116.9(6)
C(1)-Mn(1)-C(2)-O(2)	154(4)	C(2)-Mn(1)-C(5)-C(4)	-96.5(6)
C(7)-Mn(1)-C(2)-O(2)	-63(4)	C(3)-Mn(1)-C(5)-C(4)	157.8(4)
C(6)-Mn(1)-C(2)-O(2)	-35(4)	C(1)-Mn(1)-C(5)-C(4)	60.0(4)
C(8)-Mn(1)-C(2)-O(2)	-100(4)	C(7)-Mn(1)-C(5)-C(4)	-80.5(4)
C(4)-Mn(1)-C(2)-O(2)	-112(4)	C(6)-Mn(1)-C(5)-C(4)	-116.9(6)
C(5)-Mn(1)-C(2)-O(2)	-48(5)	C(8)-Mn(1)-C(5)-C(4)	-37.1(4)
C(2)-Mn(1)-C(3)-O(3)	-25(9)	C(4)-C(5)-C(6)-C(7)	-0.8(6)
C(1)-Mn(1)-C(3)-O(3)	-120(9)	Mn(1)-C(5)-C(6)-C(7)	-61.4(4)
C(7)-Mn(1)-C(3)-O(3)	65(9)	C(4)-C(5)-C(6)-Mn(1)	60.6(4)
C(6)-Mn(1)-C(3)-O(3)	92(9)	C(2)-Mn(1)-C(6)-C(7)	-50.1(4)
C(8)-Mn(1)-C(3)-O(3)	91(9)	C(3)-Mn(1)-C(6)-C(7)	-141.0(4)
C(4)-Mn(1)-C(3)-O(3)	148(8)	C(1)-Mn(1)-C(6)-C(7)	114.3(5)
C(5)-Mn(1)-C(3)-O(3)	129(9)	C(8)-Mn(1)-C(6)-C(7)	38.5(4)

C(4)-Mn(1)-C(6)-C(7)	81.5(4)	C(3)-Mn(1)-C(8)-C(7)	-36.1(10)
C(5)-Mn(1)-C(6)-C(7)	119.6(6)	C(1)-Mn(1)-C(8)-C(7)	175.8(4)
C(2)-Mn(1)-C(6)-C(5)	-169.7(4)	C(6)-Mn(1)-C(8)-C(7)	-37.5(4)
C(3)-Mn(1)-C(6)-C(5)	99.4(4)	C(4)-Mn(1)-C(8)-C(7)	-116.3(5)
C(1)-Mn(1)-C(6)-C(5)	-5.3(6)	C(5)-Mn(1)-C(8)-C(7)	-79.4(4)
C(7)-Mn(1)-C(6)-C(5)	-119.6(6)	C(11)-Mn(2)-C(9)-O(9)	-139.0(4)
C(8)-Mn(1)-C(6)-C(5)	-81.1(4)	C(10)-Mn(2)-C(9)-O(9)	-50.1(4)
C(4)-Mn(1)-C(6)-C(5)	-38.1(4)	C(16)-Mn(2)-C(9)-O(9)	119.5(5)
C(5)-C(6)-C(7)-C(8)	0.4(6)	C(12)-Mn(2)-C(9)-O(9)	85.2(5)
Mn(1)-C(6)-C(7)-C(8)	-62.3(4)	C(15)-Mn(2)-C(9)-O(9)	123.4(5)
C(5)-C(6)-C(7)-Mn(1)	62.7(4)	C(14)-Mn(2)-C(9)-O(9)	56.2(7)
C(2)-Mn(1)-C(7)-C(6)	136.6(4)	C(13)-Mn(2)-C(9)-O(9)	53.1(5)
C(3)-Mn(1)-C(7)-C(6)	48.1(5)	C(11)-Mn(2)-C(9)-C(22)	50.3(4)
C(1)-Mn(1)-C(7)-C(6)	-123.8(4)	C(10)-Mn(2)-C(9)-C(22)	139.1(4)
C(8)-Mn(1)-C(7)-C(6)	-117.0(5)	C(16)-Mn(2)-C(9)-C(22)	-51.2(4)
C(4)-Mn(1)-C(7)-C(6)	-78.8(4)	C(12)-Mn(2)-C(9)-C(22)	-85.6(5)
C(5)-Mn(1)-C(7)-C(6)	-36.2(4)	C(15)-Mn(2)-C(9)-C(22)	-47.3(6)
C(2)-Mn(1)-C(7)-C(8)	-106.4(4)	C(14)-Mn(2)-C(9)-C(22)	-114.6(6)
C(3)-Mn(1)-C(7)-C(8)	165.1(4)	C(13)-Mn(2)-C(9)-C(22)	-117.7(4)
C(1)-Mn(1)-C(7)-C(8)	-6.7(6)	C(22)-C(9)-O(9)-C(34)	-11(3)
C(6)-Mn(1)-C(7)-C(8)	117.0(5)	Mn(2)-C(9)-O(9)-C(34)	177(3)
C(4)-Mn(1)-C(7)-C(8)	38.2(4)	C(22)-C(9)-O(9)-C(29)	172.4(4)
C(5)-Mn(1)-C(7)-C(8)	80.8(4)	Mn(2)-C(9)-O(9)-C(29)	0.1(6)
C(5)-C(4)-C(8)-C(7)	-0.7(6)	C(22)-C(9)-O(9)-Fe(2)	-106.2(4)
Mn(1)-C(4)-C(8)-C(7)	61.3(3)	Mn(2)-C(9)-O(9)-Fe(2)	81.4(4)
C(5)-C(4)-C(8)-Mn(1)	-62.0(4)	C(11)-Mn(2)-C(10)-O(10)	-48(6)
C(6)-C(7)-C(8)-C(4)	0.2(6)	C(9)-Mn(2)-C(10)-O(10)	-142(6)
Mn(1)-C(7)-C(8)-C(4)	-62.1(3)	C(16)-Mn(2)-C(10)-O(10)	64(6)
C(6)-C(7)-C(8)-Mn(1)	62.3(4)	C(12)-Mn(2)-C(10)-O(10)	124(6)
C(2)-Mn(1)-C(8)-C(4)	-166.6(4)	C(15)-Mn(2)-C(10)-O(10)	42(6)
C(3)-Mn(1)-C(8)-C(4)	80.2(9)	C(14)-Mn(2)-C(10)-O(10)	70(6)
C(1)-Mn(1)-C(8)-C(4)	-67.9(4)	C(13)-Mn(2)-C(10)-O(10)	107(6)
C(7)-Mn(1)-C(8)-C(4)	116.3(5)	C(10)-Mn(2)-C(11)-O(11)	72(5)
C(6)-Mn(1)-C(8)-C(4)	78.9(4)	C(9)-Mn(2)-C(11)-O(11)	168(5)
C(5)-Mn(1)-C(8)-C(4)	36.9(3)	C(16)-Mn(2)-C(11)-O(11)	-86(5)
C(2)-Mn(1)-C(8)-C(7)	77.0(4)	C(12)-Mn(2)-C(11)-O(11)	-101(5)

C(15)-Mn(2)-C(11)-O(11)	-49(5)
C(14)-Mn(2)-C(11)-O(11)	-21(6)
C(13)-Mn(2)-C(11)-O(11)	-39(6)
C(11)-Mn(2)-C(12)-C(16)	24.2(6)
C(10)-Mn(2)-C(12)-C(16)	-145.5(5)
C(9)-Mn(2)-C(12)-C(16)	117.7(5)
C(15)-Mn(2)-C(12)-C(16)	-37.4(5)
C(14)-Mn(2)-C(12)-C(16)	-79.6(5)
C(13)-Mn(2)-C(12)-C(16)	-117.2(7)
C(11)-Mn(2)-C(12)-C(13)	141.3(5)
C(10)-Mn(2)-C(12)-C(13)	-28.3(7)
C(9)-Mn(2)-C(12)-C(13)	-125.1(5)
C(16)-Mn(2)-C(12)-C(13)	117.2(7)
C(15)-Mn(2)-C(12)-C(13)	79.8(5)
C(14)-Mn(2)-C(12)-C(13)	37.6(5)
C(16)-C(12)-C(13)-C(14)	0.6(7)
Mn(2)-C(12)-C(13)-C(14)	-61.4(5)
C(16)-C(12)-C(13)-Mn(2)	62.1(4)
C(11)-Mn(2)-C(13)-C(14)	25.7(10)
C(10)-Mn(2)-C(13)-C(14)	-82.7(5)
C(9)-Mn(2)-C(13)-C(14)	177.2(5)
C(16)-Mn(2)-C(13)-C(14)	79.4(5)
C(12)-Mn(2)-C(13)-C(14)	117.2(7)
C(15)-Mn(2)-C(13)-C(14)	37.0(5)
C(11)-Mn(2)-C(13)-C(12)	-91.5(9)
C(10)-Mn(2)-C(13)-C(12)	160.1(5)
C(9)-Mn(2)-C(13)-C(12)	60.0(6)
C(16)-Mn(2)-C(13)-C(12)	-37.8(5)
C(15)-Mn(2)-C(13)-C(12)	-80.2(6)
C(14)-Mn(2)-C(13)-C(12)	-117.2(7)
C(12)-C(13)-C(14)-C(15)	-0.5(7)
Mn(2)-C(13)-C(14)-C(15)	-61.4(4)
C(12)-C(13)-C(14)-Mn(2)	60.9(4)
C(11)-Mn(2)-C(14)-C(15)	-49.5(6)
C(10)-Mn(2)-C(14)-C(15)	-139.8(5)
C(9)-Mn(2)-C(14)-C(15)	113.2(6)
C(16)-Mn(2)-C(14)-C(15)	37.5(5)
C(12)-Mn(2)-C(14)-C(15)	80.4(6)
C(13)-Mn(2)-C(14)-C(15)	118.1(7)
C(11)-Mn(2)-C(14)-C(13)	-167.6(5)
C(10)-Mn(2)-C(14)-C(13)	102.1(5)
C(9)-Mn(2)-C(14)-C(13)	-4.9(8)
C(16)-Mn(2)-C(14)-C(13)	-80.7(6)
C(12)-Mn(2)-C(14)-C(13)	-37.8(5)
C(15)-Mn(2)-C(14)-C(13)	-118.1(7)
C(13)-C(14)-C(15)-C(16)	0.1(7)
Mn(2)-C(14)-C(15)-C(16)	-61.8(4)
C(13)-C(14)-C(15)-Mn(2)	61.9(5)
C(11)-Mn(2)-C(15)-C(16)	-104.4(6)
C(10)-Mn(2)-C(15)-C(16)	166.4(5)
C(9)-Mn(2)-C(15)-C(16)	-6.1(8)
C(12)-Mn(2)-C(15)-C(16)	37.8(5)
C(14)-Mn(2)-C(15)-C(16)	117.6(7)
C(13)-Mn(2)-C(15)-C(16)	80.4(6)
C(11)-Mn(2)-C(15)-C(14)	137.9(5)
C(10)-Mn(2)-C(15)-C(14)	48.8(5)
C(9)-Mn(2)-C(15)-C(14)	-123.7(5)
C(16)-Mn(2)-C(15)-C(14)	-117.6(7)
C(12)-Mn(2)-C(15)-C(14)	-79.8(5)
C(13)-Mn(2)-C(15)-C(14)	-37.2(5)
C(14)-C(15)-C(16)-C(12)	0.3(7)
Mn(2)-C(15)-C(16)-C(12)	-62.2(4)
C(14)-C(15)-C(16)-Mn(2)	62.5(5)
C(13)-C(12)-C(16)-C(15)	-0.6(7)
Mn(2)-C(12)-C(16)-C(15)	62.4(5)
C(13)-C(12)-C(16)-Mn(2)	-63.0(5)
C(11)-Mn(2)-C(16)-C(15)	79.5(6)
C(10)-Mn(2)-C(16)-C(15)	-30.3(12)
C(9)-Mn(2)-C(16)-C(15)	176.2(5)
C(12)-Mn(2)-C(16)-C(15)	-117.4(7)
C(14)-Mn(2)-C(16)-C(15)	-37.3(5)
C(13)-Mn(2)-C(16)-C(15)	-79.7(6)

C(11)-Mn(2)-C(16)-C(12)	-163.2(5)
C(10)-Mn(2)-C(16)-C(12)	87.0(10)
C(9)-Mn(2)-C(16)-C(12)	-66.5(5)
C(15)-Mn(2)-C(16)-C(12)	117.4(7)
C(14)-Mn(2)-C(16)-C(12)	80.1(5)
C(13)-Mn(2)-C(16)-C(12)	37.7(4)
O(1)-C(1)-C(17)-C(21)	4.7(6)
Mn(1)-C(1)-C(17)-C(21)	178.7(3)
O(1)-C(1)-C(17)-C(18)	-179.0(4)
Mn(1)-C(1)-C(17)-C(18)	-5.0(6)
O(1)-C(1)-C(17)-Fe(1)	93.8(4)
Mn(1)-C(1)-C(17)-Fe(1)	-92.2(4)
C(18)-Fe(1)-C(17)-C(21)	-117.2(4)
C(23)-Fe(1)-C(17)-C(21)	126.9(3)
C(26)-Fe(1)-C(17)-C(21)	47.1(5)
C(25)-Fe(1)-C(17)-C(21)	-156.4(6)
C(20)-Fe(1)-C(17)-C(21)	-37.0(3)
C(19)-Fe(1)-C(17)-C(21)	-79.8(4)
C(24)-Fe(1)-C(17)-C(21)	169.1(3)
C(22)-Fe(1)-C(17)-C(21)	83.2(3)
C(23)-Fe(1)-C(17)-C(18)	-115.9(3)
C(26)-Fe(1)-C(17)-C(18)	164.3(4)
C(21)-Fe(1)-C(17)-C(18)	117.2(4)
C(25)-Fe(1)-C(17)-C(18)	-39.2(7)
C(20)-Fe(1)-C(17)-C(18)	80.1(3)
C(19)-Fe(1)-C(17)-C(18)	37.4(3)
C(24)-Fe(1)-C(17)-C(18)	-73.8(3)
C(22)-Fe(1)-C(17)-C(18)	-159.6(3)
C(18)-Fe(1)-C(17)-C(1)	120.7(5)
C(23)-Fe(1)-C(17)-C(1)	4.8(4)
C(26)-Fe(1)-C(17)-C(1)	-74.9(6)
C(21)-Fe(1)-C(17)-C(1)	-122.1(5)
C(25)-Fe(1)-C(17)-C(1)	81.5(8)
C(20)-Fe(1)-C(17)-C(1)	-159.1(4)
C(19)-Fe(1)-C(17)-C(1)	158.1(5)
C(24)-Fe(1)-C(17)-C(1)	47.0(5)
C(22)-Fe(1)-C(17)-C(1)	-38.8(4)
C(21)-C(17)-C(18)-C(19)	-1.8(5)
C(1)-C(17)-C(18)-C(19)	-178.8(4)
Fe(1)-C(17)-C(18)-C(19)	-61.3(3)
C(21)-C(17)-C(18)-Fe(1)	59.5(3)
C(1)-C(17)-C(18)-Fe(1)	-117.5(4)
C(23)-Fe(1)-C(18)-C(19)	-157.2(4)
C(26)-Fe(1)-C(18)-C(19)	-42.4(8)
C(21)-Fe(1)-C(18)-C(19)	80.0(4)
C(25)-Fe(1)-C(18)-C(19)	-74.5(5)
C(20)-Fe(1)-C(18)-C(19)	36.5(4)
C(17)-Fe(1)-C(18)-C(19)	118.8(5)
C(24)-Fe(1)-C(18)-C(19)	-115.1(4)
C(22)-Fe(1)-C(18)-C(19)	167.6(5)
C(23)-Fe(1)-C(18)-C(17)	84.0(3)
C(26)-Fe(1)-C(18)-C(17)	-161.2(5)
C(21)-Fe(1)-C(18)-C(17)	-38.9(3)
C(25)-Fe(1)-C(18)-C(17)	166.6(3)
C(20)-Fe(1)-C(18)-C(17)	-82.3(3)
C(19)-Fe(1)-C(18)-C(17)	-118.8(5)
C(24)-Fe(1)-C(18)-C(17)	126.1(3)
C(22)-Fe(1)-C(18)-C(17)	48.8(7)
C(17)-C(18)-C(19)-C(20)	1.9(6)
Fe(1)-C(18)-C(19)-C(20)	-59.0(4)
C(17)-C(18)-C(19)-Fe(1)	60.9(3)
C(18)-Fe(1)-C(19)-C(20)	120.3(5)
C(23)-Fe(1)-C(19)-C(20)	171.7(4)
C(26)-Fe(1)-C(19)-C(20)	-75.5(4)
C(21)-Fe(1)-C(19)-C(20)	37.4(3)
C(25)-Fe(1)-C(19)-C(20)	-116.1(3)
C(17)-Fe(1)-C(19)-C(20)	81.8(3)
C(24)-Fe(1)-C(19)-C(20)	-157.4(3)
C(22)-Fe(1)-C(19)-C(20)	-43.6(9)
C(23)-Fe(1)-C(19)-C(18)	51.4(7)
C(26)-Fe(1)-C(19)-C(18)	164.2(3)
C(21)-Fe(1)-C(19)-C(18)	-82.9(4)

C(25)-Fe(1)-C(19)-C(18)	123.6(4)
C(20)-Fe(1)-C(19)-C(18)	-120.3(5)
C(17)-Fe(1)-C(19)-C(18)	-38.5(3)
C(24)-Fe(1)-C(19)-C(18)	82.3(4)
C(22)-Fe(1)-C(19)-C(18)	-163.9(6)
C(18)-C(19)-C(20)-C(21)	-1.2(6)
Fe(1)-C(19)-C(20)-C(21)	-59.2(3)
C(18)-C(19)-C(20)-Fe(1)	58.0(4)
C(18)-Fe(1)-C(20)-C(19)	-37.0(3)
C(23)-Fe(1)-C(20)-C(19)	-166.6(7)
C(26)-Fe(1)-C(20)-C(19)	122.8(3)
C(21)-Fe(1)-C(20)-C(19)	-119.6(5)
C(25)-Fe(1)-C(20)-C(19)	80.6(4)
C(17)-Fe(1)-C(20)-C(19)	-81.8(4)
C(24)-Fe(1)-C(20)-C(19)	47.4(6)
C(22)-Fe(1)-C(20)-C(19)	164.8(3)
C(18)-Fe(1)-C(20)-C(21)	82.6(3)
C(23)-Fe(1)-C(20)-C(21)	-47.0(9)
C(26)-Fe(1)-C(20)-C(21)	-117.6(3)
C(25)-Fe(1)-C(20)-C(21)	-159.8(3)
C(19)-Fe(1)-C(20)-C(21)	119.6(5)
C(17)-Fe(1)-C(20)-C(21)	37.8(3)
C(24)-Fe(1)-C(20)-C(21)	166.9(4)
C(22)-Fe(1)-C(20)-C(21)	-75.6(3)
C(19)-C(20)-C(21)-C(17)	0.0(5)
Fe(1)-C(20)-C(21)-C(17)	-59.6(3)
C(19)-C(20)-C(21)-Fe(1)	59.6(4)
C(18)-C(17)-C(21)-C(20)	1.1(5)
C(1)-C(17)-C(21)-C(20)	178.0(4)
Fe(1)-C(17)-C(21)-C(20)	59.9(3)
C(18)-C(17)-C(21)-Fe(1)	-58.8(3)
C(1)-C(17)-C(21)-Fe(1)	118.2(4)
C(18)-Fe(1)-C(21)-C(20)	-80.4(3)
C(23)-Fe(1)-C(21)-C(20)	165.8(3)
C(26)-Fe(1)-C(21)-C(20)	80.3(3)
C(25)-Fe(1)-C(21)-C(20)	44.1(6)
C(19)-Fe(1)-C(21)-C(20)	-36.9(3)
C(17)-Fe(1)-C(21)-C(20)	-119.6(4)
C(24)-Fe(1)-C(21)-C(20)	-156.3(7)
C(22)-Fe(1)-C(21)-C(20)	124.4(3)
C(18)-Fe(1)-C(21)-C(17)	39.2(3)
C(23)-Fe(1)-C(21)-C(17)	-74.6(3)
C(26)-Fe(1)-C(21)-C(17)	-160.0(3)
C(25)-Fe(1)-C(21)-C(17)	163.8(4)
C(20)-Fe(1)-C(21)-C(17)	119.6(4)
C(19)-Fe(1)-C(21)-C(17)	82.7(3)
C(24)-Fe(1)-C(21)-C(17)	-36.6(9)
C(22)-Fe(1)-C(21)-C(17)	-116.0(3)
O(9)-C(9)-C(22)-C(23)	5.1(6)
Mn(2)-C(9)-C(22)-C(23)	177.7(3)
O(9)-C(9)-C(22)-C(26)	-177.8(4)
Mn(2)-C(9)-C(22)-C(26)	-5.2(6)
O(9)-C(9)-C(22)-Fe(1)	94.1(4)
Mn(2)-C(9)-C(22)-Fe(1)	-93.3(4)
C(18)-Fe(1)-C(22)-C(23)	48.7(6)
C(26)-Fe(1)-C(22)-C(23)	-116.6(4)
C(21)-Fe(1)-C(22)-C(23)	127.7(3)
C(25)-Fe(1)-C(22)-C(23)	-79.5(3)
C(20)-Fe(1)-C(22)-C(23)	168.9(3)
C(19)-Fe(1)-C(22)-C(23)	-158.0(7)
C(17)-Fe(1)-C(22)-C(23)	84.2(3)
C(24)-Fe(1)-C(22)-C(23)	-36.7(3)
C(18)-Fe(1)-C(22)-C(9)	-73.7(7)
C(23)-Fe(1)-C(22)-C(9)	-122.5(5)
C(26)-Fe(1)-C(22)-C(9)	120.9(5)
C(21)-Fe(1)-C(22)-C(9)	5.2(4)
C(25)-Fe(1)-C(22)-C(9)	158.0(4)
C(20)-Fe(1)-C(22)-C(9)	46.5(5)
C(19)-Fe(1)-C(22)-C(9)	79.5(9)
C(17)-Fe(1)-C(22)-C(9)	-38.3(4)
C(24)-Fe(1)-C(22)-C(9)	-159.2(4)
C(18)-Fe(1)-C(22)-C(26)	165.4(5)

C(23)-Fe(1)-C(22)-C(26)	116.6(4)
C(21)-Fe(1)-C(22)-C(26)	-115.7(3)
C(25)-Fe(1)-C(22)-C(26)	37.1(3)
C(20)-Fe(1)-C(22)-C(26)	-74.4(3)
C(19)-Fe(1)-C(22)-C(26)	-41.4(8)
C(17)-Fe(1)-C(22)-C(26)	-159.2(2)
C(24)-Fe(1)-C(22)-C(26)	79.9(3)
C(9)-C(22)-C(23)-C(24)	178.1(4)
C(26)-C(22)-C(23)-C(24)	0.5(5)
Fe(1)-C(22)-C(23)-C(24)	59.8(3)
C(9)-C(22)-C(23)-Fe(1)	118.3(4)
C(26)-C(22)-C(23)-Fe(1)	-59.3(3)
C(18)-Fe(1)-C(23)-C(24)	79.7(3)
C(26)-Fe(1)-C(23)-C(24)	-81.1(3)
C(21)-Fe(1)-C(23)-C(24)	166.0(3)
C(25)-Fe(1)-C(23)-C(24)	-37.5(3)
C(20)-Fe(1)-C(23)-C(24)	-156.9(7)
C(19)-Fe(1)-C(23)-C(24)	43.5(6)
C(17)-Fe(1)-C(23)-C(24)	123.9(3)
C(22)-Fe(1)-C(23)-C(24)	-120.8(4)
C(18)-Fe(1)-C(23)-C(22)	-159.5(3)
C(26)-Fe(1)-C(23)-C(22)	39.6(2)
C(21)-Fe(1)-C(23)-C(22)	-73.2(3)
C(25)-Fe(1)-C(23)-C(22)	83.3(3)
C(20)-Fe(1)-C(23)-C(22)	-36.2(8)
C(19)-Fe(1)-C(23)-C(22)	164.3(5)
C(17)-Fe(1)-C(23)-C(22)	-115.3(3)
C(24)-Fe(1)-C(23)-C(22)	120.8(4)
C(22)-C(23)-C(24)-C(25)	-0.2(5)
Fe(1)-C(23)-C(24)-C(25)	59.5(3)
C(22)-C(23)-C(24)-Fe(1)	-59.7(3)
C(18)-Fe(1)-C(24)-C(25)	122.8(3)
C(23)-Fe(1)-C(24)-C(25)	-118.7(4)
C(26)-Fe(1)-C(24)-C(25)	-37.0(3)
C(21)-Fe(1)-C(24)-C(25)	-166.4(7)
C(20)-Fe(1)-C(24)-C(25)	48.3(6)
C(19)-Fe(1)-C(24)-C(25)	80.8(4)
C(17)-Fe(1)-C(24)-C(25)	164.5(3)
C(22)-Fe(1)-C(24)-C(25)	-81.7(3)
C(18)-Fe(1)-C(24)-C(23)	-118.5(3)
C(26)-Fe(1)-C(24)-C(23)	81.7(3)
C(21)-Fe(1)-C(24)-C(23)	-47.7(9)
C(25)-Fe(1)-C(24)-C(23)	118.7(4)
C(20)-Fe(1)-C(24)-C(23)	167.0(4)
C(19)-Fe(1)-C(24)-C(23)	-160.5(3)
C(17)-Fe(1)-C(24)-C(23)	-76.9(3)
C(22)-Fe(1)-C(24)-C(23)	37.0(3)
C(23)-C(24)-C(25)-C(26)	-0.1(5)
Fe(1)-C(24)-C(25)-C(26)	58.7(3)
C(23)-C(24)-C(25)-Fe(1)	-58.9(3)
C(18)-Fe(1)-C(25)-C(24)	-75.6(4)
C(23)-Fe(1)-C(25)-C(24)	38.1(3)
C(26)-Fe(1)-C(25)-C(24)	120.4(4)
C(21)-Fe(1)-C(25)-C(24)	172.0(4)
C(20)-Fe(1)-C(25)-C(24)	-157.0(3)
C(19)-Fe(1)-C(25)-C(24)	-116.0(3)
C(17)-Fe(1)-C(25)-C(24)	-45.3(8)
C(22)-Fe(1)-C(25)-C(24)	82.3(3)
C(18)-Fe(1)-C(25)-C(26)	164.0(3)
C(23)-Fe(1)-C(25)-C(26)	-82.3(3)
C(21)-Fe(1)-C(25)-C(26)	51.6(6)
C(20)-Fe(1)-C(25)-C(26)	82.6(3)
C(19)-Fe(1)-C(25)-C(26)	123.6(3)
C(17)-Fe(1)-C(25)-C(26)	-165.7(6)
C(24)-Fe(1)-C(25)-C(26)	-120.4(4)
C(22)-Fe(1)-C(25)-C(26)	-38.1(3)
C(24)-C(25)-C(26)-C(22)	0.5(5)
Fe(1)-C(25)-C(26)-C(22)	59.8(3)
C(24)-C(25)-C(26)-Fe(1)	-59.3(3)
C(23)-C(22)-C(26)-C(25)	-0.6(4)
C(9)-C(22)-C(26)-C(25)	-178.3(4)
Fe(1)-C(22)-C(26)-C(25)	-59.9(3)

C(23)-C(22)-C(26)-Fe(1)	59.3(3)
C(9)-C(22)-C(26)-Fe(1)	-118.3(4)
C(18)-Fe(1)-C(26)-C(25)	-43.0(7)
C(23)-Fe(1)-C(26)-C(25)	80.5(3)
C(21)-Fe(1)-C(26)-C(25)	-156.7(3)
C(20)-Fe(1)-C(26)-C(25)	-115.0(3)
C(19)-Fe(1)-C(26)-C(25)	-74.7(4)
C(17)-Fe(1)-C(26)-C(25)	169.2(4)
C(24)-Fe(1)-C(26)-C(25)	36.6(3)
C(22)-Fe(1)-C(26)-C(25)	119.6(4)
C(18)-Fe(1)-C(26)-C(22)	-162.6(6)
C(23)-Fe(1)-C(26)-C(22)	-39.1(2)
C(21)-Fe(1)-C(26)-C(22)	83.7(3)
C(25)-Fe(1)-C(26)-C(22)	-119.6(4)
C(20)-Fe(1)-C(26)-C(22)	125.5(3)
C(19)-Fe(1)-C(26)-C(22)	165.8(3)
C(17)-Fe(1)-C(26)-C(22)	49.7(5)
C(24)-Fe(1)-C(26)-C(22)	-82.9(3)
C(1)-O(1)-C(27)-C(28)	-178.6(5)
C(9)-O(9)-C(29)-C(30)	-174.1(5)

Appendix 8

Crystallographic data of Complex 27

Table 1. Crystal data and structure refinement for Complex **27**.

Identification code	db61a5_abs	
Empirical formula	$C_{34} H_{18} Fe O_{20} Re_4$	
Formula weight	1547.13	
Temperature	293(2) K	
Wavelength	0.71073 Å	
Crystal system	Triclinic	
Space group	$P\bar{1}$	
Unit cell dimensions	a = 15.5600(14) Å	a= 98.175(1)°.
	b = 16.0269(14) Å	b= 91.337(1)°.
	c = 16.5632(14) Å	g = 90.100(1)°.
Volume	4087.4(6) $Å^3$	
Z	4	
Density (calculated)	2.514 Mg/m^3	
Absorption coefficient	12.227 mm^{-1}	
F(000)	2832	
Crystal size	0.34 x 0.08 x 0.01 mm^3	
Theta range for data collection	2.34 to 26.52°.	
Index ranges	-19<=h<=19, -19<=k<=20, -20<=l<=6	
Reflections collected	22399	
Independent reflections	14796 [R(int) = 0.0532]	
Completeness to θ = 25.00°	97.7 %	
Absorption correction	Semi-empirical from equivalents	
Max. and min. transmission	0.885 and 0.348	
Refinement method	Full-matrix least-squares on F^2	
Data / restraints / parameters	14796 / 0 / 1064	
Goodness-of-fit on F^2	0.997	
Final R indices [I>2σ(I)]	R1 = 0.0545, wR2 = 0.1265	
R indices (all data)	R1 = 0.0995, wR2 = 0.1568	
Extinction coefficient	0.00078(6)	
Largest diff. peak and hole	2.547 and -2.452 e.$Å^{-3}$	

Table 2. Atomic coordinates (x 10^4) and equivalent isotropic displacement parameters ($Å^2$x 10^3) for Complex **27**. U(eq) is defined as one third of the trace of the orthogonalized U^{ij} tensor.

	x	y	z	U(eq)
Re(1)	5620(1)	2995(1)	4048(1)	46(1)
Re(2)	7212(1)	1853(1)	3705(1)	47(1)
C(1)	4676(13)	3721(12)	4400(11)	70(5)
O(1)	4098(10)	4123(9)	4637(8)	93(4)
C(2)	6485(12)	3893(11)	4397(10)	57(4)
O(2)	7027(10)	4406(8)	4534(9)	90(4)
C(3)	5642(16)	3297(14)	2910(11)	94(7)
O(3)	5631(10)	3485(10)	2283(8)	102(5)
C(4)	4828(11)	2065(11)	3606(10)	59(4)
O(4)	4381(8)	1533(9)	3333(8)	87(4)
C(5)	5673(16)	2640(13)	5136(12)	88(7)
O(5)	5631(10)	2408(9)	5763(8)	93(5)
C(6)	8134(13)	1115(11)	3340(10)	68(5)
O(6)	8688(9)	672(9)	3128(9)	90(4)
C(7)	6954(14)	1287(12)	4667(10)	79(6)
O(7)	6927(10)	1038(8)	5287(7)	85(4)
C(8)	7945(13)	2572(11)	4483(13)	76(5)
O(8)	8412(12)	2990(10)	4920(10)	124(6)
C(9)	7493(12)	2719(11)	3014(10)	61(4)
O(9)	7680(9)	3266(8)	2670(8)	83(4)
C(10)	6384(10)	1129(9)	2848(9)	48(4)
O(10)	5883(7)	460(7)	2944(6)	60(3)
Re(3)	9018(1)	-1125(1)	-2004(1)	55(1)
Re(4)	7478(1)	64(1)	-1765(1)	45(1)
C(11)	10006(13)	-1855(12)	-2158(10)	72(5)
O(11)	10600(10)	-2306(10)	-2269(9)	105(5)
C(12)	9317(11)	-605(11)	-2976(10)	63(5)
O(12)	9426(9)	-333(9)	-3566(7)	88(4)
C(13)	8251(15)	-1937(13)	-2691(13)	86(7)
O(13)	7820(12)	-2418(11)	-3090(11)	140(8)
C(14)	8610(13)	-1560(13)	-1013(12)	88(7)
O(14)	8426(13)	-1853(10)	-469(9)	136(8)

C(15)	9668(12)	-210(13)	-1308(12)	72(5)
O(15)	10046(9)	287(11)	-892(10)	106(5)
C(16)	6491(12)	767(11)	-1624(10)	64(5)
O(16)	5889(9)	1191(9)	-1508(8)	91(4)
C(17)	8204(12)	910(11)	-2154(9)	61(4)
O(17)	8638(9)	1371(8)	-2474(8)	86(4)
C(18)	7274(11)	-262(11)	-2952(10)	61(5)
O(18)	7132(10)	-420(9)	-3640(7)	98(5)
C(19)	6877(11)	-988(11)	-1627(9)	56(4)
O(19)	6547(9)	-1627(8)	-1628(7)	74(3)
C(20)	7791(9)	359(9)	-511(8)	44(3)
O(20)	8292(7)	973(7)	-138(6)	58(3)
Fe(1)	6662(2)	462(1)	1006(1)	48(1)
C(21)	6257(11)	1241(10)	1994(8)	53(4)
C(22)	6775(11)	1684(10)	1490(8)	54(4)
C(23)	6383(15)	1617(12)	691(10)	76(6)
C(24)	5614(14)	1120(14)	691(10)	84(7)
C(25)	5523(11)	875(12)	1468(10)	69(5)
C(26)	7478(10)	-91(9)	156(9)	50(4)
C(27)	6732(14)	-586(11)	168(9)	70(5)
C(28)	6631(17)	-856(12)	959(11)	88(7)
C(29)	7331(15)	-486(12)	1423(11)	83(7)
C(30)	7862(12)	-25(11)	974(10)	65(5)
C(31)	5863(11)	117(10)	3707(9)	60(4)
C(32)	5219(15)	-594(13)	3558(13)	100(7)
C(33)	8596(12)	1687(11)	-494(10)	68(5)
C(34)	8933(16)	2306(12)	186(13)	104(8)
Re(41)	6038(1)	3816(1)	-2014(1)	53(1)
Re(42)	7546(1)	5077(1)	-1841(1)	45(1)
C(41)	5093(13)	3049(12)	-2156(11)	73(5)
O(41)	4499(9)	2589(9)	-2228(9)	99(5)
C(42)	6488(10)	3424(11)	-992(11)	62(5)
O(42)	6747(10)	3187(9)	-424(9)	102(5)
C(43)	6804(13)	3001(11)	-2672(12)	72(5)
O(43)	7253(12)	2551(11)	-3038(11)	133(7)
C(44)	5723(11)	4308(12)	-3019(10)	65(5)

O(44)	5588(9)	4571(9)	-3609(8)	97(5)
C(45)	5346(14)	4660(14)	-1366(11)	81(6)
O(45)	4910(10)	5129(10)	-959(10)	106(5)
C(46)	8514(11)	5808(11)	-1702(11)	64(5)
O(46)	9124(9)	6240(9)	-1572(9)	93(4)
C(47)	6808(10)	5928(10)	-2281(10)	53(4)
O(47)	6417(9)	6358(8)	-2633(8)	88(4)
C(48)	7731(10)	4670(10)	-3020(8)	54(4)
O(48)	7840(9)	4459(9)	-3676(7)	88(4)
C(49)	8173(11)	4062(10)	-1601(8)	53(4)
O(49)	8510(7)	3437(7)	-1527(7)	65(3)
C(50)	7258(9)	5414(9)	-606(8)	42(3)
O(50)	6689(7)	5943(7)	-247(6)	63(3)
Re(43)	9363(1)	8021(1)	4155(1)	46(1)
Re(44)	7759(1)	6867(1)	3817(1)	45(1)
C(51)	10304(13)	8773(12)	4545(10)	65(5)
O(51)	10873(10)	9189(9)	4772(9)	106(6)
C(52)	10148(11)	7121(11)	3684(11)	62(5)
O(52)	10635(9)	6647(9)	3385(8)	92(5)
C(53)	9268(12)	8370(11)	3053(9)	66(5)
O(53)	9267(10)	8608(9)	2434(8)	95(5)
C(54)	8472(13)	8877(12)	4517(11)	67(5)
O(54)	7940(10)	9363(8)	4692(9)	91(4)
C(55)	9411(14)	7594(11)	5216(11)	74(5)
O(55)	9400(10)	7383(9)	5840(7)	89(4)
C(56)	6830(12)	6122(11)	3416(11)	66(5)
O(56)	6288(9)	5671(9)	3151(10)	104(5)
C(57)	8078(11)	6188(12)	4718(10)	63(5)
O(57)	8188(11)	5933(8)	5301(8)	98(5)
C(58)	7045(13)	7527(12)	4661(11)	71(5)
O(58)	6590(12)	7930(10)	5096(10)	122(6)
C(59)	7450(10)	7758(10)	3165(9)	52(4)
O(59)	7202(8)	8333(7)	2886(7)	73(3)
C(60)	8551(10)	6255(9)	2920(8)	49(4)
O(60)	9067(7)	5600(7)	2936(6)	59(3)
Fe(41)	8347(2)	5713(2)	1015(1)	55(1)

C(61)	7657(11)	5051(11)	52(10)	62(5)
C(62)	7297(12)	4944(10)	821(10)	62(5)
C(63)	7921(15)	4593(11)	1310(12)	81(6)
C(64)	8694(18)	4472(13)	878(13)	108(10)
C(65)	8541(13)	4746(13)	105(10)	85(6)
C(66)	8604(12)	6494(10)	2078(8)	55(4)
C(67)	7945(13)	6801(10)	1615(9)	64(5)
C(68)	8275(18)	6964(13)	861(11)	94(8)
C(69)	9123(16)	6700(17)	867(12)	107(9)
C(70)	9317(13)	6402(13)	1588(12)	81(6)
C(71)	6241(11)	6569(10)	-671(11)	62(5)
C(72)	5694(15)	7074(13)	-51(13)	100(7)
C(73)	9168(13)	5156(11)	3628(11)	77(6)
C(74)	9766(19)	4455(14)	3412(15)	140(11)

Table 3. Bond lengths [Å] and angles [°] for Complex **27**.

Re(1)-C(1)	1.924(19)	C(11)-O(11)	1.18(2)
Re(1)-C(5)	1.96(2)	C(12)-O(12)	1.142(18)
Re(1)-C(4)	1.979(19)	C(13)-O(13)	1.15(2)
Re(1)-C(2)	1.99(2)	C(14)-O(14)	1.117(19)
Re(1)-C(3)	2.013(18)	C(15)-O(15)	1.13(2)
Re(1)-Re(2)	3.0974(9)	C(16)-O(16)	1.161(19)
Re(2)-C(6)	1.915(19)	C(17)-O(17)	1.187(19)
Re(2)-C(8)	1.95(2)	C(18)-O(18)	1.147(18)
Re(2)-C(9)	1.975(18)	C(19)-O(19)	1.146(18)
Re(2)-C(7)	1.991(17)	C(20)-O(20)	1.327(16)
Re(2)-C(10)	2.111(15)	C(20)-C(26)	1.493(19)
C(1)-O(1)	1.15(2)	O(20)-C(33)	1.444(18)
C(2)-O(2)	1.17(2)	Fe(1)-C(22)	2.014(15)
C(3)-O(3)	1.121(19)	Fe(1)-C(25)	2.021(16)
C(4)-O(4)	1.135(19)	Fe(1)-C(30)	2.024(18)
C(5)-O(5)	1.16(2)	Fe(1)-C(27)	2.026(17)
C(6)-O(6)	1.15(2)	Fe(1)-C(21)	2.027(15)
C(7)-O(7)	1.156(18)	Fe(1)-C(26)	2.028(14)
C(8)-O(8)	1.16(2)	Fe(1)-C(29)	2.035(18)
C(9)-O(9)	1.152(18)	Fe(1)-C(23)	2.038(17)
C(10)-O(10)	1.355(17)	Fe(1)-C(24)	2.041(17)
C(10)-C(21)	1.460(19)	Fe(1)-C(28)	2.104(19)
O(10)-C(31)	1.449(16)	C(21)-C(22)	1.43(2)
Re(3)-C(11)	1.93(2)	C(21)-C(25)	1.49(2)
Re(3)-C(12)	1.979(16)	C(22)-C(23)	1.43(2)
Re(3)-C(13)	1.98(2)	C(22)-H(22)	0.9300
Re(3)-C(14)	1.989(17)	C(23)-C(24)	1.44(3)
Re(3)-C(15)	1.99(2)	C(23)-H(23)	0.9300
Re(3)-Re(4)	3.0632(9)	C(24)-C(25)	1.41(2)
Re(4)-C(16)	1.905(18)	C(24)-H(24)	0.9300
Re(4)-C(17)	1.952(18)	C(25)-H(25)	0.9300
Re(4)-C(19)	1.970(18)	C(26)-C(27)	1.41(2)
Re(4)-C(18)	1.980(16)	C(26)-C(30)	1.46(2)
Re(4)-C(20)	2.108(14)	C(27)-C(28)	1.45(2)

C(27)-H(27)	0.9300	C(48)-O(48)	1.109(16)
C(28)-C(29)	1.40(3)	C(49)-O(49)	1.151(17)
C(28)-H(28)	0.9300	C(50)-O(50)	1.319(17)
C(29)-C(30)	1.40(2)	C(50)-C(61)	1.44(2)
C(29)-H(29)	0.9300	O(50)-C(71)	1.471(18)
C(30)-H(30)	0.9300	Re(43)-C(51)	1.93(2)
C(31)-C(32)	1.51(2)	Re(43)-C(55)	1.975(19)
C(31)-H(31A)	0.9700	Re(43)-C(52)	1.98(2)
C(31)-H(31B)	0.9700	Re(43)-C(53)	1.986(16)
C(32)-H(32A)	0.9600	Re(43)-C(54)	1.99(2)
C(32)-H(32B)	0.9600	Re(43)-Re(44)	3.0962(9)
C(32)-H(32C)	0.9600	Re(44)-C(56)	1.919(19)
C(33)-C(34)	1.48(2)	Re(44)-C(59)	1.963(17)
C(33)-H(33A)	0.9700	Re(44)-C(58)	1.991(19)
C(33)-H(33B)	0.9700	Re(44)-C(57)	2.021(17)
C(34)-H(34A)	0.9600	Re(44)-C(60)	2.090(15)
C(34)-H(34B)	0.9600	C(51)-O(51)	1.13(2)
C(34)-H(34C)	0.9600	C(52)-O(52)	1.14(2)
Re(41)-C(41)	1.904(19)	C(53)-O(53)	1.143(18)
Re(41)-C(45)	1.95(2)	C(54)-O(54)	1.15(2)
Re(41)-C(44)	1.993(17)	C(55)-O(55)	1.133(19)
Re(41)-C(43)	1.99(2)	C(56)-O(56)	1.148(19)
Re(41)-C(42)	2.000(17)	C(57)-O(57)	1.111(18)
Re(41)-Re(42)	3.0771(9)	C(58)-O(58)	1.15(2)
Re(42)-C(46)	1.895(16)	C(59)-O(59)	1.151(17)
Re(42)-C(49)	1.983(17)	C(60)-O(60)	1.324(17)
Re(42)-C(47)	1.989(16)	C(60)-C(66)	1.502(19)
Re(42)-C(48)	1.997(14)	O(60)-C(73)	1.440(19)
Re(42)-C(50)	2.100(14)	Fe(41)-C(67)	1.990(17)
C(41)-O(41)	1.17(2)	Fe(41)-C(70)	2.007(18)
C(42)-O(42)	1.130(18)	Fe(41)-C(65)	2.031(18)
C(43)-O(43)	1.13(2)	Fe(41)-C(69)	2.03(2)
C(44)-O(44)	1.132(19)	Fe(41)-C(62)	2.036(16)
C(45)-O(45)	1.17(2)	Fe(41)-C(63)	2.039(19)
C(46)-O(46)	1.172(18)	Fe(41)-C(66)	2.041(14)
C(47)-O(47)	1.133(18)	Fe(41)-C(64)	2.045(19)

Fe(41)-C(68)	2.06(2)
Fe(41)-C(61)	2.062(16)
C(61)-C(62)	1.44(2)
C(61)-C(65)	1.47(2)
C(62)-C(63)	1.42(2)
C(62)-H(62)	0.9300
C(63)-C(64)	1.41(3)
C(63)-H(63)	0.9300
C(64)-C(65)	1.43(3)
C(64)-H(64)	0.9300
C(65)-H(65)	0.9300
C(66)-C(70)	1.39(2)
C(66)-C(67)	1.40(2)
C(67)-C(68)	1.42(2)
C(67)-H(67)	0.9300
C(68)-C(69)	1.39(3)
C(68)-H(68)	0.9300
C(69)-C(70)	1.38(3)
C(69)-H(69)	0.9300
C(70)-H(70)	0.9300
C(71)-C(72)	1.50(2)
C(71)-H(71A)	0.9700
C(71)-H(71B)	0.9700
C(72)-H(72A)	0.9600
C(72)-H(72B)	0.9600
C(72)-H(72C)	0.9600
C(73)-C(74)	1.47(3)
C(73)-H(73A)	0.9700
C(73)-H(73B)	0.9700
C(74)-H(74A)	0.9600
C(74)-H(74B)	0.9600
C(74)-H(74C)	0.9600

C(1)-Re(1)-C(5)	88.9(8)
C(1)-Re(1)-C(4)	91.8(8)
C(5)-Re(1)-C(4)	93.0(8)
C(1)-Re(1)-C(2)	92.7(8)
C(5)-Re(1)-C(2)	90.6(7)
C(4)-Re(1)-C(2)	174.3(6)
C(1)-Re(1)-C(3)	95.6(8)
C(5)-Re(1)-C(3)	175.6(10)
C(4)-Re(1)-C(3)	86.9(8)
C(2)-Re(1)-C(3)	89.2(8)
C(1)-Re(1)-Re(2)	172.9(5)
C(5)-Re(1)-Re(2)	84.9(7)
C(4)-Re(1)-Re(2)	91.8(5)
C(2)-Re(1)-Re(2)	84.2(4)
C(3)-Re(1)-Re(2)	90.7(7)
C(6)-Re(2)-C(8)	93.3(8)
C(6)-Re(2)-C(9)	95.4(7)
C(8)-Re(2)-C(9)	81.5(7)
C(6)-Re(2)-C(7)	95.0(8)
C(8)-Re(2)-C(7)	83.6(8)
C(9)-Re(2)-C(7)	162.3(7)
C(6)-Re(2)-C(10)	89.0(7)
C(8)-Re(2)-C(10)	177.1(6)
C(9)-Re(2)-C(10)	96.5(6)
C(7)-Re(2)-C(10)	98.0(7)
C(6)-Re(2)-Re(1)	172.0(5)
C(8)-Re(2)-Re(1)	93.3(5)
C(9)-Re(2)-Re(1)	81.3(5)
C(7)-Re(2)-Re(1)	90.1(6)
C(10)-Re(2)-Re(1)	84.2(4)
O(1)-C(1)-Re(1)	176.3(17)
O(2)-C(2)-Re(1)	173.9(15)
O(3)-C(3)-Re(1)	178(2)
O(4)-C(4)-Re(1)	178.3(16)
O(5)-C(5)-Re(1)	174(2)
O(6)-C(6)-Re(2)	179.4(17)
O(7)-C(7)-Re(2)	168.0(19)
O(8)-C(8)-Re(2)	177(2)
O(9)-C(9)-Re(2)	174.3(15)

O(10)-C(10)-C(21)	104.8(13)
O(10)-C(10)-Re(2)	129.2(10)
C(21)-C(10)-Re(2)	125.9(12)
C(10)-O(10)-C(31)	122.0(12)
C(11)-Re(3)-C(12)	90.5(7)
C(11)-Re(3)-C(13)	93.4(8)
C(12)-Re(3)-C(13)	90.0(8)
C(11)-Re(3)-C(14)	95.9(7)
C(12)-Re(3)-C(14)	173.7(7)
C(13)-Re(3)-C(14)	89.8(9)
C(11)-Re(3)-C(15)	93.7(8)
C(12)-Re(3)-C(15)	89.2(7)
C(13)-Re(3)-C(15)	172.9(8)
C(14)-Re(3)-C(15)	90.3(9)
C(11)-Re(3)-Re(4)	178.8(6)
C(12)-Re(3)-Re(4)	88.7(5)
C(13)-Re(3)-Re(4)	87.5(6)
C(14)-Re(3)-Re(4)	84.9(5)
C(15)-Re(3)-Re(4)	85.4(5)
C(16)-Re(4)-C(17)	95.1(7)
C(16)-Re(4)-C(19)	95.8(7)
C(17)-Re(4)-C(19)	164.4(6)
C(16)-Re(4)-C(18)	94.5(7)
C(17)-Re(4)-C(18)	81.4(6)
C(19)-Re(4)-C(18)	86.6(6)
C(16)-Re(4)-C(20)	90.1(6)
C(17)-Re(4)-C(20)	97.7(6)
C(19)-Re(4)-C(20)	93.4(6)
C(18)-Re(4)-C(20)	175.3(7)
C(16)-Re(4)-Re(3)	177.8(5)
C(17)-Re(4)-Re(3)	86.9(5)
C(19)-Re(4)-Re(3)	82.1(5)
C(18)-Re(4)-Re(3)	84.7(5)
C(20)-Re(4)-Re(3)	90.7(4)
O(11)-C(11)-Re(3)	178.5(18)
O(12)-C(12)-Re(3)	174.3(17)
O(13)-C(13)-Re(3)	179(2)
O(14)-C(14)-Re(3)	174.5(17)
O(15)-C(15)-Re(3)	177.2(18)
O(16)-C(16)-Re(4)	177.5(16)
O(17)-C(17)-Re(4)	172.6(15)
O(18)-C(18)-Re(4)	176.9(17)
O(19)-C(19)-Re(4)	173.0(13)
O(20)-C(20)-C(26)	104.9(12)
O(20)-C(20)-Re(4)	128.7(10)
C(26)-C(20)-Re(4)	126.4(11)
C(20)-O(20)-C(33)	125.5(12)
C(22)-Fe(1)-C(25)	70.7(7)
C(22)-Fe(1)-C(30)	106.8(7)
C(25)-Fe(1)-C(30)	158.8(6)
C(22)-Fe(1)-C(27)	158.7(6)
C(25)-Fe(1)-C(27)	121.2(8)
C(30)-Fe(1)-C(27)	68.7(8)
C(22)-Fe(1)-C(21)	41.5(6)
C(25)-Fe(1)-C(21)	43.1(6)
C(30)-Fe(1)-C(21)	121.2(7)
C(27)-Fe(1)-C(21)	158.8(7)
C(22)-Fe(1)-C(26)	122.1(6)
C(25)-Fe(1)-C(26)	156.9(7)
C(30)-Fe(1)-C(26)	42.2(6)
C(27)-Fe(1)-C(26)	40.6(7)
C(21)-Fe(1)-C(26)	158.7(7)
C(22)-Fe(1)-C(29)	123.8(8)
C(25)-Fe(1)-C(29)	122.6(7)
C(30)-Fe(1)-C(29)	40.4(7)
C(27)-Fe(1)-C(29)	67.1(8)
C(21)-Fe(1)-C(29)	107.3(7)
C(26)-Fe(1)-C(29)	68.7(6)
C(22)-Fe(1)-C(23)	41.5(6)
C(25)-Fe(1)-C(23)	69.6(8)
C(30)-Fe(1)-C(23)	123.2(8)
C(27)-Fe(1)-C(23)	122.3(7)

C(21)-Fe(1)-C(23)	70.1(6)	C(24)-C(23)-H(23)	126.1
C(26)-Fe(1)-C(23)	106.3(7)	Fe(1)-C(23)-H(23)	127.5
C(29)-Fe(1)-C(23)	160.3(10)	C(25)-C(24)-C(23)	109.1(17)
C(22)-Fe(1)-C(24)	69.7(8)	C(25)-C(24)-Fe(1)	69.0(9)
C(25)-Fe(1)-C(24)	40.6(7)	C(23)-C(24)-Fe(1)	69.3(10)
C(30)-Fe(1)-C(24)	159.7(7)	C(25)-C(24)-H(24)	125.5
C(27)-Fe(1)-C(24)	106.9(8)	C(23)-C(24)-H(24)	125.5
C(21)-Fe(1)-C(24)	70.3(7)	Fe(1)-C(24)-H(24)	127.9
C(26)-Fe(1)-C(24)	121.6(6)	C(24)-C(25)-C(21)	107.8(17)
C(29)-Fe(1)-C(24)	157.8(10)	C(24)-C(25)-Fe(1)	70.5(10)
C(23)-Fe(1)-C(24)	41.2(8)	C(21)-C(25)-Fe(1)	68.6(9)
C(22)-Fe(1)-C(28)	158.6(7)	C(24)-C(25)-H(25)	126.1
C(25)-Fe(1)-C(28)	105.6(9)	C(21)-C(25)-H(25)	126.1
C(30)-Fe(1)-C(28)	68.7(9)	Fe(1)-C(25)-H(25)	126.4
C(27)-Fe(1)-C(28)	41.0(6)	C(27)-C(26)-C(30)	105.9(14)
C(21)-Fe(1)-C(28)	121.6(6)	C(27)-C(26)-C(20)	128.7(14)
C(26)-Fe(1)-C(28)	69.5(7)	C(30)-C(26)-C(20)	125.2(15)
C(29)-Fe(1)-C(28)	39.5(8)	C(27)-C(26)-Fe(1)	69.6(9)
C(23)-Fe(1)-C(28)	158.5(9)	C(30)-C(26)-Fe(1)	68.8(9)
C(24)-Fe(1)-C(28)	121.8(10)	C(20)-C(26)-Fe(1)	121.6(10)
C(22)-C(21)-C(10)	129.7(15)	C(26)-C(27)-C(28)	111.1(18)
C(22)-C(21)-C(25)	106.2(13)	C(26)-C(27)-Fe(1)	69.8(9)
C(10)-C(21)-C(25)	124.1(15)	C(28)-C(27)-Fe(1)	72.4(10)
C(22)-C(21)-Fe(1)	68.8(8)	C(26)-C(27)-H(27)	124.4
C(10)-C(21)-Fe(1)	126.8(11)	C(28)-C(27)-H(27)	124.4
C(25)-C(21)-Fe(1)	68.3(8)	Fe(1)-C(27)-H(27)	125.0
C(21)-C(22)-C(23)	109.1(16)	C(29)-C(28)-C(27)	103.8(18)
C(21)-C(22)-Fe(1)	69.7(9)	C(29)-C(28)-Fe(1)	67.6(11)
C(23)-C(22)-Fe(1)	70.2(10)	C(27)-C(28)-Fe(1)	66.6(10)
C(21)-C(22)-H(22)	125.4	C(29)-C(28)-H(28)	128.1
C(23)-C(22)-H(22)	125.4	C(27)-C(28)-H(28)	128.1
Fe(1)-C(22)-H(22)	126.2	Fe(1)-C(28)-H(28)	129.1
C(22)-C(23)-C(24)	107.7(16)	C(28)-C(29)-C(30)	112.5(17)
C(22)-C(23)-Fe(1)	68.4(9)	C(28)-C(29)-Fe(1)	72.9(12)
C(24)-C(23)-Fe(1)	69.5(10)	C(30)-C(29)-Fe(1)	69.4(10)
C(22)-C(23)-H(23)	126.1	C(28)-C(29)-H(29)	123.8

C(30)-C(29)-H(29)	123.8
Fe(1)-C(29)-H(29)	125.5
C(29)-C(30)-C(26)	106.6(18)
C(29)-C(30)-Fe(1)	70.2(11)
C(26)-C(30)-Fe(1)	69.1(9)
C(29)-C(30)-H(30)	126.7
C(26)-C(30)-H(30)	126.7
Fe(1)-C(30)-H(30)	125.6
O(10)-C(31)-C(32)	104.9(14)
O(10)-C(31)-H(31A)	110.8
C(32)-C(31)-H(31A)	110.8
O(10)-C(31)-H(31B)	110.8
C(32)-C(31)-H(31B)	110.8
H(31A)-C(31)-H(31B)	108.8
C(31)-C(32)-H(32A)	109.5
C(31)-C(32)-H(32B)	109.5
H(32A)-C(32)-H(32B)	109.5
C(31)-C(32)-H(32C)	109.5
H(32A)-C(32)-H(32C)	109.5
H(32B)-C(32)-H(32C)	109.5
O(20)-C(33)-C(34)	106.7(14)
O(20)-C(33)-H(33A)	110.4
C(34)-C(33)-H(33A)	110.4
O(20)-C(33)-H(33B)	110.4
C(34)-C(33)-H(33B)	110.4
H(33A)-C(33)-H(33B)	108.6
C(33)-C(34)-H(34A)	109.5
C(33)-C(34)-H(34B)	109.5
H(34A)-C(34)-H(34B)	109.5
C(33)-C(34)-H(34C)	109.5
H(34A)-C(34)-H(34C)	109.5
H(34B)-C(34)-H(34C)	109.5
C(41)-Re(41)-C(45)	91.0(8)
C(41)-Re(41)-C(44)	92.8(7)
C(45)-Re(41)-C(44)	90.3(8)
C(41)-Re(41)-C(43)	92.4(8)
C(45)-Re(41)-C(43)	176.6(7)
C(44)-Re(41)-C(43)	89.4(7)
C(41)-Re(41)-C(42)	94.8(7)
C(45)-Re(41)-C(42)	89.9(8)
C(44)-Re(41)-C(42)	172.4(7)
C(43)-Re(41)-C(42)	90.0(7)
C(41)-Re(41)-Re(42)	178.0(5)
C(45)-Re(41)-Re(42)	89.1(5)
C(44)-Re(41)-Re(42)	85.2(5)
C(43)-Re(41)-Re(42)	87.5(5)
C(42)-Re(41)-Re(42)	87.2(5)
C(46)-Re(42)-C(49)	95.7(7)
C(46)-Re(42)-C(47)	93.0(7)
C(49)-Re(42)-C(47)	167.7(6)
C(46)-Re(42)-C(48)	95.6(7)
C(49)-Re(42)-C(48)	87.2(6)
C(47)-Re(42)-C(48)	83.3(6)
C(46)-Re(42)-C(50)	90.0(7)
C(49)-Re(42)-C(50)	91.4(6)
C(47)-Re(42)-C(50)	97.3(6)
C(48)-Re(42)-C(50)	174.3(6)
C(46)-Re(42)-Re(41)	176.5(5)
C(49)-Re(42)-Re(41)	80.9(5)
C(47)-Re(42)-Re(41)	90.5(5)
C(48)-Re(42)-Re(41)	85.2(5)
C(50)-Re(42)-Re(41)	89.1(4)
O(41)-C(41)-Re(41)	178(2)
O(42)-C(42)-Re(41)	178.5(17)
O(43)-C(43)-Re(41)	178.5(18)
O(44)-C(44)-Re(41)	176.0(17)
O(45)-C(45)-Re(41)	176.1(18)
O(46)-C(46)-Re(42)	175.9(16)
O(47)-C(47)-Re(42)	170.6(14)
O(48)-C(48)-Re(42)	178.6(17)
O(49)-C(49)-Re(42)	173.9(12)
O(50)-C(50)-C(61)	104.2(12)

O(50)-C(50)-Re(42)	131.3(10)
C(61)-C(50)-Re(42)	124.4(11)
C(50)-O(50)-C(71)	122.7(12)
C(51)-Re(43)-C(55)	88.2(7)
C(51)-Re(43)-C(52)	92.7(7)
C(55)-Re(43)-C(52)	90.8(8)
C(51)-Re(43)-C(53)	95.9(7)
C(55)-Re(43)-C(53)	175.6(7)
C(52)-Re(43)-C(53)	87.5(7)
C(51)-Re(43)-C(54)	93.3(7)
C(55)-Re(43)-C(54)	93.2(7)
C(52)-Re(43)-C(54)	172.9(6)
C(53)-Re(43)-C(54)	88.1(7)
C(51)-Re(43)-Re(44)	170.8(5)
C(55)-Re(43)-Re(44)	84.3(6)
C(52)-Re(43)-Re(44)	92.8(5)
C(53)-Re(43)-Re(44)	91.7(5)
C(54)-Re(43)-Re(44)	81.8(5)
C(56)-Re(44)-C(59)	95.8(7)
C(56)-Re(44)-C(58)	93.2(8)
C(59)-Re(44)-C(58)	84.0(7)
C(56)-Re(44)-C(57)	93.0(7)
C(59)-Re(44)-C(57)	165.8(7)
C(58)-Re(44)-C(57)	84.4(8)
C(56)-Re(44)-C(60)	90.0(7)
C(59)-Re(44)-C(60)	93.2(6)
C(58)-Re(44)-C(60)	176.0(7)
C(57)-Re(44)-C(60)	97.9(6)
C(56)-Re(44)-Re(43)	170.0(5)
C(59)-Re(44)-Re(43)	79.9(4)
C(58)-Re(44)-Re(43)	95.2(5)
C(57)-Re(44)-Re(43)	93.1(5)
C(60)-Re(44)-Re(43)	81.4(4)
O(51)-C(51)-Re(43)	177.6(17)
O(52)-C(52)-Re(43)	174.7(17)
O(53)-C(53)-Re(43)	174.8(16)
O(54)-C(54)-Re(43)	177.0(15)
O(55)-C(55)-Re(43)	175.8(19)
O(56)-C(56)-Re(44)	177.7(18)
O(57)-C(57)-Re(44)	167.3(18)
O(58)-C(58)-Re(44)	174(2)
O(59)-C(59)-Re(44)	169.6(14)
O(60)-C(60)-C(66)	106.3(13)
O(60)-C(60)-Re(44)	130.4(10)
C(66)-C(60)-Re(44)	123.3(11)
C(60)-O(60)-C(73)	123.6(12)
C(67)-Fe(41)-C(70)	67.8(8)
C(67)-Fe(41)-C(65)	161.4(7)
C(70)-Fe(41)-C(65)	122.5(9)
C(67)-Fe(41)-C(69)	67.3(9)
C(70)-Fe(41)-C(69)	39.8(7)
C(65)-Fe(41)-C(69)	109.6(9)
C(67)-Fe(41)-C(62)	106.6(7)
C(70)-Fe(41)-C(62)	160.9(7)
C(65)-Fe(41)-C(62)	68.6(8)
C(69)-Fe(41)-C(62)	156.8(8)
C(67)-Fe(41)-C(63)	120.8(9)
C(70)-Fe(41)-C(63)	125.0(7)
C(65)-Fe(41)-C(63)	68.2(9)
C(69)-Fe(41)-C(63)	161.9(10)
C(62)-Fe(41)-C(63)	40.7(7)
C(67)-Fe(41)-C(66)	40.5(6)
C(70)-Fe(41)-C(66)	40.0(7)
C(65)-Fe(41)-C(66)	157.0(7)
C(69)-Fe(41)-C(66)	66.9(7)
C(62)-Fe(41)-C(66)	124.0(7)
C(63)-Fe(41)-C(66)	107.7(7)
C(67)-Fe(41)-C(64)	155.9(8)
C(70)-Fe(41)-C(64)	108.3(9)
C(65)-Fe(41)-C(64)	41.0(8)
C(69)-Fe(41)-C(64)	126.0(12)
C(62)-Fe(41)-C(64)	68.8(9)

C(63)-Fe(41)-C(64)	40.5(9)	Fe(41)-C(63)-H(63)	126.7
C(66)-Fe(41)-C(64)	121.1(7)	C(63)-C(64)-C(65)	106.9(17)
C(67)-Fe(41)-C(68)	41.0(7)	C(63)-C(64)-Fe(41)	69.5(11)
C(70)-Fe(41)-C(68)	67.5(9)	C(65)-C(64)-Fe(41)	69.0(11)
C(65)-Fe(41)-C(68)	124.8(8)	C(63)-C(64)-H(64)	126.6
C(69)-Fe(41)-C(68)	39.6(9)	C(65)-C(64)-H(64)	126.6
C(62)-Fe(41)-C(68)	121.1(9)	Fe(41)-C(64)-H(64)	126.5
C(63)-Fe(41)-C(68)	156.6(11)	C(64)-C(65)-C(61)	109.8(19)
C(66)-Fe(41)-C(68)	68.2(7)	C(64)-C(65)-Fe(41)	70.1(10)
C(64)-Fe(41)-C(68)	161.6(11)	C(61)-C(65)-Fe(41)	70.2(10)
C(67)-Fe(41)-C(61)	122.7(7)	C(64)-C(65)-H(65)	125.1
C(70)-Fe(41)-C(61)	157.5(8)	C(61)-C(65)-H(65)	125.1
C(65)-Fe(41)-C(61)	41.9(6)	Fe(41)-C(65)-H(65)	126.3
C(69)-Fe(41)-C(61)	121.9(7)	C(70)-C(66)-C(67)	106.4(14)
C(62)-Fe(41)-C(61)	41.0(6)	C(70)-C(66)-C(60)	125.8(16)
C(63)-Fe(41)-C(61)	69.3(7)	C(67)-C(66)-C(60)	127.7(17)
C(66)-Fe(41)-C(61)	159.9(7)	C(70)-C(66)-Fe(41)	68.7(10)
C(64)-Fe(41)-C(61)	70.3(7)	C(67)-C(66)-Fe(41)	67.8(9)
C(68)-Fe(41)-C(61)	106.3(7)	C(60)-C(66)-Fe(41)	125.5(11)
C(62)-C(61)-C(50)	127.9(15)	C(66)-C(67)-C(68)	109.3(19)
C(62)-C(61)-C(65)	104.4(15)	C(66)-C(67)-Fe(41)	71.7(10)
C(50)-C(61)-C(65)	127.6(16)	C(68)-C(67)-Fe(41)	72.1(12)
C(62)-C(61)-Fe(41)	68.5(9)	C(66)-C(67)-H(67)	125.4
C(50)-C(61)-Fe(41)	125.2(12)	C(68)-C(67)-H(67)	125.4
C(65)-C(61)-Fe(41)	67.9(9)	Fe(41)-C(67)-H(67)	122.4
C(63)-C(62)-C(61)	109.8(18)	C(69)-C(68)-C(67)	105.3(19)
C(63)-C(62)-Fe(41)	69.8(11)	C(69)-C(68)-Fe(41)	69.2(15)
C(61)-C(62)-Fe(41)	70.5(10)	C(67)-C(68)-Fe(41)	66.8(10)
C(63)-C(62)-H(62)	125.1	C(69)-C(68)-H(68)	127.4
C(61)-C(62)-H(62)	125.1	C(67)-C(68)-H(68)	127.4
Fe(41)-C(62)-H(62)	126.2	Fe(41)-C(68)-H(68)	128.0
C(64)-C(63)-C(62)	109.1(18)	C(70)-C(69)-C(68)	109.9(19)
C(64)-C(63)-Fe(41)	70.0(13)	C(70)-C(69)-Fe(41)	69.0(12)
C(62)-C(63)-Fe(41)	69.5(10)	C(68)-C(69)-Fe(41)	71.2(13)
C(64)-C(63)-H(63)	125.4	C(70)-C(69)-H(69)	125.1
C(62)-C(63)-H(63)	125.4	C(68)-C(69)-H(69)	125.1

Fe(41)-C(69)-H(69)	126.3
C(69)-C(70)-C(66)	108.9(19)
C(69)-C(70)-Fe(41)	71.2(12)
C(66)-C(70)-Fe(41)	71.3(10)
C(69)-C(70)-H(70)	125.5
C(66)-C(70)-H(70)	125.5
Fe(41)-C(70)-H(70)	123.6
O(50)-C(71)-C(72)	106.5(15)
O(50)-C(71)-H(71A)	110.4
C(72)-C(71)-H(71A)	110.4
O(50)-C(71)-H(71B)	110.4
C(72)-C(71)-H(71B)	110.4
H(71A)-C(71)-H(71B)	108.6
C(71)-C(72)-H(72A)	109.5
C(71)-C(72)-H(72B)	109.5
H(72A)-C(72)-H(72B)	109.5
C(71)-C(72)-H(72C)	109.5
H(72A)-C(72)-H(72C)	109.5
H(72B)-C(72)-H(72C)	109.5
O(60)-C(73)-C(74)	108.1(16)
O(60)-C(73)-H(73A)	110.1
C(74)-C(73)-H(73A)	110.1
O(60)-C(73)-H(73B)	110.1
C(74)-C(73)-H(73B)	110.1
H(73A)-C(73)-H(73B)	108.4
C(73)-C(74)-H(74A)	109.5
C(73)-C(74)-H(74B)	109.5
H(74A)-C(74)-H(74B)	109.5
C(73)-C(74)-H(74C)	109.5
H(74A)-C(74)-H(74C)	109.5
H(74B)-C(74)-H(74C)	109.5

Symmetry transformations used to generate equivalent atoms:

Table 4. Anisotropic displacement parameters ($Å^2$x 10^3)for Complex **27**. The anisotropic displacement factor exponent takes the form: $-2p^2[h^2a^{*2}U^{11} + ... + 2 h k a^* b^* U^{12}]$

	U^{11}	U^{22}	U^{33}	U^{23}	U^{13}	U^{12}
Re(1)	45(1)	48(1)	45(1)	8(1)	5(1)	9(1)
Re(2)	47(1)	48(1)	48(1)	10(1)	5(1)	11(1)
C(1)	80(14)	65(12)	67(11)	11(9)	7(10)	29(11)
O(1)	107(12)	82(9)	96(9)	28(8)	47(9)	45(9)
C(2)	61(11)	54(10)	59(9)	12(8)	17(9)	21(9)
O(2)	87(10)	68(9)	112(11)	4(8)	-14(9)	-21(8)
C(3)	120(20)	110(18)	58(11)	30(11)	19(12)	5(15)
O(3)	116(13)	133(13)	69(8)	50(9)	15(8)	22(10)
C(4)	53(11)	62(11)	57(9)	-5(8)	6(8)	11(9)
O(4)	55(8)	104(11)	92(9)	-15(8)	16(7)	-7(8)
C(5)	130(20)	74(14)	61(12)	-7(10)	1(12)	-10(13)
O(5)	128(13)	92(10)	63(8)	24(7)	6(8)	0(9)
C(6)	80(14)	59(11)	67(11)	12(9)	7(10)	15(10)
O(6)	66(9)	88(10)	116(11)	9(8)	22(8)	33(8)
C(7)	108(17)	82(14)	49(10)	16(9)	20(10)	-2(12)
O(7)	113(12)	87(9)	60(7)	28(7)	5(7)	18(8)
C(8)	72(14)	53(11)	105(15)	15(10)	-2(12)	18(10)
O(8)	132(15)	110(13)	118(12)	-14(10)	-55(11)	-11(11)
C(9)	66(12)	54(11)	63(10)	4(8)	-4(9)	10(9)
O(9)	98(11)	65(9)	92(9)	27(7)	16(8)	-8(8)
C(10)	39(9)	49(9)	59(9)	12(7)	6(7)	13(7)
O(10)	62(8)	58(7)	62(6)	15(5)	4(6)	-2(6)
Re(3)	55(1)	57(1)	56(1)	20(1)	18(1)	16(1)
Re(4)	43(1)	47(1)	45(1)	11(1)	6(1)	4(1)
C(11)	84(14)	86(13)	52(9)	27(9)	38(9)	16(12)
O(11)	91(11)	120(12)	112(11)	31(9)	41(9)	56(10)
C(12)	52(11)	75(12)	67(10)	22(9)	24(9)	-4(9)
O(12)	95(11)	116(11)	61(7)	33(7)	19(7)	17(9)
C(13)	95(17)	67(13)	95(15)	0(11)	60(13)	9(12)
O(13)	121(15)	122(14)	153(16)	-63(12)	48(12)	-52(12)
C(14)	77(14)	113(16)	90(13)	58(12)	59(11)	60(13)
O(14)	200(20)	116(12)	112(12)	79(10)	88(12)	76(13)

C(15)	46(11)	92(15)	85(13)	36(11)	14(10)	18(11)
O(15)	60(10)	135(14)	113(12)	-19(10)	-9(9)	18(9)
C(16)	68(12)	54(10)	67(10)	0(8)	4(9)	18(9)
O(16)	81(10)	90(10)	100(10)	9(8)	6(8)	39(8)
C(17)	73(12)	62(11)	50(9)	18(8)	1(9)	6(9)
O(17)	91(11)	82(9)	92(9)	38(8)	24(8)	-8(8)
C(18)	63(12)	72(12)	52(9)	15(8)	8(8)	-15(9)
O(18)	115(13)	123(12)	56(8)	16(8)	8(8)	-16(10)
C(19)	53(10)	64(11)	46(8)	-7(8)	8(8)	-7(9)
O(19)	83(10)	60(8)	76(8)	0(6)	17(7)	-19(7)
C(20)	37(8)	43(8)	53(8)	10(7)	-6(7)	3(7)
O(20)	47(7)	60(7)	69(7)	15(6)	5(6)	-5(6)
Fe(1)	49(1)	57(1)	41(1)	10(1)	8(1)	8(1)
C(21)	55(10)	63(10)	44(8)	15(7)	8(7)	5(8)
C(22)	61(11)	56(10)	43(8)	3(7)	17(8)	7(8)
C(23)	102(17)	71(13)	59(10)	18(9)	8(11)	33(12)
C(24)	81(15)	121(18)	51(10)	21(11)	-1(10)	57(14)
C(25)	43(10)	105(15)	57(10)	6(9)	17(8)	15(10)
C(26)	51(10)	37(8)	67(9)	20(7)	26(8)	23(7)
C(27)	100(16)	66(12)	48(9)	14(8)	30(10)	-1(11)
C(28)	140(20)	62(13)	61(11)	2(9)	39(13)	-6(13)
C(29)	120(19)	78(14)	59(11)	33(10)	43(12)	41(13)
C(30)	73(13)	66(11)	60(10)	21(9)	22(9)	22(10)
C(31)	67(12)	65(11)	55(9)	24(8)	35(8)	0(9)
C(32)	100(18)	96(17)	114(17)	41(13)	24(14)	-20(14)
C(33)	71(13)	64(12)	71(11)	18(9)	-6(10)	-4(10)
C(34)	130(20)	60(13)	121(18)	15(12)	-11(16)	-40(14)
Re(41)	50(1)	48(1)	62(1)	11(1)	-9(1)	-2(1)
Re(42)	40(1)	50(1)	45(1)	8(1)	1(1)	4(1)
C(41)	77(14)	61(12)	86(12)	29(10)	-23(11)	-11(11)
O(41)	73(10)	88(10)	135(12)	20(9)	-15(9)	-44(9)
C(42)	43(10)	66(11)	77(11)	10(9)	-13(9)	6(9)
O(42)	115(13)	96(11)	103(10)	47(9)	-41(10)	-23(9)
C(43)	70(13)	50(11)	92(13)	4(10)	-30(11)	-9(10)
O(43)	129(15)	111(13)	140(15)	-43(11)	-29(12)	67(12)
C(44)	39(10)	91(14)	67(11)	14(10)	-15(8)	6(9)

O(44)	88(11)	118(12)	95(10)	52(9)	-29(8)	-14(9)
C(45)	80(15)	92(16)	71(12)	6(11)	7(11)	-48(13)
O(45)	83(11)	105(12)	128(13)	-4(10)	55(10)	8(9)
C(46)	37(9)	67(12)	91(12)	20(10)	3(9)	-14(9)
O(46)	58(9)	105(11)	115(11)	17(9)	0(8)	-29(8)
C(47)	48(10)	46(9)	63(9)	0(8)	13(8)	14(8)
O(47)	98(11)	71(9)	100(10)	33(7)	-18(8)	16(8)
C(48)	55(10)	73(11)	33(7)	5(7)	4(7)	21(9)
O(48)	94(11)	114(11)	59(8)	25(7)	15(7)	27(9)
C(49)	65(11)	56(10)	34(7)	-3(7)	0(7)	-3(9)
O(49)	61(8)	64(8)	66(7)	2(6)	-9(6)	19(6)
C(50)	39(8)	44(8)	42(7)	-1(6)	-6(7)	-9(7)
O(50)	66(8)	65(7)	57(6)	10(5)	9(6)	26(6)
Re(43)	45(1)	43(1)	50(1)	8(1)	-2(1)	-4(1)
Re(44)	49(1)	43(1)	45(1)	8(1)	3(1)	-6(1)
C(51)	70(13)	69(12)	58(10)	17(9)	-9(9)	9(10)
O(51)	105(12)	83(10)	136(13)	41(9)	-60(11)	-41(9)
C(52)	47(10)	69(12)	71(11)	9(9)	-8(9)	-8(9)
O(52)	71(9)	120(12)	74(8)	-21(8)	4(7)	41(9)
C(53)	77(13)	74(12)	47(9)	10(8)	0(9)	-25(10)
O(53)	101(11)	115(11)	75(8)	41(8)	-14(8)	-28(9)
C(54)	74(13)	61(12)	68(11)	21(9)	-21(10)	-16(10)
O(54)	90(11)	55(8)	122(11)	-6(8)	8(9)	30(8)
C(55)	103(17)	58(12)	57(10)	-3(9)	1(11)	-8(11)
O(55)	120(13)	95(10)	54(7)	19(7)	-2(8)	-10(9)
C(56)	62(12)	59(11)	76(11)	11(9)	2(10)	-4(10)
O(56)	79(10)	92(11)	139(13)	19(9)	-41(10)	-30(9)
C(57)	50(10)	87(13)	54(9)	16(9)	-2(8)	-11(10)
O(57)	160(15)	68(9)	68(8)	28(7)	-28(9)	-30(9)
C(58)	69(13)	67(12)	76(12)	1(10)	30(10)	-12(10)
O(58)	124(14)	111(13)	123(13)	-21(10)	71(11)	-4(11)
C(59)	34(9)	61(11)	60(9)	7(8)	6(7)	2(8)
O(59)	77(9)	53(7)	90(8)	15(6)	-8(7)	7(7)
C(60)	53(10)	52(9)	42(7)	10(7)	-5(7)	8(8)
O(60)	71(8)	57(7)	46(6)	4(5)	-12(5)	14(6)
Fe(41)	58(2)	70(2)	37(1)	7(1)	2(1)	-5(1)

C(61)	50(11)	73(12)	61(10)	-7(8)	10(8)	9(9)
C(62)	66(12)	43(9)	76(11)	0(8)	-4(10)	-17(9)
C(63)	107(18)	59(12)	76(13)	17(10)	-44(13)	-8(12)
C(64)	140(20)	78(15)	90(15)	-20(11)	-76(16)	51(15)
C(65)	67(13)	134(18)	44(9)	-15(10)	-14(9)	16(12)
C(66)	72(12)	56(10)	36(7)	8(7)	-6(8)	-16(9)
C(67)	86(14)	50(10)	57(9)	13(8)	-6(9)	-12(9)
C(68)	150(20)	85(15)	51(10)	26(10)	-8(13)	-57(16)
C(69)	92(18)	180(30)	54(11)	36(14)	9(12)	-56(19)
C(70)	59(13)	105(16)	80(13)	18(12)	-11(11)	-16(12)
C(71)	54(11)	49(10)	85(12)	11(9)	9(9)	17(8)
C(72)	109(19)	79(15)	112(17)	8(13)	9(15)	33(14)
C(73)	80(14)	70(12)	78(12)	10(10)	-18(10)	34(11)
C(74)	210(30)	82(17)	130(20)	34(15)	20(20)	60(19)

Table 5. Hydrogen coordinates (x 10^4) and isotropic displacement parameters (Å^{2}x 10^3) for Complex **27**.

	x	y	z	U(eq)
H(22)	7284	1969	1654	64
H(23)	6590	1853	251	92
H(24)	5236	983	248	100
H(25)	5083	543	1624	82
H(27)	6354	-722	-275	84
H(28)	6201	-1197	1120	106
H(29)	7433	-539	1968	100
H(30)	8361	266	1161	78
H(31A)	5684	542	4147	72
H(31B)	6425	-90	3846	72
H(32A)	5176	-856	4042	151
H(32B)	5403	-1002	3116	151
H(32C)	4668	-376	3422	151
H(33A)	8129	1930	-781	82
H(33B)	9046	1516	-878	82
H(34A)	9148	2792	-25	157
H(34B)	9389	2056	468	157
H(34C)	8480	2473	558	157
H(62)	6739	5083	975	75
H(63)	7835	4464	1832	97
H(64)	9204	4255	1062	129
H(65)	8942	4733	-304	102
H(67)	7380	6886	1776	76
H(68)	7985	7198	451	113
H(69)	9503	6721	445	129
H(70)	9841	6175	1725	98
H(71A)	5887	6290	-1119	75
H(71B)	6652	6931	-885	75
H(72A)	5391	7495	-301	151
H(72B)	6052	7341	391	151
H(72C)	5288	6708	153	151
H(73A)	8616	4941	3769	92

H(73B)	9393	5534	4095	92
H(74A)	9838	4147	3865	209
H(74B)	10312	4674	3281	209
H(74C)	9539	4087	2948	209

Table 6. Torsion angles [°] for Complex **27**.

C(5)-Re(1)-Re(2)-C(8)	-66.7(8)	C(13)-Re(3)-Re(4)-C(18)	-44.2(7)
C(4)-Re(1)-Re(2)-C(8)	-159.5(8)	C(14)-Re(3)-Re(4)-C(18)	-134.2(9)
C(2)-Re(1)-Re(2)-C(8)	24.4(7)	C(15)-Re(3)-Re(4)-C(18)	135.2(7)
C(3)-Re(1)-Re(2)-C(8)	113.5(9)	C(12)-Re(3)-Re(4)-C(20)	-133.4(7)
C(5)-Re(1)-Re(2)-C(9)	-147.6(8)	C(13)-Re(3)-Re(4)-C(20)	136.5(7)
C(4)-Re(1)-Re(2)-C(9)	119.6(7)	C(14)-Re(3)-Re(4)-C(20)	46.5(8)
C(2)-Re(1)-Re(2)-C(9)	-56.4(6)	C(15)-Re(3)-Re(4)-C(20)	-44.2(7)
C(3)-Re(1)-Re(2)-C(9)	32.7(8)	C(16)-Re(4)-C(20)-O(20)	-91.6(14)
C(5)-Re(1)-Re(2)-C(7)	16.9(8)	C(17)-Re(4)-C(20)-O(20)	3.5(14)
C(4)-Re(1)-Re(2)-C(7)	-75.9(7)	C(19)-Re(4)-C(20)-O(20)	172.6(13)
C(2)-Re(1)-Re(2)-C(7)	108.0(7)	Re(3)-Re(4)-C(20)-O(20)	90.5(13)
C(3)-Re(1)-Re(2)-C(7)	-162.9(9)	C(16)-Re(4)-C(20)-C(26)	87.9(13)
C(5)-Re(1)-Re(2)-C(10)	114.9(7)	C(17)-Re(4)-C(20)-C(26)	-177.0(12)
C(4)-Re(1)-Re(2)-C(10)	22.1(6)	C(19)-Re(4)-C(20)-C(26)	-8.0(13)
C(2)-Re(1)-Re(2)-C(10)	-154.0(6)	Re(3)-Re(4)-C(20)-C(26)	-90.1(12)
C(3)-Re(1)-Re(2)-C(10)	-64.9(8)	C(26)-C(20)-O(20)-C(33)	-165.8(14)
C(6)-Re(2)-C(10)-O(10)	91.6(14)	Re(4)-C(20)-O(20)-C(33)	14(2)
C(9)-Re(2)-C(10)-O(10)	-173.1(13)	O(10)-C(10)-C(21)-C(22)	-161.1(16)
C(7)-Re(2)-C(10)-O(10)	-3.3(14)	Re(2)-C(10)-C(21)-C(22)	17(2)
C(6)-Re(2)-C(10)-C(21)	-86.2(14)	O(10)-C(10)-C(21)-C(25)	18(2)
C(9)-Re(2)-C(10)-C(21)	9.1(14)	Re(2)-C(10)-C(21)-C(25)	-164.0(12)
C(7)-Re(2)-C(10)-C(21)	178.9(14)	O(10)-C(10)-C(21)-Fe(1)	-69.2(16)
Re(1)-Re(2)-C(10)-C(21)	89.6(13)	Re(2)-C(10)-C(21)-Fe(1)	109.1(14)
C(21)-C(10)-O(10)-C(31)	176.8(13)	C(25)-Fe(1)-C(21)-C(22)	-118.5(14)
Re(2)-C(10)-O(10)-C(31)	-1(2)	C(30)-Fe(1)-C(21)-C(22)	80.0(11)
C(12)-Re(3)-Re(4)-C(17)	-35.7(7)	C(27)-Fe(1)-C(21)-C(22)	-167.2(19)
C(13)-Re(3)-Re(4)-C(17)	-125.8(7)	C(26)-Fe(1)-C(21)-C(22)	46.4(19)
C(14)-Re(3)-Re(4)-C(17)	144.2(9)	C(29)-Fe(1)-C(21)-C(22)	121.9(11)
C(15)-Re(3)-Re(4)-C(17)	53.6(7)	C(23)-Fe(1)-C(21)-C(22)	-37.4(11)
C(12)-Re(3)-Re(4)-C(19)	133.2(7)	C(24)-Fe(1)-C(21)-C(22)	-81.4(11)
C(13)-Re(3)-Re(4)-C(19)	43.1(7)	C(28)-Fe(1)-C(21)-C(22)	162.7(11)
C(14)-Re(3)-Re(4)-C(19)	-46.9(8)	C(22)-Fe(1)-C(21)-C(10)	-124.4(19)
C(15)-Re(3)-Re(4)-C(19)	-137.5(7)	C(25)-Fe(1)-C(21)-C(10)	117.1(19)
C(12)-Re(3)-Re(4)-C(18)	45.9(7)	C(30)-Fe(1)-C(21)-C(10)	-44.4(17)

C(27)-Fe(1)-C(21)-C(10)	68(3)	Fe(1)-C(22)-C(23)-C(24)	58.5(13)
C(26)-Fe(1)-C(21)-C(10)	-78(2)	C(21)-C(22)-C(23)-Fe(1)	-59.0(11)
C(29)-Fe(1)-C(21)-C(10)	-2.5(17)	C(25)-Fe(1)-C(23)-C(22)	83.5(11)
C(23)-Fe(1)-C(21)-C(10)	-161.9(17)	C(30)-Fe(1)-C(23)-C(22)	-77.4(12)
C(24)-Fe(1)-C(21)-C(10)	154.2(17)	C(27)-Fe(1)-C(23)-C(22)	-161.7(11)
C(28)-Fe(1)-C(21)-C(10)	38.2(18)	C(21)-Fe(1)-C(23)-C(22)	37.5(10)
C(22)-Fe(1)-C(21)-C(25)	118.5(14)	C(26)-Fe(1)-C(23)-C(22)	-120.4(11)
C(30)-Fe(1)-C(21)-C(25)	-161.5(10)	C(29)-Fe(1)-C(23)-C(22)	-48(3)
C(27)-Fe(1)-C(21)-C(25)	-49(2)	C(24)-Fe(1)-C(23)-C(22)	119.9(16)
C(26)-Fe(1)-C(21)-C(25)	164.9(15)	C(28)-Fe(1)-C(23)-C(22)	164.4(19)
C(29)-Fe(1)-C(21)-C(25)	-119.6(12)	C(22)-Fe(1)-C(23)-C(24)	-119.9(16)
C(23)-Fe(1)-C(21)-C(25)	81.1(11)	C(25)-Fe(1)-C(23)-C(24)	-36.3(10)
C(24)-Fe(1)-C(21)-C(25)	37.1(11)	C(30)-Fe(1)-C(23)-C(24)	162.7(10)
C(28)-Fe(1)-C(21)-C(25)	-78.8(13)	C(27)-Fe(1)-C(23)-C(24)	78.4(13)
C(10)-C(21)-C(22)-C(23)	-179.9(16)	C(21)-Fe(1)-C(23)-C(24)	-82.4(11)
C(25)-C(21)-C(22)-C(23)	1.1(18)	C(26)-Fe(1)-C(23)-C(24)	119.7(11)
Fe(1)-C(21)-C(22)-C(23)	59.3(11)	C(29)-Fe(1)-C(23)-C(24)	-168.2(18)
C(10)-C(21)-C(22)-Fe(1)	120.8(17)	C(28)-Fe(1)-C(23)-C(24)	45(3)
C(25)-C(21)-C(22)-Fe(1)	-58.2(11)	C(22)-C(23)-C(24)-C(25)	0(2)
C(25)-Fe(1)-C(22)-C(21)	39.5(9)	Fe(1)-C(23)-C(24)-C(25)	57.5(13)
C(30)-Fe(1)-C(22)-C(21)	-118.3(9)	C(22)-C(23)-C(24)-Fe(1)	-57.8(12)
C(27)-Fe(1)-C(22)-C(21)	167(2)	C(22)-Fe(1)-C(24)-C(25)	-83.6(12)
C(26)-Fe(1)-C(22)-C(21)	-161.9(9)	C(30)-Fe(1)-C(24)-C(25)	-167(2)
C(29)-Fe(1)-C(22)-C(21)	-77.4(12)	C(27)-Fe(1)-C(24)-C(25)	118.5(12)
C(23)-Fe(1)-C(22)-C(21)	120.3(15)	C(21)-Fe(1)-C(24)-C(25)	-39.3(11)
C(24)-Fe(1)-C(22)-C(21)	82.8(10)	C(26)-Fe(1)-C(24)-C(25)	160.4(11)
C(28)-Fe(1)-C(22)-C(21)	-44(3)	C(29)-Fe(1)-C(24)-C(25)	48(3)
C(25)-Fe(1)-C(22)-C(23)	-80.8(12)	C(23)-Fe(1)-C(24)-C(25)	-121.4(17)
C(30)-Fe(1)-C(22)-C(23)	121.4(12)	C(28)-Fe(1)-C(24)-C(25)	76.2(14)
C(27)-Fe(1)-C(22)-C(23)	47(3)	C(22)-Fe(1)-C(24)-C(23)	37.7(10)
C(21)-Fe(1)-C(22)-C(23)	-120.3(15)	C(25)-Fe(1)-C(24)-C(23)	121.4(17)
C(26)-Fe(1)-C(22)-C(23)	77.8(13)	C(30)-Fe(1)-C(24)-C(23)	-46(3)
C(29)-Fe(1)-C(22)-C(23)	162.3(12)	C(27)-Fe(1)-C(24)-C(23)	-120.1(11)
C(24)-Fe(1)-C(22)-C(23)	-37.5(11)	C(21)-Fe(1)-C(24)-C(23)	82.0(11)
C(28)-Fe(1)-C(22)-C(23)	-164(2)	C(26)-Fe(1)-C(24)-C(23)	-78.3(13)
C(21)-C(22)-C(23)-C(24)	0(2)	C(29)-Fe(1)-C(24)-C(23)	169.5(18)

C(28)-Fe(1)-C(24)-C(23)	-162.4(10)	C(23)-Fe(1)-C(26)-C(27)	-121.0(11)
C(23)-C(24)-C(25)-C(21)	1(2)	C(24)-Fe(1)-C(26)-C(27)	-78.8(13)
Fe(1)-C(24)-C(25)-C(21)	58.6(12)	C(28)-Fe(1)-C(26)-C(27)	36.8(11)
C(23)-C(24)-C(25)-Fe(1)	-57.7(13)	C(22)-Fe(1)-C(26)-C(30)	79.4(11)
C(22)-C(21)-C(25)-C(24)	-1.2(19)	C(25)-Fe(1)-C(26)-C(30)	-162.1(17)
C(10)-C(21)-C(25)-C(24)	179.7(15)	C(27)-Fe(1)-C(26)-C(30)	-117.2(13)
Fe(1)-C(21)-C(25)-C(24)	-59.8(12)	C(21)-Fe(1)-C(26)-C(30)	44.8(19)
C(22)-C(21)-C(25)-Fe(1)	58.6(11)	C(29)-Fe(1)-C(26)-C(30)	-38.1(11)
C(10)-C(21)-C(25)-Fe(1)	-120.5(15)	C(23)-Fe(1)-C(26)-C(30)	121.8(11)
C(22)-Fe(1)-C(25)-C(24)	81.1(13)	C(24)-Fe(1)-C(26)-C(30)	164.0(12)
C(30)-Fe(1)-C(25)-C(24)	168(2)	C(28)-Fe(1)-C(26)-C(30)	-80.5(11)
C(27)-Fe(1)-C(25)-C(24)	-79.3(14)	C(22)-Fe(1)-C(26)-C(20)	-39.7(15)
C(21)-Fe(1)-C(25)-C(24)	119.2(17)	C(25)-Fe(1)-C(26)-C(20)	79(2)
C(26)-Fe(1)-C(25)-C(24)	-47(2)	C(30)-Fe(1)-C(26)-C(20)	-119.1(17)
C(29)-Fe(1)-C(25)-C(24)	-160.5(14)	C(27)-Fe(1)-C(26)-C(20)	123.7(17)
C(23)-Fe(1)-C(25)-C(24)	36.9(12)	C(21)-Fe(1)-C(26)-C(20)	-74(2)
C(28)-Fe(1)-C(25)-C(24)	-121.0(14)	C(29)-Fe(1)-C(26)-C(20)	-157.1(16)
C(22)-Fe(1)-C(25)-C(21)	-38.1(9)	C(23)-Fe(1)-C(26)-C(20)	2.7(15)
C(30)-Fe(1)-C(25)-C(21)	49(3)	C(24)-Fe(1)-C(26)-C(20)	44.9(17)
C(27)-Fe(1)-C(25)-C(21)	161.5(9)	C(28)-Fe(1)-C(26)-C(20)	160.4(16)
C(26)-Fe(1)-C(25)-C(21)	-166.0(14)	C(30)-C(26)-C(27)-C(28)	-1.3(19)
C(29)-Fe(1)-C(25)-C(21)	80.3(13)	C(20)-C(26)-C(27)-C(28)	-175.5(15)
C(23)-Fe(1)-C(25)-C(21)	-82.3(10)	Fe(1)-C(26)-C(27)-C(28)	-60.8(13)
C(24)-Fe(1)-C(25)-C(21)	-119.2(17)	C(30)-C(26)-C(27)-Fe(1)	59.5(10)
C(28)-Fe(1)-C(25)-C(21)	119.8(10)	C(20)-C(26)-C(27)-Fe(1)	-114.8(15)
O(20)-C(20)-C(26)-C(27)	156.1(15)	C(22)-Fe(1)-C(27)-C(26)	42(3)
Re(4)-C(20)-C(26)-C(27)	-23(2)	C(25)-Fe(1)-C(27)-C(26)	161.1(9)
O(20)-C(20)-C(26)-C(30)	-17.1(19)	C(30)-Fe(1)-C(27)-C(26)	-39.8(9)
Re(4)-C(20)-C(26)-C(30)	163.3(11)	C(21)-Fe(1)-C(27)-C(26)	-162.0(16)
O(20)-C(20)-C(26)-Fe(1)	67.9(15)	C(29)-Fe(1)-C(27)-C(26)	-83.5(11)
Re(4)-C(20)-C(26)-Fe(1)	-111.7(12)	C(23)-Fe(1)-C(27)-C(26)	76.8(13)
C(22)-Fe(1)-C(26)-C(27)	-163.4(10)	C(24)-Fe(1)-C(27)-C(26)	119.2(11)
C(25)-Fe(1)-C(26)-C(27)	-45(2)	C(28)-Fe(1)-C(27)-C(26)	-121.3(17)
C(30)-Fe(1)-C(26)-C(27)	117.2(13)	C(22)-Fe(1)-C(27)-C(28)	163(2)
C(21)-Fe(1)-C(26)-C(27)	162.1(15)	C(25)-Fe(1)-C(27)-C(28)	-77.5(15)
C(29)-Fe(1)-C(26)-C(27)	79.2(12)	C(30)-Fe(1)-C(27)-C(28)	81.5(14)

C(21)-Fe(1)-C(27)-C(28)	-41(3)
C(26)-Fe(1)-C(27)-C(28)	121.3(17)
C(29)-Fe(1)-C(27)-C(28)	37.8(13)
C(23)-Fe(1)-C(27)-C(28)	-161.9(14)
C(24)-Fe(1)-C(27)-C(28)	-119.4(14)
C(26)-C(27)-C(28)-C(29)	2(2)
Fe(1)-C(27)-C(28)-C(29)	-57.7(13)
C(26)-C(27)-C(28)-Fe(1)	59.2(12)
C(22)-Fe(1)-C(28)-C(29)	-46(3)
C(25)-Fe(1)-C(28)-C(29)	-122.7(11)
C(30)-Fe(1)-C(28)-C(29)	35.7(11)
C(27)-Fe(1)-C(28)-C(29)	117.4(18)
C(21)-Fe(1)-C(28)-C(29)	-78.6(13)
C(26)-Fe(1)-C(28)-C(29)	81.0(12)
C(23)-Fe(1)-C(28)-C(29)	163(2)
C(24)-Fe(1)-C(28)-C(29)	-163.7(11)
C(22)-Fe(1)-C(28)-C(27)	-163.3(19)
C(25)-Fe(1)-C(28)-C(27)	119.8(13)
C(30)-Fe(1)-C(28)-C(27)	-81.7(13)
C(21)-Fe(1)-C(28)-C(27)	164.0(12)
C(26)-Fe(1)-C(28)-C(27)	-36.4(12)
C(29)-Fe(1)-C(28)-C(27)	-117.4(18)
C(23)-Fe(1)-C(28)-C(27)	46(3)
C(24)-Fe(1)-C(28)-C(27)	78.9(14)
C(27)-C(28)-C(29)-C(30)	-1(2)
Fe(1)-C(28)-C(29)-C(30)	-58.3(13)
C(27)-C(28)-C(29)-Fe(1)	57.0(13)
C(22)-Fe(1)-C(29)-C(28)	161.6(10)
C(25)-Fe(1)-C(29)-C(28)	74.1(13)
C(30)-Fe(1)-C(29)-C(28)	-122.9(16)
C(27)-Fe(1)-C(29)-C(28)	-39.3(11)
C(21)-Fe(1)-C(29)-C(28)	119.0(11)
C(26)-Fe(1)-C(29)-C(28)	-83.2(12)
C(23)-Fe(1)-C(29)-C(28)	-161.9(19)
C(24)-Fe(1)-C(29)-C(28)	39(2)
C(22)-Fe(1)-C(29)-C(30)	-75.5(12)
C(25)-Fe(1)-C(29)-C(30)	-163.0(10)
C(27)-Fe(1)-C(29)-C(30)	83.6(12)
C(21)-Fe(1)-C(29)-C(30)	-118.1(11)
C(26)-Fe(1)-C(29)-C(30)	39.7(11)
C(23)-Fe(1)-C(29)-C(30)	-39(3)
C(24)-Fe(1)-C(29)-C(30)	161.9(17)
C(28)-Fe(1)-C(29)-C(30)	122.9(16)
C(28)-C(29)-C(30)-C(26)	1(2)
Fe(1)-C(29)-C(30)-C(26)	-59.8(11)
C(28)-C(29)-C(30)-Fe(1)	60.3(15)
C(27)-C(26)-C(30)-C(29)	0.5(18)
C(20)-C(26)-C(30)-C(29)	175.0(14)
Fe(1)-C(26)-C(30)-C(29)	60.5(12)
C(27)-C(26)-C(30)-Fe(1)	-60.1(11)
C(20)-C(26)-C(30)-Fe(1)	114.5(14)
C(22)-Fe(1)-C(30)-C(29)	122.8(12)
C(25)-Fe(1)-C(30)-C(29)	43(3)
C(27)-Fe(1)-C(30)-C(29)	-79.2(12)
C(21)-Fe(1)-C(30)-C(29)	79.9(14)
C(26)-Fe(1)-C(30)-C(29)	-117.6(16)
C(23)-Fe(1)-C(30)-C(29)	165.3(12)
C(24)-Fe(1)-C(30)-C(29)	-160(2)
C(28)-Fe(1)-C(30)-C(29)	-35.0(11)
C(22)-Fe(1)-C(30)-C(26)	-119.6(9)
C(25)-Fe(1)-C(30)-C(26)	160.6(19)
C(27)-Fe(1)-C(30)-C(26)	38.4(9)
C(21)-Fe(1)-C(30)-C(26)	-162.6(9)
C(29)-Fe(1)-C(30)-C(26)	117.6(16)
C(23)-Fe(1)-C(30)-C(26)	-77.1(12)
C(24)-Fe(1)-C(30)-C(26)	-43(3)
C(28)-Fe(1)-C(30)-C(26)	82.6(10)
C(10)-O(10)-C(31)-C(32)	178.7(14)
C(20)-O(20)-C(33)-C(34)	165.7(16)
C(45)-Re(41)-Re(42)-C(49)	134.3(7)
C(44)-Re(41)-Re(42)-C(49)	-135.3(7)
C(43)-Re(41)-Re(42)-C(49)	-45.7(7)

C(42)-Re(41)-Re(42)-C(49)	44.4(6)
C(45)-Re(41)-Re(42)-C(47)	-54.5(7)
C(44)-Re(41)-Re(42)-C(47)	35.8(7)
C(43)-Re(41)-Re(42)-C(47)	125.5(7)
C(42)-Re(41)-Re(42)-C(47)	-144.5(7)
C(45)-Re(41)-Re(42)-C(48)	-137.7(7)
C(44)-Re(41)-Re(42)-C(48)	-47.4(7)
C(43)-Re(41)-Re(42)-C(48)	42.2(7)
C(42)-Re(41)-Re(42)-C(48)	132.3(7)
C(45)-Re(41)-Re(42)-C(50)	42.8(7)
C(44)-Re(41)-Re(42)-C(50)	133.1(7)
C(43)-Re(41)-Re(42)-C(50)	-137.2(7)
C(42)-Re(41)-Re(42)-C(50)	-47.2(6)
C(46)-Re(42)-C(50)-O(50)	100.6(14)
C(49)-Re(42)-C(50)-O(50)	-163.6(14)
C(47)-Re(42)-C(50)-O(50)	7.6(15)
Re(41)-Re(42)-C(50)-O(50)	-82.8(13)
C(46)-Re(42)-C(50)-C(61)	-82.2(14)
C(49)-Re(42)-C(50)-C(61)	13.6(14)
C(47)-Re(42)-C(50)-C(61)	-175.2(13)
Re(41)-Re(42)-C(50)-C(61)	94.5(13)
C(61)-C(50)-O(50)-C(71)	168.4(14)
Re(42)-C(50)-O(50)-C(71)	-14(2)
C(55)-Re(43)-Re(44)-C(59)	149.9(7)
C(52)-Re(43)-Re(44)-C(59)	-119.6(7)
C(53)-Re(43)-Re(44)-C(59)	-32.0(7)
C(54)-Re(43)-Re(44)-C(59)	55.9(6)
C(55)-Re(43)-Re(44)-C(58)	66.9(8)
C(52)-Re(43)-Re(44)-C(58)	157.5(8)
C(53)-Re(43)-Re(44)-C(58)	-114.9(8)
C(54)-Re(43)-Re(44)-C(58)	-27.1(7)
C(55)-Re(43)-Re(44)-C(57)	-17.7(8)
C(52)-Re(43)-Re(44)-C(57)	72.8(7)
C(53)-Re(43)-Re(44)-C(57)	160.4(8)
C(54)-Re(43)-Re(44)-C(57)	-111.8(7)
C(55)-Re(43)-Re(44)-C(60)	-115.3(7)
C(52)-Re(43)-Re(44)-C(60)	-24.7(6)
C(53)-Re(43)-Re(44)-C(60)	62.9(7)
C(54)-Re(43)-Re(44)-C(60)	150.7(6)
C(56)-Re(44)-C(60)-O(60)	-90.3(15)
C(59)-Re(44)-C(60)-O(60)	173.9(15)
C(57)-Re(44)-C(60)-O(60)	2.7(15)
Re(43)-Re(44)-C(60)-O(60)	94.7(14)
C(56)-Re(44)-C(60)-C(66)	87.5(13)
C(59)-Re(44)-C(60)-C(66)	-8.3(13)
C(57)-Re(44)-C(60)-C(66)	-179.5(13)
Re(43)-Re(44)-C(60)-C(66)	-87.5(12)
C(66)-C(60)-O(60)-C(73)	-177.1(14)
Re(44)-C(60)-O(60)-C(73)	1(2)
O(50)-C(50)-C(61)-C(62)	27(2)
Re(42)-C(50)-C(61)-C(62)	-150.7(14)
O(50)-C(50)-C(61)-C(65)	-149.5(18)
Re(42)-C(50)-C(61)-C(65)	33(2)
O(50)-C(50)-C(61)-Fe(41)	-61.8(16)
Re(42)-C(50)-C(61)-Fe(41)	120.4(11)
C(67)-Fe(41)-C(61)-C(62)	-77.3(12)
C(70)-Fe(41)-C(61)-C(62)	170.6(19)
C(65)-Fe(41)-C(61)-C(62)	116.7(16)
C(69)-Fe(41)-C(61)-C(62)	-159.2(13)
C(63)-Fe(41)-C(61)-C(62)	36.7(12)
C(66)-Fe(41)-C(61)-C(62)	-48(2)
C(64)-Fe(41)-C(61)-C(62)	80.0(13)
C(68)-Fe(41)-C(61)-C(62)	-119.0(12)
C(67)-Fe(41)-C(61)-C(50)	44.7(17)
C(70)-Fe(41)-C(61)-C(50)	-67(3)
C(65)-Fe(41)-C(61)-C(50)	-121(2)
C(69)-Fe(41)-C(61)-C(50)	-37.1(19)
C(62)-Fe(41)-C(61)-C(50)	122.1(18)
C(63)-Fe(41)-C(61)-C(50)	158.8(17)
C(66)-Fe(41)-C(61)-C(50)	74(3)
C(64)-Fe(41)-C(61)-C(50)	-158.0(18)
C(68)-Fe(41)-C(61)-C(50)	3.0(17)

C(67)-Fe(41)-C(61)-C(65)	166.0(11)	C(62)-Fe(41)-C(63)-C(64)	120.6(16)
C(70)-Fe(41)-C(61)-C(65)	54(2)	C(66)-Fe(41)-C(63)-C(64)	-117.5(11)
C(69)-Fe(41)-C(61)-C(65)	84.1(16)	C(68)-Fe(41)-C(63)-C(64)	166.8(16)
C(62)-Fe(41)-C(61)-C(65)	-116.7(16)	C(61)-Fe(41)-C(63)-C(64)	83.6(11)
C(63)-Fe(41)-C(61)-C(65)	-79.9(13)	C(67)-Fe(41)-C(63)-C(62)	79.6(13)
C(66)-Fe(41)-C(61)-C(65)	-165.0(18)	C(70)-Fe(41)-C(63)-C(62)	162.7(12)
C(64)-Fe(41)-C(61)-C(65)	-36.7(14)	C(65)-Fe(41)-C(63)-C(62)	-82.1(12)
C(68)-Fe(41)-C(61)-C(65)	124.3(13)	C(69)-Fe(41)-C(63)-C(62)	-168(2)
C(50)-C(61)-C(62)-C(63)	-177.4(16)	C(66)-Fe(41)-C(63)-C(62)	121.9(12)
C(65)-C(61)-C(62)-C(63)	-0.1(19)	C(64)-Fe(41)-C(63)-C(62)	-120.6(16)
Fe(41)-C(61)-C(62)-C(63)	-58.9(12)	C(68)-Fe(41)-C(63)-C(62)	46(2)
C(50)-C(61)-C(62)-Fe(41)	-118.6(18)	C(61)-Fe(41)-C(63)-C(62)	-37.0(11)
C(65)-C(61)-C(62)-Fe(41)	58.7(12)	C(62)-C(63)-C(64)-C(65)	0(2)
C(67)-Fe(41)-C(62)-C(63)	-118.1(13)	Fe(41)-C(63)-C(64)-C(65)	-59.1(15)
C(70)-Fe(41)-C(62)-C(63)	-48(3)	C(62)-C(63)-C(64)-Fe(41)	58.6(13)
C(65)-Fe(41)-C(62)-C(63)	81.0(13)	C(67)-Fe(41)-C(64)-C(63)	46(3)
C(69)-Fe(41)-C(62)-C(63)	171(2)	C(70)-Fe(41)-C(64)-C(63)	122.9(11)
C(66)-Fe(41)-C(62)-C(63)	-77.2(14)	C(65)-Fe(41)-C(64)-C(63)	-118.4(17)
C(64)-Fe(41)-C(62)-C(63)	36.8(12)	C(69)-Fe(41)-C(64)-C(63)	163.5(11)
C(68)-Fe(41)-C(62)-C(63)	-160.4(13)	C(62)-Fe(41)-C(64)-C(63)	-37.0(10)
C(61)-Fe(41)-C(62)-C(63)	120.9(17)	C(66)-Fe(41)-C(64)-C(63)	80.8(13)
C(67)-Fe(41)-C(62)-C(61)	121.0(10)	C(68)-Fe(41)-C(64)-C(63)	-163(2)
C(70)-Fe(41)-C(62)-C(61)	-169(2)	C(61)-Fe(41)-C(64)-C(63)	-80.9(11)
C(65)-Fe(41)-C(62)-C(61)	-39.9(10)	C(67)-Fe(41)-C(64)-C(65)	164.8(18)
C(69)-Fe(41)-C(62)-C(61)	50(3)	C(70)-Fe(41)-C(64)-C(65)	-118.7(13)
C(63)-Fe(41)-C(62)-C(61)	-120.9(17)	C(69)-Fe(41)-C(64)-C(65)	-78.1(15)
C(66)-Fe(41)-C(62)-C(61)	162.0(10)	C(62)-Fe(41)-C(64)-C(65)	81.4(13)
C(64)-Fe(41)-C(62)-C(61)	-84.0(12)	C(63)-Fe(41)-C(64)-C(65)	118.4(17)
C(68)-Fe(41)-C(62)-C(61)	78.7(12)	C(66)-Fe(41)-C(64)-C(65)	-160.8(12)
C(61)-C(62)-C(63)-C(64)	0(2)	C(68)-Fe(41)-C(64)-C(65)	-45(3)
Fe(41)-C(62)-C(63)-C(64)	-58.9(14)	C(61)-Fe(41)-C(64)-C(65)	37.5(12)
C(61)-C(62)-C(63)-Fe(41)	59.3(12)	C(63)-C(64)-C(65)-C(61)	0(2)
C(67)-Fe(41)-C(63)-C(64)	-159.9(10)	Fe(41)-C(64)-C(65)-C(61)	-59.1(14)
C(70)-Fe(41)-C(63)-C(64)	-76.8(14)	C(63)-C(64)-C(65)-Fe(41)	59.5(14)
C(65)-Fe(41)-C(63)-C(64)	38.4(10)	C(62)-C(61)-C(65)-C(64)	0(2)
C(69)-Fe(41)-C(63)-C(64)	-48(3)	C(50)-C(61)-C(65)-C(64)	177.2(17)

Fe(41)-C(61)-C(65)-C(64)	59.0(14)
C(62)-C(61)-C(65)-Fe(41)	-59.2(11)
C(50)-C(61)-C(65)-Fe(41)	118.2(18)
C(67)-Fe(41)-C(65)-C(64)	-160(2)
C(70)-Fe(41)-C(65)-C(64)	80.6(17)
C(69)-Fe(41)-C(65)-C(64)	122.8(16)
C(62)-Fe(41)-C(65)-C(64)	-81.9(15)
C(63)-Fe(41)-C(65)-C(64)	-38.0(13)
C(66)-Fe(41)-C(65)-C(64)	46(3)
C(68)-Fe(41)-C(65)-C(64)	164.3(16)
C(61)-Fe(41)-C(65)-C(64)	-120.9(19)
C(67)-Fe(41)-C(65)-C(61)	-40(3)
C(70)-Fe(41)-C(65)-C(61)	-158.5(11)
C(69)-Fe(41)-C(65)-C(61)	-116.3(13)
C(62)-Fe(41)-C(65)-C(61)	39.0(11)
C(63)-Fe(41)-C(65)-C(61)	82.9(12)
C(66)-Fe(41)-C(65)-C(61)	166.8(16)
C(64)-Fe(41)-C(65)-C(61)	120.9(19)
C(68)-Fe(41)-C(65)-C(61)	-74.8(16)
O(60)-C(60)-C(66)-C(70)	-31(2)
Re(44)-C(60)-C(66)-C(70)	150.5(15)
O(60)-C(60)-C(66)-C(67)	144.5(16)
Re(44)-C(60)-C(66)-C(67)	-34(2)
O(60)-C(60)-C(66)-Fe(41)	56.6(18)
Re(44)-C(60)-C(66)-Fe(41)	-121.6(12)
C(67)-Fe(41)-C(66)-C(70)	-119.2(15)
C(65)-Fe(41)-C(66)-C(70)	48(2)
C(69)-Fe(41)-C(66)-C(70)	-37.7(13)
C(62)-Fe(41)-C(66)-C(70)	165.7(11)
C(63)-Fe(41)-C(66)-C(70)	123.8(12)
C(64)-Fe(41)-C(66)-C(70)	81.6(15)
C(68)-Fe(41)-C(66)-C(70)	-80.6(13)
C(61)-Fe(41)-C(66)-C(70)	-158.1(19)
C(70)-Fe(41)-C(66)-C(67)	119.2(15)
C(65)-Fe(41)-C(66)-C(67)	167.4(19)
C(69)-Fe(41)-C(66)-C(67)	81.5(13)
C(62)-Fe(41)-C(66)-C(67)	-75.1(12)
C(63)-Fe(41)-C(66)-C(67)	-117.0(12)
C(64)-Fe(41)-C(66)-C(67)	-159.2(13)
C(68)-Fe(41)-C(66)-C(67)	38.6(12)
C(61)-Fe(41)-C(66)-C(67)	-39(2)
C(67)-Fe(41)-C(66)-C(60)	121(2)
C(70)-Fe(41)-C(66)-C(60)	-119(2)
C(65)-Fe(41)-C(66)-C(60)	-71(3)
C(69)-Fe(41)-C(66)-C(60)	-157.2(19)
C(62)-Fe(41)-C(66)-C(60)	46.2(18)
C(63)-Fe(41)-C(66)-C(60)	4.4(18)
C(64)-Fe(41)-C(66)-C(60)	-38(2)
C(68)-Fe(41)-C(66)-C(60)	159.9(19)
C(61)-Fe(41)-C(66)-C(60)	82(2)
C(70)-C(66)-C(67)-C(68)	-4.8(19)
C(60)-C(66)-C(67)-C(68)	178.8(15)
Fe(41)-C(66)-C(67)-C(68)	-62.8(12)
C(70)-C(66)-C(67)-Fe(41)	58.0(12)
C(60)-C(66)-C(67)-Fe(41)	-118.5(16)
C(70)-Fe(41)-C(67)-C(66)	-37.3(10)
C(65)-Fe(41)-C(67)-C(66)	-165(2)
C(69)-Fe(41)-C(67)-C(66)	-80.6(12)
C(62)-Fe(41)-C(67)-C(66)	123.2(10)
C(63)-Fe(41)-C(67)-C(66)	81.2(12)
C(64)-Fe(41)-C(67)-C(66)	48(3)
C(68)-Fe(41)-C(67)-C(66)	-118.2(17)
C(61)-Fe(41)-C(67)-C(66)	165.1(10)
C(70)-Fe(41)-C(67)-C(68)	80.8(13)
C(65)-Fe(41)-C(67)-C(68)	-46(3)
C(69)-Fe(41)-C(67)-C(68)	37.6(12)
C(62)-Fe(41)-C(67)-C(68)	-118.6(13)
C(63)-Fe(41)-C(67)-C(68)	-160.6(13)
C(66)-Fe(41)-C(67)-C(68)	118.2(17)
C(64)-Fe(41)-C(67)-C(68)	166(2)
C(61)-Fe(41)-C(67)-C(68)	-76.7(15)
C(66)-C(67)-C(68)-C(69)	4(2)

Fe(41)-C(67)-C(68)-C(69)	-58.9(16)
C(66)-C(67)-C(68)-Fe(41)	62.5(12)
C(67)-Fe(41)-C(68)-C(69)	117.9(17)
C(70)-Fe(41)-C(68)-C(69)	36.4(12)
C(65)-Fe(41)-C(68)-C(69)	-78.4(14)
C(62)-Fe(41)-C(68)-C(69)	-162.7(11)
C(63)-Fe(41)-C(68)-C(69)	163.9(16)
C(66)-Fe(41)-C(68)-C(69)	79.8(13)
C(64)-Fe(41)-C(68)-C(69)	-44(3)
C(61)-Fe(41)-C(68)-C(69)	-120.6(12)
C(70)-Fe(41)-C(68)-C(67)	-81.5(12)
C(65)-Fe(41)-C(68)-C(67)	163.7(11)
C(69)-Fe(41)-C(68)-C(67)	-117.9(17)
C(62)-Fe(41)-C(68)-C(67)	79.4(13)
C(63)-Fe(41)-C(68)-C(67)	46(2)
C(66)-Fe(41)-C(68)-C(67)	-38.1(11)
C(64)-Fe(41)-C(68)-C(67)	-162(2)
C(61)-Fe(41)-C(68)-C(67)	121.4(12)
C(67)-C(68)-C(69)-C(70)	-1(3)
Fe(41)-C(68)-C(69)-C(70)	-58.3(17)
C(67)-C(68)-C(69)-Fe(41)	57.4(13)
C(67)-Fe(41)-C(69)-C(70)	82.1(14)
C(65)-Fe(41)-C(69)-C(70)	-117.6(14)
C(62)-Fe(41)-C(69)-C(70)	161.2(18)
C(63)-Fe(41)-C(69)-C(70)	-38(4)
C(66)-Fe(41)-C(69)-C(70)	37.9(13)
C(64)-Fe(41)-C(69)-C(70)	-74.7(16)
C(68)-Fe(41)-C(69)-C(70)	121(2)
C(61)-Fe(41)-C(69)-C(70)	-162.5(13)
C(67)-Fe(41)-C(69)-C(68)	-38.9(11)
C(70)-Fe(41)-C(69)-C(68)	-121(2)
C(65)-Fe(41)-C(69)-C(68)	121.3(12)
C(62)-Fe(41)-C(69)-C(68)	40(3)
C(63)-Fe(41)-C(69)-C(68)	-159(3)
C(66)-Fe(41)-C(69)-C(68)	-83.1(13)
C(64)-Fe(41)-C(69)-C(68)	164.3(11)
C(61)-Fe(41)-C(69)-C(68)	76.5(14)
C(68)-C(69)-C(70)-C(66)	-2(3)
Fe(41)-C(69)-C(70)-C(66)	-61.6(14)
C(68)-C(69)-C(70)-Fe(41)	59.6(17)
C(67)-C(66)-C(70)-C(69)	4(2)
C(60)-C(66)-C(70)-C(69)	-179.3(17)
Fe(41)-C(66)-C(70)-C(69)	61.6(16)
C(67)-C(66)-C(70)-Fe(41)	-57.4(11)
C(60)-C(66)-C(70)-Fe(41)	119.1(16)
C(67)-Fe(41)-C(70)-C(69)	-80.7(15)
C(65)-Fe(41)-C(70)-C(69)	81.7(17)
C(62)-Fe(41)-C(70)-C(69)	-157(2)
C(63)-Fe(41)-C(70)-C(69)	166.4(16)
C(66)-Fe(41)-C(70)-C(69)	-118(2)
C(64)-Fe(41)-C(70)-C(69)	124.7(17)
C(68)-Fe(41)-C(70)-C(69)	-36.2(15)
C(61)-Fe(41)-C(70)-C(69)	42(3)
C(67)-Fe(41)-C(70)-C(66)	37.8(10)
C(65)-Fe(41)-C(70)-C(66)	-159.8(11)
C(69)-Fe(41)-C(70)-C(66)	118(2)
C(62)-Fe(41)-C(70)-C(66)	-39(3)
C(63)-Fe(41)-C(70)-C(66)	-75.1(15)
C(64)-Fe(41)-C(70)-C(66)	-116.8(13)
C(68)-Fe(41)-C(70)-C(66)	82.3(12)
C(61)-Fe(41)-C(70)-C(66)	160.4(17)
C(50)-O(50)-C(71)-C(72)	-176.9(15)
C(60)-O(60)-C(73)-C(74)	178.2(18)

Appendix 9

Crystallographic data of Complex 28

Table 1. Crystal data and structure refinement for Complex **28**.

Identification code	db61a3_c2c	
Empirical formula	$C_{32.50}\ H_{29}\ Cl_3\ Fe_2\ O_8\ Re_2$	
Formula weight	1138.01	
Temperature	293(2) K	
Wavelength	0.71073 Å	
Crystal system	Monoclinic	
Space group	C 2/c	
Unit cell dimensions	a = 22.2670(16) Å	a= 90°.
	b = 15.2017(11) Å	b= 100.1860(10)°.
	c = 21.6438(15) Å	g = 90°.
Volume	7210.9(9) Å^3	
Z	8	
Density (calculated)	2.097 Mg/m^3	
Absorption coefficient	7.751 mm^{-1}	
F(000)	4328	
Crystal size	0.40 x 0.36 x 0.26 mm^3	
Theta range for data collection	2.38 to 26.25°.	
Index ranges	-27<=h<=16, -12<=k<=18, -23<=l<=26	
Reflections collected	18498	
Independent reflections	6671 [R(int) = 0.0367]	
Completeness to theta = 25.00°	99.2 %	
Absorption correction	Semi-empirical from equivalents	
Max. and min. transmission	0.133 and 0.069	
Refinement method	Full-matrix least-squares on F^2	
Data / restraints / parameters	6671 / 0 / 431	
Goodness-of-fit on F^2	1.156	
Final R indices [I>2σ(I)]	R1 = 0.0346, wR2 = 0.0885	
R indices (all data)	R1 = 0.0386, wR2 = 0.0927	
Extinction coefficient	0	
Largest diff. peak and hole	2.194 and -0.856 e.Å^{-3}	

Table 2. Atomic coordinates (x 10^4) and equivalent isotropic displacement parameters (Å^{2}x 10^3) for Complex **28**. U(eq) is defined as one third of the trace of the orthogonalized U^{ij} tensor.

Re(1)	1923(1)	4253(1)	503(1)	41(1)
Re(2)	561(1)	2891(1)	-405(1)	43(1)
Cl(1)	790(1)	4375(1)	106(1)	48(1)
Cl(2)	1700(1)	2769(1)	-14(1)	47(1)
C(1)	2066(3)	4734(5)	-295(4)	63(2)
O(1)	2152(3)	5031(5)	-755(3)	100(2)
C(2)	2778(3)	4114(4)	737(3)	51(2)
O(2)	3302(2)	4083(3)	863(3)	66(1)
C(3)	2045(3)	5377(5)	869(3)	54(2)
O(3)	2135(2)	6074(4)	1086(3)	80(2)
C(4)	1727(3)	3645(4)	1353(3)	45(1)
O(4)	1333(2)	3916(3)	1703(2)	62(1)
C(5)	737(4)	3363(6)	-1196(4)	74(2)
O(5)	834(4)	3650(6)	-1650(3)	131(3)
C(6)	404(3)	1793(5)	-808(3)	61(2)
O(6)	282(3)	1144(4)	-1075(3)	98(2)
C(7)	-273(3)	3150(5)	-693(3)	54(2)
O(7)	-765(2)	3323(4)	-901(3)	73(1)
C(8)	410(3)	2416(4)	499(3)	42(1)
O(8)	643(2)	1699(3)	796(2)	62(1)
Fe(1)	2703(1)	2856(1)	2307(1)	58(1)
C(9)	1968(3)	2817(4)	1602(3)	46(1)
C(10)	1834(4)	2406(5)	2161(3)	62(2)
C(11)	2235(4)	1693(5)	2311(4)	67(2)
C(12)	2626(3)	1653(4)	1872(4)	62(2)
C(13)	2469(3)	2333(4)	1429(3)	50(1)
C(14)	3042(7)	4096(7)	2442(5)	107(4)
C(15)	2789(6)	3809(8)	2982(5)	109(4)
C(16)	3139(7)	3065(8)	3203(5)	111(4)
C(17)	3568(6)	2904(8)	2815(6)	110(4)
C(18)	3498(5)	3541(9)	2361(6)	107(4)
Fe(2)	-836(1)	2488(1)	860(1)	56(1)
C(19)	46(3)	2850(4)	895(3)	42(1)
C(20)	-354(3)	3590(4)	735(3)	48(1)
C(21)	-669(3)	3726(5)	1231(3)	60(2)
C(22)	-491(3)	3082(5)	1696(3)	64(2)
C(23)	-50(3)	2537(5)	1497(3)	53(2)

C(24)	-1129(6)	1670(9)	133(5)	111(4)
C(25)	-1526(6)	2362(10)	98(6)	113(4)
C(26)	-1760(4)	2332(10)	644(8)	121(4)
C(27)	-1500(5)	1655(10)	1033(6)	116(4)
C(28)	-1093(5)	1213(7)	695(6)	102(3)
C(29)	1028(5)	4762(6)	1635(4)	85(3)
C(30)	833(9)	5005(8)	2168(6)	177(8)
C(31)	998(5)	1047(6)	522(5)	91(3)
C(32)	1155(7)	346(7)	947(6)	125(4)
Cl(3)	645(3)	605(4)	2546(3)	187(2)
C(33)	0	-75(18)	2500	250(20)

Table 3. Bond lengths [Å] and angles [°] for Complex **28**.

Re(1)-C(3)	1.882(7)
Re(1)-C(2)	1.894(7)
Re(1)-C(1)	1.953(7)
Re(1)-C(4)	2.171(6)
Re(1)-Cl(1)	2.5252(15)
Re(1)-Cl(2)	2.5289(15)
Re(2)-C(6)	1.887(8)
Re(2)-C(7)	1.892(7)
Re(2)-C(5)	1.959(8)
Re(2)-C(8)	2.166(6)
Re(2)-Cl(1)	2.5249(15)
Re(2)-Cl(2)	2.5351(15)
C(1)-O(1)	1.140(8)
C(2)-O(2)	1.150(8)
C(3)-O(3)	1.162(8)
C(4)-O(4)	1.321(7)
C(4)-C(9)	1.437(9)
O(4)-C(29)	1.451(9)
C(5)-O(5)	1.131(9)
C(6)-O(6)	1.151(9)
C(7)-O(7)	1.140(8)
C(8)-O(8)	1.324(7)
C(8)-C(19)	1.441(8)
O(8)-C(31)	1.457(9)
Fe(1)-C(10)	2.024(8)
Fe(1)-C(9)	2.030(6)
Fe(1)-C(14)	2.032(9)
Fe(1)-C(16)	2.035(9)
Fe(1)-C(18)	2.039(10)
Fe(1)-C(13)	2.040(6)
Fe(1)-C(15)	2.043(9)
Fe(1)-C(17)	2.044(11)
Fe(1)-C(12)	2.050(7)
Fe(1)-C(11)	2.054(8)
C(9)-C(10)	1.440(9)
C(9)-C(13)	1.440(9)
C(10)-C(11)	1.405(10)
C(10)-H(10)	0.9800
C(11)-C(12)	1.400(10)

C(11)-H(11)	0.9800
C(12)-C(13)	1.410(9)
C(12)-H(12)	0.9800
C(13)-H(13)	0.9800
C(14)-C(18)	1.354(16)
C(14)-C(15)	1.453(16)
C(14)-H(14)	0.9800
C(15)-C(16)	1.408(16)
C(15)-H(15)	0.9800
C(16)-C(17)	1.400(17)
C(16)-H(16)	0.9800
C(17)-C(18)	1.369(16)
C(17)-H(17)	0.9800
C(18)-H(18)	0.9800
Fe(2)-C(24)	2.022(10)
Fe(2)-C(19)	2.027(6)
Fe(2)-C(23)	2.027(7)
Fe(2)-C(27)	2.032(8)
Fe(2)-C(20)	2.033(6)
Fe(2)-C(28)	2.035(9)
Fe(2)-C(26)	2.042(9)
Fe(2)-C(22)	2.046(8)
Fe(2)-C(21)	2.054(7)
Fe(2)-C(25)	2.055(10)
C(19)-C(23)	1.437(8)
C(19)-C(20)	1.438(8)
C(20)-C(21)	1.399(9)
C(20)-H(20)	0.9800
C(21)-C(22)	1.410(11)
C(21)-H(21)	0.9800
C(22)-C(23)	1.408(10)
C(22)-H(22)	0.9800
C(23)-H(23)	0.9800
C(24)-C(25)	1.367(18)
C(24)-C(28)	1.391(15)
C(24)-H(24)	0.9800
C(25)-C(26)	1.373(18)
C(25)-H(25)	0.9800
C(26)-C(27)	1.388(17)
C(26)-H(26)	0.9800

C(27)-C(28)	1.429(17)
C(27)-H(27)	0.9800
C(28)-H(28)	0.9800
C(29)-C(30)	1.355(12)
C(29)-H(29A)	0.9700
C(29)-H(29B)	0.9700
C(30)-H(30A)	0.9600
C(30)-H(30B)	0.9600
C(30)-H(30C)	0.9600
C(31)-C(32)	1.411(13)
C(31)-H(31A)	0.9700
C(31)-H(31B)	0.9700
C(32)-H(32A)	0.9600
C(32)-H(32B)	0.9600
C(32)-H(32C)	0.9600
Cl(3)-C(33)	1.758(16)
C(33)-Cl(3)#1	1.758(16)
C(33)-H(33A)	0.9700
C(33)-H(33B)	0.9700

C(3)-Re(1)-C(2)	85.8(3)
C(3)-Re(1)-C(1)	90.0(3)
C(2)-Re(1)-C(1)	88.0(3)
C(3)-Re(1)-C(4)	93.7(3)
C(2)-Re(1)-C(4)	94.0(3)
C(1)-Re(1)-C(4)	175.9(3)
C(3)-Re(1)-Cl(1)	97.90(19)
C(2)-Re(1)-Cl(1)	175.2(2)
C(1)-Re(1)-Cl(1)	88.9(2)
C(4)-Re(1)-Cl(1)	88.90(16)
C(3)-Re(1)-Cl(2)	176.8(2)
C(2)-Re(1)-Cl(2)	97.3(2)
C(1)-Re(1)-Cl(2)	89.6(2)
C(4)-Re(1)-Cl(2)	86.67(16)
Cl(1)-Re(1)-Cl(2)	78.97(5)
C(6)-Re(2)-C(7)	86.6(3)
C(6)-Re(2)-C(5)	88.2(4)
C(7)-Re(2)-C(5)	88.4(3)
C(6)-Re(2)-C(8)	94.4(3)
C(7)-Re(2)-C(8)	93.9(2)

C(5)-Re(2)-C(8)	176.6(3)
C(6)-Re(2)-Cl(1)	178.1(2)
C(7)-Re(2)-Cl(1)	93.9(2)
C(5)-Re(2)-Cl(1)	89.9(3)
C(8)-Re(2)-Cl(1)	87.38(16)
C(6)-Re(2)-Cl(2)	100.5(2)
C(7)-Re(2)-Cl(2)	172.2(2)
C(5)-Re(2)-Cl(2)	88.6(2)
C(8)-Re(2)-Cl(2)	88.88(15)
Cl(1)-Re(2)-Cl(2)	78.86(5)
Re(2)-Cl(1)-Re(1)	101.28(5)
Re(1)-Cl(2)-Re(2)	100.90(5)
O(1)-C(1)-Re(1)	178.5(8)
O(2)-C(2)-Re(1)	175.5(6)
O(3)-C(3)-Re(1)	177.8(6)
O(4)-C(4)-C(9)	107.4(5)
O(4)-C(4)-Re(1)	127.4(4)
C(9)-C(4)-Re(1)	125.0(4)
C(4)-O(4)-C(29)	124.3(5)
O(5)-C(5)-Re(2)	178.7(9)
O(6)-C(6)-Re(2)	176.2(7)
O(7)-C(7)-Re(2)	175.9(6)
O(8)-C(8)-C(19)	107.6(5)
O(8)-C(8)-Re(2)	127.1(4)
C(19)-C(8)-Re(2)	125.3(4)
C(8)-O(8)-C(31)	123.8(5)
C(10)-Fe(1)-C(9)	41.6(3)
C(10)-Fe(1)-C(14)	131.1(5)
C(9)-Fe(1)-C(14)	111.4(4)
C(10)-Fe(1)-C(16)	118.8(5)
C(9)-Fe(1)-C(16)	154.9(5)
C(14)-Fe(1)-C(16)	67.4(4)
C(10)-Fe(1)-C(18)	168.0(5)
C(9)-Fe(1)-C(18)	129.4(4)
C(14)-Fe(1)-C(18)	38.9(5)
C(16)-Fe(1)-C(18)	66.6(5)
C(10)-Fe(1)-C(13)	69.2(3)
C(9)-Fe(1)-C(13)	41.4(2)
C(14)-Fe(1)-C(13)	121.5(4)
C(16)-Fe(1)-C(13)	161.5(5)

C(18)-Fe(1)-C(13)	109.2(4)
C(10)-Fe(1)-C(15)	108.5(4)
C(9)-Fe(1)-C(15)	121.3(4)
C(14)-Fe(1)-C(15)	41.8(5)
C(16)-Fe(1)-C(15)	40.4(4)
C(18)-Fe(1)-C(15)	68.1(5)
C(13)-Fe(1)-C(15)	156.8(4)
C(10)-Fe(1)-C(17)	151.6(4)
C(9)-Fe(1)-C(17)	164.3(5)
C(14)-Fe(1)-C(17)	66.3(5)
C(16)-Fe(1)-C(17)	40.2(5)
C(18)-Fe(1)-C(17)	39.2(5)
C(13)-Fe(1)-C(17)	125.2(5)
C(15)-Fe(1)-C(17)	68.2(5)
C(10)-Fe(1)-C(12)	68.1(3)
C(9)-Fe(1)-C(12)	68.8(3)
C(14)-Fe(1)-C(12)	153.2(5)
C(16)-Fe(1)-C(12)	124.3(4)
C(18)-Fe(1)-C(12)	118.9(5)
C(13)-Fe(1)-C(12)	40.3(3)
C(15)-Fe(1)-C(12)	161.9(4)
C(17)-Fe(1)-C(12)	105.9(4)
C(10)-Fe(1)-C(11)	40.3(3)
C(9)-Fe(1)-C(11)	68.7(3)
C(14)-Fe(1)-C(11)	166.9(5)
C(16)-Fe(1)-C(11)	106.6(4)
C(18)-Fe(1)-C(11)	151.1(5)
C(13)-Fe(1)-C(11)	67.8(3)
C(15)-Fe(1)-C(11)	126.2(5)
C(17)-Fe(1)-C(11)	117.3(4)
C(12)-Fe(1)-C(11)	39.9(3)
C(4)-C(9)-C(10)	125.2(6)
C(4)-C(9)-C(13)	127.3(6)
C(10)-C(9)-C(13)	106.4(6)
C(4)-C(9)-Fe(1)	117.0(4)
C(10)-C(9)-Fe(1)	68.9(4)
C(13)-C(9)-Fe(1)	69.6(4)
C(11)-C(10)-C(9)	108.1(6)
C(11)-C(10)-Fe(1)	71.0(5)
C(9)-C(10)-Fe(1)	69.4(4)

C(11)-C(10)-H(10)	125.9
C(9)-C(10)-H(10)	125.9
Fe(1)-C(10)-H(10)	125.9
C(12)-C(11)-C(10)	108.8(6)
C(12)-C(11)-Fe(1)	69.9(4)
C(10)-C(11)-Fe(1)	68.7(4)
C(12)-C(11)-H(11)	125.6
C(10)-C(11)-H(11)	125.6
Fe(1)-C(11)-H(11)	125.6
C(11)-C(12)-C(13)	108.8(6)
C(11)-C(12)-Fe(1)	70.2(4)
C(13)-C(12)-Fe(1)	69.4(4)
C(11)-C(12)-H(12)	125.6
C(13)-C(12)-H(12)	125.6
Fe(1)-C(12)-H(12)	125.6
C(12)-C(13)-C(9)	107.9(6)
C(12)-C(13)-Fe(1)	70.2(4)
C(9)-C(13)-Fe(1)	68.9(4)
C(12)-C(13)-H(13)	126.0
C(9)-C(13)-H(13)	126.0
Fe(1)-C(13)-H(13)	126.0
C(18)-C(14)-C(15)	108.9(11)
C(18)-C(14)-Fe(1)	70.8(6)
C(15)-C(14)-Fe(1)	69.5(6)
C(18)-C(14)-H(14)	125.5
C(15)-C(14)-H(14)	125.5
Fe(1)-C(14)-H(14)	125.5
C(16)-C(15)-C(14)	104.1(11)
C(16)-C(15)-Fe(1)	69.5(6)
C(14)-C(15)-Fe(1)	68.7(5)
C(16)-C(15)-H(15)	127.9
C(14)-C(15)-H(15)	127.9
Fe(1)-C(15)-H(15)	127.9
C(17)-C(16)-C(15)	109.4(11)
C(17)-C(16)-Fe(1)	70.3(6)
C(15)-C(16)-Fe(1)	70.1(5)
C(17)-C(16)-H(16)	125.3
C(15)-C(16)-H(16)	125.3
Fe(1)-C(16)-H(16)	125.3
C(18)-C(17)-C(16)	107.7(12)

C(18)-C(17)-Fe(1)	70.2(6)
C(16)-C(17)-Fe(1)	69.5(7)
C(18)-C(17)-H(17)	126.2
C(16)-C(17)-H(17)	126.2
Fe(1)-C(17)-H(17)	126.2
C(14)-C(18)-C(17)	109.9(12)
C(14)-C(18)-Fe(1)	70.3(6)
C(17)-C(18)-Fe(1)	70.6(7)
C(14)-C(18)-H(18)	125.1
C(17)-C(18)-H(18)	125.1
Fe(1)-C(18)-H(18)	125.1
C(24)-Fe(2)-C(19)	112.0(4)
C(24)-Fe(2)-C(23)	132.3(5)
C(19)-Fe(2)-C(23)	41.5(2)
C(24)-Fe(2)-C(27)	67.3(5)
C(19)-Fe(2)-C(27)	153.4(5)
C(23)-Fe(2)-C(27)	117.8(4)
C(24)-Fe(2)-C(20)	120.6(4)
C(19)-Fe(2)-C(20)	41.5(2)
C(23)-Fe(2)-C(20)	69.4(3)
C(27)-Fe(2)-C(20)	163.0(5)
C(24)-Fe(2)-C(28)	40.1(4)
C(19)-Fe(2)-C(28)	120.4(4)
C(23)-Fe(2)-C(28)	109.7(4)
C(27)-Fe(2)-C(28)	41.1(5)
C(20)-Fe(2)-C(28)	154.2(4)
C(24)-Fe(2)-C(26)	64.9(6)
C(19)-Fe(2)-C(26)	166.0(5)
C(23)-Fe(2)-C(26)	150.8(5)
C(27)-Fe(2)-C(26)	39.8(5)
C(20)-Fe(2)-C(26)	126.8(5)
C(28)-Fe(2)-C(26)	66.9(5)
C(24)-Fe(2)-C(22)	168.2(5)
C(19)-Fe(2)-C(22)	68.8(3)
C(23)-Fe(2)-C(22)	40.4(3)
C(27)-Fe(2)-C(22)	106.5(4)
C(20)-Fe(2)-C(22)	68.3(3)
C(28)-Fe(2)-C(22)	128.7(4)
C(26)-Fe(2)-C(22)	117.3(5)
C(24)-Fe(2)-C(21)	151.6(5)

C(19)-Fe(2)-C(21)	68.3(2)
C(23)-Fe(2)-C(21)	68.0(3)
C(27)-Fe(2)-C(21)	125.9(5)
C(20)-Fe(2)-C(21)	40.0(2)
C(28)-Fe(2)-C(21)	165.3(4)
C(26)-Fe(2)-C(21)	107.5(5)
C(22)-Fe(2)-C(21)	40.2(3)
C(24)-Fe(2)-C(25)	39.2(5)
C(19)-Fe(2)-C(25)	129.6(4)
C(23)-Fe(2)-C(25)	169.1(5)
C(27)-Fe(2)-C(25)	67.8(5)
C(20)-Fe(2)-C(25)	107.9(4)
C(28)-Fe(2)-C(25)	67.8(5)
C(26)-Fe(2)-C(25)	39.2(5)
C(22)-Fe(2)-C(25)	149.5(6)
C(21)-Fe(2)-C(25)	117.2(5)
C(23)-C(19)-C(20)	107.0(5)
C(23)-C(19)-C(8)	125.3(5)
C(20)-C(19)-C(8)	127.2(5)
C(23)-C(19)-Fe(2)	69.3(3)
C(20)-C(19)-Fe(2)	69.5(3)
C(8)-C(19)-Fe(2)	119.7(4)
C(21)-C(20)-C(19)	107.7(6)
C(21)-C(20)-Fe(2)	70.8(4)
C(19)-C(20)-Fe(2)	69.0(3)
C(21)-C(20)-H(20)	126.2
C(19)-C(20)-H(20)	126.2
Fe(2)-C(20)-H(20)	126.2
C(20)-C(21)-C(22)	109.2(6)
C(20)-C(21)-Fe(2)	69.2(4)
C(22)-C(21)-Fe(2)	69.6(4)
C(20)-C(21)-H(21)	125.4
C(22)-C(21)-H(21)	125.4
Fe(2)-C(21)-H(21)	125.4
C(23)-C(22)-C(21)	108.3(6)
C(23)-C(22)-Fe(2)	69.1(4)
C(21)-C(22)-Fe(2)	70.2(4)
C(23)-C(22)-H(22)	125.9
C(21)-C(22)-H(22)	125.9
Fe(2)-C(22)-H(22)	125.9

C(22)-C(23)-C(19)	107.8(6)
C(22)-C(23)-Fe(2)	70.5(4)
C(19)-C(23)-Fe(2)	69.2(3)
C(22)-C(23)-H(23)	126.1
C(19)-C(23)-H(23)	126.1
Fe(2)-C(23)-H(23)	126.1
C(25)-C(24)-C(28)	111.7(12)
C(25)-C(24)-Fe(2)	71.7(7)
C(28)-C(24)-Fe(2)	70.5(6)
C(25)-C(24)-H(24)	124.2
C(28)-C(24)-H(24)	124.2
Fe(2)-C(24)-H(24)	124.2
C(24)-C(25)-C(26)	105.5(12)
C(24)-C(25)-Fe(2)	69.1(6)
C(26)-C(25)-Fe(2)	69.9(6)
C(24)-C(25)-H(25)	127.2
C(26)-C(25)-H(25)	127.2
Fe(2)-C(25)-H(25)	127.2
C(25)-C(26)-C(27)	111.4(13)
C(25)-C(26)-Fe(2)	70.9(6)
C(27)-C(26)-Fe(2)	69.7(6)
C(25)-C(26)-H(26)	124.3
C(27)-C(26)-H(26)	124.3
Fe(2)-C(26)-H(26)	124.3
C(26)-C(27)-C(28)	105.9(11)
C(26)-C(27)-Fe(2)	70.5(6)
C(28)-C(27)-Fe(2)	69.5(5)
C(26)-C(27)-H(27)	127.0
C(28)-C(27)-H(27)	127.0
Fe(2)-C(27)-H(27)	127.0
C(24)-C(28)-C(27)	105.5(11)
C(24)-C(28)-Fe(2)	69.4(6)
C(27)-C(28)-Fe(2)	69.3(6)
C(24)-C(28)-H(28)	127.2
C(27)-C(28)-H(28)	127.2
Fe(2)-C(28)-H(28)	127.2
C(30)-C(29)-O(4)	111.7(8)
C(30)-C(29)-H(29A)	109.3
O(4)-C(29)-H(29A)	109.3
C(30)-C(29)-H(29B)	109.3

O(4)-C(29)-H(29B)	109.3
H(29A)-C(29)-H(29B)	107.9
C(29)-C(30)-H(30A)	109.5
C(29)-C(30)-H(30B)	109.5
H(30A)-C(30)-H(30B)	109.5
C(29)-C(30)-H(30C)	109.5
H(30A)-C(30)-H(30C)	109.5
H(30B)-C(30)-H(30C)	109.5
C(32)-C(31)-O(8)	109.8(8)
C(32)-C(31)-H(31A)	109.7
O(8)-C(31)-H(31A)	109.7
C(32)-C(31)-H(31B)	109.7
O(8)-C(31)-H(31B)	109.7
H(31A)-C(31)-H(31B)	108.2
C(31)-C(32)-H(32A)	109.5
C(31)-C(32)-H(32B)	109.5
H(32A)-C(32)-H(32B)	109.5
C(31)-C(32)-H(32C)	109.5
H(32A)-C(32)-H(32C)	109.5
H(32B)-C(32)-H(32C)	109.5
Cl(3)-C(33)-Cl(3)#1	108.0(15)
Cl(3)-C(33)-H(33A)	110.1
Cl(3)#1-C(33)-H(33A)	110.1
Cl(3)-C(33)-H(33B)	110.1
Cl(3)#1-C(33)-H(33B)	110.1
H(33A)-C(33)-H(33B)	108.4

Symmetry transformations used to generate equivalent atoms:

#1 -x,y,-z+1/2

Table 4. Anisotropic displacement parameters (Å^{2}x 10^3) for Complex **28**. The anisotropic displacement factor exponent takes the form: $-2\pi^2[h^2a^{*2}U^{11} + ... + 2 h k a^* b^* U^{12}]$

	U^{11}	U^{22}	U^{33}	U^{23}	U^{13}	U^{12}
Re(1)	39(1)	43(1)	42(1)	1(1)	14(1)	-2(1)
Re(2)	42(1)	53(1)	36(1)	1(1)	11(1)	-3(1)
Cl(1)	44(1)	43(1)	59(1)	4(1)	10(1)	2(1)
Cl(2)	44(1)	51(1)	47(1)	-7(1)	13(1)	3(1)
C(1)	57(4)	72(5)	63(5)	14(4)	18(3)	-2(3)
O(1)	119(5)	120(5)	71(4)	39(4)	46(4)	1(4)
C(2)	48(4)	54(4)	55(4)	-5(3)	20(3)	-4(3)
O(2)	45(3)	75(3)	81(4)	-5(3)	18(2)	-1(2)
C(3)	43(3)	57(4)	64(4)	4(3)	14(3)	-1(3)
O(3)	59(3)	68(3)	116(5)	-30(3)	26(3)	-11(3)
C(4)	49(3)	51(3)	40(3)	-6(3)	18(3)	-1(3)
O(4)	67(3)	69(3)	60(3)	8(2)	35(2)	15(2)
C(5)	62(4)	103(6)	58(5)	16(4)	16(4)	2(4)
O(5)	143(7)	186(9)	74(4)	62(5)	49(4)	10(6)
C(6)	46(3)	79(5)	59(4)	-15(4)	9(3)	-3(3)
O(6)	90(4)	90(4)	111(5)	-54(4)	10(4)	-7(3)
C(7)	52(4)	64(4)	46(4)	-2(3)	10(3)	-4(3)
O(7)	48(3)	98(4)	68(3)	3(3)	-5(2)	3(3)
C(8)	45(3)	39(3)	42(3)	4(2)	12(2)	-2(2)
O(8)	76(3)	56(3)	62(3)	18(2)	33(2)	20(2)
Fe(1)	75(1)	53(1)	45(1)	3(1)	4(1)	-1(1)
C(9)	46(3)	49(3)	43(3)	-2(3)	12(3)	-2(2)
C(10)	74(5)	59(4)	60(4)	10(3)	31(4)	-1(3)
C(11)	95(6)	49(4)	59(4)	10(3)	17(4)	1(4)
C(12)	69(4)	44(3)	71(5)	6(3)	11(4)	7(3)
C(13)	59(4)	47(3)	46(3)	-1(3)	13(3)	4(3)
C(14)	151(11)	68(6)	82(7)	-3(5)	-32(7)	-34(6)
C(15)	139(10)	101(8)	80(7)	-48(6)	0(7)	-9(7)
C(16)	161(12)	101(8)	54(6)	5(5)	-24(7)	-17(8)
C(17)	109(9)	116(9)	87(8)	9(7)	-29(7)	-11(6)
C(18)	89(7)	129(10)	97(8)	-11(7)	1(6)	-40(7)
Fe(2)	47(1)	67(1)	56(1)	3(1)	17(1)	-11(1)
C(19)	38(3)	45(3)	43(3)	2(2)	10(2)	-3(2)
C(20)	47(3)	49(3)	48(3)	-8(3)	11(3)	-1(3)
C(21)	58(4)	63(4)	62(4)	-12(3)	23(3)	7(3)
C(22)	67(4)	78(5)	52(4)	-3(3)	26(3)	-3(4)
C(23)	60(4)	59(4)	41(3)	5(3)	15(3)	-3(3)

C(24)	116(9)	134(10)	86(7)	-35(7)	22(6)	-79(8)
C(25)	81(7)	143(11)	103(9)	27(8)	-19(6)	-48(7)
C(26)	52(5)	141(11)	167(13)	18(10)	11(7)	-25(6)
C(27)	90(7)	164(12)	96(8)	21(8)	22(6)	-73(8)
C(28)	103(8)	72(6)	124(9)	1(6)	1(7)	-44(5)
C(29)	106(6)	79(5)	85(6)	15(5)	57(5)	41(5)
C(30)	350(20)	96(8)	106(9)	3(7)	105(12)	100(12)
C(31)	119(7)	60(5)	109(7)	22(5)	64(6)	39(5)
C(32)	184(13)	71(6)	127(10)	15(6)	49(9)	50(7)
Cl(3)	205(5)	171(4)	184(4)	9(3)	30(4)	84(4)
C(33)	350(50)	130(20)	220(30)	0	-110(30)	0

Table 5. Hydrogen coordinates (x 10^4) and isotropic displacement parameters ($Å^2$x 10^3) for Complex **28**.

	x	y	z	U(eq)
H(10)	1514	2586	2393	75
H(11)	2249	1302	2674	81
H(12)	2957	1229	1875	74
H(13)	2668	2457	1069	60
H(14)	2905	4607	2178	128
H(15)	2464	4089	3166	131
H(16)	3086	2710	3568	133
H(17)	3868	2426	2863	131
H(18)	3738	3585	2024	128
H(20)	-395	3941	350	57
H(21)	-979	4181	1245	72
H(22)	-650	3019	2088	77
H(23)	156	2037	1728	63
H(24)	-893	1522	-194	134
H(25)	-1634	2776	-250	136
H(26)	-2056	2754	755	145
H(27)	-1594	1494	1443	139
H(28)	-850	686	826	122
H(29A)	1307	5204	1528	102
H(29B)	682	4732	1294	102
H(30A)	585	4545	2295	213
H(30B)	597	5534	2094	213
H(30C)	1179	5106	2494	213
H(31A)	761	826	133	109
H(31B)	1365	1318	426	109
H(32A)	1309	578	1357	187
H(32B)	1463	-9	810	187
H(32C)	801	-6	963	187
H(33A)	39	-448	2869	304
H(33B)	-39	-448	2131	304

Table 6. Torsion angles [°] for Complex **28**.

C(7)-Re(2)-Cl(1)-Re(1)	-177.3(2)
C(5)-Re(2)-Cl(1)-Re(1)	-89.0(2)
C(8)-Re(2)-Cl(1)-Re(1)	88.97(16)
Cl(2)-Re(2)-Cl(1)-Re(1)	-0.40(5)
C(3)-Re(1)-Cl(1)-Re(2)	180.0(2)
C(1)-Re(1)-Cl(1)-Re(2)	90.2(2)
C(4)-Re(1)-Cl(1)-Re(2)	-86.42(16)
Cl(2)-Re(1)-Cl(1)-Re(2)	0.40(5)
C(2)-Re(1)-Cl(2)-Re(2)	-177.3(2)
C(1)-Re(1)-Cl(2)-Re(2)	-89.4(2)
C(4)-Re(1)-Cl(2)-Re(2)	89.12(16)
Cl(1)-Re(1)-Cl(2)-Re(2)	-0.40(5)
C(6)-Re(2)-Cl(2)-Re(1)	178.5(2)
C(7)-Re(2)-Cl(2)-Re(1)	23.6(15)
C(5)-Re(2)-Cl(2)-Re(1)	90.6(3)
C(8)-Re(2)-Cl(2)-Re(1)	-87.15(16)
Cl(1)-Re(2)-Cl(2)-Re(1)	0.40(5)
C(6)-Re(2)-C(8)-O(8)	48.6(6)
C(7)-Re(2)-C(8)-O(8)	135.5(6)
Cl(1)-Re(2)-C(8)-O(8)	-130.7(5)
Cl(2)-Re(2)-C(8)-O(8)	-51.8(5)
C(6)-Re(2)-C(8)-C(19)	-133.4(5)
C(7)-Re(2)-C(8)-C(19)	-46.5(5)
Cl(1)-Re(2)-C(8)-C(19)	47.3(5)
Cl(2)-Re(2)-C(8)-C(19)	126.2(5)
C(19)-C(8)-O(8)-C(31)	174.8(7)
Re(2)-C(8)-O(8)-C(31)	-6.9(10)
O(4)-C(4)-C(9)-C(10)	-4.4(9)
Re(1)-C(4)-C(9)-C(10)	-179.3(5)
O(4)-C(4)-C(9)-C(13)	-170.8(6)
Re(1)-C(4)-C(9)-C(13)	14.3(9)
O(4)-C(4)-C(9)-Fe(1)	-86.7(6)
Re(1)-C(4)-C(9)-Fe(1)	98.4(5)
C(10)-Fe(1)-C(9)-C(4)	119.8(6)
C(14)-Fe(1)-C(9)-C(4)	-8.6(7)
C(16)-Fe(1)-C(9)-C(4)	73.6(10)
C(18)-Fe(1)-C(9)-C(4)	-49.1(8)
C(13)-Fe(1)-C(9)-C(4)	-122.5(6)
C(15)-Fe(1)-C(9)-C(4)	37.0(7)

C(17)-Fe(1)-C(9)-C(4)	-87.1(15)
C(12)-Fe(1)-C(9)-C(4)	-159.7(5)
C(11)-Fe(1)-C(9)-C(4)	157.3(5)
C(14)-Fe(1)-C(9)-C(10)	-128.4(6)
C(16)-Fe(1)-C(9)-C(10)	-46.2(10)
C(18)-Fe(1)-C(9)-C(10)	-168.9(6)
C(13)-Fe(1)-C(9)-C(10)	117.8(5)
C(15)-Fe(1)-C(9)-C(10)	-82.7(6)
C(17)-Fe(1)-C(9)-C(10)	153.1(14)
C(12)-Fe(1)-C(9)-C(10)	80.5(4)
C(11)-Fe(1)-C(9)-C(10)	37.5(4)
C(10)-Fe(1)-C(9)-C(13)	-117.8(5)
C(14)-Fe(1)-C(9)-C(13)	113.9(6)
C(16)-Fe(1)-C(9)-C(13)	-164.0(9)
C(18)-Fe(1)-C(9)-C(13)	73.3(7)
C(15)-Fe(1)-C(9)-C(13)	159.5(6)
C(17)-Fe(1)-C(9)-C(13)	35.4(16)
C(12)-Fe(1)-C(9)-C(13)	-37.3(4)
C(11)-Fe(1)-C(9)-C(13)	-80.2(4)
C(4)-C(9)-C(10)-C(11)	-169.7(6)
C(13)-C(9)-C(10)-C(11)	-0.9(8)
Fe(1)-C(9)-C(10)-C(11)	-60.8(6)
C(4)-C(9)-C(10)-Fe(1)	-108.9(6)
C(13)-C(9)-C(10)-Fe(1)	59.9(4)
C(9)-Fe(1)-C(10)-C(11)	118.7(6)
C(14)-Fe(1)-C(10)-C(11)	-165.8(6)
C(16)-Fe(1)-C(10)-C(11)	-81.7(6)
C(18)-Fe(1)-C(10)-C(11)	164.2(19)
C(13)-Fe(1)-C(10)-C(11)	79.9(5)
C(15)-Fe(1)-C(10)-C(11)	-124.6(6)
C(17)-Fe(1)-C(10)-C(11)	-46.4(11)
C(12)-Fe(1)-C(10)-C(11)	36.5(4)
C(14)-Fe(1)-C(10)-C(9)	75.4(6)
C(16)-Fe(1)-C(10)-C(9)	159.6(5)
C(18)-Fe(1)-C(10)-C(9)	45(2)
C(13)-Fe(1)-C(10)-C(9)	-38.8(4)
C(15)-Fe(1)-C(10)-C(9)	116.7(5)
C(17)-Fe(1)-C(10)-C(9)	-165.1(9)
C(12)-Fe(1)-C(10)-C(9)	-82.2(4)
C(11)-Fe(1)-C(10)-C(9)	-118.7(6)

C(9)-C(10)-C(11)-C(12)	1.2(9)
Fe(1)-C(10)-C(11)-C(12)	-58.5(6)
C(9)-C(10)-C(11)-Fe(1)	59.8(5)
C(10)-Fe(1)-C(11)-C(12)	120.7(6)
C(9)-Fe(1)-C(11)-C(12)	82.0(5)
C(14)-Fe(1)-C(11)-C(12)	175.0(16)
C(16)-Fe(1)-C(11)-C(12)	-124.1(6)
C(18)-Fe(1)-C(11)-C(12)	-52.5(10)
C(13)-Fe(1)-C(11)-C(12)	37.2(4)
C(15)-Fe(1)-C(11)-C(12)	-164.1(6)
C(17)-Fe(1)-C(11)-C(12)	-82.1(6)
C(9)-Fe(1)-C(11)-C(10)	-38.7(4)
C(14)-Fe(1)-C(11)-C(10)	54.3(18)
C(16)-Fe(1)-C(11)-C(10)	115.2(6)
C(18)-Fe(1)-C(11)-C(10)	-173.2(8)
C(13)-Fe(1)-C(11)-C(10)	-83.5(5)
C(15)-Fe(1)-C(11)-C(10)	75.2(6)
C(17)-Fe(1)-C(11)-C(10)	157.2(6)
C(12)-Fe(1)-C(11)-C(10)	-120.7(6)
C(10)-C(11)-C(12)-C(13)	-1.1(9)
Fe(1)-C(11)-C(12)-C(13)	-58.9(5)
C(10)-C(11)-C(12)-Fe(1)	57.8(6)
C(10)-Fe(1)-C(12)-C(11)	-36.8(4)
C(9)-Fe(1)-C(12)-C(11)	-81.7(5)
C(14)-Fe(1)-C(12)-C(11)	-177.5(8)
C(16)-Fe(1)-C(12)-C(11)	74.0(7)
C(18)-Fe(1)-C(12)-C(11)	154.0(6)
C(13)-Fe(1)-C(12)-C(11)	-120.0(6)
C(15)-Fe(1)-C(12)-C(11)	45.6(15)
C(17)-Fe(1)-C(12)-C(11)	113.8(6)
C(10)-Fe(1)-C(12)-C(13)	83.2(4)
C(9)-Fe(1)-C(12)-C(13)	38.3(4)
C(14)-Fe(1)-C(12)-C(13)	-57.5(10)
C(16)-Fe(1)-C(12)-C(13)	-166.0(6)
C(18)-Fe(1)-C(12)-C(13)	-85.9(6)
C(15)-Fe(1)-C(12)-C(13)	165.6(13)
C(17)-Fe(1)-C(12)-C(13)	-126.2(6)
C(11)-Fe(1)-C(12)-C(13)	120.0(6)
C(11)-C(12)-C(13)-C(9)	0.5(8)
Fe(1)-C(12)-C(13)-C(9)	-58.8(4)

C(11)-C(12)-C(13)-Fe(1)	59.3(5)
C(4)-C(9)-C(13)-C(12)	168.7(6)
C(10)-C(9)-C(13)-C(12)	0.2(8)
Fe(1)-C(9)-C(13)-C(12)	59.6(5)
C(4)-C(9)-C(13)-Fe(1)	109.0(6)
C(10)-C(9)-C(13)-Fe(1)	-59.4(5)
C(10)-Fe(1)-C(13)-C(12)	-80.3(5)
C(9)-Fe(1)-C(13)-C(12)	-119.2(6)
C(14)-Fe(1)-C(13)-C(12)	153.5(6)
C(16)-Fe(1)-C(13)-C(12)	39.1(15)
C(18)-Fe(1)-C(13)-C(12)	112.4(6)
C(15)-Fe(1)-C(13)-C(12)	-168.7(11)
C(17)-Fe(1)-C(13)-C(12)	71.8(6)
C(11)-Fe(1)-C(13)-C(12)	-36.9(4)
C(10)-Fe(1)-C(13)-C(9)	39.0(4)
C(14)-Fe(1)-C(13)-C(9)	-87.3(6)
C(16)-Fe(1)-C(13)-C(9)	158.3(13)
C(18)-Fe(1)-C(13)-C(9)	-128.4(5)
C(15)-Fe(1)-C(13)-C(9)	-49.5(12)
C(17)-Fe(1)-C(13)-C(9)	-169.0(5)
C(12)-Fe(1)-C(13)-C(9)	119.2(6)
C(11)-Fe(1)-C(13)-C(9)	82.4(4)
C(10)-Fe(1)-C(14)-C(18)	-170.4(6)
C(9)-Fe(1)-C(14)-C(18)	-126.8(7)
C(16)-Fe(1)-C(14)-C(18)	80.3(8)
C(13)-Fe(1)-C(14)-C(18)	-81.5(8)
C(15)-Fe(1)-C(14)-C(18)	119.8(10)
C(17)-Fe(1)-C(14)-C(18)	36.4(8)
C(12)-Fe(1)-C(14)-C(18)	-41.7(12)
C(11)-Fe(1)-C(14)-C(18)	145.4(16)
C(10)-Fe(1)-C(14)-C(15)	69.8(8)
C(9)-Fe(1)-C(14)-C(15)	113.5(7)
C(16)-Fe(1)-C(14)-C(15)	-39.5(7)
C(18)-Fe(1)-C(14)-C(15)	-119.8(10)
C(13)-Fe(1)-C(14)-C(15)	158.7(6)
C(17)-Fe(1)-C(14)-C(15)	-83.3(8)
C(12)-Fe(1)-C(14)-C(15)	-161.5(8)
C(11)-Fe(1)-C(14)-C(15)	26(2)
C(18)-C(14)-C(15)-C(16)	0.8(11)
Fe(1)-C(14)-C(15)-C(16)	60.9(7)

C(18)-C(14)-C(15)-Fe(1)	-60.1(7)
C(10)-Fe(1)-C(15)-C(16)	113.1(8)
C(9)-Fe(1)-C(15)-C(16)	157.1(7)
C(14)-Fe(1)-C(15)-C(16)	-115.1(11)
C(18)-Fe(1)-C(15)-C(16)	-79.2(9)
C(13)-Fe(1)-C(15)-C(16)	-166.8(9)
C(17)-Fe(1)-C(15)-C(16)	-36.8(8)
C(12)-Fe(1)-C(15)-C(16)	37.3(18)
C(11)-Fe(1)-C(15)-C(16)	71.9(9)
C(10)-Fe(1)-C(15)-C(14)	-131.8(7)
C(9)-Fe(1)-C(15)-C(14)	-87.8(8)
C(16)-Fe(1)-C(15)-C(14)	115.1(11)
C(18)-Fe(1)-C(15)-C(14)	36.0(7)
C(13)-Fe(1)-C(15)-C(14)	-51.7(14)
C(17)-Fe(1)-C(15)-C(14)	78.3(8)
C(12)-Fe(1)-C(15)-C(14)	152.4(12)
C(11)-Fe(1)-C(15)-C(14)	-173.0(7)
C(14)-C(15)-C(16)-C(17)	-0.9(12)
Fe(1)-C(15)-C(16)-C(17)	59.5(8)
C(14)-C(15)-C(16)-Fe(1)	-60.4(6)
C(10)-Fe(1)-C(16)-C(17)	154.8(7)
C(9)-Fe(1)-C(16)-C(17)	-172.0(7)
C(14)-Fe(1)-C(16)-C(17)	-79.5(8)
C(18)-Fe(1)-C(16)-C(17)	-37.2(8)
C(13)-Fe(1)-C(16)-C(17)	43.2(17)
C(15)-Fe(1)-C(16)-C(17)	-120.3(11)
C(12)-Fe(1)-C(16)-C(17)	72.8(8)
C(11)-Fe(1)-C(16)-C(17)	112.9(7)
C(10)-Fe(1)-C(16)-C(15)	-84.9(8)
C(9)-Fe(1)-C(16)-C(15)	-51.7(13)
C(14)-Fe(1)-C(16)-C(15)	40.8(8)
C(18)-Fe(1)-C(16)-C(15)	83.1(9)
C(13)-Fe(1)-C(16)-C(15)	163.6(11)
C(17)-Fe(1)-C(16)-C(15)	120.3(11)
C(12)-Fe(1)-C(16)-C(15)	-166.9(7)
C(11)-Fe(1)-C(16)-C(15)	-126.8(8)
C(15)-C(16)-C(17)-C(18)	0.7(13)
Fe(1)-C(16)-C(17)-C(18)	60.1(7)
C(15)-C(16)-C(17)-Fe(1)	-59.4(7)
C(10)-Fe(1)-C(17)-C(18)	-170.3(8)

C(9)-Fe(1)-C(17)-C(18)	48.8(19)
C(14)-Fe(1)-C(17)-C(18)	-36.2(8)
C(16)-Fe(1)-C(17)-C(18)	-118.6(12)
C(13)-Fe(1)-C(17)-C(18)	76.8(9)
C(15)-Fe(1)-C(17)-C(18)	-81.6(9)
C(12)-Fe(1)-C(17)-C(18)	116.5(8)
C(11)-Fe(1)-C(17)-C(18)	157.8(8)
C(10)-Fe(1)-C(17)-C(16)	-51.7(13)
C(9)-Fe(1)-C(17)-C(16)	167.4(12)
C(14)-Fe(1)-C(17)-C(16)	82.5(8)
C(18)-Fe(1)-C(17)-C(16)	118.6(12)
C(13)-Fe(1)-C(17)-C(16)	-164.6(6)
C(15)-Fe(1)-C(17)-C(16)	37.0(7)
C(12)-Fe(1)-C(17)-C(16)	-124.9(7)
C(11)-Fe(1)-C(17)-C(16)	-83.5(8)
C(15)-C(14)-C(18)-C(17)	-0.5(12)
Fe(1)-C(14)-C(18)-C(17)	-59.7(8)
C(15)-C(14)-C(18)-Fe(1)	59.3(7)
C(16)-C(17)-C(18)-C(14)	-0.1(13)
Fe(1)-C(17)-C(18)-C(14)	59.6(8)
C(16)-C(17)-C(18)-Fe(1)	-59.7(8)
C(10)-Fe(1)-C(18)-C(14)	37(2)
C(9)-Fe(1)-C(18)-C(14)	74.7(8)
C(16)-Fe(1)-C(18)-C(14)	-82.5(8)
C(13)-Fe(1)-C(18)-C(14)	116.8(7)
C(15)-Fe(1)-C(18)-C(14)	-38.5(7)
C(17)-Fe(1)-C(18)-C(14)	-120.6(12)
C(12)-Fe(1)-C(18)-C(14)	159.9(6)
C(11)-Fe(1)-C(18)-C(14)	-164.5(7)
C(10)-Fe(1)-C(18)-C(17)	157.5(18)
C(9)-Fe(1)-C(18)-C(17)	-164.8(7)
C(14)-Fe(1)-C(18)-C(17)	120.6(12)
C(16)-Fe(1)-C(18)-C(17)	38.1(8)
C(13)-Fe(1)-C(18)-C(17)	-122.6(8)
C(15)-Fe(1)-C(18)-C(17)	82.0(9)
C(12)-Fe(1)-C(18)-C(17)	-79.5(9)
C(11)-Fe(1)-C(18)-C(17)	-43.9(13)
O(8)-C(8)-C(19)-C(23)	-1.2(8)
Re(2)-C(8)-C(19)-C(23)	-179.5(5)
O(8)-C(8)-C(19)-C(20)	-171.5(6)

Re(2)-C(8)-C(19)-C(20)	10.2(9)
O(8)-C(8)-C(19)-Fe(2)	-85.7(6)
Re(2)-C(8)-C(19)-Fe(2)	96.0(5)
C(24)-Fe(2)-C(19)-C(23)	-129.7(6)
C(27)-Fe(2)-C(19)-C(23)	-46.9(10)
C(20)-Fe(2)-C(19)-C(23)	118.4(5)
C(28)-Fe(2)-C(19)-C(23)	-85.7(6)
C(26)-Fe(2)-C(19)-C(23)	156(2)
C(22)-Fe(2)-C(19)-C(23)	37.6(4)
C(21)-Fe(2)-C(19)-C(23)	81.0(4)
C(25)-Fe(2)-C(19)-C(23)	-171.0(7)
C(24)-Fe(2)-C(19)-C(20)	111.9(6)
C(23)-Fe(2)-C(19)-C(20)	-118.4(5)
C(27)-Fe(2)-C(19)-C(20)	-165.3(9)
C(28)-Fe(2)-C(19)-C(20)	155.8(5)
C(26)-Fe(2)-C(19)-C(20)	37(2)
C(22)-Fe(2)-C(19)-C(20)	-80.8(4)
C(21)-Fe(2)-C(19)-C(20)	-37.5(4)
C(25)-Fe(2)-C(19)-C(20)	70.5(7)
C(24)-Fe(2)-C(19)-C(8)	-10.1(7)
C(23)-Fe(2)-C(19)-C(8)	119.6(6)
C(27)-Fe(2)-C(19)-C(8)	72.8(11)
C(20)-Fe(2)-C(19)-C(8)	-121.9(6)
C(28)-Fe(2)-C(19)-C(8)	33.9(7)
C(26)-Fe(2)-C(19)-C(8)	-84(2)
C(22)-Fe(2)-C(19)-C(8)	157.2(6)
C(21)-Fe(2)-C(19)-C(8)	-159.4(5)
C(25)-Fe(2)-C(19)-C(8)	-51.4(8)
C(23)-C(19)-C(20)-C(21)	1.2(7)
C(8)-C(19)-C(20)-C(21)	173.0(6)
Fe(2)-C(19)-C(20)-C(21)	60.6(5)
C(23)-C(19)-C(20)-Fe(2)	-59.3(4)
C(8)-C(19)-C(20)-Fe(2)	112.4(6)
C(24)-Fe(2)-C(20)-C(21)	152.2(7)
C(19)-Fe(2)-C(20)-C(21)	-118.5(6)
C(23)-Fe(2)-C(20)-C(21)	-80.0(4)
C(27)-Fe(2)-C(20)-C(21)	38.6(14)
C(28)-Fe(2)-C(20)-C(21)	-172.8(8)
C(26)-Fe(2)-C(20)-C(21)	72.1(7)
C(22)-Fe(2)-C(20)-C(21)	-36.5(4)

C(25)-Fe(2)-C(20)-C(21)	111.2(6)
C(24)-Fe(2)-C(20)-C(19)	-89.3(7)
C(23)-Fe(2)-C(20)-C(19)	38.5(4)
C(27)-Fe(2)-C(20)-C(19)	157.1(12)
C(28)-Fe(2)-C(20)-C(19)	-54.3(10)
C(26)-Fe(2)-C(20)-C(19)	-169.4(6)
C(22)-Fe(2)-C(20)-C(19)	82.0(4)
C(21)-Fe(2)-C(20)-C(19)	118.5(6)
C(25)-Fe(2)-C(20)-C(19)	-130.3(6)
C(19)-C(20)-C(21)-C(22)	-1.3(8)
Fe(2)-C(20)-C(21)-C(22)	58.1(5)
C(19)-C(20)-C(21)-Fe(2)	-59.4(4)
C(24)-Fe(2)-C(21)-C(20)	-57.5(10)
C(19)-Fe(2)-C(21)-C(20)	38.8(4)
C(23)-Fe(2)-C(21)-C(20)	83.7(4)
C(27)-Fe(2)-C(21)-C(20)	-167.0(6)
C(28)-Fe(2)-C(21)-C(20)	167.6(15)
C(26)-Fe(2)-C(21)-C(20)	-127.0(6)
C(22)-Fe(2)-C(21)-C(20)	121.2(6)
C(25)-Fe(2)-C(21)-C(20)	-85.7(6)
C(24)-Fe(2)-C(21)-C(22)	-178.7(8)
C(19)-Fe(2)-C(21)-C(22)	-82.4(4)
C(23)-Fe(2)-C(21)-C(22)	-37.4(4)
C(27)-Fe(2)-C(21)-C(22)	71.8(6)
C(20)-Fe(2)-C(21)-C(22)	-121.2(6)
C(28)-Fe(2)-C(21)-C(22)	46.4(16)
C(26)-Fe(2)-C(21)-C(22)	111.8(6)
C(25)-Fe(2)-C(21)-C(22)	153.1(6)
C(20)-C(21)-C(22)-C(23)	0.9(8)
Fe(2)-C(21)-C(22)-C(23)	58.8(5)
C(20)-C(21)-C(22)-Fe(2)	-57.9(5)
C(24)-Fe(2)-C(22)-C(23)	57(2)
C(19)-Fe(2)-C(22)-C(23)	-38.6(4)
C(27)-Fe(2)-C(22)-C(23)	113.8(6)
C(20)-Fe(2)-C(22)-C(23)	-83.3(4)
C(28)-Fe(2)-C(22)-C(23)	74.0(6)
C(26)-Fe(2)-C(22)-C(23)	155.3(6)
C(21)-Fe(2)-C(22)-C(23)	-119.6(6)
C(25)-Fe(2)-C(22)-C(23)	-172.0(7)
C(24)-Fe(2)-C(22)-C(21)	176.9(19)

C(19)-Fe(2)-C(22)-C(21)	81.1(4)
C(23)-Fe(2)-C(22)-C(21)	119.6(6)
C(27)-Fe(2)-C(22)-C(21)	-126.6(6)
C(20)-Fe(2)-C(22)-C(21)	36.3(4)
C(28)-Fe(2)-C(22)-C(21)	-166.3(6)
C(26)-Fe(2)-C(22)-C(21)	-85.0(6)
C(25)-Fe(2)-C(22)-C(21)	-52.4(9)
C(21)-C(22)-C(23)-C(19)	-0.1(8)
Fe(2)-C(22)-C(23)-C(19)	59.4(4)
C(21)-C(22)-C(23)-Fe(2)	-59.5(5)
C(20)-C(19)-C(23)-C(22)	-0.7(7)
C(8)-C(19)-C(23)-C(22)	-172.6(6)
Fe(2)-C(19)-C(23)-C(22)	-60.2(5)
C(20)-C(19)-C(23)-Fe(2)	59.5(4)
C(8)-C(19)-C(23)-Fe(2)	-112.5(6)
C(24)-Fe(2)-C(23)-C(22)	-166.5(6)
C(19)-Fe(2)-C(23)-C(22)	118.8(6)
C(27)-Fe(2)-C(23)-C(22)	-82.8(7)
C(20)-Fe(2)-C(23)-C(22)	80.3(4)
C(28)-Fe(2)-C(23)-C(22)	-127.1(6)
C(26)-Fe(2)-C(23)-C(22)	-49.5(11)
C(21)-Fe(2)-C(23)-C(22)	37.3(4)
C(25)-Fe(2)-C(23)-C(22)	158(2)
C(24)-Fe(2)-C(23)-C(19)	74.7(6)
C(27)-Fe(2)-C(23)-C(19)	158.3(6)
C(20)-Fe(2)-C(23)-C(19)	-38.5(3)
C(28)-Fe(2)-C(23)-C(19)	114.0(5)
C(26)-Fe(2)-C(23)-C(19)	-168.3(9)
C(22)-Fe(2)-C(23)-C(19)	-118.8(6)
C(21)-Fe(2)-C(23)-C(19)	-81.6(4)
C(25)-Fe(2)-C(23)-C(19)	39(2)
C(19)-Fe(2)-C(24)-C(25)	-126.4(7)
C(23)-Fe(2)-C(24)-C(25)	-170.0(6)
C(27)-Fe(2)-C(24)-C(25)	82.3(8)
C(20)-Fe(2)-C(24)-C(25)	-80.8(8)
C(28)-Fe(2)-C(24)-C(25)	122.0(11)
C(26)-Fe(2)-C(24)-C(25)	38.7(7)
C(22)-Fe(2)-C(24)-C(25)	142.4(19)
C(21)-Fe(2)-C(24)-C(25)	-41.7(12)
C(19)-Fe(2)-C(24)-C(28)	111.6(7)

C(23)-Fe(2)-C(24)-C(28)	68.0(9)
C(27)-Fe(2)-C(24)-C(28)	-39.6(7)
C(20)-Fe(2)-C(24)-C(28)	157.2(7)
C(26)-Fe(2)-C(24)-C(28)	-83.3(8)
C(22)-Fe(2)-C(24)-C(28)	20(2)
C(21)-Fe(2)-C(24)-C(28)	-163.7(7)
C(25)-Fe(2)-C(24)-C(28)	-122.0(11)
C(28)-C(24)-C(25)-C(26)	-1.5(12)
Fe(2)-C(24)-C(25)-C(26)	-60.8(8)
C(28)-C(24)-C(25)-Fe(2)	59.3(7)
C(19)-Fe(2)-C(25)-C(24)	75.7(8)
C(23)-Fe(2)-C(25)-C(24)	43(3)
C(27)-Fe(2)-C(25)-C(24)	-80.7(8)
C(20)-Fe(2)-C(25)-C(24)	116.7(7)
C(28)-Fe(2)-C(25)-C(24)	-36.1(7)
C(26)-Fe(2)-C(25)-C(24)	-116.4(11)
C(22)-Fe(2)-C(25)-C(24)	-165.7(7)
C(21)-Fe(2)-C(25)-C(24)	159.1(6)
C(24)-Fe(2)-C(25)-C(26)	116.4(11)
C(19)-Fe(2)-C(25)-C(26)	-167.9(7)
C(23)-Fe(2)-C(25)-C(26)	159.0(19)
C(27)-Fe(2)-C(25)-C(26)	35.6(9)
C(20)-Fe(2)-C(25)-C(26)	-126.9(8)
C(28)-Fe(2)-C(25)-C(26)	80.2(9)
C(22)-Fe(2)-C(25)-C(26)	-49.4(13)
C(21)-Fe(2)-C(25)-C(26)	-84.5(9)
C(24)-C(25)-C(26)-C(27)	2.3(13)
Fe(2)-C(25)-C(26)-C(27)	-58.0(8)
C(24)-C(25)-C(26)-Fe(2)	60.3(7)
C(24)-Fe(2)-C(26)-C(25)	-38.7(8)
C(19)-Fe(2)-C(26)-C(25)	42(2)
C(23)-Fe(2)-C(26)-C(25)	-172.0(8)
C(27)-Fe(2)-C(26)-C(25)	-122.6(13)
C(20)-Fe(2)-C(26)-C(25)	71.9(10)
C(28)-Fe(2)-C(26)-C(25)	-82.7(9)
C(22)-Fe(2)-C(26)-C(25)	154.3(8)
C(21)-Fe(2)-C(26)-C(25)	111.8(9)
C(24)-Fe(2)-C(26)-C(27)	84.0(9)
C(19)-Fe(2)-C(26)-C(27)	164.3(16)
C(23)-Fe(2)-C(26)-C(27)	-49.4(14)

C(20)-Fe(2)-C(26)-C(27)	-165.4(7)
C(28)-Fe(2)-C(26)-C(27)	39.9(8)
C(22)-Fe(2)-C(26)-C(27)	-83.1(9)
C(21)-Fe(2)-C(26)-C(27)	-125.5(9)
C(25)-Fe(2)-C(26)-C(27)	122.6(13)
C(25)-C(26)-C(27)-C(28)	-2.2(13)
Fe(2)-C(26)-C(27)-C(28)	-60.9(7)
C(25)-C(26)-C(27)-Fe(2)	58.7(8)
C(24)-Fe(2)-C(27)-C(26)	-77.6(9)
C(19)-Fe(2)-C(27)-C(26)	-171.6(9)
C(23)-Fe(2)-C(27)-C(26)	155.2(8)
C(20)-Fe(2)-C(27)-C(26)	43.6(17)
C(28)-Fe(2)-C(27)-C(26)	-116.2(11)
C(22)-Fe(2)-C(27)-C(26)	113.1(9)
C(21)-Fe(2)-C(27)-C(26)	73.3(10)
C(25)-Fe(2)-C(27)-C(26)	-35.1(9)
C(24)-Fe(2)-C(27)-C(28)	38.7(7)
C(19)-Fe(2)-C(27)-C(28)	-55.3(12)
C(23)-Fe(2)-C(27)-C(28)	-88.5(7)
C(20)-Fe(2)-C(27)-C(28)	159.9(11)
C(26)-Fe(2)-C(27)-C(28)	116.2(11)
C(22)-Fe(2)-C(27)-C(28)	-130.7(7)
C(21)-Fe(2)-C(27)-C(28)	-170.5(6)
C(25)-Fe(2)-C(27)-C(28)	81.2(8)
C(25)-C(24)-C(28)-C(27)	0.2(11)
Fe(2)-C(24)-C(28)-C(27)	60.3(7)
C(25)-C(24)-C(28)-Fe(2)	-60.0(8)
C(26)-C(27)-C(28)-C(24)	1.2(11)
Fe(2)-C(27)-C(28)-C(24)	-60.4(6)
C(26)-C(27)-C(28)-Fe(2)	61.5(7)
C(19)-Fe(2)-C(28)-C(24)	-88.7(8)
C(23)-Fe(2)-C(28)-C(24)	-133.3(8)
C(27)-Fe(2)-C(28)-C(24)	116.6(11)
C(20)-Fe(2)-C(28)-C(24)	-50.1(13)
C(26)-Fe(2)-C(28)-C(24)	77.9(8)
C(22)-Fe(2)-C(28)-C(24)	-174.7(7)
C(21)-Fe(2)-C(28)-C(24)	148.4(14)
C(25)-Fe(2)-C(28)-C(24)	35.4(8)
C(24)-Fe(2)-C(28)-C(27)	-116.6(11)
C(19)-Fe(2)-C(28)-C(27)	154.8(6)

C(23)-Fe(2)-C(28)-C(27)	110.2(7)
C(20)-Fe(2)-C(28)-C(27)	-166.7(8)
C(26)-Fe(2)-C(28)-C(27)	-38.6(7)
C(22)-Fe(2)-C(28)-C(27)	68.7(8)
C(21)-Fe(2)-C(28)-C(27)	31.9(19)
C(25)-Fe(2)-C(28)-C(27)	-81.2(8)
C(4)-O(4)-C(29)-C(30)	-157.8(11)
C(8)-O(8)-C(31)-C(32)	-177.4(9)

Appendix 10

Crystallographic data of Complex 33

Table 1. Crystal data and structure refinement for Complex **33**.

Identification code	db55a3a_abs	
Empirical formula	$C_{40} H_{22} Fe O_{22} Re_4 Ti$	
Formula weight	1703.13	
Temperature	293(2) K	
Wavelength	0.71073 Å	
Crystal system	Triclinic	
Space group	P $\bar{1}$	
Unit cell dimensions	a = 10.7406(7) Å	a= 90.9060(10)°.
	b = 12.1924(8) Å	b= 94.7320(10)°.
	c = 18.4356(12) Å	g = 95.6650(10)°.
Volume	2393.5(3) $Å^3$	
Z	2	
Density (calculated)	2.363 Mg/m^3	
Absorption coefficient	10.607 mm^{-1}	
F(000)	1572	
Crystal size	0.17 x 0.17 x 0.01 mm^3	
Theta range for data collection	2.41 to 26.33°.	
Index ranges	-13<=h<=5, -14<=k<=13, -21<=l<=22	
Reflections collected	12826	
Independent reflections	8569 [R(int) = 0.0308]	
Completeness to theta = 25.00°	97.2 %	
Absorption correction	Semi-empirical from equivalents	
Max. and min. transmission	0.727 and 0.215	
Refinement method	Full-matrix least-squares on F^2	
Data / restraints / parameters	8569 / 0 / 608	
Goodness-of-fit on F^2	1.025	
Final R indices [I>2sigma(I)]	R1 = 0.0503, wR2 = 0.1319	
R indices (all data)	R1 = 0.0778, wR2 = 0.1520	
Extinction coefficient	0.00036(10)	
Largest diff. peak and hole	3.273 and -1.699 e.$Å^{-3}$	

Table 2. Atomic coordinates (x 10^4) and equivalent isotropic displacement parameters (Å^{2}x 10^3) for Complex **33**. U(eq) is defined as one third of the trace of the orthogonalized U^{ij} tensor.

	x	y	z	U(eq)
Re(1)	2508(1)	8347(1)	-291(1)	45(1)
Re(2)	2014(1)	7706(1)	1271(1)	44(1)
Re(3)	8470(1)	2372(1)	4638(1)	62(1)
Re(4)	6893(1)	3587(1)	3518(1)	46(1)
Fe(1)	3470(2)	4021(1)	1560(1)	40(1)
Ti(1)	5958(2)	6973(2)	2524(1)	38(1)
C(1)	2876(15)	8806(12)	-1244(9)	60(4)
O(1)	3129(13)	9049(10)	-1824(7)	85(4)
C(2)	2566(12)	6755(11)	-514(8)	50(3)
O(2)	2549(12)	5873(9)	-691(7)	75(3)
C(3)	669(15)	8112(13)	-566(10)	67(4)
O(3)	-366(10)	7975(12)	-768(9)	103(5)
C(4)	2327(16)	9851(13)	60(10)	70(5)
O(4)	2261(13)	10736(9)	266(8)	91(4)
C(5)	4269(14)	8509(12)	116(9)	57(4)
O(5)	5290(10)	8622(10)	366(8)	87(4)
C(6)	1575(14)	7272(15)	2215(11)	69(5)
O(6)	1305(12)	7038(14)	2775(8)	101(5)
C(7)	700(12)	6645(12)	785(9)	54(4)
O(7)	-132(10)	6105(10)	506(8)	90(4)
C(8)	870(20)	8825(14)	1210(8)	91(8)
O(8)	-41(11)	9337(10)	1165(8)	87(4)
C(9)	3316(15)	8954(13)	1565(9)	60(4)
O(9)	4011(12)	9683(10)	1728(8)	86(4)
C(10)	3505(10)	6617(10)	1393(6)	35(3)
O(10)	4543(7)	6928(6)	1772(5)	42(2)
C(11)	9543(19)	1747(15)	5365(11)	86(6)
O(11)	10214(16)	1371(15)	5786(11)	142(7)
C(12)	8492(15)	1241(14)	3886(11)	70(5)
O(12)	8444(14)	587(11)	3431(10)	107(5)
C(13)	6870(19)	1610(14)	4923(11)	79(5)
O(13)	5963(15)	1160(12)	5092(8)	104(5)
C(14)	8200(20)	3605(18)	5320(10)	83(6)
O(14)	7967(18)	4285(14)	5703(9)	122(6)
C(15)	9900(17)	3206(14)	4193(12)	80(5)
O(15)	10656(14)	3685(12)	3927(10)	113(5)
C(16)	6062(13)	2065(12)	3327(8)	50(3)

O(16)	5589(10)	1201(8)	3228(7)	69(3)
C(17)	5717(19)	3751(14)	4248(10)	72(5)
O(17)	5007(17)	3852(13)	4645(9)	119(6)
C(18)	7950(17)	4939(14)	3862(10)	70(4)
O(18)	8589(14)	5689(10)	4110(8)	96(4)
C(19)	8014(14)	3469(13)	2824(9)	66(5)
O(19)	8722(13)	3305(13)	2341(8)	102(5)
C(20)	5707(13)	4386(9)	2820(7)	42(3)
O(20)	5833(7)	5407(6)	2681(4)	39(2)
C(21)	3482(11)	5526(10)	1068(7)	42(3)
C(22)	4573(12)	4980(11)	933(7)	43(3)
C(23)	4168(13)	3959(11)	570(7)	48(3)
C(24)	2871(13)	3834(11)	480(8)	51(3)
C(25)	2412(12)	4764(11)	795(8)	49(3)
C(26)	4472(12)	3829(10)	2532(7)	44(3)
C(27)	4222(14)	2800(12)	2140(8)	59(4)
C(28)	2872(17)	2562(14)	1998(10)	76(5)
C(29)	2296(14)	3412(15)	2318(9)	68(5)
C(30)	3256(14)	4211(13)	2622(8)	56(4)
C(31)	7000(14)	7108(15)	1423(9)	67(5)
C(32)	7621(15)	6427(14)	1866(11)	71(5)
C(33)	8156(14)	7032(19)	2480(10)	78(5)
C(34)	7891(16)	8081(15)	2399(11)	75(5)
C(35)	7127(15)	8138(13)	1773(11)	71(5)
C(36)	4557(18)	7016(17)	3455(11)	86(7)
C(37)	5770(20)	6912(18)	3790(9)	89(7)
C(38)	6463(18)	7850(20)	3677(11)	84(6)
C(39)	5720(20)	8507(14)	3263(11)	80(5)
C(40)	4600(9)	7991(7)	3162(5)	79(5)
O(21)	1887(9)	112(7)	3125(5)	127(7)
O(22)	2301(9)	1241(7)	4453(5)	127(6)

Table 3. Bond lengths [Å] and angles [°] for Complex **33**.

O(5)-C(5)	1.149(18)	Ti(1)-C(37)	2.361(17)
Re(1)-C(1)	1.912(17)	Ti(1)-C(32)	2.381(15)
Re(1)-C(5)	1.967(15)	Ti(1)-C(36)	2.377(15)
Re(1)-C(4)	1.968(17)	Ti(1)-C(40)	2.376(8)
Re(1)-C(2)	1.985(14)	Ti(1)-C(34)	2.392(14)
Re(1)-C(3)	1.989(17)	Ti(1)-C(31)	2.398(16)
Re(1)-Re(2)	3.0712(8)	C(1)-O(1)	1.161(18)
Re(2)-C(6)	1.909(19)	C(2)-O(2)	1.117(16)
Re(2)-C(8)	1.923(14)	C(3)-O(3)	1.138(19)
Re(2)-C(7)	1.965(15)	C(4)-O(4)	1.150(18)
Re(2)-C(9)	1.999(17)	C(6)-O(6)	1.129(19)
Re(2)-C(10)	2.178(11)	C(7)-O(7)	1.138(17)
Re(3)-C(11)	1.912(18)	C(8)-O(8)	1.209(18)
Re(3)-C(12)	1.94(2)	C(9)-O(9)	1.123(18)
Re(3)-C(13)	1.98(2)	C(10)-O(10)	1.286(14)
Re(3)-C(15)	1.999(19)	C(10)-C(21)	1.448(17)
Re(3)-C(14)	2.00(2)	C(11)-O(11)	1.15(2)
Re(3)-Re(4)	3.0569(8)	C(12)-O(12)	1.14(2)
Re(4)-C(19)	1.84(2)	C(13)-O(13)	1.14(2)
Re(4)-C(17)	1.941(18)	C(14)-O(14)	1.14(2)
Re(4)-C(18)	1.972(18)	C(15)-O(15)	1.11(2)
Re(4)-C(16)	1.991(15)	C(16)-O(16)	1.129(16)
Re(4)-C(20)	2.059(13)	C(17)-O(17)	1.11(2)
Fe(1)-C(30)	2.003(14)	C(18)-O(18)	1.151(19)
Fe(1)-C(25)	2.019(13)	C(19)-O(19)	1.24(2)
Fe(1)-C(22)	2.025(12)	C(20)-O(20)	1.272(14)
Fe(1)-C(28)	2.033(15)	C(20)-C(26)	1.481(18)
Fe(1)-C(23)	2.032(13)	C(21)-C(22)	1.440(17)
Fe(1)-C(26)	2.043(13)	C(21)-C(25)	1.454(17)
Fe(1)-C(24)	2.043(14)	C(22)-C(23)	1.416(18)
Fe(1)-C(27)	2.038(14)	C(22)-H(22)	0.9300
Fe(1)-C(29)	2.058(15)	C(23)-C(24)	1.382(19)
Fe(1)-C(21)	2.059(12)	C(23)-H(23)	0.9300
Ti(1)-O(20)	1.929(8)	C(24)-C(25)	1.417(19)
Ti(1)-O(10)	1.968(9)	C(24)-H(24)	0.9300
Ti(1)-C(39)	2.343(16)	C(25)-H(25)	0.9300
Ti(1)-C(35)	2.347(14)	C(26)-C(27)	1.430(19)
Ti(1)-C(33)	2.363(15)	C(26)-C(30)	1.45(2)
Ti(1)-C(38)	2.363(17)	C(27)-C(28)	1.45(2)

C(27)-H(27)	0.9300
C(28)-C(29)	1.40(2)
C(28)-H(28)	0.9300
C(29)-C(30)	1.42(2)
C(29)-H(29)	0.9300
C(30)-H(30)	0.9300
C(31)-C(32)	1.36(2)
C(31)-C(35)	1.39(2)
C(31)-H(31)	0.9300
C(32)-C(33)	1.39(2)
C(32)-H(32)	0.9300
C(33)-C(34)	1.35(2)
C(33)-H(33)	0.9300
C(34)-C(35)	1.37(2)
C(34)-H(34)	0.9300
C(35)-H(35)	0.9300
C(36)-C(40)	1.31(2)
C(36)-C(37)	1.41(3)
C(36)-H(36)	0.9300
C(37)-C(38)	1.34(3)
C(37)-H(37)	0.9300
C(38)-C(39)	1.37(3)
C(38)-H(38)	0.9300
C(39)-C(40)	1.30(2)
C(39)-H(39)	0.9300
C(40)-H(40)	0.9300

C(1)-Re(1)-C(5)	94.9(7)
C(1)-Re(1)-C(4)	93.9(6)
C(5)-Re(1)-C(4)	89.6(7)
C(1)-Re(1)-C(2)	94.5(6)
C(5)-Re(1)-C(2)	91.9(6)
C(4)-Re(1)-C(2)	171.4(6)
C(1)-Re(1)-C(3)	93.1(7)
C(5)-Re(1)-C(3)	171.9(7)
C(4)-Re(1)-C(3)	90.1(7)
C(2)-Re(1)-C(3)	87.3(6)
C(1)-Re(1)-Re(2)	177.1(5)
C(5)-Re(1)-Re(2)	82.9(5)
C(4)-Re(1)-Re(2)	84.2(5)
C(2)-Re(1)-Re(2)	87.6(4)
C(3)-Re(1)-Re(2)	89.0(5)
C(6)-Re(2)-C(8)	93.2(6)
C(6)-Re(2)-C(7)	92.2(7)
C(8)-Re(2)-C(7)	89.8(8)
C(6)-Re(2)-C(9)	98.9(7)
C(8)-Re(2)-C(9)	84.7(9)
C(7)-Re(2)-C(9)	167.8(6)
C(6)-Re(2)-C(10)	87.6(5)
C(8)-Re(2)-C(10)	172.2(8)
C(7)-Re(2)-C(10)	98.0(5)
C(9)-Re(2)-C(10)	87.5(5)
C(6)-Re(2)-Re(1)	175.5(5)
C(8)-Re(2)-Re(1)	84.7(4)
C(7)-Re(2)-Re(1)	83.8(5)
C(9)-Re(2)-Re(1)	84.8(5)
C(10)-Re(2)-Re(1)	95.0(3)
C(11)-Re(3)-C(12)	97.4(8)
C(11)-Re(3)-C(13)	96.5(8)
C(12)-Re(3)-C(13)	88.9(8)
C(11)-Re(3)-C(15)	93.4(8)
C(12)-Re(3)-C(15)	87.6(8)
C(13)-Re(3)-C(15)	169.9(8)
C(11)-Re(3)-C(14)	91.4(8)
C(12)-Re(3)-C(14)	170.8(7)
C(13)-Re(3)-C(14)	87.4(8)
C(15)-Re(3)-C(14)	94.6(8)
C(11)-Re(3)-Re(4)	174.5(6)
C(12)-Re(3)-Re(4)	86.7(5)
C(13)-Re(3)-Re(4)	87.3(5)
C(15)-Re(3)-Re(4)	83.0(5)
C(14)-Re(3)-Re(4)	84.8(5)
C(19)-Re(4)-C(17)	178.6(7)
C(19)-Re(4)-C(18)	86.4(7)
C(17)-Re(4)-C(18)	92.5(8)
C(19)-Re(4)-C(16)	93.9(7)
C(17)-Re(4)-C(16)	87.4(7)
C(18)-Re(4)-C(16)	167.6(6)
C(19)-Re(4)-C(20)	92.3(5)
C(17)-Re(4)-C(20)	87.0(6)

C(18)-Re(4)-C(20)	94.9(6)
C(16)-Re(4)-C(20)	97.4(5)
C(19)-Re(4)-Re(3)	92.5(4)
C(17)-Re(4)-Re(3)	88.3(5)
C(18)-Re(4)-Re(3)	86.6(5)
C(16)-Re(4)-Re(3)	81.1(4)
C(20)-Re(4)-Re(3)	175.1(3)
C(30)-Fe(1)-C(25)	121.4(6)
C(30)-Fe(1)-C(22)	128.2(6)
C(25)-Fe(1)-C(22)	69.4(5)
C(30)-Fe(1)-C(28)	68.9(7)
C(25)-Fe(1)-C(28)	122.6(6)
C(22)-Fe(1)-C(28)	153.4(7)
C(30)-Fe(1)-C(23)	164.8(6)
C(25)-Fe(1)-C(23)	68.3(6)
C(22)-Fe(1)-C(23)	40.8(5)
C(28)-Fe(1)-C(23)	117.3(7)
C(30)-Fe(1)-C(26)	42.0(6)
C(25)-Fe(1)-C(26)	157.9(6)
C(22)-Fe(1)-C(26)	108.0(5)
C(28)-Fe(1)-C(26)	70.0(6)
C(23)-Fe(1)-C(26)	124.9(6)
C(30)-Fe(1)-C(24)	155.1(6)
C(25)-Fe(1)-C(24)	40.8(5)
C(22)-Fe(1)-C(24)	68.2(6)
C(28)-Fe(1)-C(24)	104.4(6)
C(23)-Fe(1)-C(24)	39.7(6)
C(26)-Fe(1)-C(24)	160.3(6)
C(30)-Fe(1)-C(27)	69.3(7)
C(25)-Fe(1)-C(27)	160.0(6)
C(22)-Fe(1)-C(27)	119.2(6)
C(28)-Fe(1)-C(27)	41.8(6)
C(23)-Fe(1)-C(27)	105.5(6)
C(26)-Fe(1)-C(27)	41.0(5)
C(24)-Fe(1)-C(27)	122.5(6)
C(30)-Fe(1)-C(29)	40.9(6)
C(25)-Fe(1)-C(29)	107.3(6)
C(22)-Fe(1)-C(29)	165.9(7)
C(28)-Fe(1)-C(29)	40.1(7)
C(23)-Fe(1)-C(29)	152.0(6)
C(26)-Fe(1)-C(29)	69.7(6)
C(24)-Fe(1)-C(29)	118.9(6)
C(27)-Fe(1)-C(29)	68.8(7)
C(30)-Fe(1)-C(21)	109.6(6)
C(25)-Fe(1)-C(21)	41.8(5)
C(22)-Fe(1)-C(21)	41.3(5)
C(28)-Fe(1)-C(21)	162.1(6)
C(23)-Fe(1)-C(21)	69.0(5)
C(26)-Fe(1)-C(21)	121.7(5)
C(24)-Fe(1)-C(21)	69.1(5)
C(27)-Fe(1)-C(21)	155.8(5)
C(29)-Fe(1)-C(21)	127.2(7)
O(20)-Ti(1)-O(10)	96.1(3)
O(20)-Ti(1)-C(39)	133.5(6)
O(10)-Ti(1)-C(39)	104.4(6)
O(20)-Ti(1)-C(35)	133.6(5)
O(10)-Ti(1)-C(35)	88.1(5)
C(39)-Ti(1)-C(35)	89.0(7)
O(20)-Ti(1)-C(33)	91.2(6)
O(10)-Ti(1)-C(33)	133.4(5)
C(39)-Ti(1)-C(33)	103.3(8)
C(35)-Ti(1)-C(33)	55.8(6)
O(20)-Ti(1)-C(38)	106.9(7)
O(10)-Ti(1)-C(38)	135.4(6)
C(39)-Ti(1)-C(38)	34.0(7)
C(35)-Ti(1)-C(38)	101.7(8)
C(33)-Ti(1)-C(38)	84.7(7)
O(20)-Ti(1)-C(37)	78.5(6)
O(10)-Ti(1)-C(37)	125.0(7)
C(39)-Ti(1)-C(37)	55.5(7)
C(35)-Ti(1)-C(37)	134.4(9)
C(33)-Ti(1)-C(37)	101.6(8)
C(38)-Ti(1)-C(37)	32.8(7)
O(20)-Ti(1)-C(32)	78.5(5)
O(10)-Ti(1)-C(32)	102.9(6)
C(39)-Ti(1)-C(32)	133.9(7)
C(35)-Ti(1)-C(32)	55.7(6)
C(33)-Ti(1)-C(32)	34.1(6)
C(38)-Ti(1)-C(32)	118.6(7)
C(37)-Ti(1)-C(32)	128.4(7)

O(20)-Ti(1)-C(36)	84.7(6)
O(10)-Ti(1)-C(36)	90.6(6)
C(39)-Ti(1)-C(36)	54.3(6)
C(35)-Ti(1)-C(36)	141.6(7)
C(33)-Ti(1)-C(36)	136.0(7)
C(38)-Ti(1)-C(36)	55.3(6)
C(37)-Ti(1)-C(36)	34.7(7)
C(32)-Ti(1)-C(36)	159.4(8)
O(20)-Ti(1)-C(40)	116.1(4)
O(10)-Ti(1)-C(40)	81.3(4)
C(39)-Ti(1)-C(40)	32.1(5)
C(35)-Ti(1)-C(40)	110.3(5)
C(33)-Ti(1)-C(40)	135.0(6)
C(38)-Ti(1)-C(40)	54.4(6)
C(37)-Ti(1)-C(40)	55.0(5)
C(32)-Ti(1)-C(40)	164.6(5)
C(36)-Ti(1)-C(40)	32.0(6)
O(20)-Ti(1)-C(34)	124.0(6)
O(10)-Ti(1)-C(34)	121.5(6)
C(39)-Ti(1)-C(34)	78.9(6)
C(35)-Ti(1)-C(34)	33.5(6)
C(33)-Ti(1)-C(34)	32.9(6)
C(38)-Ti(1)-C(34)	75.7(7)
C(37)-Ti(1)-C(34)	105.1(8)
C(32)-Ti(1)-C(34)	55.2(6)
C(36)-Ti(1)-C(34)	129.5(6)
C(40)-Ti(1)-C(34)	109.9(5)
O(20)-Ti(1)-C(31)	101.9(5)
O(10)-Ti(1)-C(31)	77.6(5)
C(39)-Ti(1)-C(31)	122.9(6)
C(35)-Ti(1)-C(31)	34.1(6)
C(33)-Ti(1)-C(31)	55.9(6)
C(38)-Ti(1)-C(31)	131.2(6)
C(37)-Ti(1)-C(31)	157.4(8)
C(32)-Ti(1)-C(31)	33.0(6)
C(36)-Ti(1)-C(31)	167.0(8)
C(40)-Ti(1)-C(31)	138.2(6)
C(34)-Ti(1)-C(31)	55.6(6)
O(1)-C(1)-Re(1)	177.3(14)
O(2)-C(2)-Re(1)	174.5(14)
O(3)-C(3)-Re(1)	175.6(17)
O(4)-C(4)-Re(1)	177.9(15)
O(5)-C(5)-Re(1)	178.3(14)
O(6)-C(6)-Re(2)	178.5(17)
O(7)-C(7)-Re(2)	173.7(12)
O(8)-C(8)-Re(2)	166.0(19)
O(9)-C(9)-Re(2)	177.3(14)
O(10)-C(10)-C(21)	113.0(10)
O(10)-C(10)-Re(2)	120.6(8)
C(21)-C(10)-Re(2)	126.4(8)
C(10)-O(10)-Ti(1)	161.3(8)
O(11)-C(11)-Re(3)	178(2)
O(12)-C(12)-Re(3)	176.5(15)
O(13)-C(13)-Re(3)	178.9(18)
O(14)-C(14)-Re(3)	175.5(19)
O(15)-C(15)-Re(3)	177.1(18)
O(16)-C(16)-Re(4)	179.2(13)
O(17)-C(17)-Re(4)	177.2(19)
O(18)-C(18)-Re(4)	175.0(16)
O(19)-C(19)-Re(4)	174.8(14)
O(20)-C(20)-C(26)	112.8(11)
O(20)-C(20)-Re(4)	125.7(10)
C(26)-C(20)-Re(4)	120.6(8)
C(20)-O(20)-Ti(1)	176.2(8)
C(22)-C(21)-C(10)	125.3(11)
C(22)-C(21)-C(25)	105.4(11)
C(10)-C(21)-C(25)	129.3(11)
C(22)-C(21)-Fe(1)	68.1(7)
C(10)-C(21)-Fe(1)	129.4(9)
C(25)-C(21)-Fe(1)	67.6(7)
C(23)-C(22)-C(21)	108.5(11)
C(23)-C(22)-Fe(1)	69.9(7)
C(21)-C(22)-Fe(1)	70.6(7)
C(23)-C(22)-H(22)	125.8
C(21)-C(22)-H(22)	125.8
Fe(1)-C(22)-H(22)	125.3
C(24)-C(23)-C(22)	109.1(12)
C(24)-C(23)-Fe(1)	70.6(8)
C(22)-C(23)-Fe(1)	69.3(7)
C(24)-C(23)-H(23)	125.4

C(22)-C(23)-H(23)	125.4
Fe(1)-C(23)-H(23)	126.2
C(23)-C(24)-C(25)	108.7(12)
C(23)-C(24)-Fe(1)	69.7(8)
C(25)-C(24)-Fe(1)	68.7(8)
C(23)-C(24)-H(24)	125.6
C(25)-C(24)-H(24)	125.6
Fe(1)-C(24)-H(24)	127.5
C(24)-C(25)-C(21)	108.2(11)
C(24)-C(25)-Fe(1)	70.5(8)
C(21)-C(25)-Fe(1)	70.6(7)
C(24)-C(25)-H(25)	125.9
C(21)-C(25)-H(25)	125.9
Fe(1)-C(25)-H(25)	124.6
C(27)-C(26)-C(30)	105.9(12)
C(27)-C(26)-C(20)	127.9(13)
C(30)-C(26)-C(20)	126.2(12)
C(27)-C(26)-Fe(1)	69.3(8)
C(30)-C(26)-Fe(1)	67.5(8)
C(20)-C(26)-Fe(1)	129.3(9)
C(26)-C(27)-C(28)	108.4(15)
C(26)-C(27)-Fe(1)	69.7(8)
C(28)-C(27)-Fe(1)	68.9(8)
C(26)-C(27)-H(27)	125.8
C(28)-C(27)-H(27)	125.8
Fe(1)-C(27)-H(27)	127.2
C(29)-C(28)-C(27)	108.2(14)
C(29)-C(28)-Fe(1)	70.9(9)
C(27)-C(28)-Fe(1)	69.3(8)
C(29)-C(28)-H(28)	125.9
C(27)-C(28)-H(28)	125.9
Fe(1)-C(28)-H(28)	125.5
C(28)-C(29)-C(30)	108.0(14)
C(28)-C(29)-Fe(1)	69.0(9)
C(30)-C(29)-Fe(1)	67.5(8)
C(28)-C(29)-H(29)	126.0
C(30)-C(29)-H(29)	126.0
Fe(1)-C(29)-H(29)	129.1
C(29)-C(30)-C(26)	109.4(14)
C(29)-C(30)-Fe(1)	71.7(9)
C(26)-C(30)-Fe(1)	70.5(8)
C(29)-C(30)-H(30)	125.3
C(26)-C(30)-H(30)	125.3
Fe(1)-C(30)-H(30)	124.2
C(32)-C(31)-C(35)	106.8(16)
C(32)-C(31)-Ti(1)	72.8(10)
C(35)-C(31)-Ti(1)	70.9(9)
C(32)-C(31)-H(31)	126.6
C(35)-C(31)-H(31)	126.6
Ti(1)-C(31)-H(31)	121.5
C(31)-C(32)-C(33)	108.5(16)
C(31)-C(32)-Ti(1)	74.2(9)
C(33)-C(32)-Ti(1)	72.2(9)
C(31)-C(32)-H(32)	125.8
C(33)-C(32)-H(32)	125.8
Ti(1)-C(32)-H(32)	119.7
C(34)-C(33)-C(32)	107.8(16)
C(34)-C(33)-Ti(1)	74.7(9)
C(32)-C(33)-Ti(1)	73.7(9)
C(34)-C(33)-H(33)	126.1
C(32)-C(33)-H(33)	126.1
Ti(1)-C(33)-H(33)	117.5
C(33)-C(34)-C(35)	108.6(15)
C(33)-C(34)-Ti(1)	72.4(9)
C(35)-C(34)-Ti(1)	71.4(8)
C(33)-C(34)-H(34)	125.7
C(35)-C(34)-H(34)	125.7
Ti(1)-C(34)-H(34)	122.1
C(34)-C(35)-C(31)	108.1(16)
C(34)-C(35)-Ti(1)	75.1(9)
C(31)-C(35)-Ti(1)	75.0(8)
C(34)-C(35)-H(35)	125.9
C(31)-C(35)-H(35)	125.9
Ti(1)-C(35)-H(35)	116.1
C(40)-C(36)-C(37)	106.7(16)
C(40)-C(36)-Ti(1)	73.9(8)
C(37)-C(36)-Ti(1)	72.0(10)
C(40)-C(36)-H(36)	126.6
C(37)-C(36)-H(36)	126.6
Ti(1)-C(36)-H(36)	119.4

C(38)-C(37)-C(36)	106.4(17)	C(40)-C(39)-C(38)	108.0(16)
C(38)-C(37)-Ti(1)	73.7(11)	C(40)-C(39)-Ti(1)	75.4(8)
C(36)-C(37)-Ti(1)	73.3(10)	C(38)-C(39)-Ti(1)	73.8(10)
C(38)-C(37)-H(37)	126.8	C(40)-C(39)-H(39)	126.0
C(36)-C(37)-H(37)	126.8	C(38)-C(39)-H(39)	126.0
Ti(1)-C(37)-H(37)	118.3	Ti(1)-C(39)-H(39)	116.8
C(37)-C(38)-C(39)	107.9(18)	C(36)-C(40)-C(39)	111.0(15)
C(37)-C(38)-Ti(1)	73.5(11)	C(36)-C(40)-Ti(1)	74.0(8)
C(39)-C(38)-Ti(1)	72.2(10)	C(39)-C(40)-Ti(1)	72.6(8)
C(37)-C(38)-H(38)	126.1	C(36)-C(40)-H(40)	124.5
C(39)-C(38)-H(38)	126.1	C(39)-C(40)-H(40)	124.5
Ti(1)-C(38)-H(38)	120.0	Ti(1)-C(40)-H(40)	120.5

Symmetry transformations used to generate equivalent atoms:

Table 4. Anisotropic displacement parameters (Å^{2}x 10^3)for Complex **33**. The anisotropic displacement factor exponent takes the form: -2p^2[h^{2}a*^{2}U^{11} + ... + 2 h k a* b* U^{12}]

	U^{11}	U^{22}	U^{33}	U^{23}	U^{13}	U^{12}
O(5)	47(6)	87(9)	122(11)	0(8)	0(7)	-5(6)
Re(1)	40(1)	38(1)	57(1)	0(1)	4(1)	8(1)
Re(2)	33(1)	43(1)	56(1)	1(1)	3(1)	9(1)
Re(3)	62(1)	48(1)	71(1)	11(1)	-23(1)	1(1)
Re(4)	50(1)	37(1)	48(1)	1(1)	-8(1)	5(1)
Fe(1)	38(1)	34(1)	45(1)	0(1)	-4(1)	2(1)
Ti(1)	37(1)	29(1)	46(1)	-4(1)	-1(1)	3(1)
C(1)	74(10)	45(8)	61(11)	-2(7)	6(8)	10(7)
O(1)	110(10)	87(9)	60(8)	16(7)	30(7)	0(7)
C(2)	51(8)	38(8)	62(10)	10(7)	13(7)	7(6)
O(2)	93(8)	45(6)	90(9)	2(6)	9(7)	10(6)
C(3)	61(10)	53(9)	89(13)	-3(8)	9(9)	18(7)
O(3)	36(6)	109(11)	156(14)	3(9)	-20(7)	-2(6)
C(4)	77(11)	50(9)	92(13)	21(9)	38(10)	23(8)
O(4)	104(10)	45(7)	129(12)	-11(7)	28(9)	12(6)
C(5)	46(8)	62(9)	67(11)	-5(8)	12(7)	10(7)
C(6)	47(8)	89(12)	76(13)	14(10)	13(8)	21(8)
O(6)	73(8)	166(15)	68(9)	26(9)	24(7)	17(8)
C(7)	36(7)	49(8)	76(11)	5(7)	-10(7)	10(6)
O(7)	49(6)	69(7)	145(13)	-10(8)	-27(7)	7(6)
C(8)	180(19)	88(12)	35(9)	38(8)	70(11)	101(13)
O(8)	71(7)	75(8)	124(11)	13(7)	21(7)	41(6)
C(9)	62(9)	55(9)	66(11)	-3(8)	13(8)	18(8)
O(9)	83(8)	60(7)	107(11)	-14(7)	-18(7)	-13(6)
C(10)	31(6)	40(6)	31(7)	2(5)	-2(5)	0(5)
O(10)	39(4)	32(4)	52(6)	-7(4)	-4(4)	1(3)
C(11)	90(13)	71(12)	92(15)	26(11)	-29(11)	8(10)
O(11)	115(12)	127(13)	170(17)	74(13)	-63(12)	-9(10)
C(12)	54(9)	57(10)	96(14)	6(10)	-22(9)	11(7)
O(12)	108(11)	67(8)	144(14)	-34(9)	-20(10)	25(8)
C(13)	93(13)	55(10)	83(14)	18(9)	-13(11)	-4(9)
O(13)	107(11)	92(10)	106(12)	21(9)	7(9)	-18(9)
C(14)	104(14)	93(14)	42(10)	13(10)	-13(10)	-22(11)
O(14)	162(16)	107(12)	86(11)	-34(9)	6(11)	-27(11)
C(15)	62(10)	57(10)	114(16)	8(10)	-8(10)	-6(8)
O(15)	92(10)	96(11)	144(15)	13(10)	10(10)	-20(8)
C(16)	52(8)	51(9)	45(8)	5(7)	-8(6)	5(6)

O(16)	71(7)	42(6)	90(9)	-4(5)	-12(6)	-5(5)
C(17)	97(13)	66(11)	59(11)	9(8)	23(10)	20(9)
O(17)	156(15)	113(12)	99(12)	-1(9)	54(11)	34(11)
C(18)	86(12)	57(10)	66(11)	0(8)	-2(9)	10(9)
O(18)	119(11)	50(7)	106(11)	-1(7)	-43(9)	-13(7)
C(19)	52(8)	70(10)	67(11)	45(9)	-28(8)	-18(7)
O(19)	87(9)	129(12)	92(11)	1(9)	26(8)	2(8)
C(20)	68(8)	29(6)	29(7)	0(5)	12(6)	5(6)
O(20)	47(5)	36(5)	31(5)	-8(4)	-2(4)	-1(4)
C(21)	39(6)	43(7)	40(8)	3(6)	-8(5)	0(5)
C(22)	44(7)	49(7)	38(7)	5(6)	8(6)	9(6)
C(23)	56(8)	42(7)	46(8)	-11(6)	7(6)	-3(6)
C(24)	60(8)	40(7)	50(9)	-11(6)	-9(7)	-1(6)
C(25)	36(6)	50(8)	59(9)	6(7)	-12(6)	1(6)
C(26)	55(8)	35(7)	39(8)	2(6)	-1(6)	-5(5)
C(27)	67(9)	47(8)	57(10)	6(7)	-29(8)	1(7)
C(28)	85(12)	58(10)	72(12)	17(9)	-32(10)	-32(9)
C(29)	42(8)	93(13)	62(11)	8(9)	4(7)	-22(8)
C(30)	65(9)	63(9)	38(8)	-6(7)	4(7)	-3(7)
C(31)	49(8)	85(12)	60(11)	-14(9)	10(8)	-32(8)
C(32)	57(9)	62(10)	100(15)	-3(10)	31(10)	7(8)
C(33)	45(8)	124(17)	66(12)	19(12)	0(8)	18(10)
C(34)	60(10)	75(12)	83(13)	-28(10)	16(9)	-29(9)
C(35)	52(9)	52(9)	110(15)	33(10)	17(10)	-4(7)
C(36)	76(12)	106(15)	74(13)	-52(12)	42(11)	-26(11)
C(37)	150(20)	90(14)	37(10)	4(9)	8(11)	67(15)
C(38)	74(12)	113(17)	62(12)	-39(12)	1(10)	1(12)
C(39)	107(15)	43(9)	89(14)	-18(9)	23(12)	-1(9)
C(40)	71(11)	91(14)	82(14)	-21(11)	13(10)	42(11)
O(21)	176(15)	86(10)	121(13)	-48(9)	95(12)	-29(9)
O(22)	172(16)	101(11)	110(12)	-37(9)	-41(11)	71(11)

Table 5. Hydrogen coordinates (x 10^4) and isotropic displacement parameters (Å^{2}x 10^3) for Complex **33**.

	x	y	z	U(eq)
H(22)	5402	5252	1062	51
H(23)	4692	3454	416	58
H(24)	2381	3236	250	62
H(25)	1572	4870	824	59
H(27)	4822	2358	1999	71
H(28)	2460	1952	1740	91
H(29)	1436	3445	2329	81
H(30)	3125	4876	2843	67
H(31)	6572	6922	972	81
H(32)	7679	5682	1775	86
H(33)	8615	6760	2875	93
H(34)	8178	8669	2717	90
H(35)	6757	8757	1610	86
H(36)	3863	6494	3444	103
H(37)	6030	6308	4041	106
H(38)	7298	8036	3847	101
H(39)	5981	9196	3087	95
H(40)	3918	8276	2914	95

Table 6. Torsion angles [°] for Complex **33**.

C(5)-Re(1)-Re(2)-C(8)	127.0(9)
C(4)-Re(1)-Re(2)-C(8)	36.7(9)
C(2)-Re(1)-Re(2)-C(8)	-140.8(9)
C(3)-Re(1)-Re(2)-C(8)	-53.4(9)
C(5)-Re(1)-Re(2)-C(7)	-142.7(6)
C(4)-Re(1)-Re(2)-C(7)	127.1(7)
C(2)-Re(1)-Re(2)-C(7)	-50.5(6)
C(3)-Re(1)-Re(2)-C(7)	36.9(6)
C(5)-Re(1)-Re(2)-C(9)	41.9(6)
C(4)-Re(1)-Re(2)-C(9)	-48.4(7)
C(2)-Re(1)-Re(2)-C(9)	134.1(6)
C(3)-Re(1)-Re(2)-C(9)	-138.6(6)
C(5)-Re(1)-Re(2)-C(10)	-45.1(5)
C(4)-Re(1)-Re(2)-C(10)	-135.4(6)
C(2)-Re(1)-Re(2)-C(10)	47.1(5)
C(3)-Re(1)-Re(2)-C(10)	134.4(5)
C(12)-Re(3)-Re(4)-C(19)	-50.6(7)
C(13)-Re(3)-Re(4)-C(19)	-139.7(8)
C(15)-Re(3)-Re(4)-C(19)	37.4(8)
C(14)-Re(3)-Re(4)-C(19)	132.7(7)
C(12)-Re(3)-Re(4)-C(17)	130.6(8)
C(13)-Re(3)-Re(4)-C(17)	41.6(8)
C(15)-Re(3)-Re(4)-C(17)	-141.4(8)
C(14)-Re(3)-Re(4)-C(17)	-46.0(8)
C(12)-Re(3)-Re(4)-C(18)	-136.8(7)
C(13)-Re(3)-Re(4)-C(18)	134.1(8)
C(15)-Re(3)-Re(4)-C(18)	-48.8(8)
C(14)-Re(3)-Re(4)-C(18)	46.5(8)
C(12)-Re(3)-Re(4)-C(16)	42.9(7)
C(13)-Re(3)-Re(4)-C(16)	-46.1(7)
C(15)-Re(3)-Re(4)-C(16)	130.9(7)
C(14)-Re(3)-Re(4)-C(16)	-133.7(7)
C(6)-Re(2)-C(10)-O(10)	-79.8(11)
C(7)-Re(2)-C(10)-O(10)	-171.7(10)
C(9)-Re(2)-C(10)-O(10)	19.3(10)
Re(1)-Re(2)-C(10)-O(10)	103.8(9)
C(6)-Re(2)-C(10)-C(21)	101.7(12)
C(7)-Re(2)-C(10)-C(21)	9.8(12)
C(9)-Re(2)-C(10)-C(21)	-159.2(11)
Re(1)-Re(2)-C(10)-C(21)	-74.7(10)
C(19)-Re(4)-C(20)-C(26)	110.1(11)
C(17)-Re(4)-C(20)-C(26)	-71.2(11)
C(18)-Re(4)-C(20)-C(26)	-163.4(11)
C(16)-Re(4)-C(20)-C(26)	15.9(11)
O(10)-C(10)-C(21)-C(22)	-21.8(18)
Re(2)-C(10)-C(21)-C(22)	156.8(10)
O(10)-C(10)-C(21)-C(25)	159.8(13)
Re(2)-C(10)-C(21)-C(25)	-21.6(19)
O(10)-C(10)-C(21)-Fe(1)	67.7(14)
Re(2)-C(10)-C(21)-Fe(1)	-113.7(10)
C(10)-C(21)-C(22)-C(23)	-176.5(12)
C(25)-C(21)-C(22)-C(23)	2.3(14)
C(21)-C(22)-C(23)-C(24)	-0.8(16)
C(22)-C(23)-C(24)-C(25)	-1.0(17)
C(23)-C(24)-C(25)-C(21)	2.5(16)
C(22)-C(21)-C(25)-C(24)	-2.9(15)
C(10)-C(21)-C(25)-C(24)	175.8(13)
O(20)-C(20)-C(26)-C(27)	134.1(14)
Re(4)-C(20)-C(26)-C(27)	-56.0(17)
O(20)-C(20)-C(26)-C(30)	-48.6(17)
Re(4)-C(20)-C(26)-C(30)	121.3(13)
C(26)-C(27)-C(28)-C(29)	-1.9(18)
C(27)-C(28)-C(29)-C(30)	3.3(19)
C(28)-C(29)-C(30)-C(26)	-3.6(18)
C(27)-C(26)-C(30)-C(29)	2.4(16)
C(20)-C(26)-C(30)-C(29)	-175.4(13)
C(31)-C(32)-C(33)-C(34)	-1.7(19)
C(32)-C(31)-C(35)-C(34)	3.9(17)
C(40)-C(36)-C(37)-C(38)	0.4(18)
C(36)-C(37)-C(38)-C(39)	-2(2)
C(37)-C(38)-C(39)-C(40)	3(2)
C(37)-C(36)-C(40)-C(39)	1.4(17)
C(38)-C(39)-C(40)-C(36)	-2.7(18)

Table 7. Selected least-squares planes and deviations from the planes (Åx10^3) for Complex **33**.

Plane 1 4.491(33)x + 4.487(62)y - 15.695(65)z = 2.365(59)

Atoms *	Re(2)	C(10)	O(10)	C(21)	rms	[Ti(1)]
Deviations	2(3)	-8(10)	3(4)	3(3)	5	[-552(18)]

Plane 2 -5.907(49)x + 3.672(59)y + 15.374(29)z = 2.637(59)

Atoms *	Re(4)	C(20)	O(20)	C(26)	rms	[Ti(1)]
Deviations	17(3)	-62(10)	25(4)	20(3)	36	[285(17)]

Plane 3 0.523(76)x + 5.578(76)y - 16.520(57)z = 1.485(45)

Atoms *	C(21)	C(22)	C(23)	C(24)	C(25)	rms	[Fe(1)]
Deviations	15(8)	-10(8)	0(9)	10(9)	-16(9)	12	[-1638(6)]

Plane 4 -0.492(80)x - 6.016(84)y + 16.178(70)z = 1.563(49)

Atoms *	C(26)	C(27)	C(28)	C(29)	C(30)	rms	[Fe(1)]
Deviations	8(9)	4(9)	-15(10)	20(10)	-17(9)	14	[-1631(6)]

Plane 5 9.090(45)x + 1.928(94)y - 10.101(120) z = 6.282(77)

Atoms *	C(31)	C(32)	C(33)	C(34)	C(35)	rms	[Ti(1)]
Deviations	15(9)	1(10)	-16(10)	26(10)	-25(9)	19	[-2071(7)]

Plane 6 -4.011 (78)x + 5.098(98)y + 15.916(675)5 z = 7.250(82)

Atoms *	C(36)	C(37)	C(38)	C(39)	C(40)	rms	[Ti(1)]
Deviations	-2(9)	-7(11)	14(11)	-15(10)	11(9)	11	[-2068(7)]

Dihedral angles between planes (º):

Planes 1 and 2:	39.3(4)	Planes 3 and 4:	2.4(9)
Planes 1 and 3:	21.9(7)	Planes 5 and 6	51.4(7)
Planes 2 and 4:	53.8(4)		

* rms = root mean square deviation from the plane;
atoms not involved in calculating the plane are shown in brackets [ ].